INSIGHT
Gut microbes and health

nature

THE INTERNATIONAL WEEKLY JOURNAL OF SCIENCE

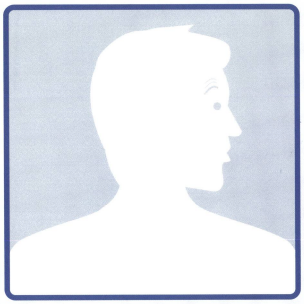

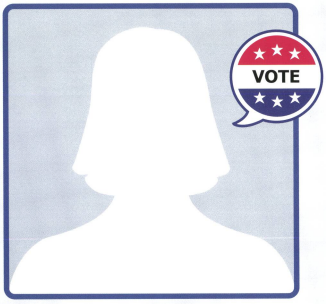

0 1 2 2 6 0 3 0 0
People on Facebook Voted

Close friendships beat weaker Facebook links in test of election-day influence PAGES 212 & 295

MICROWAVE WARFARE

UNEXPLODED MYTH?

The Pentagon's quest for the e-bomb

PAGE 198

RESEARCH CAREERS

PICKING WINNERS

A formula to predict your future h*-index*

PAGE 201

LITERATURE

FORGOTTEN FUTURES

When science fiction came of age

PAGE 204

NATURE.COM/NATURE
13 September 2012 £10
Vol. 489, No. 7415
37
9 770028 083095

R&D Systems Tools for Cell Biology Research™

NEW Interactive Pathways & Processes

✓ Designed by scientists for scientists

✓ One click to access the widest collection of products

✓ Request a printed copy, which includes additional resources

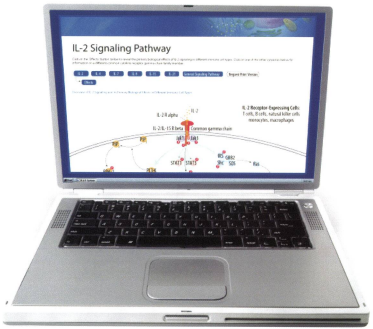

R&D Systems is excited to announce the addition of Interactive Pathways & Processes to the growing list of reference tools available on our website. These new fully-interactive pathways allow you to explore a variety of biological processes, including Apoptosis, Wnt Signaling, and Th1 Differentiation.

Start exploring today
www.RnDSystems.com/**Pathways**

R&D SYSTEMS®

nature OUTLOOK

Published in the 30 August issue of *Nature* and available free online for six months

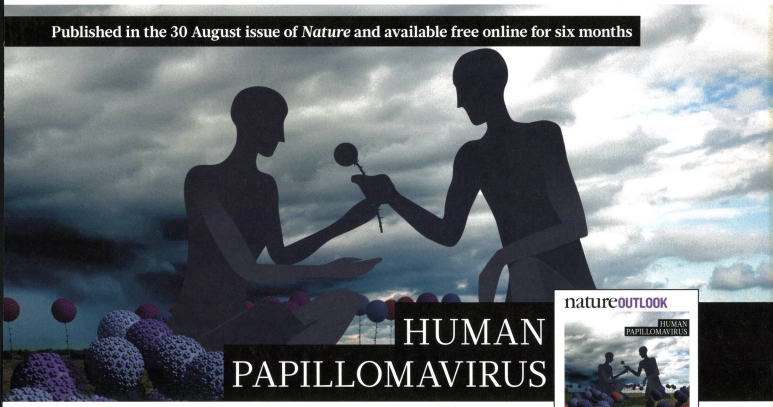

It is tempting to characterize the human papillomavirus (HPV) story as a triumph of science. It might have taken 30 years from identification of HPV as the cause of cervical cancer to the first vaccine reaching the market, but there is still much to understand about HPV biology and an urgent need to improve on existing vaccines and diagnostic tests. The story of HPV is still being written.

Access the Outlook free online for six months.
nature.com/nature/outlook/hpv_2012

Scan this tag to access the Outlook on your smartphone

Produced with support from: Vactia · FINNISH MEDICAL ASSOCIATION · PreHdict

If you would be interested in partnering with *Nature* on a similar project please contact: sponsorship@nature.com

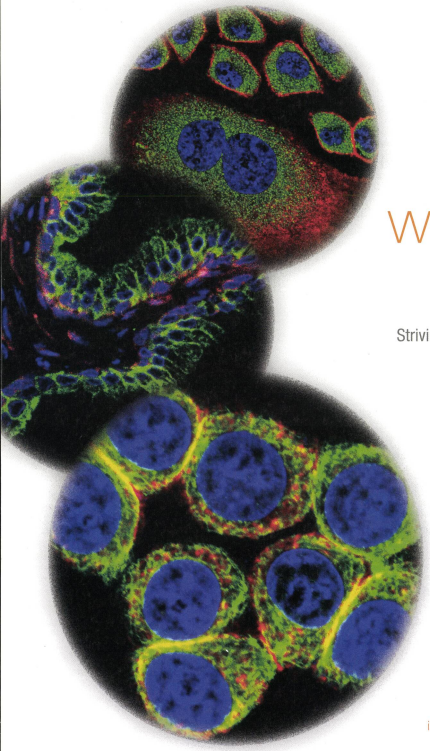

Proteome-wide antibody coverage.

Striving towards an antibody for each human protein.

Unsurpassed development capabilities built over the last ten years allow Abgent to produce more than 5,000 new antibodies per year. Protein A and peptide affinity purification, along with rigorous antibody validation, ensures antibody quality and assay flexibility. The end result is a broad offering of in-house developed, high quality antibodies tailored to your research and drug discovery needs.

Applications: Western Blot, Immunohistochemistry, Immunofluorescence, Flow Cytometry, ELISA, and more.

20µg Evaluation Size Vials
available for most new products.

Visit our website at **www.abgent.com** for more information on Abgent's product and service offerings.

© 2012 ABGENT. All rights reserved. It's all about New, is a trademark of ABGENT. For Research Use Only. Not For Use In Diagnostic Procedures. ABG-00104-0612

It's all about New™
Unsurpassed Development Capabilities

ABGENT ANTIBODIES ARE ESSENTIAL TOOLS FOR THE STUDY OF CANCER, NEURODEGENERATIVE DISEASES, METABOLIC SYNDROME, IMMUNOLOGY, APOPTOSIS, AUTOPHAGY, DEVELOPMENT AND MORE.

Visit our website for a complete product listing.

www.abgent.com

药明康德 WuXi AppTec | ABGENT

CONTENTS

13 September 2012 / Vol 489 / Issue No 7415

THIS WEEK

EDITORIALS

177 METRICS
Count on me
There is a responsible way to assess a scientific career

177 DEFENCE RESEARCH
Secret weapons
Clandestine research programmes do no one any favours

178 TAXONOMY
The name game
Zoologist embrace the world of online publishing

WORLD VIEW

179 **Predatory publishers are corrupting open access**
Jeffrey Beall
The author-pays model is being abused — and that is harming science

RESEARCH HIGHLIGHTS

180 SELECTIONS FROM THE SCIENTIFIC LITERATURE
Lost supernova companion / Hopes high for hydrogels / Bioluminescence marks seals' prey / Fewer sunspots mean cooler winters

SEVEN DAYS

182 THE NEWS IN BRIEF
The Yangtze turns red / The SKA gets a new director / *Chikyu* drills record core

CAREERS

327 COLUMN
Two for one
Mary Anne Holmes
How to solve the two-body problem

328 TURNING POINT
Astrobiologist Alberto Gonzalez Fairén was one of many inspired by Carl Sagan's *Cosmos* series

NATUREJOBS ADVERTISING FEATURE
Spotlight on Latin America

NEWS IN FOCUS

185 CLIMATE
Record summer melt in the Arctic raises questions over ice models

187 DISEASE SURVEILLANCE
Invasive mosquitoes bring exotic diseases to Europe

188 EUROPE
Politicians begin fight over Horizon 2020's budget

189 RESEARCH ETHICS
Official report offers clouded view of psychologist's misconduct

190 COSMOLOGY
Surveys seek answers on dark energy

192 PUBLIC HEALTH
India launches bid to battle antibiotic resistance

FEATURES

194 DEEP-SEA RESEARCH
Dive master
As the submersible *Alvin* gets a refit, is the tide turning against ocean research?

MICROWAVE WEAPONS
Firing blanks
The US military's bid to create an electromagnetic bomb has been less than successful
PAGE 198

COMMENT

201 RESEARCH CAREERS
Predicting scientific success
Daniel E Acuna, Stefano Allesina & Konrad P Kording
A formula to work out a researcher's future *h*-index

203 NIH GRANTS
Well-funded investigators should receive extra scrutiny
Jeremy M Berg
The NIH will benefit from additional reviews of elite grant-holders

Q&A

Pieces of ice

James Balog's time-lapse photographs record climate change

PAGE 206

BOOKS & ARTS

204 SCIENCE FICTION
The radium age
Joshua Glenn

205 BOOKS IN BRIEF

207 PHYSICS
Modelling Feynman
Daniel Cressey

CORRESPONDENCE

208 Uncertainty in climate models / ENCODE as a role model / Same-sex behaviour misrepresented / Europe lags on conduct code / Wallace the first astrobiologist

FUTURES

330 **Communicant**
John Gilbey

This month in *Nature Reviews*

Neural mechanisms of atrial arrhythmias

M. J. Shen, E. Choi, A. Y. Tan, S. Lin, M. C. Fishbein, L. S. Chen & P. Chen

Ectopic foci in pulmonary veins can trigger episodes of atrial fibrillation (AF), but how these foci arise remains unclear. This review highlights the role of the autonomic nervous system in the induction and maintenance of atrial arrhythmias, and explores neural modulation as a treatment strategy for AF.

www.nature.com/nrcardio

The worldwide epidemiology of type 2 diabetes mellitus—present and future perspectives

L. Chen, D. J. Magliano & P. Z. Zimmet

Zimmet and colleagues review the current worldwide trends of the diabetes epidemic and discuss the associated major risk factors, particularly genetic and epigenetic factors. The authors also discuss the potential impact of the use of HbA_{1c} as an alternative diagnostic tool on global diabetes surveillance.

www.nature.com/nrendo

MRI in Crohn's disease—current and future clinical applications

G. Fiorino, C. Bonifacio, A. Malesci, L. Balzarini & S. Danese

Fiorino *et al.* discuss the development of objective MRI-based scores to evaluate the extent of intestinal damage in patients with Crohn's disease and speculate about how this could form part of a 'damage-driven' treatment paradigm.

www.nature.com/nrgastro

The podocyte cytoskeleton—key to a functioning glomerulus in health and disease

G. I. Welsh & M. A. Saleem

This Review outlines the most recent concepts and advances in podocyte biology, and discusses how an improved understanding of the podocyte cytoskeleton is starting to shape advances in delineating the pathogenesis of common glomerular diseases.

www.nature.com/nrneph

Depression in Parkinson disease—epidemiology, mechanisms and management

D. Aarsland, S. Påhlhagen, C. G. Ballard, U. Ehrt & P. Svenningsson

Depression is common in patients with Parkinson disease (PD). Aarsland *et al.* discuss the course of depression and the mechanisms that contribute to enhanced susceptibility to depression in PD. Management strategies are also highlighted.

www.nature.com/nrneurol

Cancer immunology—analysis of host and tumor factors for personalized medicine

S. Ogino, J. Galon, C. S. Fuchs & G. Dranoff

Cancer immunology is an interactive field that requires the skills of oncologists and immunologists, in addition to other aspects, such as pathology. This Review uses colorectal cancer as a prototypical cancer and describes how molecular features and immune reactions are inter-related.

www.nature.com/nrclinonc

Cardiovascular safety of biologic therapies for the treatment of RA

J. D. Greenberg, V. Furer & M. E. Farkouh

Comorbid cardiovascular disease is a substantial problem for patients with rheumatoid arthritis (RA). Here, the authors summarize the evidence—and knowledge gaps—regarding the influence of biologic therapies on cardiovascular risk parameters in patients with RA.

www.nature.com/nrrheum

Image-guided radiation therapy for muscle-invasive bladder cancer

J. Thariat et al.

The hollow and mobile nature of the bladder causes variations in its volume, shape and position, making delivery of radiation therapy to bladder tumors challenging. Here, Thariat *et al.* describe using imaging to improve the accuracy and effectiveness of radiation therapy for bladder cancer.

www.nature.com/nrurol

CONTENTS

13 September 2012 / Vol 489 / Issue No 7415

RESEARCH

NEW ONLINE

209 Papers published this week at nature.com

NEWS & VIEWS

210 AGEING
Mixed results for dieting monkeys
Calorie restriction does not increase longevity in rhesus monkeys
Steven N Austad SEE LETTER P.318

211 BIOGEOCHEMISTRY
Drought and tropical soil emissions
Denitrification in tropical soils is lowered by drought
Cory C Cleveland & Benjamin W Sullivan

212 SOCIAL SCIENCE
Poked to vote
A Facebook message spreads change in voting behaviour among friends
Sinan Aral SEE LETTER P.295

214 ORGANIC SYNTHESIS
A biochemical messenger made easily
Prostaglandin $F_{2\alpha}$ synthesized in just seven steps
Erik J Sorensen SEE LETTER P.278

215 CELL BIOLOGY
Dormant and restless skin stem cells
Not all stem cells are equal in mouse epidermis
Laura De Rosa & Michele De Luca
SEE ARTICLE P.257

217 ENVIRONMENTAL SCIENCE
The rainforest's water pump
Evidence that deforestation greatly lowers tropical rainfall
Luiz E O C Aragão SEE LETTER P.282

ARTICLES

257 STEM CELLS **Distinct contribution of stem and progenitor cells to epidermal maintenance**
G Mascré et al. SEE N&V P.215

263 CELL BIOLOGY **RPN-6 determines *C. elegans* longevity under proteotoxic stress conditions**
D Vilchez et al.

LETTERS

269 INFORMATION TECHNOLOGY **Quantum teleportation over 143 kilometres using active feed-forward**
X-S Ma et al.

ON THE COVER

Poll of polls

Millions of US Facebook users on Election Day 2010 received either a message with information about voting and an 'I voted' button, or the message plus profile photos of Facebook friends who had already clicked the button. Their responses reveal much about the way we communicate. PAGES 212 & 295

274 PHYSICS **Stabilization of Leidenfrost vapour layer by textured superhydrophobic surfaces**
I U Vakarelski, N A Patankar, J O Marston, D Y C Chan & S T Thoroddsen

278 CHEMISTRY **Stereocontrolled organocatalytic synthesis of prostaglandin $PGF_{2\alpha}$ in seven steps**
G Coulthard, W Erb & V K Aggarwal
SEE N&V P.214

282 CLIMATE SCIENCE **Observations of increased tropical rainfall preceded by air passage over forests**
D V Spracklen, S R Arnold & C M Taylor
SEE N&V P.217

286 ENVIRONMENTAL SCIENCE **Ploughing the deep sea floor**
P Puig et al.

290 ENVIRONMENTAL SCIENCE **Averting biodiversity collapse in tropical forest protected areas**
W F Laurance et al.

295 SOCIAL SCIENCE **A 61-million-person experiment in social influence and political mobilization**
R M Bond et al. SEE N&V P.212

299 NEUROSCIENCE **Activity in motor–sensory projections reveals distributed coding in somatosensation**
L Petreanu et al.

304 STEM CELLS **Increased proteasome activity in human embryonic stem cells is regulated by PSMD11**
D Vilchez et al.

309 CANCER **Chronic lymphocytic leukaemia is driven by antigen-independent cell-autonomous signalling**
M Dühren-von Minden et al.

313 GENETICS **HDAC8 mutations in Cornelia de Lange syndrome affect the cohesin acetylation cycle**
M A Deardorff et al.

318 PHYSIOLOGY **Impact of caloric restriction on health and survival in rhesus monkeys from the NIA study**
J A Mattison et al. SEE N&V P.210

322 STEM CELLS **Human ES-cell-derived cardiomyocytes electrically couple and suppress arrhythmias in injured hearts**
Y Shiba et al.

326 CORRIGENDUM **Recurrent network activity drives striatal synaptogenesis**
Y Kozorovitskiy, A Saunders, C A Johnson, B B Lowell & B L Sabatini

326 ERRATUM **Non-invasive prenatal measurement of the fetal genome**
H C Fan et al.

326 CORRIGENDUM **Biodiversity loss and its impact on humanity**
B J Cardinale et al.

326 ERRATUM **An origin of the radio jet in M87 at the location of the central black hole**
K Hada et al.

KELLY KRAJESKI/NATURE

ENVIRONMENTAL SCIENCE

Plough mark

Bottom trawling fisheries leave their mark on the sea bed. PAGE 286

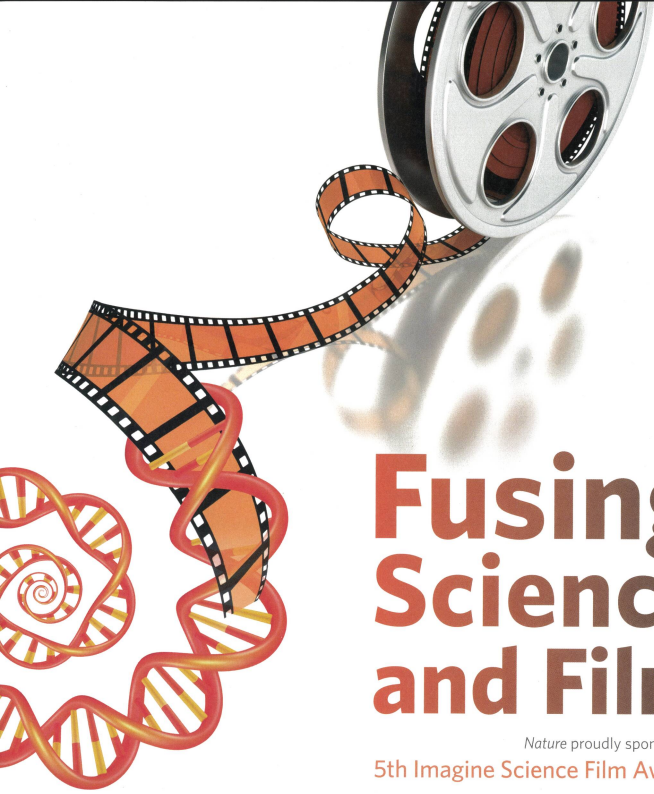

Fusing Science and Film

Nature proudly sponsors the

5th Imagine Science Film Awards

Submit your film and compete for the
$2,500 *Nature* Scientific Merit Award
and the **$1,000 *Nature* Audience Award**

www.imaginesciencefilms.org

nature

imagine SCIENCE Film Festival

nature publishing group npg

INSIGHT

13 September 2012 / Vol 489 / Issue No 7415

GUT MICROBES AND HEALTH

REVIEWS

220 Diversity, stability and resilience of the human gut microbiota
The human microbiota is hugely diverse; it varies between individuals, over time and with changes in environmental factors such as diet, medication and disease state. Ecological principles can help to explain how the microbial communities in our bodies are assembled and how they respond to alterations in their environment, and how, in turn, these dynamics may affect the physiological processes of the human host. Understanding the functional interplay between the microbiota and the environment the host provides may, ultimately, allow strategies to be devised that promote a healthy microbial state.
Catherine A. Lozupone et al.

231 Reciprocal interactions of the intestinal microbiota and immune system
The emergence of the adaptive immune system in vertebrates set the stage for a symbiotic relationship between an increasingly complex intestinal microbiota and the vertebrate host, which has co-evolved ever since. How the adaptive immune system copes with the remarkable number and diversity of microbes that colonize the intestinal tract immediately after birth, and how the adaptive immune response is integrated with more primitive innate immune responses to the microbiota, are key to understanding homeostatic immune regulation and the dysregulation that leads to chronic immune-mediated diseases.
Craig L. Maynard et al.

242 Functional interactions between the gut microbiota and host metabolism
The microbes that colonize the intestine of humans can influence the metabolic processes of their host, which may contribute to obesity and other metabolic diseases. The microbiota not only aids digestion by fermenting dietary carbohydrates, but their metabolic products can also act as signal molecules. Owing to the complexity of the microbiota — and its variability between and within individuals — it is difficult to determine the causal links between individual microbial species, active molecules and processes. Increasing our knowledge of the mechanistic basis of these interactions may be useful in fighting the worldwide increase in metabolic disease.
Valentina Tremaroli & Fredrik Bäckhed

250 Genomic approaches to studying the human microbiota
Studying the vast array of microbes that make up the complex community within the human gut is a considerable task. Development of new sequencing techniques has allowed the community to be studied as a whole. This is a crucial advance because many of the bacteria that constitute the microbiota cannot be cultured independently. The emerging data are helping researchers to understand the differences that exist both between and within gut microbial communities. Information about community structure is built up through a combination of targeting regions of genes and shotgun sequencing, and comparing these data to reference genomes and databases. At present, these sequence-based technologies are being used to teach us about the communities of microbes in the gut, but ultimately they may have a diagnostic application.
George M. Weinstock

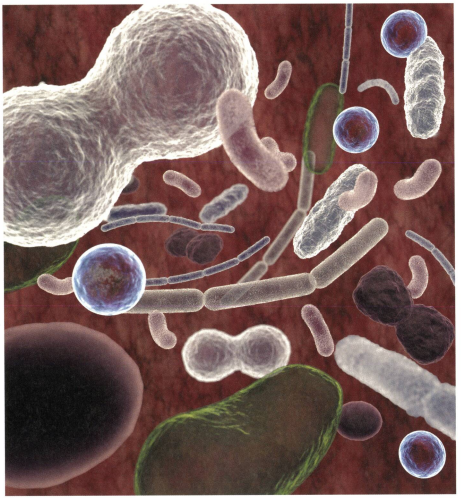

nature

13 September 2012 / Vol 489 / Issue No. 7415

EDITORIAL

LONDON, MUNICH, WASHINGTON DC, NEW YORK, BOSTON, PARIS, SAN FRANCISCO, TOKYO nature@nature.com

EDITOR-IN-CHIEF: Philip Campbell
EXECUTIVE EDITOR: Nick Campbell
PUBLISHING EXECUTIVE EDITOR: Maxine Clarke **EXECUTIVE EDITOR:** Véronique Kiermer
CHIEF MAGAZINE EDITOR: Tim Appenzeller
THIS WEEK/NEWS/FEATURES: Alison Abbott, David Adam, Ananyo Bhattacharya, Geoff Brumfiel, Declan Butler, Ewen Callaway, Erika Check Hayden, Daniel Cressey, David Cyranoski, Natasha Gilbert, Eric Hand, Heidi Ledford, Corie Lok, Brendan Maher, Emma Marris, Richard Monastersky, Brian Owens, Helen Pearson, Mark Peplow, Eugenie Samuel Reich, Ivan Semeniuk, Quirin Schiermeier, Jeff Tollefson, Richard Van Noorden, Meredith Wadman, M Mitchell Waldrop **COMMENT:** Sara Abdulla, Joanne Baker, Rosalind Cotter, Barbara Kiser, Alison McCook, Lucy Odling-Smee, Sarah Tomlin **NATURE PODCAST/VIDEO:** Adam Rutherford, Thea Cunningham, Geoff Marsh, Kerri Smith, Charlotte Stoddart **NEWS AND VIEWS:** Sadaf Shadan, Ana Lopes, Andrew Mitchinson, Cesar Sanchez, Marian Turner **RESEARCH:** Ritu Dhand, Karl Ziemelis, Francesca Cesari, I-han Chou, Tanguy Chouard, Rosamund Daw, Alex Eccleston, Angela Eggleston, Joshua Finkelstein, Henry Gee, Patrick Goymer, Noah Gray, Marie-Thérèse Heemels, Magdalena Helmer, Karen Howell, Claudia Lupp, Barbara Marte, Andrew Mitchinson, Juliane Mössinger, Deepa Nath, Wayne Peng, Leslie Sage, Magdalena Skipper, Clare Thomas, Maria Trejkovska, John VanDecar, Liesbeth Venema, Ursula Weiss, Michael White **INSIGHTS/REVIEWS/PERSPECTIVES:** Ursula Weiss **CAREERS:** Gene Russo, Karen Kaplan **TECHNOLOGY FEATURES:** Monya Baker **FUTURES:** Colin Sullivan **SUPPLEMENTS:** Herb Brody, Michelle Grayson, Tony Scully **SUBEDITORS:** Colin Sullivan, Mary Abraham, Sarah Archibald, Nicola Bailey, Anne Blewett, Nicolas Fanget, Isobel Flanagan, Paul Fletcher, Sasha Lewis, Dinah Loon, Louisa Lyon, Anna Novitzky, Yukie Ozawa, Katherine Perry, David Price, Jenny Rooke, David Winters, Anna York **PRODUCTION:** Jenny Henderson, Leonora Dawson-Bowling, Dan Foley, Stewart Fraser, Susan Gray, Simon Gribbin, Hazel Mayhew, James McQuat, Emilia Oviss, Yvonne Strong, Robert Sullivan, Roberta Tarran, Charles Wenz **ART AND DESIGN:** Kelly Buckheit Krause, Wesley Fernandes, Madeline Hutchinson, Barbara Izdebska, Paul Jackman, Jasiek Krzystofiak, Annthea Lewis, Chris Ryan, Nik Spencer, Claire Welsh, Mark Wood **JAPAN EDITION:** Eiji Matsuda, Mika Ishida, Mitsuyo Utsugi, Sayaka Ayame **PRESS OFFICE:** Ruth Francis, Neda Afsarmanesh, Lisa Boucher, Rachel Twinn, Rebecca Walton **ADMINISTRATION:** Paul Sng, Liz Bankes, Roseann Campbell, Peter Cary, Fifon Cleverley, Dana Coles, Faye Fornasier, Ashlee Gagui, Peter Hewitt, Amy Invernizzi, Caroline McLean, Rina Nozawa, Anastasia Panoutsou, Kenneth Simpson, Diane Yorke

PUBLISHING

LONDON feedback@nature.com

MANAGING DIRECTOR & PUBLISHER: Steven Inchcoombe
ASSOCIATE PUBLISHER: Arash Hejazi
PUBLISHING PROJECT MANAGERS: Claudia Deasy, Christian Manco
TOKYO feedback@natureasia.com
REGIONAL MANAGING DIRECTOR — ASIA-PACIFIC: David Swinbanks
DIRECTOR — ASIA-PACIFIC: Antoine E Bocquet
OPERATIONS DIRECTOR — ASIA-PACIFIC: Hiroshi Minemura

DISPLAY ADVERTISING, SPONSORSHIP & NATUREJOBS

GLOBAL HEAD: Andrew Douglas a.douglas@nature.com
DISPLAY ADVERTISING AND SPONSORSHIP
GLOBAL HEAD: Gerard Preston g.preston@nature.com
ASSISTANT SPONSORSHIP MANAGER: Reya Silao Tel: +44 (0)20 7843 4977 (rsilao@nature.com)

EUROPE/REST OF WORLD display@nature.com Tel: +44 (0)20 7843 4960
GERMANY/SWITZERLAND/AUSTRIA: Sabine Hugi-Fürst Tel: +41 52761 3386
UK/IRELAND/SCANDINAVIA/SPAIN/PORTUGAL: Evelina Rubio Hakansson Tel: +44 (0)20 7843 4079
FRANCE/BELGIUM/THE NETHERLANDS/LUXEMBOURG/ITALY/OTHER EUROPE: Nicola Wright
Tel: +44 (0)20 7843 4959

NORTH AMERICA display@natureny.com
NEW ENGLAND/ EASTERN CANADA: Sheila Reardon Tel: +1 617 494 4900
NEW YORK/ MID-ATLANTIC/ SOUTHEAST: Jim Beaudt Tel: +1 212 726 9334
MIDWEST: Mike Rossi Tel: +1 212 726 9255
WEST COAST/ WESTERN CANADA: George Lui Tel: +1 415 781 3804
WEST COAST NORTH: Kayla McCutchan Tel: +1 415 403 9038

ASIA-PACIFIC display@naturesia.com
ASIA-PACIFIC HEAD: Kate Yoneyama
JAPAN: Ken Mikami Tel: +81 3 3267 8765
GREATER CHINA/SINGAPORE: Gloria To Tel: +852 2811 7191
INDIA: Vikas Chawla Tel: +91 124 288 1057

SPONSORSHIP
BUSINESS DEVELOPMENT MANAGER: David Bagshaw Tel: +1 212 726 9215
BUSINESS DEVELOPMENT MANAGER: Patrick Murphy Tel: +1 617 475 9216

NATUREJOBS naturejobs@nature.com
EUROPEAN HEAD OFFICE, LONDON: Tel: +44 (0)20 7843 4961
EUROPEAN SALES MANAGER: Nils Moeller (n.moeller@nature.com) **BUSINESS DEVELOPMENT MANAGER, MIDDLE EAST:** Jon Giuliani (j.giuliani@nature.com) **ADVERTISING PRODUCTION MANAGER:** Stephen Russell **NATUREJOBS ONLINE PRODUCTION:** Dennis Chu
US HEAD OFFICE, NEW YORK: naturejobs@natureny.com **US SALES MANAGER:** Ken Finnegan
JAPAN HEAD OFFICE, TOKYO: Tel: +81 3 3267 8765 **ASIA-PACIFIC HEAD:** Kate Yoneyama
ASIA-PACIFIC SALES & BUSINESS DEVELOPMENT MANAGER: Yuki Fujiwara **BUSINESS DEVELOPMENT MANAGER, GREATER CHINA, SINGAPORE:** Gloria To Tel: +852 2811 7191
INDIA: Vikas Chawla Tel: +91 1242881057 (v.chawla@nature.com)

MARKETING & SUBSCRIPTIONS

USA/CANADA/LATIN AMERICA subscriptions@us.nature.com
Tel: (USA/Canada)+1 866 363 7860; (outside USA/Canada) +1 212 726 9223
MARKETING: Sara Girard **FULFILMENT:** Karen Dawson

JAPAN/CHINA/KOREA subscriptions@natureasia.com
Tel: +81 3 3267 8751 **MARKETING:** Sachiyo Ikeda **FULFILMENT:** Masayo Tanaka

EUROPE/REST OF WORLD subscriptions@nature.com
Tel: +44 (0)1256 329242
MARKETING: Elena Woodstock, Marcus Parker, Hannah Phipps **FULFILMENT:** Jean Burrows

INDIA npgindia@nature.com
Tel: +91 124 2881053/54
HEAD OF BUSINESS DEVELOPMENT, INDIA: Debashish Brahmachari **MARKETING:** Harpal Singh Gill

ANNUAL SUBSCRIPTIONS (UK/Europe, including post and packing)
FULL RATE: £1,400
PERSONAL RATES: UK £135; Europe €209; Rest of World £210
STUDENT RATES: UK £79; Europe €122; Rest of World £125
Individual rates apply to payments by personal cheque or credit card. Back issues: £20.00.

ANNUAL SUBSCRIPTIONS (USA, including post and packing)
INSTITUTIONAL/CORPORATE RATE: $2,730 ; **PERSONAL RATE:** $199; **STUDENT RATE:** $99;
POSTDOC RATE: $119
Printed in USA. Individual rates available only to subscribers paying by personal check or credit card. Orders for student/postdoc subscriptions must be accompanied by a copy of student ID. Rates apply to USA, Canada, Mexico/Central & South America. Add 7% GST tax in Canada (Canadian GST number 140911595). **BACK ISSUES:** US$20.00.

ANNUAL SUBSCRIPTIONS (Asia, including post and packing)
JAPAN: 年間購読料金: *Nature* のみ 437,800 円 +21,890 円 (消費税) =459,690 円 (合計)
Nature + *Nature Digest* 466,550 円 +23,328 円 (消費税) =489,878 (合計)
お問い合わせ: 日本出版貿易株式会社 国内営業 1 部
〒101-0064 東京都千代田区猿楽町 1-2-1 Tel: 03-3292-3767 Fax: 03-3292-8766
個人/学生購読について
NPG エイチャーアジア パシフィック フルフィルメント & カスタマーサービス
〒162-0843 東京都新宿区市谷田町 2-37 千代田ビル Tel: 03-3267-8759 Fax: 03-3267-8752
CHINA: www.natureasia.com/cn/subscribe; **KOREA:** www.natureasia.com/korea/subscribe

NATURE ONLINE WWW.NATURE.COM/NATURE

CHIEF TECHNOLOGY OFFICER: Howard Ratner **ASSOCIATE DIRECTOR, NATURE.COM:** Daniel Pollock
PLATFORM DEVELOPMENT: Jeremy Macdonald **WEB PRODUCTION:** Alexander Thurrell, Deborah Anthony **WEB DESIGN:** Juan-Carlos Sobrino, Luke Stavenhagen **PLATFORM INTERFACES:** Amanda Ward

SITE LICENCES, FULFILMENT & CUSTOMER SERVICES

SITE LICENCES: npg.nature.com/libraries feedback@nature.com
CHIEF OPERATIONS OFFICER: John Carroll **ASSOCIATE DIRECTOR OF OPERATIONS:** Dominic Pettit
CUSTOMER SERVICE: Liz Davidson **ORDER PROCESSING OPERATIONS:** Steve Poulter

NATURE PUBLISHING GROUP OFFICES

LONDON: The Macmillan Building, 4 Crinan Street, London N1 9XW Tel: +44 (0)20 7833 4000 Fax: +44 (0)20 7843 4596/7

BASINGSTOKE: Nature Publishing Group, Subscriptions, Brunel Road, Basingstoke, Hants RG21 6XS, UK Tel: +44 (0)1256 329242

WASHINGTON DC: 968 National Press Building, 529 14th St NW, Washington DC 20045-1938 Tel: +1 202 737 2355

NEW YORK: 75 Varick St, 9th Floor, New York, NY 10013-1917 Tel: +1 212 726 9200

BOSTON: 25 First Street, Suite 104, Cambridge, MA 02141 Tel: +1 617 475 9275

SAN FRANCISCO: 225 Bush Street, Suite 1453, San Francisco, CA 94104 Tel: +1 415 403 9027

MUNICH: Nymphenburger Strasse 14, D-80335 München Tel: +49 89 549057-13

PARIS: Moulin de Malicorne, Sainte Maure de Touraine, Paris 37800 Tel: +33 2 47 35 72 15

TOKYO: Chiyoda Building, 2-37 Ichigayatamachi, Shinjuku-ku, Tokyo 162-0843 Tel: +81 3 3267 8751

INDIA: Nature Publishing Group, 3A, 4th Floor, DLF Corporate Park, Gurgaon 122002 Tel: +91 124 2881053/54

Nature® (ISSN 0028-0836) is published by Nature Publishing Group, a division of Macmillan Publishers Ltd (The Macmillan Building, 4 Crinan Street, London N19XW). Registered as a newspaper at the British Post Office. North and South American orders to subscriptions@nature.com (Tel: +44 (0)1256 329242; Fax +44 (0)1256 812358). Authorization to photocopy material for internal or personal use, or internal or personal use of specific clients, is granted by *Nature* to libraries and others registered with the Copyright Clearance Center (CCC) Transactional Reporting Service, provided the relevant copyright fee is paid direct to CCC, 222 Rosewood Drive, Danvers MA 01923, USA. Identification code for *Nature*: 0028-0836/03. CPC PUB AGREEMENT #40032744. In the US, *Nature* (ISSN 0028-0836) is published weekly on Thursday, except the last week in December by Nature Publishing Group, 75 Varick St, 9th Fl, New York NY 10013-1917, USA, US Periodicals postage paid at New York NY, and additional mailing post offices. US POSTMASTER: send address changes to *Nature*, Subscription Dept, 75 Varick St, 9th Fl, New York NY 10013-1917, USA. Published in Japan by NPG Nature Asia-Pacific, Chiyoda Building, 2-37 Ichigayatamachi, Shinjuku-ku, Tokyo 162-0843, Japan. ©

2012 Macmillan Publishers Limited. All rights reserved.

THIS WEEK

EDITORIALS

ZOOLOGY Online-only species naming made official at last **p.178**

WORLD VIEW The corruption of open-access scientific publishing **p.179**

COOLING Horses sweat, people perspire and model houses glow **p.180**

Count on me

Sometimes, the use of metrics to assess the value of scientists is unavoidable. So let's come up with the best measure possible.

In an ideal world, scientists applying for grants or jobs would be judged holistically — balancing quantitative measures such as their publication record against indications of their potential from recommendation letters, personal interactions and other activities. So even if a candidate had not generated many papers, it would count in their favour if the few they had published had received positive post-publication review (comments, tweets and blog posts, for instance). Also favourable would be a tendency to ask insightful questions at talks that lead to valuable discussions and new experiments, or a willingness to share reagents and expertise with their colleagues. That would be ideal. But that is not the world in which most scientists live.

Instead, hiring committees and grant reviewers sweat through hundreds of applications, often with only enough time to give each submission a cursory glance. In 2010, a *Nature* poll found that most administrators say that metrics — quantifiable measures of scientists' achievements — matter less in job decisions than scientists often think (see *Nature* **465**, 860–862; 2010), but good peer review is often simply not possible.

As a result, evaluators are increasingly turning to metrics, such as total citation count and the *h*-index, a measure of both the quality and quantity of papers (a scientist has an *h*-index of 12 if they have published 12 papers that have each received at least 12 citations). Naturally, many scientists object to such cold quantification of their contribution. Plus, all metrics have obvious flaws — a paper may gather many citations not because of its importance, but because it is in a large field that publishes frequently, so generates more opportunities for citations. Review articles, which may not add much to the research, count the same as original research papers, which contribute a great deal. And all existing metrics capture only what a scientist has done, not what he or she might be capable of. Clearly, there is a need for more and better measures.

On page 201, Daniel Acuna, Stefano Allesina and Konrad Kording suggest an alternative: the future *h*-index. Unlike other metrics, this index estimates a scientist's publication prowess five years or so into the future — a useful timescale for tenure decisions.

Using publicly available data on the history of publication, citation and funding for thousands of neuroscientists, researchers working on the fruitfly *Drosophila* and evolutionary biologists, the authors constructed an algorithm that converts information on a typical scientist's CV — the number of journals published in and articles in top journals for instance — into a number that represents their probable *h*-index in the years that follow.

Outraged? Please send complaints to the usual address. Interested? Calculate your own future *h*-index here: go.nature.com/z4rroc.

Nature receives thousands of submissions a year, some of which point out the flaws in existing metrics and propose alternatives. We accepted the piece by Acuna *et al.* after submitting it to peer review. The reviewers and our editors felt that the authors had used appropriate methods to obtain their algorithm, and its predictive values seemed realistic. Furthermore, the authors are cautious about its value, pointing out that it is probably less accurate for scientists in other disciplines, and should not be considered a replacement for peer review. At the very least, the future *h*-index should help to address some problems with the current *h*-index, which tends to favour established scientists because they have had more time to accrue citations. A forward-looking metric may give a leg up to promising, early-career scientists who don't yet have impressive CVs.

"There is no substitute for examining the research itself to appreciate its value."

Nevertheless, no one wants their career potential to be reduced to a number. *Nature* publishes many scientific gems that nevertheless achieve few citations; there is no substitute for examining the research itself to appreciate its value. We know that the idea of a new metric published in these pages will raise some anxieties, and a few hackles. But metrics are already being used, so it is important that they create the most accurate picture possible of someone's potential. Plus, they do hold some advantages over peer review, by helping to eliminate the unconscious biases that can creep into personal evaluations.

In that vein, scientists should continue to hunt for metrics that capture a scientist's true value, including aspects such as teaching, reviewing and public-speaking ability, as well as online responses to publications in blogs and comments — 'alt-metrics'. We may not live in an ideal world, but we can still improve the recruitment, reward and opportunities for scientists. ■

Secret weapons

US military furtiveness is hindering progress and the development of technology.

In the 1940s, with the Second World War in full swing, Japanese scientists sketched out a plan to build a microwave weapon to shoot down enemy bombers. That idea, perhaps the earliest description of an electromagnetic bomb, encapsulates much of what military officials still hope to achieve with such weapons: disabling electronics (or, in some cases, people) using a powerful energy beam, without causing any collateral physical damage. The US military's attempts to make a practical weapon based on this idea have so far resulted in only one system — at least as far as it has revealed publicly. The Air Force

has built the Active Denial System, a non-lethal high-power microwave weapon supposedly able to deter an angry mob by creating the sensation of being burned.

For decades, the US military has conducted much of its research on such weapons in secret. It has often hinted that it is on the verge of a breakthrough, yet high-power microwave weapons are noticeably absent from modern battlefields and scenes of civil unrest. The military, for the most part, won't discuss its progress — or lack thereof — citing secrecy in the name of national security.

There is nothing unique about the classification of this research: nuclear weapons, stealth aircraft and satellite reconnaissance systems were all developed in secret. Although such furtiveness can legitimately protect US weapons and capabilities, it can also prevent much-needed dissemination of scientific research. And it has all too often concealed a lack of progress.

As we discuss on page 198, this has been the problem with the programme to develop high-power microwave weapons: the little information that has been released points to obvious scientific and technological problems. Crucially, power sources for such devices are often too unwieldy to use. More than ten years after the Active Denial System was first revealed to the public, its size and complexity mean that it is still nearly impossible to deploy. The military rejected the system for use at checkpoints in Iraq because it would have taken 16 hours to cool down the weapon's pulse generator to superconducting temperatures to fire it.

Many records related to the Active Denial System remain classified and inaccessible to the public and the scientific community. The US Air Force's unwillingness to reveal the full scope of its research into the biological effects of high-power microwaves in the 1990s, which included work on their auditory and lethal effects, flies in the face of the defence department's claims that it is interested in classifying only weapons technology, and not science. If, as the Air Force says, the biological research never led to weapons, then there is no reason not to release it.

Work on high-power microwaves designed to take out electronics has not fared much better. Advocates can always claim that classified programmes are yielding great progress, but information in the public sphere does not paint a rosy picture. Military officials and academics acknowledge that developing compact power sources remains the biggest hurdle. The Air Force and a contractor have touted efforts to develop a high-power microwave cruise missile, but neither will release details that might allow independent experts to judge the programme's potential. The Pentagon is staying quiet on a system developed to take out improvised explosive devices, but what little information is available indicates that — like the Active Denial System — it has proved too cumbersome to use effectively.

"The government must be willing to share data and findings between military labs and academia."

This is not to say that all government spending on high-power microwaves is a waste. Academic funding under Multidisciplinary University Research Initiatives is contributing to a host of peer-reviewed publications and collaborative research. But for the government to take full advantage of that research, it must be willing to share data and findings between military labs and academia. The defence department's own science board has found that reluctance to share is a barrier to progress.

Getting to the truth about high-power microwaves requires transparency. Independent experts must be able to scrutinize technology to enable scientific–military cooperation and to provide a reality check for those who make fantastic claims about a weapon's potential.

By the time it cancelled the Airborne Laser programme earlier this year, the US defence department had poured billions of dollars into the weapon: a chemical laser in the nose of an aircraft, designed to shoot down ballistic missiles. In the end, the question was not whether the laser would work, but whether it would be usable, given the scientific and technological practicalities of integrating such a complex system. "There's nobody in uniform that I know who believes that this is a workable concept," concluded former US defence secretary Robert Gates, when he finally moved to kill the project. The same concerns would probably be expressed about high-power microwaves — if more information about them were available. ■

The name game

After several years of wrangling, zoologists can now name new species online only.

With access to the Internet, the (official) world of animals and plants will soon be at your fingertips. In a landmark ruling, zoologists last week agreed that newly identified species can be named in online-only publications. Previously, the first official description of anything that crawled, flew, wriggled, walked or swam across Earth needed to be formally written up and recorded in print, where it would remain in perpetuity for future scientists to reference.

That made sense when Henry Fairfield Osborn described *Tyrannosaurus rex* in 1905; less so when Rob Gay named a new theropod, *Kayentavenator elysiae*, in 2010, which helps to explain why Gay broke with convention and claimed the first description of the species in a self-published print-on-demand book.

As technology blurred the distinction between what is published and what is not, some predicted online anarchy, with 'taxonomic vandals' taking to the Internet to self-publish reports of new species. An obvious solution to the problem would have been to extend the rules from print to cover online scientific journals, and to draw the line there. But there were concerns about whether online journals would endure. In a messy compromise, online journals that published descriptions of new species printed and bound several dozen copies of the paper — in case a twenty-second-century palaeontologist should call. In an even messier compromise, some scientists printed papers from journal websites and posted them to libraries themselves.

No more. The International Commission on Zoological Nomenclature (ICZN), which sets the rules for the naming of new species, announced on 4 September that it was relaxing its code to encompass publication in online-only publications. The change, which followed a vote of 23 in favour to 3 against, with one abstention, comes into force at the start of next year. The amendment allows for descriptions of new species in "widely accessible electronic copies with fixed content and layout". New animal species will also need to be registered with ZooBank.org, the official registry of the ICZN.

It is a sensible move, and one that most in the field should welcome. It comes a year after the International Botanical Congress endorsed online-only publication for new types of plant. In an Editorial at the time (*Nature* **475**, 424; 2011), which called on zoologists to follow suit, *Nature* said: "At this point, it seems that there is little reason to continue to demand paper on a shelf to make a species name official."

On hearing the news from the ICZN, one member of *Nature*'s staff quipped: "Now to name a dinosaur you don't have to behave like one." But that is a little unfair. Proper taxonomy and a robust archive are crucial to science, and the zoologists were right to consider with care the possible negative aspects of such a change, as well as listening to the clamour to embrace the new. True, the change has been a long time coming. It is overdue, even. Still, when you have been dead and waiting for a name since the Mesozoic era, what are a few extra years? ■

➲ **NATURE.COM**
To comment online, click on Editorials at:
go.nature.com/xhunqv

J. SANCHEZ

Predatory publishers are corrupting open access

Journals that exploit the author–pays model damage scholarly publishing and promote unethical behaviour by scientists, argues **Jeffrey Beall**.

When e-mail first became available, it was a great innovation that made communication fast and cheap. Then came spam — and suddenly, the innovation wasn't so great. It meant having to filter out irrelevant, deceptive and sometimes offensive messages. It still does.

The same corruption of a great idea is now occurring with scholarly open-access publishing.

Early experiments with open-access publishing, such as the *Journal of Medical Internet Research* and BioMed Central, were very promising. Set up more than a decade ago, they helped to inspire a social movement that has changed academic publishing for the better, lowered costs and expanded worldwide access to the latest research.

Then came predatory publishers, which publish counterfeit journals to exploit the open-access model in which the author pays. These predatory publishers are dishonest and lack transparency. They aim to dupe researchers, especially those inexperienced in scholarly communication. They set up websites that closely resemble those of legitimate online publishers, and publish journals of questionable and downright low quality. Many purport to be headquartered in the United States, United Kingdom, Canada or Australia but really hail from Pakistan, India or Nigeria.

Some predatory publishers spam researchers, soliciting manuscripts but failing to mention the required author fee. Later, after the paper is accepted and published, the authors are invoiced for the fees, typically US$1,800. Because the scientists are often asked to sign over their copyright to the work as part of the submission process (against the spirit of open access) they feel unable to withdraw the paper and send it elsewhere.

I monitor predatory publishers on my blog, Scholarly Open Access, which has become a forum in which scientists can raise their concerns over the practice. They send me hundreds of e-mails passing on spam solicitations or asking whether a particular publisher is legitimate.

I also get e-mails from the predators' victims. Some have been named as members of editorial boards without their knowledge or permission. Others have had an article partially or completely plagiarized in a predatory journal. Many ask me for advice on where to publish or how to withdraw an article that they wish they hadn't submitted. As a librarian, I do my best to answer the questions I receive, but they often require expertise in the author's field of study. So it is important that more scientists are made aware of the problem.

The predatory publishers and journals often have lofty titles that make them seem legitimate in a list of publications on a CV. Scholarly publishing's traditional role of vetting the best research is disappearing. Now there is a journal willing to accept almost every article, as long as the author is willing to pay the fee. Authors, rather than libraries, are the customers of open-access publishers, so a powerful incentive to maintain quality has been removed.

Perhaps nowhere are these abuses more acute than in India, where new predatory publishers or journals emerge each week. They are appearing because of the market need — hundreds of thousands of scientists in India and its neighbouring countries need to get published to earn tenure and promotion.

Here, the problem is not just with the publishers. Scientists themselves are also to blame. Many are taking unethical shortcuts and paying for the publication of plagiarized or self-plagiarized work.

Honest scientists stand to lose the most in this unethical quagmire. When a researcher's work is published alongside articles that are plagiarized, that report on conclusions gained from unsound methodologies or that contain altered photographic figures, it becomes tainted by association. Unethical scientists gaming the system are earning tenure and promotion at the expense of the honest.

The competition for author fees among fraudulent publishers is a serious threat to the future of science communication. To compete in a crowded market, legitimate open-access publishers are being forced to promise shorter submission-to-publication times; this weakens the peer-review process, which takes time to do properly.

To tackle the problem, scholars must resist the temptation to publish quickly and easily. The research community needs to use scholarly social networks such as Connotea and Mendeley to identify and share information on publishers that deceive, lack transparency or otherwise fail to follow industry standards. Scientific literacy must include the ability to recognize publishing fraud, and libraries must remove predatory publishers from their online catalogues. The worst offenders can usually be discovered without too much effort: their websites are littered with grammatical errors and they list bogus contact details. The borderline cases are more difficult to spot — here, we need open-access zealots to open their eyes to the growing quality problems.

SCIENTIFIC LITERACY MUST INCLUDE THE ABILITY TO RECOGNIZE PUBLISHING FRAUD.

Conventional scholarly publishers have had an important role in validating research, yet too often advocates of open access seem to overlook the importance of validation in online publishing. They promote access at the expense of quality: a shortcoming that tacitly condones the publication of unworthy scientific research. ■

➲ **NATURE.COM**
Discuss this article online at:
go.nature.com/bnuuly

Jeffrey Beall *is Scholarly Initiatives Librarian at the University of Colorado Denver.*
e-mail: jeffrey.beall@ucdenver.edu

RESEARCH HIGHLIGHTS

Selections from the scientific literature

ASTRONOMY

On the origin of Ia supernovae

Using a computer model, astronomers in Japan present evidence to support one theory about the origin of type Ia supernovae, which are of predictable luminosity and are therefore useful for estimating distances to remote galaxies. These supernovae are generated when a compact star called a carbon–oxygen white dwarf siphons off a critical amount of matter from a companion star. However, astronomers have yet to directly observe a companion star.

Izumi Hachisu at the University of Tokyo and his team offer a solution to this conundrum. Their model, which accounts for the rotation of white dwarfs, shows that many companion stars have evolved to a state too faint to be seen. The model is consistent with observations of supernova 2011fe.

Astrophys. J. 756, L4 (2012)

E. CAMPRASSE/C. GUINET FIELD TEAM CEBC-CNRS

ANIMAL BEHAVIOUR

Seals see glowing prey

Female southern elephant seals are thought to locate their food in deep, dark waters by detecting the bioluminescence of their prey. The seals see best at the wavelength of light produced by bioluminescent organisms.

Jade Vacquié-Garcia at the Chizé Centre for Biological Studies in Villiers-en-Bois, part of the French National Centre for Scientific Research, and her team tested the idea by studying four female southern elephant seals (*Mirounga leonina*; pictured) living on the Kerguelen islands in the southern Indian Ocean. The researchers used satellite tracking to follow the animals as they made a total of 3,386 dives, and a light sensor to measure bioluminescence. During the dives, the seals' foraging intensity was positively related to the number of bioluminescence events.

PLoS ONE 7, e43565 (2012)

MATERIALS

Hydrogel makes buildings sweat

Just as mammals can reduce their body temperature by sweating, so a coating of heat-sensitive hydrogel could 'sweat' to cool buildings.

Wendelin Stark and his colleagues at the Swiss Federal Institute of Technology in Zurich produced a 3-millimetre-thick layer of thermoresponsive hydrogel. When heated to roughly 32 °C, the gel undergoes a phase transition from a wet state to a dry state, and releases water. With this water could go much of a building's heat.

Miniature model houses (**pictured**) with roofs coated with the substance were up to 20 °C cooler than uncoated models when exposed to simulated tropical midday Sun. The authors estimate that this translates into annual savings of 220 kilowatt-hours of energy for a detached house. A brief 'rain' recharged the hydrogel with water.

Adv. Mater. http://dx.doi.org/10.1002/adma.201202574 (2012)

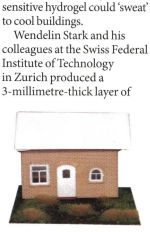

WILEY-VCH VERLAG GMBH & CO. KGAA, WEINHEIM

MOLECULAR BIOLOGY

Red-blood-cell regulator

Human genome-wide association studies have indicated that a common single nucleotide sequence variant influences the size and number of red blood cells. A team led by Harvey Lodish of the Whitehead Institute, and Eric Lander of the Broad Institute, both in Cambridge, Massachusetts, found that this variant in the non-coding sequence reduces the expression of the nearby gene *CCND3*, which is involved in controlling the cell cycle.

Reducing the expression of the gene in human and mouse red-blood-cell precursors caused the cells to go through fewer divisions, resulting in fewer, but bigger, red blood cells.

Genes Dev. http://dx.doi.org/10.1101/gad.197020.112 (2012)

MICROBIOLOGY

Populations cooperate

Populations of naturally co-occurring bacteria work together, an analysis suggests.

To test whether bacteria aggregate for reasons beyond access to resources such as food, Martin Polz at the

Massachusetts Institute of Technology in Cambridge and his team created a network map of interactions between 185 strains of Vibrionaceae bacteria. They found that antagonistic interactions were much less likely between strains that are as closely related as those within naturally occurring populations.

The authors suggest that the populations act as cohesive units that can defend themselves against other groups of bacteria. The coordination seems to have arisen through horizontal gene transfer, in which population members capable of producing antibiotics passed on antibiotic-resistance genes to their neighbours.

Science 337, 1228–1231 (2012)

MICROBIOLOGY

Ecosystems compete

Bacterial species seem to compete more than they cooperate.

Kevin Foster at the University of Oxford, UK, and Thomas Bell at Imperial College London tested the theory that different bacterial species can form cooperative 'superorganisms'. The team measured the productivity — in terms of CO_2 given off through respiration — of a range of multi-species microbial cultures. After both one week and one month, species in the mixtures were less productive than they would have been if grown separately, suggesting that social living comes at a cost.

Curr. Biol. http://dx.doi.org/10.1016/j.cub.2012.08.005 (2012)

NEUROSCIENCE

A treatable form of autism

A rare form of autism that is accompanied by epilepsy and intellectual disability could be treatable with dietary supplements.

Joseph Gleeson and Gaia Novarino at the University of California, San Diego, and their team identified three affected families that carry mutated versions of a gene called *BCKDK*. The gene encodes an enzyme that slows the breakdown of branched-chain amino acids such as leucine and valine. Mice that lack both copies of the gene had low serum and brain levels of these amino acids, and showed neurological abnormalities and stunted growth. Enriching the animals' diets in branched-chain amino acids reversed these deficits.

Similar dietary enrichment normalized serum levels of branched-chain amino acids in people affected by the *BCKDK* mutation.

Science http://dx.doi.org/10.1126/science.1224631 (2012)

CONSERVATION BIOLOGY

Tigers and people can coexist

As the world becomes more crowded, setting aside time, as well as space, for other species could help humans to live harmoniously alongside wildlife.

Jianguo Liu of Michigan State University in East Lansing and his team came up with the idea after analysing footage from motion-activated cameras they had set up in and around Nepal's Chitwan National Park. The team detected high levels of both human and tiger activity in the park, and found that the geographical activity patterns of the two species overlapped: any given camera was likely to collect images of both. Yet there was little conflict between humans and tigers in the park, probably because 80% of tiger detections occurred at night, when humans are generally at home. Outside the park, where humans are even thicker on the ground, 95% of tiger detections were at night.

Proc. Natl Acad. Sci. USA http://dx.doi.org/10.1073/pnas.1210490109 (2012)

COMMUNITY CHOICE

The most viewed papers in science

CLIMATE SCIENCE

Calm Sun promotes chilly winters

HIGHLY READ on www.agu.org 27 Aug–2 Sept

Unusually cold central European winters — such as those of the past two years — could be due to atmospheric circulation anomalies caused by weak solar activity.

Frank Sirocko of the Johannes Gutenberg University of Mainz, Germany, and his team compared historical records of freezing of the river Rhine with a time series of observed sunspot activity. The researchers found that 10 of the 14 major freezing events that have occurred since 1780 took place in or around years with minimal numbers of sunspots, when solar activity was weak.

The effects of weak solar activity may propagate to the lowest layer of Earth's atmosphere, leading to changes in pressure systems over the North Atlantic. These changes would favour the sustained flow of chilly Arctic air to central Europe during winter months, the team suggests.

Geophys. Res. Lett. http://dx.doi.org/10.1029/2012GL052412 (2012)

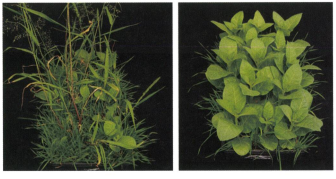

PLANT BIOTECHNOLOGY

Engineered plants can use phosphite

Many crops depend on phosphorus-based fertilizers and are threatened by herbicide-resistant weeds. Genetically modified plants that can digest an alternative phosphorus source that normally inhibits plant growth could solve both problems.

Damar López-Arredondo and Luis Herrera-Estrella at the National Polytechnic Institute's Centre for Research and Advanced Studies in Irapuato, Mexico, engineered the model plant *Arabidopsis*, and tobacco plants, to metabolize phosphite, in addition to the orthophosphate found in standard fertilizer. When phosphite was available, the transgenic plants needed 30–50% less phosphorus to generate the same amount of biomass as that produced in the presence of orthophosphate. The researchers also tested the transgenic plants against weeds. In the presence of orthophosphate, weeds dominated the transgenic plants, but with the addition of phosphite, transgenic tobacco plants easily outcompeted weeds (**pictured**).

Nature Biotechnol. http://dx.doi.org/10.1038/nbt.2346 (2012)

NATURE.COM

For the latest research published by *Nature* visit:
www.nature.com/latestresearch

SEVEN DAYS *The news in brief*

POLICY

Missile defence

The US missile-defence programme should end costly efforts to catch missiles in the early stages of launch and strengthen its ability to intercept them in mid-course, says *Making Sense of Ballistic Missile Defence*, a study from the National Academy of Sciences published on 11 September. Research into expensive space-based radars should be slashed, and efforts to distinguish warheads from dummies intensified, it says.

Climate-model plan

US climate modellers should work towards better ways of developing, interpreting and comparing climate and weather models, the National Research Council concludes in a report released on 7 September. *A National Strategy for Advancing Climate Modeling* recommends that the community try to standardize software platforms so that they are ready for the next generation of supercomputers. See go.nature.com/b2ymhi for more.

Nuclear future

The United Arab Emirates has started to build its first nuclear reactor, making it the first country to embark on a commercial nuclear programme since China in 1985. On 30 August, reactor unit 1 at Barakah was reported by the International Atomic Energy Agency in Vienna as being officially "under construction". The reactor is the first of four that will be supplied by a South Korean consortium at a total cost of US$20 billion. The 1,400-megawatt pressurized water reactor is scheduled to begin operations in 2017.

JOURNALISM AWARD

Gayathri Vaidyanathan, who worked at *Nature* during a fellowship from the International Development Research Centre in Ottawa, Canada, has won the Evert Clark/Seth Payne Award for young journalists. The award cited 'The wheat stalker' (*Nature* **474,** 563–565; 2011) and 'The cultured chimpanzees' (*Nature* **476,** 266–269; 2011), and two pieces published elsewhere.

CHINAFOTOPRESS VIA GETTY IMAGES

Yellow river turns red

A stretch of the Yangtze River near Chongqing in southwest China turned red on 6 September. What caused the sudden change in the river's colour is still unclear, but freshwater scientists contacted by *Nature* say that it is unlikely to be attributable to an algal bloom because such algae do not grow in oxygen-rich, fast-flowing river waters. Last December, the Jian River in northern China turned red as a result of dye pollution.

Shale-gas risks

Drilling for shale gas might contaminate water resources, damage biodiversity and pollute the air — and such environmental risks are not adequately mitigated by existing legislation, says a study published by the European Commission on 7 September. A second study notes that European shale gas would generate more greenhouse-gas emissions than conventional gas — but fewer than would be produced by importing gas into the European Union.

BUSINESS

Oil exploration

On 9 September, Shell began oil exploration in the Chukchi Sea off Alaska, the first offshore drilling in the sea for more than 20 years. The drilling is designed to reach an oil reservoir at a depth of 2,400 metres, but is unlikely to be finished this year: Shell's current permit is valid only until 24 September because of the threat of encroaching sea ice. Shell has requested an extension, arguing that sea ice is likely to arrive later this year. See go.nature.com/kjdtih for more.

RESEARCH

New species online

Animal species can now be described and named in electronic-only publications, the International Commission on Zoological Nomenclature announced on 4 September. Previously, descriptions of new animal species had to be published in print to be considered bona fide. Botanists endorsed electronic publication last year (see go.nature.com/ufq7sv). See page 178 and go.nature.com/pta96e for more.

Drilling depth

The deep-sea drilling vessel *Chikyu* has recovered rock samples from more than 2.1 kilometres beneath the sea floor, the Japan Agency for Marine-Earth Science and Technology announced on 6 September. *Chikyu* is drilling

WHEELER STUDIOS/SKA.ORG

off the coast of Japan north of the fault zone responsible for the 2011 Tohoku earthquake. Although oil wells frequently reach deeper, this is the first scientific expedition to retrieve core samples from such depths. See go.nature.com/vxrcrg for more.

Dengue trial

A dengue vaccine protected Thai schoolchildren from some forms of the mosquito-borne virus, reports a study published on 10 September (A. Sabchareon *et al. Lancet* http://doi.org/jbq; 2012). Overall, 2.8% of 2,669 children who received the vaccine developed dengue, compared with 4.4% of the 1,333 in a control group, a result that was not statistically significant. But a secondary analysis found that the vaccine was 60–90% effective against three out of four genetic forms of dengue.

PEOPLE

Telescope chief

The world's largest radio-telescope project has chosen a director-general. On 5 September, the board of the Square Kilometre Array appointed Phil Diamond to oversee construction of the €1.5-billion (US$1.9-billion) project, which will have sites in Australia and South Africa (see *Nature* **485,** 555–556; 2012). Diamond (**pictured**) is currently serving as the head of astronomy and space science at Australia's Commonwealth Scientific and Industrial Research Organisation in Marsfield. He replaces Michiel van Haarlem, who has served as interim director-general since December 2011.

Hauser disciplined

Marc Hauser, a former psychologist at Harvard University in Cambridge, Massachusetts, engaged in research misconduct, the US Office of Research Integrity concluded on 5 September. He neither admits nor denies the charges. See page 189 for more.

FUNDING

Football donation

The US National Football League (NFL) is donating US$30 million to the Foundation for the National Institutes of Health to support research into brain injuries. The money will help to establish a Sports and Health Research Program at the National Institutes of Health, to fund research on chronic traumatic encephalopathy and other sport-related brain injuries. Meanwhile, a study in *Neurology* (E. J. Lehman *et al. Neurology* http://doi.org/h97; 2012) has reported that professional American football players are more likely than the general population to have Alzheimer's disease or the neurodegenerative disease amyotrophic lateral sclerosis as an underlying cause of death.

AWARDS

Balzan prizes

Kurt Lambeck, a geophysicist at the Australian National University in Canberra, has been awarded one of this year's two 750,000-Swiss-franc (US$790,000) Balzan prizes in science for his research on sea-level changes and glacial cycles. Plant scientist David Baulcombe of the University of Cambridge, UK, won the other for his work on epigenetics.

Lasker award

The US$250,000 Albert Lasker Basic Medical Research Award has been awarded to biologist Michael Sheetz of Columbia University in New York city, biochemist James Spudich of the Stanford University School of Medicine in California and cell biologist Ronald Vale of the University of California, San Francisco, for their work on cytoskeletal motor proteins, which underlie cellular transport and muscle contraction. Winners of the award often go on to receive a Nobel prize.

COMING UP

14 SEPTEMBER
More details on the workings of the US National Institutes of Health's youngest centre, the National Center for Advancing Translational Sciences, are revealed at two key meetings in Bethesda, Maryland. The centre's advisory council and its Cures Acceleration Network Review Board both convene.
go.nature.com/zablws

17–21 SEPTEMBER
Nuclear safety and security are discussed at the annual general conference of the International Atomic Energy Agency in Vienna.
go.nature.com/dfaznk

EVENTS

Dawn departure

NASA's mission to explore the asteroid belt's two most massive bodies departed from its first target, Vesta, on 5 September. The Dawn probe had been mapping Vesta since July 2011. It is now heading for an early-2015 appointment with Ceres, the dwarf planet that is thought to harbour substantial amounts of subterranean ice. See go.nature.com/pgoftk for more.

TREND WATCH

The world's network of protected areas is growing rapidly, but not fast enough to meet the 2020 Aichi biodiversity targets, according to the trend detailed in the United Nations' *Protected Planet* report, released on 7 September at the IUCN World Conservation Congress in Jeju, South Korea. The proportion of area managed exclusively by governments has fallen, as conservation schemes based on local community management (often by indigenous peoples) play a growing part. See go.nature.com/dgve5x for more.

SOURCE: UNEP-WCMC

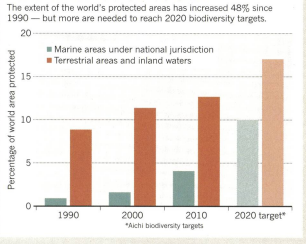

NATURE.COM
For daily news updates see:
www.nature.com/news

King Abdullah International Medical Research Center

Got Ethics?

We do. Ethics is doing the right thing, even if nobody is watching.

KAIMRC aims to disseminate biomedical ethic concepts into the health care system and community through education and public awareness. In an Islamic matrix of ethics and morality, we strive to set our own trends to formulate policies and guidelines, carry out and coordinate teaching and research, stimulate informed public debate, and provide a resource service for health professionals in our community and beyond. Ethical work behavior is a crucial part of success; all our employees possess a high degree of integrity and an outstanding level of professionalism.

At KAIMRC, a segment in the enormous healthcare system of King Abdulaziz Medical City, we felt the overwhelming sense of obligation towards both the healthcare profession and our institution to launch a Masters Degree program in Biomedical Ethics with the incorporation of Islamic Law. Healthcare professionals who show genuine interest in applying their knowledge and expertise to the ethical aspects of healthcare would be considered for program.

KAIMRC takes pride in its Bioethics Section, as it is home for the UNESCO chair of Saudi Arabia, held by its head Dr. Amin Kashmeery.

"*Whoever works righteousness, man or woman, and has faith, verily, to them will We give a new Life, a life that is good and pure, and We will bestow on such their reward according to the best of their actions.*" - Holy Qur'an, Chapter 16, Verse 97

"*It is better for a leader to make a mistake in forgiving than to make a mistake in punishing.*"- Prophet Mohammed (PBUH)

"*In law a man is guilty when he violates the rights of others. In ethics he is guilty if he only thinks of doing so.*" – Immanuel Kant

"*Ethics is knowing the difference between what you have a right to do and what is right to do.*" – Potter Stewart

Scientists Vacancies at King Abdullah International Medical Research Center

KAIMRC provides an opportunity to serve in a dynamic, multicultural environment with state-of-the-art facilities for competent and motivated persons who are willing to dedicate themselves and make a difference in the world of scientific medical research. If you are interested in being involved in demanding and innovative projects within one of the leading medical research centers worldwide, then search KAIMRC on Naturejobs.com to find our latest vacancies or apply with us by sending your resume to recruitment@kaimrc.med.sa. Please identify the position that you are applying to in the subject heading of your e mail.

Today's Question, Tomorrow's Answer

KAIMRC Is Looking To Hire The Following:

1. Senior Research Scientist:

Education & Qualifications:

- Doctorate Degree (PhD) in Health Science or in a related discipline from an accredited university(Essential).

Experience:

- Minimum of twelve (12) years of experience in a well recognized research institution, coupled with two (2) years supervisory experience in a senior management position(Essential).

2. Research Scientist:

Education & Qualifications:

- PhD IN Science/Pathology or in a related discipline from an accredited University (Essential).

Preferably post-doctoral research experience

Experience:

- Eight (8) years working experience in clinical /research institution or Five (5) years experience with one or more publication as Principal Investigator in journal with 12 or more impact factor(Essential).

3. Associate research scientist:

Education & Qualifications:

- Doctorate Degree (PhD) in Health Science or equivalent from an accredited university (Essential).

Experience:

- Completion of Post Doctoral Fellowship (Essential).
- Minimum of three (3) years of experience in a clinical/research institution(Essential).

4. Research Assistant:

Education & Qualifications:

- Master's Degree in Health Science/ Health Management/Public Health or equivalent from an accredited college or university(Essential).

Experience:

- Minimum of four (4) years working experience in clinical research or scientific field(Essential).

5. Research Associate:

Education & Qualifications:

- Master's Degree in Health Science/ Health Management/Public Health or equivalent from an accredited college or university (Essential).

Experience:

- Minimum of seven (7) years of experience in a clinical/research institution(Essential).

For further information
Please visit our website: www.kaimrc.med.sa
To know more about our activities, the available positions or our collaboration policies,
Email: research1@ngha.med.sa

CUSTOM MONOCLONAL ANTIBODIES
Rat mAb ◦ Mouse mAb ◦ Ascites

CUSTOM PROTEIN EXPRESSION
HEK293 ◦ Baculovirus ◦ *E. coli*

Superior Quality • Unrivaled Expertise
www.promab.com
1.866.339.0871 | info@promab.com
ProMab Biotechnologies, Inc

nature**MIDDLE EAST**
Emerging science in the Arab world
twitter facebook google+

RESEARCH, NEWS, JOBS, BLOGS, EVENTS

Ensure you're part of the scientific and medical community gaining access to **the latest research in the region**.

Nature Middle East is your free comprehensive portal keeping you at the centre of science in the Arabic speaking Middle East.

nature.com/nmiddleeast

Download the free app for your phone at http://gettag.mobi

Sponsored by

nature publishing group npg

nature**jobs**

Scientists stay informed of the latest:

- **Hot jobs**
- **Career news**
- **Announcements**

Sign-up to our **FREE** jobseeker newsletter:
www.naturejobs.com/newsletter

SCIENTIFIC AMERICAN™

Gain complete online access to the latest in science, technology and medicine at your institution

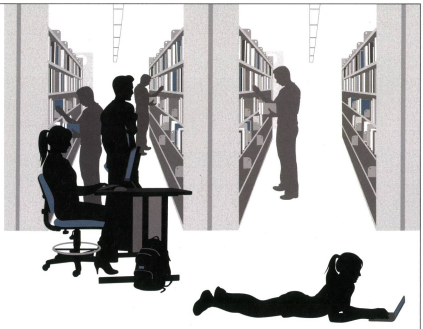

Recommend site license access to your library today!
www.nature.com/scientificamerican

™ Scientific American, Inc.

nature publishing group npg

NEWS IN FOCUS

PUBLIC HEALTH Europe seeks early warning of invading mosquitoes **p.187**

MISCONDUCT Guilty verdict settles Marc Hauser case — but not the questions **p.189**

ASTRONOMY Distorted galaxies scrutinized for dark energy **p.190**

OCEANOGRAPHY *Alvin* upgraded while projects founder **p.194**

E. BACCEGA/AGE FOTOSTOCK/ROBERT HARDING PICTURE LIBRARY

Larger areas of open ocean and warming surface waters will alter evaporation, cloudiness, precipitation and storm patterns across the Arctic and beyond.

CLIMATE

Ice loss shifts Arctic cycles

Record shrinkage confounds models and portends atmospheric and ecological change.

BY QUIRIN SCHIERMEIER

Before indifferent satellite eyes, the top of the world is undergoing a transformation. The Arctic ice pack, a primary indicator of climate change, has shrunk in recent weeks to an extent that no computer model and few scientists had thought possible.

After five years that all saw less ice than previously documented in the 34-year satellite record, this year's record loss has scientists questioning their models. They are also striving to understand the complex cascade of effects — from shifting weather patterns to displaced marine species — that the accelerating retreat could trigger.

The US National Snow and Ice Data Center (NSIDC) in Boulder, Colorado, announced the record decline on 26 August, saying that the ice extent had dropped to 4.10 million square kilometres (see 'Going, going...'). The figure is 70,000 square kilometres less than the previous record low, set in 2007, and it came at least two weeks before the annual low is typically reached. According to the NSIDC, by 9 September that figure had dropped by another 14%, to around 3.52 million square kilometres.

The massive melt has occurred in relatively normal weather conditions, with only one strong summer storm to hasten the break-up of the pack ice. Mark Serreze, director of the NSIDC, says that much of the Arctic pack is now thin first-year ice — frozen only last winter — which requires much less energy to break apart and disperse than multi-year ice. "We have entered a new regime," he says. "The sea ice is in such poor health in spring that large parts of it can't survive the summer melt season, even without boosts from extreme weather."

Computer models that simulate how the ice will respond to a warming climate project that the Arctic will be seasonally 'ice free' (definitions of this vary) some time between 2040 and the end of the century. But the observed downward trend in sea-ice cover suggests that summer sea ice could disappear completely as early as 2030, something that none of ▶

➲ NATURE.COM
For more on the receding Arctic ice, see:
go.nature.com/s5w2pr

▶ the models used for the next report by the Intergovernmental Panel on Climate Change comes close to forecasting[1].

"There's a tremendous spread between observations and model projections," says Serreze. "It might be that natural variability is larger than assumed, or perhaps models don't get the change in ice thickness right." Uncertainty also remains over the strength of various natural 'feedbacks'. For example, an exposed ocean is darker than an ice-covered surface and so absorbs more solar heat, causing yet more warming and melting.

A lack of fine detail about circulation patterns in the Arctic Ocean could also be throwing off the models. For example, a survey carried out in 2008 revealed 20 formerly unobserved eddies, each some 15 to 20 kilometres in diameter, in waters north of Canada. "Whether these are new features, and what role they might play for ocean-mixing processes, we don't know yet," says Yves Gratton, an oceanographer and Arctic researcher at the National Institute of Scientific Research in Montreal, Canada.

Ice loss could also accelerate if the ice pack's underlying waters warm up. Unlike in most of the world's oceans, the coldest water in the Arctic, at –1 °C to –2 °C, is at the surface; below a depth of 200–300 metres, saltier and warmer water of about 1 °C flows in from the Atlantic. The cold surface layer — called the halocline — isolates the sea ice from the warmer water below.

But the halocline is vulnerable to warming from above, says Henning Bauch, a marine geologist at the GEOMAR research centre in Kiel, Germany. A thinning halocline — something that has not yet been observed — would not only jeopardize the sea ice but could also melt the carbon-rich permafrost beneath shallow coastal waters[2], releasing greenhouse gases into the atmosphere.

Meanwhile, Arctic biology is already changing, as the retreat and thinning of sea ice allows more sunlight to penetrate the upper ocean and deprives certain species of habitat, says Jørgen Berge, a marine biologist at the University of Tromsø in Norway. For example, the dominant Arctic zooplankton — the copepods *Calanus hyperboreus* and *C. glacialis* — are being replaced by Atlantic *C. finmarchicus*. Meanwhile, Arctic cod (*Arctogadus glacialis*) is increasingly being out-competed by its larger Atlantic cousin *Gadus morhua*[3].

Other species are showing unexpected resilience. In January, a research cruise into the pack ice north of Svalbard, Norway, found evidence that *Apherusa glacialis* — amphipods, or small crustaceans, that feed on algae growing beneath the ice and are the main food source for many Arctic sea birds — are less dependent on extensive sea ice than previously thought. Just as some coastal organisms drift with the tide to retain their positions in river estuaries, these amphipods can sink to depths at which pole-ward ocean currents sweep them farther north, where they can find and colonize surviving sea ice[4].

"This looks like an adaptive trait that allows key Arctic-ice fauna to persist in changing sea-ice environments," says Berge, who led the study. He points out that the Arctic Ocean has been ice-free during the summer several times during the past 2.5 million years, and that as recently as 8,000–6,500 years ago, during a period known as the Holocene Thermal Maximum, much more of the Arctic was ice-free than it is today[5] — with no mass-extinction events known to have occurred.

Farther afield, this year's record sea-ice melt might foreshadow a harsh winter in parts of Europe and North America. Recent research, although preliminary, suggests a connection between late-summer Arctic sea-ice extent and the location of areas of high and low atmospheric pressure over the northern Atlantic. The highs and lows can remain relatively fixed for weeks, shaping storm tracks and seasonal weather patterns such as extended cold surges[6].

Ralf Jaiser, a climate scientist at the Alfred Wegener Institute for Polar and Marine Research in Potsdam, Germany, found a significant correlation in 1989–2011 meteorological data between late-summer Arctic sea-ice extent and atmospheric-pressure anomalies that favour extreme weather such as prolonged cold snaps in winter[7]. He reasons that in autumn, the open Arctic Ocean sheds heat to the high-latitude atmosphere. The warming tends to reduce the large-scale atmospheric-pressure gradient and weakens the dominant westerly winds in the Northern Hemisphere. Those winds normally sweep warm, moist Atlantic air to western Europe; their weakening leaves the region more prone to persistent cold.

"The impacts will become more apparent in autumn, once the freeze-up is under way and we see how circulation patterns have influenced the geographical distribution of sea ice," says Judith Curry, a climate researcher at the Georgia Institute of Technology in Atlanta. But, she adds, "We can probably expect somewhere in the mid/high latitudes of the Northern Hemisphere to have a snowy and cold winter."■

1. Stroeve, J. C. *et al. Geophys. Res. Lett.* **39**, L16502 (2012).
2. Vonk, J. E. *et al. Nature* **489**, 137–140 (2012).
3. Schiermeier, Q. *Nature* **446**, 133–135 (2007).
4. Berge, J. *et al. Biol. Lett.* http://dx.doi.org/10.1098/rsbl.2012.0517 (2012).
5. Funder, S. *et al. Science* **333**, 747–750 (2011).
6. Liu, J., Curry, J. A., Wang, H., Song, M. & Horton, R. M. *Proc. Natl Acad. Sci. USA* **109**, 4074–4079 (2012).
7. Jaiser, R., Dethloff, K., Handorf, D., Rinke, A. & Cohen, J. *Tellus A* **64**, 11595 (2012).

NATIONAL SNOW AND ICE DATA CENTER

MORE ONLINE

TOP STORY

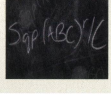

'Astounding' solution to complex maths puzzle
go.nature.com/2lz9lk

MORE NEWS

- Science wins over creationism in South Korea go.nature.com/abfuyd
- Rabbit grimaces unlock animal pain go.nature.com/qenfku
- Dietary supplements may offer a way to treat rare form of autism go.nature.com/ghevdf

SLIDESHOW

Glittering African fruit has nature's brightest hue go.nature.com/o39pay

P. MOULT

F. SCHAFFNER/AVIA-GIS

The Asian tiger mosquito (*Aedes albopictus*) can transmit at least 22 different viruses.

DISEASE CONTROL

Europe on alert for flying invaders

Spread of disease-carrying mosquitoes prompts guidelines for boosting surveillance.

BY DECLAN BUTLER

The buzz of tiny wings has been growing ever louder in Europe over the past decade, as invasive mosquitoes carrying exotic diseases such as chikungunya and dengue fever have taken up residence around the continent. Now Europe's entomologists and public-health experts are joining forces to defend the region against the growing threat.

On 28 August, the European Centre for Disease Prevention and Control (ECDC) in Stockholm released guidelines that should help European countries to develop mosquito surveillance, which had become mostly unnecessary after malaria was largely eradicated from the continent in the mid-twentieth century. But the need for better vigilance has been growing again since the late 1990s, as the increased globalization of trade gives species such as the Asian tiger mosquito (*Aedes albopictus*) more opportunities to penetrate into Europe.

The surveillance data will feed into the three-year-old VBORNET consortium, a Europe-wide network of some 400 medical entomologists, microbiologists and public-health experts that is funded by the ECDC. The wealth of data they are assembling should help researchers to better understand how invasive mosquitoes are spreading and the risks they pose, and so to develop control strategies.

The latest guidelines provide an A–Z of mosquito surveillance, covering topics ranging from what sort of mosquito traps should be used in particular circumstances to resource management and policy-making advice. Francis Schaffner, head of integrated pest management at the consultancy Avia-GIS in Zoersel, Belgium, and one of the lead authors of the guidelines, hopes that they will encourage scientists, local authorities and governments to carry out more comprehensive surveillance. By recommending standardized surveillance reporting, the guidelines should also allow data generated by different researchers in different countries to be seamlessly combined into pan-European databases, he says.

NATURE.COM
Read more on vector control in this Outlook:
go.nature.com/udwjuu

A key target of surveillance is the Asian tiger mosquito, which can transmit at least 22 different viruses, including chikungunya and dengue. After it was reported in Albania in 1979, this native of southeast Asia spread to Italy in 1990 and has now expanded along the Mediterranean coast to nations such as France and Spain, as well as around the Black Sea (see 'Multiplying mosquitoes') (J. M. Medlock *et al. Vector-Borne Zoonotic Dis.* **12,** 435–447; 2012). At least five other invasive mosquitoes capable of spreading diseases are also gaining ground in Europe, including *Aedes aegypti*, which can transmit dengue and other diseases.

The international tyre business brings most of the unwanted arrivals. Mosquitoes can breed in small volumes of water, such as rainwater in tyres, and invasive forms have drought-resistant eggs that enable stowaways to survive long-distance transport before being revived by rain once they reach their destinations. The invaders can also hitch a ride on imported plants, such as lucky bamboo (*Dracaena* species). In the future, climate change could accelerate the spread of these subtropical and tropical species: predictive models suggest that invasive mosquitoes could find suitable habitats in northern Europe by 2030.

In 2007, Italy saw an outbreak of several hundred cases of chikungunya, which causes nausea, vomiting and debilitating joint pain. Dengue fever, which causes similar symptoms and can be fatal, hit a handful of people in France and Croatia in 2010. And there has been a steady rise in cases of West Nile virus, the fever that is currently notching up a record year for infections in the United States.

Surveillance remains patchy or non-existent in many of the most affected countries around Europe, including Portugal, Greece, Turkey and those bordering the Black Sea. Monitoring insects is expensive and time-consuming, and governments that are preoccupied with existing health challenges may be reluctant to put funds towards tracking potential future threats. But one underlying message of the report is that early surveillance is ultimately cheaper than dealing with an established pest, which can require widespread spraying with insecticides.

The latest guidelines provide an A–Z of mosquito surveillance.

In the Netherlands, for example, Asian tiger mosquitoes are introduced every year, but surveillance and control measures have so far prevented them from becoming established, says Marieta Braks, an entomologist at the National Institute for Public Health and the Environment in Bilthoven, and leader of VBORNET's strategic consultation group. The Dutch authorities pay close attention to companies that import tyres from countries harbouring dangerous mosquitoes, and that stock tyres outdoors, ▶

▶ where rain could allow mosquito eggs to hatch. In countries such as Italy, where the tiger mosquito is already widespread, surveillance is instead geared more towards keeping numbers under control.

VBORNET's geographical information system allows scientists to combine surveillance data with environmental factors, including temperature and humidity, to better track the main invasive mosquito species. Models based on these combined data can reveal, for example, how environmental conditions can affect mosquitoes' ability to transmit pathogens, and so provide information on the likelihood of outbreaks in various regions.

The maps may also perform a useful peer-pressure function, says Braks, by highlighting where researchers and authorities have failed to supply and share data. "What we hope is that no one will want to be a blank on the map." ■

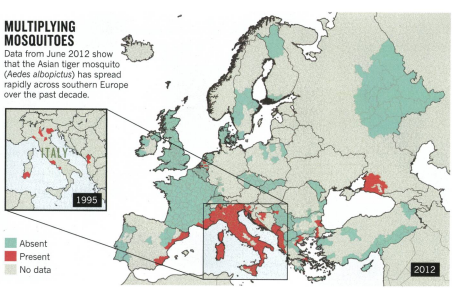

FUNDING

EU battles over research billions

Politicians will spend the next few months negotiating cuts to Horizon 2020's budget.

BY NATASHA GILBERT

Tens of billions of euros are at stake as negotiations ramp up to shape Europe's next seven-year research programme. The discussions will cover familiar divisions over applied versus basic research and conflicting national agendas, but the continent's ongoing financial problems will add an extra measure of anxiety.

The European Commission proposed the general size and shape of the Horizon 2020 research and innovation programme in November 2011 (see *Nature* http://doi.org/dtvtbx; 2011). European Union (EU) member states and members of the European Parliament will negotiate and agree on the budget and final details of the programme, which will run from 2014 to 2020, over the next 15 months.

Last year, the commission requested €77.6 billion (US$99 billion) for Horizon 2020, out of a total European budget for 2014–20 of about €1 trillion (at constant 2011 prices). But many members of the European Parliament (MEPs) want research to get €100 billion, twice as much as was allocated to Horizon 2020's predecessor, the Seventh Framework Programme (FP7), which runs from 2007 until 2013 (see 'Budget breakdown'). Most scientists and EU science officials say that such a large jump is unrealistic, and there are growing fears that even the lower budget proposed by the commission is unlikely, given Europe's shaky economy.

At a meeting on 30 August, high-level ministers said that cuts to the proposed EU budget are "inevitable", implying that spending on Horizon 2020 will be eroded. Ministers are aiming to reach a consensus on the size and shape of the EU budget by the end of the year, but in the meantime, MEPs, scientists and member-state officials will fight over which of Horizon 2020's ambitions should bear the brunt of any budget reductions. The first sortie will come on 17–18 September, when MEPs on the European Parliament's Industry, Research and Energy (ITRE) committee will begin discussing around 3,000 suggested amendments to the Horizon 2020 budget.

Most likely to feel the pinch is the European Institute of Innovation and Technology (EIT), a virtual institute headquartered in Budapest and made up of scientific 'communities' that conduct research on themes such as climate change and sustainable energy. The institute also runs postgraduate education programmes and knowledge-transfer activities to disseminate the fruits of research to businesses and policy-makers (see *Nature* **440**, 8–9; 2006). The EIT concept was developed and championed by the European Commission, which now suggests that the institute's budget should win €2.8 billion from Horizon 2020, 3.6% of the total research budget and vastly more than the €309 million in European funds allocated to it between 2008 and 2013.

However, few outside the commission want the EIT to claim so much; some argue that the

institute has yet to prove its scientific worth. Teresa Madurell, a Spanish social-democrat MEP on the ITRE committee, suggests that the EIT should get no more than 3.1% of Horizon 2020's funds. Paul Rübig, an Austrian Christian Democrat MEP who also sits on the committee, wants to trim that even further, suggesting that the EIT's remit be reduced to knowledge-transfer activities only.

The EIT's critics say that the money would be better spent on initiatives with a proven track record. The most popular programmes include the European Research Council (ERC), which dispenses excellence-based grants for frontier science, and the Marie Curie Actions programme, which provides career-development grants to young researchers. The commission proposed that the ERC's budget should rise by 77% to €13.3 billion, but Luke Georghiou, who studies European research policy at the University of Manchester, UK, expects opposition from member states in eastern Europe, which could hold up the budget negotiations. Scientists in those countries often lose out to those from research powerhouses such as the United Kingdom and Germany when ERC grants are allocated. Some say that the ERC should also fund those scientists with the 'potential for excellence'. Vicky Ford, a British Conservative member of the ITRE committee, counters that ERC funding should go only to excellent research.

The ERC tends to fund individual researchers, so during FP7 larger collaborations have relied on separate funding streams. But some scientists are concerned that funding for applied research has squeezed out support for basic science in these programmes. Over the past four years, calls for collaborative proposals in areas of basic science such as epigenetics and protein regulation have become less frequent, says Karin Metzlaff, executive director of the European Plant Science Organisation in Brussels. She hopes that the ITRE committee meeting can help to make basic-science projects a bigger priority in Horizon 2020's collaborative-research programme, dubbed Societal Challenges.

Overall, research is likely to be spared the EU budget's most severe cuts, because politicians recognize that investing in science is central to boosting economic growth. Indeed, countries such as Spain, which has slashed domestic science spending owing to the financial crisis, will become more reliant on Horizon 2020 funds. That may even prompt them to give ground in negotiations on contentious issues such as human embryonic stem-cell research, says Georghiou. "They need to replace their national funding shortage," he says. ■

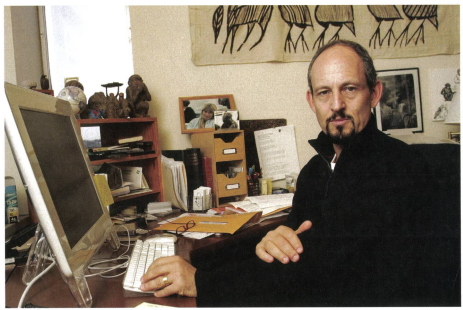

R. FREEMAN/THE NEW YORK TIMES/REDUX/EYEVINE

Marc Hauser left Harvard University in 2011 after the institution found him guilty of misconduct.

RESEARCH ETHICS

Misconduct ruling is silent on intent

Psychologist Marc Hauser admits errors but not fraud.

BY EUGENIE SAMUEL REICH

Mavens of research ethics often insist that there is a clear difference between sloppy science and scientific fraud. But if ever there was a case that blurs that line, it is that of Marc Hauser, a high-flying evolutionary psychologist who resigned from Harvard University in Cambridge, Massachusetts, in 2011, after the university found him guilty of misconduct.

In a finding published on 6 September in the *Federal Register*, the US Office of Research Integrity (ORI) in Rockville, Maryland, which oversees science funded by the National Institutes of Health (NIH), has also concluded that Hauser "engaged in research misconduct". The office found that he: "published fabricated data" in the journal *Cognition* in 2002[1]; "falsified" results in an unpublished study; and made false statements in four other instances. But the ORI did not state whether Hauser acted intentionally — its definition of misconduct also covers cases in which misrepresentations are "reckless".

That has provided enough wiggle room for both supporters and critics to claim the finding as a vindication. "It isn't a strong case for intentional misconduct. It seems it's peccadilloes," says Pierre Pica, a linguist at the French National Center for Scientific Research in Paris, who has criticized the investigation. But Gerry Altmann, a psychologist at the University of York, UK, and editor-in-chief of *Cognition*, disagrees. "The number of instances [in the investigated body of work] suggests it is extremely unlikely it was not intentional," he says.

Harvard had found Hauser guilty of eight counts of misconduct in 2010, after a three-year internal investigation of some of his studies of cognition in non-human primates. To the annoyance of many scientists, the university did not release its findings, so exactly what Hauser had done remained unclear. The ORI provides details on six counts of misconduct, three of which were published[2,3].

In a statement sent to *Nature*, Hauser acknowledges mistakes and errors, but not scientific fraud or research misconduct, which the ORI says he neither admits nor denies. "Although I have fundamental differences with some of the findings in the ORI report," Hauser says, "I acknowledge that I made mistakes. I let important details get away from my control, and as head of the lab, I take responsibility for all errors made within the lab, whether or not I was directly involved." No one else who worked in Hauser's lab has been charged with misconduct.

The ORI often resolves allegations ▶

against scientists through a settlement agreement, which helps the reputedly overstretched office to save on legal resources. Hauser's settlement means that he escapes the harshest possible punishment — a ban on future NIH funding — and must instead submit a supervisory plan that will ensure integrity if he applies to the agency for any future research grants. (The agency spent at least US$790,000 on grants that funded work affected by the misconduct.)

Bennett Galef, an expert in animal behaviour at McMaster University in Hamilton, Canada, reviewed evidence used in the Harvard investigation at the request of Hauser's lawyer, and questions the ORI's use of the word "fabricated" to describe the errors in the *Cognition* paper[1]. "That is a conceivable read of what happened, but it's slanted," he says. According to Galef, lab records show that in the study, which examined habituation to sound patterns, two groups of tamarin monkeys were played the same stimuli instead of different ones, as the paper reported. Galef says that this was because of an error in the computer program that played the stimuli, which the authors plausibly didn't know about because the protocol called for them to be blinded to the stimuli at the time they coded the monkeys' responses. "It was a big mistake. It was definitely a disaster, but whether there was any fabrication, you don't know," says Galef.

ORI officials familiar with Hauser's case could not comment because of government privacy rules. The inspector-general of the National Science Foundation, which also funded Hauser, is still looking into one of the misconduct counts found by Harvard; the remaining instance was referred to the ORI but has been deemed outside its statute of limitations. Harvard says that the graduate students and postdocs who were working in Hauser's lab have been relocated to other labs within the university.

Hauser has now begun a different chapter in his life, working with at-risk youth. His website states that he has co-founded a company called Gamience, which develops computer games to teach self-control and other cognitive skills, and is working with a non-profit company that serves schools on Cape Cod, called the Cape Cod Collaborative, in Bourne, Massachusetts. "This work is deeply satisfying and I look forward to making new contributions to human welfare, education and the role of scientific knowledge in understanding human nature," Hauser says. ■

1. Hauser, M. D., Weiss, D. & Marcus, G. *Cognition* **86,** B15–B22 (2002).
2. Hauser, M. D., Glynn, D. & Wood, J. *Proc. R. Soc. B* **274,** 1913–1918 (2007).
3. Wood, J. N., Glynn, D. D., Phillips, B. C. & Hauser, M. D. *Science* **317,** 1402–1405 (2007).

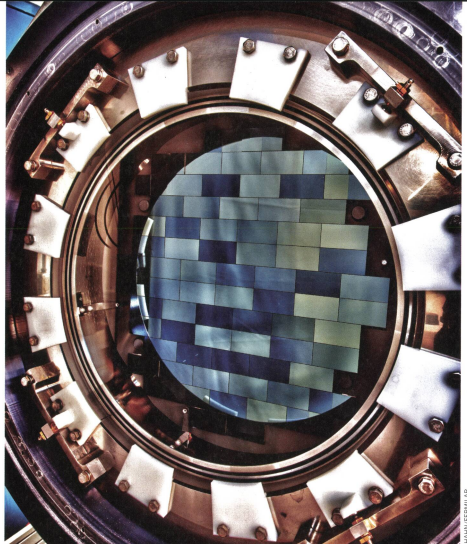

R. HAHN/FERMILAB

The Dark Energy Survey camera will investigate millions of galaxies for the subtle effects of weak lensing.

COSMOLOGY

Cameras to focus on dark energy

A pair of detectors that measure minute distortions in images of distant galaxies will probe the riddle of cosmic acceleration.

BY ERIC HAND

Even the best pictures of a distant galaxy are a bit lopsided. But this is an attribute, not a bug. Because mass distorts space-time, light coming from distant galaxies is bent as it passes through intervening shoals of invisible matter, leaving the images of these distant objects minutely sheared and stretched.

Two astronomical surveys now scheduled to come online seek to take advantage of this effect, which is known as weak gravitational lensing. The surveys aim to use the technique to get a firmer handle on dark energy, the mysterious force that is apparently speeding up the expansion of the Universe. By observing the patterns of distortions across large swathes of sky (see 'Falling into line'), astronomers hope to map the density and distribution of dark matter, the web-like invisible scaffolding around which visible matter is thought to have first coalesced. Then, by looking at changes in this hidden web across cosmic time, they hope to discern the imprint of dark energy.

Observers already study the effects of dark energy by tracking cosmic landmarks: the standard candles of distant supernovae and the

NATURE.COM
Read more about the search for dark energy at:
go.nature.com/cz3f64

standard rulers of ripples in the distribution of galaxies. But those techniques reveal only how the Universe's expansion rate has changed because of dark energy. Weak lensing offers an extra prize: the distortions hold clues to the action of gravity at far-off locales. The technique can thus address an increasingly pressing question for theorists: what if the Universe's accelerated expansion is not the result of dark energy's mysterious anti-gravitational force, but is instead a sign that gravity behaves differently in different parts of the Universe?

"It provides unfettered insight into the properties of gravity that we can't get by other techniques," says Rachel Bean, an astrophysicist at Cornell University in Ithaca, New York. "Its potential is massive, but so are the challenges."

Unlike strong gravitational lensing, in which a major concentration of mass markedly distorts the image of a single galaxy, the subtle effects of weak lensing can be detected only in detailed surveys of millions of galaxies. One of the new efforts will use the Hyper Suprime-Cam (HSC), which achieved first light on 28 August on the 8.2-metre Subaru telescope in Hawaii. By 2018, it aims to have imaged 10 million galaxies over a 1,500-square-degree-swathe of the sky, says Satoshi Miyazaki of the National Astronomical Observatory of Japan in Mitaka, who is the principal investigator of the HSC survey.

A rival project, the Dark Energy Survey (DES), is set to start operating later this month on the 4-metre Blanco telescope in Chile, says its principal investigator, Josh Frieman of the Fermi National Accelerator Laboratory in Batavia, Illinois. Being the main project for the Blanco telescope, the DES will get more observing nights than the HSC, allowing it to image 300 million galaxies over 5,000 square degrees by 2018. But its smaller telescope means that it will not be able to peer as deeply into the distant Universe as the HSC survey.

Even with these massive digital cameras — 870 million pixels for the HSC and 570 million pixels for the DES — weak lensing "is a very, very difficult measurement to make", says Bean. To detect the subtle distortions caused by lensing, for example, astronomers must subtract aberrations caused by the optics of the telescope and by Earth's atmosphere.

Doing the measurements from space could help. The European Space Agency is planning to launch a dark-energy probe called Euclid in 2019. And in the United States, an as-yet-unfunded dark-energy mission called the Wide-Field Infrared Survey Telescope, which would dedicate much of its time to weak-lensing measurements, was ranked as the top priority for space-based astronomy in a 2010 decadal survey.

Some astronomers doubt that the technique can outperform supernova surveys and measurements of baryonic acoustic oscillations — ripples in cosmic structure dating from several hundred thousand years after the Big Bang. "I think the jury's still out," says David Schlegel, principal investigator of the Baryon Oscillation Spectroscopic Survey at the Lawrence Berkeley National Laboratory in Berkeley, California. He points out, for instance, that a key assumption in weak lensing — that galaxies are oriented randomly — is turning out not to be true, forcing astronomers to correct for a systematic effect.

"The technique's potential is massive, but so are the challenges."

But others say that it is important to take diverse approaches to the dark-energy mystery. Chris Stubbs, an astrophysicist at Harvard University in Cambridge, Massachusetts, says that, a decade ago, astronomers were intent on simply proving that the effect was real. Now there is little doubt, and they need techniques such as weak lensing to explore more-detailed questions — for instance, whether the effect varies with distance, direction or the density of matter, and whether the effects of dark energy can be distinguished from those of variable gravity. "We are only now entering an era where we're attacking the dark-energy problem with instruments and experiments that were explicitly optimized for that purpose," says Stubbs. ■

FALLING INTO LINE

When light from a randomly oriented group of galaxies passes through a region influenced by the gravity of a large concentration of dark matter, the galaxy images show a slight alignment along a particular direction. Such distortions can reveal the changing concentrations of matter at different cosmic times.

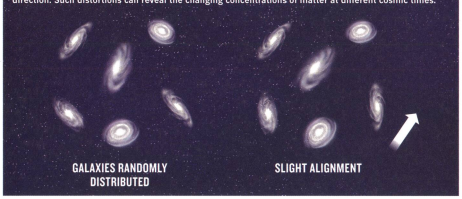

Flow Cytometry by Stratedigm
Cytometry Without Compromise

S1000Ex -
Up to 4 lasers, 14 colors

S1000 -
Up to 4 lasers, 8 colors

SE520 -
2 lasers, 4 colors

A600 -
High throughput autosampler

Industry leading sensitivity in a compact footprint.

Stratedigm
Cytometry Without Compromise

www.stratedigm.com
408.512.3910 info@stratedigm.com

P. VISWANATHAN/THE NEW YORK TIMES/REDUX/EYEVINE

Soaring sales of antibiotics at Indian pharmacies are compounding drug-resistance problems.

PUBLIC HEALTH

India moves to tackle antibiotic resistance

Drug regulator aims to restrict over-the-counter sales.

BY ERICA WESTLY IN CHENNAI, INDIA

Kumar Prabhash's voice is sombre as he describes how he is losing a key weapon in the fight against hospital infections. At the Tata Memorial Centre in Mumbai, where the oncologist works, at least half of bacterial samples from patients with infections are resistant to carbapenems — a class of 'second-line' antibiotics used to treat infections that are already resistant to other drugs. Just a few years ago, the resistance rate in such samples was only 30%. "That is really scary for us," says Prabhash.

Antibiotic resistance is a problem worldwide, but is particularly worrying in India, where hospital standards are inconsistent and antibiotics are readily available over the counter at pharmacies. Prabhash's story was all too familiar to the physicians who heard it at India's first joint medical-society meeting on antibiotic resistance, held on 24 August in Chennai. The symposium is part of an ongoing campaign by Indian clinicians for a national policy to curb misuse of these vital drugs.

"As physicians, we have a responsibility for the future of India," said J. A. Jayalal, who represented the Indian Medical Association at the meeting. "If we're not raising our voices about this, future generations will not forgive us."

Last week, physicians moved a step closer to their goal when India's drug regulators announced a plan that would put tight restrictions on the sale of antibiotics. Carbapenems and many other antibiotics are already on a list of 536 drugs in India that require a prescription. But studies have shown that such drugs are easy to purchase at retail pharmacies without a physician's signature (U. P. Rathnaker *et al. J. Clin. Diagn. Res.* **6**, 951–954 (2012) and A. Kotwani *et al. J. Clin. Pharm. Ther.* **37**, 308–312; 2012). Under the new regulations, carbapenems and other antibiotics with declining efficacy would be treated as a special category of prescription drugs. They would carry prominent red labels, and surprise inspections by the regulator would check whether pharmacies were selling them over the counter.

Drug misuse is a key factor that leads to antibiotic resistance, says Arjun Srinivasan, a medical epidemiologist at the US Centers for Disease Control and Prevention in Atlanta, Georgia. A patient's risk of developing a life-threatening infection that is resistant to carbapenems is 15 times greater if he or she has been exposed to the drug class before, he notes. "Improved antibiotic use will be essential to combat drug resistance," he adds.

There is ample evidence of excessive carbapenem use in India. A survey (go.nature.com/rpsg2r) published earlier this year by the Center for Disease Dynamics, Economics and Policy, a non-profit health-research organization headquartered in Washington DC, found that Indian pharmacy sales of carbapenems increased by nearly six times between 2005 and 2010 (see 'Antibiotics for all').

Limited access to basic medical care is one reason for the overuse of carbapenems and other second-line antibiotics. About 70% of India's 1.2 billion citizens live in rural areas, where, despite government efforts, hospitals are often understaffed and lacking basic equipment and medication. Rather than relying on physicians, many rural patients turn to local pharmacists and whatever drugs they have in stock.

In 2010, India's government created a task force to develop a national antibiotic policy. But last year, Indian health minister Ghulam Nabi Azad rejected the task force's recommendations to ban over-the-counter sales of antibiotics and prohibit the use of carbapenems and other second-line antibiotics except in major hospitals. Azad argued that the bans could have a devastating effect on health in rural areas.

The health ministry did not respond to *Nature*'s questions about the latest recommendation from India's drug regulator, but a health-ministry representative told the *Times of India* that the office did intend to approve the antibiotic restrictions, possibly as early as this week.

Infectious-disease specialist Abdul Ghafur, who organized the joint society meeting in Chennai, hopes to use momentum from the latest restrictions to push for a national antibiotic policy to regulate India's 24,000 hospitals and hundreds of thousands of physicians, as well as its pharmacies. "I am now trying to follow up with the health minister's office to arrange a meeting with the various medical societies," he says. "There are still many more steps ahead." ■

ANTIBIOTICS FOR ALL

Carbapenem antibiotics are increasingly available without prescription in India, compared with Western nations. This is driving the emergence of microbial resistance to the drugs in the country.

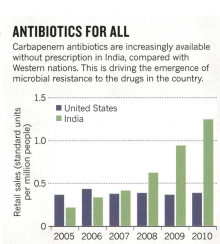

SOURCE: CDDEP

Introducing the BD FACSJazz™

Perfectly tuned cell sorting from BD Biosciences.

BD

Helping all people live healthy lives

Breathtaking solo performance.

The BD FACSJazz™ system begins a new era in cell sorting with stellar performance, benchtop fit, and an affordable price.

The BD FACSJazz can be configured with up to 3 lasers and 8 parameters to support your application needs—offloading sorting demand at core labs or meeting the needs of individuals.

Requiring less than 2 x 2 ft (20 x 20 in, 51 x 51 cm) of bench space, the BD FACSJazz also addresses biosafety concerns with an optional custom designed biosafety cabinet that meets personnel and product protection standards for both a Class II Type A2 biosafety cabinet and the National Sanitation Foundation International Standard 49.

In addition to factory-optimized settings, the BD FACSJazz comes standard with BD FACS™ Sortware sorter software to simplify use. This innovative software is specifically designed for cell sorting and features comprehensive control for acquisition, sorting, and analysis.

For legendary results, just add your creativity. Learn how at **bdbiosciences.com/go/jazz**

Class 1 Laser Product.
For Research Use Only. Not for use in diagnostic or therapeutic procedures.
BD, BD Logo and all other trademarks are property of Becton, Dickinson and Company. © 2012 BD
23-14201-00

BD Biosciences
2350 Qume Drive
San Jose, CA 95131
bdbiosciences.com

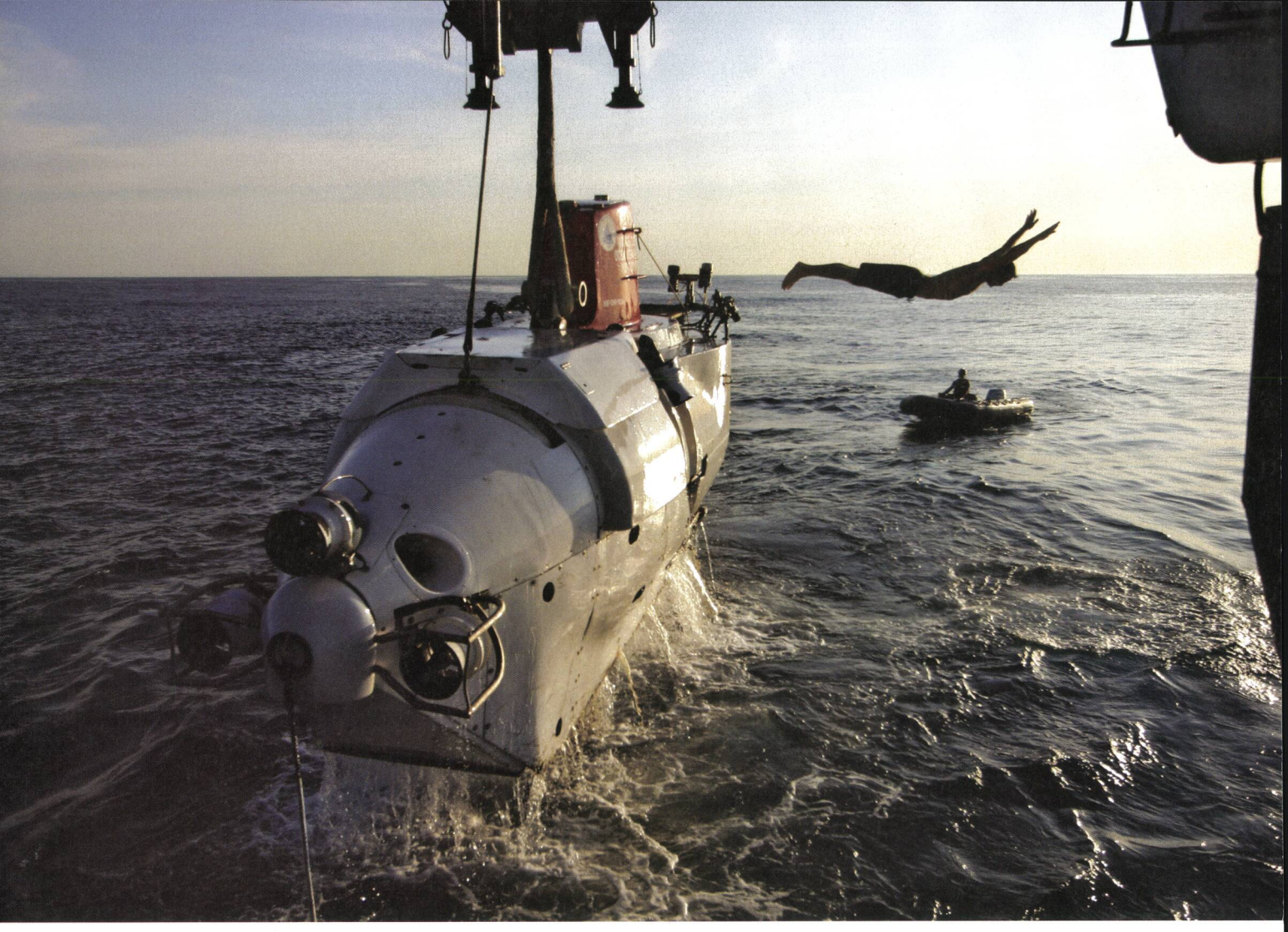

L. WILLS/WOODS HOLE OCEANOGRAPHIC INSTITUTION

DIVE MASTER

The US flagship submersible *Alvin* is getting a partial upgrade. But deep-sea exploration faces some rough water.

BY RICHARD MONASTERSKY

At an industrial hangar in Woods Hole, Massachusetts, a plush toy dog stands guard next to a 5-tonne titanium sphere. Polished to a high shine, the 2.2-metre orb reflects the lights overhead and the faces of passing scientists, who come to ogle the US$11-million engineering marvel — a container strong enough to ferry researchers 6,500 metres down to the bottom of the ocean.

The sphere will be the new heart of the *Alvin* submersible, the United States' workhorse in the deep sea. Over its five-decade career, *Alvin* has dived to the sea floor more than any other research submersible and has made some of the most important oceanographic discoveries of the past few generations. But in the past few years, it has been showing its age and other countries have surged past with vehicles that can venture far deeper than *Alvin*'s current limit of 4,500 metres. In 2010, *Alvin*'s caretakers at the Woods Hole Oceanographic Institution (WHOI) took the venerable submersible out of commission for a $40-million redesign.

The massive upgrade was a long time coming. "I started here in 1996 and there was talk about building a new sub then," says Bruce Strickrott, an *Alvin* pilot and expedition leader at WHOI, who is managing the sub's reconstruction.

This month, Strickrott and his crew will start to rebuild the sub around the passenger sphere, readying it for a series of a final tests off the coast of Bermuda by March. Assuming it passes, *Alvin* will resume a full schedule of scientific dives, joining a suite of tools that are giving US researchers unprecedented ways to study the deep sea — from manned subs like *Alvin* to remotely controlled robots and autonomous mappers.

But after celebrating the revamped sub's maiden voyage, researchers will wake up to some sobering realities. Budget problems have constrained the current *Alvin* upgrade, so researchers must wait for the completion of a second construction phase, in 3–5 years, before they can take advantage of the greater depth limit allowed by the new sphere. That leaves the United States well behind France, Russia, Japan and now China, which sent its research submersible below 7,000 metres in June. And as wealthy entrepreneurs such as film director James Cameron capture public attention with dives in privately built subs, the United States is making painful cuts to many of its deep-sea assets. The administration of President Barack Obama is proposing to cut off funding next year for a pair of manned submersibles in Hawaii that can dive to 2,000 metres.

The *Alvin* submersible was taken out of service for upgrades in 2010 and will dive again next year.

"America has one submersible capa-

the couple-of-miles range — which these days isn't that deep," says Cameron. "What is the future of deep submergence research?"

That future once looked boundless. On 17 February 1977, *Alvin* skimmed along the ocean bottom about 400 kilometres northeast of the Galapagos Islands. Days before, sensors towed by a ship had identified a spike in water temperatures near the sea floor. *Alvin* explored the region and brought researchers face to face, for the first time, with hydrothermal vents, fissures in the sea floor that spew streams of warm, shimmering brine into the near-freezing water. In what was supposed to be a barren desert at the ocean bottom — far from the reaches of life-powering sunlight — *Alvin* revealed oases of clams, crabs, shrimp and alien-like white tube worms crowned with crimson tops.

Two years after the Galapagos dives, an *Alvin* expedition witnessed a more violent scene: jets of black fluids, superheated to 400 °C, shooting out of gigantic chimneys of rock, which were dubbed black smokers. Later, in the geologically quieter Gulf of Mexico, *Alvin* found vents that were releasing cooler methane-rich fluids. These 'cold seeps' also support communities of animals, including slow-growing tube worms thought to be hundreds of years old — some of the most ancient creatures alive on the planet. The discovery of such ecosystems, powered by microbes that harness chemical energy from vent waters, raised questions about where life originated on Earth and where it may reside on other worlds.

Alvin's string of accomplishments silenced early critics — some of the top geoscientists of the 1960s and 1970s — who initially regarded the submersible as little more than a toy. And ever since, the vehicle has been in high demand, trekking to the sea floor 100–150 times a year. Although some countries can dive more deeply, *Alvin* "is the most reliable submersible there is", says Susan Humphris, a geochemist at WHOI and principal investigator of the *Alvin* overhaul. "We need a workhorse at the bottom of the ocean. That's what *Alvin* has been and that's what *Alvin* will continue to be."

AT THE HELM

Cindy Van Dover knows the submersible better than any other scientist. Now the director of the Duke University Marine Laboratory in Beaufort, North Carolina, Van Dover spent nearly three years training and working as an *Alvin* pilot after getting her doctorate at Woods Hole. She is the only researcher, and the only woman, to have piloted the craft, choosing to detour from a conventional research career because the job offered opportunities that few researchers can get. "I wanted to do a lot of dives," she says. "It was about wanting to see the environment that I was studying."

In 1991, when Van Dover gave up her pilot's seat and went back to being an occasional passenger in *Alvin*, one of the things she missed most was the view. The old sphere, built in 1973, had three 13-centimetre-wide viewports, one on each side for passengers and one at the front for the pilot. Through those saucer-sized side ports, Van Dover says, "sometimes it was a great view but often it wasn't, so you'd end up watching a video of what the pilot was doing". The new sphere retains the side windows but has three 18-centimetre-wide ones at the front, giving researchers a field of view that overlaps with the pilot's (see 'Voyager to the bottom of the sea').

The space inside the sphere has also grown, which should make for less-painful rides. With an internal diameter of less than 2 metres, the old sphere had no room for seats; scientists had to huddle on the floor, and lean awkwardly against the sloped walls. After a 2-hour descent to the bottom, limbs would stiffen up. "You switch your position because your legs are so uncomfortable and you rock the whole submersible," says Chris German, a marine geochemist at WHOI and chief scientist for the US National Deep Submergence Facility in Woods Hole, which coordinates the use of *Alvin*. "That can compromise taking the samples."

The new sphere has 18% more interior space and will have ergonomically designed seats. And while sampling or exploring, researchers will be able to take advantage of brighter lights and improved camera systems.

Scientists are keen to use the tools to explore the geology and biology of the mid-ocean ridges, the 60,000-kilometre-long chain of volcanic fissures that forge new ocean crust. So far, oceanographers have surveyed only a tiny fraction of the ridge system. The ridges and their flanks hide a subsurface plumbing network of fissures and pores so extensive that it circulates a volume of water equal to the entire ocean about every million years or so, altering the chemistry of the seas. Future dives will also target the communities of microbes living beneath the sea floor, which has been estimated to constitute as much as one-third of the planet's biomass. And marine scientists want to study the vast abyssal plains, which cover more than half of Earth's surface and are poorly explored; most of the species that researchers pull up in samples from abyssal sites are new to science.

"WHAT IS THE FUTURE OF DEEP SUBMERGENCE RESEARCH?"

But some places that scientists want to visit lie deeper than 4,500 metres and so will remain off-limits to *Alvin* for now. The National Science Foundation, which is funding most of the *Alvin* redesign, could not afford to build a 6,500-metre-class sub all at once. In particular, such deep dives require more energy and it would be prohibitively expensive to build a submersible that uses current battery technology to dive frequently and to greater depths.

Rich Lutz, an oceanographer at Rutgers University in New Brunswick, New Jersey, who has racked up more *Alvin* dives than perhaps any scientist, was surprised to learn that the current overhaul won't add to the sub's depth range. "I certainly would have assumed that one of those improvements would be the capability of going down to 6,500 metres," he says.

BOTTOM DWELLER

Yet depth isn't everything. Despite the excitement over record-breaking dives by China's *Jiaolong* (7,020 metres) and Cameron's *Deepsea Challenger* (11,000 metres), researchers don't go deep very often. Fewer than 10% of the dives by the French and Japanese submersibles approach their limits. Vincent Rigaud, manager of the underwater systems department at the French Research Institute for Exploration of the Sea in La Seyne-sur-Mer, says that research is increasingly focusing on shallower depths. "The science today is linked to [minerals] exploitation or areas where there is an impact from man's activities or man's interests," he says.

Some US researchers are more upset about other limitations of the new *Alvin*. "It's a superb tool for what it does but it could have been a hell of a lot better," says Bruce Robison, a marine ecologist at the Monterey Bay Aquarium Research Institute in Moss Landing, California. In 2004, Robison was a member of a committee of the National Research Council that assessed the future needs of deep submergence science. One of his biggest wishes was for a human-occupied vehicle (HOV) that could adjust its buoyancy to stop at any depth, allowing researchers to work well above the ocean floor. Most of the biological and chemical process in the ocean take place in the water column, not on the sea floor, Robison says. Yet neither the old *Alvin* nor the rebuilt sub can adjust its buoyancy enough to linger above the sea floor without draining its batteries. So nearly all trips go straight to the bottom.

Along with concerns over *Alvin*'s limitations, US researchers also lament the loss of several scientific submersibles. Funding woes forced Florida International University's Harbor Branch Oceanographic Institute in Fort Pierce to retire its two submersibles, the Johnson Sea Links, last year. And the National Oceanic and Atmospheric Administration plans to stop funding the National Undersea Research Program, which supports two *Pisces* submersibles located in Hawaii. The two HOVs are known for their work exploring seamounts in the Pacific Ocean, including the newest Hawaiian volcano. Robison bemoans the loss of

VOYAGER TO THE BOTTOM OF THE SEA

A US$40-million upgrade to *Alvin* will lead to noticeable improvements for researchers, but the submersible will have the same depth limit, 4,500 metres, as the previous one. Only five nations — and entrepreneur James Cameron — have research submersibles that can go deeper than 4,000 metres.

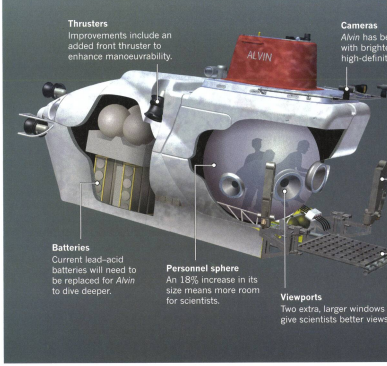
ALVIN
Thrusters
Improvements include an added front thruster to enhance manoeuvrability.
Cameras
Alvin has been outfitted with brighter lights and high-definition cameras.
Manipulator arms
Improvements nearly double the reachable area.
Work basket
The space for transporting equipment and samples has been increased 45%.
Batteries
Current lead-acid batteries will need to be replaced for *Alvin* to dive deeper.
Personnel sphere
An 18% increase in its size means more room for scientists.
Viewports
Two extra, larger windows give scientists better views.

ALVIN ILLUSTRATION BY MEGAN CARROLL. © WOODS HOLE OCEANOGRAPHIC INSTITUTION

all the other US scientific submersibles. "As good as *Alvin* is," he says "that isn't enough."

Veteran explorer Robert Ballard is not shedding any tears over the HOVs. "I consider that a dead paradigm," says the marine geologist who discovered the *Titanic* and co-led the cruise that discovered the first hydrothermal vents; he used *Alvin* to explore them both. He now relies on autonomous underwater vehicles (AUVs) and remotely operated vehicles (ROVs), which can be controlled by researchers on a ship or from halfway across the world. "AUVs augmented with ROVs is where I see the future. I don't need any people in them."

Alvin is limited to 4–5 hours of work at depth, whereas ROVs can spend days on the bottom and some AUVs can explore for months. And unmanned vehicles don't require such large support ships and crews as HOVs, which can trim the cost of a mission substantially. Thanks to their data links, ROVs also enable essentially unlimited numbers of researchers around the world to take part in missions.

The ROV Jason 2 has become a favourite tool of US marine geologists, who love its flexibility in exploring and collecting samples down to 6,500 metres. But its heavy steel cable, which supplies power and transmits data, prevents the ROV from diving deeper and complicates missions.

Just up the hill from where *Alvin* is taking shape at Woods Hole, researchers are working on an experimental vehicle that will sever that troublesome umbilical cord while retaining the advantages of an ROV. Canary yellow and the size of a delivery van, Nereus made headlines in 2009 by reaching the bottom of Challenger Deep in the South Pacific — at 11,000 metres, the lowest spot on Earth. Nereus can operate either autonomously or connected to a surface ship through a fibre-optic cable.

But the tether, just three times the thickness of a human hair, breaks easily. So the Woods Hole team is now working to cut the physical link with the surface. This month, off Guam, the crew will test a laser system on Nereus that sends the data to a receiver hanging down from a ship. Researchers will control Nereus using acoustic signals from the ship.

➲ NATURE.COM
For an interview with filmmaker James Cameron visit:
go.nature.com/uvjdyw

Despite the advantages of ROVs, most scientists say that there is no substitute for exploring the depths in person. "There is still a place for having a human brain and eyes at the bottom of the ocean," says Humphris. To those who say there is no need for HOVs, she says "It's a little bit like saying, 'Why would you go to the Grand Canyon rather than watching a movie about it?'."

Alvin is also one of the best recruiting tools in marine science. "It's what has brought the very best minds to the deep-sea oceanographic community," says Lutz. "You're able to tell them, 'You come work with us and we're going to take you a mile and a half down to the bottom of the sea in a submersible,' as opposed to saying, 'We're going to take you out on a ship and you're going to watch it on a television screen.'"

Private money could help to preserve some opportunities for deep-sea science. Eric Schmidt, former chief executive of Google, purchased an 83-metre-long ship in 2010 that he retrofitted for oceanographic science. His Schmidt Ocean Institute will start research cruises with the vessel next year and will test existing ROVs with the aim of purchasing one in a couple of years and making it available for researchers.

And Cameron's dive aboard his one-person *Deepsea Challenger* fired up the imagination of researchers such as Lutz. "You look at it as a scientist and say, 'Shit! I'd go down in that thing.'"

Cameron says that his sub is available for anyone willing to put up the money for further expeditions. "I'm more than happy to put in the sub and the technology. It's not doing any good sitting in my barn," he says.

In the meantime, the hopes of the US oceanographic community ride on *Alvin*, which currently rests in pieces at Woods Hole. Looking up at the gleaming passenger sphere, Strickrott takes a moment to picture the day his crew has completed all its work and *Alvin* is ready to dive once again. "When it gets rolled out here, it's spotless," he says. "It's a beautiful thing." ■

Richard Monastersky *is a features editor for* Nature.

Principles of **Biology**

by nature **EDUCATION**

Bringing biology to life

To learn more about *Principles of Biology*, the first interactive textbook from Nature Education, visit **www.nature.com/principles**

nature publishing group npg

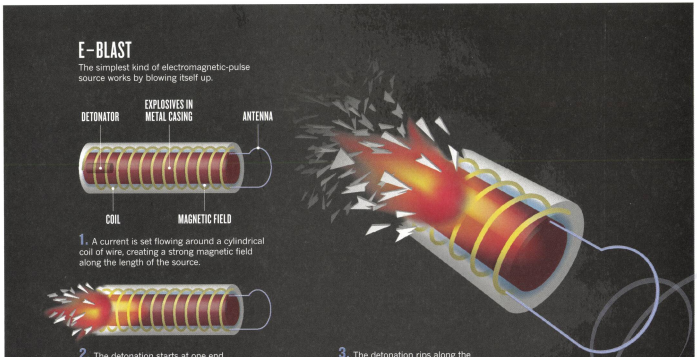
E–BLAST
The simplest kind of electromagnetic-pulse source works by blowing itself up.
DETONATOR
EXPLOSIVES IN METAL CASING
ANTENNA
COIL
MAGNETIC FIELD
1. A current is set flowing around a cylindrical coil of wire, creating a strong magnetic field along the length of the source.
2. The detonation starts at one end, compressing the field as it forces the metal casing against the coil and short-circuits it.
3. The detonation rips along the midline, squeezing the compressed field out as an electromagnetic pulse.
ELECTROMAGNETIC PULSE

WASTED ENERGY

DESPITE 50 YEARS OF RESEARCH ON HIGH-POWER MICROWAVES, THE US MILITARY HAS YET TO PRODUCE A USABLE WEAPON.

BY SHARON WEINBERGER

For some Pentagon officials, the demonstration in October 2007 must have seemed like a dream come true — an opportunity to blast reporters with a beam of energy that causes searing pain.

The event in Quantico, Virginia, was to be a rare public showing for the US Air Force's Active Denial System: a prototype non-lethal crowd-control weapon that emits a beam of microwaves at 95 gigahertz. Radiation at that frequency penetrates less than half a millimetre into the skin, so the beam was supposed to deliver an intense burning sensation to anyone in its path, forcing them to move away, but without, in theory, causing permanent damage.

However, the day of the test was cold and rainy. The water droplets in the air did what moisture always does: they absorbed the microwaves. And when some of the reporters volunteered to expose themselves to the attenuated beam, they found that on such a raw day, the warmth was very pleasant.

A demonstration of the system on a sunny day this March proved more successful. But that hasn't changed a fundamental reality for the Pentagon's only acknowledged, fully developed high-power microwave (HPM) weapon: no one seems to want it. Although the Active Denial System works (mostly) as advertised, its massive size, energy consumption and technical complexity make it effectively unusable on the battlefield.

The story is much the same in other areas of HPM weapons development, which began as an East–West technology race nearly 50 years ago. In the United States, where spending on electromagnetic weapons is down from cold-war levels, but remains at some US$47 million per year, progress is elusive. "There's lots of smoke and mirrors," says Peter Zimmerman, an emeritus nuclear physicist at King's College London and former chief scientist of the US Arms Control and Disarmament Agency in Washington DC. Although future research may yield scientific progress, he adds, "I cannot see they will build a useful, deployable weapon".

For many critics, the US HPM programme has become a study in wishful thinking, exacerbated by a culture of secrecy that makes real progress even more difficult.

The quest to build an electromagnetic weapon — an e-bomb, in military jargon — was sparked on 8 July 1962, when the United States carried out Starfish Prime, the largest high-altitude nuclear test that had ever been attempted. The 1.4-megaton thermonuclear warhead, detonated 400 kilometres above the central Pacific Ocean at 9 seconds past 11 p.m., Hawaii time, blasted huge swarms of charged particles outwards along Earth's magnetic field. Their gyrations generated a pulse of microwave energy that drove measuring instruments off the scale. Artificial auroras lit up the night across swathes of ocean. And in Honolulu, more than 1,300 kilometres from the detonation point, the pulse set off burglar alarms, knocked out street lights and tripped power-line circuit breakers.

Nothing like Starfish Prime has been seen since August 1963, when the Partial Test Ban Treaty outlawed nuclear explosions anywhere but underground. But the test showcased the potential destructiveness of an electromagnetic pulse to military planners on both sides of the cold-war divide, and launched them into a race to harness it as a weapon using a non-nuclear source.

POWER CUT

The US Air Force has been the main funder of the country's HPM programme from the beginning. At first, its goal was a weapon capable of taking out an enemy's computers, communication systems and other electronics. In theory, the idea remains compelling: an e-bomb would be able to fire microwave 'bullets' at the speed of light and, if tuned to the right frequencies, disable its targets without collateral damage. Cars could be stopped in their tracks, radars blinded and computers destroyed, with no need for high explosives.

But that goal has foundered on the HPM weapon's main technical challenge: generating a pulse that is directed enough to pick out a specific target and powerful enough to have an effect when it gets there, ideally using a generator that is small and light enough for an aeroplane or missile to lift.

A battery-powered device can generate an HPM pulse, but producing the kind of highly concentrated power needed to destroy electronics typically requires detonating a conventional explosive inside a device that destroys itself in the act of pulsing (see 'E-blast'). Because doing this inside a piloted aircraft is risky — "a few pounds in the right place will take down anything", notes Zimmerman — the Air Force has in recent years pursued HPM weapons designed for single-use missiles.

For example, the Counter-electronics High-power Microwave Advanced Missile Project (CHAMP) is an experimental cruise missile designed to take out electronic targets such as production sites for weapons of mass destruction. Neither the Air Force nor Boeing, its main contractor for CHAMP, will discuss technical details of the programme. But the project is just

> "I'D RATHER TERRORISTS SPENT ALL THEIR TIME WORKING ON AN HPM WEAPON THAN CAR BOMBS."

a prototype; when CHAMP was flight-tested last year, it still didn't include the HPM payload.

It is possible to make a microwave generator compact enough for a missile. Engineers at Texas Tech University in Lubbock have developed an experimental explosive-based source less than 2 metres long and 16 centimetres in diameter (M. A. Elsayed *et al. Rev. Sci. Instrum.* **83**, 024705; 2012). But lead developer Andreas Neuber points out that there are physical limits: to maximize the microwave power while keeping the system small, the engineers had to increase the internal electrical field. The result can be a catastrophic failure of the system's insulating materials that short-circuits it before the system can build up much power.

Even if the military succeeds in packaging an HPM system, there is serious doubt over how effective the pulses will be when they hit their targets. In the late 1980s, a device called Gypsy successfully took out a bank of personal computers during the Air Force's first unclassified test of a microwave weapon. But building on that success "became an incredibly difficult research project", says Doug Beason, a physicist who was associate director for threat reduction at the Los Alamos National Laboratory in New Mexico until 2008, and wrote *The E-Bomb* (Da Capo, 2005), a discussion of directed-energy weapons. "You could understand how microwaves affected components of electronic circuits — transistors, capacitors, inductors and all that. But when you started putting them together in complex circuits, it became more of a stochastic process and you wouldn't always get the same results each time."

There is similar uncertainty over how electromagnetic energy flows through enclosures such as buildings. The process is chaotic, says Edl Schamiloglu, an electrical engineer at the University of New Mexico in Albuquerque who is involved in a multi-university research initiative funded by the US defence department to improve such predictions. "When an electromagnetic ray or wave-beam enters the enclosure," he says, "it will continue bouncing around and not repeat its trajectory."

In short, more than 20 years after the Gypsy test, scientists still can't reliably predict the damage a weapon would do. And that is without even considering the countermeasures that an adversary might use, which could be as elementary as surrounding sensitive electronics with a Faraday cage — the equivalent of the aluminium mesh used to shield microwave ovens.

The effort to disable electronics has remained mostly secret. But in 2001, the Air Force publicly announced that it had made substantial progress in developing microwave weapons that target people, when it unveiled the Active Denial System.

Development of the system began in the 1990s with the Air Force's efforts to explore the biological effects of microwaves. A project code-named Hello studied how to modulate the clicking or buzzing sounds produced by microwave heating in the inner ear, to produce psychologically devastating 'voices in the head'. 'Goodbye' explored the use of microwaves for crowd control. And 'Good Night' looked at whether they could be used to kill people.

HELLO GOODBYE

Only the Goodbye effect went into development as a weapon. Further bioeffects research was conducted in secrecy at Brooks Air Force Base near San Antonio in Texas, but even that programme almost stalled when the weapon was ready to move from animal to human testing. Hans Mark, a nuclear engineer at the University of Texas at Austin who was then the Pentagon's director of defence research and engineering, paid a visit to Brooks in the 2000 to check out the work. "Dr Mark didn't believe in the effect," recalls Beason, "and he actually had a shouting match with one of the main researchers." But Mark's approval was needed to advance the project, so he agreed to be subjected to the beam.

The Air Force got its human tests. The Brooks scientists joke that "you've never seen a political appointee run so fast", says Beason.

Mark says that his doubts about the Goodbye effect were rooted in what he calls the "extravagant claims" made by its advocates. If nothing else, he says, the superconducting electromagnet that powered the system's pulse generator required a cooling system too big and cumbersome to be used in the

LOS ALAMOS NATL LAB ARCHIVES

The 1962 Starfish Prime nuclear test set off an electromagnetic pulse that sparked a weapons programme.

field. Mark says that he allowed the system to proceed to human testing not because he was convinced that it would work, but because after exposing himself to the beam, he decided that human testing at least wouldn't harm anyone. "Almost all of this programme has been a waste of money," he says.

Mark's concerns have proved prescient: efforts to deploy the weapon have been futile. At the 2001 unveiling, the defence department touted the Active Denial System for use in peacekeeping missions in places such as Kosovo and Somalia. But after the invasion of Iraq in 2003, when the US Joint Non-Lethal Weapons Directorate offered to deploy the Active Denial System to the region, it was rebuffed.

"We knew it wasn't reliable," said Franz Gayl, the Marine Corps's science and technology adviser, in an interview last year. Worse, he said, the pulse generator was so big that it had to be carried on its own utility vehicle. "That was a recipe for disaster," said Gayl, "because the operators are going to be a target." And worst of all, he said, before use the system had to be cooled down to 4 kelvin — a process that took 16 hours.

The defence department tried to deploy the weapon in Afghanistan in 2010, but it was sent home unused. In the same year, California rejected a smaller version meant for use in prisons. The device was built by defence contractor Raytheon of Waltham, Massachusetts, which declines to discuss it.

Other weapons have fared little better. The Air Force Research Laboratory developed an HPM system called MAXPOWER to detonate roadside bombs remotely, but it was the size of an articulated lorry — too unwieldy to be deployed in Afghanistan. The Joint Improvised Explosive Device Defeat Organization, the defence department's bomb-fighting agency, declined to discuss the system, citing classification issues. But it did say that, as of 2011, it was not funding MAXPOWER.

In July, General Norton Schwartz, the Air Force chief who retired last month, warned that the service would have to withdraw from some science efforts amid budget cuts, but that HPM technology would still be pursued. It "clearly has potential", he told the trade magazine *Aviation Week & Space Technology*, warning that countries such as Russia could be ahead of the United States.

THE MICROWAVE GAP

The concern that other nations, or even terrorists, could be working on similar technology seems to have been one of the prime motivations for the US military to continue investing in microwave weaponry, despite the apparent lack of progress. According to a 2009 briefing on non-lethal technologies prepared by the Office of Naval Research and obtained under the Freedom of Information Act, Russia, China and even Iran are pursuing HPM programmes — and the UK Defence Science and Technology Laboratory at Fort Halstead is sponsoring a classified car-stopping programme.

But such programmes are not necessarily proof that the cold-war HPM arms race is still going on. At least some countries may — like the United States — be conducting research out of fear of becoming vulnerable to such weapons. Modern technologies such as mobile phones are particularly susceptible to HPMs, says Michael Suhrke, head of the electromagnetic effects and threats business unit at the Fraunhofer Institute for Technological Trend Analysis in Euskirchen, Germany.

➲ NATURE.COM
For more about electromagnetic military research:
go.nature.com/xloydm

As for HPM weapons in the hands of terrorists, many scientists regard that threat as far-fetched at best. Even if terrorist groups had the sophistication to carry out the necessary testing, says Yousaf Butt, a physicist in the high-energy astrophysics division at the Harvard-Smithsonian Center for Astrophysics in Cambridge, Massachusetts, why would they? A microwave weapon of any magnitude would probably have to be powered by explosives. And if they had that kind of material, he says, "why wouldn't they just explode it?"

"Is it conceivable?" asks Philip Coyle, who in 2010–11 served as associate director for national security and international affairs in the White House Office of Science and Technology Policy, and is now a senior fellow at the Center for Arms Control and Non-Proliferation, a think tank based in Washington DC. "Barely, I think. I wouldn't take it for granted that terrorists couldn't do it. But I'd rather terrorists spent all their time working on [an HPM weapon] than car bombs."

Experts still disagree on whether HPMs might eventually make useful weapons. But one thing is clear: the mythical e-bomb capable of stopping cars or planes has not yet materialized on the battlefield. Asked whether the Air Force had produced any operational weapons, its research lab said only: "Due to operational concerns, we are unable to respond to this question."

The secrecy that surrounds HPM weapons research seems to have greatly exacerbated technical obstacles to the programme. In 2007, for example, a report on directed-energy weapons by the Defense Science Board said that the Pentagon had not effectively used data collected by university researchers to understand microwave effects. The Air Force claims that sharing is better now. But working in a field shrouded in secrecy still affects how information is disseminated. Neuber, for example, could agree to answer questions for this article only if he replied in writing, and only after his responses had been cleared through the US Army office that sponsors his team's work.

"Working in an area that is to a large extent of military interest requires playing by a set of different rules to some extent," he wrote. "Some flow of information is not as free as in other areas of the research endeavour."

To John Alexander, a retired army colonel who once headed the non-lethal weapons programme at Los Alamos National Laboratory, the secrecy reinforces the air of fantasy around the whole endeavour. "My point is always: chemistry and physics work the same way for everyone, and there are smart folks out there, so who are you trying to fool?" he says. "The people not getting adequate information were our own commanders." ■ SEE EDITORIAL P.177

Sharon Weinberger *is a freelance writer in Washington DC.*

COMMENT

FUNDING In defence of more scrutiny for elite grant-holders at the NIH **p.203**

NOVELS Celebrating the acerbic 'radium age' of science fiction **p.204**

CLIMATE Glacier photographer captures vanishing frozen landscapes **p.206**

ART Information designer Edward Tufte sculpts Feynman equations **p.207**

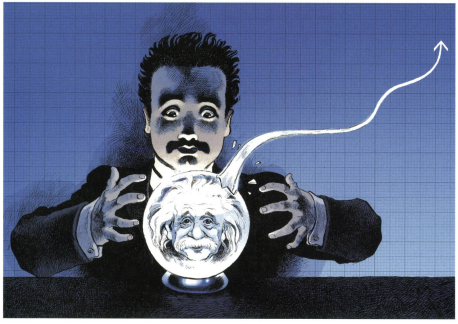

ILLUSTRATION BY DAVID PARKINS

Predicting scientific success

Daniel E. Acuna, Stefano Allesina and **Konrad P. Kording** present a formula to estimate the future *h*-index of life scientists.

We research scientists often worry about the future of our careers. Is our research an exciting path or a dead end that will end our careers prematurely? Predicting scientific trajectories is a daily task for hiring committees, funding agencies and department heads who probe CVs searching for signs of scientific potential.

One popular measure of success is physicist Jorge Hirsch's *h*-index[1], which captures the quality (citations) and quantity (number) of papers, thus representing scientific achievements better than either factor alone. A scientist has an *h*-index of *n* if he or she has published *n* articles receiving at least *n* citations each[2]. Einstein, Darwin and Feynman, for example, have impressive *h*-indices of 96, 63 and 53, respectively. According to Hirsch, an *h*-index of 12 for a physicist — meaning 12 papers with at least 12 citations each — could qualify him or her for tenure at a major university.

However, the *h*-index[3] and similar metrics[4] can capture only past accomplishments, not future achievements[5]. Here we attempt to predict the future *h*-index of scientists on the basis of features found in most CVs.

We maintain that the best way of predicting a scientist's future success is for peers to evaluate scientific contributions and research depth, but think that our methods could be valuable complementary tools.

The typical research CV contains information on the number of publications, those in high-profile journals, the *h*-index and collaborators. One can also infer interdisciplinary breadth, the length and quality of training, the amount of funding received and even the standing of the scientist's PhD adviser. Such factors are taken into account for hiring decisions, but how should they be weighted? Fortunately, obtaining data on the scientific activities of individual researchers has never been easier. Using all of these features, we can begin to probe the scientific enterprise statistically.

VITAL STATISTICS

To construct a formula to predict future *h*-index, we assembled a large data set and analysed it using machine-learning techniques. Our initial sample from academic-tree.org — a crowd-sourced website listing scientists' mentors, trainees and collaborators — contains the names and institutions of about 34,800 neuroscientists, 2,000 scientists studying the fruitfly *Drosophila* and 1,300 evolutionary researchers. We matched these authors to records in Scopus, an online database of academic papers and citation data. We restricted our analysis to authors who had accrued an *h*-index greater than 4 (to exclude inactive scientists); to publications after 1995 (because electronic records are sparse before then); to authors who had published their first manuscript in the past 5–12 years; and to authors who were identifiable in Scopus.

That left us with 3,085 neuroscientists, 57 *Drosophila* researchers and 151 evolutionary scientists for whom we constructed a history of publication, citation and funding.

For each year since the first article published by a given scientist, we used the features that were available at the time to forecast their *h*-index a number of years into the future. For example, we reconstructed how the CV features of a scientist looked five years after publishing his or her first article, and found a relationship between those features and the reconstructed *h*-index five years on.

Starting with neuroscientists, we attempted to predict the *h*-index of each scientist 5 years ahead — a timescale relevant for tenure decisions — using a linear regression with elastic net regularization[6] (see Supplementary Information at go.nature.com/mtvuzr). The ▶

➲ NATURE.COM
For more on science metrics, see:
go.nature.com/nj2xqk

METRICS

Predict your future h-index

These are approximate equations for predicting the *h*-index of neuroscientists in the future. They are probably reasonably precise for life scientists, but likely to be less meaningful for the other sciences. Try it for yourself online at go.nature.com/z4rroc.

- **Predicting next year** ($R^2 = 0.92$):
$$h_{+1} = 0.76 + 0.37\sqrt{n} + 0.97h - 0.07y + 0.02j + 0.03q$$
- **Predicting 5 years into the future** ($R^2 = 0.67$):
$$h_{+5} = 4 + 1.58\sqrt{n} + 0.86h - 0.35y + 0.06j + 0.2q$$
- **Predicting 10 years into the future** ($R^2 = 0.48$):
$$h_{+10} = 8.73 + 1.33\sqrt{n} + 0.48h - 0.41y + 0.52j + 0.82q$$

Key: *n*, number of articles written; *h*, current *h*-index; *y*, years since publishing first article; *j*, number of distinct journals published in; *q*, number of articles in *Nature*, *Science*, *Nature Neuroscience*, *Proceedings of the National Academy of Sciences* and *Neuron*.

PATHS TO SUCCESS

The accuracy of future *h*-index prediction decreases over time, but the Acuna *et al.* formula predicts future *h*-index better than does current *h*-index alone (left). The contribution of each factor to the formula accuracy also changes over time (right). Shading indicates 95% confidence error bars.

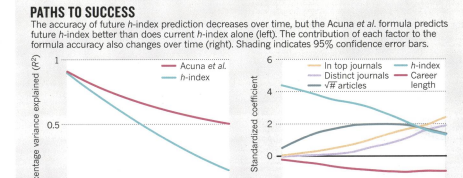

model predicted the future *h*-index accurately, yielding a respectable $R^2 = 0.67$, cross-validated across scientists (an R^2 of 1 would imply that the model predicts the data perfectly). A simplified model containing only the number of published articles, the *h*-index, years since first publication, number of publications in prestigious neuroscience journals (*Nature*, *Science*, *Nature Neuroscience*, *Neuron* and the *Proceedings of the National Academy of Sciences*) and the number of distinct journals still performed nearly equally well ($R^2 = 0.66$; see 'Predict your future *h*-index').

Predicting the future careers of *Drosophila* and evolutionary scientists leads to somewhat worse predictions ($R^2 = 0.54$ and $R^2 = 0.61$, respectively, based on scientists 3–15 years into their careers) but still better than predictions based on the *h*-index alone ($R^2 = 0.38$ and $R^2 = 0.39$, respectively). This indicates that generalizations to other fields within and outside of life science may be limited[1]. But for neuroscientists, at least, the predictions extend well to longer periods of time, such as ten years into the future ($R^2 = 0.52$). Over time, using just the *h*-index performs much worse than taking all features into account (see 'Paths to success', left panel).

The main five predictive features change in importance for predicting *h*-indices over increasingly longer periods (see 'Paths to success', right panel). The power of the *h*-index declines. The number of articles written, the diversity of publication in distinct journals and the number of articles published in five prestigious journals all become increasingly influential over time.

FUTURE FORTUNES

It is risky to make any causal interpretations of these results. However, we will briefly speculate on why these features might be important predictors of future success. Some features directly affect the potential for a high *h*-index, such as the number of articles written. These features can also indirectly affect a scientist's future success, because scientists who are productive and publish many papers tend to remain productive. Publishing in many different journals may lead to fewer overlapping populations of scientists who cite the work, and hence higher growth potential for articles. A scientist who has published in several distinct journals is also likely to be someone with broad training who contributes in many ways. The number of publications in leading journals can increase the visibility of a scientist's other papers, past and future.

If promotion, hiring or funding were largely based on indices (*h*-index, the model used here or any other measure), then some scientists would adapt their behaviour to maximize their chances of success. Models such as ours that take into account several dimensions of scientific careers should be more difficult for researchers to game than those that focus on a single measure.

Our formula is particularly useful for funding agencies, peer reviewers and hiring committees who have to deal with vast numbers of applications and can give each only a cursory examination. Statistical techniques have the advantage of returning results instantaneously and in an unbiased way. Building and analysing massive data sets to track scientific careers could also help to identify potential gender, racial and other biases[7–9] and advance our understanding of how science develops.

Although our findings and predictions may not alleviate scientists' angst over their careers, the results offer some comfort by showing that the future is not so random. The occasional rejection of a paper may feel unjust and indiscriminate, but in the long run, such factors seem to average out, rendering *h*-index trajectories relatively predictable. ■

Daniel E. Acuna *is a research associate at the Rehabilitation Institute of Chicago, Illinois 60611, USA, and a research affiliate in biomedical engineering at Northwestern University, Evanston, Illinois 60208, USA.*
Stefano Allesina *is assistant professor in ecology and evolution and at the Computation Institute at the University of Chicago, Illinois 60637, USA.*
Konrad P. Kording *is associate professor of physical medicine and rehabilitation, physiology, and applied mathematics at Northwestern University, and at the Rehabilitation Institute of Chicago.*
e-mail: daniel.acuna@northwestern.edu

1. Hirsch, J. E. *Proc. Natl Acad. Sci. USA* **102,** 16569–16572 (2005).
2. Redner, S. *J. Stat. Mech. Theory Exp.* **3,** L03005 (2010).
3. Peterson, I. *ScienceNews* 2 December 2005; available at http://go.nature.com/iawd5o.
4. Alonso, S., Cabrerizo, F. J., Herrera-Viedma, E. & Herrera, F. *J. Informetr.* **3,** 273–289 (2009).
5. Hirsch, J. E. *Proc. Natl Acad. Sci. USA* **104,** 19193–19198 (2007).
6. Zou, H. & Hastie, T. *J. Roy. Stat. Soc. B* **67,** 301–320 (2005).
7. Dwan, K. *et al. PLoS ONE* **3,** e3081 (2008).
8. Ginther, D. K. *et al. Science* **333,** 1015–1019 (2011).
9. Allesina, S. *PLoS ONE* **6,** e21160 (2011).

Well-funded investigators should receive extra scrutiny

An added layer of review for elite grant-holders upholds the mission of the National Institutes of Health, says **Jeremy M. Berg**.

The US National Institutes of Health (NIH) receives many more grant applications proposing outstanding scientific projects than its budget can support. The overall success rate for grants in fiscal year 2011 was 18% — a historic low.

Last month, the agency announced a policy that will apply to the next round of R01 grants. Applications from investigators who receive more than US$1 million a year in funding from the NIH (not including 'indirect costs' that go to the investigator's university) will be subjected to extra review. The agency's advisory councils will examine how distinct the proposed project is from the investigator's other funded work. If it is a grant renewal, they will consider whether the project has been productive, and look at its value to the investigator's research programme and collaborations. This analysis will be provided to NIH programme staff, who will make funding recommendations.

The policy has been criticized for adding to the NIH's administrative burden, and for potentially penalizing the most productive scientists. However, I believe that it will complement peer review and help to determine the best possible portfolio of NIH-funded research, short and long term.

The National Institute of General Medical Sciences (NIGMS) in Bethesda, Maryland — where I was director between 2003 and 2011 — has, for around two decades, given extra scrutiny to applications from investigators receiving more than $750,000 per year in costs from all funding sources, including the pending NIGMS application. This policy is not a cap; rather, it is a useful tool for managing taxpayer resources to achieve the goals of the NIGMS and the NIH. The scrutiny has influenced the distribution of resources, either by denying or reducing funding for well-off applicants, or providing grants on the condition that others will not be renewed. This frees up money for other investigators and allows those who are well-funded to change the course of their research. Assuming that the NIH policy can be implemented effectively, it is a step in the right direction.

Critics of the NIH policy argue that although peer review is not perfect, it is the best system for evaluating scientific projects. Many reviewers try to ensure that a new project does not overlap significantly with one that is already funded. But they do not have full access to NIH portfolio data, nor the time to analyse the information.

Peer review has several limitations. To compare and rank grant applications across hundreds of NIH sections, administrators assign each peer-review score a percentile value. The first percentile (the top 1%) corresponds to the most highly rated applications. These percentile values have uncertainties that stem from the potential biases of primary reviewers, the characteristics of the process used to calculate percentiles, and the fact that an application is judged by whether it will be an important future scientific advance — which is inherently difficult to predict.

SCORE DRAW

Higher grant scores do not imply more papers. Renewal grants show no significant differences up to the 13th percentile; new grants showed no significant correlation over the entire range.

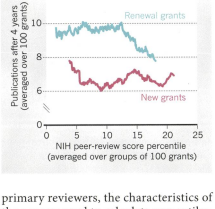

SOURCE: J. M. BERG/NIGMS

BANG FOR BUCK

During my time as director of the NIGMS, I analysed the power of peer-review scores to predict scientific productivity. This was judged by various measures, including numbers of publications, citations and highly cited publications four years after the grants were funded. The distribution of percentile scores for applications did correlate with future differences in productivity to some extent. But applications that were separated by five or even ten percentile points did not differ significantly in subsequent productivity (see 'Score draw'). Therefore, funding grants in strict percentile order does not necessarily mean that ensuing investigations will be of higher quality. So percentile score should not be the only factor taken into consideration when making funding decisions.

There are good reasons to consider how much other funding an investigator is receiving. Projects in one lab almost always overlap, even if they are addressing different questions, so some of the running costs will already be covered. Giving another grant to the same investigator might have less impact than giving it to someone with nearly the same percentile score who has little or no other funding. In another NIGMS analysis, I showed that research productivity (measured by numbers of publications or citations and averaged over groups of investigators with similar levels of support) did not increase consistently as the level of support increased, but reached a plateau near $700,000 in annual direct costs per investigator.

Some investigators are better than others at managing large amounts of resources. If an investigator is not performing as expected given the level of support, using the funds to support another researcher might be a better investment. The NIH needs to invest in a broad range of research; if scientists are well funded, their area could already be receiving enough support from other sources.

The layer of extra scrutiny is not ideal. I would prefer the limit to be less than $1 million and to include funding outside the NIH. Exceptions to the policy also mean that it might be easy to dodge. For example, grants with multiple principal investigators are scrutinized only if all receive more than $1 million in NIH funding, so I am concerned that some applicants may avoid extra review by adding a co-investigator who receives less.

I believe that special consideration should be given to investigators with strong proposals who have few or no other sources of funding, such as those at the beginning of their careers or established, productive investigators. Funding these applicants would probably have a bigger impact — by helping to develop a new lab or keeping an effective one functioning — rather than providing incremental support to an investigator who already has substantial other support. ■

Jeremy M. Berg *is associate senior vice-chancellor for science strategy and planning (health sciences) at the University of Pittsburgh, Pennsylvania 15260, USA. e-mail: jberg@pitt.edu*

LWCURREY.COM/IWKBOOKS.COM

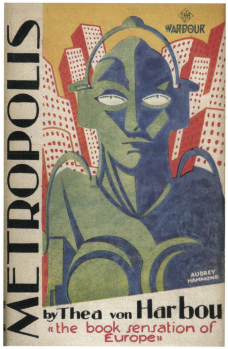

Speculative fiction from 1904 to 1933 is often overshadowed by later 'golden age' work.

SCIENCE FICTION

The radium age

Joshua Glenn explores the dark, fascinating, largely forgotten science fiction of the early twentieth century.

We think we know science fiction. There were the 'scientific romance' years that stretched from around the mid-1860s to 1903, after which H. G. Wells lost his touch. And there was the 'golden age', from 1934 to the mid-1960s. But between those periods — and overshadowed by them — was a fascinating era that gave us such enduring memes as the berserk robot, the tyrannical superman and the sinister telepath.

I call that period, from 1904 to 1933, sci-fi's 'radium age'. It emerged when the speed of change in science and technology was inducing vertigo on both sides of the Atlantic. More cynical than its Victorian precursor yet less hard-boiled than the generation that followed, this is sci-fi offering a dizzying, visionary blend of acerbic social commentary and shock tactics. It yields telling insights into its context, the early twentieth century. Plus, it is fun to read.

The scientific romances that preceded this era were strong on the fantastical but otherwise very different. The utopian fantasies of Edward Bulwer-Lytton (*The Coming Race*, 1871), for instance, and the fantastic voyages by writers such as Jules Verne (*Journey to the Centre of the Earth*, 1864) and Edgar Allan Poe (*The Unparalleled Adventure of One Hans Pfaall*, 1835) were largely sentimental literature. They were by and for people who were inspired by US inventor Thomas Edison and believed that modern science and technology would improve the human condition and usher in the triumph of millennia-old Christian values.

Radium-age writers were not out to beguile. They depict a human condition subverted or perverted by science and technology, not improved or redeemed. Aldous Huxley's 1932 *Brave New World*, with its devastating satire on corporate tyranny, behavioural conditioning and the advancement of biotechnology, is far from unique. Radium-age sci-fi tends towards the prophetic and uncanny, reflecting an era that saw the rise of nuclear physics and the revelation that the familiar — matter itself — is strange, even alien. The 1896 discovery of radioactivity, which led to the early twentieth-century insight that the atom is, at least in part, a state of energy, constantly in movement, is the perfect metaphor for an era in which life itself seemed out of control.

As demonstrated by Philipp Blom in *The Vertigo Years: Europe 1900–1914* (Basic Books, 2008), the actual experience of time and space was altered in this period by the proliferation of a range of stunning technological developments, from the telegraph and the telephone to aeroplanes and cinematic film. Thinking and perception were radically reoriented by developments in science, philosophy and the arts. These included Einstein's special theory of relativity; the work of phenomenological philosophers such as Edmund Husserl, who sought to objectively describe the subjective workings of consciousness; and Cubism, the artistic movement spearheaded by Pablo Picasso and Georges Braque that explored distortion and deconstruction. Social and cultural forms and norms, such as women's subordination to men — once regarded as natural, permanent 'elements' — were disintegrating.

During this astonishing period, sci-fi writers were obsessed with the future. The scientific romantics had conjured up simplistic utopias that remained firmly grounded in contemporary realities. By contrast, the radium-age novels, stories, movies and plays (see 'Key radium-age works') often lift off into previously unexplored realms.

Instead of offering progressive solutions

NATURE.COM
For more on science fiction, see the *Nature* Web Focus:
go.nature.com/mqc2jd

NOVEL VISIONS

Key radium-age works

Karel Čapek *R.U.R.* (1920)
Arthur Conan Doyle *The Lost World* (1912)
Hugo Gernsback *Ralph 124C 41+* (1911–12)
H. Rider Haggard *When the World Shook* (1919)
William Hope Hodgson *The Night Land* (1912)
Aldous Huxley *Brave New World* (1932)
Rudyard Kipling *With the Night Mail* (1905)
Jack London *The Scarlet Plague* (1912)
Charlotte Perkins Gilman *Herland* (1915)
Edward Shanks *The People of the Ruins* (1920)
George Bernard Shaw *Back to Methuselah* (1921)
Olaf Stapledon *Last and First Men* (1930)
Thea von Harbou *Metropolis* (1926)
Philip Wylie *Gladiator* (1930)
Yevgeny Zamyatin *WE* (1921)

to social unrest, writers satirized and exaggerated its causes and effects. The out-of-control robot can be read as a criticism of the efficiency-oriented theories of Frederick Winslow Taylor and the practices of industrialist Henry Ford. So *R.U.R.* (Czechoslovakian writer Karel Čapek's 1920 play, which introduced the term 'robot' to the English language) portrays mass production as alienating at best. In Jack London's post-apocalyptic *The Scarlet Plague* (1912), a race of barbarians descended from San Francisco's brutalized underclass roam the city's devastated remains after the fatal pandemic of 2013. And Charlotte Perkins Gilman's feminist novel *Herland* (1915) imagines an ideal community in which women aren't merely emancipated, but have done away with men altogether.

Politics are inevitably part of the mix — this is an era that encompassed the First World War, the Russian revolutions, and the rise of radical left- and right-wing movements. Many sci-fi authors, such as Čapek and Yevgeny Zamyatin, were leftists and liberals. But more conservative authors shared their utopianism and cynicism. For instance, Arthur Conan Doyle, inventor of Sherlock Holmes, wrote a series of ripping yarns starring a Professor Challenger, who discovers surviving dinosaurs, travels to Earth's "sensory cortex" and witnesses the end of life on the planet — all the while making the case for reconciling imagination and intuition with a sceptical scientific method.

Similarly, H. Rider Haggard, who had made his name with *King Solomon's Mines* (1885) and the Quartermain novels of the 1880s, created a disputatious trio in 1919's *When the World Shook* — an idealistic Anglican minister, a sardonic doctor and an adventurer whose world view hovers somewhere in between. Meanwhile, both the leftist London (in *The Scarlet Plague*) and the conservative English poet Edward Shanks (in *The People of the Ruins*) agree that the destruction of modern western society wouldn't be an entirely bad thing.

Fans of Philip K. Dick or Ursula K. Le Guin — writers belonging to what literary theorist Fredric Jameson has termed the "anti-anti-utopian" trend of the late 1960s and early 1970s — will find provocative antecedents here. Reading the dangerous visions of radium-age sci-fi, published in times as volatile as our own, destabilizes everything we take for granted. These books remind us that we need to regard our twenty-first-century forms and norms without sentimentality. ■

Joshua Glenn *edits the blog HiLobrow, and co-founded HiLoBooks to reissue 'radium age' science fiction. HiLoBooks' edition of Arthur Conan Doyle's* The Poison Belt *is out now; H. Rider Haggard's* When the World Shook *is published in October.*
e-mail: jglenn@hilobrow.com

Books in brief

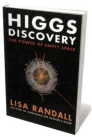

Higgs Discovery: The Power of Empty Space
Lisa Randall BODLEY HEAD *64 pp. £4.99 (2012)*
The Higgs bombshell on 4 July rocked the world of physics. In this slim volume, theoretical physicist Lisa Randall analyses the significance and implications of that momentous finding at Switzerland's Large Hadron Collider. She offers clear accounts of the Higgs mechanism and the role and modes of the Higgs's decay; follows the seven-month lead-up to the discovery; and speculates about what it all might mean for other areas of exploration, such as supersymmetry. A lucid, deft and engaging summation of dogged determination and "heroic engineering".

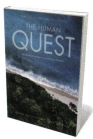

The Human Quest: Prospering Within Planetary Boundaries
Johan Rockström and Mattias Klum STOCKHOLM TEXT *314 pp. $9.99 (2012)*
In 2009, Johan Rockström of the Stockholm Resilience Centre and his colleagues set out in *Nature* nine 'planetary boundaries' — numerical limits for processes that affect Earth's capacity to support human life, such as freshwater use and climate change. This lavishly illustrated e-book — with a foreword by former US president Bill Clinton and video clips from photographer Mattias Klum — extends this idea, laying out pressures and tipping points. Paramount among the changes needed, Rockström says, is a big shift in behaviour.

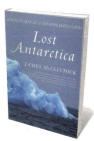

Lost Antarctica: Adventures in a Disappearing Land
James McClintock PALGRAVE MACMILLAN *256 pp. £16.99 (2012)*
The sight of 50,000 king penguins on the Crozet Island Archipelago in the early 1980s sparked marine biologist James McClintock's fascination with Antarctic fauna. Now a veteran of the extreme south, McClintock shares the otherworldly wonders unveiled by decades of research. The book is packed with joys, from soft-coral 'trees' that replant themselves to the snoozing Weddell seal, stinking of putrid fish, that the author encountered in a dive hut. Running like a chill current through all is the climate-driven decimation of the ice on which these ecosystems depend.

Before Galileo: The Birth of Modern Science in Medieval Europe
John Freely OVERLOOK PRESS *352 pp. £18.51 (2012)*
A thousand years before Galileo, the transmission of knowledge that survived the burning of the ancient Library of Alexandria began. Physicist John Freely traces this "tenuous Ariadne's thread" of classical learning that unspooled from Egypt through Byzantium and the Islamic world, finally emerging as Latin texts. Focusing on the trailblazers through this extraordinary millennium — from Bede, Averroës and al-Khwarizmi to Adelard of Bath, Robert Grosseteste and Roger Bacon — Freely ends with a coda on Copernicus, Kepler, Galileo himself and Newton. Shoulders of giants indeed.

The Scientists: An Epic of Discovery
edited by Andrew Robinson THAMES & HUDSON *304 pp. £24.95 (2012)*
The human face of scientific breakthroughs from the sixteenth to the twentieth centuries is spotlit in this sumptuously illustrated volume. Science writer Andrew Robinson, editing contributions from a stellar team of authors, groups 43 greats into six broad areas: Universe, Earth, Molecules and Matter, Inside the Atom, Life, and Body and Mind. From Alan Turing and Marie Curie to William Harvey and Chandrasekhar Venkata Raman, this is a sampler of the driven, complex, fascinating characters who fomented scientific revolutions.

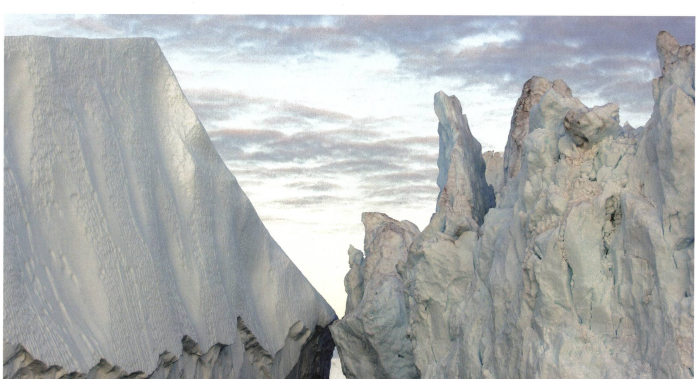

J. BALOG/EXTREME ICE SURVEY

James Balog has developed new photographic equipment to monitor changes in glaciers such as the Ilulissat in Greenland.

Q&A James Balog
Archivist of ice

For six years, photographer James Balog has trained his lens on ice, capturing time-lapse images that have helped scientists to study how glaciers and ice sheets respond to climate conditions. With the documentary Chasing Ice *soon to debut in US cinemas, Balog talks about the loss of landscapes.*

Why are you interested in frozen landscapes?

When I was six years old, I had to walk home from school in a heavy snowstorm. It was a great contest between myself and nature. As a young man, I started ice climbing and mountaineering in the White Mountains in New Hampshire. When I looked at photographs of glaciers in Alaska I knew I wanted to spend time there.

When did you start photographing glaciers in time lapse?

After being blown away by the glacial retreat I saw while shooting a *National Geographic* cover story, 'The big thaw', in 2006. The next year I created the Extreme Ice Survey, deploying time-lapse cameras to monitor retreating ice in the Arctic and mountain areas, some so remote that our team was probably the first to visit them. Temperatures could reach –40 °C and the winds 150 miles per hour. We had to tackle deep snow, torrential rain and falling rocks. Off-the-shelf gear wasn't robust enough, and it took six months of experimenting to come up with a reliable time-lapse system. Right now, we have 27 such cameras at 18 glaciers in Alaska, Greenland, Iceland, the Rocky Mountains and at Mount Everest. Shooting every half-hour of daylight year-round, each one generates 8,500 frames per year. The footage provides scientists with information on the mechanics of glacial melting and gives the public evidence of how rapidly Earth's climate is changing.

Portraits of Vanishing Glaciers
Rizzoli International: 2012. 288 pp. £29.95

Chasing Ice
Jeff Orlowski: 2012

What is the most dramatic moment you've caught?

Every year there are calving events in which ice falls off glaciers into the sea. The rate of ice loss in Greenland has doubled during the past 20 years, and this summer we've seen unprecedented rates of surface melting. We expected the Ilulissat Glacier on the west coast of Greenland to have a massive discharge of ice, so in summer 2008 two of my team members stood watch for weeks. They caught the biggest calving event ever recorded on film. It was as if the entire lower tip of Manhattan had broken off and fallen into the ocean, like an urban skyline toppling, with skyscraper-sized blocks of ice submerging and resurfacing.

What's the aim of the Extreme Ice Survey?

The problem of climate change is perception. Human brains and our economic system favour the status quo. We aim to collect powerful visual evidence so that people can understand what's really happening.

ILLUSTRATION: N. HIGGINS
PHOTO: J. ORLOWSKI/EXTREME ICE SURVEY

When satellites capture retreating glaciers from hundreds of kilometres away, the images may be beautiful but they're removed from human experience. We live on the ground. Retreating glaciers are where you can see climate change as it happens.

What have scientists learned from your images?

In 2006, on the Greenland Ice Sheet, I met glaciologists who said that glaciers are big lumbering things that respond to climate change on a scale of decades or centuries. We have learned that glaciers respond hourly to atmospheric conditions. Our visuals also suggest that subglacial floods may trigger some of the bigger calving events. We have nearly a million pictures in the archive now, although there's a lot of analysis yet to do.

How do you fund the ice survey?

A significant part of our initial funding was from the Expedition Council at *National Geographic*. Nikon gave us hardware. By partnering with scientists, we got help from the US National Science Foundation and NASA. But most of the funding over the past five years has been from private donors. It has been an absurdly difficult project to run without 'big science' government-scale funding and logistical support.

Do you have a science background?

For my master's in geomorphology, I researched Colorado's Big Thompson River flash flood of 1976. But I would not presume to call myself a scientist. When I was finishing my thesis, I remember looking at a stack of manila punchcards and deciding that I'd rather see the world through a camera than through data analysis. The data are incredibly important, but my calling is to understand the world through art.

What next?

The underlying theme of my work is the collision between human needs and nature. I'd like to do more with energy, in part because my grandfather died in a Pennsylvania coalmine collapse. We worked in the Gulf of Mexico after the Deepwater Horizon oil spill and are documenting changes in forest cover in the Rockies. And I am trying to make the ice survey financially stable so that the cameras can keep going for a long time. I feel a tremendous obligation to preserve a pictorial memory of these vanishing landscapes for the people of the future.

INTERVIEW BY JASCHA HOFFMAN

PHYSICS

Modelling Feynman

Daniel Cressey marvels at a gleaming depiction of the subatomic by the world's leading information designer.

Before the explosion in 'infographics' describing everything from cocktail mixology to US health-care spending, there was Edward Tufte.

Tufte, a statistician, is perhaps the world's most celebrated information designer. In *All Possible Photons* at his Manhattan gallery, ET Modern, Tufte has unleashed his love of artistic explanation in a series of sculptures instantly recognizable to anyone with a passing knowledge of particle physics. Minimalist 'graphics' consisting of stainless-steel tubing formed into straight and undulating lines, Tufte's rendering of Feynman diagrams transforms recondite scientific notation into abstract, glinting art. Tufte also plans to show versions more than five metres high at his sculpture park in Woodbury, Connecticut.

US physicist Richard Feynman created elegant traceries of lines, dots and arrows to describe and predict how subatomic particles interact. Feynman was not unaware of his diagrams' aesthetic appeal, and famously drove a van painted with a selection of them.

Tufte's matt or polished steel sculptures, mounted on the walls, are shorn of explanations as well as much of the detail that makes them scientifically useful, such as arrows and labels. Some are large and dominate their wall space. The most powerful artwork on display is the collection of 120 smaller pieces that give the show its name — a cluster representing all possible space and time paths of a particular interaction of photons. These form what Tufte calls "a complete enumeration of everything that could happen" in that instance.

All Possible Photons: The Conceptual and Cognitive Art of Feynman Diagrams
ET Modern, New York.
Until spring 2013; official opening 15 September.

This isn't the first time Tufte has ventured into Feynman territory. The diagrams feature as models of good design in Tufte's book *Beautiful Evidence* (Graphics, 2006). They are also referenced in one of his enormous *Rocket Science* sculptures of fantastical space probes attached to giant bazooka-style launchers. In the *Airstream Interplanetary Explorer* (2011), the probe is an iconic silvery Airstream caravan adorned with Feynman diagrams. Tufte's contention is that because subatomic particles everywhere in the Universe behave as shown by Feynman diagrams, these could work as communiqués to other worlds. As he has put it, "Better the cosmopolitan verbs of Nature's laws on spacecraft than the local proper nouns of national flags, earthly Gods and Goddesses, and government agency logos."

By focusing on the diagrams alone, the sculptures in *All Possible Photons* bring home the power of Feynman's achievement. There is beauty in his diagrams, but the real deal is what they can potentially describe — which is everything. ■

Daniel Cressey *is a reporter for* Nature.

A. SEVERNY

Edward Tufte adjusts his *All Possible 6-Photon Scattering (120 Space-Time Feynman Diagrams)* (2012).

Correspondence

Clarify the limits of climate models

Mark Maslin and Patrick Austin suggest that scientists should explain the statistical uncertainties in models of climate-change impacts (*Nature* **486,** 183–184; 2012), but these models are tools for insight, not prediction. A diversity of models benefits both science and science-based policy guidance.

We believe that future models will be more informative than those of today. The public-image problem of current models stems partly from scientists' failures to identify the limitations openly. It is important to distinguish between questions for which current models are useful as prediction engines and those for which the models merely probe possibilities. The role of science is to reflect on the plausibility and relevance of such possibilities.

Deep uncertainty is not foreign to policy-makers, who often have to weigh the advantages of deciding to wait against the potentially high costs of waiting.

David A. Stainforth, Leonard A. Smith *London School of Economics, UK. d.a.stainforth@lse.ac.uk*

ENCODE leads the way on big data

The ENCODE project offers a fresh perspective on big data by providing an organized framework for genomics (www.nature.com/encode). Other big-data efforts tend to focus on rapidly locating needles in petabyte-sized haystacks (such as finding the Higgs boson, for instance), whereas ENCODE aims to supply a structured overview.

ENCODE's organization of information is hierarchical, with raw data at the bottom and layers of annotation above. The processed summaries become progressively broader — for example, starting at the level of signals representing the degree to which DNA is bound by transcription factors, moving on to the locations of sites where these factors bind, and then to overviews of regulatory networks. At the summit are the linked publications documenting the annotation.

The ENCODE data model could be useful in other fields: for example, astronomy and Earth science are in the process of organizing their reams of data (M. J. Raddick and A. S. Szalay *Science* **329,** 1028–1029; 2010), but don't yet compare with ENCODE in terms of the level of integration.

Mark Gerstein *Yale University, New Haven, Connecticut, USA. mark.gerstein@yale.edu*

Animal variants in sexual behaviour

Andrew Barron and Mark Brown suggest that journalists, by merging animal and human behaviour, promote the myth that minority sexual preferences are an 'illness' (*Nature* **488,** 151–152; 2012). They include one of my articles among their examples — 'Bat bugs turn transsexual to avoid stabbing penises' (see go.nature.com/9iwdpb) — presumably because it uses 'transsexual' to describe insect behaviour. I contend that this term is valid shorthand for what the insects are doing, as well as catching the reader's attention.

Reporting of same-sex behaviour in animals can stray into troubling territory. In one example given by Barron and Brown, *The Sunday Times* wrote in 2006 that a study of male-oriented behaviour in sheep "could pave the way for breeding out homosexuality in humans". However, the problem here is not the terms used to describe animals' sex lives, but the leverage of the research paper to make a political point.

Homosexual behaviour is condemned as unnatural in some places around the world. By describing the huge variation in sexual behaviour across the animal kingdom, the media may be helping to destroy forever the idea that gay, lesbian, bisexual and transgender people represent some kind of aberration.

Rowan Hooper *London, UK. rowan.hooper@newscientist.com*

A code of conduct for European scientists

Progress in safeguarding research integrity is lamentably slow in Europe compared with the United States (*Nature* **488,** 7; 2012). Many European universities are still unsure of their responsibilities in policing research conduct.

Punishing misconduct makes no sense without prevention, given that one study found that up to one-third of all researchers engage in questionable research practices (D. Fanelli *PLoS ONE* **4,** e5738; 2009). What is needed is for each research institution to provide a detailed standard of responsible research conduct, along with mandatory education, so that researchers know how to uphold this standard in day-to-day practice.

We suggest that a European forum should be set up to educate researchers and their mentors in all matters relating to this standard. The forum would develop educational material, train and accredit teachers and remove discrepancies between research institutions.

Every university would need to set up a 'research integrity unit' to guide and supervise its research activities, and to ensure compliance with international standards.

We urge public and private research funders to lend their support to this venture, which would help to free European research from questionable research practices and make life harder for fraudsters.

Nils Axelsen *Statens Serum Institut, Copenhagen, Denmark.* **Xavier Bosch** *Department of Internal Medicine, Hospital Clínic, University of Barcelona, Spain. xavbosch@clinic.ub.es*

Wallace pioneered astrobiology too

The field of astrobiology, called 'exobiology' during the space programmes of the 1960s (*Nature* **488,** 160; 2012), was anticipated six decades earlier by Alfred Russel Wallace, better known as the co-discoverer of the principle of natural selection.

Next year is the centenary of Wallace's death, when his seminal contribution to biogeography and evolution will be celebrated. But he should also be remembered as a pioneer in astrobiology, whose hypotheses are still alive today.

Wallace introduced the concept of "astro-biology" in his popular book *Man's Place in the Universe* (Chapman & Hall, 1903). He reviewed the physical conditions required for organic life in terrestrial ecosystems and concluded that Earth is the only habitable planet in the Solar System.

He later published a monograph (*Is Mars Habitable?* Macmillan, 1907) evaluating astronomer Percival Lowell's suggestion that Mars could be "inhabited by a race of highly intelligent beings" (see *Nature* **74,** 587–589; 1906). After analysing what was then known about the Martian climate, temperature, possible presence of water and the 'canals' thought by Lowell to indicate intelligent life, Wallace roundly refuted this idea.

U. Kutschera *Institute of Biology, University of Kassel, Germany. kut@uni-kassel.de*

CORRECTION

The obituary of Andrew Fielding Huxley (*Nature* **486,** 474; 2012) omitted to mention that Hugh Huxley and Jean Hanson also proposed a sliding-filament model of muscle contraction, based on myofibril experiments. Their work was published (*Nature* **173,** 973; 1954) alongside A. F. Huxley's *Nature* paper.

RESEARCH

NEW ONLINE

Papers published this week at Nature.com/nature

NEWS & VIEWS How tropical soils offset greenhouse-gas emissions during drought **p.211**

LETTER Quantum teleportation across a 'record' 143 kilometres of free space **p.269**

LETTER Bubble-free boiling could prove useful in nuclear plants and elsewhere **p.274**

PUBLISHED 9/10 SEPTEMBER 2012

MOLECULAR BIOLOGY

DNA primed for repair

For breakages in double-stranded DNA to be repaired, the 5′ terminal strand is resected to yield a 3′ terminal single-stranded tail. How this resection occurs was unknown. Two groups now report that the yeast protein Fun30 and human protein SMARCAD1 are the chromatin remodellers that facilitate resection. Fun30 is also required to overcome resection inhibition that occurs due to binding of the checkpoint adaptor protein Rad9 to the 5′ end of the break.

The yeast Fun30 and human SMARCAD1 chromatin remodellers promote DNA end resection
T Costelloe *et al.*
doi:10.1038/nature11353

The Fun30 nucleosome remodeller promotes resection of DNA double-strand break ends
X Chen *et al.*
doi:10.1038/nature11355

CANCER GENOMICS

Lung-cancer genomes analysed

The Cancer Genome Atlas consortium has analysed 178 lung squamous-cell carcinomas, a common lung cancer for which comprehensive genomic analyses have not been available. This tumour type is characterized by complex genomic alterations, with recurrent mutations in 18 genes, including *TP53*, in nearly all samples. These analyses identify potential therapeutic targets worthy of further investigation.

Comprehensive genomic characterization of squamous cell lung cancers
The Cancer Genome Atlas Research Network
doi:10.1038/nature11404

MOLECULAR BIOLOGY

Initiation of transcription-coupled repair characterized at single-molecule resolution
K Howan *et al.*
doi:10.1038/nature11430

VIROLOGY

Efficacy of HIV vaccine

A clinical trial involving more than 16,000 volunteers, known as the RV144 trial, tested a combination of the vaccines ALVAC-HIV and AIDSVAX B/E gp120 for its safety and ability to prevent HIV infection. The regimen was 31% effective against HIV-1, and antibodies against HIV-1 envelope variable loops 1 and 2 (V1/V2) correlated inversely with infection risk. Rolland *et al.* present a genetic analysis of breakthrough infections in trial participants and identify signatures associated with vaccine-induced immune pressure.

Increased HIV-1 vaccine efficacy against viruses with genetic signatures in Env V2
M Rolland *et al.*
doi:10.1038/nature11519

PUBLISHED 12 SEPTEMBER 2012

NEUROSCIENCE

Stem cells check hearing loss

Auditory neuropathy is a type of hearing loss in which the hair cells of the inner ear are often relatively unscathed, so cochlear implants alone are ineffective. Rather it is the next step in the auditory pathway that is impaired by damage sustained by the spiral ganglion neurons, and there are no routine treatments to counter sensory neuron loss. Wei Chen *et al.* now report the generation of ear-cell progenitors from human embryonic stem cells, and show that the progenitors can differentiate into functional cells involved in auditory response. Transplantation of the progenitors into chemically damaged gerbil ears restores auditory evoked response in the brainstem, suggesting that when combined with cochlear implants, the procedure could form the basis of a cell-based therapy for some types of deafness.

Restoration of auditory evoked responses by human ES-cell-derived otic progenitors
W Chen *et al.*
doi:10.1038/nature11415

CLIMATE SCIENCE

Rain in the afternoon

Soil moisture is known to influence precipitation across a range of scales in time and space, and most models suggest that wetter soils promote higher atmospheric moisture and favour the local development of storms. But an analysis of global precipitation data from a combination of weather satellites shows that — especially in semi-arid regions — afternoon precipitation is more likely over dry soil than over wet soil. The findings suggest that current climate models may be missing fundamental processes regulating convection and land–atmosphere interactions.

Afternoon rain more likely over drier soils
C M Taylor *et al.*
doi:10.1038/nature11377

APPLIED PHYSICS

Networks of the liked and alike

Preferential attachment is a mechanism attempting to explain the emergence of scaling in growing networks. If new connections are established preferentially to more popular nodes in a network, then the network is scale-free. So, because 'popularity is attractive', does preferential attachment predict network evolution? Fragkiskos Papadopoulos *et al.* show that popularity is a strong force shaping the complex network structure and dynamics, but so too is similarity. They develop a model that increases the accuracy of network evolution predictions by considering the trade-offs between popularity and similarity. The model accurately describes large-scale evolution of technological (Internet), social and metabolic networks, predicting the probability of new links with high precision.

Popularity versus similarity in growing networks
F Papadopoulos *et al.*
doi:10.1038/nature11459

Luck or reason
A-L Barabási
doi:10.1038/nature11486

CELL BIOLOGY

Small heat-shock proteins protect from heat-stroke-associated neurodegeneration
N Kourtis *et al.*
doi:10.1038/nature11417

NEUROSCIENCE

Attention deficits without cortical neuronal deficits
A Zénon & R J Krauzlis
doi:10.1038/nature11497

AGEING

Mixed results for dieting monkeys

According to previous studies, a low-calorie diet provides health benefits and increases lifespan in mammals, including primates. Yet a long-term investigation in rhesus monkeys finds no effect on longevity. SEE LETTER P.318

STEVEN N. AUSTAD

For more than 75 years, we have known that reducing food consumption increases longevity and preserves various aspects of health in mice and rats. For many researchers, these observations offered an investigational tool for probing underlying mechanisms of the ageing process. For other researchers and for the public at large, however, the observations suggested the more immediate hope that calorie restriction might improve health and extend life in humans — the fountain of youth could be as close as one's dinner plate.

To address whether such simple dietary intervention might have beneficial effects in primates that are long-lived like humans, two independent studies using rhesus monkeys were initiated in the late 1980s, one at the US National Institute on Aging (NIA) in Bethesda, Maryland, and the other at the Wisconsin National Primate Research Center (WNPRC) in Madison. Periodic reports from the studies have provided some indications of improved health[1,2] and, possibly, increased lifespan[1] in the animals. However, on page 318 of this issue, Mattison *et al.*[4] report that the NIA data indicate that calorie restriction has no effect on the animals' longevity*.

In the NIA study, rhesus monkeys of different ages were subjected to a 30% calorie restriction (Fig. 1). The authors grouped the data into a young-onset group (animals that were 1–14 years old when enrolled in the study) and an old-onset group (aged 16–23 when enrolled). To give perspective to these ages, sexual maturity in captive rhesus monkeys occurs at 4–5 years of age, and median longevity had previously been reported[3] as 27 years. Mattison *et al.* found that, for both age groups, the treated animals lived no longer than untreated monkeys. Nearly 50% of the young-onset animals are still alive, but the researchers' projections from current survival patterns indicate a likelihood of less than 0.1% that the calorie-restricted animals will survive longer than the controls.

To explore possible health benefits of the treatment, the authors regularly took blood samples from the animals to measure levels of glucose, cholesterol and triglyceride lipids. Cholesterol levels were significantly lower in treated males than in untreated males, but were unaffected in females. Moreover, the calorie-restricted old-onset monkeys had significantly lower triglyceride levels, as well as marginally lower glucose, than the controls. However, the young-onset treated animals showed no difference in glucose concentrations, and their triglyceride levels were marginally lower in males only, when compared with untreated controls of the same age group.

Figure 1 | Thinner but not longer lived. Mattison *et al.*[4] report that restricting calorie intake in rhesus monkeys does not increase survival, although it improves certain metabolic parameters in some of the animals. The image shows two 27-year-old male monkeys, one of which had been placed on a calorie-restricted diet (left), with the other being untreated. (Housing for photo purposes only. Photo courtesy of the National Institute on Aging/NIH.)

Calorie restriction did not alter causes of death. It may be premature to predict the final effect on ageing-related diseases because half of the animals in the young-onset group are still alive, but the dietary intervention seems to have reduced the incidence of cancer and, possibly, diabetes — although it might have slightly increased the incidence of cardiovascular disease. All of these ageing-related diseases did appear marginally later in the restricted monkeys, however.

Mattison and colleagues' results contrast in some ways with those reported for the WNPRC study[2], which enrolled only young rhesus monkeys (7–14 years old). The WNPRC researchers found no statistically significant effect of calorie restriction on overall longevity, but the survival patterns (with roughly 50% of the animals still alive) suggested a clear trend towards longer life for the treated subjects. Moreover, when deaths due to non-ageing-related causes such as gastrointestinal bloat or anaesthesia (which was required for some experimental procedures) were eliminated from the WNPRC analysis, calorie restriction did show a statistically significant, positive effect on survival.

However, some of us in the field were concerned about the interpretation of the WNPRC study. The deaths that had been eliminated from the analysis made up nearly half of the total deaths, and there were more of such deaths in the restricted group than in the control group. So, it was possible that some of the non-ageing-related deaths might be linked to the treatment. Interestingly, Mattison and colleagues' data also indicate a higher incidence of

*This article and the paper under discussion[4] were published online on 29 August 2012.

non-ageing-related deaths in calorie-restricted young-onset animals than in controls.

What might account for the differences between the studies' results? One possibility is diet composition. Whereas the diets were broadly similar in their overall content of carbohydrates, proteins and fats, they differed in the specific types of such nutrients. For instance, sucrose made up 28.5% of the WNPRC diet, but only 3.9% of the NIA diet. Possibly related to this difference, more than 40% of the WNPRC control animals and only 12.5% of the NIA controls developed diabetes — although this metabolic malfunction was completely absent in the WNPRC calorie-restricted animals, but not in the treated animals in the NIA study.

Another difference is that the NIA controls were given an apportioned amount of food to prevent obesity, whereas the WNPRC controls were fed *ad libitum* (that is, they could eat as much as they pleased). Consequently, NIA control animals weighed less and were considerably longer-lived than the WNPRC controls. One interpretation of this observation is that the NIA controls were partially restricted, which would account for the lack of a survival effect of the treatment in the NIA study. Nevertheless, all animals in both studies — even in the calorie-restricted groups — weighed more than wild-caught monkeys[6].

Taken together, the contrasting results raise an intriguing question about the nature and robustness of restricting calorie intake in primates. Is calorie restriction anything more than the elimination of excess fat? That might be concluded if one interprets the control animals in the NIA study as being restricted to a healthy weight, such that further restriction had little additional effect on longevity. However, researchers who use rodent models have long assumed that calorie restriction results in more than just leanness and that it extends life beyond its normal limits. It is known, for instance, that calorie restriction improves survival in obese and non-obese mice and rats[7], even at very high restriction levels[8], and that survival is affected by calorie restriction in a different way from exercise-driven leanness[9].

The same question arises in ongoing studies comparing overweight[10,11] or lean[12] people with normal-weight controls. If calorie restriction defines only the food intake needed to maintain a healthy body weight, then pharmacological mimicry of such an effect might improve the health of only the fraction of the population that is overweight. And, in that case — somewhat disappointingly — no spectacular increase in health or longevity should be expected. ■

Steven N. Austad *is at the Barshop Institute for Longevity and Aging Studies, Department of Cellular and Structural Biology, University of Texas Health Science Center at San Antonio, San Antonio, Texas 78245, USA.*
e-mail: austad@uthscsa.edu

1. Messaoudi, I. *et al. Proc. Natl Acad. Sci. USA* **103,** 19448–19453 (2006).
2. Colman, R. J., Beasley, T. M., Allison, D. B. & Weindruch, R. *J. Gerontol. A* **63,** 556–559 (2008).
3. Colman, R. J. *et al. Science* **325,** 201–204 (2009).
4. Mattison, J. A. *et al. Nature* **489,** 318–321 (2012).
5. Colman, R. J. & Kemnitz, J. W. in *Methods in Aging Research* (ed. Yu, B. P.) 249–267 (CRC Press, 1998).
6. Leutenegger, W. & Cheverud, J. *Int. J. Primatol.* **3,** 387–402 (1982).
7. Turturro, A. *et al. J. Gerontol. A* **54,** B492–B501 (1999).
8. Weindruch, R., Walford, R. L., Fligiel, S. & Guthrie, D. *J. Nutr.* **116,** 641–654 (1986).
9. Holloszy, J. O. *J. Appl. Physiol.* **82,** 399–403 (1997).
10. Heilbronn, L. K. *et al. J. Am. Med. Assoc.* **295,** 1539–1548 (2006).
11. Fontana, L. *et al. Am. J. Physiol. Endocrinol. Metab.* **293,** E197–E202 (2007).
12. Fontana, L., Meyer, T. E., Klein, S. & Holloszy, J. O. *Proc. Natl Acad. Sci. USA* **101,** 6659–6663 (2004).

BIOGEOCHEMISTRY

Drought and tropical soil emissions

Past research implied that positive feedback might exist between climate change and greenhouse-gas emissions from soil. A study finds that drought-induced declines in such emissions from tropical forests could counter climate change.

CORY C. CLEVELAND & BENJAMIN W. SULLIVAN

Tropical forests have been aptly described as the planet's lungs. Tropical vegetation inhales vast amounts of carbon dioxide and exhales oxygen to the atmosphere, and in so doing, provides a vital climate benefit by absorbing some of the nearly 9 petagrams (1 petagram is 10^{15} g) of carbon that human activities release into the atmosphere each year[1]. What's more, tropical soils influence climate by releasing large amounts of CO_2 as a by-product of the decomposition of organic matter, and through several other soil microbial processes that both emit and consume greenhouse gases, including nitrous oxide and methane[2].

Important questions remain about the effect of climate change on greenhouse-gas fluxes from soil, and hence to what extent the beneficial climate services provided by tropical forests will persist in the future. Writing in *Global Biogeochemical Cycles*, Wood and Silver[3] report that an experimentally induced drought had reduced greenhouse-gas emissions from tropical soil to the atmosphere, an effect that represents a negative feedback to climate change.

Many of the scenarios used to predict future climate focus on rising temperature, but changes in the water balance of tropical forests might have more immediate and pronounced effects. Although substantial uncertainty remains, most climate models predict significant declines in rainfall across large areas of the tropics[4,5]. So how might such declines alter the net balance of the gases that contribute to climate change?

To address this question, Wood and Silver manipulated rainfall in a Puerto Rican tropical forest (Fig. 1) to test how drought affects soil emissions of CO_2, methane and nitrous oxide. Such experimental manipulations remain the gold standard for directly assessing the potential effects of environmental change on ecosystem processes, and can provide critical input to the development of better Earth-system models. The authors simulated the effects of a prolonged dry season by preventing rainfall from reaching the forest floor for three months, and measured greenhouse-gas emissions from soil before, during and after the experiment.

After the simulated drought, Wood and Silver documented profound declines in the efflux of CO_2 from soil and increases in soil consumption of methane. In addition, the drought elicited surprising reductions in denitrification (the production of nitrous oxide), a process that is carried out by a tiny fraction of the soil's microbial community. Together, these effects lowered the global-warming potential of the soil emissions. When the heat-trapping ability of nitrous oxide is taken into account, a substantial reduction in total global-warming potential from all three gases was accounted for by the decline of denitrification. Because tropical forest soils are a major source of nitrous oxide emissions to the atmosphere[6], this result implies that a drier climate could cause substantial reductions in global emissions of nitrous oxide from soil.

However, extrapolating results from experiments such as these is particularly challenging for tropical forests. In Wood and Silver's experiment, drought effects varied depending on landscape position: ridge and valley plots had larger responses to experimental drought than did those on slopes. This variation has considerable implications for models used to simulate biogeochemical responses to climate

JERRY BAUER

Figure 1 | Luquillo Experimental Forest. Wood and Silver[7] have studied the effect of drought on greenhouse gases emitted from soils in the Luquillo Experimental Forest, Puerto Rico.

change, none of which is able to capture the complex interplay of factors that can create substantial biogeochemical heterogeneity within and across tropical forests[7]. The authors' results are a prime example of the challenge facing scientists — many tropical regions have highly complex landscapes with varying nutrient availability, which in turn can regulate biological processes that influence greenhouse-gas production[8,9].

The possibility of positive feedback between climate change and greenhouse-gas emissions from soil has been recognized for decades. Wood and Silver's results suggest the opposite: declines in greenhouse-gas emissions following drought would reduce climate forcing. But as the authors highlight, the handful of studies in which rainfall has been excluded from tropical forests have shown positive, negative or no net effects of drought on soil greenhouse-gas emissions. Moreover, although it is crucial to consider the effects of drought alone, real-world emissions will hinge on the combined effects of changing precipitation and temperature, along with chronic shifts in atmospheric CO_2 levels and nutrient deposition — factors that were not manipulated in the authors' experiment. Finally, studies[10,11] have shown that the growth and carbon uptake of trees in the tropics are highly sensitive to climate, but the experimental plots used in Wood and Silver's study (1.54 square metres) were not large enough to simulate the potentially negative effects of drought on carbon uptake through tree growth. The overall effects of drought on the greenhouse-gas balance of the sites therefore remain unknown.

In recent decades, tropical forests have given us a discount on anthropogenic CO_2 emissions by absorbing more greenhouse gases than human activity produces. Wood and Silver's findings suggest that tropical soils may continue to offset greenhouse-gas emissions during drought. Perhaps more notably, their study highlights the need for additional large-scale experiments that can more completely resolve the potential effects of climate change on trace gas emissions in tropical forests. The authors' data are critical for improving and validating models that predict ecosystem and climate responses over large spatial and temporal scales. Considering the pivotal role of tropical ecosystems in basic human health and welfare, our understanding of fundamental ecosystem processes, and their potential response to climate change, remains woefully incomplete in complex and diverse tropical forests. ■

Cory C. Cleveland *and* **Benjamin W. Sullivan** *are in the Department of Ecosystem and Conservation Sciences, University of Montana, Missoula, Montana 59812, USA.*
e-mails: cory.cleveland@cfc.umt.edu; benjamin.sullivan@cfc.umt.edu

1. Le Quéré, C. *et al. Nature Geosci.* **2,** 831–836 (2009).
2. Montzka, S. A., Dlugokencky, E. J. & Butler, J. H. *Nature* **476,** 43–50 (2011).
3. Wood, T. E. & Silver, W. L. *Glob. Biogeochem. Cycles* **26,** GB3005 http://dx.doi.org/10.1029/2010GB004014 (2012).
4. Cox, P. M. *et al. Theor. Appl. Climatol.* **78,** 137–156 (2004).
5. Neelin, J. D., Münnich, M., Su, H., Meyerson, J. E. & Holloway, C. E. *Proc. Natl Acad. Sci. USA* **103,** 6110–6115 (2006).
6. Matson, P. A. & Vitousek, P. M. *BioScience* **40,** 667–672 (1990).
7. Townsend, A. R., Asner, G. P. & Cleveland, C. C. *Trends Ecol. Evol.* **23,** 424–431 (2008).
8. Vitousek, P. M. *et al. Ecosystems* **6,** 762–772 (2003).
9. Porder, S. & Hilley, G. E. *Biogeochemistry* **102,** 153–166 (2011).
10. Clark, D. A., Piper, S. C., Keeling, C. D. & Clark, D. B. *Proc. Natl Acad. Sci. USA* **100,** 5852–5857 (2003).
11. Zhao, M. & Running, S. W. *Science* **329,** 940–943 (2010).

SOCIAL SCIENCE

Poked to vote

A Facebook message sent out during the 2010 US congressional elections influenced the voting behaviour of millions of people. The experiment illustrates the power of digital social networks to spread behavioural change. SEE LETTER P.295

SINAN ARAL

Social networks are the pathways through which information, advice, resources and support flow between people. They are essential for many people's decision-making, cooperation and complex interdependence. Yet although humans have almost always lived in networks, advances in computing power and new social technologies have only recently facilitated the development of forms of networked communication that are automating and accelerating the social signals that pulse through the human network on a daily basis. The rapid dissemination of social signals in these digital networks — status updates, tweets, likes, posts, shares and so on — raises serious scientific questions: how, when and to what extent do these signals influence decision-making and the spread of behaviours in society? If social influence drives behaviour, then digital social signals could be used to promote widespread behaviour change and thus to transform commerce, politics and public health. On page 295 of this issue, Bond *et al.*[1] present some of the most convincing evidence to date that peer influence and digital social signals can affect political mobilization.

Political mobilization has been central to recent discourse about the transformative effects of social media — for example, the part that technologies such as Facebook or Twitter played in the protests collectively known as the Arab Spring, or may play in the forthcoming US presidential election. The question is: what role do peer influence and digital social signals have in mobilizing political expression? Do our friends' behaviours inspire us to be politically active, to protest or to vote?

These questions may seem relatively simple to answer, given the right data. But several statistical challenges make it difficult to quantitatively estimate peer influence in networks. For example, networks are homophilous — we tend to make friends with people like ourselves and thus have preferences that are highly correlated with those of our friends[2]. If two friends adopt a behaviour, one immediately after the

BOX 1

Networking behaviour

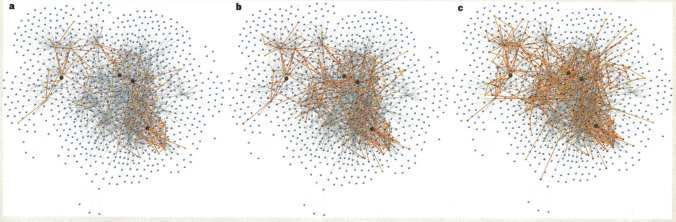

The images shown display the uptake of a personalized mobile-phone application across a network of Yahoo! customers communicating over the company's instant-messenger service[3]. Each panel displays a snapshot of one cluster of the network at 33 days (**a**), 41 days (**b**) and 62 days (**c**) after the application's launch. The four large black nodes represent customers who were initial adopters of the application; yellow nodes are new adopters in each period; red nodes are those who adopted in previous periods; and blue nodes are non-adopters. Orange lines highlight connections between previous adopters and new adopters that are activated as the product diffuses through the population.

A key question is how much the spread of behaviours such as product adoption is due to social influence — or homophily (correlated preferences among friends) — and/or other confounding factors.

Such confounding factors mimic the influence that the spread of behaviours in social networks has on the resulting diffusion patterns. Separating that influence from homophily and other factors, and establishing estimates of the degree to which peer-induced action is responsible for the adoption of a behaviour, are essential for creating effective policies that promote positive behaviours in society and contain negative ones. **S.A.**

other, it is difficult to distinguish whether this is due to peer influence or homophily. Network peers are also likely to be exposed to similar environmental stimuli: we work together and thus receive the same employee incentives; we live together and so are exposed to the same neighbourhood events; and because we have the same preferences, we tend to browse the same websites and watch the same television shows, so we see the same advertisements. This correlated exposure to external stimuli could also contribute to correlations in peer behaviours over time.

Methods are now available that can separate peer influence from homophily and other confounding factors in observational data[3]. This is useful because most data on these questions are observational. But controlling for unobservable factors, such as latent homophily, remains difficult[4]. As an alternative to observational data, experimental network studies using random assignment can provide a more robust means of identifying causal peer effects in networks and distinguishing between influence and confounding factors. Such experiments have demonstrated a role for peer influence in product adoption[5–7] (Box 1), health behaviours[8] and altruism[9].

However, although it has been postulated that voting is also motivated by interactions with friends, neighbours and family members[10], most research and many 'get out the vote' mobilization campaigns have focused on the individual[11,12] (for an exception, see ref. 13 for experimental evidence of peer influence on voting behaviour in two-person households). By contrast, Bond and colleagues used a randomized experiment — involving 61 million people within the intricate social network of Facebook — to show that digital social signals directly influence political self-expression, information-seeking and real-world voting behaviour.

The experiment was conducted during the 2010 US congressional elections. The targeted Facebook users saw a statement at the top of their 'News Feed' that encouraged them to vote, provided a link to information on local polling places, contained a clickable 'I voted' button and showed a counter of Facebook users who had voted (see Fig. 1 of the paper[1]). This was the 'informational' message, received by a control group of users. Another group received a 'social' message, which additionally included six randomly selected profile pictures of Facebook friends of the user who had already clicked the 'I voted' button. The researchers categorized these friends into either ordinary friends or close friends on the basis of the degree of Facebook interaction.

The results show that users who received the social message were 2.08% more likely to report that they themselves voted, 0.26% more likely to seek information about a polling location, and 0.39% more likely to actually vote than users receiving the informational message (the authors estimated actual voting using data on 6.3 million users in their sample that could be matched to publicly available voting records). The authors also examined 'contagion' effects of the messages on users who themselves received neither the social nor the informational message, but who had a friend who received a message. Here, in the validated voting sample, individuals were 0.224% more likely to vote, for each close friend who received a message, than they would have been had their friend received no message.

Although these estimates may seem small, they translate into significant numbers of votes. A social message saying that a Facebook friend had voted generated 886,000 additional 'expressed' votes (clicks on the 'I voted' button), and messages involving a close friend generated an additional 559,000 expressed votes. In terms of real-world voting, the authors were able to validate 282,000 additional votes cast by people receiving a message that a close Facebook friend had voted.

This work has important implications for our understanding of how signals in social networks influence an individual's behaviour. But there is more work to be done. In particular, future work modelling the degree to which contamination or leakage in networked experiments[4] (also called interference[14]) affects

inference, examination of how peer influence varies across behaviours[5], and evaluation of the social and structural conditions under which influence is more or less likely to propagate will all be essential to our understanding of the spread of behaviour change through human populations.

Advancing our understanding of peer influence in networks is the first step towards designing 'network interventions' that can promote positive behaviours in human populations, or contain negative ones[15]. It is perhaps obvious that this is relevant to, for example, targeted advertising and viral marketing. But such interventions also have the potential to promote positive social changes, such as increasing the rate of HIV testing, reducing violence, improving adherence to exercise, or increasing political mobilization and awareness. In this way, the science of social influence may have dramatic implications for products, politics and public health. ■

Sinan Aral *is at the Leonard N. Stern School of Business, New York University, New York, New York 10012, USA.*
e-mail: sinan@stern.nyu.edu

1. Bond, R. M. *et al. Nature* **489,** 295–298 (2012).
2. McPherson, M., Smith-Lovin, L. & Cook, J. M. *Annu. Rev. Sociol.* **27,** 415–444 (2001).
3. Aral, S., Muchnik, L. & Sundararajan, A. *Proc. Natl Acad. Sci. USA* **106,** 21544–21549 (2009).
4. Shalizi, C. R. & Thomas, A. C. *Sociol. Methods Res.* **40,** 211–239 (2011).
5. Aral, S. & Walker, D. *Mgmt Sci.* **57,** 1623–1639 (2011).
6. Aral, S. & Walker, D. *Science* **337,** 337–341 (2012).
7. Bakshy, E., Eckles, D., Yan, R. & Rosenn, I. *Proc. 13th ACM Conf. Electron. Comm.* 146–161 (ACM, 2012).
8. Centola, D. *Science* **329,** 1194–1197 (2010).
9. Leider, S., Möbius, M. M., Rosenblat, T. & Do, Q.-A. *Q. J. Econ.* **124,** 1815–1851 (2009).
10. McClurg, S. D. *Am. Polit. Res.* **32,** 406–443 (2004).
11. Rosenstone, S. J. & Hansen, J. M. *Mobilization, Participation and Democracy in America* (Macmillan, 1993).
12. Green, D. P., Gerber, A. S. & Nickerson, D. W. *J. Polit.* **65,** 1083–1096 (2003).
13. Nickerson, D. W. *Am. Polit. Sci. Rev.* **102,** 49–57 (2008).
14. Aronow, P. M. & Samii, C. *Estimating Average Causal Effects Under General Interference* New York Univ. Work. Pap. (2012).
15. Valente, T. W. *Science* **337,** 49–53 (2012).

ORGANIC SYNTHESIS

A biochemical messenger made easily

Biochemicals known as prostaglandins are challenging targets for synthetic organic chemistry. Yet by channelling the reactivity of a simple reactant, a powerful synthesis of one such compound has been achieved. SEE LETTER P.278

ERIK J. SORENSEN

Chemical messengers called prostaglandins are present in nearly all mammalian tissues. These elusive molecules mediate an extraordinary number of biological processes — including the regulation of body temperature, the contraction and relaxation of the human uterus, the aggregation of platelets in blood and cellular responses to inflammation. They have therefore been the targets of wide-ranging research[1] since the 1930s. In particular, their unique molecular architectures and great therapeutic potential have fired the creative imagination of synthetic organic chemists[2,3]. Writing on page 278 of this issue, Coulthard *et al.*[4] report one of the cleverest syntheses of one such molecule, prostaglandin $F_{2\alpha}$ ($PGF_{2\alpha}$), to date. The conciseness of their approach may open up new opportunities for drug discovery.

Prostaglandins contain two fat-soluble hydrocarbon chains on opposite sides of a ring of five carbon atoms (Fig. 1). Nature synthesizes $PGF_{2\alpha}$ and its analogues from arachidonic acid (a polyunsaturated fatty acid) and two molecules of oxygen, with a little help from some key enzymes. Although nearly every nucleated cell is capable of biosynthesizing prostaglandins, these compounds are short-lived and exceedingly difficult to isolate from biological samples. Since the late 1960s, chemists have therefore devised creative strategies for producing prostaglandins from simple chemicals in the laboratory. The development of dependable laboratory syntheses has contributed substantially to our knowledge of the compounds' remarkable range of pharmacological properties, as well as their relevance to human health.

Ideas about the preparation of $PGF_{2\alpha}$ have resulted in a diversity of pathways[5–9] — a diversity that demonstrates how well the principles of organic chemistry can be used to plan and execute synthetic routes to structurally complex molecules (Fig. 1). The approach now reported by Coulthard *et al.* will be praised for its remarkable brevity and for the bold strategy that guided it. The structural relationship between the simple starting material, succindialdehyde, and the coveted target is distant, and yet the authors perceived that a union of two molecules of succindialdehyde in a single laboratory operation might produce an intermediate hemiacetal compound that is tantalizingly close to the structure of $PGF_{2\alpha}$ (Fig. 2).

The risky aspect of the authors' strategy concerns the intrinsic reactivity of succindialdehyde and its potential to take part in undesired, polymer-forming reactions. Few chemists, even those of adventurous spirit, would have believed that a useful synthesis of the hemiacetal could be achieved as Coulthard *et al.* anticipated, through the direct pairing of two molecules of succindialdehyde in sequential carbon–carbon-bond-forming reactions known as aldol reactions. The great thing is that, not only did this direct approach work well, but it also achieved high stereoselectivity — it produced mostly one mirror-image isomer (enantiomer) of the product. This is crucial, because the biological activity of prostaglandins depends on their enantiomeric form.

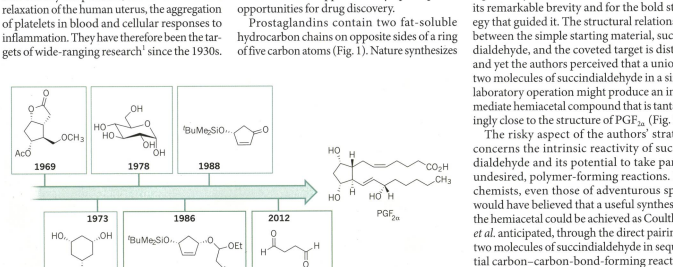

Figure 1 | Landmark syntheses of prostaglandin $F_{2\alpha}$ ($PGF_{2\alpha}$). The $PGF_{2\alpha}$ biochemical has long acted as a testing ground for organic synthesis. The dates of selected syntheses[5–9] are indicated, along with the molecule that acted as the starting point or key intermediate for each synthesis. Coulthard *et al.*[4] now report a concise synthesis of $PGF_{2\alpha}$ that starts from succindialdehyde. Ac is acetyl, $COCH_3$; Me is methyl, CH_3; Et is ethyl, C_2H_5; ^tBu is tertiary butyl, $(CH_3)_3C$.

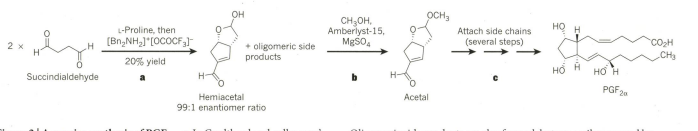

Figure 2 | A concise synthesis of $PGF_{2\alpha}$. **a**, In Coulthard and colleagues' synthesis[8], two equivalents of succindialdehyde react with each other to produce a hemiacetal when treated with catalytic L-proline, and then with another catalyst (an amine salt, $[Bn_2NH_2]^+[OCOCF_3]^-$), in the same reaction vessel. The product is obtained in 20% yield as a 99:1 ratio of enantiomers (mirror-image isomers); the major isomer is depicted. Oligomeric side products are also formed, but are easily removed by filtration. Bn is benzyl, $CH_2C_6H_5$. **b**, The hemiacetal is treated with methanol (CH_3OH), an acid (Amberlyst-15) and magnesium sulphate ($MgSO_4$) to yield an acetal, which contains most of the features needed for the ring component of $PGF_{2\alpha}$. **c**, The authors completed the synthesis by attaching two side chains to the acetal.

The authors discovered that the sequential addition of two organic catalysts to a solution of succindialdehyde is key to the formation of the desired hemiacetal. The first catalyst was the amino acid proline, and the second was an amine salt. The development of this process was supported by earlier studies of proline-catalysed aldol reactions[10–12] and ring-forming aldol reactions induced by amine salts[13] at room temperature.

Although the yield of hemiacetal isolated from the reaction was moderate (20%), Coulthard *et al.* removed most of the undesired oligomeric side products by filtration. A simple chromatographic purification step then afforded the product as the major component of a 99:1 mixture of enantiomers. Any possible concerns about the yield for this impressive transformation are assuaged by the authors' demonstration that 15 grams of a key prostaglandin building block (an acetal; Fig. 2) can be produced in only two steps from succindialdehyde — a large quantity to take forward for the rest of the synthesis.

With its ring of five carbon atoms and newly formed stereogenic centres (carbon atoms around which different geometric arrangements of bonds generate different enantiomers), the acetal building block is a close approximation of the core structure of the prostaglandins. By exploiting the reactive alkene group and the rigid molecular shape of the building block, Coulthard *et al.* attached one of the two hydrocarbon side chains of $PGF_{2\alpha}$ to the desired site on the five-membered ring. Then, in the final phase of the synthesis, the authors efficiently connected the second side chain using a reaction developed by E. J. Corey in his influential syntheses of prostaglandins[7]. In all, only seven operations were needed to transmute the simple compound succindialdehyde into $PGF_{2\alpha}$. For comparison, Corey's synthesis required 17 steps, starting from the simple molecule cyclopentadiene.

➲ NATURE.COM
For more on prostaglandin synthesis, see:
go.nature.com/thqz85

Finding a way to prepare prostaglandins and their analogues in a few steps from commonplace chemicals is still highly alluring for many researchers, especially those in the pharmaceutical industry. The brevity of Coulthard and colleagues' synthesis of $PGF_{2\alpha}$ sets a new standard, and their approach should be applicable to other members of the prostaglandin class, as well as to new structures that have some of the molecular features of prostaglandins. The authors' achievement also calls to mind a much earlier groundbreaking use of succindialdehyde in chemical synthesis — Robert Robinson's synthesis of tropinone[14], a precursor to the drug atropine, in 1917. Some of the power and simplicity of that classic work is seen in Coulthard and colleagues' remarkable solution to the problem of building prostaglandins. ■

Erik J. Sorensen *is in the Department of Chemistry, Princeton University, Princeton, New Jersey 08544, USA.*
e-mail: ejs@princeton.edu

1. Bergström, S., Carlson, L. A. & Weeks, J. R. *Pharmacol. Rev.* **20**, 1–48 (1968).
2. Bindra, J. S. & Bindra, R. *Prostaglandin Synthesis* (Academic, 1977).
3. Mitra, A. *The Synthesis of Prostaglandins* (Wiley-Interscience, 1977).
4. Coulthard, G., Erb, W. & Aggarwal, V. K. *Nature* **489**, 278–281 (2012).
5. Corey, E. J., Weinshenker, N. M., Schaaf, T. K. & Huber, W. *J. Am. Chem. Soc.* **91**, 5675–5677 (1969).
6. Woodward, R. B. *et al. J. Am. Chem. Soc.* **95**, 6853–6855 (1973).
7. Stork, G., Takahashi, T., Kawamoto, I. & Suzuki, T. *J. Am. Chem. Soc.* **100**, 8272–8373 (1978).
8. Stork, G., Sher, P. M. & Chen, H.-L. *J. Am. Chem. Soc.* **108**, 6384–6385 (1986).
9. Suzuki, M., Yanagisawa, A. & Noyori, R. *J. Am. Chem. Soc.* **110**, 4718–4726 (1988).
10. List, B., Lerner, R. A. & Barbas, C. F. III *J. Am. Chem. Soc.* **122**, 2395–2396 (2000).
11. Northrup, A. B. & MacMillan, D. W. C. *Science* **305**, 1752–1755 (2004).
12. Mukherjee, S., Yang, J. W., Hoffmann, S. & List, B. *Chem. Rev.* **107**, 5471–5569 (2007).
13. Corey, E. J. *et al. J. Am. Chem. Soc.* **100**, 8031–8034 (1978).
14. Robinson, R. *J. Chem. Soc.* 762–768 (1917).

CELL BIOLOGY

Dormant and restless skin stem cells

It has been unclear whether a uniform group of stem cells gives rise to most cells in the epidermis. A study reveals the presence of at least two stem-cell populations that have different proliferative abilities. SEE ARTICLE P.257

LAURA DE ROSA & MICHELE DE LUCA

All renewing tissues, such as blood and skin, are sustained and repaired by a small population of resident stem cells. These cells have the ability to self-renew and to generate committed progenitor cells that differentiate into the cell lineages of the tissue of origin. However, the nature and the specific activities of stem and progenitor cells at different body sites are a matter of debate. For example, several theories have been proposed regarding the epidermis, the outer covering of the skin (Fig. 1). On page 257 of this issue, Mascré *et al.*[1] provide compelling evidence for the existence of two cell populations that differ in their proliferative dynamics, their gene-expression profile and their ability to repair the epidermis after injury.

To investigate the origin, location, proliferation and fate of stem cells in mouse-tail epidermis, the authors used genetic lineage tracing — a technique that allows *in vivo* fluorescent marking of specific cell types and

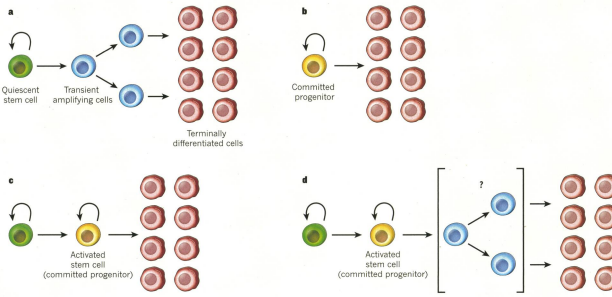

Figure 1 | Models for self-renewal of the epidermis. **a,** One model[2] of epidermal renewal relies on quiescent stem cells that generate transient actively dividing (amplifying) cells, which in turn generate non-dividing, differentiated cells. Curly arrows indicate self-renewing cells. **b,** A second model[3,4] posits the existence of a single population of actively cycling, committed progenitor cells that directly generate differentiated cells. **c,** Mascré and colleagues' results[1] suggest that epidermal renewal is sustained by slowly dividing stem cells that persist during the lifetime of the animal and contribute to both repair and long-term regeneration of the epidermis. These cells give rise to actively cycling, self-renewing stem cells (or committed progenitors) that persist for various periods of time, replenish differentiated cells and make only a short-term contribution to wound healing. **d,** We suggest that slowly dividing stem cells generate activated stem cells that give rise to transient amplifying progenitors, which eventually produce differentiated cells. A similar model has previously been proposed for other tissues[5–10].

their progeny — as well as elegant studies of individual clones (cells derived from a single initial cell). The specificity of the marking depends on the nature of the promoters (regulatory DNA sequences) that are employed to trigger permanent expression of a fluorescent protein. This is useful because different promoters are active in different cell types.

Mascré *et al.* used two distinct promoters (K14 and Inv) and unambiguously identified two cell populations. One of these populations consisted of slowly dividing cells, which represented the stem-cell reservoir and contributed to wound repair. These stem cells gave rise to a second population that comprised actively dividing committed progenitors, which eventually generated differentiated cells. The K14 promoter targeted both stem cells and committed progenitors, whereas the Inv promoter targeted only progenitors.

The results confirm the notion that the epidermis contains long-lived quiescent stem cells as well as cells endowed with differing proliferative abilities[2], and argues against the model proposing that a single progenitor-cell pool sustains self-renewal and regeneration of the mouse epidermis[3,4] (Fig. 1a–c). Moreover, the authors' study provides an explanation for previous findings that seemed to suggest a single-progenitor model[3,4]. These earlier studies had used a promoter (Ach) that targets just one group of actively cycling cells that make only a short-term contribution to epidermal repair — in other words, the Ach-marked cells behaved in a similar way to Mascré and colleagues' Inv-targeted progenitor cells.

Interestingly, the two cell populations described by the authors both possess a fundamental stem-cell property, namely, self-renewal. However, the slowly cycling stem cells persist throughout the animal's lifetime and contribute to the repair and long-term regeneration of the epidermis, whereas the actively dividing progenitors endure for shorter periods (up to several months) and make only a short-term contribution to wound healing. Therefore, these actively dividing progenitors are not the canonical 'transient amplifying cells' proposed by a previous model (Fig. 1a).

How can we define the K14- and Inv-labelled cells from a functional point of view? To try to answer this question, it may be useful to discuss what happens in other tissues. It has been shown[5] that the bone marrow contains a pool of quiescent haematopoietic (blood-forming) stem cells that generate a population of rapidly cycling stem cells. K14-marked stem cells are functionally similar to quiescent haematopoietic stem cells, whereas Inv-marked progenitors mirror actively cycling, self-renewing haematopoietic stem cells. A similar situation has been described for tissues such as hair follicles and the small intestine[6,7]. In all of these tissues, stem cells can switch between quiescence and activation depending on the functional status of the tissue; that is, normal self-renewal or acute wound healing. In our opinion, Mascré and colleagues' data support a model envisaging the coexistence of quiescent and activated stem cells as a general strategy for tissue renewal (Fig. 1c).

The notion that the mammalian epidermis contains cells endowed with different proliferative dynamics raises interesting questions that need further investigation. What factors specify the fate of these two cell populations? What are the molecular pathways that regulate stem-cell quiescence and activation in the epidermis, especially upon injury? And is the switch from quiescence to activation a cell-autonomous process, or is it controlled by environmental cues?

The study also highlights the limitations of genetic lineage tracing. Results obtained with this technique are influenced by the dynamics of the stem-cell populations in the tissues analysed, as well as by the types of promoter used and by how the promoters are activated. For instance, the authors did not detect transient amplifying progenitors, but it is not clear whether such cells are genuinely absent from the mouse epidermis or whether they were not detected owing to the lack

of an appropriate promoter (Fig. 1d).

Mascré and colleagues' work sheds light on the heterogeneity of the proliferative cell populations in mouse epidermis, and has increased our understanding of stem-cell biology. But does this knowledge apply to human tissues? Caution is required when inferring aspects of human tissue physiology from animal data. For instance, clonal analyses of several human squamous epithelia (tissues such as the epidermis, cornea and conjunctiva) have unambiguously shown the existence of self-renewing cells endowed with stem-cell properties, as well as non-self-renewing cells with differing capacities for multiplication, including canonical transient amplifying cells[8,9]. Both cell types participate in the regeneration of these epithelia in the clinic[10]. ■

Laura De Rosa *and* **Michele De Luca** *are at the Center for Regenerative Medicine 'Stefano Ferrari', University of Modena and Reggio Emilia, Modena 41125, Italy.*
e-mail: michele.deluca@unimore.it

1. Mascré, G. *et al. Nature* **489,** 257–262 (2012).
2. Potten, C. S. *Cell Tissue Kinet.* **7,** 77–88 (1974).
3. Clayton, E. *et al. Nature* **446,** 185–189 (2007).
4. Doupé, D. P. *et al. Dev. Cell* **18,** 317–323 (2010).
5. Wilson, A. *et al. Cell* **135,** 1118–1129 (2008).
6. Barker, N. *et al. Nature* **449,** 1003–1007 (2007).
7. Jaks, V. *et al. Nature Genet.* **40,** 1291–1299 (2008).
8. Barrandon, Y. & Green, H. *Proc. Natl Acad. Sci. USA* **84,** 2302–2306 (1987).
9. Pellegrini, G. *et al. J. Cell Biol.* **145,** 769–782 (1999).
10. Rama, P. *et al. N. Engl. J. Med.* **363,** 147–155 (2010).

ENVIRONMENTAL SCIENCE

The rainforest's water pump

An investigation of naturally occurring water recycling in rainforests finally marries the results of global climate models with observations. Alarmingly, it also suggests that deforestation can greatly reduce tropical rainfall. SEE LETTER P.282

LUIZ E. O. C. ARAGÃO

The humid tropics contain more than 35% of global forests, covering an area of 11,564,000 square kilometres (ref. 1). Tropical trees can extract deep soil water and pump it back to the atmosphere through a process called evapotranspiration. As a result, 25–56% of the rainfall in these regions can be recycled within the ecosystem[2]. Large-scale climate models indicate that this mechanism — which maintains atmospheric moisture and so feeds far-inland regions with rainfall — may be weakened by the removal of existing tropical forests[3,4]. Yet, paradoxically, an increase in local rainfall over deforested areas has been observed[5].

On page 282 of this issue, Spracklen *et al.*[6] report an analysis of tropical rainfall that combines models of atmospheric transport with satellite observations of rainfall and vegetation cover*. The authors conclude that, for more than 60% of pan-tropical land (that is, the tropics across all continents), air masses that have travelled over extensive vegetated surfaces can generate at least twice as much rainfall as air masses that have flowed over deforested lands. On the basis of their findings, the authors predict a potentially widespread reduction of rainfall in the Amazon basin, if deforestation in the region were to continue at the rate[7] that occurred from 1997 to 2002.

Sustaining high rates of global human-population growth requires an increase in farmable land, energy and timber supplies. Without adequate planning, these needs tend to be met by cutting down rainforests. Because ecological processes and human activities (such as agriculture) depend on water provision, scientists have, for at least two decades, investigated the impact of tropical deforestation on the hydrological cycle, especially in Amazonia.

Pioneering studies[3,4] using global climate models (GCMs) found that vegetation removal can disrupt the water cycle. For example, models show that changes in land surface characteristics cause a reduction in evapotranspiration rates and so induce basin-wide decreases in Amazonian rainfall[3]. Another simulation shows that removing around 40% of the original forest cover could drive Amazonia into an irreversible, drier climate mode[8].

These findings, however, are at odds with observations. Studies indicate that rainfall over deforested areas is, in fact, higher than in adjacent forests[5]. This is because increased surface heating in deforested areas induces upward air motion, reducing air pressure and drawing moist air from neighbouring forests into the openings. The moist air rises, and so generates

*This article and the paper under discussion[6] were published online on 5 September 2012.

Promoter Analysis without Lysing Cells

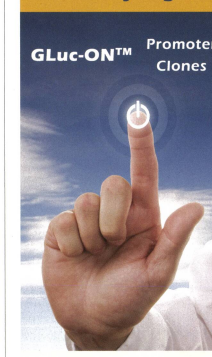

- Dual secreted reporters
- No co-transfection
- No cell lysis
- HTS compatible
- Pre-designed or custom

Search for Yours Online!

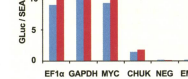

GeneCopoeia™
Expressway to Discovery
genecopoeia.com/promoter
866-360-9531

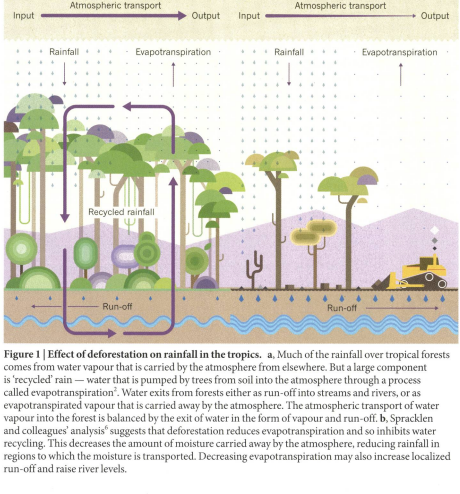

Figure 1 | Effect of deforestation on rainfall in the tropics. **a**, Much of the rainfall over tropical forests comes from water vapour that is carried by the atmosphere from elsewhere. But a large component is 'recycled' rain — water that is pumped by trees from soil into the atmosphere through a process called evapotranspiration[2]. Water exits from forests either as run-off into streams and rivers, or as evapotranspirated vapour that is carried away by the atmosphere. The atmospheric transport of water vapour into the forest is balanced by the exit of water in the form of vapour and run-off. **b**, Spracklen and colleagues' analysis[6] suggests that deforestation reduces evapotranspiration and so inhibits water recycling. This decreases the amount of moisture carried away by the atmosphere, reducing rainfall in regions to which the moisture is transported. Decreasing evapotranspiration may also increase localized run-off and raise river levels.

convective rainfall over the openings.

The problem for scientists is that models and observations capture processes at different scales, and so are not directly comparable. But with deforestation rates reaching 50,000 square kilometres per year (an area approximately the size of England) in the humid tropics[1], resolving this issue is crucial for strategically planning the conservation of tropical biomes and for maintaining the well-being of human populations.

Enter Spracklen *et al.*, who have beautifully reconciled the scale of observations with that of models. Specifically, for each $1° \times 1°$ grid-cell across the pan-tropics, the authors have quantified the amount of rainfall generated by air masses that travelled over areas of varying leaf area index (LAI, the amount of leaf area per square metre of ground). The authors combined satellite observations of LAI and rainfall with the outputs of an atmospheric-transport model, which they used to estimate the trajectories of air masses in the 10 days before they arrived at each grid location. This analysis highlighted a clear connection between rainfall and the cumulative amount of LAI over which air masses travelled: for air masses exposed to low-to-medium vegetation cover, there is a nonlinear increase of 0.3 to 0.4 millimetres per day of rainfall for every additional LAI unit, with a subsequent saturation of rainfall over densely vegetated surfaces.

Drawing on previous observations, Spracklen and colleagues' results corroborate the large-scale rainfall-driving mechanisms described by GCMs. Simply put, densely vegetated surfaces recycle water efficiently through evapotranspiration (which averages around 3–4 millimetres per day in Amazonian forests[6]), maintaining the specific humidity of the air masses over these regions (Fig. 1a). Air travelling over sparsely vegetated surfaces, however, loses moisture during continental transport because of reduced water recycling (Fig. 1b). Using a scenario of Amazonian deforestation[7] for 2050 that assumes that the environmental policies of the early 2000s are continued into the future, the authors go on to demonstrate that forest loss is likely to reduce basin-wide rainfall by 12% during wet seasons, and by 21% during dry seasons.

The projected decline in rainfall caused by deforestation in eastern and southern Amazonia (see Fig. 4 of the paper[6]) overlaps regions that, according to GCMs, already have a high probability of increased drought frequency by the end of this century, assuming that global temperature rises by about 3 °C (ref. 10). The potential ecological and economic impacts of this overlap could be huge. Changes in regional climate could exacerbate drought-related tree mortality, which in turn would reduce carbon stocks, increase fire risk and lower biodiversity[11]. Such changes might also directly threaten agriculture, which generates US$15 billion per year in Amazonia[12], and the hydropower industry, which supplies 65% of Brazil's electricity[13]. Society should therefore take urgent action now, to curb tropical deforestation and avert future environmental problems.

That said, Brazil is committed by its National Plan on Climate Change to limit historical deforestation rates by 80% by the year 2020 (ref. 14), and so the scenario used by Spracklen *et al.* for their prediction is likely to overestimate the extent and magnitude of rainfall reduction in the mid-twenty-first century. An explicit consideration of temporal changes in atmospheric circulation and vegetation characteristics is also needed to refine projections of rainfall. And to provide an independent test of the patterns proposed by Spracklen *et al.*, current pan-tropical rainfall trends should be quantified.

Nevertheless, the authors have presented the first observational assessment of the influence of vegetation on tropical rainfall patterns at a spatial resolution and coverage compatible with the outputs of GCMs. Their cutting-edge methodology will allow observations to be used consistently to examine large-scale deforestation impacts on rainfall, and to refine and evaluate current models to support conservation planning in the tropics. ■

Luiz E. O. C. Aragão *is at the College of Life and Environmental Sciences, University of Exeter, Exeter EX4 4RJ, UK.*
e-mail: l.aragao@exeter.ac.uk

1. Hansen, M. C., Stehman, S. V. & Potapov, P. V. *Proc. Natl Acad. Sci. USA* **107**, 8650–8655 (2010).
2. Eltahir, E. A. & Bras, R. L. *Rev. Geophys.* **34**, 367–378 (1996).
3. Lean, J. & Warrilow, D. A. *Nature* **342**, 411–413 (1989).
4. Shukla, J., Nobre, C. & Sellers, P. *Science* **247**, 1322–1325 (1990).
5. Negri, A. J., Adler, R. F., Xu, L. & Surratt, J. J. *Clim.* **17**, 1306–1319 (2004).
6. Spracklen, D. V., Arnold, S. R. & Taylor, C. M. *Nature* **489**, 282–285 (2012).
7. Soares-Filho, B. S. *et al. Nature* **440,** 520–523 (2006).
8. Sampaio, G. *et al. Geophys. Res. Lett.* **34,** L17709 (2007).
9. Aragão, L. E. O. C. *et al. Geophys. Res. Lett.* **34,** L07701 (2007).
10. Malhi, Y. *et al. Science* **319**, 169–172 (2008).
11. Davidson, E. A. *et al. Nature* **481,** 321–328 (2012).
12. Brazilian Institute for Geography and Statistics. *System for Automatic Data Recovery* www.sidra.ibge.gov.br (accessed August 2012).
13. Brazilian Agency for Electric Energy. *Energy Generation Database* www.aneel.gov.br/aplicacoes/capacidadebrasil/capacidadebrasil.asp (accessed August 2012).
14. Nepstad, D. *et al. Science* **326,** 1350–1351 (2009).

nature INSIGHT

GUT MICROBES AND HEALTH

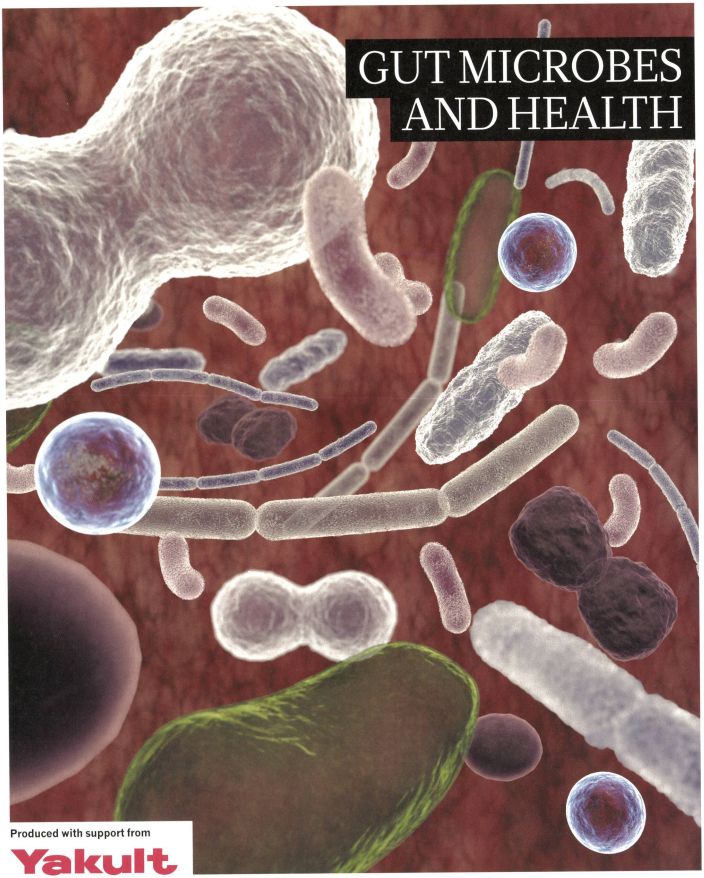

Produced with support from
Yakult

nature

A key thread in your scientific career

Since 1869 we've made it our mission to share the greatest developments in science and advance the discussion among the global scientific community. Whether in print, online or mobile, *Nature* is always at the forefront of science and is your forum to read, watch, listen and engage with key research, news and opinion.

How will you access the next landmark discovery?

➲ NATURE.COM/NATURE

nature publishing group npg

nature INSIGHT

GUT MICROBES AND HEALTH

13 September 2012 / Vol 489 / Issue No 7415

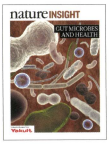

Cover illustration
by Nik Spencer

Editor, *Nature*
Philip Campbell

Publishing
Nick Campbell
Claudia Deasy

Production Editor
Jenny Rooke

Art Editor
Nik Spencer

Sponsorship
Yuki Fujiwara
Yvette Smith
Gerard Preston

Production
Emilia Orviss

Marketing
Elena Woodstock
Hannah Phipps

Editorial Assistant
Anastasia Panoutsou

Now is an exciting time to study the microbes that are associated with the body — the human microbiota. Although the beneficial effects of some of these microbes have been documented for more than a century, only with recent technological advances can the composition of the diverse microbial communities be described and compared within and between individuals. Two major funding initiatives — the US Human Microbiome Project and the European Metagenomics of the Human Intestinal Tract — are well under way, and with the contributions of individual pioneer research groups, we are beginning to understand what constitutes a healthy microbiota and how changes in its structure correlate with and affect health and disease. The more we learn about these microbes, the more we realize that they are influencing many aspects of our physiology.

This Insight focuses on the gut — the body site that is most densely populated with microbes. The greatest challenge in microbiota research is the number and diversity of species in the intestine. Rob Knight and colleagues provide a view on intestinal microbiota using principles derived from macroecology, and discuss how these principles can help to unravel the factors that shape microbial communities and may offer ways to target the microbiota for clinical intervention. Casey Weaver and colleagues review the interplay between the microbiota and the immune system by discussing the mechanisms that maintain a healthy balance, as well as the pathological consequences following perturbation. One of the main functions of gut microbes is to aid nutrient acquisition from otherwise indigestible fibres. Valentina Tremaroli and Fredrik Bäckhed explore the interactions between microbes and metabolic processes, and describe how these exchanges can lead to either a healthy equilibrium or metabolic disease. Much of the research would not have been possible without advances in sequencing technology and analysis of the microbial community genome — the microbiome. George Weinstock reviews the genomic tools that researchers can use to analyse the microbiota.

We hope that these Reviews capture some of the most exciting insights into microbiota research. We are pleased to acknowledge the financial support of Yakult Honsha in producing this Insight. As always, *Nature* carries sole responsibility for all editorial content.

Claudia Lupp, Magdalena Skipper & Ursula Weiss
Senior Editors

CONTENTS

REVIEWS

220 **Diversity, stability and resilience of the human gut microbiota**
Catherine A. Lozupone, Jesse I. Stombaugh, Jeffrey I. Gordon, Janet K. Jansson & Rob Knight

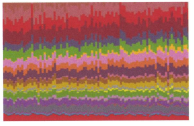

231 **Reciprocal interactions of the intestinal microbiota and immune system**
Craig L. Maynard, Charles O. Elson, Robin D. Hatton & Casey T. Weaver

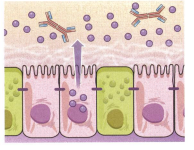

242 **Functional interactions between the gut microbiota and host metabolism**
Valentina Tremaroli & Fredrik Bäckhed

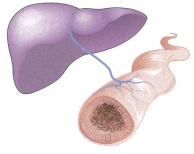

250 **Genomic approaches to studying the human microbiota**
George M. Weinstock

REVIEW

doi:10.1038/nature11550

Diversity, stability and resilience of the human gut microbiota

Catherine A. Lozupone[1], Jesse I. Stombaugh[1], Jeffrey I. Gordon[2], Janet K. Jansson[3,4] & Rob Knight[1,5,6]

Trillions of microbes inhabit the human intestine, forming a complex ecological community that influences normal physiology and susceptibility to disease through its collective metabolic activities and host interactions. Understanding the factors that underlie changes in the composition and function of the gut microbiota will aid in the design of therapies that target it. This goal is formidable. The gut microbiota is immensely diverse, varies between individuals and can fluctuate over time — especially during disease and early development. Viewing the microbiota from an ecological perspective could provide insight into how to promote health by targeting this microbial community in clinical treatments.

Most gut microbes are either harmless or of benefit to the host. The gut microbiota protects against enteropathogens[1,2], extracts nutrients and energy from our diets[3,4], and contributes to normal immune function[5]. Disruptions to the normal balance between the gut microbiota and the host have been associated with obesity[6,7], malnutrition[8], inflammatory bowel disease (IBD)[9,10], neurological disorders[11] and cancer[12]. Understanding how the gut microbiota affects health and disease requires a shift in focus from individual pathogens to an ecological approach that considers the community as a whole.

The first step in understanding the symbiotic relationship between gut microbes and their host is to characterize the baseline healthy microbiota and the differences that are associated with disease. Large-scale projects such as the European Metagenomics of the Human Intestinal Tract (MetaHIT)[13] and the US Human Microbiome Project (HMP)[14] have made substantial progress towards this goal. Once the healthy composition and functional states of gut microbiota are understood, the features that, when disrupted, are associated with disease can be determined. However, the complexity of the microbiota, and the variation between and within individuals complicates the definition of what this ideal state may be within a population or an individual.

Ecological principles can aid in understanding the host–microbe interactions and specific functions of the gut microbiota. Improvements in sequencing methods and technologies such as proteomics and metabolomics, coupled with metabolic network modelling[15,16], show how host and environmental factors can affect gut microbial ecology over a lifetime. The composition, diversity and function of gut microbial communities have the potential to inform personalized nutritional and drug treatment strategies (Fig. 1). In this Review, we summarize the progress that has been made towards characterizing the diversity and function of microbial communities in the healthy human gut, describe the ways in which this ecosystem can go awry and discuss the prospects for restoring a degraded ecosystem.

Taxonomic diversity in the healthy gut

Until the advent of higher-throughput sequencing, even basic questions — such as how many different species there are, how diverse their genetic make-up is, which features are ubiquitous and which are unique to an individual, and whether community function can be predicted from species present — remained unanswered.

Culture-based studies suggest that all healthy adults share most of the same gut bacterial species — a core microbiota. For example, *Escherichia coli* can be isolated from most people. However, culture-independent sequencing studies (Fig. 2) have demonstrated a vast microbial diversity that is highly variable over time and across populations. Each of us harbours more than 1,000 'species-level' phylotypes: clusters of sequences that have as much diversity in their small subunit ribosomal RNA genes as named species[17]. Most of these phylotypes are bacteria belonging to just a few phyla. In adults, Bacteroidetes and Firmicutes usually dominate the microbiota, whereas Actinobacteria, Proteobacteria and Verrucomicrobia, although found in many people, are generally minor constituents[18] (Fig. 3). Methanogenic archaea (mainly *Methanobrevibacter smithii*), eukaryotes (mainly yeasts) and viruses (mainly phage) are also present[19]. Despite the consistency of these main components, their relative proportions and the species present vary markedly across individuals (Figs 3 and 4). Attempts to find a core set of species-level phylotypes in the adult microbiota have identified several main players, including *Faecalibacterium prausnitzii, Roseburia intestinalis* and *Bacteroides uniformis*[13], but in some individuals even these can represent less than 0.5% of the microbes present[20]. As the data set expands to include developing countries and a broader age range[4,21], the concept that there is a core set of species in the microbiota is becoming more unlikely.

Functional diversity in the healthy gut

Knowing the composition of the microbial community alone does not necessarily lead to an understanding of its function. Functional information comes, in part, from studying cultured isolates that have well-characterized genome content and *ex vivo* phenotypes, and from sequencing community DNA. Functional screening by shotgun metagenomics relies on the sequencing of the total microbial community DNA, including from uncultured members, and matching the sequences to known functional genes (Fig. 2). Identifying the genes involved in specific metabolic pathways can predict functional capabilities, but without messenger RNA, protein and metabolite profiling these are still predictions. The process of mapping short gene

[1]Department of Chemistry and Biochemistry, University of Colorado, Boulder, Colorado, USA. [2]Center for Genome Sciences and Systems Biology, Washington University in St. Louis, St. Louis, Missouri, USA. [3]Earth Sciences Division, Lawrence Berkeley National Laboratory, Berkeley, California, USA. [4]Joint Genome Institute, Lawrence Berkeley National Laboratory, Walnut Creek, California, USA. [5]Howard Hughes Medical Institute, Boulder, Colorado, USA. [6]Biofrontiers Institute, University of Colorado, Boulder, Colorado, USA.

sequence fragments to organisms and functions is improving as more human gut microbial genomes are sequenced and annotated[23], and as more complementary 'omics' data sets become available[23,24].

Despite the highly divergent compositions of gut microbiota across individuals, the functional gene profiles are quite similar (Fig. 4). This similarity was reported in a study of 18 females who shared more than 93% of the enzyme-level functional groups, but few genus-level phylotypes[20], and was confirmed in much larger populations in HMP and MetaHIT data[13,14].

The gut microbiota all contain pathways for central, carbohydrate and amino-acid metabolism[20]. However, not all pathways are represented, and grouping genes into broad functional categories can conceal the finer differences in function between individuals. Variable functions that are restricted to a species or strain — including pathogenicity islands, vitamin and drug catabolism, motility and nutrient transporters — are possible targets for personalized diets and therapeutic strategies.

Many genes are expressed only under specific conditions. Shotgun sequencing approaches that measure levels of mRNA (metatranscriptomics) or shotgun proteomics (metaproteomics) may uncover functional variation with factors such as disease or diet that DNA studies overlook. For example, genes involved in carbohydrate metabolism and energy generation have been found to be expressed as proteins at higher levels than predicted from metagenomic data, underscoring the importance of these processes in the gut[23].

The observation that we share a functional core microbiome but not a core microbiota can be related to macroecosystems. For instance, rainforests that look the same and have many of the same functions can be composed of different species that have independently evolved. The challenge of ecological studies of the gut is to understand which members of the community have similar functional niches and which ones can be substituted for one another. Although taxonomic composition is far more variable than functional gene composition, at a general process level at least, several studies have shown a correlation between the two[8,14,25]. Functional gene composition variation that is not well explained by taxonomic variation can indicate that phylogenetically unrelated taxa have converged on similar functions and may be crucial for identifying and understanding functional components associated with altered physiological states (Fig. 2).

Factors that drive normal variation

Having established that the healthy gut microbiota is highly variable, we must next understand why it varies, so that this information can be used to tailor therapies or clinical trials. For example, the extent to which members of the same family harbour similar microbes will determine whether the family history of microbiota-driven disease is informative. How much the microbiota varies with age or pregnancy should be taken into account when designing cohorts. The sensitivity of the microbiota to external factors, such as diet, will inform strategies for treating microbiome-linked diseases.

Age

Marked changes in the gut microbiota occur early on in life, with an increase in diversity and stability over the first three years[4,26,27] (Fig. 5). The maturation of the human microbiota is an example of ecological succession[4,26,27]. After the initial colonization, communities undergo consecutive changes in composition and function until a relatively stable climax community is established.

The microbiota in infants is relatively volatile. Variation in microbial communities and functional gene repertoires between individuals is greater in infants than in adults. This has been seen in rural communities in Malawi and Venezuela, and in US metropolitan populations of European and African descent[4]. However, infant microbiomes do share characteristic properties across individuals and populations, both compositional (many bifidobacteria, and lower species richness than in adults) and functional (more genes that encode enzymes involved in folate biosynthesis[4]).

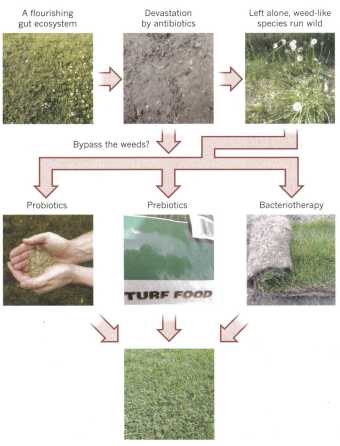

Figure 1 | Maintaining our gut microbial lawn. In some ways, maintaining a healthy microbiota is like lawn care: severe interventions can take the ecosystem back to bare earth, so it has to be re-established. Although many people recover naturally, this is not guaranteed, and weed-like species that are adapted to perturbed ecosystems often run wild. Several strategies can be used to restore the ecosystem: reseeding with a few well-defined 'good' microbes (probiotics), adding compounds that are thought to specifically promote the growth of beneficial microbes (prebiotics) and transplanting the entire microbial ecosystem, for example from a stool sample (faecal bacteriotherapy). The weed stage could be bypassed by administering the treatment immediately after the disturbance before the weeds can establish themselves. An additional strategy (not shown) is to use specific drugs, such as narrow-spectrum antibiotics, that target undesirable members of the microbial community. Although we are beginning to learn what a healthy microbial community looks like, and to recognize signs of weed species, our understanding of which strategies for altering the microbiota work best, and predicting which will work for a given individual, is still in its infancy.

The microbiota of infants is affected by antibiotic use, whether they were breastfed and the method of delivery, although whether differences in the microbiota in early life affect the composition of the adult microbiota is not well understood[28,29]. However, differences in composition driven by factors in infancy may affect susceptibility to immunological diseases into adulthood, such as asthma and atopic diseases[29]. A possible mechanism for this susceptibility has been demonstrated in germ-free mice that accumulate invariant natural-killer T (iNKT) cells in the colonic lamina propria and lungs. The mice were protected from the associated pathology of this accumulation if colonization with a conventional microbiota occurred in neonatal, but not adult germ-free mice, indicating that infancy is a crucial time for contact with the microbiota[5]. Identifying the components of the human microbiota that shape our immune system in early life is now needed.

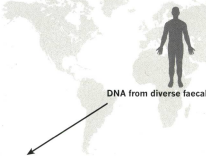

DNA from diverse faecal samples

SSU ribosomal RNA targeted gene sequencing

	S1	S2	S3	S4
OTU01	0	1	5	0
OTU02	1	2	0	7
OTU03	0	0	0	0
OTU04	1	5	2	0
OTU05	0	2	1	0
OTU06	5	1	0	4
OTU07	0	0	2	1

Cultured isolates from faecal samples

Genome sequencing

Genome sequences relate functions to species

Shotgun metagenomic sequencing

	S1	S2	S3	S4
Gene 1	0	1	5	0
Gene 2	1	2	0	7
Gene 3	0	0	0	0
Gene 4	1	5	2	0
Gene 5	0	2	1	0
Gene 6	5	1	0	4
Gene 7	0	0	2	1

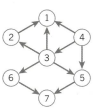

Alpha diversity

Which microbiota are the most compositionally diverse, with the most phylotypes or longest branch length?

If additional taxa (compositional diversity) do not increase the number of functions (functional diversity), there is functional redundancy.

Which microbiota are the most functionally diverse, with the most gene families?

Beta diversity

Which factors, such as age, culture or disease state, correlate with differences in the overall composition of phylotypes or phylogenetic lineages?

Beta diversity plots on the basis of taxonomic and functional composition are usually highly correlated. Therefore, functional genes have considerable phylogenetic signal.

Which factors, such as age, culture or disease state, correlate with differences in the overall composition of functional genes?

Machine learning or classical statistics

Are there phylotypes or collections of phylotypes that discriminate or significantly differ between the microbiota of individuals in different groups – diets or disease states?

Functional differences are often reflective of taxonomic differences. Selected functions that cannot be explained by selected taxonomic groups indicate potential functional convergence.

Are there particular gene families or functions that discriminate or significantly differ between the microbiomes of individuals in different groups – diets or disease states?

Co-occurrence

Which phylotypes co-distribute across people? Positive correlations are driven by shared environmental preferences, symbiotic or syntrophic relationships. Negative correlations are driven by divergent environmental preferences or competitive relationships.

Performing co-occurrence analyses on species with complete genomes can allow for further exploration of the driving factors of positive or negative correlations. For example, genes or functions that are shared by phylogenetically unrelated bacteria that co-occur can indicate potential environmental driving factors.

Which genes co-distribute across people? Positive correlations will largely be driven by genes that co-occur in the same genome (phylotype). Genes with high rates of horizontal gene transfer and strong environmental selection may co-distribute independently.

Metabolic network modelling

What metabolic activities are predicted for a collection of phylotypes?

Metabolic predictions can, in principle, be made for collections of phylotypes if associated reference genome sequences are available.

What overall metabolic activities are predicted for microbiota? What spectrum of metabolites would microbiota produce from a defined diet? Promising for designing personalized therapeutic diets, but has challenges.

Figure 2 | Tools for evaluating microbiota diversity. Targeted sequencing of phylogenetically informative genes (usually small subunit (SSU) ribosomal RNA) or random sequencing of all genes (shotgun metagenomic sequencing) can be used to assess DNA extracted from faecal samples. Genome sequences from cultured isolates link these two data sets by indicating which species contain which genes, and therefore functions. Shotgun metagenomic data will become substantially more useful as the number of reference genomes continues to increase with additional strain sequencing efforts. SSU rRNA gene sequences are related to each other in the form of phylogenetic trees because related phylotypes (clusters of similar sequences defined by sequence similarity) generally have more similar functional attributes. Genes that encode proteins that perform known enzymatic reactions are related using metabolic networks, because genes that participate in the same metabolic pathway can work together to produce a phenotype. Data from SSU rRNA targeted gene and shotgun metagenomic sequencing can be analyzed by the same suite of techniques (detailed in the table and with illustrations to the right). Combining analysis results from targeted and shotgun sequencing data from the same samples, and sometimes using genome sequences to relate the two, can provide additional insight (middle column) Combining targeted sequencing with mRNA, protein and metabolite level analyses will be crucial for moving from *in silico* predictions to direct measurements of expressed community properties. OTU, operational taxonomic unit.

Genetics, environment and diet

How factors such as the environment and diet shape the human gut microbiota is still unclear, partly because these factors are often confounded. Twins and mother-daughter pairs have more similar microbiota compositions than unrelated individuals, suggesting that there could be a genetic influence over the microbiota[9,20]. However, monozygotic and dizygotic adult twins have equally similar microbiota, suggesting environment rather than genetics may drive familial similarities[20].

Populations can be separated by characteristic differences in the gut microbiota. For example, Italian children have a different microbiota from children from rural Africa[30], and both children and adults from the United States have a very different microbiota from populations in Malawi and the Amazonas state of Venezuela[4] (Fig. 5). Although genetically different, these populations also differ in other factors that could affect the microbiota, such as environmental exposures, provision of adequate sanitation and levels of cleanliness, diet and antibiotic use. Cultural factors, especially diet, may be crucial in shaping the gut microbiota. The ratio of two of the main genera of gut bacteria, *Prevotella* and *Bacteroides*, correlates well with the overall pattern of diversity across healthy adults (see discussion of enterotypes later)[31,32]. Levels of *Prevotella* were enriched in children from a rural African village who had a high-fibre diet[30], and in children and adults from Malawi and Venezuela whose diet was dominated by plant-derived polysaccharide foods such as maize and cassava. By contrast, the microbiota of those in the United States had more *Bacteroides*[4]. For healthy adults in the United States, differences in long-term diet between individuals also was correlated with these bacteria. *Bacteroides* was associated with a long-term diet rich in animal protein, several amino acids and saturated fats, and *Prevotella* was associated with carbohydrates and simple sugars[32]. The relative importance of changes in the microbiota as a result of diet, compared with other factors that affect health, remains a subject of active investigation.

Understanding how cultural traditions affect the microbiota should highlight the factors that result in the marked differences in the incidence of diseases associated with microbiota. For example, the incidence of IBD and other allergies is greater in industrialized, Western, societies than in agrarian cultures[33]. Understanding these associations will require expanded studies that sample a greater number of populations and control the confounding factors. This may come in the form of a human microbiome diversity project that parallels the Human Genome Diversity Project[34]. Especially valuable will be populations in which variables that correlate with microbiota diversity — such as history of antibiotic use, diet and environmental exposures — can be measured. Comparisons with environmental exposures may require sampling from the environment as well as from individuals. Because exposure to a microbiota in early life is particularly relevant to the development of immunological disease[5], prospective studies that include infants or even prenatal studies, will be especially valuable. When determining disease aetiology, immigrant populations can provide an opportunity to disentangle host genetics, geography and culture because the incidence of some diseases matches that present at the destination rather than at the origin[35].

Microbiota variability, and human health and medicine

Understanding the compositional and functional differences in the gut microbiota can lay the foundation to relate these differences to human health. Differences in the microbiota and the microbiome could help to explain the variation in the gut metabolic processes of individuals, including the metabolism of drugs and food[11,36]. Many of these metabolic pathways are outside the common functional core, so they can underlie host-specific responses. For example, the health benefits of diets rich in soya, such as improvements in vasomotor symptoms, osteoporosis, prostate cancer and cardiovascular disease, have been attributed to (*S*)-equol produced from the soya isoflavone daidzein by bacterial rather than human enzymes[37]. Only 25–30% of the adult population of Western countries produce (*S*)-equol with a diet of soya-rich foods, compared with 50–60% of adults from Japan, Korea or China[38]. The cancer-protective effects of soya beans that have been described in Asian populations may therefore not be true of Western populations. Similarly, the gut microbiota can indirectly determine whether the widely used analgesic paracetamol will be metabolized to paracetamol sulphate or paracetamol glucuronide, potentially altering its efficacy and toxicity[36]. The microbes mediate this metabolic phenotype by producing the compound *p*-cresol, which competes with paracetamol for human enzymes that catalyse sulphonation[36]. Substantial differences in the gut microbiota between populations and concomitant effects on drug metabolism will necessitate population-specific drug trials for examining effectiveness and toxicity. Understanding how the microbiota varies across the population, and correlating this variability with specific microbial functions, is emerging as a component of personalized medicine.

Stable configurations of healthy microbiota

The landscape of stable states for the human gut is still unknown. Samples obtained over time from the same individual are more similar to one another than those obtained from different individuals, suggesting that each person has a relatively distinct, stable community[20,39–42]. This temporal stability could be related to the concept that stable equilibrium states exist for the microbiota, for which disturbances, stochasticity and temporal dynamics of individual microbes produce change, but the community is still drawn to a central attractor[43,44].

Clinically, it would be convenient if a few clearly differentiable stable states could be used to stratify the gut microbiome across the human population. For example, if microbes in one state were known to metabolize a drug into harmful metabolites, a simple test could avoid complications for the patient, as in the case of paracetamol and liver toxicity[36]. It would be especially helpful if the same states could be applied across the board so that, for example, the same community features that correlated with the generation of toxic metabolites from a drug also correlated with obesity.

Enterotypes propose this concept. The human microbiome has been described to form three distinct host–microbial symbiotic states driven by groups of co-occurring species and genera, which are characterized by a relatively high representation of *Bacteroides*, *Prevotella* or *Ruminococcus*[31]. Although the overall clustering structure, which was based on 33 faecal shotgun metagenomes, was not statistically significant, the three enterotype clusters described the real data better than randomly generated data sets[31]. Similar patterns were reported after existing 16S rRNA data from 154 individuals from the United States[20] and metagenomic data from 85 individuals from Denmark[13] were reanalysed. However, subsequent studies of 98 healthy adults from the United States[22], 531 healthy infants, children and adults from Malawi, Venezuela and the United States[4], and 250 healthy adults from the United States[14] failed to show the same pattern. Variation among adults in these populations was, however, associated with a trade-off between *Prevotella* and *Bacteroides*, suggesting an important role for these taxa, or taxa that co-distribute with them, in structuring the microbiota. When infants were included in the analysis, variation was also associated with a trade-off between the infant-associated *Bifidobacterium* genus and lineages that were common only to adults[4] (Fig. 5). The number of unique configurations that form functional, stable communities may be large and may not be easy to classify into a manageable number of distinct 'types'. Considering this concept further in more extensive data sets made up of different ages, cultural traditions or geographic locations, and physiological or disease states will be important.

Differences in the microbiota with disease

The composition of the microbiota differs with the physiological state of the host. People who are obese harbour fewer types of microbes in their gut than people who are lean, and have a significantly different abundance of specific taxa and functional genes[6,7,45]. Classification

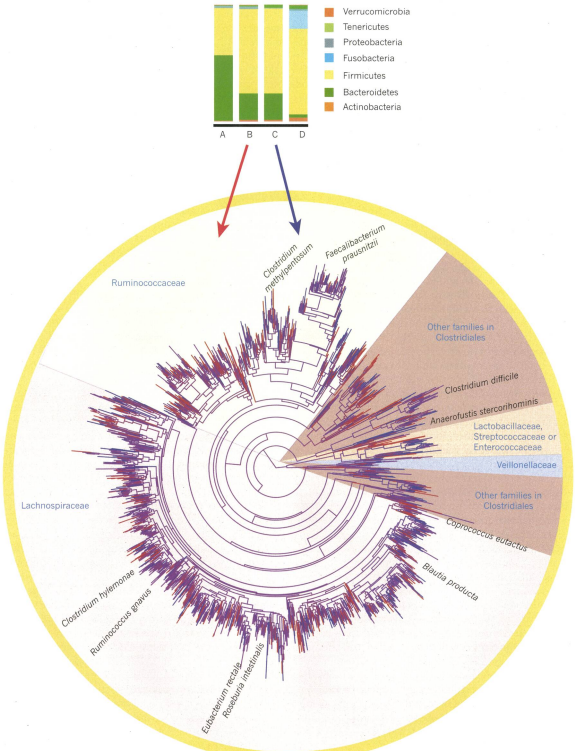

Figure 3 | Diversity of the human microbiota at different phylogenetic scales. The human microbiota is remarkably varied within and between individual hosts. Although this complexity can be simplified by evaluating communities at higher taxonomic levels, the species within each phylum have different biological properties, and significant changes detected at higher taxonomic levels are probably driven by only a subset of the species in those higher taxa. Using the 16S rRNA sequence data of four of the adults from the United States in ref. 4, the high diversity and variability among individuals, and the degree to which taxonomic grouping at high levels can mask this diversity is shown. Phylum level diversity can have a marked variation even across healthy adults in the same population. Individual A has an unusually high proportion of Bacteroidetes; individual D has an unusually high proportion of Fusobacteria; and individuals B and C are dominated by Firmicutes and Bacteroidetes, which is the more typical phylum-level distribution for this cohort. However, even B and C differ at finer scales. The tree depicts the phylogenetic relationships between species-level phylotypes in just the most diverse of the phyla, Firmicutes, in individuals B and C. Branches specific to individual B are red; branches specific to individual C are blue; and shared branches are purple. Each individual has many unique phylotypes not found in the other. As described in many surveys of the human gut[14,18,40], the Ruminococcaceae and Lachnospiraceae families are particularly rich in phylotypes.

of people as lean or obese can be made solely on the basis of their gut microbiota with 90% accuracy[46,47], but they do not separate into distinct microbiota-based clusters on commonly used principal coordinates plots, which are used to identify statistical differences between groups. Thus, multiple statistical techniques are needed to show fully the differences in the microbiota between different physiological states (Fig. 2).

Some differences in the microbiota can contribute directly to disease states. Gnotobiotic mice that were raised germ-free then colonized with the microbiota from an obese mouse gained fat more rapidly than those colonized with the microbiota of a lean mouse[7,45]. A phenotype can emerge from different compositional backgrounds, which may indicate that specific components of the microbiota can exert large effects or that many different changes can lead to the same functional result.

Differences in faecal microbial community diversity, composition and function have also been correlated with Crohn's disease[9], ulcerative colitis[10], irritable bowel syndrome (IBS)[48], *Clostridium difficile*-associated disease (CDAD)[49] and acute diarrhoea[50]. Sometimes, the nature of the microbiota deviation from health is consistent across individuals with the same disease. For instance, a twin study of IBD found marked and reproducible deviations in patients with ileal Crohn's disease relative to the controls, and more subtle, but characteristic, changes in patients with colonic Crohn's disease[51], and specific functional differences were also observed from metabolic profiling of the same samples[24]. Other diseases are associated with marked deviations from health that are inconsistent across individuals. For instance, individuals with recurrent CDAD had a phylum-level diversity that was very different from controls but not similar to each other[49]. Many disease studies are confounded by extensive use of treatments, such as antibiotics, that may obscure true disease-associated changes, highlighting the urgent need for prospective longitudinal studies that establish cause and effect.

Parallels between host physiological states

Studies of the microbiota often target one specific disease or state, but comparisons of the microbiota across many diseases can show common changes in the gut environment. Disturbed mucous layers that line the intestinal cell wall and concomitant inflammation are seen in individuals with IBD, coeliac disease, HIV enteropathy, acute diarrhoea, diverticulosis, carcinoma and IBS[52]. Given these parallels, an increase or decrease in abundance of similar microbes across different disturbances might be expected[53], but elucidation of these differences may require detailed biogeographical studies along the length of the gut — once safe and reliable means for such comprehensive sampling are developed.

Perturbed adult gut microbial communities are intriguingly similar to infant gut microbial communities. Both systems may represent successional communities in which the same opportunistic or fast-growing species can predominate[53]. For instance, *C. difficile* is a normal gut resident that can cause disease when antibiotics compromise the stable adult gut communities; it also colonizes 2–65% of infants, although most infants are asymptomatic[54,55]. *Clostridium bolteae* and *Clostridium symbiosum* are also associated with a disturbed gut and systemic infection, and are found in the infant gut[53]. The microbiota of individuals with ileal Crohn's disease can also resemble that of infants: both have increased levels of *Ruminococcus gnavus* and Enterobacteriaceae in their stools, and an under-representation of the genera that are prevalent in healthy adults, including *Faecalibacterium* and *Roseburia*[51]. These examples show the importance of understanding whether generally opportunistic members of the gut microbiota have a selective advantage during early succession or disruption caused by disease, and therefore whether they are the side effects of disease rather than causal agents.

Resilience of stable states

Resilience is the amount of stress or perturbation that a system can tolerate before its trajectory changes towards a different equilibrium state[56]. Macroecosystem studies of human interference such as

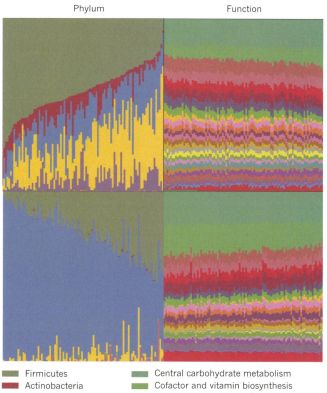

Figure 4 | Functional redundancy. The functional redundancy in microbial ecosystems may mirror that in macroecosystems. As shown in the HMP data set[14], oral communities (top panels) and faecal communities (bottom panels) analysed using 16S rRNA (coloured by microbial phyla, left panels) show tremendous abundance diversity. The same samples analysed by shotgun metagenomics (panels on right) have remarkably similar functional profiles. Reprinted with permission from ref. 14.

resource exploitation, pollution, land-use change and global warming have shown how ecological systems can be transformed into less productive or less desirable states[56]. For example, in a tropical lake community, a regime in which submerged plants dominate is preferred to one with extensive free-floating plant cover because dense mats of floating plants create anoxic conditions that reduce animal biomass and diversity. However, pollution can cause floating plants to predominate because they are better at competing for light and can exclude submerged plants when the nutrient load is high. By understanding the environmental drivers of conversion between states, interventions can be used to induce a regime change. For example, harvesting the floating plants once can induce a permanent shift to the submerged-plant-dominant state, but only if the nutrient loading is not too high[57].

Environmental studies can provide examples of the microbial response to perturbations, and perhaps an insight into how the gut microbiota might react. During the Deepwater Horizon oil spill in the Gulf of Mexico, the microbial community structure and functional gene repertoire in the deep-sea oil plume shifted, transiently, to an enrichment of microbes that were capable of hydrocarbon-degradation[58,59]. This is similar to the effect of an extreme dietary change on the gut microbiota of mice that were moved from a low-fat, plant-rich diet to a high-fat, high-sugar diet[7]. In both cases, the

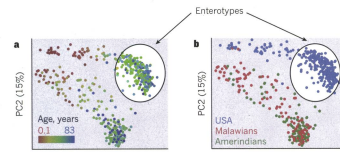

Figure 5 | Human microbial diversity and enterotypes. Enterotypes[31] were determined when evaluating only adults from the United States and Europe (circled in white). By including children from the United States and children and adults from developing countries, the picture of human-associated microbiota diversity greatly expands. The relationship between the microbiota of 531 healthy children and adults from Malawi, Amazonas state of Venezuela (Amerindians) and the United States was evaluated using sequences from the 16S rRNA gene in faecal samples and a principle coordinate analysis of unweighted UniFrac distances (adapted with permission from ref. 4). **a**, Infants differentiate strongly from adults, and **b**, adults from the United States have a distinct composition from those of Malawi and Venezuela, indicating the diversity differences are mainly owing to age and culture.

microbial communities shifted substantially, probably because of the exposure to new substrates that provided a selective advantage to certain members of the community. Whether a particular disturbance will disrupt a stable state depends on the resilience of the community to a type of perturbation.

Dietary changes

Understanding the resilience of the gut microbiota is crucial for determining the efficacy of therapeutic diets. Consuming a carbohydrate- or fat-restricted low-calorie diet for a year[8], or a high-fat and a low-fibre, or low-fat and high-fibre diet for 10 days[32] can induce statistically significant changes in the gut microbiota. However, these changes in species and gene content are small compared with the baseline variations that occur between individuals. Long-term dietary surveys and cross-cultural comparisons suggest that changes to diet might lead to regime changes over longer periods of time[8,32], perhaps by eroding the landscape of alternative stable states to allow changes that short-term 'nudges' cannot.

Antibiotics

Antibiotic administration can move the microbiota to alternative stable states. In healthy volunteers who were given two courses of ciprofloxacin in a 10-month period, the faecal microbiota reached a stable state similar to, yet distinct from, the pretreatment state[41]. However, the magnitude of disturbance that occurred after ciprofloxacin treatment, and the speed and extent of recovery to the pre-ciprofloxacin state, suggested that resilience of the microbiota varies across individuals and between ciprofloxacin treatments in the same individual[41].

Long-term studies of the microbiota after antibiotic treatment indicate that post-antibiotic equilibrium states are themselves resilient. For example, clindamycin treatment affected *Bacteroides* in the gut for up to 2 years after treatment had finished[40]. Similarly, three individuals with dyspepsia treated for 1 week with a combination of metronidazole, clarithromycin and omeprazole had a shift in their microbiota state that persisted for up to 4 years without additional antibiotic treatment[42]. In both cases, a significant increase in the antibiotic-resistance genes persisted for years[42,65], suggesting that the post-disturbance state would probably be more resilient to the same disturbance again because a greater proportion of the microbiota would be resistant. This is consistent with a case from the study of healthy volunteers given the two courses of ciprofloxacin[41]. Initial recovery of the microbiota was slow and incomplete, stabilizing in a different interim state, but after a second treatment, recovery was relatively quick. But in the same study, a different case had the opposite response, in which an essentially complete recovery occurred after the first ciprofloxacin treatment, but stabilized to a distinct state after the second treatment, suggesting that the initial antibiotic treatment decreased resilience[41], and that the resilience of the microbiota to future antibiotic treatments can vary considerably between individuals.

New species invasion

Resilience of the microbiota to challenge with exogenous microbes is also important. The gut microbiota generally shows colonization resistance, in which the native microbiota prohibits harmful (pathogenic)[1,2,63] and potentially beneficial (probiotic)[62] microbes from establishing. Challenging the gut microbiota with a foreign microbiota rather than with specific pathogens or probiotics has suggested the native community may be less resilient to colonization by exogenous microbes than previously thought. When 14 conventionally raised Lewis rats were force fed with pooled microbiota from Sprague-Dawley and Wistar strain rats, the microbiota diversity of the Lewis rats increased substantially and changed to resemble that of the Sprague-Dawley and Wistar rats, and phylotypes established from the donors persisted for up to 3 months after transplantation[63]. In contrast to ecological theory — that disturbances eliminating native species facilitate the establishment of exotic species[64] — transplantation after the resident microbiota have been depleted with two broad-spectrum antibiotics reduced rather than promoted the establishment of the donor microbiota[63].

The success of microbiota transplantation in the treatment of recurrent CDAD provides further support of the plasticity of an established gut microbiota when challenged with a complex one. Bacteriotherapy[65] involves introducing a faecal sample from a healthy donor as a homogenate by injection into the caecum using a colonoscope. In one case study, the symptoms of a patient with recurrent CDAD were resolved after faecal transplantation from a healthy donor. Before treatment, the recipient had a disturbed microbiota with *Veillonella* and *Streptococcus* predominating, whereas the donor microbiota was dominated by *Bacteroides*. A month after treatment, the patient had no *C. difficile* in stool samples, but the donor species were present, indicating that the donor microbiota persisted over this interval. Faecal transplantation for CDAD is becoming increasingly common and seems to be highly effective. A survey of 317 patients across 27 case series reported disease resolution in 92% of cases, with a single treatment being sufficient in 89% of cases[66]. The success of bacteriotherapy suggests that a previous course of antibiotic treatment reduces the resident microbiota to the extent that a donor microbiota can establish itself. However, because faecal transplantation is not a first-line therapy, there are no data on its effectiveness without antibiotics (A. Khorut, personal communication). Understanding the successional processes and which microbial taxa allow a healthy microbiota configuration to be established in faecal transplant recipients will require further studies. These studies will allow the development of a standardized way of formulating and analysing the donor specimen, design and interpretation of dosing studies, and analysis of short- and long-term safety.

Mechanisms for resilience

Understanding how the microbiota forms a stable, resilient state would allow strategies to be devised to increase the resilience of healthy states or decrease the resilience of unhealthy states. For example, a healthy state with a high resilience to exogenous microbes might mean one person at a dinner party escapes food poisoning but their companions with lower resilience fall ill. A degraded microbiota with high resilience can contribute to chronic diarrhoea or inflammation, as is inherent with CDAD, IBD and IBS.

Species and functional response diversity

The aspects of diversity that are crucial for conferring resilience in macroecosystems are probably the same features that are important in microbial ecosystems. One such parameter is the number of species present in a given system, or species richness. (In

culture-independent studies, this number depends on the number of sequences collected per sample.) Species-rich communities are less susceptible to invasion because they use limiting resources more efficiently, with different species specialized to each potentially limiting resource[64]. An excess of nutrients in water, or eutrophication, often decreases ecosystem diversity because a small number of species overgrow and outcompete everything else, with a concomitant decrease in resilience[67]. In a similar way, decreased diversity has been linked to obesity and to a diet that is high in fat and sugar compared with one that is low in fat and plant-based[4,7]. Whether this decrease in microbiota diversity results in a decrease in resilience is not known. Low microbiota diversity also correlates with IBD[51] and recurrent CDAD[49], but the effects on microbiota resilience are not known.

Functional response diversity is the degree to which species in a community that contribute to the same ecosystem function vary in their sensitivity to ecosystem changes[68]. High functional response diversity may, for instance, allow a species that is relatively rare but functionally similar to fill a niche when an abundant species is compromised by an environmental disturbance[68]. In a macroecology example, a compromised coral reef that was in a healthy state changed to an unhealthy, algal-dominated state only when both the algal-grazing fish were overfished and the sea urchins that had increased in numbers to fill this niche were compromised by a pathogen[68]. The same principle is also likely to apply to the gut microbiota. Following antibiotic treatment, a previously rare microbe may increase in abundance to fill a niche that had been dominated by a microbe with higher antibiotic sensitivity, leading to persistence of the same stable state but with a decreased resilience because of the decrease in functional redundancy.

Human-gut-adapted bacteria are likely to have high functional response diversity because phylogenetically disparate microbes often perform similar metabolic functions. For example, methanogenic Archaea, sulphate-reducing bacteria and phylogenetically diverse acetogens in humans and mice all consume hydrogen generated by other microbes during fermentation[69]. Butyrate producers of the Clostridiales order can have different ecological strategies, such as adaptation to different stages of community succession, oxygen tolerance and substrate preference. The abundance of *Anaerostipes caccae* peaks in infancy, whereas *Eubacterium hallii* and *R. intestinalis* are more abundant in adults. *A. caccae* is able to survive 10–60-minute periods of exposure to air better than *E. hallii* or *R. intestinalis*[70]. Furthermore, *E. hallii* but not *F. prausnitzii* can use lactate as a substrate[71]. Thus, butyrate production in the gut can also continue through different successional and metabolic states.

Competition and feedback loops

The densely populated gut environment means that microbes compete to use the same resources or inhibit each other directly using antimicrobial products. Phylogenetically related bacteria could be expected to compete because of their overlapping functional roles, habitats or both, yet contrary to this expectation, phylogenetically similar species tend to appear in the same samples[72]. For example, analysis of bacteria with complete or draft genome sequences from 124 individuals from Europe found that the abundance of related Enterobacter species, including *E. coli*, *Salmonella enterica*, *Citrobacter koseri* and *Enterobacter cancerogenus* were positively correlated across individuals[53]. These related species may share environmental preferences so that they are selected for simultaneously. The abundance of closely related species can also predict the susceptibility to intestinal colonization by both pathogenic and commensal bacteria in mice[73].

Feedback loops can either stabilize or destabilize the microbiota (Fig. 6). Stable physiological states are preserved by negative feedback, in which a change to the gut environment results in opposing changes that maintain homeostasis. This feedback is likely to be controlled by a tight interplay between microbial metabolic activities and host pathways. For example, microbial metabolites might induce changes in the expression of the host pathways that control gut retention time so that it rises above or below the optimum, causing diarrhoea or constipation. This deviation probably induces host signalling pathways to correct it. This is similar to body temperature regulation, in which a rise above the optimum induces thermoregulatory mechanisms such as sweating, and a fall induces mechanisms such as shivering. Stabilizing the physiological parameters that are controlled by negative feedback from the host could therefore promote resilience of the microbiota.

Negative-feedback loops that promote microbiota resilience could also operate independently of the host. For example, if the abundance of a particular microbe exceeds a certain threshold, this would result in a change in the gut environment that would decrease the growth of that microbe relative to other species. These feedback loops may involve the accumulation of a phage specific to that microbe or the accumulation of a specific toxic metabolite. Negative feedback is thought to promote high ecosystem diversity, which can promote resilience[74].

Positive feedback is thought to induce an ecosystem change because a difference from a point in one direction produces further change in the same direction. However, positive-feedback mechanisms could support stability at the individual microbe level or of the microbial consortia that promote each other's growth. Metabolic activities or interactions with host pathways in microbes may induce a physiological state that favours their growth over the growth of potential competitors, promoting resilience. The microbiota is likely to contain both important functional drivers of physiological status and microbes that co-occur with these drivers because they are able to thrive in such an environment. Invasion by microbes that do not thrive in that particular physiological state would be prevented, for example if a microbiota containing functional drivers of a low inflammatory state resists colonization by pathogens, and microbiota with functional drivers of a relatively high inflammatory state resists colonization of beneficial microbes (Fig. 6).

Positive- and negative-feedback loops are also likely to have a role in destabilizing the microbiota during regime changes, such as during succession in early development and following a disturbance (Fig. 6). Negative feedback, whereby an organism's activity alters the environment so that fitness is decreased, can induce a directional change when microbes induce a physiological state that favours their competitors. For instance, the higher redox potential in the gut of infants is probably one of the factors that explains the relative success of facultative anaerobes such as *E. coli* or some *Lactobacillus* in early development[75], but the reduction of oxygen that results from their metabolism favours their eventual replacement by a consortium dominated by strict anaerobes.

The importance of feedback for successional changes is also likely to involve a complex interplay between the microbiota and its host. For example, the same change in redox potential that directly affects microbial fitness can also affect the expression of host factors in the gut epithelium, such as hypoxia-inducible factor, in early development and inflammatory diseases of the gut[76]. Manipulating positive and negative feedback at the level of the host, the individual microbes and the entire gut ecosystem will be essential to maintaining healthy stable states and switching from an unhealthy to a healthy state.

Prospects

High-throughput sequencing of samples suggests that the microbiota of each person has some resistance to perturbation, but that this resistance can be overcome by diet, drugs, prebiotics or probiotics. Dietary changes may alter the regime in the gut over long time periods. The surprising success of whole community transplants in healthy rats and in humans with CDAD shows that exogenous microbes can colonize the gut even with resistance from an entrenched microbiota. However, which microbes will be the best colonizers is unknown; neither do we know how a particular microbial

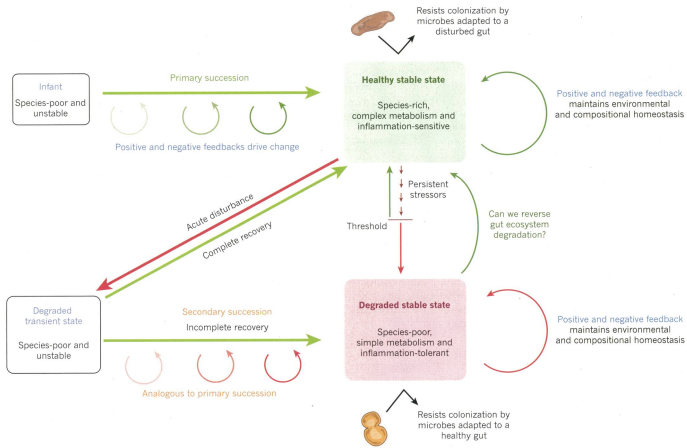
Resists colonization by microbes adapted to a disturbed gut
Infant
Species-poor and unstable
Primary succession
Positive and negative feedbacks drive change
Healthy stable state
Species-rich, complex metabolism and inflammation-sensitive
Positive and negative feedback maintains environmental and compositional homeostasis
Persistent stressors
Threshold
Acute disturbance
Complete recovery
Can we reverse gut ecosystem degradation?
Degraded transient state
Species-poor and unstable
Secondary succession
Incomplete recovery
Analogous to primary succession
Degraded stable state
Species-poor, simple metabolism and inflammation-tolerant
Positive and negative feedback maintains environmental and compositional homeostasis
Resists colonization by microbes adapted to a healthy gut

Figure 6 | Compositional transitions in the human gut microbiota. Primary succession of the gut microbiota during early development involves a systematic turnover of species until a stable adult state is reached. Positive- and negative-feedback loops probably have a role in driving primary succession and in conferring resilience to healthy stable equilibrium states. Acute disturbances, such as antibiotic administration, are often followed by an unstable state that progresses to a stable state through secondary succession. In some cases, a complete recovery occurs, in which the stable state highly resembles the pre-disturbance state, but sometimes the post-recovery stable state is distinct. Post-disturbance stable states may be both degraded and resilient; for example, IBS that forms after an initial acute disturbance of the microbiota from an enteropathogen can persist in some individuals for years and even decades[78]. Resilience of degraded states is probably driven by unique positive- and negative-feedback loops that occur both in concert with and independently of the host. Degradation to a stable state may also occur as a result of persistent stressors, such as poor diet, that slowly degrade resilience of a healthy state until a threshold is passed so that new feedback mechanisms are needed to maintain community composition and stability. Developing therapies that encourage transition from degraded to healthy stable states, or complete recovery to a healthy stable state following disturbance, may involve identifying species or combinations of species, and drivers of feedback loops. Whether interventions are more effective early in succession, when communities are more unstable but possibly stochastic, or later in succession, when convergence to the end point is more certain but the trajectory may be more difficult to change, will be important to investigate.

configuration and its functional attributes change in response to dietary components or exogenous microbes. We need to learn what conditions promote the health of desired species and exclude the undesirable ones, just as a gardener would exclude weeds.

The landscape of stable states for the microbiota and its implications for resilience is an important research direction. Small perturbations, such as short-term dietary changes, may allow the microbiota to return to its original state, but larger disturbances, such as antibiotic administration, could cause movement into a different state. The long-term implications for health are not yet well understood. Furthermore, changes to the stable equilibrium of the gut microbiota through long-term changes, such as inflammation, diet or repeated antibiotic administration, could make new states reachable with smaller perturbations. Host genetics, the factors that affect the microbiota early in development, diet and long-term drug administration may all contribute to individual differences. Consequently, the general landscape and the current community state could be important for determining individual responses to an intervention.

How resilient the microbiota is to diet, disturbance by antibiotics and challenge by exogenous microbes will have important implications for health care. The degree to which repeated applications of broad-spectrum antibiotics degrade the microbiota and its ability to function as a healthy system would need to be studied, especially in children, in whom the development of interactions between the microbiota and host is crucial[5]. However, identifying suitable controls is challenging given the large variation in and between individuals during early development. Regime change is not always instigated by acute disturbances and can occur gradually, as indicated by studies of resilience to dietary changes. Individuals whose microbiota has been degraded by long-term consumption of a high-fat and high-sugar diet may need long-term dietary changes to restore their microbiota to a healthy state.

The lower taxonomic diversity in individuals from Western cultures who have a high-fat and high-sugar diet raises the concern that global trends in diet could result in important microbial symbionts being lost from the broader population, possibly leading to the extinction of bacterial species that can provide important health benefits. Maintaining a collection of cultures from individuals in the developing world, and specifically from agrarian cultures, could help to preserve potentially important components of the microbiota.

Microbes often produce unique states in the gut through collective activities and cooperative metabolism; understanding associations

between disease states and sets of species rather than single taxa will therefore be important[83]. A central problem of culture-independent metagenomic analyses is that identified phylotypes, or collections of these, often represent species for which there is little biological knowledge. Gut microbial ecology has come full circle, with the development of methods for culturing most of the diversity present in a community being given increasing attention so that the contribution that community members make can be further explored. The human faecal microbiota is largely composed of readily cultured bacteria[77]. *In vitro* experiments with these isolates will be extremely valuable for exploring the metabolic attributes of a particular microbe or set of microbes, and the genes involved. However, because microbiota composition and function are also controlled by feedback from the host, *in vivo* studies in gnotobiotic mice will be particularly valuable. Indeed, the component of the microbiota that can be cultured has similar colonization dynamics, biogeographical distribution and response to dietary perturbations as the full microbiota, when transplanted into gnotobiotic mice[77]. A translational science pipeline is developing in which particular phylotypes and their interactions that are important for health or that contribute to disease can be identified on the basis of distribution patterns with disease. Furthermore, the biological attribute that may be driving these patterns can be predicted from the expression or prevalence of functional genes in whole communities and in genomes. Cultures and animal models can be used to test and verify these hypotheses before human application. The tools are now in place and although the path will be difficult, the direction is clearer. ■

1. Candela, M. *et al.* Interaction of probiotic *Lactobacillus* and *Bifidobacterium* strains with human intestinal epithelial cells: adhesion properties, competition against enteropathogens and modulation of IL-8 production. *Int. J. Food Microbiol.* **125,** 286–292 (2008).
2. Fukuda, S. *et al.* Bifidobacteria can protect from enteropathogenic infection through production of acetate. *Nature* **469,** 543–547 (2011).
3. Sonnenburg, J. L. *et al.* Glycan foraging *in vivo* by an intestine-adapted bacterial symbiont. *Science* **307,** 1955–1959 (2005).
4. Yatsunenko, T. *et al.* Human gut microbiome viewed across age and geography. *Nature* **486,** 222–227 (2012).
5. Olszak, T. *et al.* Microbial exposure during early life has persistent effects on natural killer T cell function. *Science* **307,** 1955–1959 (2012).
6. Ley, R. E., Turnbaugh, P. J., Klein, S. & Gordon, J. I. Microbial ecology: human gut microbes associated with obesity. *Nature* **444,** 1022–1023 (2006).
7. Turnbaugh, P. J., Backhed, F., Fulton, L. & Gordon, J. I. Diet-induced obesity is linked to marked but reversible alterations in the mouse distal gut microbiome. *Cell Host Microbe* **3,** 213–223 (2008).
8. Kau, A. L., Ahern, P. P., Griffin, N. W., Goodman, A. L. & Gordon, J. I. Human nutrition, the gut microbiome and the immune system. *Nature* **474,** 327–336 (2011).
9. Dicksved, J. *et al.* Molecular analysis of the gut microbiota of identical twins with Crohn's disease. *ISME J.* **2,** 716–727 (2008).
10. Frank, D. N. *et al.* Molecular-phylogenetic characterization of microbial community imbalances in human inflammatory bowel diseases. *Proc. Natl Acad. Sci. USA* **104,** 13780–13785 (2007).
11. Gonzalez, A. *et al.* The mind–body–microbial continuum. *Dialogues Clin. Neurosci.* **13,** 55–62 (2011).
12. Lupton, J. R. Microbial degradation products influence colon cancer risk: the butyrate controversy. *J. Nutr.* **134,** 479–482 (2004).
13. Qin, J. *et al.* A human gut microbial gene catalogue established by metagenomic sequencing. *Nature* **464,** 59–65 (2010).
14. The Human Microbiome Project Consortium. Structure, function and diversity of the healthy human microbiome. *Nature* **486,** 207–214 (2012).
15. Borenstein, E., Kupiec, M., Feldman, M. W. & Ruppin, E. Large-scale reconstruction and phylogenetic analysis of metabolic environments. *Proc. Natl Acad. Sci. USA* **105,** 14482–14487 (2008).
16. Freilich, S. *et al.* Metabolic-network-driven analysis of bacterial ecological strategies. *Genome Biol.* **10,** R61 (2009).
17. Claesson, M. J. *et al.* Comparative analysis of pyrosequencing and a phylogenetic microarray for exploring microbial community structures in the human distal intestine. *PLoS ONE* **4,** e6669 (2009).
18. Eckburg, P. B. *et al.* Diversity of the human intestinal microbial flora. *Science* **308,** 1635–1638 (2005).
19. Reyes, A. *et al.* Viruses in the faecal microbiota of monozygotic twins and their mothers. *Nature* **466,** 334–338 (2010).
20. Turnbaugh, P. J. *et al.* A core gut microbiome in obese and lean twins. *Nature* **457,** 480–484 (2009).
21. Biagi, E. *et al.* Through ageing, and beyond: gut microbiota and inflammatory status in seniors and centenarians. *PLoS ONE* **5,** e10667 (2010).
22. Nelson, K. E. *et al.* A catalog of reference genomes from the human microbiome. *Science* **328,** 994–999 (2010).
23. Verberkmoes, N. C. *et al.* Shotgun metaproteomics of the human distal gut microbiota. *ISME J.* **3,** 179–189 (2009).
24. Jansson, J. *et al.* Metabolomics reveals metabolic biomarkers of Crohn's disease. *PLoS ONE* **4,** e6386 (2009).
25. Muegge, B. D. *et al.* Diet drives convergence in gut microbiome functions across mammalian phylogeny and within humans. *Science* **332,** 970–974 (2011).
26. Koenig, J. E. *et al.* Succession of microbial consortia in the developing infant gut microbiome. *Proc. Natl Acad. Sci. USA* **108,** 4578–4585 (2011).
27. Palmer, C., Bik, E. M., DiGiulio, D. B., Relman, D. A. & Brown, P. O. Development of the human infant intestinal microbiota. *PLoS Biol.* **5,** e177 (2007).
28. Dominguez-Bello, M. G. *et al.* Delivery mode shapes the acquisition and structure of the initial microbiota across multiple body habitats in newborns. *Proc. Natl Acad. Sci. USA* **107,** 11971–11975 (2010).
29. Kozyrskyj, A. L., Bahreinian, S. & Azad, M. B. Early life exposures: impact on asthma and allergic disease. *Curr. Opin. Allergy Clin. Immunol.* **11,** 400–406 (2011).
30. De Filippo, C. *et al.* Impact of diet in shaping gut microbiota revealed by a comparative study in children from Europe and rural Africa. *Proc. Natl Acad. Sci. USA* **107,** 14691–14696 (2010).
31. Arumugam, M. *et al.* Enterotypes of the human gut microbiome. *Nature* **473,** 174–180 (2011).
This paper reports that there is an association between co-occurring microbial groups, and that *Prevotella* versus *Bacteroides* genus level abundance estimates are associated with major patterns of differentiation in the microbiota across people.
32. Wu, G. D. *et al.* Linking long-term dietary patterns with gut microbial enterotypes. *Science* **334,** 105–108 (2011).
This study found a strong correlation between microbiota diversity and long-term diets as assessed using diet inventories.
33. Loftus, E. V. Jr. Clinical epidemiology of inflammatory bowel disease: incidence, prevalence, and environmental influences. *Gastroenterology* **126,** 1504–1517 (2004).
34. Cann, H. M. *et al.* A human genome diversity cell line panel. *Science* **296,** 261–262 (2002).
35. Bach, J. F. & Chatenoud, L. The hygiene hypothesis: an explanation for the increased frequency of insulin-dependent diabetes. *Cold Spring Harb. Perspect. Med.* **2,** a007799 (2012).
36. Clayton, T. A., Baker, D., Lindon, J. C., Everett, J. R. & Nicholson, J. K. Pharmacometabonomic identification of a significant host-microbiome metabolic interaction affecting human drug metabolism. *Proc. Natl Acad. Sci. USA* **106,** 14728–14733 (2009).
37. Jackson, R. L., Greiwe, J. S. & Schwen, R. J. Emerging evidence of the health benefits of S-equol, an estrogen receptor beta agonist. *Nutr. Rev.* **69,** 432–448 (2011).
38. Setchell, K. D. & Clerici, C. Equol: history, chemistry, and formation. *J. Nutr.* **140,** 1355S–1362S (2010).
39. Caporaso, J. G. *et al.* Moving pictures of the human microbiome. *Genome Biol.* **12,** R50 (2011).
40. Costello, E. K. *et al.* Bacterial community variation in human body habitats across space and time. *Science* **326,** 1694–1697 (2009).
41. Dethlefsen, L. & Relman, D. A. Incomplete recovery and individualized responses of the human distal gut microbiota to repeated antibiotic perturbation. *Proc. Natl Acad. Sci. USA* **108,** 4554–4561 (2011).
This paper gives insight into the resilience of the human microbiota in the face of repeated disturbances, and the degree of baseline variation.
42. Jakobsson, H. E. *et al.* Short-term antibiotic treatment has differing long-term impacts on the human throat and gut microbiome. *PLoS ONE* **5,** e9836 (2010).
43. Beisner, B. E., Haydon, D. T. & Cuddington, K. Alternative stable states in ecology. *Front. Ecol. Environ.* **1,** 376–382 (2003).
44. Walker, B., Hollin, C. S., Carpenter, S. R. & Kinzig, A. Resilience, adaptability and transformability in social-ecological systems. *Ecol. Soc.* **9,** http://www.ecologyandsociety.org/vol9/iss2/art5/ (16 September, 2004).
45. Turnbaugh, P. J. *et al.* An obesity-associated gut microbiome with increased capacity for energy harvest. *Nature* **444,** 1027–1031 (2006).
46. Sun, Y. *et al.* Advanced computational algorithms for microbial community analysis using massive 16S rRNA sequence data. *Nucleic Acids Res.* **38,** e205 (2010).
47. Knights, D., Parfrey, L. W., Zaneveld, J., Lozupone, C. & Knight, R. Human-associated microbial signatures: examining their predictive value. *Cell Host Microbe* **10,** 292–296 (2011).
48. Carroll, I. M. *et al.* Molecular analysis of the luminal- and mucosal-associated intestinal microbiota in diarrhea-predominant irritable bowel syndrome. *Am. J. Physiol. Gastrointest. Liver Physiol.* **301,** G799–G807 (2011).
49. Chang, J. Y. *et al.* Decreased diversity of the fecal microbiome in recurrent *Clostridium difficile*-associated diarrhea. *J. Infect. Dis.* **197,** 435–438 (2008).
50. Young, V. B. & Schmidt, T. M. Antibiotic-associated diarrhea accompanied by large-scale alterations in the composition of the fecal microbiota. *J. Clin. Microbiol.* **42,** 1203–1206 (2004).
51. Willing, B. P. *et al.* A pyrosequencing study in twins shows that gastrointestinal microbial profiles vary with inflammatory bowel disease phenotypes. *Gastroenterology* **139,** 1844–1854 (2010).

52. Swidsinski, A., Loening-Baucke, V. & Herber, A. Mucosal flora in Crohn's disease and ulcerative colitis — an overview. *J. Physiol. Pharmacol.* **60,** 61–71 (2009).
53. Lozupone, C. *et al.* Identifying genomic and metabolic features that can underlie early successional and opportunistic lifestyles in human gut symbionts. *Genome Res.* http://dx.doi.org/10.1101/gr.138198.112 (4 June, 2012).
54. Libby, J. M., Donta, S. T. & Wilkins, T. D. Clostridium difficile toxin A in infants. *J. Infect. Dis.* **148,** 606 (1983).
55. Yamamoto-Osaki, T., Kamiya, S., Sawamura, S., Kai, M. & Ozawa, A. Growth inhibition of *Clostridium difficile* by intestinal flora of infant faeces in continuous flow culture. *J. Med. Microbiol.* **40,** 179–187 (1994).
56. Folke, C. *et al.* Regime shifts, resilience, and biodiversity in ecosystem management. *Annu. Rev. Ecol. Evol. Syst.* **35,** 557–581 (2004).
57. Scheffer, M. *et al.* Floating plant dominance as a stable state. *Proc. Natl Acad. Sci. USA* **100,** 4040–4045 (2003).
58. Hazen, T. C. *et al.* Deep-sea oil plume enriches indigenous oil-degrading bacteria. *Science* **330,** 204–208 (2010).
59. Valentine, D. L. *et al.* Dynamic autoinoculation and the microbial ecology of a deep water hydrocarbon irruption. *Proc. Natl Acad. Sci. USA* http://dx.doi.org/10.1073/pnas.1108820109 (10 January, 2012).
60. Jernberg, C., Lofmark, S., Edlund, C. & Jansson, J. K. Long-term ecological impacts of antibiotic administration on the human intestinal microbiota. *ISME J.* **1,** 56–66 (2007).
61. van der Waaij, D., Berghuis, J. M. & Lekkerkerk, J. E. Colonization resistance of the digestive tract of mice during systemic antibiotic treatment. *J. Hyg. (Lond.)* **70,** 605–610 (1972).
62. McNulty, N. P. *et al.* The impact of a consortium of fermented milk strains on the gut microbiome of gnotobiotic mice and monozygotic twins. *Sci. Transl. Med.* **3,** 106ra106 (2011).
63. Manichanh, C. *et al.* Reshaping the gut microbiome with bacterial transplantation and antibiotic intake. *Genome Res.* **20,** 1411–1419 (2010). **This study indicates that the indigenous microbiota may be more plastic than previously thought. The observation that antibiotic pretreatment interfered with, rather than promoted, establishment of the donor community indicates that low species abundance or diversity alone cannot predict low colonization resistance.**
64. Levine, J. M. & D'antonio, C. M. Elton revisited: a review of evidence linking diversity and invasibility. *Oikos* **87,** 15–26 (1999).
65. Khoruts, A., Dicksved, J., Jansson, J. K. & Sadowsky, M. J. Changes in the composition of the human fecal microbiome after bacteriotherapy for recurrent *Clostridium difficile*-associated diarrhea. *J. Clin. Gastroenterol.* **44,** 354–360 (2010).
66. Gough, E., Shaikh, H. & Manges, A. R. Systematic review of intestinal microbiota transplantation (fecal bacteriotherapy) for recurrent *Clostridium difficile* infection. *Clin. Infect. Dis.* **53,** 994–1002 (2011).
67. Hautier, Y., Niklaus, P. A. & Hector, A. Competition for light causes plant biodiversity loss after eutrophication. *Science* **324,** 636–638 (2009).
68. Elmqvist, T. *et al.* Response diversity, ecosystem change, and resilience. *Front. Ecol. Environ.* **1,** 488–494 (2003).
69. Hansen, E. E. *et al.* Pan-genome of the dominant human gut-associated archaeon, *Methanobrevibacter smithii*, studied in twins. *Proc. Natl Acad. Sci. USA* **108,** 4599–4606 (2011).
70. Flint, H. J., Duncan, S. H., Scott, K. P. & Louis, P. Interactions and competition within the microbial community of the human colon: links between diet and health. *Environ. Microbiol.* **9,** 1101–1111 (2007).
71. Louis, P. *et al.* Restricted distribution of the butyrate kinase pathway among butyrate-producing bacteria from the human colon. *J. Bacteriol.* **186,** 2099–2106 (2004).
72. Chaffron, S., Rehrauer, H., Pernthaler, J. & von Mering, C. A global network of coexisting microbes from environmental and whole-genome sequence data. *Genome Res.* **20,** 947–959 (2010).
73. Stecher, B. *et al.* Like will to like: abundances of closely related species can predict susceptibility to intestinal colonization by pathogenic and commensal bacteria. *PLoS Pathogens* **6,** e1000711 (2010).
74. Bever, J. D., Westover, K. M. & Antonovics, J. Incorporating the soil community into plant population dynamics: the utility of the feedback approach. *J. Ecol.* **85,** 561–573 (1997).
75. Stark, P. L. & Lee, A. The microbial ecology of the large bowel of breast-fed and formula-fed infants during the 1st year of life. *J. Med. Microbiol.* **15,** 189–203 (1982).
76. Glover, L. E. & Colgan, S. P. Hypoxia and metabolic factors that influence inflammatory bowel disease pathogenesis. *Gastroenterology* **140,** 1748–1755 (2011).
77. Goodman, A. L. *et al.* Extensive personal human gut microbiota culture collections characterized and manipulated in gnotobiotic mice. *Proc. Natl Acad. Sci. USA* **108,** 6252–6257 (2011).
78. Dupont, H. L. Gastrointestinal infections and the development of irritable bowel syndrome. *Curr. Opin. Infect. Dis.* **24,** 503–508 (2011).

Acknowledgements We would like to thank L. Parfrey, J. Knight and A. Knight for their comments on this manuscript.

Author Information Reprints and permissions information is available at www.nature.com/reprints. The authors declare no competing financial interests. Readers are welcome to comment on the online version of this article at go.nature.com/7l6f2m. Correspondence should be addressed to R.K. (rob.knight@colorado.edu).

REVIEW

doi:10.1038/nature11551

Reciprocal interactions of the intestinal microbiota and immune system

Craig L. Maynard[1], Charles O. Elson[2], Robin D. Hatton[1] & Casey T. Weaver[1]

The emergence of the adaptive immune system in vertebrates set the stage for evolution of an advanced symbiotic relationship with the intestinal microbiota. The defining features of specificity and memory that characterize adaptive immunity have afforded vertebrates the mechanisms for efficiently tailoring immune responses to diverse types of microbes, whether to promote mutualism or host defence. These same attributes can put the host at risk of immune-mediated diseases that are increasingly linked to the intestinal microbiota. Understanding how the adaptive immune system copes with the remarkable number and diversity of microbes that colonize the digestive tract, and how the system integrates with more primitive innate immune mechanisms to maintain immune homeostasis, holds considerable promise for new approaches to modulate immune networks to treat and prevent disease.

Every one of us enters the world devoid of microbial colonization because of the sterile environment of the womb. This germ-free existence is short-lived: birth exposes the newborn to the microbiota of the mother, setting in motion the colonization of mucosal tissues in the digestive, respiratory and urogenital tracts, and the skin by a diverse microbiota, which we coexist with throughout our lives. The complex and dynamic interaction between the microbiota and its human host is the culmination of nearly half a billion years of co-evolution with vertebrates that has reciprocally shaped the repertoires of the microbiota and the immune system, such that the microbiota in humans is normally restrained and well-tolerated. The scope of this interaction is particularly evident in the intestinal tract, in which the greatest diversity and abundance of microbes reside. Estimated at approximately 100 trillion organisms, most of which are bacteria (although archaea and eukaryotes are also represented), the microbiota numbers about ten times the total cells in the human body, with the greatest density populating the distal ileum and colon[1]. The collective genome, or metagenome, of the intestinal microbiota has more than 100 times the number of genes of the human genome. Each individual is populated by roughly 15% of the 1,000 or more species of intestinal bacteria that have been described[2], which reflects the substantial variability in the composition of the microbiota between individuals. There are, therefore, about tenfold more genes in each of our microbiomes than in each of us, encoding the greatest source of potential antigens for the immune system to cope with, substantially exceeding those of self and pathogen-derived antigens.

The relationship that has been forged between the intestinal microbiota and its human host provides mutual benefits. At homeostasis, the microbiota benefits from the warm, nutrient-rich environment of the gut so it can establish a relatively stable ecosystem. Humans in turn benefit from a highly adaptive metabolic engine that in addition to providing essential non-nutrient factors, such as vitamins, also substantially increases our ability to harvest nutrients from food. This increased digestive capacity is mainly a result of the microbiota's complementation of the limited diversity of complex-carbohydrate-metabolizing enzymes that are encoded in the human genome. In addition, by establishing robust, interlinked metabolic or nutrient networks, and biofilms among its constituents, the microbiota limits the resources available to potential pathogens that must outcompete well-adapted and entrenched resident microbes for metabolic and physical niche space. Resident microbes thereby establish a microbial buffer that limits access by those not part of the consortium.

However, the microbiota is not innocuous, and under conditions that compromise the ability of the host to limit the microbiota's entry from the intestinal lumen, some species can invade host tissues to cause disease. Furthermore, shifts in the composition of the microbiota, whether induced by dietary changes, antibiotic treatment or invasive pathogens, can disturb the balance of organisms in the microbiota and alter the metabolic network of the collective to favour the outgrowth of potentially pathogenic constituents. Referred to as dysbiosis, such changes in the microbiota can perturb immune regulatory networks that normally restrain intestinal inflammation, and may contribute to immune-mediated disease directed against antigens of the microbiota. Dysbiosis is most often associated with inflammatory bowel disease (IBD), including Crohn's disease and ulcerative colitis, and necrotizing enterocolitis in premature infants. But it is also increasingly linked to a number of extraintestinal immune-mediated diseases, including rheumatoid arthritis, multiple sclerosis, diabetes, atopic dermatitis and asthma, as well as obesity and metabolic syndrome, all of which could have their pathogenic origins in untoward reactivity of the immune system to the microbiota. Whether dysbiosis is a cause or effect of these disorders remains to be determined, but understanding the factors that lead to alterations in the composition of the microbiota in these conditions promises to be informative, irrespective of their basis.

In this Review, we highlight advances in our understanding of the immune mechanisms by which the dynamic interplay of the intestinal microbiota and its host normally favours a homeostatic, mutualistic relationship, as a basis for understanding the causes of breakdowns in this relationship that lead to disease.

Co-evolution of the microbiota and adaptive immunity

Vertebrate evolution coincided with the emergence of the adaptive immune system, the main components of which are T and B lymphocytes. The acquisition of genetic recombinatorial mechanisms for generating diverse, anticipatory antigen-recognition receptors on T cells and B cells allowed specific responses to a vast diversity of antigens, and long-lived immune memory. Although evolutionary pressures that have shaped immune strategies are often viewed in the context of host defence, it has been proposed that the emergence of adaptive immunity

[1]Department of Pathology, The University of Alabama at Birmingham, Birmingham, Alabama, USA; [2]Department of Medicine, The University of Alabama at Birmingham, Birmingham, Alabama, USA.

could have been driven as a means to foster, rather than limit, microbial colonization[3]. In this view, a substantial survival advantage would have been afforded to organisms that could harness the extended and more flexible metabolic capacity derived from a permanent, diverse intestinal microbiota, as long as the attendant infectious risk could be mitigated. Adaptive immunity might have allowed this.

By adding new layers — such as secretory IgA (sIgA) — to existing innate barrier defences, early vertebrates with adaptive immune mechanisms could begin to promote colonization of their alimentary tracts by exerting selective pressures that favoured resident microbes that were relatively innocuous, but metabolically useful. The survival benefits that accrued as a result of derivation of nutrients from a broader range of foods could have been a major factor in the evolutionary success of vertebrates[3]. The emergence of adaptive immunity provided a means to recognize, and remember, both beneficial and detrimental members of the intestinal microbiota to foster maintenance of beneficial species at the expense of detrimental ones. In doing so, the emerging adaptive immune system would have had to acquire mechanisms for tempering innate immune responses programmed only for the clearance of microbes. The development of a broad repertoire of immune cells that could suppress, as well as promote, innate inflammatory mechanisms contingent on the threat level of the microbe they recognized would become invaluable.

Support for this hypothesis comes from the study of the diversity of the microbiota in invertebrates, which seems to be far less complex than the microbiota of vertebrates[2]. Although data on comparative metagenomics are limited, the highest density of bacteria found in either organisms or the environment is in the human colon[1]. The intestinal microbiota of vertebrate species as divergent as rodents and zebrafish share similar complexity to that of humans, and their gastrointestinal tracts are similarly colonized soon after birth[4]. Further, a homologue of sIgA was recently identified in bony fish[5]. Now extending to all jawed vertebrate taxa, except cartilaginous fish and reptiles, this unique class of immunoglobulin is adapted for interactions with the commensal microbiota and mucosal pathogens. It is tempting to speculate that the development of multimeric mucosal IgA, and adaptations that effect its efficient transport across the mucosal epithelium, and the compartmentalization of the gut-associated lymphoid tissues (GALT) from the peripheral immune system were essential adaptations that allowed vertebrates to harness a complex intestinal microbiota. Although more work is needed to establish a comparative map of the microbiota in the digestive tracts of more vertebrate and non-vertebrate species, it is anticipated that the merger of comparative studies in metagenomics and immunology will yield insight into the adaptive mechanisms that have allowed vertebrates to become an evolutionary success. It may yet prove that we owe it to the bugs that have become 'us.'

The microbiota and the developing immune system

The mammalian immune system is perhaps the most elaborate example of the complex symbiotic relationship that has resulted from the co-evolution of vertebrates and their microbiota. Unlike other vertebrates, placental mammals give birth to live young that are carried to term *in utero* and are nursed with milk that is rich in maternal antibodies. These antibodies provide passive transfer of immunity from mother to infant, which has implications for the developing immune system of the infant, and the microbiota that colonize the gut.

Maternal effects on the neonatal microbiome

The greatest initial contribution to the composite human–microbiota 'superorganism' is the vertical transmission of components of the mother's microbiota to the child at birth. Normally, intestinal colonization of neonates is dominated by transmission of bacteria from the maternal vaginal flora, which is less diverse than that of the lower intestinal tract[6]. The 'pioneer' species received from the mother seem to be important, because infants born by Caesarean section — who are initially colonized by bacterial species of epidermal, rather than vaginal, origin — are predisposed to development of allergies and asthma later in life[7]. This is despite the fact that, although Caesarean-section-born infants lag behind those born transvaginally in their acquisition of the two bacterial divisions dominant in the adult microbiota (Firmicutes and Bacteroidetes), they do catch up. Conversely, mother-to-child transmission in neonates delivered transvaginally rapidly shifts to skin and oral ecologies postpartum, such that these infants are later exposed to similar species as those delivered through Caesarean section. Thus, first contact could be deterministic. That is, pioneer bacterial species might have substantial and lasting effects on the immune response, irrespective of the composition of the mature microbiota.

The neonatal microbiota varies erratically until about 1-year-old when it stabilizes, establishing a consortium that resembles that of adults[8]. During this initial period, the neonatal immune system rapidly matures under the influence of the microbiota. Although environmental factors such as diet, exposure to new microbes, xenobiotics, bacteriophages and intestinal infections have important roles in shaping the composition of the microbiota during this maturational window, the part the neonatal immune system plays is less clear. What is clear is the initial and ongoing influence of breastfeeding on the infant's microbiome. In addition to a unique mix of nutrients and antimicrobial proteins that influence the ecology of the neonatal microbiota, breast milk provides abundant sIgA, the specificities of which have been shaped by the maternal microbiota. The mucosal immune memory of the mother is thereby transmitted to her offspring. Thus, in breastfed infants delivered transvaginally, the intestinal microbiota is not only seeded by maternal bacterial species, but its composition may also be reinforced and shaped by the maternal sIgA repertoire that is influenced, in turn, by the maternal microbiota.

Maturation of the infant mucosal immune system takes months, so the passive transfer of maternal sIgA has a considerable protective role against potential pathogens that could perturb the ecological trajectory of the infant's intestinal microbiota. Maternal sIgA also shields the neonatal immune system from its own microbiota, perhaps so the neonate's defences are not overwhelmed before they are fully developed. In so far as microbial antigens that are bound by sIgA are handled by the innate immune system in a 'tolerogenic' mode, partly owing to IgA's poor fixation of complement, transfer of maternal sIgA to the infant seems to favour the establishment of regulatory immune networks in the infant that promote a mutualistic relationship with the microbiota. Thus, in addition to the direct effect of maternal sIgA on the microbiota of the infant, it also has immunomodulatory effects on the developing infant's immune repertoire so as to indirectly influence its microbiota. The maternal–neonate metagenomic bond is, therefore, extended postnatally, providing one mechanism by which microbial ecologies tend to cluster in family members.

Microbiome effects on developing host–barrier defence

Maturation of the intestinal mucosa and its GALT — Peyer's patches of the distal ileum, isolated lymphoid follicles (ILFs) and mesenteric lymph nodes (MLNs) — is initiated by, and contingent on, intestinal colonization. Peyer's patches and MLNs develop prenatally, but ILFs develop postnatally[9]. However, each of these lymphoid tissues requires signals derived from the sensing of intestinal microbiota for their complete development, recruitment of a mature complement of immune cells, or both. Similarly, non-lymphoid structures of the intestinal mucosa that contribute to the establishment of host–microbiota mutualism are driven by colonization of the neonate.

Preparation for the adaptive immune response to neonatal colonization requires the prenatal actions of a subset of innate lymphoid cells (ILCs), termed lymphoid tissue inducer (LTi) cells (Fig. 1). LTi cells are instrumental in prenatal organization of the development of lymphoid tissues, including the components of the GALT. LTi cells develop in the fetal liver from a common lymphoid precursor that gives rise to all lymphoid cells. During fetal development, LTi cells disseminate to the MLN and Peyer's patches anlagen, stimulating the development of these structures, and the recruitment and partitioning of B and T cells into B-cell follicles and T-cell zones that characterize secondary lymphoid tissues[8,10].

The development of ILFs is also dependent on LTi cells, but is initiated

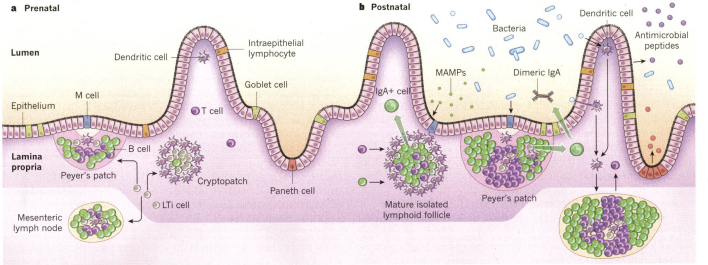

Figure 1 | The gut-associated lymphoid tissue establishes perinatal host-microbiota mutualism in the intestine. a, Prenatally, secondary lymphoid tissues (Peyer's patches and mesenteric lymph nodes) and cryptopatches develop by the spatiotemporal recruitment of lymphoid tissue inducer (LTi) cells to sites of the developing intestine and supporting neurovascular structures. This, in turn, stimulates the recruitment of dendritic cells, T cells and B cells in preparation for the immune response to the microbiota. Intraepithelial lymphocytes seed the epithelium before birth. **b**, Postnatally, bacteria colonize the neonatal intestine immediately, initiating multiple events that affect the development or functional maturation of the mucosa and gut-associated lymphoid tissues. Shown from left to right: microbe-associated molecular patterns (MAMPs) sensed by pattern-recognition receptors on intestinal epithelial cells and dendritic cells adjacent to cryptopatches stimulate the further recruitment of B cells and T cells, causing the cryptopatches to develop into mature isolated lymphoid follicles. The isolated lymphoid follicles release IgA-producing plasma cells — which are formed through T-cell-dependent and independent interactions — into the lamina propria. Microbes also cross the epithelium and enter Peyer's patches through M cells, from which they are endocytosed by dendritic cells in the subepithelial dome. Antigen-loaded dendritic cells in the Peyer's patch interact with local lymphocytes to induce T-cell differentiation and T-cell-dependent B-cell maturation in the germinal centre to induce the development of IgA-producing plasma cells that home to the lamina propria, where they release dimeric IgA for transport into the intestinal lumen. Dendritic-cell-mediated luminal sampling of microbial products or transcytosis of bacteria across the epithelium results in antigen loading of lamina propria dendritic cells, which then migrate through the afferent lymphatics vessels (not shown) to a draining mesenteric lymph node to induce differentiation of effector T cells that traffic to the lamina propria. Shown on the far right, sensing of MAMPs stimulates the proliferation of intestinal epithelial cells in crypts, resulting in their increased depth and, in the small intestine, increased density of Paneth cells. This sensing also arms the intestinal epithelial cells for release of antimicrobial peptides.

after birth when these cells cluster in the lamina propria below the intestinal crypts, forming cryptopatches[11]. ILFs develop from cryptopatches only after colonization by the intestinal microbiota. Central to sensing the colonizers of the intestinal tract is the expression of a diverse range of germline-encoded pattern-recognition receptors (PRRs) by intestinal epithelial cells (IECs) and immune cells resident in the gut. These receptors include transmembrane Toll-like receptors (TLRs) and C-type lectin receptors (CLRs) that reside on the cell surface or in endosomes, and cytosolic nucleotide-binding oligomerization domain (NOD)-like receptors (NLRs), which cells of the intestinal mucosa use to detect microbe-associated molecular patterns (MAMPs) that are expressed by constituents of the resident microbiota, as well as pathogens. MAMPs are recognized — through mechanisms that are not well understood — by cells in the neonatal gut, stimulating ILF development to generate a lymphoid structure that is capable of supporting the maturation of B cells that produce sIgA. At least one of the microbial products that induces this process is peptidoglycan derived from Gram-negative bacteria. Recognition of peptidoglycan by NOD1 in IECs elicits production of CCL20 and β-defensin 3 that direct the recruitment of B cells to LTi–dendritic-cell clusters in cryptopatches to induce the expression of sIgA (ref.12).

Unlike MLNs and Peyer's patches, for which class-switch recombination to produce IgA is T-cell dependent, IgA class-switching in ILFs can occur through T-cell-dependent and -independent pathways[13]. In addition, MLNs and Peyer's patches are unique to mammals, whereas ILFs are found in non-mammalian vertebrates, suggesting that they are the evolutionary forerunners of the secondary lymphoid tissues of the GALT[14] and may have evolved to accommodate, and promote, an increasingly complex intestinal microbiota before specialized secondary lymphoid tissues emerged. The importance of ILFs in regulating the microbiota is evident in mice that are devoid of these structures, and in which Gram-negative bacteria are over-represented[12]. Similar to Peyer's patches, ILFs develop in the intestinal mucosa in intimate association with the overlying intestinal epithelium (Fig. 1). Both structures are strategically deployed to sample the microbiota through specialized microfold, or M, cells, which transport intact microbes or their products across the epithelial barrier. In this way, the innate and adaptive immune systems constantly monitor the microbiota and are 'informed' of the dominant bacterial species that reside in proximity to the epithelium.

Like the GALT, the epithelium of the fetal and newborns' intestine is incompletely adapted to dense bacterial colonization, but responds rapidly to perinatal colonization to accommodate the microbiota. Expression of — and signalling by — TLR4, which is the receptor for the abundant product of Gram-negative bacteria, lipopolysaccharide, are significantly increased antecedent to intestinal colonization at birth[15]. Within hours of exposure to the microbiota, the response of IECs to lipopolysaccharide is markedly attenuated through the down-regulation of TLR4 and components of its signalling apparatus. This increase in TLR4 expression and signalling followed by down-regulation seems to represent a mechanism whereby the fetal epithelium is primed to transmit transient inflammatory signals on sensing the microbiota to promote an early immune response, but then becomes rapidly desensitized as an adaptation to the mounting bacterial load.

An additional immune mechanism that prepares the neonate for commensal colonization is the seeding of the intestinal epithelium with specialized intraepithelial lymphocytes before birth. Intraepithelial lymphocytes intercalate between IECs where they exist in an activated state and can respond rapidly to microbial encroachment. Throughout life, intestinal intraepithelial lymphocytes help to maintain the integrity of the epithelial-cell barrier, limit bacterial translocation and facilitate epithelium repair after injury by secreting soluble mediators, such as antimicrobial peptides[16].

Although the host has evolved elaborate developmental strategies to prepare for postnatal colonization, the microbiota reciprocates by inducing maturation of the host's immune system. Therefore, compared with conventionally raised mice, germ-free or 'germ-reduced' mice have reduced size and cellularity of secondary lymphoid tissues as well as altered numbers, frequencies or diversity of immune-cell populations at mucosal sites, and thus mount abnormal responses to infection and injury. In addition, a postnatal time window is thought to exist in which regulatory T (T_{reg}) cells[17] and invariant-natural killer T (iNK T) cells[18] that have received their 'primary education' in the thymus, receive a 'secondary education' from the microbiota to establish a durable immune repertoire that is crucial to the prevention of inflammatory diseases in childhood and adulthood.

Innate pathways to sense and restrain the microbiota

The intestinal tract is the largest barrier tissue in the human body (it has a surface area of about 300 m^2 in adults), making it the most extensive portal for entry of commensal or pathogenic microbes. Highly specialized barrier defences have evolved to confine the microbiota and resist pathogens, while maintaining its main function of nutrient uptake. The strategy is one of a layered defence that integrates a stratified mucous layer, a relatively impenetrable but highly responsive epithelium, and a lamina propria populated by innate and adaptive immune cells that actively participate in homeostatic responses to restrain the microbiota without undue inflammation, yet are poised for the induction of antimicrobial clearance responses and tissue repair, should the barrier be breached.

Reciprocity between the epithelium and the microbiota

The epithelium is central to the orchestration of intestinal defences. Not simply a passive barrier to microbial translocation, the intestinal epithelium is an active sensor of, and conduit for, the dialogue between the host and microbiota. The five main cell types that comprise the epithelium — absorptive enterocytes, goblet cells, Paneth cells, M cells and enteroendocrine cells — develop from a common stem cell located near the base of the intestinal crypts. Each cell type has a specialized, integral role in intestinal homeostasis, and is both responsive to the microbiota and conditioned by it (Fig. 1).

Maintaining the polarized structure of the epithelial barrier is crucial to its function. The tight junctions that seal the interfaces of adjacent IECs segregate the epithelium into an apical, lumen-exposed surface and a basolateral surface anchored to the basement membrane. Depending on whether the membrane-associated PRRs are arrayed on the apical or basolateral surface of the IECs and on which side of the epithelial barrier MAMPs are detected, cells of the epithelium initiate responses that either promote the release of protective factors that are directed luminally (for example, secreted mucins and antimicrobial peptides) to directly restrain the microbiota, or internally (for example, cytokines and chemokines) to either promote immune quiescence at homeostasis or activate inflammatory immune responses when the epithelial barrier has been breached.

As a mucosal tissue, the intestinal epithelium continuously produces and is invested by a layer of mucus that is a first line of defence against microbes (Fig. 2). Mucus is produced by goblet cells and is composed of heavily glycosylated mucin proteins, as well as other protective molecules, such as trefoil factor, that contribute to epithelial restitution and repair. Production of intestinal mucus is regulated by products of the microbiota. In germ-free mice the mucous layer in the colon is highly attenuated, despite normal numbers of mucin-laden goblet cells. Addition of the MAMP lipopolysaccharide or peptidoglycan stimulates the release of mucin by goblet cells and the rapid reconstitution of the colonic inner mucous layer[19]. Butyrate produced by benign constituents of the microbiota also promotes increased release of mucin, providing a positive-feedback loop for maintenance of the mucous barrier and its colonization by butyrate-producing commensals. The importance of the mucus layer is evident in mice deficient for principal intestinal mucin, Muc2. These mice have increased translocation of commensal and pathogenic bacteria[20], and spontaneously develop colitis[21]. Components of the healthy microbiota therefore directly contribute to the barrier function of the intestine through their induction of mucin production and secretion by goblet cells.

The thickness and continuity of intestinal mucus differs regionally: it is thinner and discontinuous in the proximal small intestine and becomes thicker and continuous in the distal small and large intestine[22], showing some correlation with the local bacterial load (10^3–10^5 organisms per gram of luminal contents in the duodenum and jejunum; about 10^8 organisms per gram in the ileum, and 10^{10}–10^{12} organisms per gram in the colon). The mucus is stratified into two functionally distinct layers: a compact, firmly adherent inner layer that is sparsely populated by bacteria and a more loosely structured, non-adherent outer layer that is at least tenfold more densely populated by the microbiota[22].

Although both mucous layers have a similar Muc2-dominated composition, proteolytic cleavage of Muc2's polypeptide backbone in the outer layer results in its expanded volume and accessibility to colonization by components of the microbiota[22]. Indeed, the outer mucous layer provides an anchor for the attachment of bacteria of the microbiota that can establish biofilms that exclude pathogens. Furthermore, in addition to dietary glycans, mucin glycans are nutrients for some constituents of the microbiota, such as *Bifidobacterium* and *Bacteroides* spp., thereby promoting their retention in the collective (Box 1). These bacteria ferment complex O-linked mucin glycans to produce short-chain fatty acids (SCFAs) derived from mucin catabolism (for example, acetate and lactate) that are toxic to some pathogens[23], and produce other metabolites (such as, proprionate and butyrate) that are the main nutrient source for colonic IECs. The SCFAs also signal through

BOX 1

Modulation of the microbiota by blood-group antigens

An important aspect of the microbiota's use of the intestinal mucous layer as an ecological niche is its decoration by blood-group antigens. Analogous to blood-group antigens on erythrocytes, the assembly of type A, B or Lewis-b glycans on intestinal mucins is contingent on the generation of the core H-glycan by the actions of FUT2. This protein is encoded by *FUT2*, which is functional in most individuals (secretor genotype), but is non-functional in a significant minority (about 20% of Caucasians, referred to as non-secretors) owing to a missense mutation. The presence or absence of a functional *FUT2* allele correlates strongly with the composition of the microbiota[87]. In particular, *Bifidobacterium* spp., which are a beneficial component of the microbiota, are dependent on the terminal blood-group glycans for colonization of the intestinal mucus and are less abundant in non-secretor genotypes. The non-secretor phenotype is associated with necrotizing enterocolitis and Gram-negative sepsis in premature infants[98], as well as those with Crohn's disease[99]. Therefore, it seems that the protective benefits of colonization by *Bifidobacterium* spp. are a mutually beneficial evolutionary adaptation of this commensal to its host. Given the predisposition to dysbiosis and its deleterious health effects in non-secretors, it is likely that evolutionary pressure to retain the defective *FUT2* allele in the population is a result of mucin-linked blood-group glycans also serving as sites of attachment for mucosal viruses (such as noroviruses) so that those with a non-secretor genotype are protected[100].

G-protein-coupled receptors on IECs, to downregulate host inflammatory responses[24]. Thus, colonization of the outer mucous layer by commensals is an important adaptation that supports a stable host–microbiota relationship.

In contrast with the outer mucous layer, the inner mucous layer provides a relatively impermeable barrier against the microbiota. This characteristic is a result of the layer's compact physicochemical structure and its function as a reservoir for microbicidal products of the epithelium, including antimicrobial peptides that are specialized to kill different classes of microbes and sIgA, which is retained in the mucous layer after being shuttled across the epithelium by polymeric immunoglobulin receptor (pIgR) (Fig. 2). Effectively, the inner mucous layer is a 'killing field' that few pathogens or commensals have evolved strategies to penetrate. This microbe-sparse zone is enforced, in part, by the antibacterial lectin Reg-IIIγ (ref. 25). Because Reg-IIIγ is selectively bactericidal for Gram-positive bacteria, it is likely that antimicrobial peptides specific for Gram-negative bacteria also contribute to the microbe-sparse zone. A similar spatial segregation of bacteria from the epithelium has been identified in the colon, in which a thicker inner mucous layer excludes most bacteria even in the face of a substantially higher bacterial load[22].

The region of the intestinal tract with the poorest coverage of protective mucous, the proximal small intestine[22], also has the greatest exposed epithelial surface area owing to its prominent villous structure. Although this feature favours digestion and absorption of nutrients it also seems to make the epithelium in this region particularly vulnerable to entry by the microbiota and pathogens. However, the bacterial loads in this region are the lowest along the length of the intestine, with over a million-fold fewer bacteria per unit of luminal contents than the large intestine. This is, in part, owing to the more vigorous peristaltic motility of the proximal small intestine, which rapidly clears material, including microbes, from the lumen. The lumen of the proximal small intestine is also the entry point for the contents of the gall bladder and stomach, which contain high levels of bile salts and acid that have antimicrobial effects.

In addition, the bases of the crypts of the small intestine are home to many Paneth cells. These IECs are arrayed with a range of PRRs and are specialized for the production and release of abundant antimicrobial peptides, including α-defensins, which are small, highly cationic microbicides unique to Paneth cells. In contrast with other antimicrobial peptides, such as Reg-IIIγ, synthesis of which requires signals from the microbiota[26], α-defensins are synthesized and stored in Paneth-cell granules without the need for sensing of MAMPs. However, the release of Paneth-cell granules is induced by MAMPs, and the secretion of active α-defensins has been shown to control the composition of the microbiota[27]. *NOD2*, which was the first susceptibility gene linked to Crohn's disease[28,29], encodes an NLR that is important in sensing the microbiota to control the release of antimicrobial peptides by Paneth cells. Deficiencies of antimicrobial peptide production, such as occur in NOD2 mutants, are thought to result in altered microbiota composition and density in the small intestine that heighten susceptibility to intestinal inflammation, particularly in the terminal ileum where the highest density of Paneth cells are found.

Colonic IECs also regulate the composition of microbiota through PRR-dependent mechanisms. Mice deficient in the NLRP6 inflammasome in colonic IECs have an altered microbiota that confers increased susceptibility to colitis because of damage to the colonic epithelium[30]. The increased susceptibility to colitis that results from NLRP6 deficiency is transmissible to wild-type mice, indicating that a dysbiotic flora is a contributory factor. How deficiency of the NLRP6 inflammasome results in an altered microbiota is incompletely defined, although reduced interleukin (IL)-18 levels in NLRP6-deficient mice suggests this cytokine has an important role.

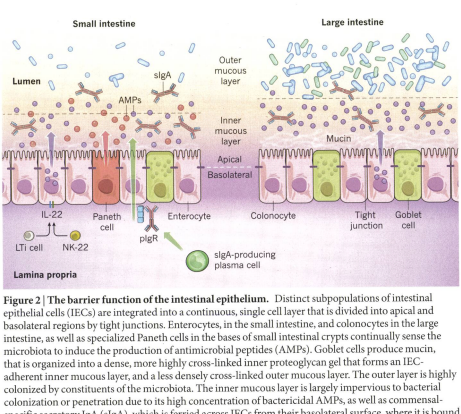

Figure 2 | The barrier function of the intestinal epithelium. Distinct subpopulations of intestinal epithelial cells (IECs) are integrated into a continuous, single cell layer that is divided into apical and basolateral regions by tight junctions. Enterocytes, in the small intestine, and colonocytes in the large intestine, as well as specialized Paneth cells in the bases of small intestinal crypts continually sense the microbiota to induce the production of antimicrobial peptides (AMPs). Goblet cells produce mucin, that is organized into a dense, more highly cross-linked inner proteoglycan gel that forms an IEC-adherent inner mucous layer, and a less densely cross-linked outer mucous layer. The outer layer is highly colonized by constituents of the microbiota. The inner mucous layer is largely impervious to bacterial colonization or penetration due to its high concentration of bactericidal AMPs, as well as commensal-specific secretory IgA (sIgA), which is ferried across IECs from their basolateral surface, where it is bound by the polymeric immunoglobulin receptor (pIgR), to the inner mucous layer where it is released by proteolytic cleavage of pIgR. Responding to the microbiota, innate lymphoid cells, including RORγt- and AhR-expressing LTi and NK-22 cells, produce IL-22, which stimulates AMP production and promotes epithelial barrier integrity.

Reciprocity between the epithelium and innate immune cells

Although the intestinal mucous layer largely insulates the intestinal epithelium from direct interactions with the microbiota, bacterial metabolites and components are able to permeate this zone and alter gene expression in IECs through PRRs[31]. In addition to the epithelial products that are secreted apically to restrict contact with the microbiota (for example, mucins and antimicrobial peptides), the epithelium also produces factors, such as chemokines and cytokines, that are secreted basolaterally. These factors signal immune cells residing internal of the epithelium, particularly in the intestinal lamina propria (Fig. 3). Activation of PRRs typically promotes pro-inflammatory innate responses, so the intestinal epithelium had to evolve strategies to mitigate these responses for commensals such that, at homeostasis, cytokine signals transmitted to mucosal immune cells limit inflammation. Several mechanisms by which this anti-inflammatory state is favoured have emerged.

The strategic distribution of TLRs and NLRs on and within IECs has a considerable effect on whether bacterial MAMPs will be recognized, and if so, whether their recognition promotes pro-inflammatory responses or represses them. Pathogenic bacteria possess virulence factors to allow them to attach to or invade IECs thereby introducing MAMPs into the IEC cytosol where they are recognized by NLRs; however, bacterial strains of the indigenous microbiota are non-invasive and therefore less potent activators of NLRs. In the intact epithelium,

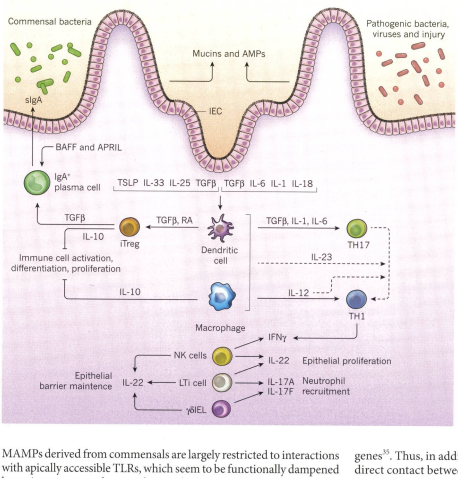

Figure 3 | The epithelial-innate-adaptive continuum in response to microbial antigens. a, In response to the microbiota, IECs secrete mucins and AMPs that limit microbial interaction with epithelial cells. Under homeostatic, eubiotic conditions, MAMPs stimulate the secretion of cytokines (including TSLP, IL-33, IL-25, and TGFβ) by IECs that promote development of tolerogenic macrophages and dendritic cells. Dendritic cells, in turn, induce the development of induced T_{reg} (iT_{reg}) cells through a TGFβ- and retinoic acid (RA)-dependent process. Through multiple mechanisms, including the secretion of TGFβ and IL-10 by iT_{reg} cells and the secretion of IL-10 by macrophages, the anti-inflammatory balance of the intestine is maintained by inhibiting or dampening potential effector responses. In addition, T_{reg} cell-derived TGFβ and epithelial-derived BAFF and APRIL promote development of IgA^+ plasma cells to ensure an abundant supply of sIgA in the lumen that further limits microbial interaction with the epithelium. **b**, In the face of pathogen invasion, mucosal injury or dysbiosis, MAMPs stimulate the secretion of pro-inflammatory cytokines by IECs (including, IL-6, IL-1 and IL-18) and intestinal dendritic cells and macrophages (including IL-6, IL-23 and IL-12) that induce development of the effector $CD4^+$ T cells T_H1 and T_H17, the latter of which can transition to the former as a result of IL-23 or IL-12 signalling. Intestinal innate lymphoid cells, including NK-like cells, LTi cells, and γδIELs, respond to pro-inflammatory cytokines to upregulate IL-22, which helps to protect the epithelial barrier, and IL-17A and IL-17F, which are involved in neutrophil recruitment.

MAMPs derived from commensals are largely restricted to interactions with apically accessible TLRs, which seem to be functionally dampened by tonic exposure to the microbiota, whether through decreased expression, impaired signalling or both.

By contrast, expression of TLRs on the basolateral aspects of IECs can signal a barrier breach by both commensals and pathogens. This is exemplified by TLR5, the receptor for flagellin, which is expressed on the basolateral aspects of the epithelium where it can detect the repeated flagellin monomers that make up bacterial flagellae[32]. Detection of flagellin on the 'host' side of the intestinal epithelial barrier results in epithelial-cell activation, which initiates inflammatory responses by innate and adaptive immune cells with the aim of eradicating the invading bacterium. The importance of flagellin as an immune-activating MAMP and an antigen targeted by adaptive immune cells is reflected in its high representation among antigens bound by serum antibodies from colitic mice and in patients with Crohn's disease[33].

Apical expression of TLRs and restricted access to cytosolic NLRs are adaptations to constrain interactions with luminal microbes, but some commensals have also evolved strategies that actively dampen TLR signalling in IECs, should contact occur. *Bacteroides* and *Lactobacillus* spp. inhibit activation of the classical NF-κB pathway, which is central to induction of pro-inflammatory gene expression downstream of all PRRs. Active NF-κB dimers are sequestered in the cytosol by association with IκB complexes. Release of NF-κB for nuclear localization is contingent on the phosphorylation of IκB, by which it is targeted for ubiquitylation and protesomal degradation downstream of PRR signalling. Contact of IECs with these commensals inhibits IκB degradation, thereby blocking nuclear transport of NF-κB (ref. 34). *Bacteroides* spp. can further dampen NF-κB signalling by enhancing the nuclear export of NF-κB by inducing increased expression of the nuclear receptor family member, peroxisome-proliferation-activated receptor-γ (PPAR-γ). PPAR-γ binds NF-κB in the nucleus and shuttles it back to the cytoplasm, thereby terminating its transactivation of pro-inflammatory genes[35]. Thus, in addition to host mechanisms that normally restrain direct contact between commensals and IECs, co-adaptation of the microbiota and host have provided mechanisms that suppress pro-inflammatory engagement of PRRs in the intact epithelium.

The epithelium also supports tolerance of the microbiota by conditioning intestinal dendritic-cells through directional release of immunomodulatory cytokines into the lamina propria. At homeostasis, IECs secrete thymic stromal lymphopoietin (TSLP), IL-33 and IL-25, which promote tolerogenic activities of a subset of intestinal dendritic-cells defined by expression of integrin $\alpha_E\beta_7$ complex (also known as CD103)[36]. Antigens presented by $CD103^+$ dendritic-cells favour the development of T_{reg} cells and IgA^+ plasma cells that 'home' to the lamina propria at which they repress inflammatory responses to the microbiota[37]. IECs also produce abundant TGF-β, which suppresses NF-κB-dependent pro-inflammatory signalling in intestinal macrophages and dendritic cells, and promotes development and maintenance of T_{reg} cells and IgA^+ plasma cells. TLR-activated IECs can directly promote T-independent development of sIgA producing plasma cells in ILFs by the release of both B-cell activating factor (BAFF) and a proliferation-inducing ligand (APRIL)[38]. In addition to cytokines, IECs express other factors that limit pro-inflammatory responses of mucosal immune cells, including products of tryptophan metabolism and prostaglandins (for example, PGE_2).

Like IECs, intestinal macrophages normally express lower levels of TLRs and are hyporesponsive to TLR signalling to dampen inflammatory responses to the commensal microbiota. This is despite their retention of highly active phagocytic and bactericidal activities[39]. Also like IECs, this inflammatory anergy is probably multifactorial, but reflects the limited entry of commensal bacteria or their products into the cytosol in which they can activate NLRs — despite their uptake and degradation in phagolysosomes. Although phagocytosis of commensal bacteria induces pro-IL-1β in intestinal macrophages, its cleavage by caspase-1 to produce the active form requires NLRP3- or NLRC4-containing inflammasomes, which are activated by MAMPs

that are more effectively delivered into the cytosol by pathogenic, rather than commensal, bacteria[40]. Therefore, phagocytes in the intestinal lamina propria are conditioned to mount inflammatory responses against pathogens that deliver MAMPs to cytosolic sensors, but to efficiently clear commensals in a non-inflammatory manner.

Innate lymphoid-cells response to epithelial barrier breach

Although LTi cells are indispensable in the development of the GALT, they are only one subset of a growing family of ILCs that have emerged as important contributors to intestinal homeostasis and barrier defence in the postnatal immune system[41,42]. The diversity of ILC subsets seems to parallel that of $CD4^+$ T cells, with which they share many functional features. However, the antigen-specific-receptor-lacking ILCs are recruited to mucosal immune responses mainly by cytokines, which are produced by IECs or intestinal myeloid cells (dendritic cells and macrophages).

ILCs are distributed in the intestinal lamina propria and GALT, in which they are poised to respond rapidly to microbes that penetrate the epithelial defences. LTi cells are particularly important to barrier defence against bacterial incursions[43], as are a subset of natural-killer-like cells (referred to as NK-22 or ILC22 cells), which seem to share many features with LTi cells[44]. Common to these cells, and to $CD4^+$ T cells of the T_H17 lineage (discussed later) is their expression of the transcription factor retinoic acid-related orphan receptor (ROR)γt, which is required for these cells' development and function[9], and production of the cytokines IL-22, IL-17A and IL-17F (ref. 45). IL-22 is a member of the IL-10 cytokine family that acts on epithelial cells of barrier tissues, including the intestine, to enhance antimicrobial defence and epithelial barrier integrity. IL-17A and IL-17F target innate immune cells, stromal cells and epithelial cells to induce cytokines and chemokines (for example, G-CSF and CXCL8) that induce increased neutrophil production and recruitment, respectively.

$ROR\gamma t^+$ ILCs seem to be the main source of IL-22 at steady state and, in a continuous feedback loop with the microbiota, release IL-22, IL-17 or both in response to microbiota-induced production of IL-23 by macrophages and dendritic cells. These cytokines stimulate epithelial-cell secretion of antimicrobial peptides that inhibit or kill bacteria in the vicinity of the epithelial cell surface. Although ILCs can contribute to intestinal pathology under certain circumstances[46], they are crucial in the early host response to enteropathogenic bacteria[41,47].

$ROR\gamma t^+$ ILCs also express the aryl hydrocarbon receptor (AhR) with which they sense microbiota metabolites and xenobiotics[45,48]. AhR signalling is required both for ILC maintenance and IL-22 production[48]. Akin to its essential role in GALT development, ILC production of lymphotoxin provides an important amplifying loop for the production of IL-22 by ILCs, stimulating dendritic cell production of IL-23 that, in turn, increases IL-22 production by ILCs[49,50]. In addition to RORγt and AhR, another transcription factor shared between innate and adaptive immune cells that influences the composition of the microbiota is T-bet. This transcription factor is involved in T_H1 cell development, and is also expressed by a distinct subset of ILCs. Under pathogen-free conditions, RAG-deficient mice, which lack B and T cells, are relatively resistant to inflammation driven by their microbiota, despite the absence of an adaptive immune system. This is largely owing to compensatory increases in ILCs. However, when deficient for T-bet, RAG-deficient mice develop spontaneous intestinal inflammation resembling ulcerative colitis (known as $T\text{-}bet^{-/-}$ $RAG^{-/-}$ ulcerative colitis (TRUC) mice)[51]. Disease is a result of overexpression of TNFα by dendritic cells and an absence of T_{reg} cells. Remarkably, transfer of the microbiota from TRUC mice to immunocompetent mice transfers disease, reflecting the outgrowth of two pathogenic bacterial strains: *Klebsiella pneumoniae* and *Proteus mirabilis*. Although details of the mechanisms responsible for T-bet-dependent restraint of the microbiota remain to be defined, the dysbiosis in TRUC mice highlights the importance of innate immune cells in regulating the composition of the microbiota and is evidence that a dysbiotic flora can drive disease in otherwise healthy hosts.

Adaptive immunity in homeostatic responses to microbiota

The interplay between the microbiota, intestinal epithelium and innate and adaptive immune cells at homeostasis favours the dominance of regulatory networks that prevent inflammation or immune-mediated disease. Remarkably, the innate defences are sufficiently robust that much of the host response to the microbiota progresses without involvement of $CD4^+$ T-cell-dependent responses. Furthermore, a portion of the sIgA response that contributes to partitioning of commensal organisms away from the epithelium is generated in ILFs without the requirement for T cells[13]. When the adaptive immune response is recruited, it is typically limited to the mucosal tissues such that systemic immunity is not generated. This compartmentalization of mucosal immunity is a result of the programming of adaptive immune cells to travel back to the mucosae following their differentiation in Peyer's patches or MLNs. Finally, at steady state, antigen presentation by intestinal dendritic cells favours the development of regulatory $CD4^+$ T cells, which suppress the development of pro-inflammatory innate and effector T-cell responses to avert excessive inflammation.

Regulatory T-cell responses to the microbiota

$CD4^+$ T_{reg} cells are essential for maintenance of mutualism with the microbiota. The frequencies of these T cells are considerably elevated in the intestine relative to other tissues[52], and microbiota-induced T_{reg} cells affect the composition of the microbiota[53]. The crucial role of T_{reg} cells in immune homeostasis to the microbiota is well-documented by the consequences of these cell's absence[54]. T_{reg}-cell deficiency, irrespective of the means by which it is induced, results in unopposed effector T-cell responses and IBD, driven by reactivity to antigens of the microbiota. Indeed, much of our understanding of the inflammatory potential of the commensal microbiota has been garnered through models in which regulatory pathways have been disrupted[54]. The largely non-overlapping TCR specificities of regulatory and effector T-cell subsets in the colonic lamina propria and associated lymphoid tissues suggest that distinct antigenic epitopes, whether derived from the same or distinct members of the microbiota, control these competing T-cell fates[55].

Regulatory $CD4^+$ T cells include subsets that are distinguished on the basis of their expression of the transcription factor, Foxp3. $Foxp3^+$ (T_{reg}) or Foxp3- (T regulatory cells 1 (Tr1)) are each characterized by their production of IL-10, one of the main immunoregulatory cytokines required for immune tolerance of the intestinal microbiota. The non-redundant role of IL-10 in intestinal immune homeostasis is well-established; IL-10-deficient mice develop spontaneous, unremitting colonic inflammation driven by IL-23 and the T_H17 pathway[56,57]. The essential role of TLR in sensing the microbiota in this process is evident by the absence of disease in germ-free IL-10-deficient mice and mice deficient for both IL-10 and MyD88 (ref. 58, 59). Although non-T-cells produce IL-10, T-cell-derived IL-10 is crucial for intestinal immune homeostasis. Thus, IL-10 deficiency that is restricted to total $CD4^+$ T cells results in spontaneous colitis that has a severity comparable with that in mice with global loss of IL-10 (ref. 60). Although deficiency of IL-10 that is limited to $Foxp3^+$ T_{reg} cells also induces colitis, its severity is reduced, indicating that $Foxp3^-$ $CD4^+$ T cells contribute to the protective IL-10 response.

Myeloid cells of the innate immune system are the main targets for regulatory actions of IL-10 (ref. 61), although IL-10 signalling in $CD4^+$ T cells also seems to be contributory[62,63]. Importantly, polymorphisms in the IL-10 locus confer susceptibility to IBD in humans[64], and early-onset IBD has been linked to mutations in IL-10 receptor components that impair signalling[65].

Remarkably, IL-10-producing T cells can be induced to develop in response to specific commensals or their products. The capsular polysaccharide-A moiety of the common commensal *Bacteroides fragilis* mediates interaction of *B. fragilis* with the colonic mucosa, facilitating both colonization and activation of an anti-inflammatory cascade[66]. Polysaccharide-A promotes expansion of colonic IL-10-expressing $Foxp3^+$ T_{reg} cells, through the TLR2–MyD88 pathway[66]. The

expression of TLR2 on CD4 T-cells suggests there is the capacity for direct regulation by microbial products that favours polysaccharide-A-dependent T_{reg}-cell responses over T_H1 responses[67], although there are other known TLR2 ligands that do not promote induction of Foxp3 or IL-10 (ref. 66).

A cocktail of Clostridium species, mostly comprised of clusters IV and XIVa, drives the efficient expansion of T_{reg} cells in the colons of germ-free mice, seemingly owing to their superior ability to elicit TGFβ production in the intestinal mucosa[68]. In contrast with induction of T_{reg} cells by *B. fragilis*, *Clostridium*-dependent T_{reg} expansion occurs independently of MyD88 through mechanisms yet to be defined[68]. To date, there are no studies using otherwise complete microbiota that are devoid of *B. fragilis* or this specific collection of Clostridium spp., leaving open the issue of the level of redundancy in this process. However, *B. fragilis* is absent from the microbiota of 20–30% of humans, indicating the existence of other pathways to T_{reg}-cell development. Accordingly, default induction or expansion of T_{reg} cells can be achieved by colonization of germ-free mice with a defined altered Schaedler flora (ASF) that consists of eight species of the microbiota dominated by *Bacteroides distasonis*, but devoid of *B. fragilis*[69]. Thus, although there seems to be a proclivity of certain components of the microbiota to promote T_{reg}-cell development, this does not seem to be a unique property of any one microbial component, reflecting substantial redundancy in the system to ensure that T_{reg}-cell dominance is established.

Effector T-cell responses to the microbiota

Similar to T_{reg} cells and B cells, the largest deployment of effector CD4$^+$ T-cells in the healthy immune system is in the intestines, and is largely driven by the microbiota. Although the intestines mount robust T_H2 responses to helminth infestations, in countries where these infections are less common the main effector T-cell subsets resident in the gut express cytokines characteristic of T_H17 and T_H1 cells.

T_H17 cells in particular, which are thought to be the most ancient of effector T-cell subsets[4], seem to have evolved to bolster mucosal barrier defences to promote mutualism with the microbiota. T_H17 cells share developmental requirements for RORγt and AhR (ref. 70) with intestinal ILCs, as well as a similar effector cytokine repertoire, including IL-17A, IL-17F and IL-22. Furthermore, T_H17 cells have developmental ties with T_{reg} cells through their mutual requirement for the abundant intestinal cytokine TGFβ (ref. 4). Finally, the T_H17 developmental pathway is distinguished by considerable plasticity[71], allowing divergent functional programs contingent on local pro- or anti-inflammatory cues. Although a last line of defence, effector CD4$^+$ T-cells are perpetually engaged in the host–microbiota dialogue by favouring regulatory benefits at homeostasis or pathological consequences when dysregulated.

The contribution of the microbiota to intestinal T_H17-cell development is highlighted by the virtual absence of this subset in germ-free mice[72]. In addition to IL-6, which is required for T_H17 differentiation and its deviation away from induced T_{reg} programming, multiple microbiota-dependent factors favour T_H17 development in the intestines, including TGFβ, IL-1β (ref. 73), IL-23 (ref. 74) and even ATP derived from commensal bacteria[75]. Similar to the ability of a limited quorum of commensal bacterial species to disproportionately influence induced T_{reg}-cell development, minor constituents of the microbiota can amplify intestinal T_H17 cell numbers. In mice, an unusually potent, but not unique, inducer of T_H17 cells[69] is the *Clostridia* sp. *Candidatus arthromitus* or segmented filamentous bacteria (SFB)[72,76]. This bacterium populates the ileum and caecum and has long been known to be a potent activator of intestinal immune responses[77]. Induction of T_H17 cells by SFB provides protection against gut pathogens[78], suggesting that general amplification of T_H17 effector cells can be host-protective. However, T_H17 induction by SFB is not entirely benign, because mono-association of mice with SFB induces T_H17-mediated inflammatory arthritis[79] and multiple-sclerosis-like symptoms in the experimental autoimmune encephalomyelitis (EAE) model[80]. Remarkably, therefore, sensing of a single constituent of the intestinal microbiota can promote autoimmunity in extraintestinal tissues. At present, it is unclear whether SFB, or related organisms, exert similar effects in humans.

Whether at steady state, responding to infection or chronically inflamed as a result of IBD, the intestine contains, in addition to effectors that express IL-17, T cells that express IFNγ or both IL-17 and IFNγ. Of note, T_H17 cells retain a high capacity for divergent cytokine expression profiles and function, or plasticity, after their commitment to the T_H17 pathway. Specifically, T_H17 cells can give rise to IFNγ producers that resemble classical T_H1 cells. This has been demonstrated in humans and mice[71,81], and has suggested that many of the T_H1 cells found in the intestine arise from the T_H17 pathway (Fig. 3). The relative contributions of T_H1 cells to immune protection or pathogenesis remain to be elucidated, whether they are derived from the T_H17 pathway or not.

Balancing regulatory and effector responses

To balance accommodation of the microbiota and the need to mount host defences against microbial invasion, the adaptive immune system has evolved to direct the development of distinct CD4$^+$ T-cell fates by different APC subsets and the microbe-induced factors they produce. Although T_{reg}-cell dominance is the default at homeostasis, the shared dependence of induced T_{reg} and T_H17-cell development on TGFβ provides an elegant means to alternately divert programming of naive CD4$^+$ T cells from a homeostatic, microbe-tolerant response to an inflammatory, microbe-clearing response contingent on the cofactors integrated with TGFβ signalling[4] (Fig. 3).

At homeostasis, naive CD4$^+$ T-cell recognition of antigens derived from the microbiota favours induced T_{reg}-cell development by virtue of the production, by intestinal dendritic cells, of the vitamin A metabolite all-trans-retinoic acid[82–84]. Vitamin A is not synthesized by the host so its influence on the regulatory tone of the mucosal immune response is predicated from adequate dietary intake. Retinoic acid is derived from vitamin A by the sequential actions of the ubiquitous enzyme, alcohol dehydrogenase and one of three retinal-specific aldehyde dehydrogenases, which are more restricted in their tissue distribution, including CD103$^+$ dendritic cells and IECs in the intestine. The potency of retinoic acid as a cofactor for TGFβ-dependent development of induced T_{reg} cells — and suppression of T_H17 development — and its constitutive production by a regulatory subset of intestinal dendritic cells at steady state reflect the robust default pathway to T-cell-mediated regulation. Under conditions in which microbial antigens promote production of pro-inflammatory cytokines by dendritic cells, retinoic acid is either repressed[85] or co-opted by pro-inflammatory pathways[86,87] to override T_{reg}-cell induction.

In common with T_H17 cells, and perhaps reflecting an aspect of shared TGFβ-dependent programming that favours multipotency, induced T_{reg} cells display developmental plasticity that influences adaptive immunity to the microbiota. When acted on by pro-inflammatory cytokines, induced T_{reg} cells can down-regulate Foxp3 and up-regulate RORγt (ref. 88), and T_{reg} cells can be converted into IL-17- or IFNγ-expressing effectors during infection[89]. Notably, although Foxp3$^+$ T_{reg} cells may be diverted to effector responses, the reverse is less apparent; established effector T cells, including T_H17 cells, seem to be more resistant to reprogramming to become Foxp3$^+$ regulatory cells. Accordingly, microbial antigens that are identified as products of a pathogen are likely to be remembered as such through their imprinting of an effector T-cell response. By contrast, microbial antigens that promote induced T_{reg} responses at homeostasis, may, in the context of an inflammatory response, reprogram induced T_{reg} cells to generate an effector T-cell response that breaks the 'tolerance' to that microbe.

In a further example of the developmental plasticity of T_{reg} cells, recent studies report their role in IgA class-switch recombination in the gut, representing another arm of T_{reg} cell function in promoting immune homeostasis to the microbiota. TGFβ has long been recognized as the principal switch factor for development of IgA-producing B cells. In a new twist on TGFβ's role in this process, induced T_{reg} cells were found to down-modulate Foxp3 and acquire features of follicular helper T cells

that promoted IgA production in Peyer's patches[90]. Depletion of T_{reg} cells also caused a rapid loss of IgA^+ plasma cells and sIgA production in the intestine[91], indicating that T_{reg} cells participate both in the development and maintenance of intestinal IgA^+ B cells. Although known to be important in host defence against infections, the main role of sIgA is to establish mutualism with the intestinal microbiota, as evidenced by its marked depletion in germ-free mice and systemic IgG response to the microbiota in animals that specifically lack sIgA. Coupled with the fact that about 75% of sIgA reactive to the microbiota develops through the T-cell-dependent pathway[91,92], this suggests that sIgA is mainly regulated by intestinal T_{reg} cells. In addition to providing evidence of further plasticity in the T_{reg} developmental program, these findings identify an additional link between adaptive immune networks that cope with the commensal flora, and extend the long-established role of TGFβ in promoting host–microbiota mutualism[4].

Dysregulated immunity to the microbiota

Owing to their defined antigenic specificity and durable memory, effector $CD4^+$ T cells are a liability when inappropriately directed against self-antigens or, in the case of the microbiota, the 'extended' self. In view of the enormous number of antigens expressed in the intestinal metagenome, it is remarkable that dysregulated effector responses to the microbiota are the exception. When they do occur, the result is IBD, including Crohn's disease or ulcerative colitis, which have distinct clinical and histopathological features, but a common requirement for the intestinal microbiota. Similar to autoimmunity directed against host self-antigens, dysregulated $CD4^+$ T-cell responses to antigens of the microbiota leads to chronic, typically relapsing and remitting disease that reflects the immune system's inability to eliminate the antigens that drive the abnormal response.

That being said, inflammatory immune responses in the intestines result in detectable alterations of the resident microbiota, irrespective of the cause[93]. This presents a challenge in our attempts to understand how certain microbes positively or negatively affect the disease process in IBD because it is difficult to draw conclusions without knowing the composition of the microbiota before diagnosis. As such, our understanding of the antigenic components of the microbiota that are the targets of immune attack in IBD are limited. However, experimental mouse models and patients with Crohn's disease show a remarkably shared reactivity to specific flagellin epitopes expressed by *Clostridium* spp., which seem to be immunodominant despite their minor representation within the commensal flora[33,94]. What attributes of these commensals make them particularly common targets in a large subset of patients with Crohn's disease — but not ulcerative colitis — are unknown. However, it is likely to reflect unique properties that place them in specific geographical niches in the microbiota or in intimate contact with the immune system where their expression of flagella, which is less typical for commensal bacteria, make them unusually proficient at inducing effector rather than regulatory responses. Irrespective of the basis, retention of these organisms in the collective despite the pathogenic risk they pose implies there is a benefit to host–microbiota mutualism that has been evolutionarily conserved and remains to be understood.

In view of the prominent role of the T_H17 pathway in adaptive immunity to the intestinal microbiota and propensity for generating inflammation promoted by both IL-17 and IFNγ, it is not surprising that this pathway has emerged as a major contributor to IBD pathogenesis. Prior to the discovery of T_H17, Crohn's disease and ulcerative colitis were viewed in the context of T_H1- and T_H2-centric mechanisms, respectively; but, increasingly, data from genome-wide association studies implicate the contributions of the T_H17 pathway in both diseases[95]. The discovery of IL-23 revolutionized views on the immunopathogenesis of autoimmunity and led to discovery of T_H17 cells[96]. It is therefore fitting that this was the first cytokine linked to IBD by genome-wide association studies; variants of its receptor (IL-23R) have been found to confer both protection and susceptibility to Crohn's disease and ulcerative colitis[95].

As the number of genome-wide association and next-generation sequencing studies has proliferated, so has the number of genes linked to the T_H17 pathway in IBD (ref. 95). This has been supplemented by genes of innate and adaptive immune pathways that are integrated with the T_H17 response and control it, spanning the gamut from epithelial barrier integrity maintenance and restitution to microbial sensing, to immunomodulatory cytokines. Because individual susceptibility alleles typically confer minor risk, multiple genetic susceptibility alleles are generally required for disease. Efforts to define this clustering of risk alleles is increasingly defining genotypes that confer substantial risk, as well as identifying interlaced susceptibility pathways that identify immunopathogenetic subsets of IBD — including those that do not directly implicate the T_H17 pathway. However, as more IBD susceptibility genotypes are found to overlap with extraintestinal immune-mediated diseases that do share a T_H17 pathogenesis, they increasingly implicate a role for the microbiota in conferring disease risk beyond the confines of the gut. As we advance into the era of integrated metagenomics of the human–microbiota 'superorganism', the opportunities for personalized medicine that were originally envisioned from sequencing of the human genome may well multiply in proportion to the increase in genes contributed by our microbiota, with attendant opportunities for more specifically targeted treatments and prevention of diseases that have their origins in the merger of vertebrates and their microbiomes millions of years ago. ■

1. Ley, R. E., Peterson, D. A. & Gordon, J. I. Ecological and evolutionary forces shaping microbial diversity in the human intestine. *Cell* **124,** 837–848 (2006).
2. Qin, J. *et al.* A human gut microbial gene catalogue established by metagenomic sequencing. *Nature* **464,** 59–65 (2010).
3. McFall-Ngai, M. Adaptive immunity: care for the community. *Nature* **445,** 153 (2007).
4. Weaver, C. T. & Hatton, R. D. Interplay between the T_H17 and T_{reg} cell lineages: a (co-)evolutionary perspective. *Nature Rev. Immunol.* **9,** 883–889 (2009).
5. Zhang, Y.-A. *et al.* IgT, a primitive immunoglobulin class specialized in mucosal immunity. *Nature Immunol.* **11,** 827–835 (2010).
6. Dominguez-Bello, M. G. *et al.* Delivery mode shapes the acquisition and structure of the initial microbiota across multiple body habitats in newborns. *Proc. Natl Acad. Sci. USA* **107,** 11971–11975 (2010).
7. Bager, P., Wohlfahrt, J. & Westergaard, T. Caesarean delivery and risk of atopy and allergic disease: meta-analyses. *Clin. Exp. Allergy* **38,** 634–642 (2008).
8. Palmer, C., Bik, E., Digiulio, D., Relman, D. & Brown, P. Development of the human infant intestinal microbiota. *PLoS Biol.* **5,** e177 (2007).
9. Cherrier, M. & Eberl, G. The development of LTi cells. *Curr. Opin. Immunol.* **24,** 178–183 (2012).
10. van de Pavert, S. A. & Mebius, R. E. New insights into the development of lymphoid tissues. *Nature Rev. Immunol.* **10,** 664–674 (2010).
11. Kanamori, Y. *et al.* Identification of novel lymphoid tissues in murine intestinal mucosa where clusters of c-kit$^+$IL-7R$^+$Thy1$^+$ lympho-hemopoietic progenitors develop. *J. Exp. Med.* **184,** 1449–1459 (1996).
12. Bouskra, D. *et al.* Lymphoid tissue genesis induced by commensals through NOD1 regulates intestinal homeostasis. *Nature* **456,** 507–510 (2008).
13. Tsuji, M. *et al.* Requirement for lymphoid tissue-inducer cells in isolated follicle formation and T cell-independent immunoglobulin A generation in the gut. *Immunity* **29,** 261–271 (2008).
14. Lane, P. J. L. *et al.* Lymphoid tissue inducer cells: bridges between the ancient innate and the modern adaptive immune systems. *Mucosal Immunol.* **2,** 472–477 (2009).
15. Lotz, M. *et al.* Postnatal acquisition of endotoxin tolerance in intestinal epithelial cells. *J. Exp. Med.* **203,** 973–984 (2006).
16. Ismail, A. S. *et al.* γδ intraepithelial lymphocytes are essential mediators of host–microbial homeostasis at the intestinal mucosal surface. *Proc. Natl Acad. Sci. USA* **108,** 8743–8748 (2011).
17. Hansen, C. H. *et al.* Patterns of early gut colonization shape future immune responses of the host. *PLoS ONE* **7,** e34043 (2012).
18. Olszak, T. *et al.* Microbial exposure during early life has persistent effects on natural killer T cell function. *Science* **336,** 489–493 (2012).
19. Peterson, J. *et al.* Importance and regulation of the colonic mucus barrier in a mouse model of colitis. *Am. J. Physiol. Gastrointest. Liver Physiol.* **300,** G327–G333 (2011).
20. Bergstrom, K. S. B. *et al.* Muc2 protects against lethal infectious colitis by disassociating pathogenic and commensal bacteria from the colonic mucosa. *PLoS Pathogens* **6,** e1000902 (2010).
21. Van der Sluis, M. *et al.* Muc2-deficient mice spontaneously develop colitis, indicating that MUC2 is critical for colonic protection. *Gastroenterology* **131,** 117–129 (2006).
22. Johansson, M. E. V., Larsson, J. M. H. & Hansson, G. C. The two mucus layers of colon are organized by the MUC2 mucin, whereas the outer layer is a legislator of host–microbial interactions. *Proc. Natl Acad. Sci. USA* **108,** 4659–4665 (2011).
23. Fukuda, S. *et al.* Bifidobacteria can protect from enteropathogenic infection through production of acetate. *Nature* **469,** 543–547 (2011).

This article reports comparative genomic and metabolic profiling of protective compared with non-protective strains of *Bifidobacterium* to identify a class of bacterial carbohydrate transporters that impart host-protective effects through the generation of acetate.

24. Maslowski, K. M. *et al.* Regulation of inflammatory responses by gut microbiota and chemoattractant receptor GPR43. **Nature 461,** 1282–1286 (2009).
25. Vaishnava, S. *et al.* The antibacterial lectin Reg-IIIγ promotes the spatial segregation of microbiota and host in the intestine. *Science* **334,** 255–258 (2011).
26. Cash, H. L., Whitham, C. V., Behrendt, C. L. & Hooper, L. V. Symbiotic bacteria direct expression of an intestinal bactericidal lectin. *Science* **313,** 1126–1130 (2006).
This study demonstrated that Reg-IIIγ, a C-type lectin produced by Paneth cells in response to the resident microbiota, has microbicidal activity, identifying a new mechanism for sequestration of constituents of the microbiota to the intestinal lumen.
27. Salzman, N. H. *et al.* Enteric defensins are essential regulators of intestinal microbial ecology. *Nature Immunol.* **11,** 76–83 (2010).
28. Hugot, J. P. *et al.* Association of NOD2 leucine-rich repeat variants with susceptibility to Crohn's disease. *Nature* **411,** 599–603 (2001).
29. Ogura, Y. *et al.* A frameshift mutation in *NOD2* associated with susceptibility to Crohn's disease. *Nature* **411,** 603–606 (2001).
References 28 and 29 identified the first major susceptibility gene for IBD. These studies also implicated a link between impaired innate immune recognition of the microbiota and dysregulated adaptive immunity in IBD pathogenesis.
30. Elinav, E. *et al.* NLRP6 inflammasome regulates colonic microbial ecology and risk for colitis. *Cell* **145,** 745–757 (2011).
31. Rakoff-Nahoum, S., Paglino, J., Eslami-Varzaneh, F., Edberg, S. & Medzhitov, R. Recognition of commensal microflora by Toll-like receptors is required for intestinal homeostasis. *Cell* **118,** 229–241 (2004).
This report established that TLR signalling in response to the resident microbiota has an important role in promoting maintenance of epithelial barrier function.
32. Vijay-Kumar, M., Aitken, J. D. & Gewirtz, A. T. Toll like receptor-5: protecting the gut from enteric microbes. Semin. Immunopathol. **30,** 11–21 (2008).
33. Lodes, M. J. *et al.* Bacterial flagellin is a dominant antigen in Crohn disease. *J. Clin. Invest.* **113,** 1296–1306 (2004).
This study reports an expression library that was made from the microbiota of spontaneously colitic mice and was screened with antibodies in their serum to identify commensal bacterial flagellins as major antigenic targets of the immune response in IBD.
34. Neish, A. S. *et al.* Prokaryotic regulation of epithelial responses by inhibition of IκB-α ubiquitination. *Science* **289,** 1560–1563 (2000).
35. Kelly, D. *et al.* Commensal anaerobic gut bacteria attenuate inflammation by regulating nuclear–cytoplasmic shuttling of PPAR-γ and RelA. *Nature Immunol.* **5,** 104–112 (2004).
36. Hill, D. A. & Artis, D. Intestinal bacteria and the regulation of immune cell homeostasis. *Annu. Rev. Immunol.* **28,** 623–667 (2010).
37. Rescigno, M. & Di Sabatino, A. Dendritic cells in intestinal homeostasis and disease. *J. Clin. Invest.* **119,** 2441–2450 (2009).
38. He, B. *et al.* Intestinal bacteria trigger T cell-independent immunoglobulin A2 class switching by inducing epithelial-cell secretion of the cytokine APRIL. *Immunity* **26,** 812–826 (2007).
39. Smythies, L. E. *et al.* Human intestinal macrophages display profound inflammatory anergy despite avid phagocytic and bacteriocidal activity. *J. Clin. Invest.* **115,** 66–75 (2005).
40. Franchi, L. *et al.* NLRC4-driven production of IL-1β discriminates between pathogenic and commensal bacteria and promotes host intestinal defense. *Nature Immunol.* **13,** 449–456 (2012).
41. Colonna, M. Interleukin-22-producing natural killer cells and lymphoid tissue inducer-like cells in mucosal immunity. *Immunity* **31,** 15–23 (2009).
42. Spits, H. & Di Santo, J. P. The expanding family of innate lymphoid cells: regulators and effectors of immunity and tissue remodeling. *Nature Immunol.* **12,** 21–27 (2011).
43. Sonnenberg, G. F., Monticelli, L. A., Elloso, M. M., Fouser, L. A. & Artis, D. CD4$^+$ lymphoid tissue-inducer cells promote innate immunity in the gut. *Immunity* **34,** 122–134 (2011).
44. Cella, M. *et al.* A human natural killer cell subset provides an innate source of IL-22 for mucosal immunity. *Nature* **457,** 722–725 (2009).
45. Takatori, H. *et al.* Lymphoid tissue inducer-like cells are an innate source of IL-17 and IL-22. *J. Exp. Med.* **206,** 35–41 (2009).
46. Buonocore, S. *et al.* Innate lymphoid cells drive interleukin-23-dependent innate intestinal pathology. *Nature* **464,** 1371–1375 (2010).
47. Sonnenberg, G. F., Fouser, L. A. & Artis, D. Border patrol: regulation of immunity, inflammation and tissue homeostasis at barrier surfaces by IL-22. *Nature Immunol.* **12,** 383–390 (2011).
48. Qiu, J. *et al.* The aryl hydrocarbon receptor regulates gut immunity through modulation of innate lymphoid cells. *Immunity* **36,** 92–104 (2012).
49. Ota, N. *et al.* IL-22 bridges the lymphotoxin pathway with the maintenance of colonic lymphoid structures during infection with *Citrobacter rodentium*. *Nature Immunol.* **12,** 941–948 (2011).
50. Tumanov, A. V. *et al.* Lymphotoxin controls the IL-22 protection pathway in gut innate lymphoid cells during mucosal pathogen challenge. *Cell Host Microbe* **10,** 44–53 (2011).
51. Garrett, W. S. *et al.* Enterobacteriaceae act in concert with the gut microbiota to induce spontaneous and maternally transmitted colitis. *Cell Host Microbe* **8,** 292–300 (2010).
52. Maynard, C. L. *et al.* Regulatory T cells expressing interleukin 10 develop from Foxp3$^+$ and Foxp3$^-$ precursor cells in the absence of interleukin 10. *Nature Immunol.* **8,** 931–941 (2007).
53. Josefowicz, S. Z. *et al.* Extrathymically generated regulatory T cells control mucosal T_H2 inflammation. *Nature* **482,** 395–399 (2012).
54. Izcue, A., Coombes, J. L. & Powrie, F. Regulatory lymphocytes and intestinal inflammation. *Annu. Rev. Immunol.* **27,** 313–338 (2009).
55. Lathrop, S. K. *et al.* Peripheral education of the immune system by colonic commensal microbiota. *Nature* **478,** 250–254 (2011).
56. Kühn, R., Löhler, J., Rennick, D., Rajewsky, K. & Müller, W. Interleukin-10-deficient mice develop chronic enterocolitis. *Cell* **75,** 263–274 (1993).
This study identified a non-redundant function for IL-10 in immune homeostasis in the intestine, and observed the importance of composition of the microbiota in modulating disease severity in genetically susceptible mice.
57. Yen, D. *et al.* IL-23 is essential for T cell-mediated colitis and promotes inflammation via IL-17 and IL-6. *J. Clin. Invest.* **116,** 1310–1316 (2006).
58. Sellon, R. K. *et al.* Resident enteric bacteria are necessary for development of spontaneous colitis and immune system activation in interleukin-10-deficient mice. *Infect. Immun.* **66,** 5224–5231 (1998).
59. Rakoff-Nahoum, S., Hao, L. & Medzhitov, R. Role of Toll-like receptors in spontaneous commensal-dependent colitis. *Immunity* **25,** 319–329 (2006).
60. Roers, A. *et al.* T cell-specific inactivation of the interleukin 10 gene in mice results in enhanced T cell responses but normal innate responses to lipopolysaccharide or skin irritation. *J. Exp. Med.* **200,** 1289–1297 (2004).
61. Takeda, K. *et al.* Enhanced Th1 activity and development of chronic enterocolitis in mice devoid of Stat3 in macrophages and neutrophils. *Immunity* **10,** 39–49 (1999).
62. Chaudhry, A. *et al.* Interleukin-10 signaling in regulatory T cells is required for suppression of Th17 cell-mediated inflammation. *Immunity* **34,** 566–578 (2011).
63. Huber, S. *et al.* Th17 cells express interleukin-10 receptor and are controlled by Foxp3$^-$ and Foxp3$^+$ regulatory CD4$^+$ T cells in an interleukin-10-dependent manner. *Immunity* **34,** 554–565 (2011).
64. Franke, A. *et al.* Sequence variants in *IL10, ARPC2* and multiple other loci contribute to ulcerative colitis susceptibility. *Nature Genet.* **40,** 1319–1323 (2008).
65. Glocker, E.-O. *et al.* Inflammatory bowel disease and mutations affecting the interleukin-10 receptor. *N. Engl. J. Med.* **361,** 2033–2045 (2009).
66. Round, J. L. *et al.* The Toll-like receptor 2 pathway establishes colonization by a commensal of the human microbiota. *Science* **332,** 974–977 (2011).
67. Wang, Q. *et al.* A bacterial carbohydrate links innate and adaptive responses through Toll-like receptor 2. *J. Exp. Med.* **203,** 2853–2863 (2006).
68. Atarashi, K. *et al.* Induction of colonic regulatory T cells by indigenous *Clostridium* species. *Science* **331,** 337–341 (2011).
69. Geuking, M. B. *et al.* Intestinal bacterial colonization induces mutualistic regulatory T cell responses. *Immunity* **34,** 794–806 (2011).
70. Sawa, S. *et al.* RORγt$^+$ innate lymphoid cells regulate intestinal homeostasis by integrating negative signals from the symbiotic microbiota. *Nature Immunol.* **12,** 320–326 (2011).
71. Lee, Y. K. *et al.* Late developmental plasticity in the T helper 17 lineage. *Immunity* **30,** 92–107 (2009).
72. Ivanov, I. I. *et al.* Specific microbiota direct the differentiation of IL-17-producing T-helper cells in the mucosa of the small intestine. *Cell Host Microbe* **4,** 337–349 (2008).
73. Shaw, M. H., Kamada, N., Kim, Y.-G. & Núñez, G. Microbiota-induced IL-1β, but not IL-6, is critical for the development of steady-state TH17 cells in the intestine. *J. Exp. Med.* **209,** 251–258 (2012).
74. Zeph, C. *et al.* Commensal dependent expression of IL-25 regulates the IL-23–IL-17 axis in the intestine. *J. Exp. Med.* **205,** 2191–2198 (2008).
75. Atarashi, K. *et al.* ATP drives lamina propria TH17 cell differentiation. *Nature* **455,** 808–812 (2008).
76. Gaboriau-Routhiau, V. *et al.* The key role of segmented filamentous bacteria in the coordinated maturation of gut helper T cell responses. *Immunity* **31,** 677–689 (2009).
77. Talham, G. L., Jiang, H. Q., Bos, N. A. & Cebra, J. J. Segmented filamentous bacteria are potent stimuli of a physiologically normal state of the murine gut mucosal immune system. *Infect. Immun.* **67,** 1992–2000 (1999).
78. Ivanov, I. I. *et al.* Induction of intestinal Th17 cells by segmented filamentous bacteria. *Cell* **139,** 485–498 (2009).
79. Wu, H.-J. *et al.* Gut-residing segmented filamentous bacteria drive autoimmune arthritis via T helper 17 cells. *Immunity* **32,** 815–827 (2010).
This study reported that a single component of the microbiota that induces increased intestinal T_H17 cells could drive the development of extraintestinal immune-mediated disease in genetically susceptible mice. This raises the possibility that antigen-independent effects of the mucosal immune response to limited constituents of the microbiota may trigger systemic autoimmunity.
80. Lee, Y. K., Menezes, J. S., Umesaki, Y. & Mazmanian, S. K. Proinflammatory T-cell responses to gut microbiota promote experimental autoimmune encephalomyelitis. *Proc. Natl Acad. Sci. USA* **108,** 4615–4622 (2011).
81. Annunziato, F. *et al.* Phenotypic and functional features of human Th17 cells. *J. Exp. Med.* **204,** 1849–1861 (2007).
82. Coombes, J. L. *et al.* A functionally specialized population of mucosal CD103$^+$ DCs induces Foxp3$^+$ regulatory T cells via a TGF-β and retinoic acid-dependent mechanism. *J. Exp. Med.* **204,** 1757–1764 (2007).
83. Sun, C. M. *et al.* Small intestine lamina propria dendritic cells promote *de novo* generation of Foxp3 T reg cells via retinoic acid. *J. Exp. Med.* **204,** 1775–1785 (2007).

84. Mucida, D. *et al.* Reciprocal TH17 and regulatory T cell differentiation mediated by retinoic acid. *Science* **317,** 256–260 (2007).
85. Maynard, C. L. *et al.* Contrasting roles for all-trans retinoic acid in TGF-β-mediated induction of *Foxp3* and *Il10* genes in developing regulatory T cells. *J. Exp. Med.* **206,** 343–357 (2009).
86. Hall, J. *et al.* Commensal DNA limits regulatory T cell conversion and is a natural adjuvant of intestinal immune responses. *Immunity* **29,** 637–649 (2008).
87. DePaolo, R. W. *et al.* Co-adjuvant effects of retinoic acid and IL-15 induce inflammatory immunity to dietary antigens. *Nature* **471,** 220–224 (2011).
88. Lee, Y. K., Mukasa, R., Hatton, R. D. & Weaver, C. T. Developmental plasticity of Th17 and T_{reg} cells. *Curr. Opin. Immunol.* **21,** 274–280 (2009).
89. Wohlfert, E. & Belkaid, Y. Plasticity of T_{reg} at infected sites. *Mucosal Immunol.* **3,** 213–215 (2010).
90. Tsuji, M. *et al.* Preferential generation of follicular B helper T cells from Foxp3$^+$ T cells in gut Peyer's patches. *Science* **323,** 1488–1492 (2009).
91. Cong, Y., Feng, T., Fujihashi, K., Schoeb, T. R. & Elson, C. O. A dominant, coordinated T regulatory cell–IgA response to the intestinal microbiota. *Proc. Natl Acad. Sci. USA* **106,** 19256–19261 (2009).
References 90 and 91 identify a central role for T_{reg} cells in the induction and maintenance of IgA-producing plasma cells in the intestines, extending the functionality of T_{reg} cells in supporting mutualism to the microbiota.
92. Macpherson, A. J. & Uhr, T. Induction of protective IgA by intestinal dendritic cells carrying commensal bacteria. *Science* **303,** 1662–1665 (2004).
93. Lupp, C. *et al.* Host-mediated inflammation disrupts the intestinal microbiota and promotes the overgrowth of Enterobacteriaceae. *Cell Host Microbe* **2,** 119–129 (2007).
94. Targan, S. R. *et al.* Antibodies to CBir1 flagellin define a unique response that is associated independently with complicated Crohn's disease. *Gastroenterology* **128,** 2020–2028 (2005).
95. Khor, B., Gardet, A. & Xavier, R. J. Genetics and pathogenesis of inflammatory bowel disease. *Nature* **474,** 307–317 (2011).
96. Kastelein, R. A., Hunter, C. A. & Cua, D. J. Discovery and biology of IL-23 and IL-27: related but functionally distinct regulators of inflammation. *Annu. Rev. Immunol.* **25,** 221–242 (2007).
97. Wacklin, P. *et al.* Secretor genotype (*FUT2* gene) is strongly associated with the composition of bifidobacteria in the human intestine. *PLoS ONE* **6,** e20113 (2011).
98. Morrow, A. L. *et al.* Fucosyltransferase 2 non-secretor and low secretor status predicts severe outcomes in premature infants. *J. Pediatr.* **158,** 745–751 (2011).
99. McGovern, D. P. B. *et al.* Fucosyltransferase 2 (*FUT2*) non-secretor status is associated with Crohn's disease. *Hum. Mol. Genet.* **19,** 3468–3476 (2010).
100. Rydell, G. E., Kindberg, E., Larson, G. & Svensson, L. Susceptibility to winter vomiting disease: a sweet matter. *Rev. Med. Virol.* **21,** 370–382 (2011).

Acknowledgements The authors thank D. Randolph and C. Morrow for discussions and critical review of this manuscript. C.T.W., C.O.E. and R.D.H. are supported by grants from the National Institutes of Health, and C.T.W. and C.L.M. are supported by grants from the Crohn's and Colitis Foundation of America. The authors extend their apologies to colleagues whose work could not be adequately acknowledged owing to space limitations.

Author Information Reprints and permissions information is available at www.nature.com/reprints. The authors declare no competing financial interests. Readers are welcome to comment on the online version of this article at go.nature.com/nqbfui. Correspondence should be addressed to C.T.W. (cweaver@uab.edu).

REVIEW

doi:10.1038/nature11552

Functional interactions between the gut microbiota and host metabolism

Valentina Tremaroli[1,2] & Fredrik Bäckhed[1,2,3]

The link between the microbes in the human gut and the development of obesity, cardiovascular disease and metabolic syndromes, such as type 2 diabetes, is becoming clearer. However, because of the complexity of the microbial community, the functional connections are less well understood. Studies in both mice and humans are helping to show what effect the gut microbiota has on host metabolism by improving energy yield from food and modulating dietary or the host-derived compounds that alter host metabolic pathways. Through increased knowledge of the mechanisms involved in the interactions between the microbiota and its host, we will be in a better position to develop treatments for metabolic disease.

Changes to lifestyle and an increase in the availability of energy-rich foods are important contributors to the worldwide obesity epidemic. The microbial inhabitants of the gut can also have an influence on metabolic processes, such as energy extraction from food, and should be considered an environmental factor that contributes to obesity and its comorbidities (such as insulin resistance, diabetes and cardiovascular disease).

Culture-independent methods to study microbial communities have advanced our knowledge of this human gut microbiota (Box 1) (see page 250 of this issue). Profiling of the common proxy for this community, the faecal microbiota, by 16S ribosomal RNA surveys and by direct sequencing of genetic material have shown that the human gut microbiota is a complex community of 100 trillion archaeal and bacterial cells distributed over more than 1,000 species[1] (Box 2). The community is dominated by bacteria, with more than 90% of the species belonging to Firmicutes and Bacteroidetes. Each person has a distinct and highly variable microbiota, but a conserved set of gut colonizers (the core gut microbiota) and genes (the core microbiome) are shared among individuals[1,2] and may be required for the correct functioning of the gut.

Germ-free mice are those born and reared without exposure to any live microbes, and they provide a powerful tool for understanding the effects of the gut microbiota on host physiology. These mice can be colonized either with selected microbial species or whole communities from mice or humans to examine the transmissibility of physiological and pathological phenotypes, and to test what role the microbiota has in a particular phenotype. The gut microbiota in these mice modulates bone-mass density[3] and promotes fat storage[4], intestinal angiogenesis[5,6] and the development of an immune response[7,8] (see page 231 of this issue). In this Review, we discuss the metagenomic and gnotobiotic-based evidence for the role of the gut microbiota in energy metabolism and the possible links with obesity.

Obesity

Gut microbiota composition is altered in people who are obese, and it can respond to changes in body weight. Genetically obese *ob*/*ob* mice[9] are hyperphagic as a result of a mutation in the gene that encodes the satiety-promoting hormone leptin. The caecal microbiota of these mice contains more Firmicutes and fewer Bacteroidetes than that of their lean wild-type littermates, even when the mice are fed the same low-fat, polysaccharide-rich diet[9]. Similar changes have also been seen in the faecal microbiota of humans who are obese[10]. Bacteroidetes levels increase when weight is reduced, either by fat- or carbohydrate-restricted diets[10], suggesting that Bacteroidetes may be responsive to calorie intake. A similar effect has also been observed in people who lost weight after a Roux-en-Y gastric bypass procedure. In these patients, increased levels of *Bacteroides* and *Prevotella* were negatively correlated with energy intake and adiposity[11]. Other studies showed no such shift in the Firmicutes–Bacteroidetes ratio[12–14], but this may be because they used different clinical criteria (such as level of obesity, age, degree of weight loss and duration of calorie restriction), geographical locations, population sizes and microbiota-profiling methodologies. Although obesity and energy intake can affect the microbial composition, whether the gut microbiota contributes to obesity in humans is unclear.

A gastric bypass promotes sustained weight reduction and diminishes the risk of diabetes and cardiovascular disease for people who are obese[15,16]. This knowledge has allowed the relationship between microbiota and obesity to be explored further. After a gastric bypass, diabetes can resolve before patients begin to lose weight, suggesting that this type of surgery has a direct antidiabetic effect. Exactly how this happens is not clear, but a shift in the composition of the faecal microbiota of humans[11,14] suggests the gut microbiota contributes to the improved metabolic phenotype after a gastric bypass. The beneficial microbe *Faecalibacterium prausnitzii*, in particular, is less abundant in patients who are obese and diabetic, but increases after surgery[11]. Levels of *F. prausnitzii* are negatively correlated with inflammatory markers, indicating that the bacterium may modulate systemic inflammation (common to diabetes and obesity) and contribute to the amelioration of diabetes. In addition, germ-free mice do not develop diet-induced obesity, and treatment of obese mice with antibiotics reduces adiposity and adipose inflammation, and improves glucose metabolism[17–19], further supporting the benefits of inducing a shift in microbiota composition.

Energy harvest

Carbohydrates are important sources of energy for human and microbial cells. Human enzymes cannot degrade most complex carbohydrates and plant polysaccharides. Instead, the non-digestible

[1]Wallenberg Laboratory for Cardiovascular and Metabolic Research, Sahlgrenska University Hospital, 413 45 Gothenburg, Sweden. [2]Department of Molecular and Clinical Medicine, University of Gothenburg, 413 45 Gothenburg, Sweden. [3]Novo Nordisk Foundation Center for Basic Metabolic Research, Faculty of Health Sciences, University of Copenhagen, Copenhagen DK-2200, Denmark.

carbohydrates, including cellulose, xylans, resistant starch and inulin, are fermented in the colon by its microbiota to yield energy for microbial growth and end products such as short-chain fatty acids (SCFAs) (Fig. 1), mainly acetate, propionate and butyrate, which have profound effects on gut health as, for example, an energy source, an inflammation modulator, a vasodilator and part of gut motility and wound healing. In addition, SCFAs are energy substrates for the colonic epithelium (butyrate) and peripheral tissues (acetate and propionate)[20]. The patterns of intestinal fermentation, and consequently the types and amount of SCFAs produced, are determined by how much carbohydrate is consumed and the composition of the gut microbiota. For example, fermentation of dietary fructans increases when gnotobiotic mice that have been colonized with *Bacteroides thetaiotaomicron*, are co-colonized with *Methanobrevibacter smithii*[21]. *B. thetaiotaomicron* produces more acetate and formate, and *M. smithii* uses formate for methanogenesis. The interactions promote more efficient carbohydrate fermentation and increased energy absorption from the gut, resulting in increased adiposity in the co-colonized mice compared with mice colonized with only *B. thetaiotaomicron*. The composition of the gut microbiota and the metabolic interactions between its species may therefore affect food digestion and energy harvest.

Direct evidence for the role of the microbiota in energy harvest and fat deposition comes from germ-free rats, which have reduced intestinal levels of SCFAs[22], and twice as much urinary and faecal excretion of calories as that of conventional rats fed the same polysaccharide-rich diet[23]. The germ-free rodents compensate for the reduced energy harvest by increasing their food intake[23]. Germ-free mice also have reduced adiposity compared with their conventional counterparts, but adiposity is normalized when they are colonized with a healthy microbiota for 14 days[4,19]. Microbial energy harvest in obesity has been investigated in conventional genetically obese *ob*/*ob* mice, which have increased amounts of SCFAs in their caecum and reduced energy content in their faeces compared with their lean littermates[24]. Metagenomic sequencing of the caecal microbiota showed an enrichment of gene functions that were related to the degradation of dietary polysaccharides in the microbiome of *ob*/*ob* mice[24]. This finding was also true of humans: the faecal microbiota of people who are obese has an increased capacity to harvest energy[2]. In mice, the obese phenotype was transmissible through microbiota transplants, and germ-free mice colonized with the microbiota from obese donors gained twice as much fat as those colonized with the microbiota from lean donors[24].

The role of the gut microbiota in promoting energy harvest from diet and fat deposition has been clearly demonstrated in mice, but most of the evidence in humans has come from indirect studies. For instance, people who are obese have higher levels of ethanol in their breath than lean people[25], indicating altered fermentation and a greater number of faecal SCFAs[13], which may suggest increased microbial energy harvest.

Diet alters the gut microbiota

Diet is known to modulate the composition of the gut microbiota in humans and mice. Long-term dietary habits have a considerable effect on the human gut microbiota. For example, children in a rural African village, who consumed high amounts of plant polysaccharides, had low levels of Firmicutes and increased levels of Bacteroidetes — mainly *Prevotella* and *Xylanibacter* — in their faecal microbiota compared with Italian children, who had high levels of Enterobacteriaceae — mainly *Shigella* and *Escherichia*[26]. *Prevotella* and *Xylanibacter* are known to degrade cellulose and xylans, and are associated with increased faecal SCFAs, suggesting that the gut microbiota of the children living in rural Africa had adapted to maximize energy extraction from a diet rich in fibre. Human gut microbiota can be divided into three discrete compositions. However, this concept is currently being challenged as enterotypes maybe more of a gradient than discrete entities. Each enterotype is dominated by a different genus — *Bacteroides*, *Prevotella* or *Ruminococcus*[27] — but not affected by gender, age or nationality[27]. Enterotypes dominated by *Bacteroides* or *Prevotella* are associated with the consumption of a diet rich in protein and animal fat, or carbohydrates, respectively[28]. The *Ruminococcus* enterotype is not well separated and is partly merged with the *Bacteroides* enterotype[28]. This division supports the association between *Prevotella* and a diet high in carbohydrates, which was seen in children from rural Africa[26]. A 10-day dietary intervention, however, was not sufficient to alter the enterotype of an individual[28],

BOX 1

Terminology

- **Enterotype** is the grouping of the microbiota of a given person into discrete configurations. But recent data have conflicted with this definition and suggest that enterotypes may be less discrete.
- **Gnotobiotics** is the study of animals living in a microbiologically defined environment, either germ-free or colonized with known bacteria.
- **Inflammasomes** are protein complexes containing an intracellular sensor (such as a nucleotide-binding oligomerization domain (NOD)-like receptor), the procaspase-1 precursor and the ASC (apoptosis-associated speck-like protein containing a caspase activation and recruitment domain) adaptor protein. These complexes recognize microbe- and the host-derived inflammatory signals, microbial-associated molecular patterns and damage-associated molecular patterns, and its activation leads to the maturation of inflammatory cytokines (such as interleukin-1β and interleukin-18). Inflammasomes participate in antimicrobial innate immune responses, but may also have a role in metabolic diseases, such as obesity, type 2 diabetes and atherosclerosis.
- **Metagenome** is the total DNA that can be extracted from an environment. The human metagenome is the aggregate of the DNA of the host and the microbiota. Metagenome and microbiome are often used interchangeably.
- **Metagenomics** is the study of the metagenome (microbiome). Metagenomics can either be targeted (usually 16S ribosomal RNA) or untargeted (shotgun sequencing).
- **Microbiota** is the collective microbial community inhabiting a specific environment. Cellular density increases along the length of the gut, and the colonic microbiota is the densest and most diverse community in the gut, and in the whole human body.
- **Microbiome** is the collective genomic content of a microbiota. It also indicates the total genetic capacity of the community.
- **Probiotics** are defined as live microorganisms that, when administered in adequate amounts, confer a health benefit for the host[85]. Many bacterial strains in the *Lactobacillus* and *Bifidobacterium* genera are considered to be probiotic.
- **Prebiotics** are non-digestible food ingredients that, when consumed in sufficient amounts, selectively stimulate the growth, activity or both of one or a limited number of microbial genera or species in the gut microbiota that confer(s) health benefits to the host[85]. Inulin and *trans*-galacto-oligosaccharides are defined as prebiotics because they are resistant to gastric digestion and hydrolysis by human enzymes; are fermented by specific members of the gut microbiota; and induce selective growth, activity or both of beneficial intestinal bacteria[86]. Both inulin and *trans*-galacto-oligosaccharides stimulate the growth of *Bifidobacterium*, an effect defined as bifidogenic.

BOX 2

Dominant microbes

The human gut microbiota is dominated by five bacterial phyla (Firmicutes, Bacteroidetes, Actinobacteria, Proteobacteria and Verrucomicrobia) and one Archaea (Euryarchaeota). The less prevalent bacterial groups are distributed among Cyanobacteria, Fusobacteria, Lentisphaerae, Spirochaetes and TM7.

The Firmicutes phylum contains relevant genera, including *Ruminococcus, Clostridium, Lactobacillus* (several strains of which are probiotics), and the butyrate producers *Eubacterium, Faecalibacterium* and *Roseburia*.

In Bacteroidetes, *Bacteroides*, *Prevotella* and *Xylanibacter* degrade a variety of complex glycans.

The Actinobacteria phylum includes *Collinsella* and *Bifidobacterium* (which contains probiotic strains). Common Proteobacteria are *Escherichia* (from the Enterobacteriaceae family) and *Desulfovibrio* (which contains sulphate-reducing bacteria). Verrucomicrobia was recently discovered and includes *Akkermansia* (which are specialized for mucus degradation). Euryarchaeota contains the prevalent Methanobrevibacter (which is involved in the continuation of intestinal methanogenesis).

suggesting that a long-term change may be required to provoke a major shift in gut microbiota composition.

Changes in daily carbohydrate intake may affect specific groups of colonic bacteria over a short period of time. Consumption of the prebiotic inulin increases the levels of *F. prausnitzii* and *Bifidobacterium* sp. in humans[29]. Similarly, prebiotics promote a selective increase in *Bifidobacterium* sp. in diet-induced obese mice, and this increase is correlated with reduced adiposity and levels of microbe-derived inflammatory molecules, such as lipopolysaccharide, compared with mice that are fed a high-fat diet without prebiotics[30]. Human diets that are supplemented with resistant starch have increased faecal levels of *Ruminococcus bromii* and *Eubacterium rectale*, which correlates with fibre fermentation[31]. Consumption of resistant starch also improves insulin sensitivity[32], but the variation in the microbial response to changes in resistant starch between individuals suggests successful dietary interventions need to be personalized[31].

The gut microbiota also reacts to dietary fat. Mice fed on high-fat diets have reduced numbers of Bacteroidetes, and increased numbers of Firmicutes and Proteobacteria[33,34]. This change is rapid, occurring within 24 hours[35]. Transplantation of the caecal microbiota from obese mice fed on high-fat diets into germ-free recipients increases adiposity significantly more than transplantation of a lean microbiota[34]. The altered microbial community of obese mice seems to have some role in promoting diet-induced obesity, but the mechanisms that cause this are unknown. A change in diet clearly alters the gut microbiota, and these alterations may contribute to the host's metabolic phenotype. Further metatranscriptomic and proteomic studies should provide insight into the response of microbial function as a result of a dietary shift.

Microbial processing of food constituents

Products of microbial metabolism act as signalling molecules and influence the host's metabolism. Microbial products directly affect intestinal function but may also affect the liver and brain, as well as adipose and muscle tissue, which consequently may affect the level of obesity and the associated comorbidities (Fig. 2). Microbial enzymatic activities can act directly on the fermentation of polysaccharides and bile-acid metabolism, or act in conjunction with the host on the metabolism of choline (Fig. 3).

Fermentation of polysaccharides

Non-digestible carbohydrates are important sources of energy for several members of the colonic microbiota. Species such as *B. thetaiotaomicron* and *Bacteroides ovatus* contain more than twice the number of glycosidase and lyase genes than the human genome and are capable of using nearly all of the main plant and host glycans (such as mucus-associated glycoproteins)[36,37]. Of the SCFAs produced from microbial fermentation, butyrate is particularly important as an energy substrate for cellular metabolism in the colonic epithelium. The colonic epithelial cells of germ-free mice are severely energy-deprived and are characterized by increased activation of AMP-activated protein kinase (AMPK), which senses cellular energy status[38]. This is also true of the liver of germ-free mice[39]. The liver metabolism of germ-free and colonized mice differs considerably, possibly because of the increased influx of SCFAs into the liver of colonized mice (Fig. 1). Acetate and propionate are taken up by the liver and used as substrates for lipogenesis and gluconeogenesis. Colonized mice have higher levels of stored triglycerides in the liver and an increase in the synthesis of very-low-density lipoproteins[40], which transport triglycerides from the liver to other tissues. Increased triglyceride production in the liver of colonized mice is associated with reduced expression of fasting-induced adipose factor, or ANGPTL4, in the small intestine[4,39]. ANGPTL4 is a potent inhibitor of the enzyme lipoprotein lipase, which mediates cellular uptake of triglycerides. Germ-free *Angptl4*-deficient mice gained as much fat mass and body weight during high-fat feeding as colonized mice, indicating that ANGPTL4 directly mediates microbial regulation of adiposity in mice[4,39].

SCFAs also affect proliferation, differentiation and modulation of gene expression in mammalian colonic epithelial cells[41]. However, these effects have been attributed to butyrate acting as a potent histone deacetylase inhibitor and, as such, it may regulate 2% of the

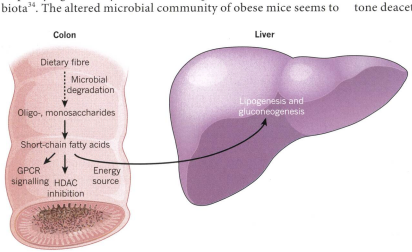

Figure 1 | Effects of colonic fermentation of dietary fibres. Complex carbohydrates, such as dietary fibre, are metabolized by the colonic microbiota to oligosaccharides and monosaccharides and then fermented to short-chain fatty acid end-products, mainly acetate, propionate and butyrate. Short-chain fatty acids are absorbed in the colon, where butyrate provides energy for colonic epithelial cells, and acetate and propionate reach the liver and peripheral organs, where they are substrates for gluconeogenesis and lipogenesis. In addition to being energy sources, short-chain fatty acids control colonic gene expression by inhibiting the enzyme histone deacetylase (HDAC) and metabolic regulation by signalling through G-protein-coupled receptors (GPCRs), such as GPR41 or GPR43.

mammalian transcriptome[41]. In addition, SCFAs can regulate gene expression by binding to the G-protein-coupled receptors (GPCRs) GPR41 (also known as FFAR3) and GPR43 (also known as FFAR2). Signalling through these receptors affects several different functions depending on the cellular type. For example, SCFAs suppress inflammation through GPR43 signalling in immune cells, such as neutrophils[42,43], and modulate secretion of the hormone GLP-1 — which improves insulin secretion and has antidiabetic effects — by enteroendocrine L-cells in the distal small intestine and colon[44]. In addition, the gut microbiota induces *Pyy* expression by L-cells through a GPR41-dependent mechanism. Conventional *Gpr41*-deficient mice have reduced adiposity compared with conventional wild-type mice, whereas germ-free wild-type and *Gpr41*-deficient mice had similar adiposity[45], indicating that the effect of the microbiota on fat deposition is dependent on this SCFA receptor.

Microbial fermentation of polysaccharides may affect host adiposity through several complementary mechanisms, so modulation of the microbiota and its fermentation capacity may provide new avenues for managing obesity.

Microbial regulation of bile-acid metabolism

The primary bile acids cholic acid and chenodeoxycholic acid are synthesized in the human liver from cholesterol, and are important for ensuring that cholesterol, dietary fats and fat-soluble vitamins from the small intestine are soluble and absorbable. Primary bile acids are conjugated to taurine in mice and to glycine in humans, and are taken up in the distal ileum for transport to the liver. However, bacteria in this part of the ileum deconjugate these bile acids, which then escape intestinal uptake and can be further metabolized by the gut microbiota into secondary bile acids. Because the gut microbiota transforms bile acids, germ-free rodents have more bile acid and a less diverse profile than their conventionally raised counterparts[46–48].

Bile acids also function as signalling molecules and bind to cellular receptors[49], such as the bile-acid-synthesis controlling nuclear receptor farnesoid X receptor (FXR)[50] and the GPCR TGR5. Both FXR and TGR5 have been implicated in the modulation of glucose metabolism in mice, but FXR impairs, whereas TGR5 promotes, glucose homeostasis[51–53]. In contrast to FXR, which is activated by primary bile acids, TGR5 binds secondary bile acids such as deoxycholic acid (formed from cholic acid) and lithocholic acid (formed from chenodeoxycholic acid). TGR5 signalling in enteroendocrine L-cells induces secretion of GLP-1, thereby improving liver and pancreatic function and enhancing glucose tolerance in obese mice[53]. Bile acids are taken up from the gut and circulated throughout the body, so activation of TGR5 and FXR in peripheral organs may contribute to overall host metabolism. Activation of TGR5 in brown adipose tissue and muscle increases energy expenditure and protects against diet-induced obesity[54]. The gut microbiota may therefore contribute to the level of obesity and type 2 diabetes by controlling lipid and glucose metabolism though the composition of bile-acid pools and the modulation of FXR and TGR5 signalling.

Microbial metabolism of choline

Choline is an important component of cell membranes and is mostly obtained from foods such as red meat and eggs, but may also be synthesized by the host[55]. Choline is also important for lipid metabolism and synthesis of very-low-density lipoprotein in the liver, and insufficient levels in the diet are associated with altered gut microbial ecology and liver steatosis in mice[56] and humans[57]. In particular, low quantities of Gamma-proteobacteria and high levels of *Erysipelotrichi* in human faecal microbiota are associated with hepatic steatosis[57]. Microbial and host enzymatic activities interact in choline's transformation into toxic methylamines, so trimethylamine that is produced by intestinal microbes can be further metabolized to trimethylamine-N-oxide in the liver[58,59]. These transformations may decrease the levels of bioavailable choline and are suggested to trigger non-alcoholic fatty liver disease (NAFLD) in mice[58]. An altered gut microbial composition and its capacity to metabolize choline may have an important role in modulating NAFLD as well as glucose homeostasis[58].

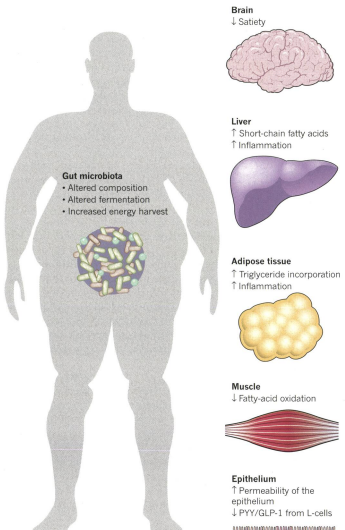

Figure 2 | Features of the gut microbiota that promote obesity and insulin resistance. Alterations to the composition and metabolic capacity of gut microbiota in obesity promote adiposity and influence metabolic processes in peripheral organs, such as the control of satiety in the brain; the release of hormones from the gut (shown as PYY and GLP-1); and the synthesis, storage or metabolism of lipids in the adipose tissue, liver and muscle. Microbial molecules also increase intestinal permeability, leading to systemic inflammation and insulin resistance.

Furthermore, plasma levels of trimethylamine-*N*-oxide and its metabolites are correlated with cardiovascular disease[60] (Fig. 3). The effect of microbial choline metabolism in cardiovascular disease is shown by the reduction of atherosclerosis in atherosclerosis-prone *Apoe*$^{-/-}$ mice treated with broad-spectrum antibiotics[60]. A gut microbiome with different capacities to process cholesterol and choline may contribute to the development of cardiovascular diseases.

Regulation of permeability and inflammation

Obesity, insulin resistance and development of type 2 diabetes are associated with systemic and adipose tissue inflammation[61]. The gut microbiota is a rich source of molecules such as lipopolysaccharide and peptidoglycan that may cause inflammation in peripheral tissues of the body. Colonization of germ-free mice with *Escherichia coli* is

sufficient to augment macrophage infiltration of adipose tissue and polarize macrophages towards the expression of pro-inflammatory cytokines[19]. Plasma lipopolysaccharide levels increase in patients with type 2 diabetes[62], and feeding lipopolysaccharide to mice for 4 weeks increase adipose tissue inflammation and reduce insulin sensitivity[63]. These findings suggest that the gut microbiota may affect host metabolism by altering adipose tissue inflammation. Higher numbers of T cells[64,65] and mast cells[66], and lower numbers of regulatory T cells[67] are also involved, but if and how the gut microbiota affects these cells and whether such interactions contribute to metabolic abnormalities is unclear.

Plasma lipopolysaccharide levels seem to rise with higher fat intake in mice[63] and humans[68,69]. Two hypotheses have been made to explain the mechanism: lipopolysaccharide is taken up with dietary fats in chylomicrons[70], or lipopolysaccharide reaches the circulation because the gut is more permeable in obese mice[63]. A connection between metabolism and the function of the epithelial barrier is thought to exist. Targeted deletion of fatty acid synthase — encoded by the *Fas* gene — in the gut epithelium of mice showed that epithelial *de novo* lipogenesis is required to maintain barrier function[71]. *Fas*-deficient epithelium has increased permeability and, as a result, increased colonic levels of proinflammatory cytokines and high serum lipopolysaccharide. These phenotypes were corrected by antibiotic treatment, suggesting a reciprocal interaction between microbiota, altered epithelial permeability and host metabolism.

A similar connection between gut permeability and type 2 diabetes in humans could also be present. Permeability is correlated with increased visceral adiposity and hepatic steatosis[72], and those with high visceral adiposity and type 2 diabetes have increased levels of bacterial DNA in their blood[73]. However, inflammation may increase permeability in the gut, and further investigation into whether increased permeability causes adipose inflammation or increased inflammation contributes to increased permeability is needed. Either way, the gut microbiota modulates permeability that may contribute to adipose inflammation and cause insulin resistance.

Lipopolysaccharide molecules bind to Toll-like receptor 4 (TLR4), and peptidoglycan to nucleotide-binding oligomerization domain (NOD) receptors, both of which activates proinflammatory signalling cascades[63,74,75]. Deletion of TLR4 in haematopoietic cells by generating bone-marrow chimaeras shows that TLR4 activation in macrophages of mice fed a high-fat diet is required for the development of fasting hyperinsulinaemia, and insulin resistance in liver and adipose tissue but not for the development of obesity[76]. The innate immune system, however, also modulates microbial composition, which may have autonomous effects on host metabolism. Mice deficient in TLR5 have an altered microbial ecology and exhibit metabolic-syndrome signs, such as obesity, insulin resistance and dyslipidaemia, which are, in part, associated with increased food consumption[77]. Transplantation of the gut microbiota from *Tlr5*-deficient and wild-type mice into germ-free recipients shows that the phenotypes are transmissible, and suggests that the gut microbiota alone can mediate disease.

Microbe-associated molecular patterns, including lipopolysaccharide and peptidoglycan, can be recognized by nucleotide-binding domain and leucine-rich-repeat-containing proteins (NLRPs), which form the inflammasome complex together with the apoptosis-associated speck-like protein containing a caspase activation and recruitment domain (ASC)[78]. Obesity is associated with increased adipose expression of NLRP3 in mice and ablation of NLRP3 enhances insulin signalling[79]. However, inflammasomes may be linked to gut microbiota and host metabolism (Fig. 4). NLRP3, NLRP6 and ASC are important regulators of microbial ecology in mice, and deletion of their genes increases the number of Bacteroidetes (Prevotellaceae) and TM7[56,80]. In particular, deficiency in *Nlrp6* results in altered gut microbial ecology that predisposes mice to colitis[80], and inflammasome complexes that do not contain NLRP3 or NLRP6 are associated with an altered gut microbiota and promote NAFLD and non-alcoholic steatohepatitis (NASH)[56]. Importantly, wild-type mice housed with disease-prone Asc$^{-/-}$ mice develop NAFLD or NASH, providing direct evidence that an altered gut microbiota may cause these diseases[56]. Alterations to gut microbiota composition are associated with an increased influx of TLR4 and TLR9 ligands — presumably lipopolysaccharide and bacterial DNA — respectively,

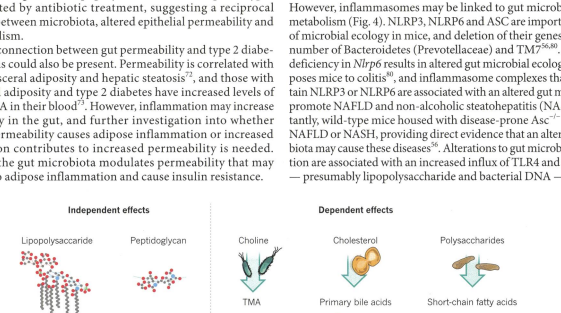

Figure 3 | Diet-independent and -dependent microbial effects on host metabolism. The gut microbiota produces pro-inflammatory molecules, such as lipopolysaccharide and peptidoglycan, which may affect host metabolism through proteins produced by the host to mediate the immune response. Choline, cholesterol and polysaccharides obtained from the diet are metabolized by the gut microbiota and either directly or through further host–microbial co-metabolization generate bioactive compounds. In the case of choline, this can lead to cardiovascular disease; for cholesterol, activation of TGR5 can increase energy expenditure and GLP-1 secretion or protection against heart disease; and for polysaccharides, short-chain fatty acids can be used as an energy source or can bind to GPR41 or GPR43 to regulate hormones and modulate inflammation. FMO, flavin-containing monooxygenase; TLR4, Toll-like receptor 4; TMA, trimethylamine; TMAO, trimethylamine-*N*-oxide.

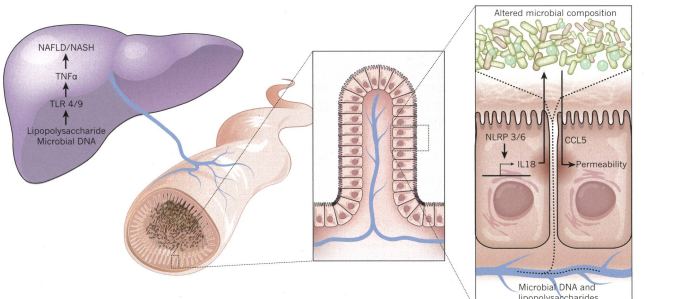

Figure 4 | Different microbial innate immune mechanisms affect host metabolism in the gut and liver. Plasma lipopolysaccharide seems to rise with higher fat intake, and those with high visceral adiposity have higher levels of microbial DNA in their blood. Both lipopolysaccharide and microbial DNA seem to be connected with gut permeability. NLRP3 and 6 are both important regulators of microbial ecology through the effector protein interleukin-18 (IL-18). The altered gut microbiota can stimulate CCL5 secretion, which can result in increased permeability and influx of microbial components. In the liver, lipopolysaccharide and bacterial DNA activate the receptors, TLR4 and 9, leading to increased tumour-necrosis-factor-α (TNFα) secretion and development of non-alcoholic fatty liver disease (NAFLD) and non-alcoholic steatohepatitis (NASH).

to the liver through the portal vein[56]. Mice deficient in TLR signalling in the liver are therefore protected from developing conditions related to metabolic syndrome such as obesity, NAFLD and NASH[56] (Fig. 4). The interaction between diet, host and gut microbiota may modulate gut permeability that leads to an influx of proinflammatory molecules and subsequent activation of inflammatory signalling pathways in peripheral tissues that may cause obesity, steatosis and insulin resistance.

Future research

The gut microbiota is increasingly being accepted as an environmental factor that affects host metabolism and contributes to associated pathological conditions, such as obesity, diabetes and cardiovascular disease. However, the contribution that the gut microbiota makes to causing obesity and diabetes in humans is unclear. This is probably because the heterogeneous aetiology of obesity and diabetes can be associated with different microbes; studies are underpowered and include participants with diverse ethnic origin and food habits; the composition of the gut microbiota has large interpersonal variation; and different methods, with specific biases, have been used to profile the microbiota. Cheaper sequencing and improved bioinformatics tools for the analysis of the gut microbiota will allow more researchers to use metagenomic sequencing and avoid primer and polymerase chain reaction biases linked to 16S rRNA gene surveys. Although useful, metagenomic approaches should be complemented by metatranscriptomics and metaproteomics to assess which microbial genes and proteins are expressed in specific conditions. One of the main challenges is to obtain robust predictive biomarkers for obesity and diabetes on the basis of the gut microbiota, for which improved study designs and analytical methods are essential. Much of the focus has been on the faecal microbiota, but many metabolic functions also occur in the small intestine. Sampling intestinal specimens might contribute to the identification of microbial biomarkers for health and disease, and although challenging, more emphasis should be placed on examining its microbiota and the effects on host metabolism.

Studies in humans tend to be correlative, so the role of the microbiota in obesity and its comorbidities in humans remains to be proven. However, this role can be examined in animal studies. Germ-free mice can be 'humanized' by colonizing them with human intestinal communities, providing tools for examining the function of a specific human microbiota and testing how it interacts with specific diets. Genetically engineered germ-free mice could help to identify the molecular mechanisms by which the gut microbiota affects host metabolism. Pigs have similar gastrointestinal tracts and diets to humans, so they could be useful animal models in which to test dietary interventions and to manipulate the gut microbiota to improve health and prevent disease.

Accumulating evidence indicates that the gut microbiota may be a target for treating metabolic diseases[81]. Supplementing the diet with non-digestible food ingredients, or prebiotics, that stimulate the expansion of specific microbes to improve metabolic regulation can be a therapy. Probiotics may be an interesting approach for prevention of obesity and related diseases. But to determine the effects of both of these therapies, double-blind, placebo-controlled studies are required. Therapies that replace unhealthy with a healthy microbiota through transplantation have been used successfully since 1958 for the treatment of antibiotic-related diarrhoeal colitis[82]. Recently, transplantation of healthy lean microbiota improved insulin signalling in participants with metabolic syndrome[83]. Although a promising technique, transmission of unknown and potentially pathogenic bacteria and viruses from an unfractionated gut microbiota may have risks for the recipient. Using microbiota-based interventions to treat obesity will require probiotics that are selected for specific clinical manifestations of metabolic syndrome. ■

1. Qin, J. *et al.* A human gut microbial gene catalogue established by metagenomic sequencing. *Nature* **464,** 59–65 (2010).
This article is the first catalogue of the human metagenome.
2. Turnbaugh, P. J. *et al.* A core gut microbiome in obese and lean twins. *Nature* **457,** 480–484 (2009).
This paper reports that the diversity of the gut microbiota differs between lean and obese individuals.
3. Sjogren, K. *et al.* The gut microbiota regulates bone mass in mice. *J. Bone Miner. Res.* **27,** 1357–1367 (2012).
4. Bäckhed, F. *et al.* The gut microbiota as an environmental factor that regulates fat storage. *Proc. Natl Acad. Sci. USA* **101,** 15718–15723 (2004).
This article reports a link between the gut microbiota and adiposity.
5. Reinhardt, C. *et al.* Tissue factor and PAR1 promote microbiota-induced intestinal vascular remodelling. *Nature* **483,** 627–631 (2012).

6. Stappenbeck, T. S., Hooper, L. V. & Gordon, J. I. Developmental regulation of intestinal angiogenesis by indigenous microbes via Paneth cells. *Proc. Natl Acad. Sci. USA* **99,** 15451–15455 (2002).
7. Larsson, E. *et al.* Analysis of gut microbial regulation of host gene expression along the length of the gut and regulation of gut microbial ecology through MyD88. *Gut* **61,** 1124–1131 (2011).
8. Gaborieau-Routhiau, V. *et al.* The key role of segmented filamentous bacteria in the coordinated maturation of gut helper T cell responses. *Immunity* **31,** 677–689 (2009).
9. Ley, R. E. *et al.* Obesity alters gut microbial ecology. *Proc. Natl Acad. Sci. USA* **102,** 11070–11075 (2005).
10. Ley, R. E., Turnbaugh, P. J., Klein, S. & Gordon, J. I. Microbial ecology: human gut microbes associated with obesity. *Nature* **444,** 1022–1023 (2006).
11. Furet, J. P. *et al.* Differential adaptation of human gut microbiota to bariatric surgery-induced weight loss: links with metabolic and low-grade inflammation markers. *Diabetes* **59,** 3049–3057 (2010).
12. Duncan, S. H. *et al.* Human colonic microbiota associated with diet, obesity and weight loss. *Int. J. Obes. (Lond.)* **32,** 1720–1724 (2008).
13. Schwiertz, A. *et al.* Microbiota and SCFA in lean and overweight healthy subjects. *Obesity* **18,** 190–195 (2010).
14. Zhang, H. *et al.* Human gut microbiota in obesity and after gastric bypass. *Proc. Natl Acad. Sci. USA* **106,** 2365–2370 (2009).
15. Sjostrom, L. *et al.* Lifestyle, diabetes, and cardiovascular risk factors 10 years after bariatric surgery. *N. Engl. J. Med.* **351,** 2683–2693 (2004).
16. Sjostrom, L. *et al.* Effects of bariatric surgery on mortality in Swedish obese subjects. *N. Engl. J. Med.* **357,** 741–752 (2007).
17. Cani, P. D. *et al.* Changes in gut microbiota control metabolic endotoxemia-induced inflammation in high-fat diet-induced obesity and diabetes in mice. *Diabetes* **57,** 1470–1481 (2008).
18. Membrez, M. *et al.* Gut microbiota modulation with norfloxacin and ampicillin enhances glucose tolerance in mice. *FASEB J.* **22,** 2416–2426 (2008).
19. Caesar, R. *et al.* Gut-derived lipopolysaccharide augments adipose macrophage accumulation but is not essential for impaired glucose or insulin tolerance in mice. *Gut* http://dx.doi.org/10.1136/gutjnl-2011-301689 (25 April, 2012).
20. Bergman, E. N. Energy contributions of volatile fatty acids from the gastrointestinal tract in various species. *Physiol. Rev.* **70,** 567–590 (1990).
21. Samuel, B. S. & Gordon, J. I. A humanized gnotobiotic mouse model of host–archaeal–bacterial mutualism. *Proc. Natl Acad. Sci. USA* **103,** 10011–10016 (2006).
22. Hoverstad, T. & Midtvedt, T. Short-chain fatty acids in germfree mice and rats. *J. Nutr.* **116,** 1772–1776 (1986).
23. Wostmann, B. S., Larkin, C., Moriarty, A. & Bruckner-Kardoss, E. Dietary intake, energy metabolism, and excretory losses of adult male germfree Wistar rats. *Lab. Anim. Sci.* **33,** 46–50 (1983).
24. Turnbaugh, P. J. *et al.* An obesity-associated gut microbiome with increased capacity for energy harvest. *Nature* **444,** 1027–1031 (2006).
This article demonstrates that the microbiota of those who are obese is enriched in genes for energy harvest and that obesity can be transmitted by transplantation of microbiota.
25. Nair, S., Cope, K., Risby, T. H. & Diehl, A. M. Obesity and female gender increase breath ethanol concentration: potential implications for the pathogenesis of nonalcoholic steatohepatitis. *Am. J. Gastroenterol.* **96,** 1200–1204 (2001).
26. De Filippo, C. *et al.* Impact of diet in shaping gut microbiota revealed by a comparative study in children from Europe and rural Africa. *Proc. Natl Acad. Sci. USA* **107,** 14691–14696 (2010).
This article demonstrates the affect of diet in shaping the gut microbiota.
27. Arumugam, M. *et al.* Enterotypes of the human gut microbiome. *Nature* **473,** 174–180 (2011).
28. Wu, G. D. *et al.* Linking long-term dietary patterns with gut microbial enterotypes. *Science* **334,** 105–108 (2011).
29. Ramirez-Farias, C. *et al.* Effect of inulin on the human gut microbiota: stimulation of *Bifidobacterium adolescentis* and *Faecalibacterium prausnitzii*. *Br. J. Nutr.* **101,** 541–550 (2009).
30. Cani, P. D. *et al.* Selective increases of bifidobacteria in gut microflora improve high-fat-diet-induced diabetes in mice through a mechanism associated with endotoxaemia. *Diabetologia* **50,** 2374–2383 (2007).
31. Walker, A. W. *et al.* Dominant and diet-responsive groups of bacteria within the human colonic microbiota. *ISME J.* **5,** 220–230 (2010).
32. Robertson, M. D., Bickerton, A. S., Dennis, A. L., Vidal, H. & Frayn, K. N. Insulin-sensitizing effects of dietary resistant starch and effects on skeletal muscle and adipose tissue metabolism. *Am. J. Clin. Nutr.* **82,** 559–567 (2005).
33. Hildebrandt, M. A. *et al.* High-fat diet determines the composition of the murine gut microbiome independently of obesity. *Gastroenterology* **137,** 1716–1724 (2009).
34. Turnbaugh, P. J., Bäckhed, F., Fulton, L. & Gordon, J. I. Diet-induced obesity is linked to marked but reversible alterations in the mouse distal gut microbiome. *Cell Host Microbe* **3,** 213–223 (2008).
35. Turnbaugh, P. J. *et al.* The effect of diet on the human gut microbiome: a metagenomic analysis in humanized gnotobiotic mice. *Sci. Transl. Med.* **1,** 6ra14 (2009).
36. Xu, J. *et al.* A genomic view of the human–*Bacteroides thetaiotaomicron* symbiosis. *Science* **299,** 2074–2076 (2003).
37. Martens, E. C. *et al.* Recognition and degradation of plant cell wall polysaccharides by two human gut symbionts. *PLoS Biol.* **9,** e1001221 (2011).
38. Donohoe, D. R. *et al.* The microbiome and butyrate regulate energy metabolism and autophagy in the mammalian colon. *Cell Metab.* **13,** 517–526 (2011).
39. Bäckhed, F., Manchester, J. K., Semenkovich, C. F. & Gordon, J. I. Mechanisms underlying the resistance to diet-induced obesity in germ-free mice. *Proc. Natl Acad. Sci. USA* **104,** 979–984 (2007).
40. Velagapudi, V. R. *et al.* The gut microbiota modulates host energy and lipid metabolism in mice. *J. Lipid Res.* **51,** 1101–1112 (2010).
41. Davie, J. R. Inhibition of histone deacetylase activity by butyrate. *J. Nutr.* **133,** 2485S–2493S (2003).
42. Maslowski, K. M. *et al.* Regulation of inflammatory responses by gut microbiota and chemoattractant receptor GPR43. *Nature* **461,** 1282–1286 (2009).
43. Sina, C. *et al.* G protein-coupled receptor 43 is essential for neutrophil recruitment during intestinal inflammation. *J. Immunol.* **183,** 7514–7522 (2009).
44. Tolhurst, G. *et al.* Short-chain fatty acids stimulate glucagon-like peptide-1 secretion via the G-protein-coupled receptor FFAR2. *Diabetes* **61,** 364–371 (2012).
45. Samuel, B. S. *et al.* Effects of the gut microbiota on host adiposity are modulated by the short-chain fatty-acid binding G protein-coupled receptor, Gpr41. *Proc. Natl Acad. Sci. USA* **105,** 16767–16772 (2008).
46. Wostmann, B. S. Intestinal bile acids and cholesterol absorption in the germfree rat. *J. Nutr.* **103,** 982–990 (1973).
47. Swann, J. R. *et al.* Systemic gut microbial modulation of bile acid metabolism in host tissue compartments. *Proc. Natl Acad. Sci. USA* **108,** 4523–4530 (2010).
48. Gustafsson, B. E., Bergstrom, S., Lindstedt, S. & Norman, A. Turnover and nature of fecal bile acids in germfree and infected rats fed cholic acid-24–14C; bile acids and steroids 41. *Proc. Soc. Exp. Biol. Med.* **94,** 467–471 (1957).
49. Hylemon, P. B. *et al.* Bile acids as regulatory molecules. *J. Lipid Res.* **50,** 1509–1520 (2009).
50. Sinal, C. J. *et al.* Targeted disruption of the nuclear receptor FXR/BAR impairs bile acid and lipid homeostasis. *Cell* **102,** 731–744 (2000).
51. van Dijk, T. H. *et al.* An increased flux through the glucose 6-phosphate pool in enterocytes delays glucose absorption in $Fxr^{-/-}$ mice. *J. Biol. Chem.* **284,** 10315–10323 (2009).
52. Prawitt, J. *et al.* Farnesoid X receptor deficiency improves glucose homeostasis in mouse models of obesity. *Diabetes* **60,** 1861–1871 (2011).
53. Thomas, C. *et al.* TGR5-mediated bile acid sensing controls glucose homeostasis. *Cell Metab.* **10,** 167–177 (2009).
54. Watanabe, M. *et al.* Bile acids induce energy expenditure by promoting intracellular thyroid hormone activation. *Nature* **439,** 484–489 (2006).
55. Vance, D. E. Role of phosphatidylcholine biosynthesis in the regulation of lipoprotein homeostasis. *Curr. Opin. Lipidol.* **19,** 229–234 (2008).
56. Henao-Mejia, J. *et al.* Inflammasome-mediated dysbiosis regulates progression of NAFLD and obesity. *Nature* **482,** 179–185 (2012).
This paper elegantly connects microbial recognition by inflammasomes in the gut with altered permeability and liver steatosis.
57. Spencer, M. D. *et al.* Association between composition of the human gastrointestinal microbiome and development of fatty liver with choline deficiency. *Gastroenterology* **140,** 976–986 (2011).
58. Dumas, M. E. *et al.* Metabolic profiling reveals a contribution of gut microbiota to fatty liver phenotype in insulin-resistant mice. *Proc. Natl Acad. Sci. USA* **103,** 12511–12516 (2006).
59. Prentiss, P. G. *et al.* The metabolism of choline by the germfree rat. *Arch. Biochem. Biophys.* **94,** 424–429 (1961).
60. Wang, Z. *et al.* Gut flora metabolism of phosphatidylcholine promotes cardiovascular disease. *Nature* **472,** 57–63 (2011).
61. Osborn, O. & Olefsky, J. M. The cellular and signaling networks linking the immune system and metabolism in disease. *Nature Med.* **18,** 363–374 (2012).
62. Creely, S. J. *et al.* Lipopolysaccharide activates an innate immune system response in human adipose tissue in obesity and type 2 diabetes. *Am. J. Physiol. Endocrinol. Metab.* **292,** E740–E747 (2007).
63. Cani, P. D. *et al.* Metabolic endotoxemia initiates obesity and insulin resistance. *Diabetes* **56,** 1761–1772 (2007).
This paper reports that endotoxin is sufficient to alter metabolic inflammation and insulin sensitivity.
64. Nishimura, S. *et al.* CD8$^+$ effector T cells contribute to macrophage recruitment and adipose tissue inflammation in obesity. *Nature Med.* **15,** 914–920 (2009).
65. Winer, S. *et al.* Normalization of obesity-associated insulin resistance through immunotherapy. *Nature Med.* **15,** 921–929 (2009).
66. Liu, J. *et al.* Genetic deficiency and pharmacological stabilization of mast cells reduce diet-induced obesity and diabetes in mice. *Nature Med.* **15,** 940–945 (2009).
67. Feuerer, M. *et al.* Lean, but not obese, fat is enriched for a unique population of regulatory T cells that affect metabolic parameters. *Nature Med.* **15,** 930–939 (2009).
68. Amar, J. *et al.* Energy intake is associated with endotoxemia in apparently healthy men. *Am. J. Clin. Nutr.* **87,** 1219–1223 (2008).
69. Erridge, C., Attina, T., Spickett, C. M. & Webb, D. J. A high-fat meal induces low-grade endotoxemia: evidence of a novel mechanism of postprandial inflammation. *Am. J. Clin. Nutr.* **86,** 1286–1292 (2007).

70. Ghoshal, S., Witta, J., Zhong, J., de Villiers, W. & Eckhardt, E. Chylomicrons promote intestinal absorption of lipopolysaccharides. *J. Lipid Res.* **50,** 90–97 (2009).
71. Wei, X. *et al.* Fatty acid synthase modulates intestinal barrier function through palmitoylation of mucin 2. *Cell Host Microbe* **11,** 140–152 (2012).
72. Gummesson, A. *et al.* Intestinal permeability is associated with visceral adiposity in healthy women. *Obesity* **19,** 2280–2282 (2011).
73. Amar, J. *et al.* Involvement of tissue bacteria in the onset of diabetes in humans: evidence for a concept. *Diabetologia* **54,** 3055–3061 (2011).
74. Amar, J. *et al.* Intestinal mucosal adherence and translocation of commensal bacteria at the early onset of type 2 diabetes: molecular mechanisms and probiotic treatment. *EMBO Mol. Med.* **3,** 559–572 (2011).
75. Schertzer, J. D. *et al.* NOD1 activators link innate immunity to insulin resistance. *Diabetes* **60,** 2206–2215 (2011).
76. Saberi, M. *et al.* Hematopoietic cell-specific deletion of Toll-like receptor 4 ameliorates hepatic and adipose tissue insulin resistance in high-fat-fed mice. *Cell Metab.* **10,** 419–429 (2009).
77. Vijay-Kumar, M. *et al.* Metabolic syndrome and altered gut microbiota in mice lacking Toll-like receptor 5. *Science* **328,** 228–231 (2010).
78. Strowig, T., Henao-Mejia, J., Elinav, E. & Flavell, R. Inflammasomes in health and disease. *Nature* **481,** 278–286 (2012).
79. Vandanmagsar, B. *et al.* The NLRP3 inflammasome instigates obesity-induced inflammation and insulin resistance. *Nature Med.* **17,** 179–188 (2011).
80. Elinav, E. *et al.* NLRP6 inflammasome regulates colonic microbial ecology and risk for colitis. *Cell* **145,** 745–757 (2011).
81. Murphy, E. F. *et al.* Divergent metabolic outcomes arising from targeted manipulation of the gut microbiota in diet-induced obesity. *Gut* http://dx.doi.org/10.1136/gutjnl-2011-300705 (16 February, 2012).
82. Eiseman, B., Silen, W., Bascom, G. S. & Kauvar, A. J. Fecal enema as an adjunct in the treatment of pseudomembranous enterocolitis. *Surgery* **44,** 854–859 (1958).
83. Vrieze, A. *et al.* Transfer of intestinal microbiota from lean donors increases insulin sensitivity in subjects with metabolic syndrome. *Gastroenterology* http://dx.doi.org/10.1053/j.gastro.2012.06.031 (20 June, 2012) **This article reports that insulin resistance in obese humans can be improved by transplantation of a lean microbiota.**
84. Food and Agriculture Organization of the United Nations and World Health Organization. *Working Group Report on Drafting Guidelines for the evaluation of Probiotics in Food.* ftp://ftp.fao.org/es/esn/food/wgreport2.pdf (FAO and WHO, 2002).
85. Robertroid, M. *et al.* Prebiotic effects: metabolic and health benefits. *Br. J. Nutr.* **104,** S1–S63 (2010).

Acknowledgements The authors are grateful to A. Hallén for contribution to the artwork and to R. Perkins for reading the manuscript. Work in the authors' laboratory is funded by the Swedish Research Council, the Swedish Foundation for Strategic Research, Torsten Söderberg's Foundation, Ragnar Söderberg's foundation, AFA Insurances, the Knut and Alice Wallenberg foundation, the Swedish heart lung foundation, the NovoNordisk foundation and the Swedish diabetes foundation.

Author Information Reprints and permissions information is available at www.nature.com/reprints. The authors declare no competing financial interests. Readers are welcome to comment on the online version of this article at go.nature.com/1azgex. Correspondence should be addressed to F.B. (Fredrik.Backhed@wlab.gu.se).

REVIEW

doi:10.1038/nature11553

Genomic approaches to studying the human microbiota

George M. Weinstock[1]

The human body is colonized by a vast array of microbes, which form communities of bacteria, viruses and microbial eukaryotes that are specific to each anatomical environment. Every community must be studied as a whole because many organisms have never been cultured independently, and this poses formidable challenges. The advent of next-generation DNA sequencing has allowed more sophisticated analysis and sampling of these complex systems by culture-independent methods. These methods are revealing differences in community structure between anatomical sites, between individuals, and between healthy and diseased states, and are transforming our view of human biology.

The microbes that exist in the human body are collectively known as the human microbiota. This amazingly complex and poorly understood group of communities has an enormous impact on humans. An increasing number of conditions are being examined for correlative and causative associations with the microbiome — which, in this Review, is used to refer to the microbiota and the habitat it colonizes (Box 1). Each one of the many microbial communities has its own structure and ecosystem, depending on the body environment it exists in. The fundamental goal of human microbiome research is to measure the structure and dynamics of microbial communities, the relationships between their members, what substances are produced and consumed, the interaction with the host, and differences between healthy hosts and those with disease.

Despite an explosion in human-microbiome research, these communities are still the dark matter of the body. The microbiome has been called another organ[1–4] because of its products, its responsiveness to the environment and its integration with other systems. Sometimes referred to as our second genome[5], the genes of microbes that make up the microbiome outnumber human genes by more than 100-fold, with over 3 million bacterial genes in the gut alone[6,7]. These extensive microbial ecosystems are not limited to the human body. Microbes and their communities dominate the environment and occupy a vast range of niches. Environmental metagenomics was developed extensively before being applied to the human body[8,9], and methods from other disciplines have had a significant effect on human-microbiome research. Defining complicated microbial ecosystems and developing tools to probe their workings is an important research enterprise of twenty-first century microbiology.

The complexity of microbial communities makes studying them challenging. There may be hundreds of different species, and enumerating what organisms are present with standard microbiological techniques is not possible because many organisms have never been grown in culture and may require special, as yet unknown, growth conditions. In addition, the abundance of some microbes can range over orders of magnitude, so deep sampling is required to detect the less-abundant members. Culture-independent methods of taking a microbial census began about 25 years ago and were based on targeted sequencing of 5S and 16S ribosomal RNA genes[10], which differ for each species and are a convenient identifier. As this became a tractable research area, next-generation sequencing (NGS) technologies (Table 1) were developed and allowed more extensive analyses, both targeted 16S rRNA gene sequencing and whole-genome shotgun sequencing of microbes in communities en masse. The number of culture-independent metagenomic investigations of the human microbiome has mushroomed, and it is one of the most studied areas of microbiology with significant potential to benefit clinical practice. This culture-independent methodology is broadly applied outside human-microbiome research and is expanding our knowledge of the environment. This Review describes how NGS approaches are transforming human-microbiome studies, and posing questions and challenges for the future.

Single organisms and microbial communities

In the past, research on microbial interactions with humans has focused on single pathogenic organisms. Studies of communities of non-pathogenic microbes in the body were limited because the organisms were thought to be benign, with minor effects on human health compared with pathogens. Microbiome research has led to new interest in the communities of non-pathogenic microbes that inhabit the human body, and the need to describe the genomes of these organisms to understand the human microbiome has been recognized.

Every community of the microbiome has its own characteristics (Table 2). For the gut community, for example, high biodiversity is associated with a healthy state and reduced biodiversity occurs in patients with conditions such as Crohn's disease[11], whereas for tissues of the vagina, a lower biodiversity exists in healthy individuals and a bloom of organisms occurs in patients with vaginosis[12]. To understand why different sites have different properties, the mechanisms that lead to the disruption of ecosystems and to disease, and exceptions to generalities about a tissue, researchers require knowledge of the structure and behaviour of microbial communities.

Microbial communities benefit the host by providing functions such as digestion of nutrients[13] or protection against infection[14]. Antibiotic treatment perturbs the microbiome[15,16] by reducing its size and altering its composition. This disturbance can lead to infection[17–19], and antibiotic-resistant organisms such as *Clostridium difficile* — normally controlled by the microbiome — can overgrow and create problems[20]. More complex community contributions also exist, such as interactions with host immune and inflammatory systems[21,22] or production of metabolites involving hybrid pathways from multiple organisms, including host–microbe pathways[23]. Understanding these phenomena will ultimately allow the

[1]The Genome Institute, Washington University, 4444 Forest Park Avenue, Campus Box 8501, St. Louis, Missouri 63108, USA.

microbiome to be manipulated so that, for example, transplants of microbial communities could treat *C. difficile* infections[24,25].

Whether the microbial ecology of the human body can be simplified to the properties of single organisms is unknown. Many organisms have never been cultured and may be adapted to life in a community environment rather than a pure culture. For organisms for which growth requirements are understood, there is a dependence on secreted products from other community members. For example, secreted siderophores[26] are small molecules that help microbes to scavenge iron, which is a limiting factor for growth in the body. So even the study of individual organisms can be dependent on studying the community.

Dissecting a microbiome

Analysis of community structure (Fig. 1) focuses on either targeted regions (such as the 16S rRNA gene) or shotgun sequencing to catalogue the genes that are present. Additional analysis involves sequencing genomes of individual organisms to produce a catalogue of reference genomes[27], and analysing RNA to describe the transcriptome and identify RNA viruses. Non-genomic analyses include proteomic and metabolomic studies, but these are not discussed here. Every sample should be well-annotated with clinical metadata, so that, ultimately, the microbiome's genetic and community structures can be correlated with the individual's phenotype.

Census of organisms

Modern metagenomic analyses of microbial communities were developed from culture-independent methods for taking a census of organisms present in a community and their abundances. Although DNA reassociation kinetics provides information on community diversity and structure[28], there is no accounting for organisms that may be tracked between samples. Methods more useful for providing information on the entire structure often focus on signature sequences that distinguish taxa (detected by hybridization to arrays of diagnostic oligonucleotides[29]), various methods for fingerprinting polymerase chain reaction (PCR) products (such as single-strand conformation polymorphisms or terminal restriction fragment length polymorphisms) or DNA sequencing of targeted PCR products. Sequencing of 16S rRNA genes is the main method of taking a community census because fingerprinting methods do not adequately measure low-abundance organisms[30].

16S rRNA differs for each bacterial species. A bacterial species is hard to define, but is often taken as organisms with 16S rRNA gene sequences having at least 97% identity — an operational taxonomic unit (OTU). A 16S rRNA gene sequence of about 1.5 kilobases has nine short hypervariable regions that distinguish bacterial taxa; the sequences of one or more of these regions are targeted in a community census.

Before the introduction of NGS methods, the prevailing approach was to clone full-length 16S rRNA genes after PCR with primers that would amplify genes from a wide range of organisms. Cloned 16S rRNA genes were sequenced by the Sanger method, which required two or three reads to cover the entire gene. Accuracy was crucial because sequencing errors led to misclassification. The cost and effort required for the Sanger method limited the depth of sampling, and studies often produced about 100 sequences per specimen. This method identified the dominant organisms in a community, but analysis of less abundant organisms was limited.

Introducing NGS to 16S rRNA gene analysis led to marked improvements in cost and depth of sampling. The Roche–454 platform has dominated microbial community analysis[31]. As the read length for 454 pyrosequencing is about 400 bases, only a portion of the 16S rRNA gene can be sampled, and many different studies have targeted between one and three of the hypervariable regions, with different hypervariable regions targeted in different studies. Using a portion of the 16S rRNA gene led to a loss of sensitivity (some taxa

BOX 1

Terminology

- **Biodiversity** is a measure of the complexity of a community. It is affected by the number of taxa (richness) and their range of abundance (evenness). High biodiversity occurs when many taxa (high richness) are present at similar abundances (an even distribution).
- **Commensals** are organisms that benefit from another organism but that have no harm or benefit themselves. Microbes of the microbiome were thought to be commensals that benefited from the human host but did no harm. Many of these organisms provide benefits to the human host and so have a mutualistic relationship.
- **Contig** is a stretch of contiguous sequence in a genome assembly.
- **Coverage** is the number of times a genome or gene is sequenced. In a genome sequenced to coverage, each nucleotide in the sequence appears, on average, in 100 reads.
- **Genome assembly** is the process of constructing a genome sequence from short subsequences by sequencing many random fragments from a sheared genome. The random short sequences are compared, and overlapping common sequences are used to determine their orientation and order with respect to each other. A consensus sequence is constructed from this layout. Usually there are gaps, but when contigs can be arranged in the correct order and orientation, these longer stretches are called scaffolds.
- **Metagenomics** was defined[83] as a process for identifying genes specifically by their function by cloning them directly from the environment and expressing genes in a surrogate host[84]. Therefore, gene function was known even if the sequence was not sufficient for functional inference, such as when it encoded a protein of previously unknown function. This definition, also known as functional metagenomics, is widely used. More recently, metagenomics refers to general analyses of microbial communities by culture-independent methods, which do not necessarily focus on function. The combined genomes of the microbes in a community are thought of as the community metagenome. Another type of metagenomic analysis focuses on the structure of these aggregate genomes in a community.
- **Microbiome** in this Review refers to the microbiota and the habitat it colonizes and is analogous to the term biome in ecology. Microbiome is also used to refer to the collective genomes of the microbes — what is now the metagenome, and may have originally been coined by Joshua Lederberg (cited by Hooper and Gordon[85]). However, it is also used for the more ecologically consistent meaning. A microbiome can be a specific body site, such as the gut microbiome, but the human microbiome is often used to refer to the collection of microbiomes of the human body.
- **Mutualism** is a type of symbiosis in which both organisms benefit. This is one type of relationship seen in the human microbiome.
- **Operational taxonomic unit** in microbiome research is a group of organisms with 16S ribosomal RNA gene sequences that show a certain level of identity. This group is often used as a surrogate for a species when the 16S rRNA sequences are at least 97% identical.
- **Pathogenic microbe** is one with the potential to cause disease.
- **Read** is the primary output of DNA sequencing, consisting of a short stretch of DNA sequence that is produced from sequencing a region of a single DNA fragment.
- **Shotgun sequencing** is the process of randomly breaking (often by shearing) a long DNA molecule (for example, a complete chromosome) and then sequencing the resultant DNA fragments, which each come from a different location in the original long DNA molecule.
- **Virome** is the collection of viruses in the microbiota.

Table 1 | DNA sequencing platforms used for microbiome analysis

Platform	Method	Characteristics	16S rRNA	Shotgun	Comments
Established					
Sanger-based or capillary-based instrument	Fluorescent, dideoxy terminator	750-base reads High accuracy	Full length sequenced with 2–3 reads	Long reads help with database comparisons	Most costly method Relatively low throughput, so low coverage of 16S or shotgun
Roche–454	Pyrosequencing light emission	400-base reads	Up to 3 variable regions per read	Long reads help with database comparisons	Cost limits shotgun coverage but 16S coverage is good
Illumina	Fluorescent, stepwise sequencing	100–150- base reads	Only 1 variable region per read	Short reads do not seem to limit analysis	Very high coverage owing to high instrument output and very low cost
Not yet widely used					
Ion Torrent	Proton detection	More than 200-base reads	Like other NGS	Like Illumina	Expect high coverage, but longer reads than Illumina
PacBio	Fluorescent, single-molecule sequencing	Up to 10- kilobase reads Low accuracy	Accuracy an issue for correct taxon identification	Long reads could help assembly	Attractive for long reads, but lower accuracy limits applications
Oxford Nanopore*	Electronic signal as DNA passes through pore Single-molecule sequencing	Long reads	Unknown	Long reads could help assembly	Not yet available

*At the time of publication, the Oxford Nanopore system was not available, and information provided is based on company presentations. Ion Torrent and PacBio are both available but have not been widely used for microbiome analysis. The Illumina MiSeq instrument is expected to provide 250-base reads in the near future.

cannot be reliably defined at the species level, although high confidence identification of higher taxonomic ranks is possible), nevertheless gains in depth of sampling and cost savings outweigh this caveat. The US Human Microbiome Project (HMP)[33] has sequenced more than 10,000 specimens from healthy adults on the 454 platform by targeting V3 to V5 regions in the 16S rRNA gene and producing, on average, 7,000 sequences per specimen[33], which is a vast expansion on the Sanger method of sequencing analysis. The results of the HMP, which sampled 18 body sites, provide an in-depth definition of the human microbiome. Another study[16] that focused on the effects of the antibiotic ciprofloxacin reported the 'rare biosphere' in the gut. This study documented perturbation of taxa and recovery from antibiotic treatment, as well as minor constituents that did not recover after antibiotic treatment. Such analyses will be important in identifying individuals who are at risk of side effects from antibiotic treatment, for example overgrowth of pathogens such as *C. difficile* or life-threatening antibiotic-associated diarrhoea.

When using 16S rRNA gene sequencing to compare individuals it is not necessary to know which organisms are present, only whether the spectra of 16S rRNA gene sequences are similar and the degree of difference between samples. Projects that compare healthy cohorts and those with disease to determine whether there is a difference in the microbiome, or examine the effects of diet, antibiotic treatment or environmental factors on the microbiome, all focus on detecting differences in communities, rather than identifying actual taxa. A loss of sensitivity for organism identification can be tolerated, and NGS allows cost-effective deep sampling of large cohorts, which is needed to reach statistically significant conclusions. The Illumina sequencing platform has been applied to metagenomics projects[34–36], but because this sequencing platform currently produces reads of 100 bases (HiSeq system) to 150 bases (MiSeq system), only a single hypervariable region can be sequenced. However, this further loss of sensitivity does not preclude the use of the Illumina platform for the comparative projects already described in this Review. An early application of this platform was its use in a study of vaginal microbiomes in patients with HIV, for which comparisons of patients with conditions such as vaginosis before and after antibiotic therapy were examined[37]. As a result of the exceptional increases in numbers of reads and the lower cost associated with the Illumina platform, it is becoming more widely used for 16S rRNA gene-sequence profiling and continues the microbiome-analysis trend of deeper sampling at lower costs.

Shotgun sequencing for cataloguing organisms

Targeted sequencing is a powerful tool for assessing the organisms that are present in microbial communities, but it is limited in terms of the functional and genetic information produced. Organisms for which the genome sequences are known (currently there are several thousand sequenced bacterial genomes) can be used to infer the genes and functional capabilities of the community (Fig. 1). However, many organisms have no reference sequence. Furthermore, a reference sequence does not completely describe the genes that are contributed by an organism. There is considerable variation in the genomes between strains of the same species. Two strains of *Escherichia coli*, O157:H7 and K-12, both have 16S rRNA gene sequences of *E. coli*, but differ in hundreds of genes. There are limits to what can be learned about the genetic content of communities from 16S rRNA gene sequences alone.

Moving beyond this level of functional inference requires a gene-based census. This catalogue of genes can be provided by shotgun sequencing of DNA that has been extracted from the community as a whole and samples the mixture of genomes that make up the metagenome (Fig. 1). In a community in excess of hundreds of species with varying abundance, deep sequencing is needed to sample minor constituents that are not necessarily unimportant. The bacterial concentration in the gut can be 10^{11} cells ml^{-1} (refs. 38, 39), so for an organism that is present at a concentration of 1 per 10^6 there are 10^5 cells ml^{-1}, which is sufficient for the organism's products, such as metabolites and toxins, to have an effect on the community and the host.

Illumina sequencing of faecal samples produced 4 gigabases per sample and 10 Gb per sample in the Metagenomics of the Human Intestinal Tract (MetaHIT)[6] and HMP[33] projects, respectively, which corresponded to tens of millions of reads per sample. At this depth of sequencing, the genomes of minor constituents such as *E. coli* (with an abundance of about 1% or lower) are sampled almost completely, and organisms with an even lower abundance have some of their genome represented. This extraordinary sampling of complex microbial communities is made possible by producing large amounts of data and by the low cost of NGS methods.

Shotgun sequence data, in addition to 16S rRNA gene analysis, provide information on the organisms that make up communities. Extracting 16S rRNA gene sequences from shotgun reads to determine the organisms present is possible; however, targeted 16S rRNA gene sequencing tends to introduce biases (owing to the broad-range PCR used to amplify 16S rRNA gene sequences or the choice of region within the 16S rRNA gene), which shotgun sequencing does not. Shotgun sequencing is less sensitive than targeted rRNA sequencing because a small fraction of the

sequences are from 16S rRNA genes. Another approach is to align shotgun sequences to bacterial reference genomes[33,40,41], allowing the relative abundance of species to be determined on the basis of the number of reads that align to each reference genome (also useful for the comparative studies already described). The MetaHIT project has used this approach to classify individuals into different groups, called enterotypes, on the basis of the community structure in their faecal samples[40]. The same enterotypes have been found in 16S rRNA gene-based analysis[42]. The vaginal microbiome has also been classified into five groups[43]. These observations suggest the human microbiome may exist in distinct states in different people, although correlation with environmental, genetic or health status is not yet clear. Stratifying future studies depending on which community class an individual belongs to may be important for identifying correlations with phenotypic data.

The need for reference genome sequences is clear both to infer genetic content of organisms identified by 16S rRNA genes and to identify sources of shotgun reads by aligning to reference genomes, and so determining organismal content of communities from shotgun data. NGS techniques have reduced the cost of bacterial sequences to less than US$1,000 per genome and led to an increase in the production of 'complete' genome sequences. Current methodology relies mainly on Illumina shotgun sequencing and a variety of methods to assemble the reads into a genome. The product is not a true complete genome, but a high-quality draft that covers almost all of the genome and results in a high-quality base sequence[27]. Programmes such as the HMP[32,44] and the Genomic Encyclopedia of Bacteria and Archaea (GEBA)[45] are producing reference genomes by the thousands.

Although bacteria are the main components of the human microbiome, eukaryotic microbes and viruses (both human viruses and bacteriophages) are also present (Table 2). The study of eukaryotic microbes is not as advanced as that of bacteria[46], but the organisms are identified by signature sequences (such as fingerprinting and 18S rRNA) and shotgun sequencing analogous to bacteria. The number of reference genomes for eukaryotic microbes is smaller than that for bacteria, and progress will depend on addressing this shortfall.

By contrast, considerable effort is being given to characterizing the genomes of human viruses[47] and bacteriophages[48], known as the virome (Box 1). This work is based on shotgun sequencing (Fig. 1), although oligonucleotides microarrays for virus detection are also used[49,50]. Viral sequences can be detected in shotgun data from different body sites, and viruses can also be enriched by processing samples before DNA extraction[51]. Virome analysis by shotgun sequencing of microbial communities (discussed later) has led to the identification of human viruses[52–54], as well as the detection of known viruses in healthy subjects and diseases of unknown aetiology[55]. Likewise, bacteriophages are found to be highly diverse at different body sites[56–58], with differences between individuals as a result of diet[59] or disease states[60,61].

Sequencing for gene catalogues and functional inference

Metagenomic shotgun data also sample community gene content, which is useful to define community capabilities and identify particular members. Deep sequencing, such as that used in the MetaHIT and the HMP, broadly samples the genomes of even minor constituents, facilitating the identification of genes present within a given community (Fig. 1). By using the sequence reads themselves, or by first assembling them into contigs (Box 1), sequence data can be compared with databases such as the National Institutes of Health's GenBank to identify which genes are present. *De novo* prediction of genes from metagenomic data is also possible[53], which provides motifs for functional inference even if the sequence does not find a match in a database. Finally, alignment of reads or contigs to reference genomes identifies which organisms are present, along with their known gene content. These methods convert metagenomic sequence data into catalogues of genes that can be further analysed.

Gene catalogues can be compared with databases such as the Kyoto Encyclopedia of Genes and Genomes (KEGG)[62], which sorts gene products into pathways and processes. Such analyses provides lists of pathways, identify which pathway genes are in the community and quantify the abundances of genes and pathways[63]. Comparing gene catalogues to specialized metabolic databases, such as the Carbohydrate-Active Enzymes database[64], is also useful. Carbohydrate-degrading capabilities of communities differ between body sites, suggesting the carbohydrate spectrum of each body site has determined which organisms and pathways are present[65].

In addition to pathway analysis, determining the presence and abundance of genes, such as antibiotic-resistance genes or virulence factors, in a community is possible using similar methods to those already described, and can shed light on pathogen burden in an individual and consequences of antibiotic treatment. The importance of functional analyses cannot be overemphasized, and functional properties of communities are thought to be more important than their taxonomic composition[66].

Computational tools and strategies

Metagenomic data are a rich source of information for the sequencing and analysis methods already discussed[67,68]. The data analysis workflow has three phases. In the first phase, primary data are processed and filtered depending on the application. For 16S rRNA gene sequencing, the quality of analysis is important so that organisms are not misclassified. Initial processing addresses read quality, chimaerism (a read formed from different 16S rRNA genes), read length after removing low-quality bases and related issues[69–73]. For shotgun sequence data[8,33] — in addition to sequence quality — artefacts such as duplicate reads must also be addressed, as well as computationally removing contamination from human sequences. Removal of human and bacterial sequences is important in read processing for virome analysis[47,55] (Fig. 1).

Following production of processed reads, the second phase involves generating various derivative data sets. For 16S rRNA gene analysis, tables of taxa and abundance are produced by comparisons with 16S rRNA sequence databases or by using software packages to

Table 2 | Characteristics of bacteria, microbial eukaryotes and viruses in the human microbiome

Characteristic	Bacteria	Viruses	Eukaryotic microbes
Genome size	0.5–10 megabases	1–1,000 kilobases	10–50 megabases
Number of taxa in the human microbiome	At least thousands	Unknown, but could be as many as bacteria	Unknown, but may be fewer than bacteria
Relative abundances	Highly variable	Highly variable	Unknown
Targeted detection methods	Sequencing of genes such as 5S and 16S rRNA	No universal method for genes, but virus-specific polymerase chain reaction assays for some	Sequencing of 18S rRNA gene Spacer region in rRNA
Shotgun approach to analyses	Alignment to reference genomes or database comparison	Database comparison	Alignment to reference genomes or database comparison
Subspecies or strain diversity	Modest sequence variation Horizontal gene transfer also contributes	High sequence variation	Unknown

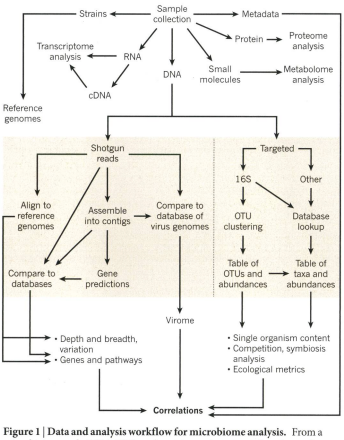

Figure 1 | Data and analysis workflow for microbiome analysis. From a microbiota sample, DNA, RNA and protein can be extracted, and metadata and strains of bacteria obtained. Data from DNA can be supplemented with proteome and transcriptome analysis. During primary analysis, shotgun techniques can produce reads from DNA, which are then aligned to reference genomes to identify variants and community population genetics, assembled into contigs to make gene predictions or compared with databases. Alternatively, targeted sequencing such as 16S rRNA gene sequencing can be used to take a community census, and these data are then compared with databases to create tables of taxa and abundance, or analysed with software programs to cluster the reads into OTUs to create tables of abundance. The derivative data is used in secondary analysis for ecological metrics or competition and symbiosis analysis. In addition, shotgun reads and comparisons with reference genomes and databases can be used to build pathways and reconstruct the capabilities of a community. The combination of these analyses will contribute to understanding the differences within and between individuals.

cluster the reads into OTUs[74,75]. Comparing shotgun reads to gene databases, such as GenBank or KEGG, by using the Basic Local Alignment Search Tool (BLAST), for example, produces lists of genes and the number of matched reads[7,13,63]. Alignment of reads to reference genomes produces tables of breadth and depth of coverage, by reads of each genome[41]. In each of these data sets, there is more biological information to be gleaned and added through further analysis. Not all reads match sequences in databases because not all organisms have a reference genome sequenced. In addition, reads may match genes whose function has not been elucidated. These sequences of unknown origin or function can be a sizeable fraction and the effect of this uninformative portion of data on analyses and conclusions is not clear.

The third phase of analysis uses these derivative data to produce trees or other representations of the similarity of communities, abundance curves, biodiversity plots, and other ecological and statistical descriptors of community structure[74,75] (Fig. 1). A list of hits from BLAST is used to build metabolic pathways for reconstruction of community capabilities[65]. Alignments to reference genomes are further analysed for variants and population genetics of communities. Computational analysis can also be used to determine which organisms co-occur or rarely co-occur as evidence for symbiosis or competition, respectively, or to follow the dynamics of community structure in longitudinal time series[76].

Some analyses pose significant computational challenges. Comparisons to gene databases at the protein level are particularly demanding because shotgun sequences must be translated into polypeptides in all six reading frames, and each must be compared with a gene database represented at the protein level. Using conventional BLASTx programs for this comparison in large data sets, such as the HMP, could take decades, so supercomputers, accelerated BLAST programs or both must be used[33]. A lack of efficient software and large enough computer clusters are often bottlenecks for metagenomic analysis, because sequencing and data production are not limiting factors. Management of large data sets and computing resources are receiving more attention, with cloud-computing services seeming to be a viable alternative[77].

Future directions and challenges

The rapid rise in metagenomic studies has solved many problems but, as the field has grown, other questions have been raised. Existing methodology is becoming more sophisticated, and sequencing technology is making exponential advances (Table 1). The Illumina platform introduced instruments that were more appropriate for sequencing smaller genomes, with faster run times and longer read lengths, offering more flexibility for metagenomic applications. The long read length of the PacBio platform has the potential to help distinguish the reads from different organisms, which is a challenge for metagenomic shotgun sequencing. The technology produced by Oxford Nanopore promises long reads and short run times in a scalable system, and is therefore a good match for microbial applications. Reducing the amount of DNA needed for shotgun sequencing will allow communities in smaller anatomical regions, such as within the gastrointestinal tract, to be studied separately rather than together with other regions as is the case with the current methodology. Short run-time instruments and reductions in sample size will also hasten the introduction of microbiome analysis to the clinic, where analyses of patient samples must be quick and able to deal with limited amounts of material. Ultimately, the aim of human-microbiome research is its application as a diagnostic, therapeutic and preventive tool in the clinic.

The main limitation of using shotgun data is the large number of organisms that have not been cultured, let alone sequenced. These organisms are therefore under-represented in databases, and their shotgun reads are anonymous. When community shotgun data are assembled into genomes to obtain genome sequences for new organisms, contig sizes are typically small as a result of lower organism abundance and the challenges associated with assembly of a complex mixture. The long read lengths of PacBio and Oxford Nanopore instruments should help with these challenges, as will the development of assembly algorithms for metagenomic data. Expanding the catalogue of reference genomes by producing reference sequences for individual uncultured organisms is an active area. Methods that use cell sorting to isolate organisms, coupled with sequencing and assembly techniques for single-cell DNA preparations, are producing new genome sequences[78,79] and, in high-throughput mode, could complement shotgun metagenomics for analysing communities.

One problem associated with genomic data is that it does not address whether an organism is alive or has succumbed to host defences or antibiotic treatment. However, the data can be complemented with transcriptome analysis, or proteomic and metabolomic data sets, which analyse gene expression and metabolic data that are more likely to be derived specifically from living cells.

The simultaneous advances in human genetics and genomics offer opportunities for combining studies of host genotype

with microbiome phenotype. Methods for viewing the microbiome as a quantitative trait and relating this to host genotype are being developed[80]. Advances in host–microbiome studies are also coming from combining immunology and human-microbiome research[81,82]. Moreover, continued development of statistical methods in microbiome research, such as advances in power analysis, will aid experimental design and future analysis. ■

1. Backhed, F., Ley, R. E., Sonnenburg, J. L., Peterson, D. A. & Gordon, J. I. Host–bacterial mutualism in the human intestine. *Science* **307,** 1915–1920 (2005).
2. Foxman, B., Goldberg, D., Murdock, C., Xi, C. & Gilsdorf, J. R. Conceptualizing human microbiota: from multicelled organ to ecological community. *Interdiscip. Perspect. Infect. Dis.* **2008,** 613979 (2008).
3. Possemiers, S., Bolca, S., Verstraete, W. & Heyerick, A. The intestinal microbiome: a separate organ inside the body with the metabolic potential to influence the bioactivity of botanicals. *Fitoterapia* **82,** 53–66 (2011).
4. Shanahan, F. The host-microbe interface within the gut. *Best Pract. Res. Clin. Gastroenterol.* **16,** 915–931 (2002).
5. Bruls, T. & Weissenbach, J. The human metagenome: our other genome? *Hum. Mol. Genet.* **20,** R142–R148 (2011).
6. Qin, J. *et al.* A human gut microbial gene catalogue established by metagenomic sequencing. *Nature* **464,** 59–65 (2010).
This paper presents initial findings on the gut microbiome from the MetaHIT project.
7. Human Microbiome Project Consortium. Structure, function and diversity of the healthy human microbiome. *Nature* **486,** 207–214 (2012).
This paper presents analysis of data from the HMP.
8. Stein, J. L., Marsh, T. L., Wu, K. Y., Shizuya, H. & DeLong, E. F. Characterization of uncultivated prokaryotes: isolation and analysis of a 40-kilobase-pair genome fragment from a planktonic marine archaeon. *J. Bacteriol.* **178,** 591–599 (1996).
9. Vergin, K. L. *et al.* Screening of a fosmid library of marine environmental genomic DNA fragments reveals four clones related to members of the order Planctomycetales. *Appl. Environ. Microbiol.* **64,** 3075–3078 (1998).
10. Olsen, G. J., Lane, D. J., Giovannoni, S. J., Pace, N. R. & Stahl, D. A. Microbial ecology and evolution: a ribosomal RNA approach. *Annu. Rev. Microbiol.* **40,** 337–365 (1986).
11. Manichanh, C. *et al.* Reduced diversity of faecal microbiota in Crohn's disease revealed by a metagenomic approach. *Gut* **55,** 205–211 (2006).
12. Fredricks, D. N., Fiedler, T. L. & Marrazzo, J. M. Molecular identification of bacteria associated with bacterial vaginosis. *N. Engl. J. Med.* **353,** 1899–1911 (2005).
13. Flint, H. J., Bayer, E. A., Rincon, M. T., Lamed, R. & White, B. A. Polysaccharide utilization by gut bacteria: potential for new insights from genomic analysis. *Nature Rev. Microbiol.* **6,** 121–131 (2008).
14. Sriskanth, C. V. & McCormick, B. A. Interactions of the intestinal epithelium with the pathogen and the mutualistic microbiota: a three-way crosstalk. *Interdiscip. Perspect. Infect. Dis.* **2008,** 626827 (2008).
15. Jakobsson, H. E. *et al.* Short-term antibiotic treatment has differing long-term impacts on the human throat and gut microbiome. *PLoS ONE* **5,** e9836 (2010).
16. Dethlefsen, L., Huse, S., Sogin, M. L. & Relman, D. A. The pervasive effects of an antibiotic on the human gut microbiota, as revealed by deep 16S rRNA sequencing. *PLoS Biol.* **6,** e280 (2008).
17. Miller, C. P., Bohnhoff, M. & Rifkind, D. The effect of an antibiotic on the susceptibility of the mouse's intestinal tract to *Salmonella* infection. *Trans. Am. Clin. Climatol. Assoc.* **68,** 51–55 (1956).
18. Sekirov, I. *et al.* Antibiotic-induced perturbations of the intestinal microbiota alter host susceptibility to enteric infection. *Infect. Immun.* **76,** 4726–4736 (2008).
19. Croswell, A., Amir, E., Teggatz, P., Barman, M. & Salzman, N. H. Prolonged impact of antibiotics on intestinal microbial ecology and susceptibility to enteric *Salmonella* infection. *Infect. Immun.* **77,** 2741–2753 (2009).
20. Mulligan, M. E. Epidemiology of *Clostridium difficile*-induced intestinal disease. *Rev. Infect. Dis.* **6,** S222–S228 (1984).
21. Jarchum, I. & Pamer, E. G. Regulation of innate and adaptive immunity by the commensal microbiota. *Curr. Opin. Immunol.* **23,** 353–360 (2011).
22. Marsland, B. J. Regulation of inflammatory responses by the commensal microbiota. *Thorax* **67,** 93–94 (2012).
23. Wang, Z. *et al.* Gut flora metabolism of phosphatidylcholine promotes cardiovascular disease. *Nature* **472,** 57–63 (2011).
24. Gough, E., Shaikh, H. & Manges, A. R. Systematic review of intestinal microbiota transplantation (fecal bacteriotherapy) for recurrent *Clostridium difficile* infection. *Clin. Infect. Dis.* **53,** 994–1002 (2011).
25. Brandt, L. J. & Reddy, S. S. Fecal microbiota transplantation for recurrent *clostridium difficile* infection. *J. Clin. Gastroenterol.* **45,** S159–S167 (2011).
26. D'Onofrio, A. *et al.* Siderophores from neighboring organisms promote the growth of uncultured bacteria. *Chem. Biol.* **17,** 254–264 (2010).
27. Human Microbiome Jumpstart Reference Strains Consortium. A catalog of reference genomes from the human microbiome. *Science* **328,** 994–999 (2010).
This paper presents methods and analysis for large-scale production of reference genome sequences from human-microbiome organisms.
28. Gans, J., Wolinsky, M. & Dunbar, J. Computational improvements reveal great bacterial diversity and high metal toxicity in soil. *Science* **309,** 1387–1390 (2005).
29. Nelson, T. A. *et al.* PhyloChip microarray analysis reveals altered gastrointestinal microbial communities in a rat model of colonic hypersensitivity. *Neurogastroenterol. Motil.* **23,** 169–177 (2011).
30. Bent, S. J. *et al.* Measuring species richness based on microbial community fingerprints: the emperor has no clothes. *Appl. Environ. Microbiol.* **73,** 2399–2401 (2007).
31. Sogin, M. L. *et al.* Microbial diversity in the deep sea and the underexplored "rare biosphere". *Proc. Natl Acad. Sci. USA* **103,** 12115–12120 (2006).
32. The NIH HMP Working Group *et al.* The NIH Human Microbiome Project. *Genome Res.* **19,** 2317–2323 (2009).
33. Human Microbiome Project Consortium. A framework for human microbiome research. *Nature* **486,** 215–221 (2012).
This paper describes the data sets and resources of the HMP.
34. Lazarevic, V. *et al.* Metagenomic study of the oral microbiota by Illumina high-throughput sequencing. *J. Microbiol. Methods* **79,** 266–271 (2009).
35. Claesson, M. J. *et al.* Comparison of two next-generation sequencing technologies for resolving highly complex microbiota composition using tandem variable 16S rRNA gene regions. *Nucleic Acids Res.* **38,** e200 (2010).
36. Gloor, G. B. *et al.* Microbiome profiling by Illumina sequencing of combinatorial sequence-tagged PCR products. *PLoS ONE* **5,** e15406 (2010).
37. Hummelen, R. *et al.* Deep sequencing of the vaginal microbiota of women with HIV. *PLoS ONE* **5,** e12078 (2010).
38. Zubrzycki, L. & Spaulding, E. H. Studies on the stability of the normal human fecal flora. *J. Bacteriol.* **83,** 969–974 (1962).
39. Luckey, T. D. Introduction to intestinal microecology. *Am. J. Clin. Nutr.* **25,** 1292–1294 (1972).
40. Arumugam, M. *et al.* Enterotypes of the human gut microbiome. *Nature* **473,** 174–180 (2011).
41. Martin, J. *et al.* Optimizing read mapping to reference genomes to determine composition and species prevalence in microbial communities. *PloS ONE* **7,** e36427 (2012).
42. Wu, G. D. *et al.* Linking long-term dietary patterns with gut microbial enterotypes. *Science* **334,** 105–108 (2011).
43. Ravel, J. *et al.* Vaginal microbiome of reproductive-age women. *Proc. Natl Acad. Sci. USA* **108,** S4680–S4687 (2011).
44. Proctor, L. M. The Human Microbiome Project in 2011 and beyond. *Cell Host Microbe* **10,** 287–291 (2011).
45. DOE Joint Genome Institute. *A Genomic Encyclopedia of Bacteria and Archaea.* http://www.jgi.doe.gov/programs/GEBA/ (US Department of Energy, 2012).
46. Parfrey, L. W., Walters, W. A. & Knight, R. Microbial eukaryotes in the human microbiome: ecology, evolution, and future directions. *Front. Microbiol.* **2,** 153 (2011).
47. Wylie, K. M., Weinstock, G. M. & Storch, G. A. Emerging view of the human virome. *Transl. Res.* http://dx.doi.org/10.1016/j.trsl.2012.03.006 (24 April 2012).
48. Breitbart, M. *et al.* Metagenomic analyses of an uncultured viral community from human feces. *J. Bacteriol.* **185,** 6220–6223 (2003).
49. Palacios, G. *et al.* Panmicrobial oligonucleotide array for diagnosis of infectious diseases. *Emerg. Infect. Dis.* **13,** 73–81 (2007).
50. Wang, D. *et al.* Viral discovery and sequence recovery using DNA microarrays. *PLoS Biol.* **1,** E2 (2003).
51. Casas, V. & Rohwer, F. Phage metagenomics. *Methods Enzymol.* **421,** 259–268 (2007).
52. Allander, T. *et al.* Cloning of a human parvovirus by molecular screening of respiratory tract samples. *Proc. Natl Acad. Sci. USA* **102,** 12891–12896 (2005).
53. Finkbeiner, S. R. *et al.* Metagenomic analysis of human diarrhea: viral detection and discovery. *PLoS Pathogens.* **4,** e1000011 (2008).
54. Breitbart, M. & Rohwer, F. Method for discovering novel DNA viruses in blood using viral particle selection and shotgun sequencing. *Biotechniques* **39,** 729–736 (2005).
55. Wylie, K. M., Mihindukulasuriya, K. A., Sodergren, E., Weinstock, G. M. & Storch, G. A. Sequence analysis of the human virome in febrile and afebrile children. *PLoS ONE* **7,** e27735 (2012).
56. Pride, D. T. *et al.* Evidence of a robust resident bacteriophage population revealed through analysis of the human salivary virome. *ISME J.* **6,** 915–926 (2011).
57. Minot, S., Grunberg, S., Wu, G. D., Lewis, J. D. & Bushman, F. D. Hypervariable loci in the human gut virome. *Proc. Natl Acad. Sci. USA* **109,** 3962–3966 (2012).
58. Breitbart, M. *et al.* Viral diversity and dynamics in an infant gut. *Res. Microbiol.* **159,** 367–373 (2008).
59. Minot, S. *et al.* The human gut virome: inter-individual variation and dynamic response to diet. *Genome Res.* **21,** 1616–1625 (2011).
60. Willner, D. & Furlan, M. Deciphering the role of phage in the cystic fibrosis airway. *Virulence* **1,** 309–313 (2010).
61. Lepage, P. *et al.* Dysbiosis in inflammatory bowel disease: a role for bacteriophages? *Gut* **57,** 424–425 (2008).
62. Kanehisa, M., Goto, S., Furumichi, M., Tanabe, M. & Hirakawa, M. KEGG for representation and analysis of molecular networks involving diseases and drugs. *Nucleic Acids Res.* **38,** D355–D360 (2010).

63. Abubucker, S. *et al.* Metabolic reconstruction for metagenomic data and its application to the human microbiome. *PLoS Comput. Biol.* **8,** e1002358 (2012).
64. Cantarel, B. L. *et al.* The Carbohydrate-Active EnZymes database (CAZy): an expert resource for glycogenomics. *Nucleic Acids Res.* **37,** D233–D238 (2009).
65. Cantarel, B. L., Lombard, V. & Henrissat, B. Complex carbohydrate utilization by the healthy human microbiome. *PLoS ONE* **7,** e28742 (2012).
66. Turnbaugh, P. J. & Gordon, J. I. The core gut microbiome, energy balance and obesity. *J. Physiol. (Lond.)* **587,** 4153–4158 (2009).
67. Raes, J., Foerstner, K. U. & Bork, P. Get the most out of your metagenome: computational analysis of environmental sequence data. *Curr. Opin. Microbiol.* **10,** 490–498 (2007).
68. Wooley, J. C., Godzik, A. & Friedberg, I. A primer on metagenomics. *PLoS Comput. Biol.* **6,** e1000667 (2010).
69. Edgar, R. C., Haas, B. J., Clemente, J. C., Quince, C. & Knight, R. UCHIME improves sensitivity and speed of chimera detection. *Bioinformatics* **27,** 2194–2200 (2011).
70. Haas, B. J. *et al.* Chimeric 16S rRNA sequence formation and detection in Sanger and 454-pyrosequenced PCR amplicons. *Genome Res.* **21,** 494–504 (2011).
71. Jumpstart Consortium Human Microbiome Project Data Generation Working Group. Evaluation of 16S rDNA-based community profiling for human microbiome research. *PLoS ONE* **7,** e39315 (2012).
72. Schloss, P. D., Gevers, D. & Westcott, S. L. Reducing the effects of PCR amplification and sequencing artifacts on 16S rRNA-based studies. *PLoS ONE* **6,** e27310 (2011).
73. Wright, E. S., Yilmaz, L. S. & Noguera, D. R. DECIPHER, a search-based approach to chimera identification for 16S rRNA sequences. *Appl. Environ. Microbiol.* **78,** 717–725 (2012).
74. Lozupone, C., Lladser, M. E., Knights, D., Stombaugh, J. & Knight, R. UniFrac: an effective distance metric for microbial community comparison. *ISME J.* **5,** 169–172 (2011).
75. Schloss, P. D. *et al.* Introducing mothur: open-source, platform-independent, community-supported software for describing and comparing microbial communities. *Appl. Environ. Microbiol.* **75,** 7537–7541 (2009).
76. Caporaso, J. G. *et al.* Moving pictures of the human microbiome. *Genome Biol.* **12,** R50 (2011).
77. Angiuoli, S. V., White, J. R., Matalka, M., White, O. & Fricke, W. F. Resources and costs for microbial sequence analysis evaluated using virtual machines and cloud computing. *PLoS ONE* **6,** e26624 (2011).
78. Chitsaz, H. *et al.* Efficient *de novo* assembly of single-cell bacterial genomes from short-read data sets. *Nature Biotechnol.* **29,** 915–921 (2011).
79. Dichosa, A. E. *et al.* Artificial polyploidy improves bacterial single cell genome recovery. *PLoS ONE* **7,** e37387 (2012).
80. Benson, A. K. *et al.* Individuality in gut microbiota composition is a complex polygenic trait shaped by multiple environmental and host genetic factors. *Proc. Natl Acad. Sci. USA* **107,** 18933–18938 (2010).
81. Elinav, E. *et al.* NLRP6 inflammasome regulates colonic microbial ecology and risk for colitis. *Cell* **145,** 745–757 (2011).
82. Hooper, L. V., Littman, D. R. & Macpherson, A. J. Interactions between the microbiota and the immune system. *Science* **336,** 1268–1273 (2012).
83. Handelsman, J., Rondon, M. R., Brady, S. F., Clardy, J. & Goodman, R. M. Molecular biological access to the chemistry of unknown soil microbes: a new frontier for natural products. *Chem. Biol.* **5,** R245–R249 (1998).
84. Riesenfeld, C. S., Schloss, P. D. & Handelsman, J. Metagenomics: genomic analysis of microbial communities. *Annu. Rev. Genet.* **38,** 525–552 (2004).
85. Hooper, L. V. & Gordon, J. I. Commensal host–bacterial relationships in the gut. *Science* **292,** 1115–1118 (2001).

Acknowledgements The author gratefully acknowledges generous support from the National Institutes of Health.

Author Information Reprints and permissions information is available at www.nature.com/reprints. The author declares no competing financial interests. Readers are welcome to comment on the online version of this article at go.nature.com/1oqsjw. Correspondence should be addressed to G.W. (gweinsto@genome.wustl.edu).

Yakult

Yakult: pursuing the glorious future of investigations into the intestinal microbiota and probiotics

Authors
Takahiro Matsuki, Satoshi Matsumoto, Kan Shida, Hirokazu Tsuji, Takuya Takahashi, Takashi Asahara & Koji Nomoto

Yakult Central Institute for Microbiological Research, 1796 Yaho, Kunitachi, Tokyo, Japan

The Yakult Central Institute for Microbiological Research has been dedicated to basic research on the intestinal microbiota, and applied studies on probiotics and prebiotics, since its foundation. As detailed analysis of the composition of the intestinal microbiota is needed for identifying its functions and defining factors, we have established the Yakult Intestinal Flora-SCAN (YIF-SCAN®) system based on quantitative polymerase chain reaction (qPCR) and reverse transcription (RT)-qPCR methods[1,2], and we are investigating the role of flora characteristics in various diseases. In addition, to understand the role of the microbiota in local regions of the intestine, Yakult is conducting studies using germ-free or gnotobiotic animals, and continuing research on the role of the intestinal microbiota in the development of the host immune system, intestinal diseases and the immunomodulatory effects of probiotics.

Significance, function and composition of intestinal microbiota

Various types of bacteria reside in the human intestinal tract, where they form a complex microbial ecosystem (the microbiota or intestinal flora). Bacteria in the human intestinal tract outnumber the total cells in the host and, at more than 2 kg, outweigh the human brain. Recent analyses targeting 16S ribosomal RNA (rRNA) gene sequences have revealed that the intestinal microbiota comprises hundreds of bacterial species per capita, differs between individuals and is dominated by two phyla (Bacteroidetes and Firmicutes), although several others (such as Actinobacteria, Proteobacteria and Verrucomicrobia) are also present[3].

Recent studies have revealed that the relationship between the intestinal microbiota and human hosts is not simply commensal, but rather is symbiotic. Germ-free animals are effective tools for understanding the relationship between the intestinal microbiota and its hosts; comparisons between germ-free and normal animals have revealed that the intestinal microbiota has various physiological effects on its hosts, including promoting immune-system development, defending against infections, controlling movement of the intestine, normalizing the structure of intestinal epithelia, producing bioactive substrates (such as vitamins and equol) and degrading polysaccharides associated with the production of short-chain fatty acids. Additionally, there has been recent interest in the findings that the intestinal microbiota is among the environmental factors involved in the onset and aggravation of obesity and metabolic syndrome, and that behaviour and brain development differ between germ-free and normal animals. Thus, the influence of the intestinal microbiota on human health has come to be widely recognized, and numerous reports have recently been published in this field.

Here, we describe some of the clinical applications of Yakult's technologies, including YIF-SCAN®, probiotics such as *Lactobacillus casei* strain Shirota (LcS) and *Bifidobacterium breve* strain Yakult (BbY), and synbiotics. We also introduce Yakult's work on the catabolism of soybean isoflavones by endogenous enterobacteria and their benefits, as well as analyses of the mechanisms underlying the immunological effects of probiotics and intestinal microbiota.

Clinical applications of YIF-SCAN®

The YIF-SCAN® method targets high copy-number rRNA molecules in microbes, and has been established as a precise and sensitive microbial assay. It is valuable for obtaining a detailed and accurate understanding of intestinal microbiota with a broad dynamic range. Recent reports have suggested applications for YIF-SCAN®

SPONSOR FEATURE

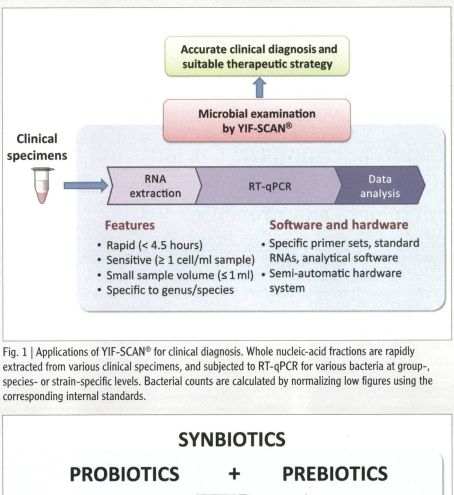
Accurate clinical diagnosis and suitable therapeutic strategy
Microbial examination by YIF-SCAN®
Clinical specimens
RNA extraction
RT-qPCR
Data analysis
Features
• Rapid (< 4.5 hours)
• Sensitive (≥ 1 cell/ml sample)
• Small sample volume (≤ 1 ml)
• Specific to genus/species
Software and hardware
• Specific primer sets, standard RNAs, analytical software
• Semi-automatic hardware system

Fig. 1 | Applications of YIF-SCAN® for clinical diagnosis. Whole nucleic-acid fractions are rapidly extracted from various clinical specimens, and subjected to RT-qPCR for various bacteria at group-, species- or strain-specific levels. Bacterial counts are calculated by normalizing low figures using the corresponding internal standards.

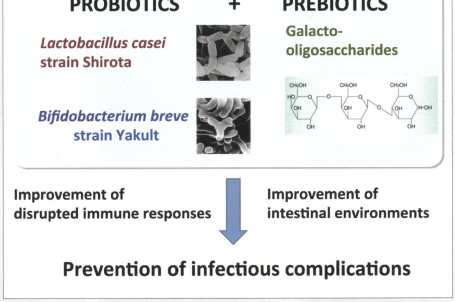

Fig. 2 | Prevention of infectious complications by synbiotics. A combination of LcS, BbY and galactooligosaccharides ameliorated disruption of the immune response and the intestinal environment in the compromised host, and prevented postoperative infectious complications.

in clinical examinations[4–6]. Moreover, YIF-SCAN® allows the rapid and sensitive detection of bacteria in the peripheral blood in cases of fever with neutropaenia, and has been reported to be an effective alternative to conventional blood-culture tests, which are time-consuming, have low detection rates for pathogenic microbes and require significant volumes of blood[4]. In addition, as a basic research tool for the rapid and accurate diagnosis of drug-resistant bacteria, YIF-SCAN® has allowed the fast and sensitive detection of methicillin-resistant *Staphylococcus aureus* (MRSA) in clinical samples by targeting 16S rRNA, the *spa* gene encoding Protein A and the *mecA* gene encoding drug resistance[5]. Furthermore, it has been suggested that YIF-SCAN® is suitable for diagnosing the risk of infectious complications after intestinal surgeries[6].

YIF-SCAN® is useful for sensitive and precise quantification not only of the intestinal microbiota, but also of pathogenic microbes in biological samples, and holds promise for further applications in the field of clinical medicine (Fig. 1).

Probiotics and synbiotics: clinical applications

Postoperative infectious complications affect the prognosis of perioperative patients. The perioperative intestinal tract is the main target of invasions, and a collapse of the balance of the intestinal microbiota and bacterial translocations are major causes of postoperative infections. Synbiotics, which combine probiotics and prebiotic selective enhancers of function and growth, have recently been established as a prophylaxis for perioperative infectious complications (Fig. 2). A randomized clinical trial involving postoperative patients with severely invasive biliary tract cancer has revealed that synbiotics comprising LcS, BbY and galactooligosaccharides have a preventive effect on infectious complications, such as wound infection, intraperitoneal abscess and sepsis, and improve patients' quality of life[7]. In the field of critical-care medicine, synbiotics have also been shown to prevent infectious complications in patients with severe systemic inflammatory-response syndrome caused by a range of serious clinical events (for example, surgery, trauma, burns, pancreatitis and infection)[8].

Beneficial effects of probiotics have been shown in the paediatric field. Synbiotics have been reported to improve nutritional status, and to have a preventive effect on enterocolitis and systemic infections in neonatal patients with severe paediatric diseases requiring surgery or intensive care[9]. Probiotics and synbiotics have been shown to ameliorate the disruption of intestinal microbiota, to improve the enteral environment (promoting the growth of beneficial bacteria, decreasing harmful bacteria and increasing short-chain fatty acids), and to aid the recovery of function in immunocompromised patients[7–9], all of which are regarded as action mechanisms for the prevention of infectious complications.

The key benefits of probiotics and synbiotics include their safety and usefulness

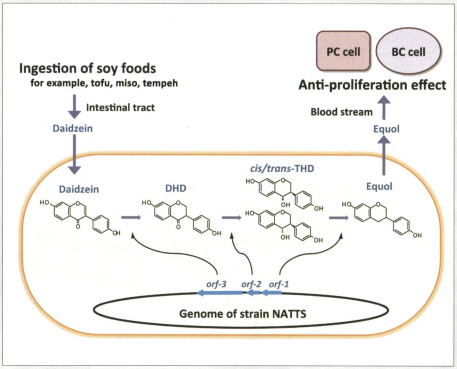

Fig. 3 | Molecular mechanism of daidzein–equol conversion in *Slackia* sp. strain NATTS. This strain has a unique enzyme system composed of three proteins that convert daidzein to equol through the intermediate products DHD and THD. BC, breast cancer; PC, prostate cancer.

against drug-resistant bacteria[10]. In this context, widespread clinical applications of probiotics and synbiotics are desirable as part of activities such as nutritional support.

Metabolism of soybean isoflavones by endogenous enterobacteria

Equol is a soybean isoflavone derivative that has a promising preventive effect on various sex hormone-dependent diseases, such as breast and prostate cancer, because of its high binding capacity to oestrogen receptor beta and strong antioxidant activity. Equol also inhibits the growth of prostate cancer cells by specifically binding to dihydrotestosterone (DHT), preventing it from forming complexes with androgen receptors. At certain concentrations, equol can be detected in human blood and urine in certain individuals known as 'equol-producers' but not in others known as 'non-equol-producers'. As equol is produced in the human intestine via enzyme reactions by certain enterobacteria from daidzein, a soybean isoflavone, it is thought that equol-producers carry these strains.

Slackia sp. strain NATTS, which has high daidzein–equol converting capacity, has been isolated from the faeces of a healthy equol-producer. This bacterium converts daidzein into equol at a high efficiency *in vitro*, and has greater daidzein–equol converting activity than any previously reported. A survey of the distribution of related bacteria using a specific primer set revealed that they were present in 40% of healthy adults[11].

Determination of the sequences of the genes directly involved in daidzein–equol conversion in the NATTS strain has suggested that they encode three proteins implicated in *cis/trans*-tetrahydrodaidzein (THD)–equol conversion, dihydrodaidzein (DHD)–*cis/trans*-THD conversion and daidzein–DHD conversion[12] (Fig. 3).

The global increase in sex hormone-dependent diseases, including prostate and breast cancers, is a topic of concern. Approaches to prevention include re-evaluating the implications of soybean ingestion, increasing the number of equol-producers and administering a preparation of equol-producing bacteria such as strain NATTS[11]. The production of equol using enzyme reactors with daidzein-equol converting enzymes might also be useful.

LcS: clinical effects through controlling host immunological functions

One mechanism by which LcS prevents infection clinically could be by ameliorating the disruption of intestinal microbiota caused by varying loads, restoring normality and stability, and enhancing colonization resistance. LcS might also prevent infection by strengthening host immunoprophylaxis.

Upper respiratory tract infection
HTLV-1-associated myelopathy
Superficial bladder cancer
Colon cancer
Ulcerative colitis

Table 1 | Promising targets of LcS for prevention and/or treatment by modulating immune responses in humans.

Athletes who consumed LcS-fermented milk for 16 weeks during winter training experienced a decreased reduction of saliva immunoglobulin A (IgA) levels and a reduced occurrence of upper respiratory infection[13]. Administrating LcS-fermented milk to patients with human T-lymphotropic virus type 1 (HTLV-1)-associated myelopathy driven by the causal virus of adult T-cell leukaemia recovered their natural killer-cell activity and improved their clinical symptoms[14].

In addition, administering a powder formulation of LcS was found to reduce the risk of disease recurrence in patients with superficial bladder cancer whose lesions were transurethrally removed, and to prevent the recurrence of tumours with moderate-to-high atypia in patients in whom more than one tumour was removed from the large intestine[14]. Enhanced biophylaxis as a result of LcS intake is thought to underlie these effects[14]. In fact, several clinical trials have demonstrated that LcS intake restores reduced natural killer-cell activity[14]. In addition, many studies in model animals strongly support the notion that LcS exerts its effect on cancers and infections by activating host immunological functions.

LcS has been reported to show efficacy against diseases caused by excessive immune responses. Administration of LcS-fermented milk for 8 weeks to patients with ulcerative colitis in its active phase was shown to ameliorate the clinical symptoms[15]. The main mechanism underlying this effect is thought to be the prevention of interleukin-6 (IL-6) production by the characteristic polysaccharide component (PS-1) on LcS cell surfaces. Furthermore, animal experiments suggest that LcS might be effective against autoimmune diseases such as type I diabetes and rheumatoid arthritis.

Thus, LcS has been shown to work in two ways, restoring biophylaxis to normal levels when immunological function is low, and preventing excessive immune responses when an inflammatory reaction is induced (Table 1).

SPONSOR FEATURE

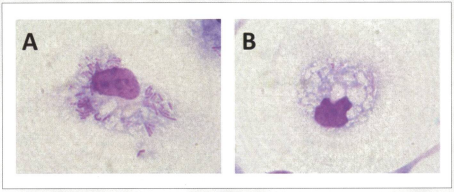

Fig. 4 | LcS cells engulfed by macrophages show resistance to intracellular digestion. (A) LcS. (B) *Lactobacillus johnsonii* ICM 2012[T].

Commensal bacteria, immune system development and intestinal diseases

Intestinal commensal bacteria affect the physiological functions of their hosts, including immune and neuroendocrine systems, via various metabolites and bacterial cellular components.

By contrast, the host controls the intestinal commensal flora through anti-microbial agents produced by intestinal epithelial cells, through recognition of commensal bacteria by the intestinal immune system, through activation of gut immunity by both innate and adaptive systems, and through intestinal transit controlled by mucins from epithelial cells and enteric neuroendocrine systems.

Host health is maintained by the establishment of symbiotic relationships with intestinal commensal bacteria. Studies in germ-free or gnotobiotic animals have shown that commensal bacteria affect intestinal epithelial cells, induce the production of glycoproteins and bioactive peptides, and promote the immunological maturation of intestinal intraepithelial lymphocytes with strong cytotoxic activity and IgA-producing plasma cells[16]. Studies have also implicated host-specific commensal species, such as segmented filamentous bacteria and clostridia, in the maturation of the gut mucosal immune system.

Disruption of the symbiotic relationship between intestinal commensal bacteria and their hosts is considered to cause intestinal diseases, including enteric infections and inflammatory bowel disease (IBD). In addition, recent studies have proposed that intestinal commensal bacteria are involved in lifestyle-related diseases, such as obesity and arteriosclerosis, and links with various disorders are being explored. Yakult has developed models of some intestinal diseases, including IBD, and has been analysing the relationship with commensal bacteria[17]. Studies of tumorigenesis in the large intestine have suggested that commensal bacteria are involved in the formation of mutagenic compounds, including nitrosamine, tryptophan metabolites and secondary bile acids, and that butyric acid, which is a metabolite of intestinal commensal bacteria, exerts an anti-tumour effect by contributing to the prevention of histone deacetylation. In recent years, it has been suggested that chronic inflammation is related to tumorigenesis in the stomach and large intestine. The Yakult Central Institute for Microbiological Research has been focusing on the relationship between commensal microbiota and chronic inflammation in tumorigenesis of the large intestine. We have found that IL-6 *trans*-signalling, which differs from classic IL-6 signalling, plays a critical role in chronic colitis-associated tumorigenesis in the large intestine, and that the activation of macrophages in the intestinal mucosa by the indigenous microbiota is implicated in this pathway[18].

Yakult intends to improve understanding of the relationship between commensal bacteria and disease further through studies combining animal models of human diseases and gnotobiology, and to continue clarifying the roles of intestinal commensal bacteria.

LcS: plasticity in induction of cytokine production

LcS has effects on macrophages and dendritic cells, and induces various cytokines, such as IL-12, IL-10 and tumour necrosis factor-alpha. IL-12 and IL-10 are particularly important in the activation of biophylaxis function and in the homeostasis of immune systems through reduced inflammatory response, respectively.

Stimulating the peritoneal macrophages of mice with different kinds of lactic-acid bacteria causes different patterns of induction of IL-12/IL-10 production depending on the strain. In particular, LcS vigorously induces IL-12 production, but weakly induces IL-10. LcS bacteria engulfed by macrophages show significant resistance to digestion, and continuous stimulation of the macrophages via the tertiary structures of the LcS cell walls increases IL-12 production[19] (Fig. 4A). Notably, LcS can induce IL-12 production in Toll-like receptor 2 (TLR2)-deficient macrophages in a similar way to in wild-type macrophages, but not in those lacking myeloid-differentiation primary response gene (88) (MyD88). Therefore, although induction of IL-12 production does not require stimulation via TLR2, it might make use of TLR signals in some way.

Recent studies have revealed that the induction patterns of cytokine production change when LcS, which has the potential to induce IL-12 production strongly, acts on macrophages in conjunction with certain kinds of bacteria and their components. For example, a minimal amount of IL-10 is induced in macrophages that are stimulated by lipoteichoic acid (LTA), which is a bacterial component characteristic of Gram-positive bacteria. However, the simultaneous addition of LTA and LcS to a macrophage culture strongly induced the production of IL-10 while weakly inducing IL-12[20]. Thus, LcS appears to change from a strong inducer of IL-12 to a strong inducer of IL-10 when it coexists with certain bacterial components. Furthermore, LTA was found to function by activating the mitogen-activated protein kinase (MAPK/ERK) pathway via the stimulation of TLR2. However, LTA did not strongly induce IL-10 production even in the presence of lactic-acid bacterial strains that were sensitive to digestion within macrophages and had a low inducing capacity for IL-12 production[19] (Fig. 4B). Therefore, the cell-wall structure, which is characteristic of LcS and resistant to digestion within macrophages, could be an important factor in the induction of IL-10 production.

There is growing evidence that LcS might differentially change the induction patterns of cytokine production depending on the conditions of macrophages and dendritic cells that it stimulates. This could be important for understanding the expression mechanisms of the various immunomodulatory effects of LcS.

Perspectives from studies on intestinal microbiota and probiotics

YIF-SCAN® has provided clear data on the composition of the intestinal microbiota, which can significantly influence host health. Although certain microbes have been shown to have critical functions, such as catabolism of bile and organic acids, it remains unclear how they are controlled in

such complex ecosystems and are regulated exogenously. It is essential to understand the effects of intestinal microbiota on host functions (such as intestinal immune and endocrine systems), and analyses in partially reconstructed systems of the intestinal microbiota in gnotobiotic animals are expected to facilitate this.

Various probiotics have been developed as food products. Normalizing the mechanisms of immunity disrupted by diseases, particularly innate immunity, and improving the intestinal microbiota and environment have been identified as crucial action mechanisms for probiotics. Understanding the distinct strain-specific mechanisms of action, such as those of LcS described above, and clinical validation of the disease-prevention effects will facilitate the classification of probiotics.

Understanding the functions of endogenous microbiota at strain-, species- and group-specific levels, and the effects of probiotics, which are exogenous ingested microbes, remain pivotal to future investigations, and should benefit the prevention and treatment of diseases involving the intestines. Yakult's efforts in this field are expected to lead to the development of novel probiotics.

References

1. Matsuda, K. *et al.* Establishment of an analytical system for the human fecal microbiota, based on reverse transcription-quantitative PCR targeting of multicopy rRNA molecules. *Appl. Environ. Microbiol.* **75**, 1961–1969 (2009).
2. Matsuki, T. *et al.* Use of 16S rRNA gene-targeted group-specific primers for real-time PCR analysis of predominant bacteria in human feces. *Appl. Environ. Microbiol.* **70,** 7220–7228 (2004).
3. Eckburg, P. B. *et al.* Diversity of the human intestinal microbial flora. *Science* **308,** 1635–1638 (2005).
4. Sakaguchi, S. *et al.* Bacterial rRNA-targeted reverse transcription-PCR used to identify pathogens responsible for fever with neutropenia. *J. Clin. Microbiol.* **48,** 1624–1628 (2010).
5. Wada, M. *et al.* Quantitative reverse transcription-PCR assay for the rapid detection of methicillin-resistant *Staphylococcus aureus*. *J. Appl. Microbiol.* **108,** 779–788 (2010).
6. Mizuno, T. *et al.* Intraoperative bacterial translocation detected by bacterium-specific ribosomal RNA-targeted reverse-transcriptase polymerase chain reaction for the mesenteric lymph node strongly predicts postoperative infectious complications after major hepatectomy for biliary malignancies. *Ann. Surg.* **252,** 1013–1019 (2010).
7. Sugawara, G. *et al.* Perioperative synbiotic treatment to prevent postoperative infectious complications in biliary cancer surgery: a randomized controlled trial. *Ann. Surg.* **244,** 706–714 (2006).
8. Shimizu, K. *et al.* Synbiotics decrease the incidence of septic complications in patients with severe SIRS: a preliminary report. *Dig. Dis. Sci.* **54,** 1071–1078 (2009).
9. Kanamori, Y. *et al.* Early use of probiotics is an important therapy in infants with severe congenital anomaly. *Pediatr. Int.* **52,** 362–367 (2010).
10. Asahara, T. *et al.* Protective effect of *Lactobacillus casei* strain Shirota against lethal infection with multi-drug resistant *Salmonella enterica* serovar Typhimurium DT104 in mice. *J. Appl. Microbiol.* **110,** 163–173 (2011).
11. Akaza, H. Prostate cancer chemoprevention by soy isoflavones-role of intestinal bacteria as the "second human genome". *Cancer Sci.* **103,** 969–975 (2012).
12. Tsuji, H. *et al.* Identification of an enzyme system for daidzein-to-equol conversion in *Slackia* sp. strain NATTS. *Appl. Environ. Microbiol.* **78,** 1228–1236 (2012).
13. Gleeson, M. *et al.* Daily probiotic's (*Lactobacillus casei* Shirota) reduction of infection incidence in athletes. *Int. J. Sport Nutr. Excerc. Metab.* **21,** 55–64 (2011).
14. Nanno, M. *et al.* Biological effects of probiotics: what impact does *Lactobacillus casei* Shirota have on us? *Int. J. Immunopathol. Pharmacol.* **24 (suppl.),** 45–50 (2011).
15. Mitsuyama, K. *et al.* Beneficial effects of *Lactobacillus casei* in ulcerative colitis: a pilot study. *J. Clin. Biochem. Nutr.* **43,** s78–s81 (2008).
16. Umesaki, Y. *et al.* Structure of the intestinal flora responsible for development of the gut immune system in a rodent model. *Microbes Infect.* **2,** 1343–1351 (2000).
17. Matsumoto S. *et al.* Inflammatory bowel disease-like enteritis and caecitis in a senescence accelerated mouse P1/Yit strain. *Gut* **43,** 71–78 (1998).
18. Matsumoto S. *et al.* Essential roles of IL-6 *trans*-signaling in colonic epithelial cells, induced by the IL-6/soluble-IL-6-receptor derived from lamina propria macrophages, on the development of colitis-associated premalignant cancer in a murine model. *J. Immunol.* **184,** 1543–1551 (2010).
19. Shida, K. *et al.* Induction of interleukin-12 by *Lactobacillus* strains having a rigid cell wall resistant to intracellular digestion. *J. Dairy Sci.* **89,** 3306–3317 (2006).
20. Kaji, R. *et al.* Bacterial teichoic acids reverse predominant IL-12 production induced by certain *Lactobacillus* strains into predominant IL-10 production via TLR2-dependent ERK activation in macrophages. *J. Immunol.* **184,** 3505–3513 (2010).

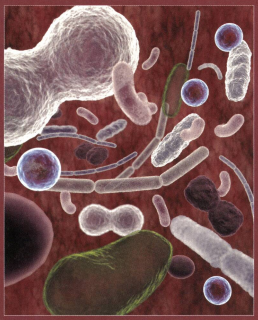

nature

www.nature.com/nature/supplements/insights

ARTICLE

doi:10.1038/nature11393

Distinct contribution of stem and progenitor cells to epidermal maintenance

Guilhem Mascré[1], Sophie Dekoninck[1], Benjamin Drogat[1], Khalil Kass Youssef[1], Sylvain Brohée[1,2], Panagiota A. Sotiropoulou[1], Benjamin D. Simons[3,4] & Cédric Blanpain[1,5]

The skin interfollicular epidermis (IFE) is the first barrier against the external environment and its maintenance is critical for survival. Two seemingly opposite theories have been proposed to explain IFE homeostasis. One posits that IFE is maintained by long-lived slow-cycling stem cells that give rise to transit-amplifying cell progeny, whereas the other suggests that homeostasis is achieved by a single committed progenitor population that balances stochastic fate. Here we probe the cellular heterogeneity within the IFE using two different inducible Cre recombinase–oestrogen receptor constructs targeting IFE progenitors in mice. Quantitative analysis of clonal fate data and proliferation dynamics demonstrate the existence of two distinct proliferative cell compartments arranged in a hierarchy involving slow-cycling stem cells and committed progenitor cells. After wounding, only stem cells contribute substantially to the repair and long-term regeneration of the tissue, whereas committed progenitor cells make a limited contribution.

Skin epidermis is comprised of a basal layer of proliferative cells and several suprabasal layers of terminally differentiated cells that are progressively enucleated, forming squames that are shed from the skin surface[1]. Depending on anatomical location and species, the minimum transit time from the basal layer to the cornified layer has been estimated at around 1–2 weeks[2]. In homeostasis, cells lost during the course of turnover must be perfectly compensated by cells generated in the basal layer. Different theories have been proposed to explain how this balance is achieved[1]. On the basis of morphological and proliferation studies, it has been proposed that the IFE is organized into discrete 'epidermal proliferative units' (EPUs), comprised of slow-cycling stem cells (SCs) together with around 10 transit-amplifying cell progeny, which undergo terminal differentiation after a fixed number of cell divisions[2–5]. Following the clonal marking of IFE cells by retroviruses[6–9] or mutagens[10,11], long-lived columns of labelled IFE cells that span the epidermis from the basal layer to the top of the cornified layer appear, lending support to the concept of EPUs. By contrast, the quantitative analysis of lineage tracing data in IFE using a ubiquitous promoter suggests that tissue is maintained by a single, equipotent, committed progenitor (CP) cell population in which the balance between proliferation and differentiation follows from seemingly random cell fate decisions[12,13]. Although this model is attractive in its simplicity, it does not easily explain the ability of tissue to respond rapidly to increased cell demand, such as during wound healing, and cannot rule out the presence of a quiescent or slow-cycling IFE population[14]. More importantly, whereas the contribution of different populations of hair follicle SCs to wound healing is well-established[15–18], little is known about the contribution of putative IFE SCs or CP cells to the repair of skin epidermis.

From a quantitative analysis of lineage tracing data using two different Cre recombinase–oestrogen receptor (Cre-ER) transgenic mice, we demonstrate the existence of two distinct populations of epidermal progenitors that form a SC/CP cell hierarchy that differentially contribute to the homoeostasis and repair of the epidermis.

Heterogeneity of epidermal progenitors

To probe the proliferative heterogeneity within the IFE, we made use of two Cre-ER transgenic mice that target IFE progenitors (Supplementary Fig. 1a, b). With a high dose of tamoxifen, Cre-ER under the control of the keratin 14 promoter (K14-Cre-ER) can target most cells in the basal layer of tail IFE[19]. A very low dose of tamoxifen (0.2 mg) to K14-Cre-ER/RosaYFP induced yellow fluorescent protein (YFP) expression at clonal density (Supplementary Fig. 1c). Although Cre-ER under the control of the involucrin promoter (Inv-Cre-ER) predominantly targets cells in the suprabasal layers, we have recently shown that some basal cells, characterized by K5 but not Inv protein expression, are also induced but at a lower frequency than K14-Cre-ER (Supplementary Fig. 1d–f)[20]. The basal cells marked by these two different Cre-ER comprise IFE progenitors, as demonstrated by their ability to proliferate, and give rise to differentiated progeny, forming columns of labelled cells (Supplementary Fig. 1c, d).

To determine whether the two induction protocols mark the same homogenous pool of progenitors, we first quantified their survival at different time points after tamoxifen administration. Although many of the clones induced by the K14-Cre-ER survived up to 1 year post-induction, most of the Inv-Cre-ER targeted clones were progressively lost (Fig. 1a–c). Whereas the population of 'surviving clones', defined as clones that retain at least one basal layer cell, drops by around 30% for K14 mice from 4 weeks to 6 months after labelling, the clone density falls by a factor of 10 in the Inv mice over the same period, indicating that IFE is maintained by a heterogeneous pool of progenitors with different survival potential.

Inv-Cre-ER targets committed progenitors

To gain further insight into the behaviour of these apparently distinct pools of progenitors, we quantified the pattern of growth of individual clones targeted by the Inv-Cre-ER at eight time points ranging from 3.5 days to 48 weeks post-induction, a period spanning more than half of the average lifetime of the mouse. At 3.5 days, 40% of surviving clones had undergone at least one round of cell division (Fig. 2a, b and

[1]Université Libre de Bruxelles, IRIBHM, Brussels B-1070, Belgium. [2]Université Libre de Bruxelles, Machine Learning Group, Brussels B-1050, Belgium. [3]Cavendish Laboratory, Department of Physics, J.J. Thomson Avenue, Cambridge CB3 0HE, UK. [4]The Wellcome Trust/Cancer Research UK Gurdon Institute, University of Cambridge, Tennis Court Road, Cambridge CB2 1QN, UK. [5]WELBIO, Université Libre de Bruxelles, Brussels B-1070, Belgium.

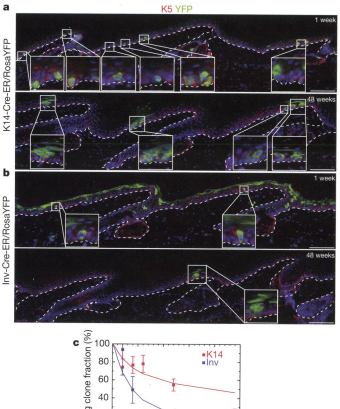

Figure 1 | K14-Cre-ER and Inv-Cre-ER target IFE progenitors with different survival characteristics. a, **b**, Immunostaining of K5 and YFP in K14-Cre-ER/RosaYFP (**a**) and Inv-Cre-ER/RosaYFP (**b**) tail epidermis at 1 week and 48 weeks post-induction showing the high survival rate of K14-Cre-ER clones. Dashed lines represent the basal lamina. Hoechst nuclear staining is represented in blue. **c**, Quantification of surviving clones in K14-Cre-ER/RosaYFP and Inv-Cre-ER/RosaYFP tail epidermis at different times following tamoxifen administration ($n = 327$ clones at least, for each time point of K14 and Inv). Symbols show experimental data and the lines represent the prediction of the mathematical modelling. The data has been normalized to the initial clone density as inferred by the fit to theory. Error bars show s.d. Scale bars, 200 μm.

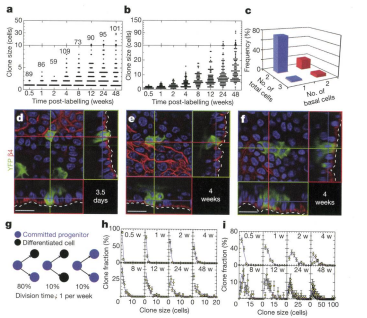

Figure 2 | Inv-Cre-ER targets IFE CP cells. a, **b**, Distribution of Inv-Cre-ER clone sizes as measured by basal (**a**) and total (**b**) cell content of surviving clones, imaged by confocal microscopy on whole-mount tail epidermis from 3.5 days to 48 weeks following tamoxifen administration. The number of analysed clones is indicated in **a** and this is identical in **b**, **h** and **i**. **c**, Size distribution of surviving clones with more than one cell at 3.5 days post-labelling disaggregated according to basal and total cell number ($n = 37$ clones). **d**–**f**, Confocal analysis of representative Inv-Cre-ER-targeted basal clones at 3.5 days (**d**) and 4 weeks (**e**, **f**) post tamoxifen. Dashed lines represent the basal lamina. Hoechst nuclear staining is represented in blue. **g**, A fit of the Inv-Cre-ER clonal fate data predicts that progenitors undergo population asymmetry through a combination of asymmetric cell division, symmetrical self-renewal and symmetrical differentiation with an average cell cycle time of approximately 1 week. **h**, **i**, Frequency distribution of basal (**h**) and total (**i**) clone size. Symbols represent experimental data and the lines correspond to the model prediction. Error bars show s.e.m. Scale bars, 10 μm.

Supplementary Fig. 2a), and the vast majority of these divisions resulted in one basal and one suprabasal cell (Fig. 2c, d). At 4 weeks post-induction, although almost all surviving clones had undergone at least one cell division, 40% of clones still contained only one basal cell (Fig. 2a, e), indicating that most of these divisions led to asymmetric fate outcome. However, the other 60% of surviving clones had also expanded basally (Fig. 2a, f), indicating that progenitors can also symmetrically self-renew.

This clonal heterogeneity increased progressively over the 48-week time course, indicating that progenitors follow divergent fates (Supplementary Fig. 2b, c). At the same time, the average size of surviving clones (as measured both by their total size and their 'footprint' on the basal layer) grew approximately linearly with time (Supplementary Fig. 2d), whereas the number of surviving clones progressively fell (Fig. 1c). Such behaviour mirrors that reported previously[12] in studies using a ubiquitous promoter, and indicates that Inv-Cre-ER targets the actively cycling CP cell population, in which stochastic cell loss through differentiation is perfectly compensated by duplication (Fig. 2g). This conclusion is reinforced by a quantitative analysis of the data, which confirms that the basal layer clone size distribution converges onto the hallmark scaling behaviour in which the chance of finding a clone larger than some multiple of the average stays constant over time (Supplementary Fig. 2e and Supplementary Methods, section 'Theory')[21]. From the detailed study of the basal and total clone size distribution over the 48 week time course (Fig. 2h, i, Supplementary Fig. 2f and Supplementary Methods, section 'Theory'), we are able to conclude that, following CP cell division (at an average rate of 1.21 ± 0.04 per week), 80% result in asymmetric fate (leading to one dividing and one differentiated cell) with the remainder leading to symmetric duplication or differentiation with approximately equal probability (Fig. 2g), consistent with the results from ref. 12. Indeed, from the 48 week time point, we are able to resolve a small (less than 1 in 14) bias towards terminal division.

K14-Cre-ER targets long-lived SCs

To determine whether the dynamics of K14 clones are different from the Inv clones, we performed extensive clonal analysis using the K14-Cre-ER mice ranging from 3.5 days to 48 weeks post-induction (Fig. 3). At just 3.5 days, 60% of K14 clones had already undergone one round of cell division (Fig. 3a, b and Supplementary Fig. 3a), whereas the fraction of clones involving two or more basal cells was greatly increased compared with Inv (Fig. 3a–d). However, following an initial abrupt expansion, the growth of K14 clones rapidly decelerates over the first few weeks, with the size distribution from 8 weeks to 6 months post-induction showing only a modest expansion (Fig. 3a–f and Supplementary Fig. 3a–c). Alongside the propensity of clones to persist, these observations are consistent with the K14 promoter targeting both the CP cell population and a second, slow-cycling, SC population. In particular, the precipitous expansion of clones (Fig. 3a–c), which is far more rapid than that found in the

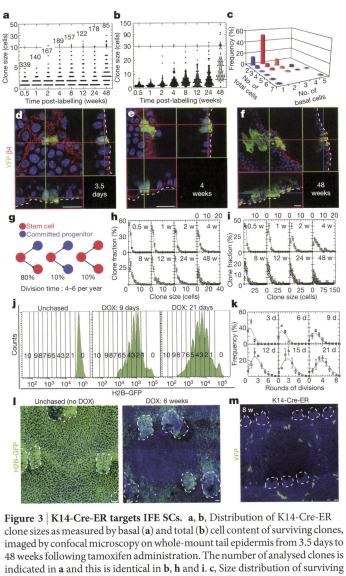

Figure 3 | K14-Cre-ER targets IFE SCs. **a**, **b**, Distribution of K14-Cre-ER clone sizes as measured by basal (**a**) and total (**b**) cell content of surviving clones, imaged by confocal microscopy on whole-mount tail epidermis from 3.5 days to 48 weeks following tamoxifen administration. The number of analysed clones is indicated in **a** and this is identical in **b**, **h** and **i**. **c**, Size distribution of surviving clones with more than one cell at 3.5 days post-labelling disaggregated according to basal and total cell number ($n = 197$ clones). **d**–**f**, Confocal analysis of representative K14-Cre-ER targeted basal clones at 3.5 days (**d**), 4 weeks (**e**) and 48 weeks (**f**) post tamoxifen. Dashed lines represent the basal lamina. Hoechst nuclear staining is represented in blue. Scale bars, 10 μm. **g**, Biophysical modelling of the clonal fate data predicts that K14-Cre-ER targets both CP cells and SCs with the latter undergoing population asymmetry through a combination of asymmetric cell division, symmetrical self-renewal and symmetric differentiation with an average cell cycle rate of between 4 and 6 per year. **h**, **i**, Frequency distribution of basal (**h**) and total (**i**) clone size. Symbols represent data and the lines correspond to the model prediction. **j**, FACS analysis of K5tTA/tet(O)-H2BGFP mice at different time point following DOX administration. **k**, Frequency of the number of cell divisions that surviving basal IFE cells undergo during the chase period as quantified by FACS analysis at different time points after DOX administration to adult K5tTA/tet(O)-H2BGFP mice. Symbols represent the average of the experimental data ($n = 3$ mice at each time point). Lines correspond to the predicted model dynamics (Supplementary Methods, section 'Theory'). **l**, **m**, Confocal analysis of H2B–GFP immunostaining in unchased mice (no DOX) (left panel) and 6 weeks after DOX administration (right panel), showing the preferential localization of the slow-cycling IFE cells in the bottom of epidermal undulations (stars) (**l**) and of YFP immunostaining in K14-Cre-ER/RosaYFP 8 weeks after tamoxifen administration (**m**). Dashed lines are hair follicles. Scale bars, 20 μm. Error bars show s.e.m. Hoechst nuclear staining is represented in blue.

Inv study (Fig. 2a–c), indicates that SCs are induced predominantly on cell cycle entry. This conclusion is consistent with the observation that, after administration of 12-*O*-tetradecanoyl phorbol-13-acetate (TPA), a drug that stimulates epidermal proliferation, there is an 80% increase in clone labelling after low dose of tamoxifen (Supplementary Fig. 4a, b). Furthermore, the deceleration in the rate of clonal expansion at subsequent times indicates that, after division, SCs re-enter a quiescent phase whereas their CP cell progeny go on to proliferate and differentiate. For these clones, the quiescent SC 'mother' provides an anchor to the basal layer (Fig. 3a–f and Supplementary Fig. 3a), leading to clonal persistence. Such behaviour is consistent with the observation that, in K14 mice, the level of positive regulators of the cell cycle, such as *Ccnb1* and *Cdc20*, decreased, whereas negative regulators of the cell cycle, such as *Cdkn1a* and *Cdkn2a*, increased in basal cells between 3.5 days and 8 weeks (Supplementary Fig. 4c–e).

With this hypothesis, if we assume that SC division can also lead to all three possible fates (Fig. 3g), the predicted model dynamics provides an excellent fit to the clone size data (basal and suprabasal) over the wide range of time points up to 1-year post-labelling (Fig. 3h, i, Supplementary Fig. 3c, d and Supplementary Methods, section 'Theory'). In particular, we find that SCs account for some $50 \pm 5\%$ of the induced proliferative cells. With a SC division rate as low as 4–6 per year, a factor of 10–20 times slower than CP cells, most of the clone size data (from 1 week to 3 months post-labelling) are largely fixed by the known characteristics of CP cells. Drawing on the early (3.5 day) time point, we are able to deduce that, in common with their progenitor cell progeny, SCs undergo population asymmetric self-renewal with some $80 \pm 10\%$ of SC divisions resulting in asymmetric fate (one SC and one CP cell), whereas the remaining divisions are equally balanced between SC duplication and symmetrical differentiation into two CPs (Fig. 3g). Finally, although the analysis points at a proliferative hierarchy, we cannot rule out the possibility that proliferative cells may switch reversibly between CP and SC behaviour if the transfer rate is sufficiently low. Moreover, the data do not allow us to infer whether the balance between SC proliferation and differentiation follows from intrinsic (cell autonomous) regulation or is controlled by environmental cues (Supplementary Methods, section 'Theory')[21].

Proliferation dynamics of the IFE

To challenge these findings, we applied further independent experimental assays to explore the IFE cell proliferation using a combination of cell cycle analysis, 5-bromo-2-deoxyuridine (BrdU) incorporation, and pulse-chase experiments using the K5tTA/tet(O)-H2B-GFP reporter mouse, that have proved useful in resolving quantitatively the proliferation dynamics of hair follicle bulge SCs[15,22–24]. We first determined the cell cycle profile of basal IFE cells by determining their DNA content. These experiments show that around 9% of $\alpha6^+CD34^-$ IFE cells were in the S/G2/M phase of the cell cycle (Supplementary Fig. 5a, b). Continuous BrdU administration labelled $28 \pm 2\%$ and $57 \pm 10\%$ of K5-expressing cells after 24 and 72 h, respectively, indicating an average cell division time of around 6 ± 1 days (Supplementary Fig. 5c, d and Supplementary Methods, section 'Theory'), consistent with the inferred CP cell division rate.

To develop a more refined method to quantify proliferation kinetics over a longer period, we used K5tTA/tet(O)-H2B-GFP mice (Supplementary Fig. 6). In the absence of doxycycline (DOX), histone 2B domain–green fluorescent protein (H2B–GFP) fusion protein is expressed at a very high level in a discrete peak of fluorescence (Supplementary Fig. 6a–c, top panels). Following DOX administration, H2B–GFP fluorescence decreases by a factor of two after cell division[15,22] (Supplementary Fig. 6a–c, bottom panels). The discrete peak of H2B–GFP fluorescence observed by fluorescence-activated cell sorting (FACS) analysis during the chase period allowed an accurate quantification of the distribution in the number of rounds of division experienced by basal layer cells ($\alpha6^+CD34^-$) at various time points following induction (Fig. 3j and Supplementary Fig. 6d). At 3 weeks post-DOX administration, dilution of H2B–GFP label shows evidence of CP cell proliferation, while a small peak at high levels of fluorescence is consistent with around 5% or less of label-retaining cells (LRCs).

From the quantification of fluorescence over the time course, the distribution of cell divisions was shown to be quantitatively consistent with the inferred SC and CP cell dynamics (Fig. 3k and Supplementary Methods, section 'Theory'). Notably, after 6 weeks of chase, the H2B–GFP label has become diluted in the vast majority of basal layer cells and only a small minority retain high levels of expression (Supplementary Fig. 6d). Intriguingly, these LRCs are localized to the bottom of the undulations of the tail epidermis (Fig. 3l), which correlate with the location of persistent clones derived by the K14 assay (Fig. 3m), and are reminiscent of the so-called rete ridges in human epidermis, where epidermal SCs were thought to reside[23,26].

Molecular characterization of SCs and CP cells

To gain further insight into the molecular properties of these two functionally distinct pools of epidermal progenitors, we transcriptionally profiled FACS-purified $\alpha6^+CD34^-$ K14-Cre-ER and Inv-Cre-ER YFP-positive IFE cells 3.5 days after tamoxifen administration (Supplementary Fig. 7). Comparison of the K14 and Inv transcriptome revealed notable differences. All markers previously associated with murine and human IFE SCs[25,27–29] were upregulated in K14-targeted cells, including α6, α2, α3, β1 integrins and *Cspg4* (Supplementary Fig. 8). Real-time quantitative reverse transcriptase-PCR (qRT–PCR) performed on independent biological samples confirmed the upregulation of these integrins in K14-targeted cells (Fig. 4a). FACS analysis showed that α6β4 integrins were expressed at a higher and more uniform level in K14- than in Inv-targeted cells. The pattern of α2β1 integrin showed a more notable difference between the two populations, with a very high and narrow peak of α2β1 expression in K14-targeted cells compared to the much lower and heterogeneous α2β1 expression in Inv-targeted cells (Fig. 4b, c and Supplementary Fig. 9). Gene ontology classification of the genes differentially expressed by more than 1.5-fold between K14- and Inv-labelled cells revealed that genes preferentially expressed in K14-positive cells are enriched with a very high statistical significance in functional groups involved in positive and negative cell cycle regulation (for example, *Ccnd2*, *Cdc20*, *Cdkn1a*, *Cdkn2a*), mitosis (for example, *Ccnb1*, *Kif11*), chromosome segregation (for example, *Cenpe*), regulation of cell proliferation (for example, *Epgn*), and DNA repair (for example, *Brca1*) (Fig. 4a, Supplementary Figs 8, 10a and Supplementary Table 1). By contrast, Inv-Cre-ER labelled cells preferentially expressed genes known to control epidermal differentiation[30–32] (for example, *Notch3*, *Grhl3*), keratinocyte differentiation and keratinization (for example, *Sppr1a*, *1b*, *2d*, *2i*)[33], and lipid metabolism (for example, *Elovl4*, *6*, *7*, *Olah*), as confirmed by qRT–PCR analysis (Fig. 4d, Supplementary Figs 8, 10b and Supplementary Table 1). Altogether these data demonstrate that K14- and Inv-targeted cells differ by their gene expression profile, and uncover many new markers preferentially expressed by IFE SC and CP cells.

To characterize further the molecular heterogeneity of basal IFE cells, we FACS-purified different populations of basal epidermal cells ($\alpha6^+CD34^-$) according to the level of β1 integrin expression which, together with α2 integrin, present the most significant difference between K14 and Inv-targeted cells at 3.5 days following tamoxifen administration (Fig. 4b and Supplementary Fig. 9). We fractionated epidermis into three distinct populations: one population (<3%) expressing very high levels of β1 integrin (which are likely to be enriched in SCs as they are only detected in K14- but not Inv-targeted cells), a second population expressing intermediate levels of β1 integrin detected in both K14 and Inv-targeted cells (which are likely to represent CP cells), and cells expressing low levels of β1 integrin only found in Inv-targeted cells (which are likely to represent the differentiated basal cells and early suprabasal cells) (Supplementary Fig. 11a). Strikingly, many markers identified as being upregulated in K14 versus Inv were also upregulated in cells expressing very high levels of β1 integrin compared to cells expressing intermediate or low levels (Supplementary Fig. 11b). Similarly, many genes preferentially expressed by Inv cells were already upregulated in cells expressing intermediate levels of β1 integrin compared to β1 integrin high cells but, nevertheless, much less expressed than in cells expressing low levels of β1 integrin (Supplementary Fig. 11c). These data demonstrate that the expression of many differentiation-associated genes is already upregulated at the earliest stage of progenitor commitment, reminiscent of the lineage priming reported in haematopoietic stem cells[34,35].

Long-term SC contribution to wound healing

In addition to their role in maintenance, adult SCs are implicated in the repair of damaged tissue following injury. Lineage tracing has shown that hair follicle SCs are mobilized to the wound area and contribute to the repair of damaged epidermis[15–18]. At the same time, genetic mouse mutants, that present a complete absence of hair follicle, heal incisional wounds with a slight delay of the reepithelialisation, demonstrating that IFE cells are also capable of tissue regeneration[36]. However, in unperturbed conditions, the contribution of IFE SCs and progenitors to wound healing is currently unknown. To address the respective contributions of K14-SCs and Inv-CPs during tissue repair, we first marked basal progenitors by titrating the dose of tamoxifen so as to label Inv and K14-Cre-ER epidermis at roughly the same density (4.5 ± 0.1 clones per mm^2 and 3.8 ± 0.5 clones per mm^2 in K14 and Inv, respectively), then subjected tail epidermis to full thickness excisional wound using punch biopsy, and assessed the contribution of marked cells to repair (Fig. 5a). Whole-mount analysis showed major recruitment of K14-Cre-ER-labelled IFE cells to the wound area, with clones migrating from the periphery towards the centre of the wound (with only 7.5% of clones from hair follicle), persisting long-term after wounding (2.6 ± 0.1 clones per mm^2 after 35 days) (Fig. 5b, c and Supplementary Fig. 12), and consisting of very large clones with a broad basal attachment and huge numbers of differentiated cells (Fig. 5d). In sharp contrast, few Inv-Cre-ER-targeted cells were recruited to the wound area, and these clones were, on average, much

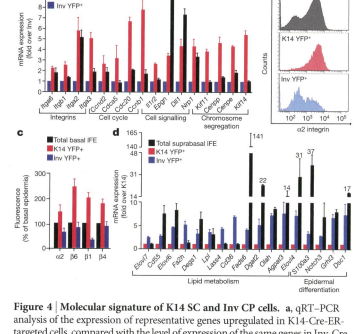

Figure 4 | Molecular signature of K14 SC and Inv CP cells. a, qRT–PCR analysis of the expression of representative genes upregulated in K14-Cre-ER-targeted cells, compared with the level of expression of the same genes in Inv-Cre-ER-targeted cells and total basal IFE cells ($n = 3$). **b**, **c**, Fluorescence histogram (**b**) and geometric mean fluorescence (**c**) of integrin cell-surface expression in all basal IFE cells, K14-Cre-ER- and Inv-Cre-ER-targeted IFE cells, as determined by FACS analysis, 3.5 days after tamoxifen ($n = 3$). **d**, qRT–PCR analysis of the expression of representative genes upregulated in Inv-Cre-ER-targeted cells, compared to the level of expression of the same genes in basal epidermal K14-Cre-ER-targeted cells and total suprabasal IFE cells ($n = 3$). Error bars show s.e.m.

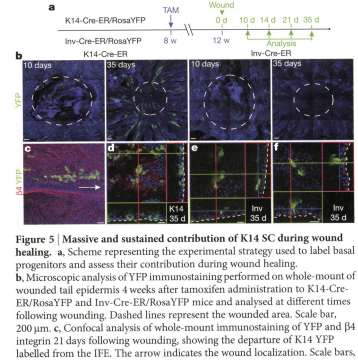

Figure 5 | Massive and sustained contribution of K14 SC during wound healing. a, Scheme representing the experimental strategy used to label basal progenitors and assess their contribution during wound healing. **b**, Microscopic analysis of YFP immunostaining performed on whole-mount of wounded tail epidermis 4 weeks after tamoxifen administration to K14-Cre-ER/RosaYFP and Inv-Cre-ER/RosaYFP mice and analysed at different times following wounding. Dashed lines represent the wounded area. Scale bar, 200 μm. **c**, Confocal analysis of whole-mount immunostaining of YFP and β4 integrin 21 days following wounding, showing the departure of K14 YFP labelled from the IFE. The arrow indicates the wound localization. Scale bars, 20 μm. **d**–**f**, Confocal analysis of representative clones from wounded tail epidermis 35 days post-wound, showing very big clones containing multiple basal cells in K14 targeted cells (**d**), whereas the rare still visible Inv marked clones are either completely detached from the basal epidermis (**e**) or very small containing one or few basal cells (**f**). Dashed lines represent the basal lamina. Scale bars, 20 μm. Hoechst nuclear staining is represented in blue.

smaller. At 35 days post-injury, few Inv clones survived (0.3 ± 0.3 clones per mm^2) and consisted of either clones of cells being shed with no basal attachment (Fig. 5e), or small clones with one or few basal cells (Fig. 5f). These data demonstrate that K14-derived SC are capable of extensive tissue regeneration, whereas Inv CP cells have only a limited contribution to wound healing.

Discussion

Our study demonstrates the existence, hierarchical organization and the proliferation dynamics of two distinct types of progenitors that effect different functions during homeostasis and repair of the IFE in adult mice. Quantitative modelling of clonal fate data suggest that both the slow-cycling SCs and the more rapidly cycling CP cells share a similar pattern of population asymmetric self-renewal in which the balance between proliferation and differentiation is achieved through stochastic fate choice (Supplementary Fig. 13). These findings provide a reconciliation of seemingly contradictory theories of IFE maintenance[4,12], and explain the proliferative heterogeneity previously reported in IFE[5,37,38]. The existence of slow-cycling SCs and more rapidly cycling progenitors is reminiscent of the situation encountered in other tissues including cornea[39], hair follicle[40], blood[41,42], muscle[43] and brain[44]. In all of these tissues, these slow-cycling SCs can switch rapidly and reversibly between quiescence and activity following injury and/or drug treatment[43,45]. Indeed, this partitioning of function—progenitors to undertake routine maintenance and quiescent SCs to effect repair—may represent a generic strategy of tissue maintenance.

The demonstration that the long-term wound healing potential is dominated by the IFE SC compartment may suggest that either SC and CP cell populations are not interchangeable, in contrast to progenitors in intestinal epithelium[46], or that their reversion rate is sufficiently slow to render its effects negligible. The seemingly short-lived contribution of Inv CP cells to the repair of the epidermis is reminiscent of the fate of K15 bulge-derived SCs during wounding[16], and demonstrates the critical role of IFE SCs for the long-term repair of the epidermis, as has been proposed[16].

METHODS SUMMARY

Clonal YFP expression in the tail IFE was performed by administrating 0.2 mg and 2.5 mg tamoxifen to K14-Cre-ER/RosaYFP and Inv-Cre-ER/RosaYFP mice, respectively. Immunostainings were performed as described[47]. Quantification of the proportion of surviving clones as well as the basal, suprabasal and total clone size was determined by counting the number of YFP^+ cells using whole-mount tail epidermis, analysed by confocal microscopy. BrdU pulse and H2B–GFP label retention was performed as described[13,43]. The wound healing assay was performed by administrating 1 mg and 10 mg tamoxifen to K14-Cre-ER/RosaYFP and Inv-Cre-ER/RosaYFP mice, respectively. Four weeks later punch biopsies were performed in the tail epidermis and analysed at different time points. Mathematical modelling of the clonal fate data was performed as described in Supplementary Methods, section 'Theory'. For further details see Supplementary Methods.

Full Methods and any associated references are available in the online version of the paper.

Received 13 March; accepted 3 July 2012.
Published online 2 September 2012.

1. Blanpain, C. & Fuchs, E. Epidermal homeostasis: a balancing act of stem cells in the skin. *Nature Rev. Mol. Cell Biol.* **10,** 207–217 (2009).
2. Potten, C. S., Saffhill, R. & Maibach, H. I. Measurement of the transit time for cells through the epidermis and stratum corneum of the mouse and guinea-pig. *Cell Tissue Kinet.* **20,** 461–472 (1987).
3. Potten, C. S. Cell replacement in epidermis (keratopoiesis) via discrete units of proliferation. *Int. Rev. Cytol.* **69,** 271–318 (1981).
4. Potten, C. S., Wichmann, H. E., Loeffler, M., Dobek, K. & Major, D. Evidence for discrete cell kinetic subpopulations in mouse epidermis based on mathematical analysis. *Cell Tissue Kinet.* **15,** 305–329 (1982).
5. Potten, C. S. & Loeffler, M. Epidermal cell proliferation. I. Changes with time in the proportion of isolated, paired and clustered labelled cells in sheets of murine epidermis. *Virchows Arch. B Cell Pathol. Incl. Mol. Pathol.* **53,** 279–285 (1987).
6. Mackenzie, I. C. Retroviral transduction of murine epidermal stem cells demonstrates clonal units of epidermal structure. *J. Invest. Dermatol.* **109,** 377–383 (1997).
7. Kolodka, T. M., Garlick, J. A. & Taichman, L. B. Evidence for keratinocyte stem cells *in vitro*: long term engraftment and persistence of transgene expression from retrovirus-transduced keratinocytes. *Proc. Natl Acad. Sci. USA* **95,** 4356–4361 (1998).
8. Ghazizadeh, S. & Taichman, L. B. Multiple classes of stem cells in cutaneous epithelium: a lineage analysis of adult mouse skin. *EMBO J.* **20,** 1215–1222 (2001).
9. Ghazizadeh, S. & Taichman, L. B. Organization of stem cells and their progeny in human epidermis. *J. Invest. Dermatol.* **124,** 367–372 (2005).
10. Ro, S. & Rannala, B. A stop-EGFP transgenic mouse to detect clonal cell lineages generated by mutation. *EMBO Rep.* **5,** 914–920 (2004).
11. Ro, S. & Rannala, B. Evidence from the stop-EGFP mouse supports a niche-sharing model of epidermal proliferative units. *Exp. Dermatol.* **14,** 838–843 (2005).
12. Clayton, E. *et al.* A single type of progenitor cell maintains normal epidermis. *Nature* **446,** 185–189 (2007).
13. Doupé, D. P., Klein, A. M., Simons, B. D. & Jones, P. H. The ordered architecture of murine ear epidermis is maintained by progenitor cells with random fate. *Dev. Cell* **18,** 317–323 (2010).
14. Jones, P. & Simons, B. D. Epidermal homeostasis: do committed progenitors work while stem cells sleep? *Nature Rev. Mol. Cell Biol.* **9,** 82–88 (2008).
15. Tumbar, T. *et al.* Defining the epithelial stem cell niche in skin. *Science* **303,** 359–363 (2004).
16. Ito, M. *et al.* Stem cells in the hair follicle bulge contribute to wound repair but not to homeostasis of the epidermis. *Nature Med.* **11,** 1351–1354 (2005).
17. Levy, V., Lindon, C., Zheng, Y., Harfe, B. D. & Morgan, B. A. Epidermal stem cells arise from the hair follicle after wounding. *FASEB J.* **21,** 1358–1366 (2007).
18. Snippert, H. J. *et al.* Lgr6 marks stem cells in the hair follicle that generate all cell lineages of the skin. *Science* **327,** 1385–1389 (2010).
19. Vasioukhin, V., Degenstein, L., Wise, B. & Fuchs, E. The magical touch: genome targeting in epidermal stem cells induced by tamoxifen application to mouse skin. *Proc. Natl Acad. Sci. USA* **96,** 8551–8556 (1999).
20. Lapouge, G. *et al.* Identifying the cellular origin of squamous skin tumors. *Proc. Natl Acad. Sci. USA* **108,** 7431–7436 (2011).
21. Klein, A. M. & Simons, B. D. Universal patterns of stem cell fate in cycling adult tissues. *Development* **138,** 3103–3111 (2011).
22. Waghmare, S. K. *et al.* Quantitative proliferation dynamics and random chromosome segregation of hair follicle stem cells. *EMBO J.* **27,** 1309–1320 (2008).
23. Zhang, Y. V., Cheong, J., Ciapurin, N., McDermitt, D. J. & Tumbar, T. Distinct self-renewal and differentiation phases in the niche of infrequently dividing hair follicle stem cells. *Cell Stem Cell* **5,** 267–278 (2009).
24. Zhang, Y. V., White, B. S., Shalloway, D. I. & Tumbar, T. Stem cell dynamics in mouse hair follicles: A story from cell division counting and single cell lineage tracing. *Cell Cycle* **9,** 1504–1510 (2010).

25. Jones, P. H., Harper, S. & Watt, F. M. Stem cell patterning and fate in human epidermis. *Cell* **80**, 83–93 (1995).
26. Lavker, R. M. & Sun, T. T. Heterogeneity in epidermal basal keratinocytes: morphological and functional correlations. *Science* **215**, 1239–1241 (1982).
27. Jones, P. H. & Watt, F. M. Separation of human epidermal stem cells from transit amplifying cells on the basis of differences in integrin function and expression. *Cell* **73**, 713–724 (1993).
28. Legg, J., Jensen, U. B., Broad, S., Leigh, I. & Watt, F. M. Role of melanoma chondroitin sulphate proteoglycan in patterning stem cells in human interfollicular epidermis. *Development* **130**, 6049–6063 (2003).
29. Tani, H., Morris, R. J. & Kaur, P. Enrichment for murine keratinocyte stem cells based on cell surface phenotype. *Proc. Natl Acad. Sci. USA* **97**, 10960–10965 (2000).
30. Rangarajan, A. *et al.* Notch signaling is a direct determinant of keratinocyte growth arrest and entry into differentiation. *EMBO J.* **20**, 3427–3436 (2001).
31. Blanpain, C., Lowry, W. E., Pasolli, H. A. & Fuchs, E. Canonical notch signaling functions as a commitment switch in the epidermal lineage. *Genes Dev.* **20**, 3022–3035 (2006).
32. Ting, S. B. *et al.* A homolog of *Drosophila* grainy head is essential for epidermal integrity in mice. *Science* **308**, 411–413 (2005).
33. Candi, E., Schmidt, R. & Melino, G. The cornified envelope: a model of cell death in the skin. *Nature Rev. Mol. Cell Biol.* **6**, 328–340 (2005).
34. Månsson, R. *et al.* Molecular evidence for hierarchical transcriptional lineage priming in fetal and adult stem cells and multipotent progenitors. *Immunity* **26**, 407–419 (2007).
35. Pina, C. *et al.* Inferring rules of lineage commitment in haematopoiesis. *Nature Cell Biol.* **14**, 287–294 (2012).
36. Langton, A. K., Herrick, S. E. & Headon, D. J. An extended epidermal response heals cutaneous wounds in the absence of a hair follicle stem cell contribution. *J. Invest. Dermatol.* **128**, 1311–1318 (2008).
37. Loeffler, M., Potten, C. S. & Wichmann, H. E. Epidermal cell proliferation. II. A comprehensive mathematical model of cell proliferation and migration in the basal layer predicts some unusual properties of epidermal stem cells. *Virchows Arch. B Cell Pathol. Incl. Mol. Pathol.* **53**, 286–300 (1987).
38. Morris, R. J., Fischer, S. M. & Slaga, T. J. Evidence that the centrally and peripherally located cells in the murine epidermal proliferative unit are two distinct cell populations. *J. Invest. Dermatol.* **84**, 277–281 (1985).
39. Cotsarelis, G., Cheng, S. Z., Dong, G., Sun, T. T. & Lavker, R. M. Existence of slow-cycling limbal epithelial basal cells that can be preferentially stimulated to proliferate: implications on epithelial stem cells. *Cell* **57**, 201–209 (1989).
40. Cotsarelis, G., Sun, T. T. & Lavker, R. M. Label-retaining cells reside in the bulge area of pilosebaceous unit: implications for follicular stem cells, hair cycle, and skin carcinogenesis. *Cell* **61**, 1329–1337 (1990).
41. Wilson, A. *et al.* Hematopoietic stem cells reversibly switch from dormancy to self-renewal during homeostasis and repair. *Cell* **135**, 1118–1129 (2008).
42. Foudi, A. *et al.* Analysis of histone 2B-GFP retention reveals slowly cycling hematopoietic stem cells. *Nature Biotechnol.* **27**, 84–90 (2009).
43. Rocheteau, P., Gayraud-Morel, B., Siegl-Cachedenier, I., Blasco, M. A. & Tajbakhsh, S. A subpopulation of adult skeletal muscle stem cells retains all template DNA strands after cell division. *Cell* **148**, 112–125 (2012).
44. Bonaguidi, M. A. *et al. In vivo* clonal analysis reveals self-renewing and multipotent adult neural stem cell characteristics. *Cell* **145**, 1142–1155 (2011).
45. Essers, M. A. *et al.* IFNα activates dormant haematopoietic stem cells *in vivo*. *Nature* **458**, 904–908 (2009).
46. Takeda, N. *et al.* Interconversion between intestinal stem cell populations in distinct niches. *Science* **334**, 1420–1424 (2011).
47. Youssef, K. K. *et al.* Identification of the cell lineage at the origin of basal cell carcinoma. *Nature Cell Biol.* **12**, 299–305 (2010).

Supplementary Information is available in the online version of the paper.

Acknowledgements We thank F. Bollet-Quivogne and J.-M. Vanderwinden for their help with confocal imaging. C.B. and P.A.S. are chercheur qualifié, G.M. and S.B. are supported by fellowship of the FRS/FNRS. B.D. is supported by TELEVIE. C.B. is an investigator of WELBIO. This work was supported by the FNRS, the program d'excellence CIBLES of the Wallonia Region, a research grant from the Fondation Contre le Cancer, the ULB fondation, the fond Gaston Ithier, the European Research Council (ERC) and the EMBO Young Investigator Program.

Author Contributions C.B., G.M., B.D., S.D., P.A.S. and B.D.S. designed the experiments and performed data analysis. G.M., S.D., B.D. and K.K.Y. performed all the experiments. S.B. performed bioinformatic analysis of the microarray. C.B. and B.D.S. wrote the manuscript.

Author Information The data discussed in this publication have been deposited in the NCBI Gene Expression Omnibus and are accessible through GEO Series accession number GSE36688. Reprints and permissions information is available at www.nature.com/reprints. The authors declare no competing financial interests. Readers are welcome to comment on the online version of the paper. Correspondence and requests for materials should be addressed to C.B. (cedric.blanpain@ulb.ac.be) or B.D.S. (bds10@cam.ac.uk).

ARTICLE

doi:10.1038/nature11315

RPN-6 determines *C. elegans* longevity under proteotoxic stress conditions

David Vilchez[1], Ianessa Morantte[1], Zheng Liu[1], Peter M. Douglas[1], Carsten Merkwirth[1], Ana P. C. Rodrigues[2]†, Gerard Manning[2]† & Andrew Dillin[1]

Organisms that protect their germ-cell lineages from damage often do so at considerable cost: limited metabolic resources become partitioned away from maintenance of the soma, leaving the ageing somatic tissues to navigate survival amid an environment containing damaged and poorly functioning proteins. Historically, experimental paradigms that limit reproductive investment result in lifespan extension. We proposed that germline-deficient animals might exhibit heightened protection from proteotoxic stressors in somatic tissues. We find that the forced re-investment of resources from the germ line to the soma in *Caenorhabditis elegans* results in elevated somatic proteasome activity, clearance of damaged proteins and increased longevity. This activity is associated with increased expression of *rpn-6*, a subunit of the 19S proteasome, by the FOXO transcription factor DAF-16. Ectopic expression of *rpn-6* is sufficient to confer proteotoxic stress resistance and extend lifespan, indicating that *rpn-6* is a candidate to correct deficiencies in age-related protein homeostasis disorders.

In nature, food sources are largely unpredictable and insufficient. The constant pressures that limited energetic resources place on an organism have long been theorized to cause a significant life-history trade-off: the absolute need for repairing and preventing damage to the germ line, and for ensuring elimination of damage in progeny, necessarily dominates resource allocation strategies, whereas conversely little or no evolutionary pressure will be placed on the maintenance of the soma[1]. Thus, ageing, post-reproductive organisms that escape predation witness the gradual deterioration of their own somatic tissues. In support of such theories, modulations of reproduction that eliminate germ cells provide effective mechanisms for extending lifespan[2,3], phenotypes that may be caused by heightened resource availability within the post-mitotic soma. Likewise, it has been proposed that animals undergoing dietary restriction adopt a strategy in which resources are re-allocated towards somatic maintenance, extending lifespan and prolonging reproduction until conditions for survival become more favourable[4].

When proliferating germline cells of *C. elegans* are removed, worms live up to 60% longer than normal and seem to be resistant to a variety of environmental stressors[5–7]. Whereas germline ablation affords an obvious protection, the downstream effectors of such protection remain ambiguous. The re-allocation of resources to the soma seems to be directed through a specific, genetically defined stress-responsive pathway. Germline removal extends lifespan by triggering an active signalling network, involving the nuclear localization and activation of DAF-16, a forkhead transcription factor (FOXO)[8] and the major downstream effector of the DAF-2–insulin–insulin-like growth factor (IGF) signalling (IIS) pathway. However, although worms with an ablated germ line exhibit a *daf-16*-dependent extension in lifespan, longevity caused by germline ablation functions in a synergistic manner with mutations in the IIS receptor, *daf-2* (ref. 6). Additionally, in germline-ablated animals, but not *daf-2* mutant worms, *kri-1*, *daf-9* and the nuclear hormone receptor *daf-12* are also required for the constitutive nuclear localization of DAF-16 (refs 9, 10).

Notably, post-mitotic somatic cells are particularly susceptible to age-onset protein aggregation diseases. As the somatic cell ages, the accumulation of damaged proteins represents a particular challenge to the ageing cell, especially as they aggregate in inclusions and aggresomes capable of overwhelming the cellular machinery required for their degradation[11,12]. These effects are probably compounded by age-related dysregulation of chaperones, a downregulation of degradation machinery itself, and a continually accelerating loss in general cellular homeostasis. As such, a rapid decline in the capacity of the cell to protect its proteome has been highly correlated with multiple age-related disorders[13]. This conversely indicates that long-lived somatic cells, such as those found in a germline-ablated animal, might exhibit a heightened capacity for clearing damaged proteins, and that this proteostatic capacity might contribute to the increased longevity in these mutants.

Increased proteasome activity in *glp-1(e2141)* worms

We hypothesized that a key aspect of the proteostasis network, the ubiquitin proteasome system (UPS), might be altered in the soma of germline-ablated animals. To test this hypothesis, we first examined the activity of the 26S/30S proteasome in several long-lived mutants using a fluorogenic peptide substrate specific for the chymotrypsin-like activity of the proteasome (Supplementary Fig. 1). We found that *glp-1(e2141)* mutant worms, which lack their germ line, displayed a marked increase (over sixfold) in the chymotrypsin-like proteasome activity (Fig. 1a and Supplementary Figs 1 and 2a–c). The proteasome inhibitors MG-132, lactacystin and PI-1 blocked activity from extracts in both the *glp-1* mutant and the control strain (Supplementary Fig. 3), indicating that the increased peptidase activity in *glp-1(e2141)* worms was due to the proteasome. The caspase-like and trypsin-like activities were also increased in *glp-1* mutant worms (Fig. 1b, c). Additionally, we found that a *C. elegans* genetic model of dietary restriction[14] also induced proteasome activity, although to a lesser extent than the *glp-1(e2141)* mutation (Supplementary Fig. 1). In contrast, neither reduced IIS signalling by mutation of *daf-2* nor reduced mitochondrial

[1]Howard Hughes Medical Institute, Glenn Center for Aging Research, Molecular and Cell Biology Laboratory, The Salk Institute for Biological Studies, 10010 North Torrey Pines Road, La Jolla, California 92037, USA. [2]Razavi Newman Center for Bioinformatics, The Salk Institute for Biological Studies, 10010 North Torrey Pines Road, La Jolla, California 92037, USA. †Present addresses: Department of Computational Medicine and Bioinformatics, University of Michigan, 100 Washtenaw Avenue, Ann Arbor, Michigan 48109-2218, USA (A.P.C.R.); Bioinformatics and Computational Biology, Genentech, 1 DNA Way, South San Francisco, California 94080, USA (G.M.).

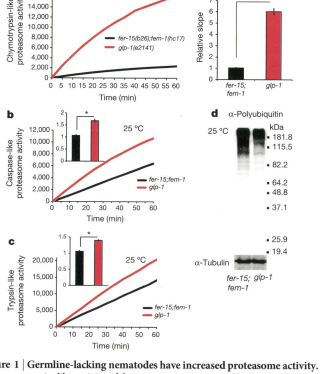

Figure 1 | Germline-lacking nematodes have increased proteasome activity. **a**, Chymotrypsin-like activity of the proteasome monitored by Z-Gly-Gly-Leu-AMC digestion in day 7 adult worm extract containing equal amounts of total protein. Proteasome activity (relative slope to control strain *fer-15(b26);fem-1(hc17)*) is shown, with error bars indicating mean ± s.e.m. ($n = 50$, $^*P = 1.83 \times 10^{-17}$). **b**, Caspase-like (Z-Leu-Leu-Glu-AMC) proteasome activity (relative slope) is shown, with error bars representing mean ± s.e.m. ($n = 8$, $^*P < 0.00001$). **c**, Trypsin-like (Ac-Arg-Leu-Arg-AMC) proteasome activity (relative slope) is shown, with error bars showing mean ± s.e.m. ($n = 7$, $^*P < 0.00001$). **d**, Representative polyubiquitinated protein immunoblot. α-Tubulin is used as the loading control.

electron transport chain activity[15] upregulated proteasome activity (Supplementary Fig. 1). Consistent with increased proteasome activity in *glp-1(e2141)* worms, we observed decreased levels of polyubiquitinated proteins in these worms (Fig. 1d). To examine further UPS activity in living animals, we used a photoconvertible fluorescent UPS reporter system for live imaging and quantification of protein degradation in *C. elegans*[16]. This proteasome reporter consists of the photoconvertible fluorescent protein Dendra2 targeted for proteasomal degradation by fusion to a mutant form of ubiquitin (UbG76V) that cannot be cleaved by ubiquitin hydrolases. Dendra2 can be irreversibly photoconverted from a green to a red fluorescent state, providing quantification of UPS activity independently of protein synthesis. We found that this reporter is degraded more rapidly in *glp-1* mutant worms compared to control strains, whereas Dendra2 lacking the UbG76V signal remained stable (Supplementary Fig. 4).

glp-1(e2141) worms differ from other types of reproductive mutants in that their entire germ line is missing. Notably, *glp-1* mutants exhibit a significantly increased lifespan in comparison to worms that are also sterile but which still contain a proliferating germ line (Supplementary Fig. 5). We observed that the increased proteasome activity of *glp-1* mutants was not due to a benefit of sterility per se, because the normal-lived, sterile control *fer-15(b26);fem-1(hc17)* animals have similar proteasome activity as wild-type animals (Supplementary Figs 2a and 6). Furthermore, treatment with 5-fluoro-2′deoxyuridine (FUdR), a drug used to block progeny production in worms[17], did not affect proteasome activity (Supplementary Fig. 6). The *glp-1(e2141)* allele is temperature-sensitive for reproduction and longevity[18]; these worms are only long-lived when they are shifted to restrictive temperature (25 °C) either during development or in early adulthood[5]. Accordingly, proteasome activity is not increased in *glp-1(e2141)* worms grown continuously at the permissive temperature (Supplementary Fig. 7). However, resembling the longevity phenotype[5], *glp-1(e2141)* worms maintained high proteasome activity when down-shifted to a permissive temperature after germline removal (Supplementary Fig. 8). These results indicate that different forms of sterility do not have similar effects on proteasome activity, but are specific to loss of the germ line.

DAF-16 regulates proteasome activity

Because DAF-16, the worm FOXO transcription factor, is essential for the increased longevity of *glp-1* mutant worms[5], we tested whether *daf-16* was also required for the increased proteasome activity found in *glp-1(e2141)* animals. Proteasome activity of *glp-1* mutant animals was suppressed to wild-type levels in *daf-16;glp-1* double mutant animals (Fig. 2a–c). *daf-16* is required during reproductive adulthood to modulate the ageing process in worms[19]. Accordingly, *daf-16* RNA interference (RNAi) treatment of *glp-1(e2141)* animals during adulthood decreased proteasome activity (Fig. 2d). In contrast, *daf-16* RNAi did not affect proteasome activity in control strains (Fig. 2d and Supplementary Fig. 9), where DAF-16 is located in the cytosol and is inactive. Loss of *daf-16* suppressed longevity and proteasome activity, but not the reproductive phenotype of *glp-1(e2141)* worms, providing further evidence that increased proteasomal activity could not be separated from the increased longevity mediated by DAF-16 in *glp-1* mutants. We examined whether other genes required to promote DAF-16/FOXO nuclear localization in the germline longevity pathway (that is, *daf-12*, *daf-9* and *kri-1*) were also necessary for increased proteasome activity. Accordingly, reduction of any one of these genes in *glp-1(e2141)* worms resulted in decreased proteasome activity, although not to the extent of *daf-16* reduction (Fig. 2e). Furthermore, reduction of *daf-12*, *daf-9* or *kri-1* did not further decrease proteasome activity of the *daf-16;glp-1* double mutant animals or the control strain (Supplementary Fig. 10a, b). In addition to *daf-16*, *glp-1*-mediated longevity requires two additional transcription factors: *hsf-1* (ref. 20) and *skn-1* (Supplementary Fig. 11). *hsf-1* is required for the regulation of adult lifespan, heat-shock and proteotoxic stress[21,22]; *skn-1* is the worm orthologue of *nrf-2* and has a central role in oxidative stress responses in worms, flies and mice[23,24]. In contrast to *daf-16*, *daf-12*, *daf-9* and *kri-1*, we observed that neither *hsf-1* nor *skn-1* was required for the increased proteasome activity in *glp-1(e2141)* worms (Fig. 2f, g). To uncover a possible redundancy of either *hsf-1* or *skn-1* with *daf-16*, we knocked down these factors in the *daf-16;glp-1* double mutant animals. However, in the context of *daf-16* loss, neither *hsf-1* nor *skn-1* further affected proteasome activity in *glp-1(e2141)* worms (Supplementary Fig. 12). The nuclear hormone receptor *nhr-80* links fatty acid desaturation to lifespan extension through germline ablation in a *daf-16*-independent manner[25]. Consistent with a requirement for *daf-16* in proteasome activity, *nhr-80* was not required for increased proteasome activity in *glp-1* mutant worms (Supplementary Fig. 13). Taken together, alterations that specifically affect DAF-16 activity, but not HSF-1, SKN-1 or NHR-80, alter proteasome activity in *glp-1* mutants, indicating that a major output for DAF-16-mediated longevity in this mutant is to increase proteasome activity.

DAF-16 regulates *rpn-6.1* levels

The 26S/30S proteasome consists of a 20S core structure that contains the proteolytic active sites and 19S cap structures that impart regulation on the activity of the holo-complex (26S, single capped, and 30S, double capped)[26]. Although 20S particles can exist in a free form, 20S particles in their most physiological form are inactive, unable to degrade denatured proteins or cleave peptides[27]. The 19S regulatory subunit is responsible for stimulating the 20S proteasome to degrade proteins, as ATPases of the regulatory particle open the 20S core, allowing substrates access to proteolytic active sites[28]. Analysis of

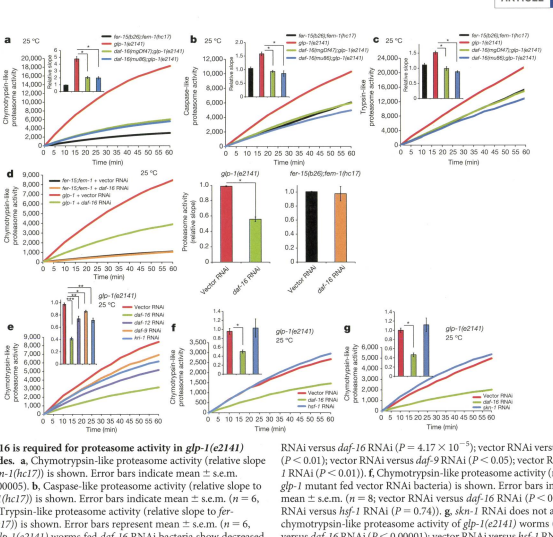

Figure 2 | DAF-16 is required for proteasome activity in *glp-1(e2141)* mutant nematodes. **a**, Chymotrypsin-like proteasome activity (relative slope to *fer-15(b26);fem-1(hc17)*) is shown. Error bars indicate mean ± s.e.m. ($n = 11$, $^*P < 0.00005$). **b**, Caspase-like proteasome activity (relative slope to *fer-15(b26);fem-1(hc17)*) is shown. Error bars indicate mean ± s.e.m. ($n = 6$, $^*P < 0.0001$). **c**, Trypsin-like proteasome activity (relative slope to *fer-15(b26);fem-1(hc17)*) is shown. Error bars represent mean ± s.e.m. ($n = 6$, $^*P < 0.005$). **d**, *glp-1(e2141)* worms fed *daf-16* RNAi bacteria show decreased chymotrypsin-like proteasome activity ($P = 8.5 \times 10^{-8}$ *glp-1* mutant fed vector RNAi bacteria versus *glp-1* mutant fed *daf-16* RNAi bacteria; $n = 16$). *daf-16* RNAi knock down does not affect proteasome activity in *fer-15;fem-1* worms ($P = 0.79$ *fer-15;fem-1* fed vector RNAi bacteria versus *fer-15;fem-1* fed *daf-16* RNAi bacteria; $n = 9$). **e**, Chymotrypsin-like proteasome activity in *glp-1(e2141)* worms fed *daf-16*, *daf-12*, *daf-9* or *kri-1* RNAi bacteria ($n = 4$; vector RNAi versus *daf-16* RNAi ($P = 4.17 \times 10^{-5}$); vector RNAi versus *daf-12* RNAi ($P < 0.01$); vector RNAi versus *daf-9* RNAi ($P < 0.05$); vector RNAi versus *kri-1* RNAi ($P < 0.01$)). **f**, Chymotrypsin-like proteasome activity (relative slope to *glp-1* mutant fed vector RNAi bacteria) is shown. Error bars indicate mean ± s.e.m. ($n = 8$; vector RNAi versus *daf-16* RNAi ($P < 0.0001$); vector RNAi versus *hsf-1* RNAi ($P = 0.74$)). **g**, *skn-1* RNAi does not affect chymotrypsin-like proteasome activity of *glp-1(e2141)* worms (vector RNAi versus *daf-16* RNAi ($P < 0.00001$); vector RNAi versus *hsf-1* RNAi ($P = 0.46$)). Chymotrypsin-like proteasome activity (relative slope to *glp-1* mutant fed vector RNAi bacteria) is shown. Error bars indicate the mean ± s.e.m. ($n = 9$; vector RNAi versus *daf-16* RNAi ($P < 0.00001$); vector RNAi versus *hsf-1* RNAi ($P = 0.46$)). All activities measured at day 5 of adulthood. All RNAi treatment was initiated at day 1 of adulthood. All statistical comparisons were made by Student's *t*-test for unpaired samples.

the messenger RNA levels of the 20S proteasome subunits revealed that α-subunits were not increased in *glp-1* mutants whereas only one of the β-subunits, *pbs-5*, was moderately increased (Supplementary Fig. 14 and Supplementary Table 1). PBS-5 is the β-type subunit that contains the chymotrypsin-like proteolytic active site[26]. With regard to the 19S proteasome subunits, we did not detect an increase of the ATPase subunits (Fig. 3a and Supplementary Table 1). Notably, only one of the non-ATPase subunits showed increased mRNA levels in *glp-1* mutant animals: *rpn-6.1*, an essential subunit for the activity of the 26S/30S proteasome that stabilizes the otherwise weak interaction between the 20S core and the 19S cap[29,30] (Fig. 3a, b and Supplementary Table 1). mRNA levels of the closely related *rpn-6.2* were not increased in *glp-1* mutants (Fig. 3a and Supplementary Table 1). *rpn-6.1* had a threefold increase in its expression in *glp-1* mutants and was by far the most increased of all subunits. Accordingly, knock down of *rpn-6.1* markedly decreased proteasome activity in *glp-1(e2141)* animals (Fig. 3c) similar to loss of *daf-16*. In contrast, loss of other non-ATPase subunits did not affect proteasome activity of *glp-1* mutants (Supplementary Fig. 15). Knock down of *rpn-6.1* induced an upregulation in the expression of the rest of the 26S proteasome subunits, probably to compensate for the reduction in proteasome activity induced by decreased levels of this critical subunit (Supplementary Table 2). Moreover, overexpression of *rpn-6.1* in wild-type animals was sufficient to increase proteasome activity (Fig. 3d). The increase in *rpn-6.1* mRNA levels did not alter the expression of other 26S proteasome subunits (Supplementary Table 3). Taken together, RPN-6.1 seems to be a key component required for activation of the proteasome machinery of the germline-lacking nematodes.

We found that DAF-16 is necessary for the increased expression of *rpn-6.1* by analysing its mRNA levels in both *daf-16;glp-1* double mutants and *daf-16* RNAi-treated animals (Fig. 3e, Supplementary Figs 16 and 17 and Supplementary Table 4). Notably, mRNA levels of other proteasome subunits, including *pbs-5*, were not decreased by loss of *daf-16* in *glp-1* mutant worms (Supplementary Fig. 17). *daf-16* RNAi did not change *rpn-6.1* expression in control worms (Supplementary Fig. 16). Therefore, these results display a correlation between *daf-16* activity, *rpn-6.1* levels and proteasome activity. Consistent with DAF-16 regulating the expression of *rpn-6.1*, we identified a potential DAF-16 binding site[31] within the first intron of *rpn-6.1* (Supplementary Fig. 18). This site is supported by a DAF-16 binding region defined by the modENCODE project[32], indicating that *rpn-6.1* is likely to be a direct DAF-16 target. To explore further *rpn-6.1* transcriptional regulation, we generated a transcriptional reporter construct. We found that *rpn-6.1* was expressed in the pharynx and posterior intestine in control worms. Notably, *rpn-6.1* expression increased markedly in the pharynx and throughout the intestine of *glp-1* mutants. In

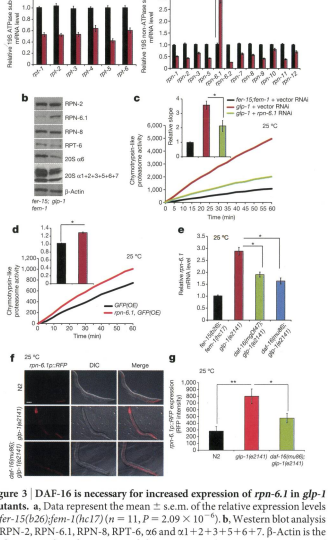

Figure 3 | DAF-16 is necessary for increased expression of *rpn-6.1* in *glp-1* mutants. a, Data represent the mean ± s.e.m. of the relative expression levels to *fer-15(b26);fem-1(hc17)* ($n = 11$, $P = 2.09 \times 10^{-6}$). **b**, Western blot analysis of RPN-2, RPN-6.1, RPN-8, RPT-6, α6 and α1+2+3+5+6+7. β-Actin is the loading control. **c**, *glp-1* mutants fed *rpn-6.1* RNAi bacteria starting day 1 of adulthood have decreased chymotrypsin-like proteasome activity ($P < 0.05$). Proteasome activity (relative slope to *fer-15(b26);fem-1(hc17)*) represents the mean ± s.e.m. ($n = 6$). **d**, Increased chymotrypsin-like proteasome activity in *rpn-6.1* overexpressing N2 worms (*rpn-6.1*, *GFP(OE)*) in day 1 adult worm extract ($P < 0.001$). Proteasome activity (relative slope to *GFP(OE)* worms) represents the mean ± s.e.m. ($n = 9$). **e**, *daf-16;glp-1* double mutants have decreased *rpn-6.1* mRNA levels ($P < 0.001$). Graph represents the mean ± s.e.m. ($n = 6$). **f**, Representative images of RFP expressed under control of the *rpn-6.1* promoter. *rpn-6.1* is expressed in the pharynx and posterior intestine in N2 worms. Increased *rpn-6.1* expression in *glp-1(e2141)* animals relative to N2. *daf-16;glp-1* mutant worms have decreased *rpn-6.1* expression compared to *glp-1* mutants. DIC, differential interference contrast microscopy. Scale bar, 100 μm. **g**, Quantification of RFP signal intensity (mean ± s.e.m. ($n = 5$)). *glp-1(e2141)* worms have increased *rpn-6.1* expression compared to N2 ($P < 0.01$) and *daf-16(mu86);glp-1(e2141)* double mutants ($P < 0.05$). All statistical comparisons were made by Student's *t*-test for unpaired samples.

daf-16;glp-1 double mutants, we found almost a twofold decreased expression of *rpn-6.1* compared to *glp-1(e2141)* worms, although *rpn-6.1* expression is still increased compared to wild-type worms (Fig. 3f, g). These results correlated with quantitative real-time polymerase chain reaction (qPCR) data indicating that *daf-16* mutations decrease *rpn-6.1* expression in *glp-1* mutants, but not to control levels (Fig. 3e, g), suggesting that a potential additional factor may be necessary for *rpn-6.1* expression in addition to DAF-16.

rpn-6.1 determines stress resistance

With the strong connection between *daf-16*, a key ageing modulator, *rpn-6.1*, a key proteasomal factor, and increased proteasome activity in long-lived *glp-1* mutant animals dependent upon both *daf-16* and *rpn-6.1*, we asked what role, if any, does *rpn-6.1* have in longevity. To assess the requirement for *rpn-6.1* during lifespan, we conducted RNAi knock down of this gene in *C. elegans*. Because proteasomal function is required during larval development[33], we initiated *rpn-6.1* RNAi treatment during adulthood, the time at which *daf-16* is required for longevity assurance[19]. Knock down of *rpn-6.1* substantially decreased the lifespan of *glp-1* mutant animals (Supplementary Fig. 19). However, loss of *rpn-6.1* also decreased lifespan of both wild-type and sterile control animals (*fer-15(b26);fem-1(hc17)*). In addition to germ-cell loss, we also examined the effects of *rpn-6.1* RNAi on other pathways that influence lifespan such as reduced IIS (*daf-2(e1370)* worms), reduced mitochondrial electron transport chain (*isp-1(qm150)* worms) and reduced food intake (*eat-2(ad1116)* worms). In all cases, knock down of *rpn-6.1* substantially decreased lifespan, confirming that this gene is essential for the viability of adult animals, making lifespan analysis by *rpn-6.1* loss of function difficult to interpret (Supplementary Fig. 19).

To explore whether *rpn-6.1* might have a positive role in longevity, we tested the impact of increased *rpn-6.1* expression. We over-expressed *rpn-6.1* in wild-type worms and conducted a series of physiological assays to measure the effects of *rpn-6.1* overexpression (OE) on resistance to challenges of oxidative stress, heat-shock and ultraviolet (UV) damage, all of which are correlated with increased longevity. *rpn-6.1(OE)* nematodes were significantly more resistant, than control strains, to oxidative stress induced by growing the worms in the presence of paraquat (Fig. 4a and Supplementary Fig. 20a). Under heat stress (34 °C), *rpn-6.1(OE)* worms lived markedly longer than control strains (Fig. 4b and Supplementary Fig. 20b). Interestingly, increased levels of *rpn-6.1* did not result in global upregulation of all stress responses because *rpn-6.1(OE)* did not protect against UV damage (Fig. 4c and Supplementary Fig. 20c). Because overexpression of *rpn-6.1* increased resistance to conditions that challenge the proteome, we examined whether it also resulted in lifespan extension. *rpn-6.1(OE)* did not extend the lifespan of worms at 20 °C but it did at 25 °C, a temperature that results in mild heat stress (Fig. 4d and Supplementary Fig. 20d). *daf-16* RNAi treatment blocked the lifespan extension induced by *rpn-6.1(OE)* at 25 °C (Fig. 4e and Supplementary Fig. 20e). Therefore, under conditions of proteome stress, overexpression of *rpn-6.1* is sufficient to promote increased survival. As a more formal test, we asked whether animals with a reduced heat-shock response via *hsf-1* downregulation had increased survival when *rpn-6.1* was overexpressed. *hsf-1*-RNAi-treated *rpn-6.1(OE)* worms were long-lived compared to control strains under the same treatment (Fig. 4f and Supplementary Fig. 20f). This last result not only indicates that the lifespan extension induced by *rpn-6.1(OE)* is *hsf-1* independent, but also suggests that these worms can significantly overcome the loss of this critical transcription factor required for adult lifespan, heat-shock and proteotoxicity responses.

Intrigued by the protection that *rpn-6.1* overexpression could confer, we hypothesized that RPN-6.1 could be a potential candidate to correct protein homeostasis deficiencies underlying diseases such as Alzheimer's, Parkinson's or Huntington's disease. Because the latter disease has been associated with proteasome failure[34], we tested whether increased levels of *rpn-6.1* could have beneficial effects in a polyglutamine (polyQ) disease model. Worm motility is markedly reduced by the aggregation of polyQ expression in neurons, with a pathogenic threshold at a length of 35–40 glutamines[35]. Notably, *rpn-6.1* overexpression substantially improved motility and reduced toxicity of worms expressing polyQ40 and polyQ67 (Fig. 5a and Supplementary Fig. 21). In addition, loss of *rpn-6.1* had a detrimental effect on the motility phenotype of polyQ67 worms even at early (day 3) adulthood stages (Fig. 5b and Supplementary Fig. 22). Furthermore,

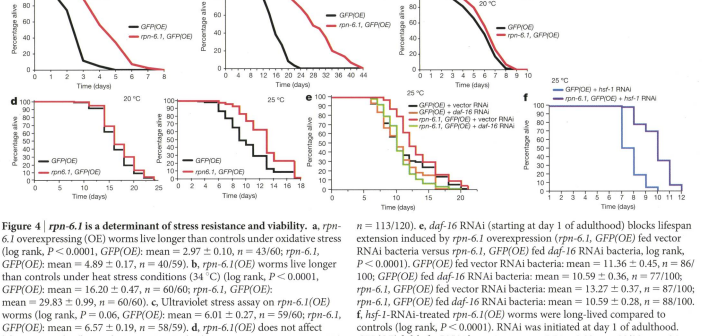

Figure 4 | *rpn-6.1* is a determinant of stress resistance and viability. **a**, *rpn-6.1* overexpressing (OE) worms live longer than controls under oxidative stress (log rank, $P < 0.0001$, *GFP(OE)*: mean = 2.97 ± 0.10, $n = 43/60$; *rpn-6.1, GFP(OE)*: mean = 4.89 ± 0.17, $n = 40/59$). **b**, *rpn-6.1(OE)* worms live longer than controls under heat stress conditions (34 °C) (log rank, $P < 0.0001$, *GFP(OE)*: mean = 16.20 ± 0.47, $n = 60/60$; *rpn-6.1, GFP(OE)*: mean = 29.83 ± 0.99, $n = 60/60$). **c**, Ultraviolet stress assay on *rpn-6.1(OE)* worms (log rank, $P = 0.06$, *GFP(OE)*: mean = 6.01 ± 0.27, $n = 59/60$; *rpn-6.1, GFP(OE)*: mean = 6.57 ± 0.19, $n = 58/59$). **d**, *rpn-6.1(OE)* does not affect lifespan at 20 °C (log rank, $P = 0.15$, *GFP(OE)*: mean = 16.33 ± 0.34, $n = 90/100$; *rpn-6.1, GFP(OE)*: mean = 17.05 ± 0.34, $n = 95/100$). *rpn-6.1* overexpression extends lifespan at 25 °C (log rank, $P < 0.0001$, *GFP(OE)*: mean = 10.19 ± 0.32, $n = 109/120$; *rpn-6.1, GFP(OE)*: mean = 12.73 ± 0.29, $n = 113/120$). **e**, *daf-16* RNAi (starting at day 1 of adulthood) blocks lifespan extension induced by *rpn-6.1* overexpression (*rpn-6.1, GFP(OE)* fed vector RNAi bacteria versus *rpn-6.1, GFP(OE)* fed *daf-16* RNAi bacteria, log rank, $P < 0.0001$). *GFP(OE)* fed vector RNAi bacteria: mean = 11.36 ± 0.45, $n = 86/100$; *GFP(OE)* fed *daf-16* RNAi bacteria: mean = 10.59 ± 0.36, $n = 77/100$; *rpn-6.1, GFP(OE)* fed vector RNAi bacteria: mean = 13.27 ± 0.37, $n = 87/100$; *rpn-6.1, GFP(OE)* fed *daf-16* RNAi bacteria: mean = 10.59 ± 0.28, $n = 88/100$. **f**, *hsf-1*-RNAi-treated *rpn-6.1(OE)* worms were long-lived compared to controls (log rank, $P < 0.0001$). RNAi was initiated at day 1 of adulthood. *GFP(OE)* fed *hsf-1* RNAi bacteria: mean = 7.74 ± 0.09, $n = 93/99$; *rpn-6.1, GFP(OE)* fed *hsf-1* RNAi bacteria: mean = 9.92 ± 0.13, $n = 94/100$. See Supplementary Table 5 for statistical analysis and replicate data of stress assays and lifespan experiments.

we observed by filter trap analysis that *rpn-6.1(OE)* reduced polyQ aggregate levels whereas polyQ67 total protein levels remained constant (Fig. 5c), suggesting that *rpn-6.1* specifically reduces aggregated, but not soluble, polyQ proteins.

Discussion

A growing body of evidence suggests that the protective modulation of various nodes of the proteostasis network, including the heat-shock response and autophagy, can contribute to the extended lifespan caused by the IIS[36,37], diet restriction[38] and germline-signalling pathways[39]. We report evidence for the requirement of an upregulated proteasome activity in the extended lifespan of germline-deficient nematodes. Our initial analysis of proteasome activity among different longevity models in the worm reveals that only *glp-1* mutant and diet-restricted animals share an increased proteasome activity, and we hypothesize that these animals may share a strategy in which resources are actively re-allocated from the germ line to the soma, resulting in an enhanced protection of the proteome within somatic cells. Furthermore, we find distinct differences in the proteasome activity between *glp-1* and *daf-2* mutant animals that is mediated by DAF-16, and in part by KRI-1, DAF-12 and DAF-9, confirming previous genetic suggestions that DAF-16 activity is differentially regulated between *glp-1* and *daf-2* mutants. Mechanistically, in germline-deficient animals, *rpn-6.1* and subsequent increases in proteasome activity seem to be direct downstream targets of DAF-16/FOXO. Our results thus provide new insights into proteostasis regulation and provide a link between the longevity regulator DAF-16 and proteasome activity regulation upon *rpn-6.1* expression.

We further define RPN-6 as a potent factor to increase resistance to proteotoxic stress, as its upregulation can delay the deleterious effects of strong adverse conditions. It is intriguing to speculate that one method to ensure survival of the soma may be the direct activation of FOXO/*daf-16*, under limited nutrient availability or loss of the germ line, resulting in increased *rpn-6.1* levels and increased proteome maintenance. Recently, it has been reported that changes in the proteasome may explain why ageing is a risk factor for neurodegenerative diseases such

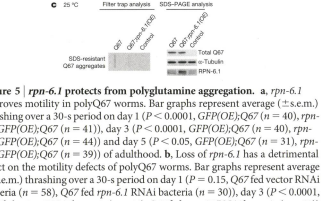

Figure 5 | *rpn-6.1* protects from polyglutamine aggregation. **a**, *rpn-6.1* improves motility in polyQ67 worms. Bar graphs represent average (±s.e.m.) thrashing over a 30-s period on day 1 ($P < 0.0001$, *GFP(OE);Q67* ($n = 40$), *rpn-6.1,GFP(OE);Q67* ($n = 41$)), day 3 ($P < 0.0001$, *GFP(OE);Q67* ($n = 40$), *rpn-6.1,GFP(OE);Q67* ($n = 44$)) and day 5 ($P < 0.05$, *GFP(OE);Q67* ($n = 31$), *rpn-6.1,GFP(OE);Q67* ($n = 39$)) of adulthood. **b**, Loss of *rpn-6.1* has a detrimental effect on the motility defects of polyQ67 worms. Bar graphs represent average (±s.e.m.) thrashing over a 30-s period on day 1 ($P = 0.15$, Q67 fed vector RNAi bacteria ($n = 58$), Q67 fed *rpn-6.1* RNAi bacteria ($n = 30$)), day 3 ($P < 0.0001$, Q67 fed vector RNAi bacteria ($n = 44$), Q67 fed *rpn-6.1* RNAi bacteria ($n = 51$)) and day 5 ($P < 0.0001$, Q67 fed vector RNAi bacteria ($n = 41$), Q67 fed *rpn-6.1* RNAi bacteria ($n = 47$)) of adulthood. All statistical comparisons were made by Student's *t*-test for unpaired samples. **c**, Filter trap analysis indicates that *rpn-6.1* overexpression results in reduced polyQ aggregates (detected by anti-GFP antibody). Right panel: SDS–PAGE analysis with antibodies to GFP, RPN-6 and α-tubulin loading control. *$P < 0.05$; **$P < 0.0001$.

as Alzheimer's, Parkinson's and Huntington's disease[40]. Therefore, RPN-6 may be a powerful candidate to correct deficiencies in disorders associated with a failure in protein homeostasis. It will be of crucial interest to explore in mammalian models whether RPN-6 could indeed alleviate the associated symptoms of these disorders.

METHODS SUMMARY

Caenorhabditis elegans were cultured using standard techniques[41] and fed on *Escherichia coli* OP50 or HT115 containing a double-stranded-RNA-expressing plasmid[42].

26S proteasome activity assays. *In vitro* 26S proteasome activity assays were performed as previously described[27]. Worms were lysed in proteasome activity assay buffer (50 mM Tris-HCl, pH 7.5, 250 mM sucrose, 5 mM $MgCl_2$, 0.5 mM EDTA, 2 mM ATP and 1 mM dithiothreitol) using a Precellys 24 homogenizer (Bertin technologies). Lysate was centrifuged at 10,000*g* for 15 min at 4 °C. A total of 25 μg of total protein lysate was transferred to a 96-well microtitre plate (BD Falcon) and incubated with fluorogenic substrate. Fluorescence (380-nm excitation, 460-nm emission) was monitored on a microplate fluorometer (Infinite M1000, Tecan) every 5 min for 1 h at 25 °C.

Motility assay. Thrashing rate was determined as previously described[35]. Worms were transferred to a drop of M9 buffer and after 30 s of adaptation the number of body bends was counted for 30 s. A body bend was defined as a change in direction of the bend at the midbody of a nematode[43].

Filter trap. Worm extracts were generated by glass bead disruption on ice in non-denaturing lysis buffer (50 mM HEPES, pH 7.4, 150 mM NaCl, 1 mM EDTA, 0.5% Triton X-100) supplemented with EDTA-free protease inhibitor cocktail (Roche). Lysate was centrifuged at 5,000*g* for 5 min. A total of 70 μg of protein extract was supplemented with SDS at a final concentration of 1% and loaded onto a cellulose acetate membrane assembled in a slot blot apparatus (BioRad). The membrane was washed with 0.1% SDS and retained Q67-GFP was assessed by immunoblotting for GFP (Roche).

A detailed description of all experimental methods including *C. elegans* strains, growth, imaging, lifespan analysis, stress assays and RNAi application is provided in Methods.

Full Methods and any associated references are available in the online version of the paper.

Received 8 August 2011; accepted 13 June 2012.
Published online 26 August 2012.

1. Kirkwood, T. B. Evolution of ageing. *Nature* **270,** 301–304 (1977).
2. Kenyon, C. A pathway that links reproductive status to lifespan in *Caenorhabditis elegans*. *Ann. NY Acad. Sci.* **1204,** 156–162 (2010).
3. Partridge, L., Gems, D. & Withers, D. J. Sex and death: what is the connection? *Cell* **120,** 461–472 (2005).
4. Shanley, D. P. & Kirkwood, T. B. Calorie restriction and aging: a life-history analysis. *Evolution* **54,** 740–750 (2000).
5. Arantes-Oliveira, N., Apfeld, J., Dillin, A. & Kenyon, C. Regulation of life-span by germ-line stem cells in *Caenorhabditis elegans*. *Science* **295,** 502–505 (2002).
6. Hsin, H. & Kenyon, C. Signals from the reproductive system regulate the lifespan of *C. elegans*. *Nature* **399,** 362–366 (1999).
7. Wang, M. C., O'Rourke, E. J. & Ruvkun, G. Fat metabolism links germline stem cells and longevity in *C. elegans*. *Science* **322,** 957–960 (2008).
8. Lin, K., Hsin, H., Libina, N. & Kenyon, C. Regulation of the *Caenorhabditis elegans* longevity protein DAF-16 by insulin/IGF-1 and germline signaling. *Nature Genet.* **28,** 139–145 (2001).
9. Berman, J. R. & Kenyon, C. Germ-cell loss extends *C. elegans* life span through regulation of DAF-16 by *kri-1* and lipophilic-hormone signaling. *Cell* **124,** 1055–1068 (2006).
10. Gerisch, B., Weitzel, C., Kober-Eisermann, C., Rottiers, V. & Antebi, A. A hormonal signaling pathway influencing *C. elegans* metabolism, reproductive development, and life span. *Dev. Cell* **1,** 841–851 (2001).
11. Bence, N. F., Sampat, R. M. & Kopito, R. R. Impairment of the ubiquitin-proteasome system by protein aggregation. *Science* **292,** 1552–1555 (2001).
12. Bennett, E. J., Bence, N. F., Jayakumar, R. & Kopito, R. R. Global impairment of the ubiquitin-proteasome system by nuclear or cytoplasmic protein aggregates precedes inclusion body formation. *Mol. Cell* **17,** 351–365 (2005).
13. Powers, E. T., Morimoto, R. I., Dillin, A., Kelly, J. W. & Balch, W. E. Biological and chemical approaches to diseases of proteostasis deficiency. *Annu. Rev. Biochem.* **78,** 959–991 (2009).
14. Lakowski, B. & Hekimi, S. The genetics of caloric restriction in *Caenorhabditis elegans*. *Proc. Natl Acad. Sci. USA* **95,** 13091–13096 (1998).
15. Dillin, A. *et al.* Rates of behavior and aging specified by mitochondrial function during development. *Science* **298,** 2398–2401 (2002).
16. Hamer, G., Matilainen, O. & Holmberg, C. I. A photoconvertible reporter of the ubiquitin-proteasome system *in vivo*. *Nature Methods* **7,** 473–478 (2010).
17. Mitchell, D. H., Stiles, J. W., Santelli, J. & Sanadi, D. R. Synchronous growth and aging of *Caenorhabditis elegans* in the presence of fluorodeoxyuridine. *J. Gerontol.* **34,** 28–36 (1979).
18. Priess, J. R., Schnabel, H. & Schnabel, R. The *glp-1* locus and cellular interactions in early *C. elegans* embryos. *Cell* **51,** 601–611 (1987).
19. Dillin, A., Crawford, D. K. & Kenyon, C. Timing requirements for insulin/IGF-1 signaling in *C. elegans*. *Science* **298,** 830–834 (2002).
20. Hansen, M., Hsu, A. L., Dillin, A. & Kenyon, C. New genes tied to endocrine, metabolic, and dietary regulation of lifespan from a *Caenorhabditis elegans* genomic RNAi screen. *PLoS Genet.* **1,** e17 (2005).
21. Cohen, E., Bieschke, J., Perciavalle, R. M., Kelly, J. W. & Dillin, A. Opposing activities protect against age-onset proteotoxicity. *Science* **313,** 1604–1610 (2006).
22. Hsu, A. L., Murphy, C. T. & Kenyon, C. Regulation of aging and age-related disease by DAF-16 and heat-shock factor. *Science* **300,** 1142–1145 (2003).
23. Alam, J. *et al.* Nrf2, a Cap'n'Collar transcription factor, regulates induction of the heme oxygenase-1 gene. *J. Biol. Chem.* **274,** 26071–26078 (1999).
24. An, J. H. & Blackwell, T. K. SKN-1 links *C. elegans* mesendodermal specification to a conserved oxidative stress response. *Genes Dev.* **17,** 1882–1893 (2003).
25. Goudeau, J. *et al.* Fatty acid desaturation links germ cell loss to longevity through NHR-80/HNF4 in *C. elegans*. *PLoS Biol.* **9,** e1000599 (2011).
26. Finley, D. Recognition and processing of ubiquitin-protein conjugates by the proteasome. *Annu. Rev. Biochem.* **78,** 477–513 (2009).
27. Kisselev, A. F. & Goldberg, A. L. Monitoring activity and inhibition of 26S proteasomes with fluorogenic peptide substrates. *Methods Enzymol.* **398,** 364–378 (2005).
28. Köhler, A. *et al.* The axial channel of the proteasome core particle is gated by the Rpt2 ATPase and controls both substrate entry and product release. *Mol. Cell* **7,** 1143–1152 (2001).
29. Pathare, G. R. *et al.* The proteasomal subunit Rpn6 is a molecular clamp holding the core and regulatory subcomplexes together. *Proc. Natl Acad. Sci. USA* **109,** 149–154 (2012).
30. Santamaria, P. G., Finley, D., Ballesta, J. P. & Remacha, M. Rpn6p, a proteasome subunit from *Saccharomyces cerevisiae*, is essential for the assembly and activity of the 26 S proteasome. *J. Biol. Chem.* **278,** 6687–6695 (2003).
31. Furuyama, T., Nakazawa, T., Nakano, I. & Mori, N. Identification of the differential distribution patterns of mRNAs and consensus binding sequences for mouse DAF-16 homologues. *Biochem. J.* **349,** 629–634 (2000).
32. Celniker, S. E. *et al.* Unlocking the secrets of the genome. *Nature* **459,** 927–930 (2009).
33. Ghazi, A., Henis-Korenblit, S. & Kenyon, C. Regulation of *Caenorhabditis elegans* lifespan by a proteasomal E3 ligase complex. *Proc. Natl Acad. Sci. USA* **104,** 5947–5952 (2007).
34. Li, X. J. & Li, S. Proteasomal dysfunction in aging and Huntington disease. *Neurobiol. Dis.* **43,** 4–8 (2011).
35. Brignull, H. R., Moore, F. E., Tang, S. J. & Morimoto, R. I. Polyglutamine proteins at the pathogenic threshold display neuron-specific aggregation in a pan-neuronal *Caenorhabditis elegans* model. *J. Neurosci.* **26,** 7597–7606 (2006).
36. Melendez, A. *et al.* Autophagy genes are essential for dauer development and life-span extension in *C. elegans*. *Science* **301,** 1387–1391 (2003).
37. Morley, J. F. & Morimoto, R. I. Regulation of longevity in *Caenorhabditis elegans* by heat shock factor and molecular chaperones. *Mol. Biol. Cell* **15,** 657–664 (2004).
38. Hansen, M. *et al.* A role for autophagy in the extension of lifespan by dietary restriction in *C. elegans*. *PLoS Genet.* **4,** e24 (2008).
39. Lapierre, L. R., Melendez, A. & Hansen, M. Autophagy links lipid metabolism to longevity in *C. elegans*. *Autophagy* **8,** 144–146 (2012).
40. Zabel, C. *et al.* Proteasome and oxidative phosphorylation changes may explain why aging is a risk factor for neurodegenerative disorders. *J. Proteomics* **73,** 2230–2238 (2010).
41. Brenner, S. The genetics of *Caenorhabditis elegans*. *Genetics* **77,** 71–94 (1974).
42. Fire, A. *et al.* Potent and specific genetic interference by double-stranded RNA in *Caenorhabditis elegans*. *Nature* **391,** 806–811 (1998).
43. Chai, Y., Shao, J., Miller, V. M., Williams, A. & Paulson, H. L. Live-cell imaging reveals divergent intracellular dynamics of polyglutamine disease proteins and supports a sequestration model of pathogenesis. *Proc. Natl Acad. Sci. USA* **99,** 9310–9315 (2002).

Supplementary Information is linked to the online version of the paper at www.nature.com/nature.

Acknowledgements We thank S. Panowski for help with the generation of transgenic strains. We thank D. Joyce for proteasome activity assays and S. Wolff for comments on the manuscript. This work was supported by HHMI and the NIA. D.V. was a recipient of the F.M. Kirby, Inc. Foundation Postdoctoral Scholar Award and Beatriu de Pinós (AGAUR) fellowship.

Author Contributions D.V. and A.D. planned and supervised the project. D.V. performed the experiments, data analysis and interpretation. I.M. performed biochemistry experiments and contributed to other assays. Z.L. performed UPS reporter experiment, lifespans and injections. P.M.D. performed the filter trap assay. C.M. performed immunoblots. A.P.C.R. and G.M. performed the transcription factor binding site analysis. The manuscript was written by D.V. and A.D. and edited by I.M. and C.M. All authors discussed the results and commented on the manuscript.

Author Information Reprints and permissions information is available at www.nature.com/reprints. The authors declare no competing financial interests. Readers are welcome to comment on the online version of this article at www.nature.com/nature. Correspondence and requests for materials should be addressed to A.D. (dillin@salk.edu).

LETTER

doi:10.1038/nature11472

Quantum teleportation over 143 kilometres using active feed-forward

Xiao-Song Ma[1,2]†, Thomas Herbst[1,2], Thomas Scheidl[1], Daqing Wang[1], Sebastian Kropatschek[1], William Naylor[1], Bernhard Wittmann[1,2], Alexandra Mech[1,2], Johannes Kofler[1,3], Elena Anisimova[4], Vadim Makarov[4], Thomas Jennewein[1,4], Rupert Ursin[1] & Anton Zeilinger[1,2]

The quantum internet[1] is predicted to be the next-generation information processing platform, promising secure communication[2,3] and an exponential speed-up in distributed computation[2,4]. The distribution of single qubits over large distances via quantum teleportation[5] is a key ingredient for realizing such a global platform. By using quantum teleportation, unknown quantum states can be transferred over arbitrary distances to a party whose location is unknown. Since the first experimental demonstrations of quantum teleportation of independent external qubits[6], an internal qubit[7] and squeezed states[8], researchers have progressively extended the communication distance. Usually this occurs without active feed-forward of the classical Bell-state measurement result, which is an essential ingredient in future applications such as communication between quantum computers. The benchmark for a global quantum internet is quantum teleportation of independent qubits over a free-space link whose attenuation corresponds to the path between a satellite and a ground station. Here we report such an experiment, using active feed-forward in real time. The experiment uses two free-space optical links, quantum and classical, over 143 kilometres between the two Canary Islands of La Palma and Tenerife. To achieve this, we combine advanced techniques involving a frequency-uncorrelated polarization-entangled photon pair source, ultra-low-noise single-photon detectors and entanglement-assisted clock synchronization. The average teleported state fidelity is well beyond the classical limit[9] of two-thirds. Furthermore, we confirm the quality of the quantum teleportation procedure without feed-forward by complete quantum process tomography. Our experiment verifies the maturity and applicability of such technologies in real-world scenarios, in particular for future satellite-based quantum teleportation.

Significant progress has been made recently in the field of quantum communication based on optical free-space links[10–19], which potentially allow much larger propagation distances compared to the existing fibre networks because of the lower photon loss per kilometre. To enable quantum communication on a global scale and among parties not having access to any fibre network, it is foreseeable that experiments will involve ground-to-satellite[10,11,15] and inter-satellite links.

Previous experiments focused on the distribution of quantum states of single photons or entangled photon pairs over optical free-space links. However, the realization of more sophisticated multiphoton quantum information protocols, such as quantum teleportation, remained an experimental challenge under real-world conditions. Quantum teleportation is based on the simultaneous creation of at least three photons, which for random photon pair sources reduces the count rate by several orders of magnitude compared to experiments using only two photons[16,19]. This decreases the signal-to-noise ratio and requires a long integration time, such that high system stability is necessary. Moreover, the complexity and environmental requirements of a quantum teleportation set-up are increased significantly compared to previous two-photon experiments, which provides significant experimental and technological challenges. The work presented in ref. 18 was a significant achievement in long-distance quantum communication, harnessing the entanglement between different degrees of freedom of a single photon. However, because the teleported qubit was not provided independently from the outside, the applicability of that scheme is limited. Most earlier experiments on teleportation of qubits and squeezed states[6–8] were in-laboratory demonstrations, and hence the communication distances were rather short. Although fibre-based teleportation has been demonstrated experimentally[20,21], the maximum transmission distance is limited by the intrinsic photon loss in optical fibre, unless quantum repeaters are involved[22]. In comparison to these previous studies, the experiment presented in this Letter achieves long-distance free-space teleportation of an independent quantum state, thus paving the way for satellite-based global quantum communication.

Quantum teleportation relies on using both a quantum channel and a classical channel between two parties, usually called Alice and Bob[5] (here located in La Palma and Tenerife respectively; Fig. 1a). The quantum channel is used by Alice and Bob to share the entangled auxiliary state[23]

$$|\Psi^-\rangle_{23}=\frac{1}{\sqrt{2}}\left(|H\rangle_2|V\rangle_3-|V\rangle_2|H\rangle_3\right) \quad (1)$$

which is one of the four maximally entangled Bell states ($|\Psi^\pm\rangle=\frac{1}{\sqrt{2}}(|H\rangle|V\rangle\pm|V\rangle|H\rangle)$ and $|\Phi^\pm\rangle=\frac{1}{\sqrt{2}}(|H\rangle|H\rangle\pm|V\rangle|V\rangle)$). $|H\rangle$ and $|V\rangle$ denote the horizontal and vertical polarization states. Alice and Bob share this entangled state, where photon 2 is with Alice and photon 3 is with Bob. Charlie provides the input photon 1 to be teleported to Alice in a general polarization state

$$|\phi\rangle_1=\alpha|H\rangle_1+\beta|V\rangle_1 \quad (2)$$

where α and β are complex numbers ($|\alpha|^2+|\beta|^2=1$), unknown to both Alice and Bob.

Alice then performs a Bell-state measurement (BSM), projecting photons 1 and 2 randomly onto one of the four Bell states each with the same probability of 25%. As a consequence, photon 3 is projected onto the input state $|\phi\rangle$, up to a unitary transformation (**U**), which depends on the outcome of the BSM. When Alice feeds the outcome of the BSM forward to Bob via the classical channel, he can implement the corresponding unitary operation in real time and thus obtain photon 3 in the initial state (equation (2)) of photon 1. If $|\Psi^-\rangle_{12}$ is detected, then **U** corresponds to the identity operation, which means that Bob needs to do nothing. If, on the other hand, $|\Psi^+\rangle_{12}$ is detected, Bob has to apply a π phase shift between the horizontal and the vertical component of his photon 3.

[1]Institute for Quantum Optics and Quantum Information (IQOQI), Austrian Academy of Sciences, Boltzmanngasse 3, A-1090 Vienna, Austria. [2]Vienna Center for Quantum Science and Technology, Faculty of Physics, University of Vienna, Boltzmanngasse 5, A-1090 Vienna, Austria. [3]Max Planck Institute of Quantum Optics, Hans-Kopfermann-Straße 1, 85748 Garching/Munich, Germany. [4]Institute for Quantum Computing and Department of Physics and Astronomy, University of Waterloo, 200 University Avenue West, Waterloo, Ontario N2L 3G1, Canada. †Present address: Department of Electrical Engineering, Yale University, New Haven, Connecticut 06520, USA.

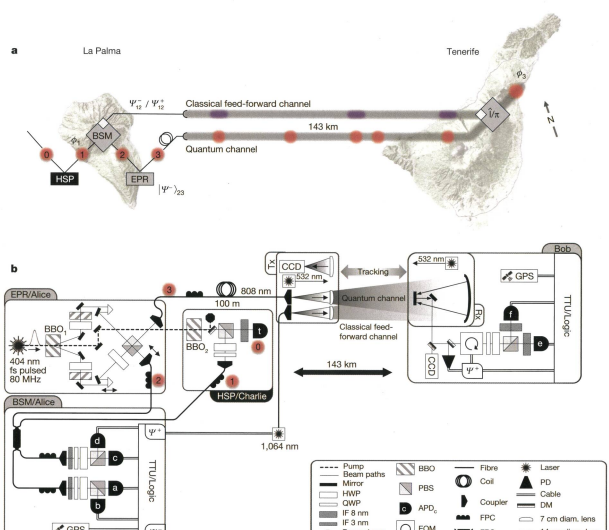

Figure 1 | Quantum teleportation between the Canary Islands La Palma and Tenerife over both quantum and classical 143-km free-space channels. **a**, Experimental scheme. Alice and Charlie are situated in La Palma, and Bob in Tenerife. Charlie prepares the teleportation input photon 1 in $|\phi\rangle_1$, using a heralded single-photon (HSP) source with a trigger photon 0 (photons are indicated by black numerals on red circles). An Einstein–Podolsky–Rosen (EPR)[23] source generates an entangled pair of photons 2 and 3 in the state $|\Psi^-\rangle_{23}$. Alice then performs a Bell-state measurement (BSM) on photons 1 and 2, and projects them onto two of the four Bell states ($|\Psi^-\rangle_{12}$/$|\Psi^+\rangle_{12}$), and sends the result via the classical feed-forward channel to Bob. Photon 3 is sent via the free-space quantum channel to Bob, who applies a unitary transformation (identity operation or π phase shift) on photon 3 depending on the BSM result and thus turns its state $|\phi\rangle_3$ into a replica of the initial quantum state $|\phi\rangle_1$. **b**, Set-up. In La Palma, a frequency-uncorrelated polarization-entangled photon pair source generated photons 2 and 3 in BBO_1 (EPR/Alice) and a collinear photon pair source generated photons 0 and 1 in BBO_2 (HSP/Charlie). All single photons were coupled into single-mode fibres. For implementing the BSM, photons 1 and 2 interfered in a fibre beam splitter (FBS) followed by polarization-resolving single-photon detection (BSM/Alice). Photon 3 was guided to the transmitter telescope via a 100-m single-mode fibre and sent to Bob in Tenerife, where the unitary transformation was implemented using an electro-optical modulator (EOM) and photon 3's polarization was measured. A real-time feed-forward operation was implemented by encoding the $|\Psi^-\rangle_{12}$ BSM result in 1,064-nm laser pulses, which were then sent to Bob via the feed-forward channel. On Bob's side, they were separated by a dichroic mirror (DM), detected with a photodetector (PD) and used to trigger the EOM to perform the required π phase shift operation. See main text for details.

Our experiment was conducted between Alice's transmitter station (at the Jacobus Kapteyn Telescope (JKT) of the Isaac Newton Group on La Palma) and Bob's receiver station (at the Optical Ground Station (OGS) of the European Space Agency on Tenerife), separated by 143 km, both at altitudes of about 2,400 m. Our experimental set-up is shown in Fig. 1b. At La Palma, near-infrared femtosecond pulses (with a central wavelength of 808 nm) emitted from a mode-locked Ti:sapphire laser, with a repetition rate of 80 MHz, were up-converted to blue pulses (with a central wavelength of 404 nm). They were used to generate two photon pairs via type-II spontaneous parametric down conversion (SPDC) in two nonlinear β-barium borate (BBO) crystals placed in sequence. The first SPDC source was aligned to emit the entangled auxiliary photon pairs (photons 2 and 3) in the $|\Psi^-\rangle_{23}$ state[24], equation (1), while the second crystal was a heralded single-photon (HSP) source providing Charlie's photon 1 to be teleported. That source delivered pairs of horizontally (photon 0) and vertically (photon 1) polarized photons in a product state. The detection of photon 0 by the avalanche photodiode (APD) t served as a trigger to herald the presence of photon 1. All photons were spectrally filtered using interference filters (IF) and coupled into single-mode fibres for spectral and spatial mode selection.

To realize the BSM, Alice's photon 2 was overlapped on a fibre beam splitter (FBS) with the teleportation input photon 1, whose polarization was arbitrarily prepared by Charlie using half- and quarter-wave plates (HWP and QWP). In each output port of the FBS, a polarizing beam splitter (PBS) was used to project these photons on either horizontal or vertical polarization. Fibre polarization controllers (FPCs) were used to compensate for unwanted polarization rotation induced

by the fibres. Our BSM can identify two out of the four Bell states, which is the optimum achievable with linear optics only[25]. For more details on our BSM, see Supplementary Information. While the BSM was being performed at Alice, photon 3 was guided to a 7-cm-aperture transmitter telescope through a 100-m-long single-mode fibre and then sent via a 143-km free-space quantum channel over to Bob in Tenerife. There, it was collected by the 1-m-aperture OGS telescope, and guided through its Coudé path to Bob.

In the first stage of our experiment, we only considered the cases where Alice detected $|\Psi^-\rangle_{12}$ in the BSM, which results in photon 3 being already in the state of the input photon, $|\phi\rangle_1$, and hence Bob was required to perform an identity operation, that is, to do nothing at all. We verified the success of the teleportation process by analysing the polarization state of photon 3, which was accomplished by a polarization analyser, consisting of a quarter- and a half-wave plate and two free-space coupled Si-APDs (silicon avalanche photodiodes) placed in each output mode of a polarizing beam splitter.

In the second stage of our experiment, we implemented a real-time feed-forward operation. When Alice obtained $|\Psi^+\rangle_{12}$, she sent this classical information to Bob. On receiving this information, Bob had to apply a π phase shift between the $|H\rangle$ and $|V\rangle$ components of photon 3 to obtain the replica of the input state $|\phi\rangle_1$. For further details on the feed-forward implementation, see Supplementary Information.

The relevant events on Alice's and Bob's sides were recorded with separate time-tagging units each disciplined to the global positioning system (GPS)[14]. First, Alice in La Palma identified the threefold coincidence events corresponding to the $|\Psi^-\rangle_{12}$ outcomes of the BSM. This was done using a coincidence logic circuit featuring two separate output signals realized with transistor-transistor logic (TTL) pulses. These TTL pulses were fed into a time-tagging unit which recorded the exact time and the BSM result into a binary file. Similarly, Bob fed either the signals of both detectors (stage 1, without feed-forward) or the coincidence between these signals and the BSM results sent via 1,064-nm laser pulses (stage 2, with feed-forward) into his time-tagging unit. After a measurement run was completed, both time-tagged data files were compared by cross-correlation, and the detection events associated with simultaneous detection of four photons originating from the same pump pulse were identified.

The real-life long-distance environment provided a number of challenges for the present teleportation experiment. These challenges resulted most significantly in the need to cope with an extremely low signal-to-noise ratio when using standard techniques—indeed, too low to perform a successful experiment. To enhance the signal-to-noise ratio to a level that made the experiment possible, we used the following advanced techniques: a frequency-uncorrelated polarization-entangled photon pair source[26–28], ultra-low-noise large-active-area single-photon detectors at Bob[29], and entanglement-assisted clock synchronization[13,14,17]. Whereas all these techniques have been implemented individually, our work is (to our knowledge) the first that combines all of them simultaneously and moreover in an outdoor environment. See Supplementary Information for details.

First we present our results without feed-forward, where we only considered the BSM outcome $|\Psi^-\rangle_{12}$. The input state $|\phi\rangle_1$ was always approximately one of the four ideal input states $|\phi_{\text{ideal}}\rangle \in \{|H\rangle, |V\rangle, |P\rangle = (|H\rangle + |V\rangle)/\sqrt{2}, |L\rangle = (|H\rangle - i|V\rangle)/\sqrt{2}\}$. We performed tomographic measurements on three consecutive nights, thereby accumulating data over 6.5 h. Figure 2 shows the state tomography results of quantum teleportation. The measured density matrix ρ for each of these teleported states was reconstructed from the experimentally obtained data using the maximum-likelihood technique[30]. The fidelity of the teleported state is defined as the overlap of the ideal teleported state $|\phi_{\text{ideal}}\rangle$ with the measured density matrix: $f = \langle\phi_{\text{ideal}}|\rho|\phi_{\text{ideal}}\rangle$. For this set of states, the teleported state fidelities are measured to be $f = 0.890(42)$, 0.865(46), 0.845(27) and 0.852(37), yielding an average $\bar{f} = 0.863(38)$, where digits in parentheses represent 1σ uncertainties, for example, $\bar{f} = 0.863 \pm 0.038$. During these measurements the link attenuation varied from 28.1 dB to 39.0 dB, which was mainly caused by rapid temperature change and strong wind. Despite such high loss in the quantum free-space channel, the classical average fidelity limit[9] of 2/3 was clearly surpassed by our observed fidelities, as shown in Fig. 3. (Note that our random sampling of the input states over the mutually unbiased bases states leads to the same classical limit as sampling over the whole Bloch sphere. Also, it does not matter whether the sampling is done over all six mutually unbiased basis states or over three states with one state per basis.) Therefore, we have explicitly demonstrated quantum teleportation over the 143-km free-space channel.

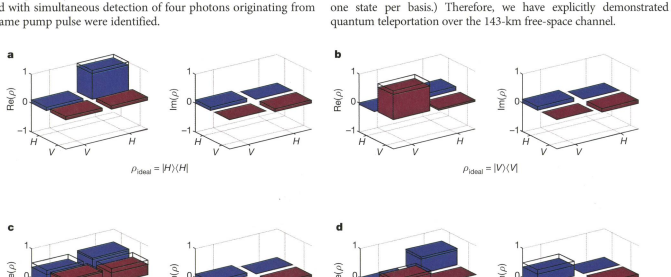

Figure 2 | State tomography results of the four quantum states without feed-forward over the 143-km free-space channel with the BSM outcome of $|\Psi^-\rangle_{12}$. The bar graphs show the reconstructed density matrices ρ for the four states teleported from Alice (La Palma) to Bob (Tenerife) over the 143-km free-space channel. The wire grid indicates the expected values for the ideal cases. The data shown comprise a total of 605 fourfold coincidence counts in about 6.5 h. The uncertainties in state fidelities extracted from these density matrices are calculated using a Monte Carlo routine assuming Poissonian errors.

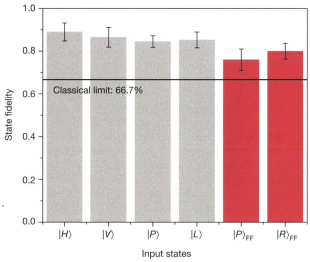

Figure 3 | Summary of the state fidelity results for the teleported quantum states with and without feed-forward. Grey bars show the results obtained in quantum teleportation without feed-forward. Bob was informed via an internet connection when Alice's BSM outcome was $|\Psi^-\rangle_{12}$, that is, those cases where he is not required to apply any operation to his photon. The uncertainties of these state fidelities are the same as presented in the main text. Red bars stand for the results obtained in quantum teleportation with feed-forward (FF). Bob was informed via the classical free-space link of Alice's BSM outcomes of $|\Psi^-\rangle_{12}$. The uncertainties of these state fidelities are derived from Poissonian statistics. All observed fidelities significantly exceed the classical average fidelity limit of 2/3 (66.7%). Error bars, $\pm 1\sigma$.

The reconstructed density matrices of the teleported quantum states allow us to fully characterize the teleportation procedure by quantum process tomography. The four input states ($\rho_{\mathrm{ideal}} = |\phi_{\mathrm{ideal}}\rangle\langle\phi_{\mathrm{ideal}}| = |H\rangle\langle H|, |V\rangle\langle V|, |P\rangle\langle P|, |L\rangle\langle L|$) are transferred to the corresponding (reconstructed) output states ρ. We can completely describe the effect of teleportation on the input states ρ_{ideal} by determining the process matrix χ, defined by $\rho = \sum_{j,k=0}^{3} \chi_{jk}\sigma_j\rho_{\mathrm{ideal}}\sigma_k$, where the σ_i are the Pauli matrices with σ_0 the identity operator. The process matrix χ can be computed analytically from these four equations for the four different input and output states[2]. The ideal process matrix of quantum teleportation χ_{ideal} has only one non-zero component, $(\chi_{\mathrm{ideal}})_{00} = 1$, meaning the input state is teleported without any reduction in quality. Figure 4a and b show respectively the real and imaginary components of χ for quantum teleportation based on our experimental results. The process fidelity of our experiment was $f_{\mathrm{process}} = \mathrm{Tr}(\chi_{\mathrm{ideal}}\chi) = 0.710(42)$. This clearly confirmed the quantum nature of our teleportation experiment as it is five standard deviations above the maximum process fidelity of 0.5, which is the limit one can reach with a classical strategy where Alice and Bob do not share any entanglement as a resource.

In the second stage of the experiment, we realized quantum teleportation including real-time feed-forward of the BSM result over the 143-km classical channel. We set $|P\rangle$ and $|R\rangle$ states ($|R\rangle = (|H\rangle + i|V\rangle)/\sqrt{2}$) as input states for which the required π phase shift between the $|H\rangle$ and the $|V\rangle$ components of photon 3 resulted in a 90° polarization rotation. However, for the $|H\rangle$ or $|V\rangle$ input state, feed-forward is irrelevant because a π phase shift would only result in a non-detectable global phase shift. Thus, the quality of teleportation of these states is already confirmed by our first-stage experiment. Realizing teleportation for the states $|P\rangle$ and $|R\rangle$ fully confirms the generality of the procedure, as these states belong to different mutually unbiased bases. In Tenerife, we analysed photon 3 in the eigenbasis of the input state, that is, the $|P\rangle/|M\rangle$ ($|R\rangle/|L\rangle$) basis when the input state was $|P\rangle$ ($|R\rangle$). Here $|M\rangle = (|H\rangle - |V\rangle)/\sqrt{2}$. The resultant fidelities of the teleported states are 0.760(50) and 0.800(37) for $|P\rangle$ and $|R\rangle$, respectively (red bars in Fig. 3). Both results are clearly above the classical fidelity bound. Note that in our experiment, the efficiency of the classical link was measured to be 21.3%, which was mainly due to amplitude fluctuations caused by atmospheric turbulence.

Using the real-time feed-forward operation, we unambiguously experimentally demonstrated quantum teleportation from La Palma to Tenerife over a 143-km free-space channel. We note that from a conceptual perspective, real-time feed-forward is part of the original teleportation proposal[5]. Ultimately, the advantage of long-distance teleportation compared to just sending the quantum state itself may lie in the following future applications: if Alice and Bob can stockpile their entangled states beforehand (with the help of quantum memories), teleportation is advantageous if the quantum channel is of low quality or if Bob's location is unknown to Alice. This is because Alice can broadcast the classical information with high quality and to arbitrary, or even unknown, locations[5]. (Also, the quantum repeater, which is of high importance for large-scale quantum networks, is based on teleportation in the form of entanglement swapping[31].) Specifically, this advantage also shows the usefulness of quantum teleportation even for quantum channels that allow only small transmission rates. We note that over the years teleportation sources have been markedly improved. We believe this development will continue and currently several new schemes are being pursued.

Our work proves the feasibility of both ground-based and satellite-based free-space quantum teleportation. Our quantum teleportation set-up was able to achieve coincidence production rates and fidelities sufficient to cope with the optical link attenuation resulting from various experimental and technical challenges; such challenges will arise in quantum transmission between a ground-based transmitter

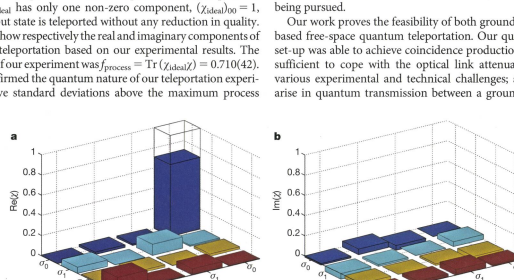

Figure 4 | Quantum process tomography of quantum teleportation without feed-forward. a, **b**, The real ($\mathrm{Re}(\chi_{lk})$; **a**) and imaginary ($\mathrm{Im}(\chi_{lk})$; **b**) values of the components of the reconstructed quantum process matrix, with $l, k = 0, 1, 2,$ and 3. The results of the state tomography of the four teleported states, $|H\rangle$, $|V\rangle$, $|P\rangle$, $|L\rangle$, are employed to reconstruct the process matrix of quantum state teleportation. The operators σ_i are the identity ($i = 0$) and the x-, y-, and z-Pauli matrices ($i = 1, 2, 3$). For the ideal case, the only non-zero component of the process matrix of quantum teleportation, χ_{ideal}, is $(\chi_{\mathrm{ideal}})_{00} = 1$, which is indicated by the wire grid. Our experiment clearly confirmed that χ_{00} (identity operation) is indeed the dominant component and surpasses the classical limit.

and a low-Earth-orbiting satellite receiver[32]. In fact, some of the demands of our experiment were even more challenging than in satellite communication since there the atmospheric distances to be overcome are certainly shorter than the distance between Tenerife and La Palma. In addition, acquiring, pointing and tracking (APT) for diffraction-limited transmitter and receiver telescopes in space is a well-established technology. Therefore, our experiment represents a crucial step towards future quantum networks in space, which require space-to-ground quantum communication. During the finalization of our manuscript, a related work was reported[33] that used a 150-Hz APT system, while our APT system operated at a few hertz, yet fast enough to fulfil the specific requirements of our experiment. The most significant distinction between ref. 33 and the experiment presented in this Letter is our implementation of an active feed-forward technique. The technology implemented in both experiments has certainly reached the required maturity for both satellite and long-distance ground communication. We expect that many of the features implemented here will be important building blocks for a new area of experiments.

Received 21 May; accepted 14 August 2012.
Published online 5 September 2012.

1. Kimble, H. J. The quantum internet. *Nature* **453,** 1023–1030 (2008).
2. Nielsen, M. & Chuang, I. *Quantum Computation and Quantum Information* (Cambridge Univ. Press, 2000).
3. Gisin, N. & Thew, R. Quantum communication. *Nature Photon.* **1,** 165–171 (2007).
4. Ladd, T. D. *et al.* Quantum computers. *Nature* **464,** 45–53 (2010).
5. Bennett, C. H. *et al.* Teleporting an unknown quantum state via dual classical and Einstein-Podolsky-Rosen channels. *Phys. Rev. Lett.* **70,** 1895–1899 (1993).
6. Bouwmeester, D. *et al.* Experimental quantum teleportation. *Nature* **390,** 575–579 (1997).
7. Boschi, D., Branca, S., De Martini, F., Hardy, L. & Popescu, S. Experimental realization of teleporting an unknown pure quantum state via dual classical and Einstein-Podolsky-Rosen channels. *Phys. Rev. Lett.* **80,** 1121–1125 (1998).
8. Furusawa, A. *et al.* Unconditional quantum teleportation. *Science* **282,** 706–709 (1998).
9. Massar, S. & Popescu, S. Optimal extraction of information from finite quantum ensembles. *Phys. Rev. Lett.* **74,** 1259–1263 (1995).
10. Hughes, R. J. *et al.* Free-space quantum key distribution in daylight. *J. Mod. Opt.* **47,** 549–562 (2000).
11. Rarity, J. G., Tapster, P. R., Gorman P. M. & Knight, P. Ground to satellite secure key exchange using quantum cryptography. *N. J. Phys.* **4,** 82 (2002).
12. Aspelmeyer, M. *et al.* Long-distance free-space distribution of quantum entanglement. *Science* **301,** 621–623 (2003).
13. Marcikic, I., Lamas-Linares, A. & Kurtsiefer, C. Free-space quantum key distribution with entangled photons. *Appl. Phys. Lett.* **89,** 101122 (2006).
14. Ursin, R. *et al.* Entanglement-based quantum communication over 144 km. *Nature Phys.* **3,** 481–486 (2007).
15. Villoresi, P. *et al.* Experimental verification of the feasibility of a quantum channel between space and Earth. *N. J. Phys.* **10,** 033038 (2008).
16. Fedrizzi, A. *et al.* High-fidelity transmission of entanglement over a high-loss free-space channel. *Nature Phys.* **5,** 389–392 (2009).
17. Scheidl, T. *et al.* Feasibility of 300 km quantum key distribution with entangled states. *N. J. Phys.* **11,** 085002 (2009).
18. Jin, X.-M. *et al.* Experimental free-space quantum teleportation. *Nature Photon.* **4,** 376–381 (2010).
19. Scheidl, T. *et al.* Violation of local realism with freedom of choice. *Proc. Natl Acad. Sci. USA* **107,** 19708–19713 (2010).
20. Marcikic, I., de Riedmatten, H., Tittel, W., Zbinden, H. & Gisin, N. Long-distance teleportation of qubits at telecommunication wavelengths. *Nature* **421,** 509–513 (2003).
21. Ursin, R. *et al.* Quantum teleportation across the Danube. *Nature* **430,** 849 (2004).
22. Briegel, H.-J., Dür, W., Cirac, J. I. & Zoller, P. Quantum repeaters: the role of imperfect local operations in quantum communication. *Phys. Rev. Lett.* **81,** 5932–5935 (1998).
23. Einstein, A., Podolsky, B. & Rosen, N. Can quantum-mechanical description of physical reality be considered complete? *Phys. Rev.* **47,** 777–780 (1935).
24. Kwiat, P. G. *et al.* New high-intensity source of polarization-entangled photon pairs. *Phys. Rev. Lett.* **75,** 4337–4341 (1995).
25. Calsamiglia, J. & Lütkenhaus, N. Maximum efficiency of a linear-optical Bell-state analyzer. *Appl. Phys. B* **72,** 67–71 (2001).
26. Kim, Y.-H., Kulik, S. P., Chekhova, M. V., Grice, W. P. & Shih, Y. Experimental entanglement concentration and universal Bell-state synthesizer. *Phys. Rev. A* **67,** 010301(R) (2003).
27. Poh, H. S., Lim, J., Marcikic, I., Lamas-Linares, A. & Kurtsiefer, C. Eliminating spectral distinguishability in ultrafast spontaneous parametric down-conversion. *Phys. Rev. A* **80,** 043815 (2009).
28. Yao, X.-C. *et al.* Observation of eight-photon entanglement. *Nature Photon.* **6,** 225–228 (2012).
29. Kim, Y.-S., Jeong, Y.-C., Sauge, S., Makarov, V. & Kim, Y.-H. Ultra-low noise single-photon detector based on Si avalanche photodiode. *Rev. Sci. Instrum.* **82,** 093110 (2011).
30. White, A. G., James, D. F. V., Eberhard, P. H. & Kwiat, P. G. Nonmaximally entangled states: production, characterization, and utilization. *Phys. Rev. Lett.* **83,** 3103–3107 (1999).
31. Żukowski, M., Zeilinger, A., Horne, M. A. & Ekert, A. K. "Event-ready-detectors" Bell experiment via entanglement swapping. *Phys. Rev. Lett.* **71,** 4287–4290 (1993).
32. Aspelmeyer, M., Jennewein, T., Pfennigbauer, M., Leeb, W. R. & Zeilinger, A. Long-distance quantum communication with entangled photons using satellites. *IEEE J. Sel. Top. Quantum Electron.* **9,** 1541–1551 (2003).
33. Yin, J. *et al.* Quantum teleportation and entanglement distribution over 100-kilometre free-space channels. *Nature* **488,** 185–188 (2012).

Supplementary Information is available in the online version of the paper.

Acknowledgements We thank the staff of IAC: F. Sanchez-Martinez, A. Alonso, C. Warden, M. Serra and J. Carlos; and the staff of ING: M. Balcells, C. Benn, J. Rey, O. Vaduvescu, A. Chopping, D. González, S. Rodríguez, M. Abreu, L. González; J. Kuusela, E. Wille and Z. Sodnik; and J. Perdigues of the OGS and ESA. X.-S.M., T.J., R.U. and A.Z. thank S. Ramelow for discussions, P. Kolenderski for discussions on the SPDC source with the Bell-state synthesizer, S. Zotter for help during the early stages of the experiment, and R. Steinacker for meteorological advice. J.K. was supported by the EU project MALICIA. E.A. and V.M. thank C. Kurtsiefer and Y.-S. Kim for detector electronics design. J. Skaar for support, and the Research Council of Norway (grant No. 180439/V30) and Industry Canada for support. This work was made possible by grants from the European Space Agency (contract 4000104180/11/NL/AF), the Austrian Science Foundation (FWF) under projects SFB F4008 and CoQuS, and the FFG for the QTS project (no. 823816) within the ASAP 7 program. We also acknowledge support by the European Commission, grant Q-ESSENCE (no. 248095) and the John Templeton Foundation.

Author Contributions X.-S.M. conceived the research, designed and carried out the experiment, and analysed data. T.H., T.S. and D.W. carried out the experiment and analysed data. S.K., W.N., B.W. and A.M. provided experimental assistance during the early stage of the experiment. J.K. provided the theoretical analysis and analysed data. E.A. and V.M. developed the ultra-low-noise detectors. T.J. provided experimental and conceptual assistance, and conceived and developed the coincidence analysis code. R.U. conceived the research, planned and carried out the experiment and analysed data. A.Z. defined the scientific goals, conceived the research, designed the experiment and supervised the project. X.-S.M., T.H., T.S., J.K., R.U. and A.Z. wrote the manuscript with assistance from all other co-authors.

Author Information Reprints and permissions information is available at www.nature.com/reprints. The authors declare no competing financial interests. Readers are welcome to comment on the online version of the paper. Correspondence and requests for materials should be addressed to X.-S.M. (Xiaosong.Ma@Univie.ac.at) or A.Z. (Anton.Zeilinger@Univie.ac.at).

LETTER

doi:10.1038/nature11418

Stabilization of Leidenfrost vapour layer by textured superhydrophobic surfaces

Ivan U. Vakarelski[1,2], Neelesh A. Patankar[3], Jeremy O. Marston[1], Derek Y. C. Chan[4,5] & Sigurdur T. Thoroddsen[1,2]

In 1756, Leidenfrost[1] observed that water drops skittered on a sufficiently hot skillet, owing to levitation by an evaporative vapour film. Such films are stable only when the hot surface is above a critical temperature, and are a central phenomenon in boiling[2]. In this so-called Leidenfrost regime, the low thermal conductivity of the vapour layer inhibits heat transfer between the hot surface and the liquid. When the temperature of the cooling surface drops below the critical temperature, the vapour film collapses and the system enters a nucleate-boiling regime, which can result in vapour explosions that are particularly detrimental in certain contexts, such as in nuclear power plants[3]. The presence of these vapour films can also reduce liquid–solid drag[4–6]. Here we show how vapour film collapse can be completely suppressed at textured superhydrophobic surfaces. At a smooth hydrophobic surface, the vapour film still collapses on cooling, albeit at a reduced critical temperature, and the system switches explosively to nucleate boiling. In contrast, at textured, superhydrophobic surfaces, the vapour layer gradually relaxes until the surface is completely cooled, without exhibiting a nucleate-boiling phase. This result demonstrates that topological texture on superhydrophobic materials is critical in stabilizing the vapour layer and thus in controlling—by heat transfer—the liquid–gas phase transition at hot surfaces. This concept can potentially be applied to control other phase transitions, such as ice or frost formation[7–9], and to the design of low-drag surfaces at which the vapour phase is stabilized in the grooves of textures without heating[10].

Heat transfer and boiling on a heated solid surface in contact with liquid are familiar phenomena observed in our daily lives, and occur in many industrial processes. As the vessel containing a liquid is progressively heated, the liquid will start to boil, with vapour bubbles forming at the hot surface. This is the nucleate-boiling regime. If the surface temperature is increased further, a continuous vapour film will form that leads to the film-boiling or Leidenfrost regime. It is known that surface properties such as roughness and wettability can alter the transition temperature from the nucleate-boiling to the film-boiling regime[11–16]. As the low thermal conductivity of the vapour layer dramatically reduces the efficiency of heat transfer, the traditional focus is to increase the temperature at which film boiling occurs[13]. However, if the vapour layer is to be used for drag reduction[4–6,17–20], lowering the temperature of film boiling is beneficial, as the presence of a Leidenfrost vapour layer can reduce the hydrodynamic drag force on a heated sphere moving in liquid by up to 85%[6].

Takata *et al.*[12] have reported that the initiation of nucleate boiling can be suppressed at what they termed "super-water-repellent" surfaces. Here we show that a textured superhydrophobic surface can eliminate the collapse of the vapour film, thus making it possible to maintain a stable vapour film at all temperatures above the boiling point of the liquid—that is, at all superheats. To this end, we investigated cooling and heating phenomena of heated surfaces that possess different degrees of hydrophobicity in water.

In our cooling experiments we use 20-mm-diameter stainless-steel spheres, and in our heating experiments 24-mm-diameter stainless-steel cylinders and stainless-steel vessels (capacity 60 ml). The stainless-steel surfaces are modified to have superhydrophilic, hydrophilic, hydrophobic or superhydrophobic wetting properties, as characterized by water-drop contact angle in air. Hydrophilic surfaces were produced by cleaning the steel surface with organic reagents, resulting in water contact angles of $<30^\circ$. Hydrophobic surfaces were produced by silanization with trichloro(1H,1H,2H,2H-perfluorooctyl)silane, giving contact angles of $\sim 100^\circ$. Superhydrophobic surfaces with water contact angles of $>160^\circ$ were produced by treatment with a commercial coating agent (Glaco Mirror Coat 'Zero', Soft 99 Co.) containing nanoparticles and organic reagent. Superhydrophilic surfaces, with contact angles of $<10^\circ$, were produced from the superhydrophobic surface by plasma cleaning to remove the organic coating, while retaining the same texture and geometric morphology (see Supplementary Information for details).

Figure 1a is an atomic-force micrograph of the superhydrophobic surface coating, showing its rough surface topography. The very high contact angle subtended by a superhydrophobic sphere at the air–water meniscus is shown in Fig. 1b. When the sphere is fully immersed in water, its surface has a silver, mirror-like sheen, caused by reflection from the thin air layer retained on the surface. This is a signature of the Cassie state[21–24], in which water is in physical contact only with the roughness peaks created by the coating (Fig. 1c). This type of air entrapment, called plastron, has been shown to reduce hydrodynamic drag on spheres moving in water[20], and is used by some aquatic insects to facilitate underwater breathing[25].

We study the cooling of superhydrophilic, hydrophilic, hydrophobic and superhydrophobic spheres that have been pre-heated in a temperature-controlled furnace and then immersed in a glass tank filled with water at 22 °C (Supplementary Fig. 4). The state of the water at the sphere surface during subsequent cooling is captured on high-speed video, and the sphere temperature is monitored by an inserted thermocouple-probe thermometer. The progress of the cooling events for the hydrophilic, hydrophobic and superhydrophobic spheres can be seen in Supplementary Movies 1, 2 and 3, respectively. The superhydrophilic and hydrophilic spheres were heated to a maximum temperature of 700 °C, but the maximum temperature to which the hydrophobic and superhydrophobic spheres could be raised was limited to ~ 400 °C by the thermal stability of the organic coating. For the superhydrophilic sphere, the maximum temperature was not high enough to initiate film boiling; when the sphere came into contact with the water, it cooled almost instantaneously, accompanied by a vigorous release of bubbles. For all other surfaces, the initial sphere temperatures were high enough to be in the film-boiling regime, in which a continuous vapour layer coated the spheres, with a single bubble dome formed on the top of the sphere by buoyancy effects. During the initial stage of cooling, the bubble dome would grow and

[1]Division of Physical Sciences and Engineering, King Abdullah University of Science and Technology (KAUST), Thuwal 23955-6900, Saudi Arabia. [2]Clean Combustion Research Center, King Abdullah University of Science and Technology (KAUST), Thuwal 23955-6900, Saudi Arabia. [3]Department of Mechanical Engineering, Northwestern University, 2145 Sheridan Road, B224, Evanston, Illinois 60208-3111, USA. [4]Department of Mathematics and Statistics, University of Melbourne, Parkville 3010, Victoria, Australia. [5]Faculty of Life and Social Sciences, Swinburne University of Technology, Hawthorn 3122, Victoria, Australia.

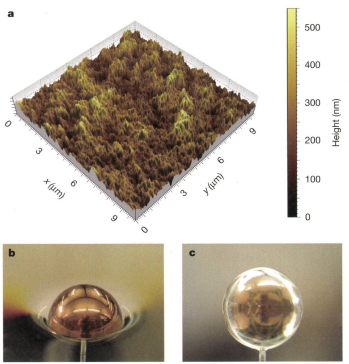

Figure 1 | Surface topography and images of the superhydrophobic sphere. **a**, Three-dimensional representation of an atomic-force micrograph of a 10-μm^2 region of the superhydrophobic surface coating. The combination of high surface roughness with an organic coating provides a high water contact angle, of >160°. **b**, Image of the superhydrophobic sphere held on the water surface, showing the high contact angle. **c**, Image of the superhydrophobic sphere immersed in water. The silver-mirror sheen of the immersed sphere is due to a thin air layer retained on the sphere surface, and is the signature appearance of a Cassie state of the water adjacent to the surface. See Supplementary Information for further details of the preparation and characterization of the superhydrophobic coating (Supplementary Figs 1, 2).

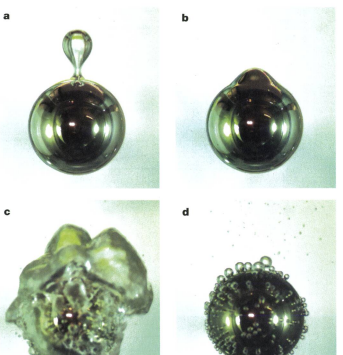

Figure 2 | High-speed camera snapshots of 20-mm steel spheres cooling in water. **a**, Bubble pinch-off from the vapour dome of a hot, superhydrophobic sphere cooling in the Leidenfrost regime. Water pool temperature is 100 °C; sphere temperature is T_s = 200 °C. **b**, Final state of the same superhydrophobic sphere, cooled to the pool temperature (T_s = 100 °C). **c**, **d**, Hydrophilic sphere cooling in water at 100 °C, at the moment of the explosive transition from film boiling to nucleate boiling (**c**, T_s = 275 °C) and during nucleate boiling (**d**, T_s = 200 °C). Sphere cooling events in water at 22 °C are shown in Supplementary Movies 1 (hydrophilic sphere), 2 (hydrophobic sphere) and 3 (superhydrophobic sphere). Supplementary Movie 4 shows hydrophilic and superhydrophobic spheres cooling in water at 100 °C.

pinch off periodically (Fig. 2a). On further cooling, the film-boiling mode on the hydrophilic sphere ended with collapse of the vapour layer, marked by an explosive release of bubbles (Fig. 2c). This was followed by a short phase of rapid cooling in the nucleate-boiling mode (Fig. 2d). Film boiling on the hydrophobic sphere also ended with an almost instantaneous collapse of the vapour layer. However, for the superhydrophobic sphere no vapour-layer collapse was observed. Instead, the vapour layer gradually relaxed over the entire sphere surface, and when cooling was complete a residual bubble dome remained on the sphere apex (Fig. 2b), and the sphere surface exhibited the silver sheen indicative of a final Cassie state of the liquid adjacent to the sphere surface (Supplementary Fig. 3).

Figure 3 shows the measured sphere temperature plotted against the immersion time. The superhydrophilic sphere (Fig. 3a) begins its cooling in the nucleate-boiling regime, and its temperature drops rapidly to the pool temperature. The cooling of the hydrophilic (Fig. 3a) and hydrophobic (Fig. 3b) spheres begins in the Leidenfrost film-boiling regime. In both cases, the vapour layer collapses at the Leidenfrost point, indicated by a sharp increase in cooling rate at ~420 °C for the hydrophilic sphere, and at ~210 °C for the hydrophobic sphere. However, for the superhydrophobic sphere, film boiling is maintained down to the pool temperature (22 °C) without vapour-layer collapse and transition to nucleate boiling (Fig. 3b).

Cooling experiments at elevated water pool temperatures of 80 and 100 °C confirmed the same trends as the room-temperature cooling experiments, with respect to the sphere hydrophobicity (Supplementary Fig. 5 and Supplementary Movie 4). In fact, as long as the water contact angle at room temperature exceeded 140°, achievable at textured superhydrophobic surfaces, no Leidenfrost transition was observed (Supplementary Figs 7, 8).

We performed heating experiments to further characterize surface properties at the boiling transition. A cartridge heater placed inside a stainless-steel cylinder (Fig. 4a and Supplementary Fig. 9) was immersed in a water-filled beaker sitting on a hot plate that heated the water to slow boiling, T_w = 100 °C. The surface temperature of the cylinder, T_s, was measured with an inserted thermocouple at constant heat flux, by controlling the applied power to the heater. We acquired high-speed video sequences along with the temperature measurements.

Figure 4d shows the measured variations of heat flux with surface temperature at steady state for the four types of surface wettability. As expected for the low values of heat flux used here, the heat exchange occurred in the nucleate-boiling regime (Fig. 4b and Supplementary Fig. 13) for the superhydrophilic and hydrophilic surfaces. However, as in the sphere-cooling experiments, the superhydrophobic surface was able to sustain a vapour layer in the Leidenfrost regime for all surface superheats. This is readily observed in both the appearance of the vapour layer and the magnitude of the increase in surface temperature with increasing heat flux (Fig. 4d).

When the temperature of the superhydrophobic cylinder was in equilibrium with the ambient water ($T_s = T_w$ = 100 °C), the cylinder's surface appeared smooth and shiny. With increasing heater power, the appearance of surface ripples[6] accompanied a gradual transition to the Leidenfrost regime (Fig. 4c, Supplementary Fig. 10 and Supplementary Movie 5). Additional experiments with the immersion heater (see Supplementary Fig. 11) showed that for the superhydrophobic surface there was no hysteresis between heating and cooling experiments.

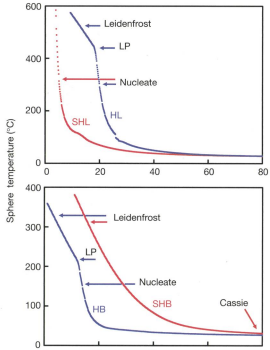

Figure 3 | Sphere temperature versus cooling time for 20-mm steel spheres held in water at 22 °C. a, Superhydrophilic sphere (contact angle <10°, SHL) and hydrophilic sphere (contact angle ~30°, HL). **b**, Hydrophobic sphere (contact angle ~100°, HB) and superhydrophobic surface sphere (contact angle >160°, SHB). Arrows indicate the Leidenfrost film-boiling regime, Leidenfrost-point transition (LP) and nucleate-boiling regime. The Leidenfrost transition in the superhydrophilic case occurs above the maximum temperature shown in the figure. In the superhydrophobic case, the Leidenfrost state relaxes to the Cassie state without passing through the nucleate-boiling regime.

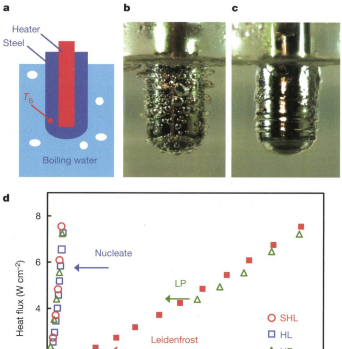

Figure 4 | Surface temperature versus heat flux in heating experiments. **a**, Schematics of the immersion heater. **b**, **c**, High-speed camera snapshots of the heater in boiling (100 °C) water for the case of (**b**) hydrophobic surface in the nucleate-boiling regime, at surface temperature $T_s = 106$ °C; and (**c**) superhydrophobic surface in the Leidenfrost regime, $T_s = 210$ °C. **d**, Dependence of the heat flux on the heater surface temperature for four types of surface in the nucleate-boiling and Leidenfrost film-boiling regimes. Abbreviations as in Fig. 3.

Keeping the surface immersed in water for up to 24 hours did not alter the smooth transition to the Leidenfrost regime (Supplementary Fig. 11). Although in such cases the surfaces appeared matte instead of shiny, suggesting that the vapour layer was not in a pure Cassie state, on heating, they returned smoothly to the Leidenfrost state (Supplementary Fig. 12). The same recovery property of superhydrophobic surfaces has been demonstrated recently using electrophoresis[26].

For the hydrophobic surface, it was possible to maintain the Leidenfrost vapour regime only if the cylinder was overheated before immersion to ~350 °C, and the heater power was maximized on immersion. When the surface temperature was allowed to fall below ~170 °C, the Leidenfrost vapour layer collapsed, and the switched to the nucleate-boiling branch (Fig. 4d).

Experiments with a stainless-steel cup placed on a hot plate showed the same behaviour as with the immersion heater (Supplementary Figs 14, 15). The good agreement among the cooling experiments and the two types of heating experiment confirm the geometry-independence and universality of the superhydrophobic surface effect in stabilizing the Leidenfrost vapour layer (compare Fig. 4d with Supplementary Figs 6 and 15).

By combining results for cooling experiments at constant initial heat content and high initial temperatures, and heating experiments at constant heating power but over a range of lower superheat temperatures, we have shown that the mode of heat transfer at the solid–liquid interface can be controlled by a combination of the surface morphology and surface chemistry of the solid surface. The observations for the hydrophilic and the hydrophobic surfaces are consistent with the standard transition between nucleate and film boiling[27]. The strong effect of the superhydrophilic surface in increasing the Leidenfrost temperature and enhancing boiling heat transfer has also been investigated recently[13]. However, we now show that for textured superhydrophobic surfaces the heat exchange always occurs in the presence of a Leidenfrost vapour layer, within the film-boiling regime. This behaviour has not been observed previously and represents a significant departure from the characteristic form of the classical boiling heat-transfer curve[10,28,29] of heat flux versus surface superheat temperature. The currently accepted form of the boiling curve comprises a critical heat-flux maximum and a Leidenfrost-point minimum that characterizes the transition between nucleate and film boiling. But at a textured superhydrophobic surface, the heat flux is a smoothly increasing function of superheat temperature, owing to the vapour layer that is always maintained at such surfaces (Supplementary Fig. 17).

The vapour layer on the superhydrophobic surface is sustained by the high surface roughness and porosity, coupled with the intrinsic, non-wetting hydrophobicity due to surface chemical treatment. These are the requisite conditions for the existence of a large non-wetting vapour layer (see Supplementary Information discussion on stabilization of vapour layers due to texture, and Supplementary Figs 18, 19). Furthermore, the three-dimensional nature of the surface roughness permits only small areas of direct contact between the peaks of the rough surface and the liquid interface. Contributions to the total heat transfer by such small areas are thus limited, and any onset of heterogeneous nucleation of bubbles will simply be taken up in the surface vapour layer that in effect will contribute to a smooth transition to the Leidenfrost regime. These conclusions are in complete accord with

what we found when repeating Leidenfrost's experiments[1] of drop evaporation at heated surfaces. For hydrophobic surfaces we observed the classical transition from nucleate to film-boiling mode, whereas at superhydrophobic surfaces nucleate boiling is absent at all superheats (Supplementary Fig. 16).

Although it has been demonstrated that the stability of the vapour layer in Leidenfrost drop experiments is sensitive to external perturbations such as vibrations, cooling rate and internal fluid circulation within the drops[31], and the hypothesis has been advanced that when the fluid drop contact angle at the surface attains the limiting value of 180°, the film-boiling regime might be possible at all superheat temperatures[32], this study has demonstrated that with the combination of surface roughness and chemical modifications Leidenfrost vapour layer stability and the film-boiling behaviour are readily achievable and remain robust under general operational conditions.

With the recent development of a wide variety of laboratory-designed and commercially available textured surface coatings with superhydrophobic[23,24], superamphiphobic[8,9], anti-frost[7] or switchable-hydrophobicity[20] properties, the effect on thermal exchange shown here opens possibilities for new applications of such coatings, ranging from the design of efficient heat-exchange devices to technologies for aqueous drag reduction.

METHODS SUMMARY

In cooling experiments we used 20-mm-diameter stainless-steel spheres (FRITSCH GmbH). In heating experiments we used an immersion heater or a 60-ml stainless-steel cup. The immersion heater is a 24-mm-diameter stainless-steel hollow cylinder with an electric heater cartridge fitted inside. All stainless-steel surfaces are modified as follows. Smooth hydrophilic surfaces are produced by cleaning with organic reagents. Smooth hydrophobic surfaces are produced by silanization with trichloro(1H,1H,2H,2H-perfluorooctyl)silane. Textured superhydrophobic surfaces are produced by treatment with a commercial superhydrophobic coating agent (Glaco Mirror Coat 'Zero', Soft 99 Co.). Textured superhydrophilic surfaces are produced by plasma cleaning of the surfaces previously treated with the superhydrophobic agent. A 2-mm hole is drilled into the spheres, the immersion-heater cylinder wall or the bottom of the cup vessel to allow the insertion of a thermocouple probe to measure the surface temperature. In cooling experiments, the heated sphere is quenched in a water-filled vessel and the sphere temperature is recorded as function of time. In heating experiments, the cylindrical heater is immersed in a water-filled glass beaker placed on a hot plate to control the water temperature, and the heater surface temperature is measured as a function of the applied power to the heater cartridge in the cylinder. The heat transfer process on the sphere surface or the immersion-heater surface is recorded using a high-speed video camera (Photron Fastcam SA-5). In the cup vessel experiments, the water-filled cup is placed on a hot plate and the vessel surface temperature is measured as a function of the hot-plate temperature. The same setup is used to measure the evaporation time of water droplets placed on the bottom of the cup. Further details of methods are available in Supplementary Information.

Received 11 February; accepted 18 July 2012.

1. Leidenfrost, J. G. *De aquae communis nonnullis qualitatibus tractatus* (Duisburg, 1756); transl. Wares, C. On the fixation of water in diverse fire. *Int. J. Heat Mass Transfer* **9,** 1153–1166 (1966).
2. Bernardin, J. D. & Mudawar, I. The Leidenfrost point: experimental study and assessment of existing models. *Trans. Am. Soc. Mech. Eng.* **121,** 894–903 (1999).
3. Berthoud, G. Vapor explosions. *Annu. Rev. Fluid Mech.* **32,** 573–611 (2000).
4. Linke, H. *et al.* Self-propelled Leidenfrost droplets. *Phys. Rev. Lett.* **96,** 154502 (2006).
5. Lagubeau, N., Le Merrer, M., Clanet, C. & Quéré, D. Leidenfrost on a ratchet. *Nature Phys.* **7,** 395–398 (2011).
6. Vakarelski, I. U., Marston, J. O., Chan, D. Y. C. & Thoroddsen, S. T. Drag reduction by Leidenfrost vapor layers. *Phys. Rev. Lett.* **106,** 214501 (2011).
7. Mishchenko, L. *et al.* Design of ice-free nanostructured surfaces based on repulsion of impacting water droplets. *ACS Nano* **4,** 7699–7707 (2010).
8. Wong, T. S. *et al.* Bioinspired self-repairing slippery surfaces with pressure-stable omniphobicity. *Nature* **477,** 443–447 (2011).
9. Deng, X. Mammen, L. Butt, H. J. & Vollmer, D. Candle soot as a template for a transparent robust superamphiphobic coating. *Science* **335,** 67–70 (2012).
10. Patankar, N. A. Supermucleating surfaces for nucleate boiling and dropwise condensation heat transfer. *Soft Matter* **6,** 1613–1620 (2010).
11. Wang, C. H. & Dhir, V. K. Effect of surface wettability on active nucleation site density during pool boiling of water on a vertical surface. *J. Heat Transfer* **115,** 659–669 (1993).
12. Takata, Y., Hidaka, S. & Kohno, M. in *Proc. Fifth Intl Conf. Enhanced, Compact and Ultra-compact Heat Exchangers: Science, Engineering and Technology* (eds Shah, R. K. *et al.*) 300–304 (Engineering Conferences International, 2005).
13. Chen, R. *et al.* Nanowires for enhanced boiling heat transfer. *Nano Lett.* **9,** 548–553 (2009).
14. Liu, G. & Craig, V. S. J. Macroscopically flat and smooth superhydrophobic surfaces: heating induced wetting transitions up to the Leidenfrost temperature. *Faraday Discuss.* **146,** 141–151 (2010).
15. Liu, G., Fu, L., Rode, A. V. & Craig, V. S. J. Water droplet motion control on superhydrophobic surfaces: exploiting the Wenzel-to-Cassie transition. *Langmuir* **27,** 2595–2600 (2011).
16. Kim, H., Truong, B., Buongiorno, J. & Hu, L. On the effect of surface roughness height, wettability, and nanoporosity on Leidenfrost phenomena. *Appl. Phys. Lett.* **98,** 083121 (2011).
17. Zvirin, Y., Hewitt, G. R. & Kenning, D. B. R. Boiling on free-falling spheres: drag and heat transfer coefficients. *Exp. Heat Transf.* **3,** 185–214 (1990).
18. Rothstein, J. P. Slip on superhydrophobic surfaces. *Annu. Rev. Fluid Mech.* **42,** 89–109 (2010).
19. Ceccio, S. L. Friction drag reduction of external flows with bubble and gas injection. *Annu. Rev. Fluid Mech.* **42,** 183–203 (2010).
20. McHale, G., Newton, M. I. & Shirtcliffe, N. J. Immersed superhydrophobic surfaces: gas exchange, slip and drag reduction properties. *Soft Matter* **6,** 714–719 (2010).
21. Cassie, A. B. D. & Baxter, S. Wettability of porous surfaces. *Trans. Faraday Soc.* **40,** 0546–0550 (1944).
22. Patankar, N. A. On the modeling of hydrophobic contact angles on rough surfaces. *Langmuir* **19,** 1249–1253 (2003).
23. Larmour, I. A., Bell, S. E. J. & Saunders, G. S. Remarkably simple fabrication of superhydrophobic surfaces using electroless galvanic deposition. *Angew. Chem. Int. Edn Engl.* **46,** 1710–1712 (2007).
24. Quéré, D. Wetting and roughness. *Annu. Rev. Mater. Res.* **38,** 71–99 (2008).
25. Flynn, M. R. & Bush, J. W. M. Underwater breathing: the mechanics of plastron respiration. *J. Fluid Mech.* **608,** 275–296 (2008).
26. Lee, C. & Kim, C.-J. Underwater restoration and retention of gases on superhydrophobic surfaces for drag reduction. *Phys. Rev. Lett.* **106,** 014502 (2011).
27. Dhir, V. K. & Purohit, G. P. Subcooled film boiling heat transfer from spheres. *Nucl. Eng. Des.* **47,** 49–66 (1978).
28. Nukiyama, S. Maximum and minimum values of heat Q transmitted from metal to boiling water under atmospheric pressure. *J. Jpn Soc. Mech. Engrs* **37,** 367–374 (1934).
29. Witte, L. C. & Lienhard, J. H. On the existence of two "transition" boiling cure. *Int. J. Heat Mass Transf.* **25,** 771–779 (1982).
30. Celestini, F. & Kirstetter, G. Effect of an electric field on a Leidenfrost droplet. *Soft Matter* **8,** 5992–5995 (2012).
31. Baumeister, K. J., Hendricks, R. C. & Hamill, T. D. *Metastable Leidenfrost States* (NASA Technical Note D3226, 1966).
32. Carey, V. P. in *Liquid-Vapor Phase-Change Phenomena* 2nd edn 353–356 (Taylor and Francis, 2008).

Supplementary Information is available in the online version of the paper.

Acknowledgements We acknowledge the KAUST Machine Workshop, KAUST Electronics Workshop and G. D. Li for assistance in setting up the cooling and heating experiments, and L. Chen and B. Chew from KAUST Advanced Nanofabrication, Imaging and Characterization Core Lab facilities for assistance in AFM and SEM imaging characterization of the superhydrophobic coating.

Author Contributions I.U.V. conceived research and designed the experiments. I.U.V. and J.O.M. carried out the experiments. N.A.P., D.Y.C.C. and S.T.T. contributed with discussions, analysis and theoretical interpretation of the experimental results. I.U.V., D.Y.C.C. and N.A.P. wrote the manuscript. All authors edited the manuscript.

Author Information Reprints and permissions information is available at www.nature.com/reprints. The authors declare no competing financial interests. Readers are welcome to comment on the online version of the paper. Correspondence and requests for materials should be addressed to I.U.V. (ivanuriev.vakarelski@kaust.edu.sa) or N.A.P. (n-patankar@northwestern.edu).

LETTER

doi:10.1038/nature11411

Stereocontrolled organocatalytic synthesis of prostaglandin $PGF_{2\alpha}$ in seven steps

Graeme Coulthard[1], William Erb[1] & Varinder K. Aggarwal[1]

Prostaglandins are hormone-like chemical messengers that regulate a broad range of physiological activities, including blood circulation, digestion and reproduction[1,2]. Their biological activities and their complex molecular architectures have made prostaglandins popular targets for synthetic organic chemists for over 40 years[3,4]. Prostaglandin analogues are widely used as pharmaceuticals and some, such as latanoprost, which is used to treat glaucoma[5,6], have become billion-dollar drugs. Previously reported syntheses of these compounds are quite lengthy, and every chemical step costs time and energy, generates waste and is accompanied by material losses. Using a new bond disconnection, here we report a concise synthesis of the most complex prostaglandin, $PGF_{2\alpha}$, with high levels of control of relative and absolute stereochemistry, and fewer steps. The key step is an aldol cascade reaction of succinaldehyde using proline organocatalysis to create a bicyclic enal in one step and an enantiomeric excess of 98%. This intermediate bicyclic enal is fully primed with the appropriate functionality for attachment of the remaining groups[7]. Access to this bicyclic enal will not only render existing prostaglandin-based drugs more affordable, but will also facilitate the rapid exploration of related chemical structures around the ubiquitous five-membered ring motif, such as potentially therapeutic prostaglandin analogues.

Prostaglandins, such as $PGF_{2\alpha}$ (Fig. 1; **1**), are hormones that are responsible for the control of a myriad of essential biological processes from sleep to pain, fever to inflammation, menstruation to birth, and constriction of blood vessels to blood clotting[1,2,8]. They are derived from arachidonic acid and are transformed by prostaglandin synthetase into a number of structurally related carbocyclic molecules. These sensitive and labile molecules are not stored in the body but are synthesized in response to stimuli. They were discovered in the early 1930s by von Euler[9] and by the mid-1960s the structures of the first family of prostaglandins was uncovered by Bergström *et al.* (see refs 2 and 10 for reviews). The complex structures of prostaglandins, together with their broad spectrum of biological activity, fuelled intense research activity into their synthesis, comparable to that generated from β-lactam antibiotics and steroids. Woodward[11], Corey[12], Stork[13], Noyori[14], Danishefsky[15] and many others contributed ingenious strategies and developed new methodologies of general use in the construction of these complex molecules[3–5]. But prostaglandins and their analogues are not only of academic interest, they have also found their way into a considerable number of pharmaceuticals. For example, an analogue of $PGF_{2\alpha}$ (**1**), latanoprost (**2**), is used in the treatment of glaucoma[16], and achieved sales of $1.75 billion in 2010 (ref. 17).

The manufacture of latanoprost[6] requires 20 steps and uses the original strategy developed by Corey *et al.*[18] in the synthesis of the related prostaglandin, $PGF_{2\alpha}$. Corey's synthesis involved the formation of a key intermediate, the Corey lactone (**3**), in nine steps from cyclopentadiene (**4**). From this lactone, they were able to assemble the entire family of prostaglandins[12], and specifically $PGF_{2\alpha}$, in eight further steps[18].

In our analysis for the synthesis of prostaglandins and in common with other syntheses of $PGF_{2\alpha}$[13,15,19] we recognized that lactol **5** was an ideal late-stage intermediate because it enabled the incorporation of the upper side-chain with control of double-bond geometry through a Wittig reaction. At this point our retrosynthetic analysis departed from all previous syntheses. We were interested in disconnecting the C12–C13 bond[20], because we recognized that the bicyclic lactol could control the stereochemistry of the 1,4-addition of the lower side-chain onto a suitable Michael acceptor **6**. By selecting an aldehyde as the electron withdrawing group of the Michael acceptor, the enal **7** could be disconnected back to a simple aldol dimerization of succinaldehyde (**8**), a process that could be rendered asymmetric through proline (**9**) catalysis[21,22].

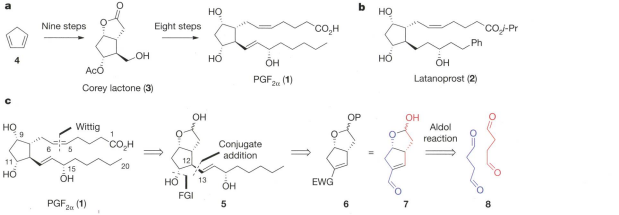

Figure 1 | Prostaglandins in nature and medicine. a, General schematic of Corey's synthesis of $PGF_{2\alpha}$. **b**, The molecular structure of latanoprost (**2**), a $PGF_{2\alpha}$ analogue used for the treatment of glaucoma. **c**, Our retrosynthetic analysis of $PGF_{2\alpha}$. The numbered carbon atoms are referred to in the main text. FGI, functional group interconversion. Ph, phenyl. EWG, electron withdrawing group. i-Pr, isopropyl, $CH(CH_3)_2$.

[1]School of Chemistry, University of Bristol, Cantock's Close, Bristol BS8 1TS, UK.

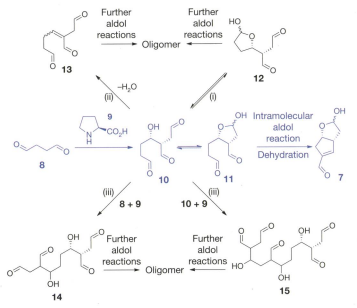

Figure 2 | Potential reaction pathways of the proline-catalysed aldol reaction of succinaldehyde. The desired pathway is shown in blue; others are labelled (i) to (iii) and described in the main text.

However, the 'simple' concept shown in the retrosynthesis belies a highly complex reaction cascade (blue, Fig. 2) with many potential pitfalls (black, Fig. 2): (i) the aldol product **10** is required to form the less favoured hemiacetal **11**, bearing *cis* substituents in the 5-membered ring, but not the *trans* hemiacetal **12**; (ii) the hemiacetal **11** is required to undergo an intramolecular second aldol and eliminate to give **7** but aldol **10** itself should not eliminate to give **13**; (iii) aldol **10** is a reactive trialdehyde which will be prone to undergo further aldol reactions with succinaldehyde (**8**) or with itself, leading to **14** and **15** and ultimately oligomers.

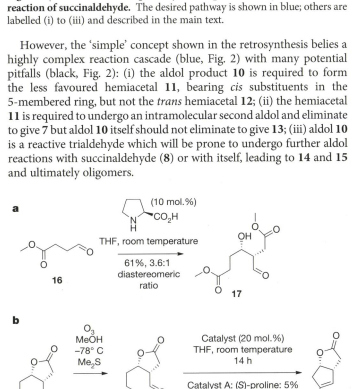

Figure 3 | Model studies. a, Model studies to investigate the intermolecular proline-catalysed aldol reaction of aldehydes bearing an ester at the 4-position. **b**, Model studies to investigate an intramolecular aldol reaction and dehydration. **c**, A transition state structure accounting for the observed enantioselectivity.

Perhaps unsurprisingly, the desired aldol proved highly challenging to realize in practice: treatment of succinaldehyde with proline in a range of solvents and under a variety of conditions did not deliver any of the desired bicyclic product but instead gave oligomeric material. We therefore deconstructed the reaction cascade to determine which of the two steps, the initial aldol step or the second aldol and dehydration step, was causing the problem.

Model aldehyde **16** was treated with proline (**9**) and aldol product **17** was obtained as a 3.6:1 mixture of diastereoisomers in moderate yield (Fig. 3a)[23]. This showed that aldol reactions of aldehydes bearing a carbonyl group in the 4-position were suitable substrates for the proline-catalysed aldol reaction.

To test the second aldol and dehydration step, model dialdehyde **18** was prepared by ozonolysis of the known lactone **19** (Fig. 3b)[24]. However, treatment of this dialdehyde with proline (catalyst A) provided only low conversion to the expected enal **20**, clearly indicating that the second step was the hurdle in the reaction cascade. We therefore explored alternative catalysts and found that $[Bn_2NH_2][OCOCF_3]$ (**21,** catalyst B)[25] was much more effective, giving enal **20** in 51% isolated yield (from **19**).

We therefore tested the aldol reaction cascade of succinaldehyde with a combination of proline and $[Bn_2NH_2][OCOCF_3]$ in a range of solvents and under a variety of conditions (see the Supplementary Information for full details). This time the reaction was successful; selected data, illustrative of the process, is summarized in Table 1. The reaction could be conducted at (unusually) low loadings of both catalysts and at relatively high concentration (2 M) (entries 1–3 in Table 1). The sequenced addition of the two catalysts and the timing was critical to the success of the reaction: if $[Bn_2NH_2][OCOCF_3]$ was present at the outset (entry 4 in Table 1), or not added at all (see earlier discussion), the reaction failed. We spent some time investigating this facet of the reaction because the low yield is a consequence of oligomerization of the intermediate trialdehyde. As the concentration of the trialdehyde builds up it is prone to undergo further aldol reactions with succinaldehyde, leading to oligomers. The second catalyst seemed to inhibit the initial proline-catalysed aldol reaction, so consecutive addition of the two catalysts was required. The optimum time to add the second catalyst was found to be dependent on the amount of proline catalyst used: using just 2% proline, the yield of the lactol **7** increased with increasing time before the addition of the second catalyst (entries 5–8 in Table 1), peaking at around 10 h. The reaction could also be conducted with just 1% proline but considerably longer reaction times were required (entry 9 in Table 1).

Table 1 | Effect of catalyst loading and time delay on yield

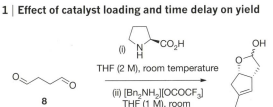

Entry	(*S*)-proline (mol.%)	Time (h)	Yield (%)
1	10	2	14
2	5	2	16
3	5	4	19
4	2	0	~2
5	2	4	10
6	2	6	16
7	2	10	20
8	2	24	20
9	1	24	18

Reactions were carried out on 200 mg of succinaldehyde **8**. 'Time' refers to the time before $[Bn_2NH_2][OCOCF_3]$ (2 mol.%) was added and the reaction was diluted to 1 M. The yield is the NMR (nuclear magnetic resonance) yield based on an internal standard (1,3,5-trimethoxybenzene); results are an average of five reactions.

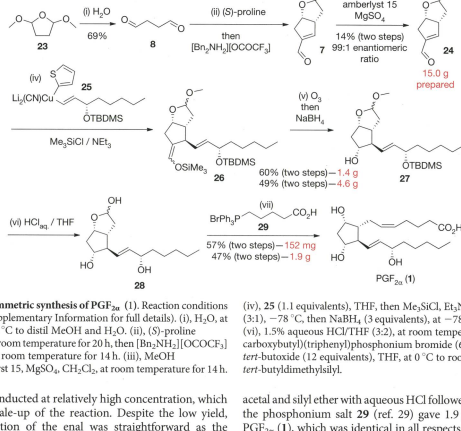

Figure 4 | A concise asymmetric synthesis of $PGF_{2\alpha}$ (1). Reaction conditions are as follows (see the Supplementary Information for full details). (i), H_2O, at 75 °C for 4 h, then at 115 °C to distil MeOH and H_2O. (ii), (*S*)-proline (2 mol.%), THF (2 M), at room temperature for 20 h, then $[Bn_2NH_2][OCOCF_3]$ (2 mol.%), THF (1 M), at room temperature for 14 h. (iii), MeOH (2.0 equivalents), amberlyst 15, $MgSO_4$, CH_2Cl_2, at room temperature for 14 h. (iv), **25** (1.1 equivalents), THF, then Me_3SiCl, Et_3N. (v), O_3, CH_2Cl_2/MeOH (3:1), −78 °C, then $NaBH_4$ (3 equivalents), at −78 °C to room temperature. (vi), 1.5% aqueous HCl/THF (3:2), at room temperature for 16 h. (vii), (4-carboxybutyl)(triphenyl)phosphonium bromide (6 equivalents), potassium *tert*-butoxide (12 equivalents), THF, at 0 °C to room temperature. TBDMS, *tert*-butyldimethylsilyl.

The reaction was conducted at relatively high concentration, which greatly assisted the scale-up of the reaction. Despite the low yield, work-up and purification of the enal was straightforward as the oligomeric side products could be largely removed by filtration, leaving a relatively pure crude material. Partial purification through a plug of silica gave the desired enal **7** in about 16% yield and with an enantiomeric ratio of 99:1, on the multigram scale. The absolute stereochemistry of the product was ultimately established through the synthesis of $PGF_{2\alpha}$ (**1**) and follows from the List–Houk model for this type of reaction (transition-state structure **22**, Fig. 3c)[26]. A mixture of diastereoisomers of trialdehyde **10** was expected to be formed (a diastereoisomeric ratio of about 3.6:1 was expected from results with the model compound **16**) but as the minor diastereoisomer cannot give the alternative diastereomeric enal it must be consumed by the formation of oligomers.

The complete synthesis of $PGF_{2\alpha}$ from commercially available materials is shown in Fig. 4. Heating 2,5-dimethoxytetrahydrofuran **23** (41 g) in water followed by evaporation and extraction gave crude dialdehyde[27] which was directly subjected to the aldol reaction as described above. The hemi-acetal **7** was converted into a 2:1 inconsequential diastereoisomeric mixture of methoxy acetals **24** which were carried through the subsequent reaction sequence. On a large scale (285 g of **23**), further modifications were required owing to the partial decomposition of the dialdehyde during the extended time needed to remove the larger volume of solvent used for extraction. Instead, we found that after distillation of the methanol (MeOH) and most of the water, azeotropic removal of the remaining water using 2-MeTHF (2-methyltetrahydrofuran) provided a solution of the dialdehyde in a solvent (2-MeTHF) that could be used directly in the aldol reaction. Using this improved and simplified protocol, from 109.5 g of inexpensive succinaldehyde we were able to obtain 15.0 g of pure methoxy acetal **24** in 14% yield over two steps. Conjugate addition of the mixed vinyl cuprate[28] **25** to 4.0 g of methoxy acetal **24** followed by trapping with TMSCl (trimethylsilyl chloride) furnished the silyl enol ether **26**. Subsequent controlled ozonolysis followed by treatment with $NaBH_4$ gave the alcohol **27** (4.6 g, 49% over two steps). As planned, these two steps occurred with complete stereocontrol at the newly created stereogenic centres. Finally, simultaneous deprotection of the acetal and silyl ether with aqueous HCl followed by Wittig reaction with the phosphonium salt **29** (ref. 29) gave 1.9 g of the target molecule $PGF_{2\alpha}$ (**1**), which was identical in all respects to the natural product[30].

Thus, we have developed a short (seven steps) synthesis of prostaglandin $PGF_{2\alpha}$ from inexpensive 2,5-dimethoxytetrahydrofuran **23**. The key step is an organocatalytic aldol dimerization reaction of succinaldehyde, which generates the bicyclic enal **7** in high enantiomeric ratio and fully primed with functionality suitable to introduce the required side chains directly. The aldol cascade required proline to perform the first aldol reaction and a second catalyst ($[Bn_2NH_2][OCOCF_3]$) to induce an intramolecular aldol reaction and elimination. Although the aldol reaction was low-yielding, the enantioselectivity was very high, isolation and purification was straightforward and the reaction could be conducted on the multigram scale. Its application in a short synthesis of the most complex of prostaglandins, $PGF_{2\alpha}$, has been demonstrated. Indeed, the bicyclic enal **7** is an ideal building block not just for the cost-effective synthesis of the whole family of prostaglandins, but for also exploring the chemical space around the ubiquitous five-membered carbocyclic ring motif, where other biologically active molecules undoubtedly lie.

METHODS SUMMARY

Procedure for formation of methoxyacetal 24. A solution of succinaldehyde **8** (109.5 g, 1.27 mol) in 2-MeTHF (650 ml) was stirred at room temperature (20 °C) (*S*)-proline (2.93 g, 25.4 mmol, 0.02 equivalents) was added and the reaction stirred at room temperature for 20 h. THF (650 ml) was added, followed by $[Bn_2NH_2][OCOCF_3]$ (8.43 g, 25.4 mmol, 0.02 equivalents). The reaction was stirred for a further 14 h. Celite (60 g) was added to the reaction and the volume of the reaction mixture was reduced by three quarters under reduced pressure. *tert*-Butyl methyl ether (TBME) (975 ml) was added slowly and with vigorous stirring of the mixture. The mixture was stirred for 20 min before filtration of the resulting solids. The solids were washed with TBME (3 × 150 ml) and the filtrate was concentrated under reduced pressure. The material was purified by column chromatography (about 600 g silica), eluting with petrol/EtOAc (6:4 to 5:5), to give the lactol **7** (as an approximately 2:1 mixture of diastereoisomers), as a brown oil.

This residue, containing **7**, was dissolved in CH_2Cl_2 (190 ml) and stirred at room temperature. MeOH (5.47 g, 6.90 ml, 170.6 mmol, 2.0 equivalents based on about 13.4% of **7** detected by internal standard in the previous reaction) was

added via syringe. Amberlyst 15 (1.22 g) and $MgSO_4$ (25.2 g) were added in one portion and the reaction mixture was stirred at room temperature for 14 h. The reaction mixture was filtered through a sinter funnel and the solids washed with CH_2Cl_2 (3 × 60 ml). The filtrate was concentrated under reduced pressure and purified by column chromatography (about 300 g silica), eluting with petrol/EtOAc (9:1 to 4:1), to give the methyl acetal **24** (as an approximately 2:1 mixture of diastereoisomers, 15.0 g, 14.0% (over two steps from succinaldehyde)) as a yellow oil. See the Supplementary Information for characterization data.

Received 9 February; accepted 11 July 2012.
Published online 15 August 2012.

1. Funk, C. D. Prostaglandins and leukotrienes: advances in eicosanoid biology. *Science* **294,** 1871–1875 (2001).
2. Bindra, J. S. & Bindra, R. *Prostaglandin Synthesis* (Academic Press, 1977).
3. Bindra, J. S. in *The Total Synthesis of Natural Products* (ed. ApSimon, J.) Vol. 4 353–449 (Wiley, 1981).
4. Das, S., Chandrasekhar, S., Yadav, J. S. & Gree, R. Recent developments in the synthesis of prostaglandins and analogues. *Chem. Rev.* **107,** 3286–3337 (2007).
5. Collins, P. W. & Djuric, S. W. Synthesis of therapeutically useful prostaglandin and prostacyclin analogs. *Chem. Rev.* **93,** 1533–1564 (1993).
6. Nair, S. K. & Henegar, K. E. in *Modern Drug Synthesis* (eds Li, J. J. & Johnson, D. S.) Ch. 21 329–338 (Wiley, 2010).
7. Ungrin, M. D. *et al.* Key structural features of prostaglandin E_2 and prostanoid analogs involved in binding and activation of the human EP1 prostanoid receptor. *Mol. Pharmacol.* **59,** 1446–1456 (2001).
8. Stix, G. Better ways to target pain. *Sci. Am.* 68–71, http://www.scientificamerican.com/article.cfm?id=better-ways-to-target-pain (16 December 2006).
9. Von Euler, U. S. Information on the pharmacological effect of natural secretions and extracts from male accessory sexual glands. *Arch. Exp. Pathol. Pharm.* **175,** 78–84 (1934).
10. Flower, R. J. Prostaglandins, bioassay and inflammation. *Br. J. Pharmacol.* **147,** S182–S192 (2006).
11. Woodward, R. B. *et al.* Novel synthesis of prostaglandin $F_{2\alpha}$. *J. Am. Chem. Soc.* **95,** 6853–6855 (1973).
12. Corey, E. J. & Cheng, X.-M. *The Logic of Chemical Synthesis* (Wiley, 1995).
13. Stork, G., Sher, P. M. & Chen, H. L. Radical cyclization-trapping in the synthesis of natural products. A simple, stereocontrolled route to prostaglandin $F_{2\alpha}$. *J. Am. Chem. Soc.* **108,** 6384–6385 (1986).
14. Suzuki, M., Yanagisawa, A. & Noyori, R. Prostaglandin synthesis. 16. The three-component coupling synthesis of prostaglandins. *J. Am. Chem. Soc.* **110,** 4718–4726 (1988).
15. Danishefsky, S. J., Paz Cabal, M. & Chow, K. Novel stereospecific silyl group transfer reactions: practical routes to the prostaglandins. *J. Am. Chem. Soc.* **111,** 3456–3457 (1989).
16. Resul, B. *et al.* Phenyl-substituted prostaglandins: potent and selective antiglaucoma agents. *J. Med. Chem.* **36,** 243–248 (1993).
17. Pfizer reports fourth-quarter and full-year 2010 results; provides 2011 financial guidance and updates 2012 financial targets. http://www.pfizer.com/files/investors/presentations/q4performance_020111.pdf (2011).
18. Corey, E. J., Weinshenker, N. M., Schaaf, T. K. & Huber, W. Stereo-controlled synthesis of dl-prostaglandins $F_{2\alpha}$ and E_2. *J. Am. Chem. Soc.* **91,** 5675–5677 (1969).
19. Howard, C. C. *et al.* Total synthesis of prostaglandin-$F_{2\alpha}$ involving stereocontrolled and photo-induced reactions of bicyclo[3.2.0]heptanones. *J. Chem. Soc. Perkin Trans.* **1** 852–857 (1980).
20. Corey, E. J., Nicolaou, K. C. & Beames, D. J. A short synthetic route to prostaglandins utilizing position-selective epoxide opening by the vinyl Gilman reagent. *Tetrahedr. Lett.* **15,** 2439–2440 (1974).
21. Mukherjee, S., Yang, J. W., Hoffmann, S. & List, B. Asymmetric enamine catalysis. *Chem. Rev.* **107,** 5471–5569 (2007).
22. List, B., Lerner, R. A. & Barbas, C. F. Proline-catalyzed direct asymmetric aldol reactions. *J. Am. Chem. Soc.* **122,** 2395–2396 (2000).
23. Northrup, A. B. & MacMillan, D. W. C. The first direct and enantioselective cross-aldol reaction of aldehydes. *J. Am. Chem. Soc.* **124,** 6798–6799 (2002).
24. Corey, E. J. & Ravindranathan, T. A simple route to a key intermediate for the synthesis of 11-desoxyprostaglandins. *Tetrahedr. Lett.* **12,** 4753–4755 (1971).
25. Corey, E. J. *et al.* Stereospecific total synthesis of gibberellic acid. A key tricyclic intermediate. *J. Am. Chem. Soc.* **100,** 8031–8034 (1978).
26. Bahmanyar, S., Houk, K. N., Martin, H. J. & List, B. Quantum mechanical predictions of the stereoselectivities of proline-catalyzed asymmetric intermolecular aldol reactions. *J. Am. Chem. Soc.* **125,** 2475–2479 (2003).
27. Gourlay, B. S., Molesworth, P. P., Ryan, J. H. & Smith, J. A. A new and high yielding synthesis of unstable pyrroles via a modified Clauson-Kaas reaction. *Tetrahedr. Lett.* **47,** 799–801 (2006).
28. Lipshutz, B. H., Kozlowski, J. A., Parker, D. A., Nguyen, S. L. & McCarthy, K. E. More highly mixed, higher order cyanocuprates "R_2(2-thienyl)Cu(CN)Li_2". Efficient reagents which promote selective ligand transfer. *J. Organomet. Chem.* **285,** 437–447 (1985).
29. de los Angeles Rey, M. *et al.* New synthetic strategies to vitamin D analogues modified at the side chain and D ring. Synthesis of 1α,25-dihydroxy-16-ene-vitamin D_3 and C-20 analogues. *J. Org. Chem.* **64,** 3196–3206 (1999).
30. Sheddan, N. A. & Mulzer, J. Cross metathesis as a general strategy for the synthesis of prostacyclin and prostaglandin analogues. *Org. Lett.* **8,** 3101–3104 (2006).

Supplementary Information is available in the online version of the paper.

Acknowledgements We thank EPSRC and the European Research Council (FP7/2007-2013, ERC grant no. 246785) for financial support. V.K.A. thanks the Royal Society for a Wolfson Research Merit Award and EPSRC for a Senior Research Fellowship.

Author Contributions G.C. and W.E. were involved in the discovery and subsequent development of the aldol reaction and G.C. applied it to $PGF_{2\alpha}$. V.K.A. conceived and directed the investigations and composed the manuscript with revisions provided by G.C. and W.E.

Author Information Reprints and permissions information is available at www.nature.com/reprints. The authors declare no competing financial interests. Readers are welcome to comment on the online version of the paper. Correspondence and requests for materials should be addressed to V.K.A. (v.aggarwal@bristol.ac.uk).

LETTER

doi:10.1038/nature11390

Observations of increased tropical rainfall preceded by air passage over forests

D. V. Spracklen[1], S. R. Arnold[1] & C. M. Taylor[2]

Vegetation affects precipitation patterns by mediating moisture, energy and trace-gas fluxes between the surface and atmosphere[1]. When forests are replaced by pasture or crops, evapotranspiration of moisture from soil and vegetation is often diminished, leading to reduced atmospheric humidity and potentially suppressing precipitation[2,3]. Climate models predict that large-scale tropical deforestation causes reduced regional precipitation[4–10], although the magnitude of the effect is model[9,11] and resolution[8] dependent. In contrast, observational studies have linked deforestation to increased precipitation locally[12–14] but have been unable to explore the impact of large-scale deforestation. Here we use satellite remote-sensing data of tropical precipitation and vegetation, combined with simulated atmospheric transport patterns, to assess the pan-tropical effect of forests on tropical rainfall. We find that for more than 60 per cent of the tropical land surface (latitudes 30 degrees south to 30 degrees north), air that has passed over extensive vegetation in the preceding few days produces at least twice as much rain as air that has passed over little vegetation. We demonstrate that this empirical correlation is consistent with evapotranspiration maintaining atmospheric moisture in air that passes over extensive vegetation. We combine these empirical relationships with current trends of Amazonian deforestation to estimate reductions of 12 and 21 per cent in wet-season and dry-season precipitation respectively across the Amazon basin by 2050, due to less-efficient moisture recycling. Our observation-based results complement similar estimates from climate models[4–10], in which the physical mechanisms and feedbacks at work could be explored in more detail.

To explore the links between vegetation and rainfall, we analysed combined satellite data on precipitation from the Tropical Rainfall Measuring Mission (TRMM) and other satellites[15] (TRMM3B42) and data on leaf area index (LAI) from the Moderate Resolution Imaging Spectroradiometer[16] (MODIS). In these data positive spatial correlations exist between annual mean precipitation and annual mean LAI (Fig. 1a, d; Pearson correlation coefficient, $r = 0.81$), highlighting the role of precipitation in controlling large-scale vegetation patterns. In this study, our aim was to investigate a causal effect of vegetation on tropical (30° S to 30° N) rainfall in subsequent days on a regional scale (over distances of hundreds to thousands of kilometres). To do this, we calculated the origin and atmospheric transport of air

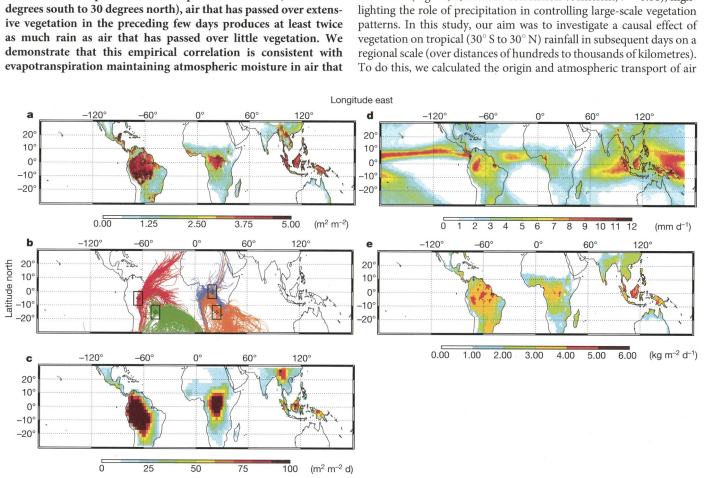

Figure 1 | Annual (2001–2007) mean vegetation, precipitation and evaporation. a, Leaf area index (LAI) from MODIS. **b**, Example 10-d back-trajectories arriving daily during 2001. Boxes illustrate the four domains analysed in detail in this study. **c**, Mean cumulative exposure of back-trajectories to LAI over the preceding 10 d. **d**, Precipitation reported by TRMM and other satellites (TRMM3B42). **e**, Evapotranspiration computed as the mean of the four GLDAS models.

[1]School of Earth and Environment, University of Leeds, Leeds LS2 9JT, UK. [2]Centre for Ecology and Hydrology, Wallingford, Oxford OX10 8BB, UK.

masses to determine the prior exposure of air to vegetation. This allowed us to evaluate whether air that had passed over more vegetation produced more rainfall.

To calculate air-mass histories, we used a Lagrangian atmospheric transport model. Such back-trajectory methods have been used previously to identify the transport of atmospheric moisture to continental regions[17,18]. We calculated atmospheric back-trajectories arriving daily at the centre of all continental $1^\circ \times 1^\circ$ grid squares over the tropical domain for 2001–2007. The trajectories were calculated using operational analysis data from the European Centre for Medium-Range Weather Forecasts (ECMWF), and are hence consistent with the large-scale atmospheric flow from the assimilated observations. We tested the sensitivity of our analysis to the length, arrival height and arrival time of the back-trajectories and found consistent results across a broad range of choices (Supplementary Figs 1, 2 and 3). Here we present results for ten-day back-trajectories arriving at the surface at 12:00 UT. Figure 1b shows example back-trajectories arriving at four tropical locations.

For each individual trajectory, we calculated the cumulative LAI (ΣLAI) encountered by the air mass during the last ten days of atmospheric transport. The resulting climatology of ΣLAI (Fig. 1c) is very similar to the *in situ* LAI, although important differences are apparent. For example, there are regions surrounding the Amazon and Congo basins where *in situ* LAI is relatively low but ΣLAI is high owing to exposure of air to large amounts of vegetation as it travels across forested regions upwind.

We analysed relationships between the daily variability in ΣLAI and the daily variability in precipitation. Figure 2a shows these relationships for air masses arriving in a ~1,000 km × 1,000 km region of Minas Gerais, Brazil, near the Amazon basin. To reduce the influence of the initial state of the air mass on our analysis, we stratified the data into that from the wet season and that from the dry season and then further according to the initial specific humidity of the trajectory, on the basis of the ECMWF analyses. We found a strong positive and significant (Student's *t*-test, $P < 0.01$) relationship between the exposure of air masses to vegetation and the precipitation those air masses produce (Fig. 2b). For air masses with low to medium exposure to precedent vegetation ($\Sigma\text{LAI} < 10\ \text{m}^2\,\text{m}^{-2}$ d), mean dry- and wet-season rainfall increases by 0.25 mm d^{-1} and, respectively, 0.4 mm d^{-1} for every additional unit of exposure to LAI that is encountered in the preceding 10 d. The impact of vegetation exposure tends to saturate, especially during the wet season, with less sensitivity of rainfall where $\Sigma\text{LAI} > 10\ \text{m}^2\,\text{m}^{-2}$ d. Although we find that the initial specific humidity of the air mass does affect precipitation, with moister air masses typically producing more precipitation, the positive trend between precipitation and exposure to LAI is similar for all subsets of the data. Qualitatively similar results are found in a 1,000 km × 1,000 km region south of the tropical forests of the Congo basin (Fig. 2b). Over the moist tropical forests themselves, differences in rainfall between air masses with low and high exposures to LAI are notably smaller (Fig. 2b), although for the Congo basin the differences are significant in the dry season ($P < 0.01$). We note that the positive relationships found between precipitation and ΣLAI are not due to the length of time the trajectories have spent over land, with distance travelled and ΣLAI often poorly correlated (Supplementary Table 1), or to the average topographic height the trajectory has crossed. When we repeated our analysis using the distance travelled by the trajectory over land or the average elevation of the topography crossed by the trajectory (in place of ΣLAI), the relationships were substantially weaker and in some cases negative (Supplementary Figs 4 and 5).

We extended this regional analysis to explore relationships between precipitation and vegetation across the tropics (Fig. 2c). For more than 60% of the tropical land surface, precipitation is a factor of at least two greater in air masses that have been exposed to extensive vegetation in the preceding days (defined as the top decile of ΣLAI), relative to air masses that have been exposed to little (defined as the bottom decile of

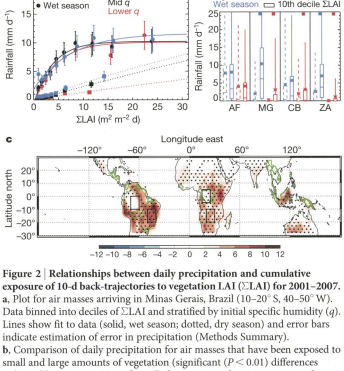

Figure 2 | Relationships between daily precipitation and cumulative exposure of 10-d back-trajectories to vegetation LAI (ΣLAI) for 2001–2007. **a**, Plot for air masses arriving in Minas Gerais, Brazil (10–20° S, 40–50° W). Data binned into deciles of ΣLAI and stratified by initial specific humidity (q). Lines show fit to data (solid, wet season; dotted, dry season) and error bars indicate estimation of error in precipitation (Methods Summary). **b**, Comparison of daily precipitation for air masses that have been exposed to small and large amounts of vegetation (significant ($P < 0.01$) differences indicated by squares at top of panel) during atmospheric transport to the Amazon basin (AB; 10–0° S, 60–70° W), Minas Gerais (MG), the Congo basin (CB; 5° N–5° S, 15–25° E) and south of Congo (ZA; 10–20° S, 20–30° E) (mean, star; median, line; 25th and 75th percentiles, box; 5th and 95th percentiles, whiskers). **c**, Number of calendar months with significant ($P < 0.01$; red, positive; blue, negative) relationships between precipitation and ΣLAI. Stippling denotes regions where precipitation is a factor of at least two greater in air with large exposure to vegetation than in air with small exposure. Green contour delimits areas with >3 $\text{m}^2\,\text{m}^{-2}$ annual mean LAI. Black boxes mark the four regions in **b**.

ΣLAI). Significant ($P < 0.01$) positive correlations between precipitation and ΣLAI are common features for much of the year in areas surrounding the Amazon (southern Brazil and Paraguay) and Congo (southern and eastern Africa) forests, matching where previous studies have found large continental precipitation recycling ratios[18]. We find few tropical regions with significant negative correlations, although the relationships between vegetation and precipitation are typically weaker in moist tropical forests. The weaker signal at the centre of extensive forests is probably due to the lack of variability in air-mass exposure to vegetation (Supplementary Fig. 6); however, saturation of the MODIS LAI retrievals for dense tropical forest canopies[19] may have a role.

This analysis demonstrates that there are strong positive relationships between the cumulative exposure of air to vegetation and the amount of precipitation that air will produce, suggestive of a water-cycle feedback. To explore potential mechanisms underlying these relationships, we evaluated the change in atmospheric moisture that occurs along our back-trajectories. To do this we calculated the net change in specific humidity (Δq) that occurred during continental transport in the ECMWF humidity analyses along the 10-d back-trajectories (Fig. 3a). In general, air becomes drier during atmospheric transport over land, owing to lower continental evaporation rates as compared with the oceans. Figure 3a demonstrates that air masses that have been exposed to more vegetation remain significantly moister ($P < 0.01$), and in some cases air can actually moisten when crossing densely vegetated regions. Analysis of the latter cases indicates that typically 70–90% of increases in q occur during the hours of daylight,

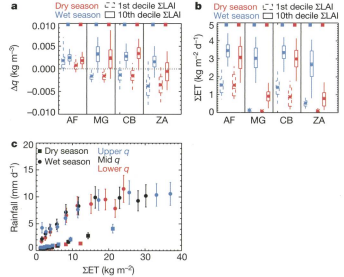

Figure 3 | Atmospheric water-budget components along back-trajectories. **a**, Same as Fig. 2b, but for net change in atmospheric specific humidity (Δq) as a function of ΣLAI. **b**, Same as Fig. 2b, but for cumulative surface evaporation (ΣET) as a function of ΣLAI. **c**, Same as Fig. 2a, but for precipitation as a function of ΣET.

consistent with a dominant forcing from evapotranspiration (Supplementary Fig. 7).

To quantify the contribution of evapotranspiration to the air-mass water budget, we used output from four global land surface models that use the best available estimates of meteorological forcing (those from the Global Land Data Assimilation System[20] (GLDAS)) (Fig. 1e). Figure 3b shows significant ($P < 0.01$) positive relationships between the multi-model mean cumulative surface evaporation (ΣET) and ΣLAI in all four regions examined. Figure 3c shows rainfall as a function of ΣET for the Minas Gerais region, demonstrating that additional moisture from evapotranspiration emitted into air masses with large exposure to vegetation is substantially greater than the additional precipitation observed in these air masses. Indeed, for all four regions the extra ΣET emitted into air masses with large vegetation exposure exceeds the observed additional precipitation by a factor of at least four (Supplementary Table 2).

Our analysis explores the role of regional-scale vegetation patterns on precipitation. Through evapotranspiration, forests maintain atmospheric moisture that can return to land as rainfall downwind. These processes operate on timescales of days over distances of 100–1,000 km (ref. 18) such that large-scale land-use change may alter precipitation hundreds to thousands of kilometres from the region of vegetation change. Land-use patterns and small-scale deforestation may also alter precipitation locally, through changes in the thermodynamic profile and the development of surface-induced mesoscale circulations[21,22]. Natural and pyrogenic emissions from vegetation can also have a role in rainfall initiation over tropical forest regions[23]. The impact of cloud microphysical processes on precipitation is highly uncertain[24], and biogenic emissions could contribute to our observed relationship between rainfall and exposed vegetation. However, our water-balance calculations imply that cumulative increases in evapotranspiration over upstream forested regions more than account for the increase in downstream rainfall.

Rapid land-use change is occurring across large regions of the tropics: 40% of the Amazon is predicted to be deforested by 2050 under a business-as-usual scenario[25]. We used this scenario to explore the potential sensitivity of rainfall to changes in moisture recycling as a result of deforestation. We combined the deforestation scenario with present-day LAI to produce a new spatial distribution of LAI

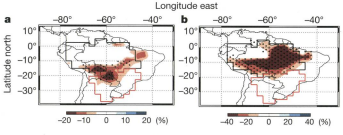

Figure 4 | Simulated percentage change in precipitation due to 2000–2050 business-as-usual deforestation of the Amazon basin. **a**, Wet season; **b**, dry season. Stippling denotes regions where the simulated precipitation anomaly differs from the present-day (1998–2010) rainfall by more than 1 s.d. The Amazon (black) and Rio de la Plata (red) basins are marked.

(Supplementary Fig. 8) and then used our trajectories to calculate ΣLAI under the deforested scenario. We then applied our empirical relationships between ΣLAI and rainfall (Fig. 2b) to estimate the change in rainfall that might occur as a result of this extensive deforestation. In this calculation, we implicitly assumed there to be no change in the large-scale circulation and that the local effects of deforestation on rainfall were negligible downstream. Despite these assumptions, our estimates are broadly consistent with estimates of basin-wide deforestation from climate models[4–10]. Using this method, we estimated a 12% reduction in wet-season precipitation and a 21% reduction in dry-season precipitation across the Amazon basin (Fig. 4). This sensitivity is not restricted to the region of deforestation, and we estimate a 4% decrease in annual total precipitation for the Rio de la Plata basin. Through comparison with TRMM3B42 data, we calculate that the estimated reduction in precipitation is equivalent to the basin-wide drought experienced across the Amazon in 2010. Such a reduction in precipitation may have consequences for the future of remaining Amazonian forests[26,27] and for rainfall-reliant industries both within and outside the Amazon basin, including agriculture and hydroelectric power generation, which contribute substantially to South American economies. The successful efforts to curb Amazon deforestation that have been applied in recent years[28] must be maintained if large-scale clearance of the Amazon and the resulting impacts on regional rainfall are to be avoided.

METHODS SUMMARY

Remote-sensed data. We used precipitation retrievals from the 3B42 3-h 0.25° × 0.25° product of TRMM and other satellites[15] to calculate daily accumulated (24-h) rainfall. We used monthly mean LAI from MODIS[16] using the MOD15_BU_V5 product available at 0.25° × 0.25° resolution. We spatially averaged both products to 1° × 1° resolution. We apply this temporal and spatial averaging to the precipitation data to reduce random error[29]. We estimate the total error to be the random error, estimated according to ref. 28, plus a systematic error estimated as 0.2 times the absolute precipitation[30], combined in quadrature.

Land surface models. We used 1° × 1° monthly mean evaporation from four global land surface models archived on GLDAS[20]. The models are forced by a combination of meteorological data sets including atmospheric analysis, and precipitation from merged gauge–satellite products.

Atmospheric transport. We calculated kinematic atmospheric back-trajectories arriving four times daily (00:00, 06:00, 12:00 and 18:00 UT) on a 1° × 1° grid for the period 2001–2007 using the OFFLINE trajectory model. The position of each trajectory is calculated every 30 min and output every 6 h. We calculated 3-, 5- and 10-d trajectories arriving at the surface and three altitudes above the surface (corresponding to air pressures of 900, 800 and 700 hPa) that are likely to be within the deep tropical boundary layer.

Analysis. For each trajectory, we calculated the total distance travelled over land, the cumulative exposure to LAI (ΣLAI), the average elevation of the topography over which the trajectory travelled and the cumulative evapotranspiration (ΣET; specified by GLDAS). We fitted rainfall data with a function of the form $f(x) = ae^{bx} + c$ (Supplementary Table 2). We calculated ΣLAI regardless of trajectory pressure. Restricting the calculation to when trajectory pressure is greater than 850 hPa gives similar results (Supplementary Fig. 9).

Full Methods and any associated references are available in the online version of the paper.

Received 16 April; accepted 29 June 2012.
Published online 5 September; corrected online 12 September 2012 (see full-text HTML version for details).

1. Bonan, G. B. Forests and climate change: forcings, feedbacks, and the climate benefit of forests. *Science* **320,** 1444–1449 (2008).
2. Shukla, J. & Mintz, Y. Influence of land-surface evapotranspiration on the Earth's climate. *Science* **215,** 1498–1501 (1982).
3. Eltahir, E. A. B. & Bras, R. L. Precipitation recycling in the Amazon basin. *Q. J. R. Meteorol. Soc.* **120,** 861–880 (1994).
4. Henderson-Sellers, A. & Gornitz, V. Possible climatic impacts of land cover transformations, with particular emphasis on tropical deforestation. *Clim. Change* **6,** 231–257 (1984).
5. Lean, J. & Warrilow, D. A. Simulation of the regional climatic impact of Amazon deforestation. *Nature* **342,** 411–413 (1989).
6. Shukla, J., Nobre, C. & Sellers, P. Amazon deforestation and climate change. *Science* **247,** 1322–1325 (1990).
7. Werth, D. & Avissar, R. The local and global effects of Amazon deforestation. *J. Geophys. Res.* **107,** 8087 (2002).
8. Ramos da Silva, R., Werth, D. & Avissar, R. Regional impacts of future land-cover changes on the Amazon basin wet-season climate. *J. Clim.* **21,** 1153–1170 (2008).
9. Hasler, N., Werth, D. & Avissar, R. Effects of tropical deforestation on global hydroclimate: a multimodel ensemble analysis. *J. Clim.* **22,** 1124–1141 (2009).
10. Nobre, P. *et al.* Amazon deforestation and climate change in a coupled model simulation. *J. Clim.* **22,** 5686–5697 (2009).
11. Pitman, A. J. *et al.* Uncertainties in climate responses to past land cover change: first results from the LUCID intercomparison study. *Geophys. Res. Lett.* **36,** L14814 (2009).
12. Butt, N., de Oliveira, P. A. & Costa, M. H. Evidence that deforestation affects the onset of the rainy season in Rondonia, Brazil. *J. Geophys. Res.* **116,** D11120 (2011).
13. Negri, A. J., Adler, R. F., Xu, L. & Surratt, J. The impact of Amazonian deforestation on dry season rainfall. *J. Clim.* **17,** 1306–1319 (2004).
14. Chagnon, F. J. F. & Bras, R. L. Contemporary climate change in the Amazon. *Geophys. Res. Lett.* **32,** L13703 (2005).
15. Huffman, G. *et al.* The TRMM multisatellite precipitation analysis (TMPA): quasi-global, multiyear, combined-sensor precipitation estimates at fine scales. *J. Hydrometeorol.* **8,** 38–55 (2007).
16. Myneni, R. B. *et al.* Global products of vegetation leaf area index and fraction absorbed PAR from year one of MODIS data. *Remote Sens. Environ.* **83,** 214–231 (2002).
17. Gimeno, L., Drumond, A., Nieto, R., Trigo, R. M. & Stohl, A. On the origin of continental precipitation. *Geophys. Res. Lett.* **37,** L13804 (2010).
18. van der Ent, R. J., Savenije, H. H. G., Schaefli, B. & Steele-Dunne, S. C. Origin and fate of atmospheric moisture over continents. *Wat. Resour. Res.* **46,** W09525 (2010).
19. Aragão, L. E. O. C. *et al.* Spatial validation of collection 4 MODIS LAI product in eastern Amazonia. *IEEE Trans. Geosci. Rem. Sens.* **43,** 2526–2534 (2005).
20. Rodell, M. *et al.* The global land data assimilation system. *Bull. Am. Meteorol. Soc.* **85,** 381–394 (2004).
21. Wang, J. F., Bras, R. L. & Eltahir, E. A. B. The impact of observed deforestation on the mesoscale distribution on the mesoscale distribution of rainfall and clouds in Amazonia. *J. Hydrometeorol.* **1,** 267–286 (2000).
22. Garcia-Carreras, L. & Parker, D. J. How does local tropical deforestation affect rainfall? *Geophys. Res. Lett.* **38,** L19802 (2011).
23. Andreae, M. O. *et al.* Smoking rain clouds over the Amazon. *Science* **303,** 1337–1342 (2004).
24. Koren, I. *et al.* Aerosol-induced intensification of rain from the tropics to mid-latitudes. *Nature Geosci.* **5,** 118–122 (2012).
25. Soares-Filho, B. S. *et al.* Modelling conservation in the Amazon basin. *Nature* **440,** 520–523 (2006).
26. Phillips, O. L. *et al.* Drought sensitivity of the Amazon rainforest. *Science* **323,** 1344–1347 (2009).
27. Aragão, L. E. O. C. *et al.* Spatial patterns and fire response of recent Amazonian droughts. *Geophys. Res. Lett.* **34,** L07701 (2007).
28. Davidson, E. A. *et al.* The Amazon basin in transition. *Nature* **481,** 321–328 (2012).
29. Huffman, G. J. Estimates of root-mean-square random error for finite samples of estimated precipitation. *J. Appl. Meteorol.* **36,** 1191–1201 (1997).
30. Smith, T. M., Arkin, P. A., Bates, J. J. & Huffman, G. J. Estimating bias of satellite precipitation estimates. *J. Hydrometeorol.* **7,** 841–856 (2006).

Supplementary Information is available in the online version of the paper.

Acknowledgements D.V.S. acknowledges a Natural Environment Research Council grant (NE/G015015/1). The GLDAS data used in this study were acquired as part of the mission of NASA's Earth Science Division and were archived and distributed by the Goddard Earth Sciences Data and Information Services Center.

Author Contributions D.V.S. and S.R.A. initiated the project. All authors participated in discussions, conducted the analysis, assisted with data interpretation and wrote the manuscript.

Author Information Reprints and permissions information is available at www.nature.com/reprints. The authors declare no competing financial interests. Readers are welcome to comment on the online version of the paper. Correspondence and requests for materials should be addressed to D.V.S. (d.v.spracklen@leeds.ac.uk).

LETTER

doi:10.1038/nature11410

Ploughing the deep sea floor

Pere Puig[1], Miquel Canals[2], Joan B. Company[1], Jacobo Martin[1], David Amblas[2], Galderic Lastras[2], Albert Palanques[1] & Antoni M. Calafat[2]

Bottom trawling is a non-selective commercial fishing technique whereby heavy nets and gear are pulled along the sea floor. The direct impact of this technique on fish populations[1,2] and benthic communities[3,4] has received much attention, but trawling can also modify the physical properties of seafloor sediments, water–sediment chemical exchanges and sediment fluxes[5,6]. Most of the studies addressing the physical disturbances of trawl gear on the seabed have been undertaken in coastal and shelf environments[7,8], however, where the capacity of trawling to modify the seafloor morphology coexists with high-energy natural processes driving sediment erosion, transport and deposition[9]. Here we show that on upper continental slopes, the reworking of the deep sea floor by trawling gradually modifies the shape of the submarine landscape over large spatial scales. We found that trawling-induced sediment displacement and removal from fishing grounds causes the morphology of the deep sea floor to become smoother over time, reducing its original complexity as shown by high-resolution seafloor relief maps. Our results suggest that in recent decades, following the industrialization of fishing fleets, bottom trawling has become an important driver of deep seascape evolution. Given the global dimension of this type of fishery, we anticipate that the morphology of the upper continental slope in many parts of the world's oceans could be altered by intensive bottom trawling, producing comparable effects on the deep sea floor to those generated by agricultural ploughing on land.

Continental slopes are at the transition between shallow continental shelves and deep basins and are often cut by submarine canyons. They represent the steepest part of continental margins, which extend from the shelf break, usually at depths of 100–200 m, to the upper continental rise at depths of 1,500–3,000 m. At fine spatial and temporal scales (that is, excluding tectonics), continental-slope morphological features form as a result of mechanisms governed by erosional and depositional processes[10]. Slope failures and sediment gravity flows[11], geostrophic contour-flowing bottom currents[12], internal waves[13] and dense shelf water cascading[14] are some of the main processes shaping continental slopes.

Bottom trawling is recurrently practised in numerous continental slopes of the world's oceans (Fig. 1). Driven by technical improvements and the exhaustion of traditional fish stocks, trawling fleets have progressively expanded their activities from the continental shelf towards deeper regions[15,16], where background energy levels controlling natural sedimentary processes are generally low except for infrequent, localized events[11,14].

The northwestern Mediterranean continental slope is a region where deep-sea trawling has been practised for a long time. A monospecific fishery targeting blue and red deep-sea shrimp *Aristeus antennatus* (Risso, 1816) was active in this area as early as the 1930s (ref. 17). However, fishing effort (a measure of the amount of fishing, generally defined as the fleet capacity times days at sea) was negligible until the mid-1960s, when the trawling fleet became fully industrialized. This trend notably accelerated in the 1970s in terms of engine power[18] and, subsequently, of gear size, fishing depth and trawled area per haul. The slope fishing grounds in the northern Catalan margin are currently being regularly exploited by 180 large bottom trawlers (that is, each over 15 m in overall length) down to 800 m depth, with greater depths being reached occasionally (Fig. 2).

Time series observations were carried out on the flank of a trawled submarine canyon (La Fonera Canyon, Fig. 2) to measure sediment transport induced by fishing activities. Following an earlier study on sedimentary processes[19], an instrumented mooring was placed at 980 m depth within a tributary valley on the canyon flank to capture the occurrence of trawl-induced sediment gravity flows. The new observations reveal a highly active scenario with the nearly daily occurrence of sediment transport events linked to the passage of the

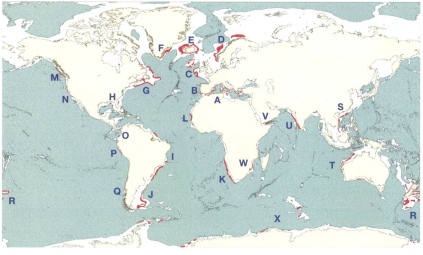

Figure 1 | Map of known trawling grounds on the world continental slopes. Red areas illustrate the extent of the trawling and the letters refer to the main fishery operating in each area, as detailed in the Supplementary Information. Darker blue regions represent water depths exceeding 2,000 m.

[1]Marine Sciences Institute, CSIC, E-08003 Barcelona, Spain. [2]CRG Marine Geosciences, University of Barcelona, E-08028 Barcelona, Spain.

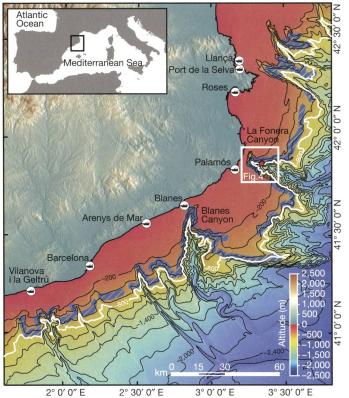

Figure 2 | Bathymetric map of the study area. Bathymetric map of the northern Catalan margin (northwestern Mediterranean) showing the main trawling grounds on the open continental slope and canyon flanks (blue hatching). Data was obtained from the VMS. The largest ports of the area (vessels in white circles) and the 800-m isobath (white thick contour) are highlighted. The location of Fig. 4 and the mooring station (red star in white box; see Fig. 3 and Supplementary Fig. 1) in La Fonera (also named Palamós) Canyon are indicated.

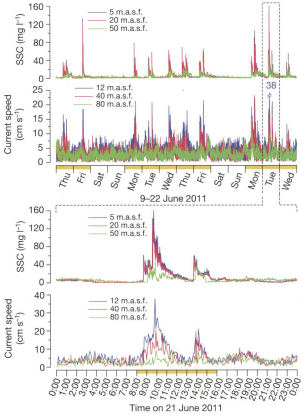

Figure 3 | Time series observations of trawling-induced sediment gravity flows. Graphs showing near-bottom suspended sediment concentration (SSC) and current speed records observed at the northern flank of La Fonera Canyon during a two-week period at different heights above the sea floor (m.a.s.f., metres above sea floor). Sediment transport events were observed during weekdays (that is, working days for the fishery), but not on weekends. The detail of a one-day record (21 June 2011) shows two sharp increases in SSC and the consequent intensification of the current speed (directed downslope towards 192°), with higher velocities closer to the sea floor that denote the occurrence of sediment gravity flows. The two peaks correspond to the two main hauls of the trawling fleet, the first one heading offshore and the second one heading to port. Orange bars on the *x* axes denote working days and working hours, respectively. Note the change in scale of the current-speed *y* axes. See mooring location in Figs 2 and 4 and Supplementary Figs 2 and 3.

trawling fleet upslope of the mooring site (Fig. 3). Increases of near-bottom suspended sediment concentrations and current velocities from trawl-induced sediment gravity flows were observed repeatedly during weekdays at working hours, indicating a periodic sediment removal from fishing grounds. Such flows reached maximum downslope velocities of up to 38 cm s^{-1} and concentrations of up to 236 mg l^{-1} (Fig. 3; Supplementary Fig. 1a). Maximum instantaneous sediment fluxes at 4–6 m above the sea floor (m.a.s.f.) were 34 g m^{-2} s^{-1} and accounted for a cumulative transport of about 1.1 tonnes m^{-2} during the observational period (Supplementary Fig. 1b). This near-bottom transport is of the same order of magnitude as the wintertime downslope cumulative transport induced by storms and dense shelf water cascading in the nearby Cap de Creus and Lacaze–Duthiers submarine canyon heads[14,20]. Integrating the sediment transport from 4 to 50 m.a.s.f., a minimum of 5.4×10^3 tonnes of sediment is estimated to have been exported downslope through the monitored tributary valley in 136 days as a consequence of trawling activities (Supplementary Fig. 1c). These recurrent trawl-induced low-concentration sediment gravity flows only travel a few kilometres downslope from the canyon flank to the main canyon axis where they deposit their sediment load[19]. Consequently, after the industrialization of the fishing fleet, a twofold increase of the sediment accumulation rates occurred in the canyon axis[18].

In 2007 a high-resolution multibeam bathymetry survey was conducted in La Fonera Canyon (Fig. 4). Analysis of the bathymetry data revealed a noticeable smoothing of bottom topography along the northern canyon flank at depths shallower than 800 m (Fig. 4a), which had been tentatively interpreted as being caused by dense shelf water cascading flowing southwards[21]. Canyon flank smoothing, however, was also observed locally in the southern canyon flank (Fig. 4a), away from the region potentially affected by cascading flows, challenging previous hypotheses. The fact that the lower limit of the smoothed bathymetric range coincided with the maximum trawled depths reported by the fishermen operating in the area pointed to trawling as a potential seafloor shaping agent within this depth range.

Plotting four years (2007–2010) of satellite-based navigation tracks from all large bottom trawlers operating in the area on top of the multibeam bathymetry of La Fonera Canyon revealed that navigation tracks coincided with the smoothed canyon flanks at depths shallower than 800 m (Fig. 4b) in a region characterized by homogeneous slopes (Fig. 4c) and low rugosity (a dimensionless measure of surface roughness) values (Supplementary Fig. 2). In contrast, untrawled canyon flank segments are dominated by a dense network of tributary valleys that progress upslope from the main canyon axis, reaching up to five orders of bifurcation[21]. Such complex morphology is missing in the trawled depth range and slightly below. Here the sea floor becomes smoother and only the main branches of the tributary valley networks are preserved (Fig. 4, Supplementary Fig. 3). Therefore, a causative relationship can be established between trawling-induced sediment erosion effects and the reduction of morphological complexity in the studied area. Contrasts between untrawled and trawled seafloor

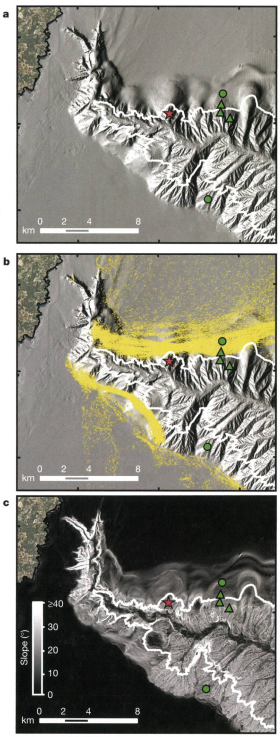

Figure 4 | Seafloor morphology and bottom trawling in La Fonera Canyon. **a**, Shaded relief image from a 15-m resolution bathymetric grid showing gullied and smoothed seafloor regions, the latter at depths shallower than 800 m (white contour) especially on the northern flank but also in parts of the southern flank. **b**, Positioning data (small yellow arrows) of bottom trawling vessels fishing from 2007 to 2010. **c**, Slope map illustrating regions of homogeneous values between 10° and 30° in the most heavily trawled regions of the canyon flanks compared to untrawled regions where the gullied sea floor and the tributary valley networks are apparent, displaying higher (>40°) and lower (<10°) slopes in the walls and axes of the various valleys, respectively. The positions of the mooring station (red star; see Fig. 3 and Supplementary Fig. 1), sediment cores (green dots; see Supplementary Fig. 4) and ROV images (green triangles; see Supplementary Fig. 5) are also indicated.

regions are also evident in sediment cores (Supplementary Fig. 4) and remote operated vehicle (ROV) footage from canyon flanks (Supplementary Fig. 5). Considering only the satellite-based navigation tracks from 2010, we determine that an area of 41.6 km^2 was affected in the northern canyon flank alone. This represents 76.3% of the canyon flank area that is shallower than 800 m.

To provide an estimate of the volume of sediment that can be remobilized downslope by trawling activities, the integrated sediment transport during the observational period (Supplementary Fig. 1c) was converted to volume using a mean dry bulk density of 0.6 g cm^{-3} (Supplementary Fig. 4) and extrapolated to one year. Using a drainage basin of 4.2 km^2 (about 10% of the canyon flank trawled during 2010) for the monitored tributary valley, approximately 2.4×10^{-4} km^3 is estimated to have been exported from this fishing ground annually. Assuming an equal sediment yield since the 1970s, following the industrialization of the trawling fleet[16], a total of around 1.0×10^{-2} km^3 has potentially been removed from this canyon flank by bottom trawling, contributing to its morphological change. The actual volume remobilized over this period could easily be larger, taking into account that the surface sediments from the fishing ground are at present overconsolidated (Supplementary Fig. 4) and that downslope sediment fluxes in the past, when the morphology was rougher and the surface sediments unconsolidated and easier to resuspend, could have been much higher. Although the estimated annual volume is similar to the annual sediment volumes involved in canyon head failures, the total estimated volume remobilized from this canyon flank over four decades is two to five orders of magnitude smaller than the sediment volumes involved in open-slope submarine failures that occur over geological periods of time (Supplementary Table 1).

Recent studies assessing the impact of anthropogenic activities in the marine ecosystems have already highlighted the effects caused by bottom trawling, both at global scale[22] and in deep-sea environments, where its spatial extent has been estimated to be an order of magnitude greater than the total extent of all other anthropogenic activities[23]. Given that deep-sea bottom trawling has spread around the globe during the past decades[4,15,16] (Fig. 1), the present study raises questions over whether bottom trawling is becoming an important driver of the upper continental slope seascape evolution during the Anthropocene[24], at a scale that has been previously unnoticed.

The relevance of bottom trawling in the alteration of natural sediment fluxes over continental shelves has already been pointed out[6,25], but our results stress that, in addition to altering deep-sea sediment fluxes, bottom trawling also modifies the shape of the upper continental slope, particularly in regions that are strongly affected by this fishing technique. In these portions of the margin, the morphological complexity, as well as benthic habitat heterogeneity, has been drastically reduced, potentially affecting species diversity by regulating levels of competition, predation and physiological stress[26]. Such seascape alteration could also affect ecosystem functioning, because deep-sea ecosystems have evolved in these environments to rely upon the original morphological complexity and biogeochemical properties of untrawled surface sediments to support benthic organisms.

This process of seascape spatial levelling has many parallels with landscape evolution under anthropogenic pressures. Changes in land use during the twentieth century resulted in a reduction of landscape diversity almost everywhere through the spreading of arable land and timber plantations, which led to the gradual disappearance of both major and minor elements of topography[27]. Bottom trawling has been compared to forest clear-cutting[28], although our results suggest that a better comparison might be intensive agricultural activities. Trawled continental-slope environments are the underwater equivalent of a gullied hill slope on land, part of which has been transformed into crop fields that are ploughed regularly, thus replacing the natural contour-normal drainage pattern by levelled areas with a smaller-scale contour-parallel alignment of troughs and crests (Fig. 4, Supplementary Fig. 5). Differences exist in the processes that operate in submarine

and subaerial environments. Although farmers usually plough their land a few times per year, at sea trawling can occur on a nearly daily basis (Fig. 3, Supplementary Fig. 1). Also, agricultural activities do not generate the periodic sediment gravity flows that contribute to remove material from fishing grounds. However, the frequent repeated trawling (ploughing) over the same ground, involving displacement of sediments owing to mechanical redistribution, is what ultimately causes the levelling of the surface and produces morphological effects similar to those of a farmer's field.

Warming, sea-level rise, acidification and changes in ocean circulation have been listed as the major present and foreseeable human footprints in the ocean[29]. This work argues for the inclusion in that list of the modification of the submarine landscape by trawling, along with the ecological and biogeochemical consequences that may derive from it. Human-induced changes on Earth's geomorphology, already well documented for emerged land[30], are also present in submerged regions.

METHODS SUMMARY

This study was conducted using a unique, dedicated experimental strategy combining monitoring of contemporary sediment transport processes, sediment coring, remote operated vehicle (ROV) *in situ* observations and high-resolution multibeam bathymetric surveys, coupled with the information provided by satellite-based navigation tracks of fishing vessels. Swath bathymetry data from La Fonera (also named Palamós) Canyon were obtained during the EUROLEÓN cruise onboard RV *Hespérides* in October 2007 using two Simrad multibeam echosounders: EM-1002S in shallow and EM-120 in deep waters. A bathymetric grid of 15-m resolution was generated to obtain the Digital Terrain Model used in this study. Contemporary sediment transport processes were measured by an instrumented mooring line equipped with a downward-looking 300 kHz acoustic Doppler current profiler (ADCP) from Teledyne RDI and three turbidimeters (AQUA logger 520 from the Aquatec Group) deployed from 10 May to 22 September 2011 on the northern flank of La Fonera Canyon, at 980 m depth within the Montgri tributary valley axis. Seafloor sediment samples from the canyon flanks were collected using a six-tube multicorer from KC-Denmark during the HERMIONE-1 cruise onboard the RV *García del Cid*. A vertical slab of undisturbed sediment was removed from one of the core tubes for X-ray analysis. A second core tube was sliced at 1-cm intervals for granulometric analyses. Bottom video imagery of La Fonera canyon flanks was recorded in July 2011 during the PROMARES-OASIS DEL MAR research cruise onboard RV *Sarmiento de Gamboa* by using a high-definition Kongsberg OE14-502A camera mounted on the 2000-m-depth-rated SubAtlantic Super Mohawk 24 ROV *Lirapus* belonging to the Spanish Institute of Oceanography. The satellite-based tracking of fishing trawlers operating in the study area from the Vessel Monitoring Systems (VMS) data for 2007–2010 was provided by the Fishing Monitoring Centre of the Spanish General Secretariat of Maritime Fishing (SEGEMAR).

Full Methods and any associated references are available in the online version of the paper.

Received 20 January; accepted 10 July 2012.
Published online 5 September 2012.

1. Thurstan, R. H., Brockington, S. & Roberts, C. M. The effects of 118 years of industrial fishing on UK bottom trawl fisheries. *Nature Commun.* **1,** 15 (2010).
2. Norse, E. A. *et al.* Sustainability of deep-sea fisheries. *Mar. Policy* **36,** 307–320 (2012).
3. Watling, L. & Norse, E. A. Effects of mobile fishing gear on marine benthos. *Conserv. Biol.* **12,** 1178–1179 (1998).
4. Roberts, J. M., Wheeler, A. J. & Freiwald, A. Reefs of the deep: the biology and geology of cold-water coral ecosystems. *Science* **312,** 543–547 (2006).
5. Jones, J. B. Environmental impact of trawling on the seabed: a review. *N. Z. J. Mar. Freshwat. Res.* **26,** 59–67 (1992).
6. Churchill, J. H. The effect of commercial trawling on sediment resuspension and transport over the Middle Atlantic Bight continental-shelf. *Cont. Shelf Res.* **9,** 841–865 (1989).
7. Schwinghamer, P. *et al.* Effects of experimental otter trawling on surficial sediment properties of a sandy-bottom ecosystem on the Grand Banks of Newfoundland. *Conserv. Biol.* **12,** 1215–1222 (1998).
8. Brown, E. J., Finney, B., Dommisse, M. & Hills, S. Effects of commercial otter trawling on the physical environment of the southeastern Bering Sea. *Cont. Shelf Res.* **25,** 1281–1301 (2005).
9. Nittrouer, C. A. & Wright, L. D. Transport of particles across continental shelves. *Rev. Geophys.* **32,** 85–113 (1994).
10. Pratson, L. F. *et al.* in *Continental-Margin Sedimentation: from Sediment Transport to Sequence Stratigraphy* (eds Nittrouer, C. A. *et al.*) 339–380 (Blackwell, 2007).
11. Piper, D. J. W. & Normark, W. R. Processes that initiate turbidity currents and their influence on turbidites: a marine geology perspective. *J. Sediment. Res.* **79,** 347–362 (2009).
12. Heezen, B. C., Hollister, C. D. & Ruddiman, W. F. Shaping of the continental rise by deep geostrophic contour currents. *Science* **152,** 502–508 (1966).
13. Cacchione, D. A., Pratson, L. F. & Ogston, A. S. The shaping of continental slopes by internal tides. *Science* **296,** 724–727 (2002).
14. Canals, M. *et al.* Flushing submarine canyons. *Nature* **444,** 354–357 (2006).
15. Gordon, J. D. M., Bergstad, O. A., Figueiredo, I. & Menezes, G. Deep-water fisheries of the Northeast Atlantic: I. Description and current trends. *J. Northwest Atlantic Fish. Sci.* **31,** 137–150 (2003).
16. Morato, T., Watson, R., Pitcher, T. J. & Pauly, D. Fishing down the deep. *Fish Fish.* **7,** 24–34 (2006).
17. Tobar, R. & Sardà, F. Análisis de la evolución de las capturas de gamba rosada, *Aristeus antennatus* (Risso, 1816), en los últimos decenios en Cataluña. *Inf. Técn. Inv. Pesq.* **142,** 3–20 (1987).
18. Martín, J., Puig, P., Palanques, A., Masqué, P. & García-Orellana, J. Effect of commercial trawling on the deep sedimentation in a Mediterranean submarine canyon. *Mar. Geol.* **252,** 150–155 (2008).
19. Palanques, A. *et al.* Evidence of sediment gravity flows induced by trawling in the Palamós (Fonera) submarine canyon (northwestern Mediterranean). *Deep-Sea Res.* **53,** 201–214 (2006).
20. Palanques, A. *et al.* Suspended sediment fluxes and transport processes in the Gulf of Lions submarine canyons. The role of storms and dense water cascading. *Mar. Geol.* **234,** 43–61 (2006).
21. Lastras, G. *et al.* Understanding sediment dynamics of two large submarine valleys from seafloor data: Blanes and La Fonera canyons, northwestern Mediterranean Sea. *Mar. Geol.* **280,** 20–39 (2011).
22. Halpern, B. S. *et al.* A global map of human impact on marine ecosystems. *Science* **319,** 948–952 (2008).
23. Benn, A. R. *et al.* Human activities on the deep seafloor in the North East Atlantic: an assessment of spatial extent. *PLoS ONE* **5,** e12730 (2010).
24. Crutzen, P. J. Geology of mankind. *Nature* **415,** 23 (2002).
25. Ferré, B., Durrieu de Madron, X., Estournel, C., Ulses, C. & Le Corre, G. Impact of natural (waves and currents) and anthropogenic (trawl) resuspension on the export of particulate matter to the open ocean: application to the Gulf of Lion (NW Mediterranean). *Cont. Shelf Res.* **28,** 2071–2091 (2008).
26. Levin, L. A., Sibuet, M., Gooday, A. J., Smith, C. R. & Vanreusel, A. The roles of habitat heterogeneity in generating and maintaining biodiversity on continental margins: an introduction. *Mar. Ecol.* **31,** 1–5 (2010).
27. Csorba, P. in *Anthropogenic Geomorphology* (eds Szabó, J., Dávid, L. & Dénes, L.) 39–52 (Springer, 2010).
28. Watling, L. & Norse, E. A. Disturbance of the seabed by mobile fishing gear: a comparison with forest clear-cutting. *Conserv. Biol.* **12,** 1180–1197 (1998).
29. Tyrrell, T. Anthropogenic modification of the oceans. *Phil. Trans. R. Soc. Lond. A* **369,** 887–908 (2011).
30. Price, S. J., Ford, J. R., Cooper, A. H. & Neal, C. Humans as major geological and geomorphological agents in the Anthropocene: the significance of artificial ground in Great Britain. *Phil. Trans. R. Soc. A* **369,** 1056–1084 (2011).

Supplementary Information is available in the online version of the paper.

Acknowledgements This work was supported by various research projects: HERMIONE (226354 and CTM2010-11084-E), DOS MARES (CTM2010-21810-C03), OASIS DEL MAR—Obra Social "la Caixa", GRACCIE-CONSOLIDER (CSD2007-00067) and REDECO (CTM2008-04973-E). We also received support from Catalan Government Grups de Recerca Consolidats grants (2009 SGR 899 and 1305). VMS data and support were provided by the Spanish General Secretariat of Maritime Fishing (SEGEMAR). Assistance at sea by the crews of RV *Hespérides*, RV *Sarmiento de Gamboa* and RV *García del Cid* is also acknowledged. J.M. was funded through a JAE-DOC contract granted by Consejo Superior de Investigaciones Cientificas and co-financed by the European Social Fund. F. Sardà and T. Milligan provided comments on the manuscript. The final document benefited from a review by P. Talling.

Author Contributions All authors contributed to the design and implementation of the experimental strategy. P.P., M.C. and J.B.C. steered the integration and joint analysis of the data. P.P. and J.M. drafted the manuscript, which was critically revised and implemented by M.C. and J.B.C. M.C. designed and coordinated the acquisition of seafloor data, including multibeam bathymetry and ROV observations, and obtained VMS data. P.P., J.M. and A.P. acquired and processed the mooring time series and the sediment cores. J.M. and J.B.C. conducted the bibliographical survey of global slope fishing grounds. D.A., M.C. and P.P. produced the various maps in the paper, to which J.M and J.B.C. contributed. G.L. coordinated the multibeam bathymetry processing and, jointly with M.C., created the slope failures table. J.B.C. provided knowledge about local fishing activities. M.C., D.A., G.L. and A.M.C. described and interpreted the whole set of seafloor data. All authors discussed the results and commented on the final version of the manuscript.

Author Information Reprints and permissions information is available at www.nature.com/reprints. The authors declare no competing financial interests. Readers are welcome to comment on the online version of the paper. Correspondence and requests for materials should be addressed to P.P. (ppuig@icm.csic.es).

LETTER

doi:10.1038/nature11318

Averting biodiversity collapse in tropical forest protected areas

A list of the authors and their affiliations appears at the end of the paper.

The rapid disruption of tropical forests probably imperils global biodiversity more than any other contemporary phenomenon[1–3]. With deforestation advancing quickly, protected areas are increasingly becoming final refuges for threatened species and natural ecosystem processes. However, many protected areas in the tropics are themselves vulnerable to human encroachment and other environmental stresses[4–9]. As pressures mount, it is vital to know whether existing reserves can sustain their biodiversity. A critical constraint in addressing this question has been that data describing a broad array of biodiversity groups have been unavailable for a sufficiently large and representative sample of reserves. Here we present a uniquely comprehensive data set on changes over the past 20 to 30 years in 31 functional groups of species and 21 potential drivers of environmental change, for 60 protected areas stratified across the world's major tropical regions. Our analysis reveals great variation in reserve 'health': about half of all reserves have been effective or performed passably, but the rest are experiencing an erosion of biodiversity that is often alarmingly widespread taxonomically and functionally. Habitat disruption, hunting and forest-product exploitation were the strongest predictors of declining reserve health. Crucially, environmental changes immediately outside reserves seemed nearly as important as those inside in determining their ecological fate, with changes inside reserves strongly mirroring those occurring around them. These findings suggest that tropical protected areas are often intimately linked ecologically to their surrounding habitats, and that a failure to stem broad-scale loss and degradation of such habitats could sharply increase the likelihood of serious biodiversity declines.

Tropical forests are the biologically richest ecosystems on Earth[1–3]. Growing concerns about the impacts of anthropogenic pressures on tropical biodiversity and natural ecosystem services have led to increases in the number and extent of protected areas across the tropics[10]. However, much remains unknown about the likelihood of biodiversity persisting in such protected areas. Remote-sensing technologies offer a bird's-eye view of tropical forests and provide many important insights[6,11–13], but are largely unable to discern crucial on-the-ground changes in forest biodiversity and ecological functioning[14].

To appraise both the ecological integrity and threats for tropical protected areas on a global scale, we conducted a systematic and uniquely comprehensive assessment of long-term changes within 60 protected areas stratified across the world's major tropical forest regions (Supplementary Fig. 1). To our knowledge, no other existing data set includes such a wide range of biodiversity and threat indicators for such a large and representative network of tropical reserves. Our study was motivated by three broad issues: whether tropical reserves will function as 'arks' for biodiversity and natural ecosystem processes; whether observed changes are mainly concordant or idiosyncratic among different protected areas; and what the principal predictors of reserve success or failure are, in terms of their intrinsic characteristics and drivers of change.

To conduct our study we amassed expert knowledge from 262 detailed interviews, focusing on veteran field biologists and environmental scientists who averaged nearly 2 decades of experience (mean ± s.d., 19.1 ± 9.6 years) at each protected area. Each interviewed researcher completed a detailed 10-page questionnaire, augmented by a telephone or face-to-face interview (see Supplementary Information). The questionnaires focused on longer-term (approximately 20–30-year) changes in the abundance of 31 animal and plant guilds (trophically or functionally similar groups of organisms), which collectively have diverse and fundamental roles in forest ecosystems (Table 1). We also recorded data on 21 potential drivers of environmental change both inside each reserve and within a 3-km-wide buffer zone immediately surrounding it (Table 1).

Our sample of protected areas spans 36 nations and represents a geographically stratified and broadly representative selection of sites across the African, American and Asia-Pacific tropics (Supplementary Fig. 1). The reserves ranged from 160 ha to 3.6 million ha in size, but most (85%) exceeded 10,000 ha in area (median = 99,350 ha; lower decile = 7,000 ha; upper decile = 750,000 ha). The protected areas fall under various International Union for Conservation of Nature (IUCN) reserve classifications. Using data from the World Database on Protected Areas (http://www.wdpa.org), we found no significant difference ($P = 0.13$) in the relative frequency of high-protection (IUCN Categories I–IV), multiple-use (Categories V–VI) and

Table 1 | The 31 animal and plant guilds, and the 21 environmental drivers assessed both inside and immediately outside each protected area.

Guilds	Potential environmental drivers
Broadly forest-dependent guilds	
Apex predators	Changes in natural-forest cover
Large non-predatory species	Selective logging
Primates	Fires
Opportunistic omnivorous mammals	Hunting
Rodents	Harvests of non-timber forest products
Bats	Illegal mining
Understory insectivorous birds	Roads
Raptorial birds	Automobile traffic
Larger frugivorous birds	Exotic plantations
Larger game birds	Human population density
Lizards and larger reptiles	Livestock grazing
Venomous snakes	Air pollution
Non-venomous snakes	Water pollution
Terrestrial amphibians	Stream sedimentation
Stream-dwelling amphibians	Soil erosion
Freshwater fish	River & stream flows
Dung beetles	Ambient temperature
Army or driver ants	Annual rainfall
Aquatic invertebrates	Drought severity or intensity
Large-seeded old-growth trees	Flooding
Epiphytes	Windstorms
Other functional groups	
Ecological specialists	
Species requiring tree cavities	
Migratory species	
Disturbance-favouring guilds	
Lianas and vines	
Pioneer and generalist trees	
Exotic animal species	
Exotic plant species	
Disease-vectoring invertebrates	
Light-loving butterflies	
Human diseases	

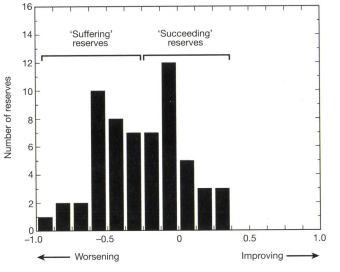

Figure 1 | Distribution of the 'reserve-health index' for 60 protected areas spanning the world's major tropical forest regions. This relative index averages changes in 10 well-studied guilds of animals and plants, including disturbance-avoiding and disturbance-favouring groups, over the past 20 to 30 years.

unclassified reserves between our sample of 60 reserves and all 16,038 reserves found in the same tropical nations (Supplementary Fig. 2). We also found no significant difference ($P = 0.08$) in the geographical isolation of our reserves (travel time to the nearest city with greater than 50,000 residents) relative to a random sample of 60 protected areas stratified across the same 36 nations (Supplementary Fig. 3).

We critically assessed the validity of our interview data by comparing them to 59 independent time-series data sets in which change in a single guild or environmental driver was assessed for one of our protected areas. Collectively, our meta-analysis included some data on 15 of the guilds, 13 of the drivers and 27 of the protected areas in our study (Supplementary Table 1). Most (86.4%) of the independent data sets supported our interview results, and in no case did an independent test report a trend opposite in sign to our interview-based findings.

Our analyses suggest that the most sensitive guilds in tropical protected areas include apex predators, large non-predatory vertebrates, bats, stream-dwelling amphibians, terrestrial amphibians, lizards and larger reptiles, non-venomous snakes, freshwater fish, large-seeded old-growth trees, epiphytes and ecological specialists (all $P < 0.0056$, with effect sizes ranging from -0.36 to -1.05; Supplementary Table 2). Several other groups were somewhat less vulnerable, including primates, understory insectivorous birds, large frugivorous birds, raptorial birds, venomous snakes, species that require tree cavities, and migratory species (all $P < 0.05$, with effect sizes from -0.27 to -0.53). In addition, five groups increased markedly in abundance in the reserves, including pioneer and generalist trees, lianas and vines, invasive animals, invasive plants and human diseases (all $P < 0.0056$, with effect sizes from 0.44 to 1.17).

To integrate these disparate data, we generated a 'reserve-health index' that focused on 10 of the best-studied guilds (data for each available at ≥ 80% of reserves), all of which seem to be sensitive to environmental changes in protected areas. Six of these are generally 'disturbance avoiders' (apex predators, large non-predatory vertebrates, primates, understory insectivorous birds, large frugivorous birds and large-seeded old-growth trees) and the remainder seem to be 'disturbance-favouring' groups (pioneer and generalist trees, lianas and vines, exotic animals and exotic plants). For each protected area, we averaged the mean values for each group, using negative values to indicate increases in abundance of the disturbance-favouring guilds.

The reserve-health index varied greatly among the different protected areas (Fig. 1). About four-fifths of the reserves had negative values, indicating some decline in reserve health. For 50% of all reserves this decline was relatively serious (mean score < -0.25), with the affected organisms being remarkable for their high functional and taxonomic diversity (Fig. 2). These included plants with varying growth forms and life-history strategies, and fauna that differed widely in body size, trophic level, foraging strategies, area needs, habitat use and other attributes. The remaining reserves generally exhibited much more positive outcomes for biodiversity (Fig. 2), although a few disturbance-favouring guilds, such as exotic plants and pioneer and generalist trees, often increased even within these areas.

An important predictor of reserve health was improving reserve management. According to our experts, reserves in which actual, on-the-ground protection efforts (see Supplementary Information) had increased over the past 20 to 30 years generally fared better than those in which protection had declined; a relationship that was consistent across all three of the world's major tropical regions (Fig. 3). Indeed, on-the-ground protection has increased in more than half of the reserves over the past 20 to 30 years, and this is assisting efforts to limit threats such as deforestation, logging, fires and hunting within these reserves (Supplementary Table 3), relative to areas immediately outside (Supplementary Table 4).

However, our findings show that protecting biodiversity involves more than just safeguarding the reserves themselves. In many instances, the landscapes and habitats surrounding reserves are under imminent threat[5,6,15] (Fig. 4 and Supplementary Tables 3 and 4). For example, 85% of our reserves suffered declines in surrounding forest cover in the last 20 to 30 years, whereas only 2% gained surrounding forest. As shown by general linear models (Supplementary Table 5), such changes can seriously affect reserve biodiversity. Among the

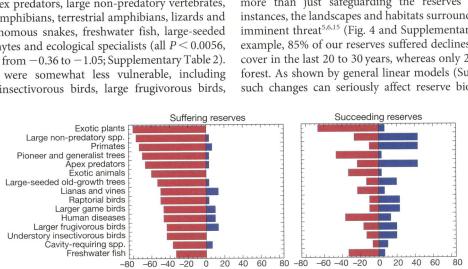

Figure 2 | Percentages of reserves that are worsening versus improving for key disturbance-sensitive guilds, contrasted between 'suffering' and 'succeeding' reserves (which are distinguished by having lower (< -0.25) versus higher (≥ -0.25) values for the reserve-health index, respectively). For disturbance-favouring organisms such as exotic plants and animals, pioneer and generalist trees, lianas and vines, and human diseases, the reserve is considered to be worsening if the group increased in abundance. For any particular guild, reserves with missing or zero values (no trend) are not included.

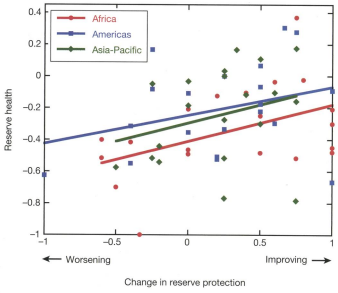

Figure 3 | Effects of improving on-the-ground protection on a relative index of reserve health. This positive relationship held across all three tropical continents (a general linear model showed that the protection term was the most effective predictor of reserve health (Akaike's information criterion weight, 0.595; deviance explained, 11.4%), with the addition of 'continent' providing only a small improvement in model fit (Akaike's information criterion weight, 0.317; deviance explained, 16.3%).

potential drivers of declining reserve health, three of the most important predictors involved ecological changes outside reserves (declining forest cover, increasing logging and increasing fires outside reserves; Supplementary Fig. 6). The remainder involved changes within reserves (particularly declining forest cover and increasing hunting, as well as increasing logging and harvests of non-timber forest products; Supplementary Table 5).

Thus, changes both inside and outside reserves determine their ecological viability, with forest disruption (deforestation, logging and fires), and overexploitation of wildlife and forest resources (hunting and harvests of non-timber forest products) having the greatest direct negative impacts. Other environmental changes, such as air and water pollution, increases in human population densities and climatic change (changes in total rainfall, ambient temperature, droughts and windstorms) generally had weaker or more indirect effects over the last 20 to 30 years (Supplementary Table 5).

Environmental degradation occurring around a protected area could affect biodiversity in many ways, such as by increasing reserve isolation, area and edge effects[15–19]. However, we discovered that its effects are also more insidious: they strongly predispose the reserve itself to similar kinds of degradation. Nearly all (19 of 21) of the environmental drivers had positive slopes when comparing their direction and magnitude inside versus outside reserves (Fig. 5). Among these, 13 were significant even with stringent Bonferroni corrections ($P < 0.0071$) and 17 would have been significant if tested individually ($P < 0.05$). As expected, the associations were strongest for climate parameters but were also strong for variables describing air and water pollution, stream sedimentation, hunting, mining, harvests of non-timber forest products and fires. To a lesser extent, trends in forest cover, human populations, road expansion and automobile traffic inside reserves also mirror those occurring outside reserves (Fig. 5).

Our findings signal that the fates of tropical protected areas will be determined by environmental changes both within and around the reserves, and that pressures inside reserves often closely reflect those occurring around them. For many reasons, larger reserves should be more resilient to such changes[15–22], although we found that removing the effects of reserve area statistically did not consistently weaken the correlations between changes inside versus outside protected areas (Supplementary Table 6).

Our study reveals marked variability in the health of tropical protected areas. It indicates that the best strategy for maintaining biodiversity within tropical reserves is to protect them against their major proximate threats, particularly habitat disruption and overharvesting. However, it is not enough to confine such efforts to reserve interiors while ignoring their surrounding landscapes, which are often being rapidly deforested, degraded and overhunted[5,6,13,15] (Fig. 5). A failure to limit interrelated internal and external threats could predispose reserves to ecological decay, including a taxonomically and functionally

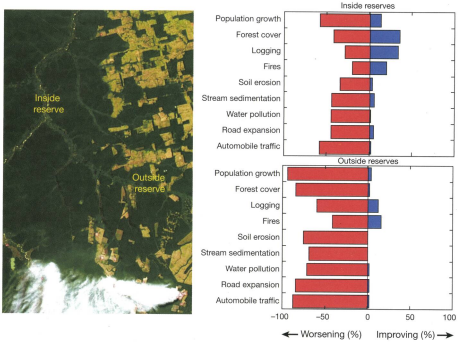

Figure 4 | Comparison of ecological changes inside versus outside protected areas, for selected environmental drivers. The image is an example of the strong distinction in disturbance inside versus outside a reserve. The bars show the percentages of reserves with improving versus worsening conditions.

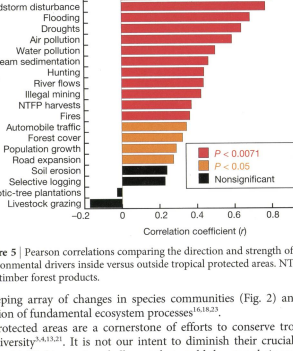

Figure 5 | Pearson correlations comparing the direction and strength of 21 environmental drivers inside versus outside tropical protected areas. NTFP, non-timber forest products.

sweeping array of changes in species communities (Fig. 2) and an erosion of fundamental ecosystem processes[16,18,23].

Protected areas are a cornerstone of efforts to conserve tropical biodiversity[3,4,13,21]. It is not our intent to diminish their crucial role but to highlight growing challenges that could threaten their success. The vital ecological functions of wildlife habitats surrounding protected areas create an imperative, wherever possible, to establish sizeable buffer zones around reserves, maintain substantial reserve connectivity to other forest areas and promote lower-impact land uses near reserves by engaging and benefiting local communities[4,15,24–27]. A focus on managing both external and internal threats should also increase the resilience of biodiversity in reserves to potentially serious climatic change[28–30] in the future.

METHODS SUMMARY

Our interview protocol, rationale, questionnaire and data analyses are detailed in the Supplementary Information. We selected protected areas broadly to span the African, American and Asia-Pacific tropics (Supplementary Fig. 1), focusing on sites with mostly tropical or subtropical forest that had at least 10 refereed publications and 4–5 researchers with long-term experience who could be identified and successfully interviewed.

We devised a robust and relatively simple statistical approach to assess temporal changes in the abundance of each guild and in each potential environmental driver across our reserve network (see Supplementary Information). In brief, this involved asking each expert whether each variable had markedly increased, remained stable or markedly declined for each reserve. These responses were scored as 1, 0 and −1, respectively. For each response, the expert was also asked to rank their degree of confidence in their knowledge. After discarding responses with lower confidence, scores from the individual experts at each site were pooled to generate a mean value (ranging from −1.0 to 1.0) to estimate the long-term trend for each variable.

The means for each variable across all 60 sites were then pooled into a single data distribution. We used bootstrapping (resampling with replacement; 100,000 iterations) to generate confidence intervals for the overall mean of the data distribution. If the confidence intervals did not overlap zero, then we interpreted the trend as being non-random. Because we tested many different guilds, we used a stringent Bonferroni correction ($P \leq 0.0056$) to reduce the likelihood of Type I statistical errors, although we also identified guilds that showed evidence of trends ($P \leq 0.05$) if tested individually. For comparison, we estimated effect sizes (bootstrapped mean divided by s.d., with negative values indicating declines) for changes in guild abundances and for potential drivers inside and outside reserves (Supplementary Tables 2–4).

Received 24 February; accepted 14 June 2012.
Published online 25 July; corrected online 12 September 2012 (see full-text HTML version for details).

1. Pimm, S. L. & Raven, P. R. Biodiversity: extinction by numbers. *Nature* **403,** 843–845 (2000).
2. Bradshaw, C. J. A., Sodhi, N. S. & Brook, B. W. Tropical turmoil—a biodiversity tragedy in progress. *Front. Ecol. Environ* **7,** 79–87 (2009).
3. Gibson, L. *et al.* Primary forests are irreplaceable for sustaining tropical biodiversity. *Nature* **478,** 378–381 (2011).
4. Bruner, A. G., Gullison, R., Rice, R. E. & da Fonseca, G. Effectiveness of parks in protecting tropical biodiversity. *Science* **291,** 125–128 (2001).
5. Curran, L. M. *et al.* Lowland forest loss in protected areas of Indonesian Borneo. *Science* **303,** 1000–1003 (2004).
6. DeFries, R., Hansen, A., Newton, A. C. & Hansen, M. C. Increasing isolation of protected areas in tropical forests over the past twenty years. *Ecol. Appl.* **15,** 19–26 (2005).
7. Lovejoy, T. E. Protected areas: A prism for a changing world. *Trends Ecol. Evol.* **21,** 329–333 (2006).
8. Possingham, H. P., Wilson, K. A., Andelman, S. J. & Vynne, C. H. in *Principles of Conservation Biology* (eds Groom, M. J., Meffe, G. K. & Carroll, C. R.) (Sinauer, 2006).
9. Joppa, L. N., Loarie, S. & Pimm, S. L. On the protection of "protected areas". *Proc. Natl Acad. Sci. USA* **105,** 6673–6678 (2008).
10. Jenkins, C. N. & Joppa, L. Expansion of the global terrestrial protected area system. *Biol. Conserv.* **142,** 2166–2174 (2009).
11. Asner, G. P. *et al.* Selective logging in the Brazilian Amazon. *Science* **310,** 480–482 (2005).
12. Wright, S. J., Sanchez-Azofeifa, G., Portillo-Quintero, C. & Davies, D. Poverty and corruption compromise tropical forest reserves. *Ecol. Appl.* **17,** 1259–1266 (2007).
13. Adeney, J. M., Christensen, N. & Pimm, S. L. Reserves protect against deforestation fires in the Amazon. *PLoS ONE* **4,** e5014 (2009).
14. Peres, C. A., Barlow, J. & Laurance, W. F. Detecting anthropogenic disturbance in tropical forests. *Trends Ecol. Evol.* **21,** 227–229 (2006).
15. Hansen, A. J. & DeFries, R. Ecological mechanisms linking protected areas to surrounding lands. *Ecol. Appl.* **17,** 974–988 (2007).
16. Laurance, W. F. *et al.* Biomass collapse in Amazonian forest fragments. *Science* **278,** 1117–1118 (1997).
17. Woodroffe, R. & Ginsberg, J. R. Edge effects and the extinction of populations inside protected areas. *Science* **280,** 2126–2128 (1998).
18. Terborgh, J. *et al.* Ecological meltdown in predator-free forest fragments. *Science* **294,** 1923–1926 (2001).
19. Laurance, W. F. *et al.* The fate of Amazonian forest fragments: a 32-year investigation. *Biol. Conserv.* **144,** 56–67 (2011).
20. Brooks, T. M., Pimm, S. L. & Oyugi, J. O. Time lag between deforestation and bird extinction in tropical forest fragments. *Conserv. Biol.* **13,** 1140–1150 (1999).
21. Peres, C. A. Why we need megareserves in Amazonia. *Conserv. Biol.* **19,** 728–733 (2005).
22. Maiorano, L., Falcucci, A. & Boitani, L. Size-dependent resistance of protected areas to land-use change. *Proc. R. Soc. B* **275,** 1297–1304 (2008).
23. Estes, J. A. *et al.* Trophic downgrading of Planet Earth. *Science* **333,** 301–306 (2011).
24. Wells, M. P. & McShane, T. O. Integrating protected area management with local needs and aspirations. *Ambio* **33,** 513–519 (2004).
25. Scherl, L. M. *et al. Can Protected Areas Contribute to Poverty Reduction? Opportunities and Limitations* (IUCN, 2004).
26. Chan, K. M. A. & Daily, G. C. The payoff of conservation investments in tropical countryside. *Proc. Natl Acad. Sci. USA* **105,** 19342–19347 (2008).
27. Porter-Bolland, L. *et al.* Community-managed forests and protected areas: an assessment of their conservation effectiveness across the tropics. *For. Ecol. Manage.* **256,** 6–17 (2012).
28. Thomas, C. D. *et al.* Extinction risk from climate change. *Nature* **427,** 145–148 (2004).
29. Sekercioglu, C. H., Schneider, S. H., Fay, J. P. & Loarie, S. R. Climate change, elevational range shifts, and bird extinctions. *Conserv. Biol.* **22,** 140–150 (2008).
30. Shoo, L. P. *et al.* Targeted protection and restoration to conserve tropical biodiversity in a warming world. *Glob. Change Biol.* **17,** 186–193 (2011).

Supplementary Information is linked to the online version of the paper at www.nature.com/nature.

Acknowledgements The study was supported by James Cook University, the Smithsonian Tropical Research Institute, an Australian Laureate Fellowship (to W.F.L.) and NSF grant RCN-0741956. We thank A. Bruner, R. A. Butler, G. R. Clements, R. Condit, C. N. Cook, S. Goosem, J. Geldmann, L. Joppa, S. L. Pimm and O. Venter for comments.

Author Contributions W.F.L. conceived the study and coordinated its design, analysis and manuscript preparation. D.C.U., J.R. and M.K. conducted the interviews; C.J.A.B. assisted with data analysis and some writing; and S.P.S., S.G.L., M.C. and W.L. organized data or collected metadata. The remaining authors provided detailed interviews on protected areas and offered feedback on the manuscript.

Author Information Reprints and permissions information is available at www.nature.com/reprints. The authors declare no competing financial interests. Readers are welcome to comment on the online version of this article at www.nature.com/nature. Correspondence and requests for materials should be addressed to W.F.L. (bill.laurance@jcu.edu.au).

William F. Laurance[1,2], D. Carolina Useche[2], Julio Rendeiro[2], Margareta Kalka[2], Corey J. A. Bradshaw[3], Sean P. Sloan[1], Susan G. Laurance[1], Mason Campbell[1], Kate

Abernethy[4], Patricia Alvarez[5], Victor Arroyo-Rodriguez[6], Peter Ashton[7], Julieta Benítez-Malvido[6], Alfred Blom[8], Kadiri S. Bobo[9], Charles H. Cannon[10], Min Cao[10], Richard Carroll[8], Colin Chapman[11], Rosamond Coates[12], Marina Cords[13], Finn Danielsen[14], Bart De Dijn[15], Eric Dinerstein[8], Maureen A. Donnelly[16], David Edwards[1], Felicity Edwards[1], Nina Farwig[17], Peter Fashing[18], Pierre-Michel Forget[19], Mercedes Foster[20], George Gale[21], David Harris[22], Rhett Harrison[10], John Hart[23], Sarah Karpanty[24], W. John Kress[25], Jagdish Krishnaswamy[26], Willis Logsdon[1], Jon Lovett[27], William Magnusson[28], Fiona Maisels[29], Andrew R. Marshall[30], Deedra McClearn[31], Divya Mudappa[32], Martin R. Nielsen[33], Richard Pearson[34], Nigel Pitman[5], Jan van der Ploeg[35], Andrew Plumptre[36], John Poulsen[37], Mauricio Quesada[6], Hugo Rainey[29], Douglas Robinson[38], Christiane Roetgers[1], Francesco Rovero[39], Frederick Scatena[40], Christian Schulze[41], Douglas Sheil[42], Thomas Struhsaker[2], John Terborgh[3], Duncan Thomas[38], Robert Timm[43], J. Nicolas Urbina-Cardona[44], Karthikeyan Vasudevan[45], S. Joseph Wright[2], Juan Carlos Arias-G.[46], Luzmila Arroyo[47], Mark Ashton[48], Philippe Auzel[11], Dennis Babaasa[49], Fred Babweteera[50], Patrick Baker[51], Olaf Banki[52], Margot Bass[53], Inogwabini Bila-Isia[54], Stephen Blake[39], Warren Brockelman[55], Nicholas Brokaw[56], Carsten A. Brühl[57], Sarayudh Bunyavejchewin[58], Jung-Tai Chao[59], Jerome Chave[60], Ravi Chellam[61], Connie J. Clark[2], José Clavijo[62], Robert Congdon[34], Richard Corlett[63], H. S. Dattaraja[64], Chittaranjan Dave[65], Glyn Davies[66], Beatriz de Mello Beisiegel[67], Rosa de Nazaré Paes da Silva[68], Anthony Di Fiore[69], Arvin Diesmos[70], Rodolfo Dirzo[71], Diane Doran-Sheehy[72], Mitchell D'Arcy[73], Louise Emmons[74], Alejandro Estrada[12], Corneille Ewango[74], Linda Fedigan[75], François Feer[19], Barbara Fruth[76], Jacalyn Giacalone Willis[77], Uromi Goodale[78], Steven Goodman[79], Juan C. Guix[80], Paul Guthiga[81], William Haber[82], Keith Hamer[83], Ilka Herbinger[84], Jane Hill[30], Zhongling Huang[85], I Fang Sung[86], Nalin Ickes[87], Akira Itoh[88], Natália Ivanauskas[89], Betsy Jackes[90], John Janovec[90], Daniel Janzen[40], Mo Jiangming[91], Chris Jordan[92], Trevor Jones[92], Hermes Justiniano[93], Elisabeth Kalko[94‡], Aventino Kasangaki[95], Timothy Killeen[96], Hen-biau King[97], Erik Klop[98], Cheryl Knott[99], Inza Koné[100], Enoka Kudavidanage[62], José Lahoz da Silva Ribeiro[101], John Lattke[102], Richard Laval[103], Robert Lawton[104], Miguel Leal[105], Mark Leighton[106], Christine Lindell[107], Caroline Leonel[108], Jeremy Lindsell[109], Lee Ling-Ling[110], K. Eduard Linsenmair[111], Elizabeth Losos[112], Ariel Lugo[113], Jeremiah Lwanga[114], Andrew L. Mack[115], Marlucia Martins[116], W. Scott McGraw[2], Roan McNab[18], Luciano Montag[117], Jo Myers Thompson[120], Jacob Nabe-Nielsen[121], Michael Nakagawa[122], Sam Nantel[123], Anuradha Nathan[124], Vojtech Novotny[125], Sean O'Donnell[126], Muse Opiang[127], Paul Ouboter[128], Kenneth Parker[129], N. Parthasarathy[130], Katia Pisciotta[131], Dewi Prawiradilaga[132], Catherine Pringle[133], Subaraj Rajathurai[134], Ulrich Reichard[135], Gay Reinartz[136], Katherine Renton[137], Glenwood Reynolds[138], Vernon Reynolds[139], Erin Riley[140], Mark Oliver Rödel[141], Jessica Rothman[142], Philip Round[143], Shoko Sakai[144], Tania Sanamxay[28], Tommaso Savini[21], Gertrud Schaab[145], John Seidensticker[146], Alhaji Siaka[147], Miles R. Silman[148], Thomas B. Smith[149], Samuel Soares de Almeida[150], Nayjot Sodhi[63], Craig Stanford[101], Kristine Stewart[132], Emma Stokes[29], Kathryn E. Stoner[151], Raman Sukumar[152], Martin Surbeck[76], Mathias Tobler[96], Tuy Tscharntke[153], Andrea Turkalo[156], Govindaswamy Umapathy[157], Merlijn van Weerd[35], Jorge Vega Rivera[137], Meena Venkataraman[158], Linda Venn[159], Carlos Verea[160], Carolina Volkmer de Castilho[161], Matthias Waltert[162], Benjamin Wang[40], David Watts[48], William Weber[29], Paige West[163], David Whitacre[164], Kofi Whitney[165], David Wilkie[29], Stephen Williams[34], Debra D. Wright[115], Patricia Wright[164], Lu Xiankai[91], Pralad Yonzon[166]‡ & Franky Zamzani[166]

[1]Centre for Tropical Environmental and Sustainability Science (TESS) and School of Marine and Tropical Biology, James Cook University, Cairns, Queensland 4878, Australia. [2]Smithsonian Tropical Research Institute, Balboa, Ancón, Panama. [3]Center for Tropical Environmental Sciences, University of Adelaide, Adelaide, South Australia 5005, Australia. [4]Stirling University, Stirling FK9 4LA, UK. [5]Duke University, Durham, North Carolina 27705, USA. [6]Universidad Nacional Autónoma de México (UNAM), Morelia, Mexico. [7]Royal Botanic Gardens, Kew, Richmond TW9 3AB, UK. [8]World Wildlife Fund (WWF), Washington DC 20037, USA. [9]University of Dschang, Dschang, Cameroon. [10]Xishuangbanna Tropical Botanical Garden, Yunnan 666303, People's Republic of China. [11]McGill University, Montreal H3A 2T7, Canada. [12]Estación de Biología Tropical Los Tuxtlas, Universidad Nacional Autónoma de México, Veracruz 95701, Mexico. [13]Columbia University, New York, New York 10027, USA. [14]Nordic Foundation for Development and Ecology, DK-1159 Copenhagen, Denmark. [15]Bart De Dijn Environmental Consultancy, Paramaribo, Suriname. [16]Florida International University, Miami, Florida 33199, USA. [17]Philipps-Universität Marburg, Marburg 35043, Germany. [18]California State University, Fullerton, California 92834, USA. [19]Muséum National d'Histoire Naturelle, 91800 Brunoy, France. [20]US Geological Survey, Smithsonian Institution, Washington DC 20013, USA. [21]King Mongkut's University of Technology Thonburi, Bangkok 10150, Thailand. [22]Royal Botanic Garden, Edinburgh, Scotland EH3 5LR, UK. [23]Tshuapa-Lomami-Lualaba Project, Democratic Republic of Congo. [24]Virginia Tech University, Blacksburg, Virginia 24061, USA. [25]National Museum of Natural History, Smithsonian Institution, Washington DC 20013, USA. [26]Ashoka Trust for Research in Ecology and the Environment (ATREE), Bangalore 560064, India. [27]University of Twente, Enschede, Netherlands. [28]Instituto Nacional de Pesquisas da Amazônia (INPA), Manaus, Amazonas 69011-970, Brazil. [29]Wildlife Conservation Society, Bronx, New York 10460, USA. [30]University of York, Heslington, York YO10 5DD, UK. [31]La Selva Biological Station, San Pedro, Costa Rica. [32]Nature Conservation Foundation, Mysore 570 002, India. [33]University of Copenhagen, Copenhagen, Denmark. [34]James Cook University, Townsville, Queensland 4811, Australia. [35]Leiden University, Leiden, Netherlands. [36]Wildlife Conservation Society, Kampala, Uganda. [37]Woods Hole Research Center, Falmouth, Massachusetts 02540, USA. [38]Oregon State University, Corvallis, Oregon 97331, USA. [39]Museo delle Scienze, 38122 Trento, Italy. [40]University of Pennsylvania, Philadelphia, Pennsylvania 19104, USA. [41]University of Vienna, 1030 Vienna, Austria. [42]Bwindi Impenetrable National Park, Kabale, Uganda. [43]University of Kansas, Lawrence, Kansas 66045, USA. [44]Pontificia Universidad Javeriana, Bogotá, Colombia. [45]Wildlife Institute of India, Dehradun, India. [46]Unidad de Parques Nacionales Naturales de Colombia, Bogotá, Colombia. [47]Museo de Historia Natural Noel Kempff, Santa Cruz, Bolivia. [48]Yale University, New Haven, Connecticut 06511, USA. [49]Institute of Tropical Forest Conservation, Kabale, Uganda. [50]Dudongo Conservation Field Station, Masindi, Uganda. [51]Monash University, Melbourne, Victoria 3800, Australia. [52]Utrecht University, Utrecht, Netherlands. [53]Finding Species, Takoma Park, Maryland 20912, USA. [54]University of Kent, Kent CT2 7NZ, UK. [55]Mahidol University Salaya, Nakhon Pathom 73170, Thailand. [56]University of Puerto Rico, San Juan 00936, Puerto Rico. [57]University Koblenz-Landau, D-76829 Landau, Germany. [58]Department of National Parks, Chatuchak, Bangkok 10900, Thailand. [59]Taiwan Forestry Research Institute, Taipei 10066, Taiwan. [60]Université Paul Sabatier, Toulouse, France. [61]Wildlife Conservation Society, Bangalore 560070, India. [62]Universidad Central de Venezuela, Aragua, Venezuela. [63]National University of Singapore, Singapore 117543. [64]Indian Institute of Science, Bangalore 560012, India. [65]World Wide Fund for Nature (WWF), New Delhi 110003, India. [66]World Wide Fund for Nature (WWF), Surrey GU7 1XR, UK. [67]Instituto Chico Mendes de Conservação de Biodiversidade, Atibaia, São Paulo 12952-011, Brazil. [68]O Conselho Regional de Engenhara, Arquitetura e Agronomia do Pará, Belém, Pará, Brazil. [69]University of Texas, Austin, Texas 78712, USA. [70]National Museum of the Philippines, Manila, Philippines. [71]Stanford University, Stanford, California 94305, USA. [72]State University of New York at Stony Brook, Stony Brook, New York 11794, USA. [73]University of Colorado, Boulder, Colorado 80309, USA. [74]Wildlife Conservation Society, Kinshasa, Democratic Republic of Congo. [75]University of Calgary, Alberta T2N 1N4, Canada. [76]Max Planck Institute for Evolutionary Anthropology, Leipzig, Germany. [77]Montclair State University, Montclair, New Jersey 07043, USA. [78]University of California, San Diego, California 92093, USA. [79]Field Museum of Natural History, Chicago, Illinois 60605, USA. [80]Universitat de Barcelona, Edifici Historic, 08028 Barcelona, Spain. [81]Kenya Institute for Public Policy Research and Analysis, Nairobi, Kenya. [82]Missouri Botanical Garden, St. Louis, Missouri 63166, USA. [83]University of Leeds, Leeds LS2 9JT, UK. [84]Wild Chimpanzee Foundation, Abidjan 23, Cote d'Ivoire. [85]Dinghushan Biosphere Reserve, Zhaoqing, People's Republic of China. [86]Tunghai University, Taichung 407, Taiwan. [87]Clemson University, Clemson, South Carolina 29634, USA. [88]Osaka City University, Osaka 558-8585, Japan. [89]Instituto Florestal, São Paulo, São Paulo 02377-000, Brazil. [90]Botanical Research Institute of Texas, Fort Worth, Texas 76107, USA. [91]South China Botanical Garden, Guangzhou 510650, People's Republic of China. [92]Anglia Ruskin University, Cambridge CB1 1PT, UK. [93]Museo de Historia Natural Noel Kempff Mercado, Santa Cruz, Bolivia. [94]Ulm University, Ulm, Germany. [95]Makerere University, Kampala, Uganda. [96]Department of National Parks, Chatuchak, Bangkok 10900, Thailand. [97]Taiwan Forestry Research Institute, Taipei 10066, Taiwan. [98]Université Paul Sabatier, Toulouse, France. [99]Wildlife Conservation Society, Bangalore 560070, India. [100]Universidad Central de Venezuela, Aragua, Venezuela. [101]Museu Nacional/UFRJ, Rio Piedras, Puerto Rico 00926. [102]Museo de Historia Natural Noel Kempff Mercado, Santa Cruz, Bolivia. [103]Universidad Nacional Autónoma de México, Veracruz 95701, Mexico. [104]Columbia University, New York, New York 10027, USA. [105]Nordic Foundation for Development and Ecology, DK-1159 Copenhagen, Denmark. [106]Bart De Dijn Environmental Consultancy, Paramaribo, Suriname. [107]Florida International University, Miami, Florida 33199, USA. [108]Philipps-Universität Marburg, Marburg 35043, Germany. [109]California State University, Fullerton, California 92834, USA. [110]Muséum National d'Histoire Naturelle, 91800 Brunoy, France. [111]Smithsonian Institution, Washington DC 20013, USA. [112]King Mongkut's University of Technology Thonburi, Bangkok 10150, Thailand. [113]Royal Botanic Garden, Edinburgh, Scotland EH3 5LR, UK. [114]Tshuapa-Lomami-Lualaba Project, Democratic Republic of Congo. [115]Virginia Tech University, Blacksburg, Virginia 24061, USA. [116]National Museum of Natural History, Smithsonian Institution, Washington DC 20013, USA. [117]Ashoka Trust for Research in Ecology and the Environment (ATREE), Bangalore 560064, India. [118]University of Twente, Enschede, Netherlands. [119]Instituto Nacional de Pesquisas da Amazônia (INPA), Manaus, Amazonas 69011-970, Brazil. [120]Wildlife Conservation Society, Bronx, New York 10460, USA. [121]University of York, Heslington, York YO10 5DD, UK. [122]La Selva Biological Station, San Pedro, Costa Rica. [123]Nature Conservation Foundation, Mysore 570 002, India. [124]University of Copenhagen, Copenhagen, Denmark. [125]James Cook University, Townsville, Queensland 4811, Australia. [126]Leiden University, Leiden, Netherlands. [127]Wildlife Conservation Society, Kampala, Uganda. [128]Woods Hole Research Center, Falmouth, Massachusetts 02540, USA. [129]Oregon State University, Corvallis, Oregon 97331, USA. [130]Museo delle Scienze, 38122 Trento, Italy. [131]University of Pennsylvania, Philadelphia, Pennsylvania 19104, USA. [132]University of Vienna, 1030 Vienna, Austria. [133]Bwindi Impenetrable National Park, Kabale, Uganda. [134]University of Kansas, Lawrence, Kansas 66045, USA. [135]Pontificia Universidad Javeriana, Bogotá, Colombia. [136]Wildlife Institute of India, Dehradun, India. [137]Unidad de Parques Nacionales Naturales de Colombia, Bogotá, Colombia. [138]Museo de Historia Natural Noel Kempff, Santa Cruz, Bolivia. [139]Yale University, New Haven, Connecticut 06511, USA. [140]Institute of Tropical Forest Conservation, Kabale, Uganda. [141]Museo de Historia Natural Noel Kempff, Santa Cruz, Bolivia. [142]Yale University, New Haven, Connecticut 06511, USA. [143]Institute of Tropical Forest Conservation, Kabale, Uganda. [144]Durrell Wildlife Conservation Trust, Jersey JE3 5BP, UK. [145]Universität Koblenz-Landau, D-76829 Landau, Germany. [146]Smithsonian Conservation Biology Institute, Front Royal, Virginia 22630, USA. [147]Fourah Bay College, University of Sierra Leone, Freetown, Sierra Leone. [148]Wake Forest University, Winston-Salem, North Carolina 27106, USA. [149]University of California, Los Angeles, California 90095, USA. [150]Av. Maalhães Barata 376, Belém, Pará 66040-170, Brazil. [151]University of Southern California, Los Angeles, California 90089, USA. [152]Institute of Applied Ethnobotany, Pomano Beach, Florida 33069, USA. [153]Texas A & M University, Kingsville, Texas 78363, USA. [154]Indian Institute of Science, Bangalore, India. [155]Georg-August-Universität, Göttingen, Germany. [156]Wildlife Conservation Society, Bangui, Central African Republic. [157]Centre for Cellular and Molecular Biology, Hyderabad, India. [158]701, Vesta B, Lodha Paradise, Thane, India. [159]Paluma Environmental Education Centre, Paluma, Queensland 4816, Australia. [160]Universidad Central de Venezuela, Maracay, Venezuela. [161]Embrapa Roraima, Boa Vista, Roraima, Brazil. [162]Treasure Valley Math and Science Center, Boise, Idaho 83714, USA. [163]Rice University, Houston, Texas 77005, USA. [164]Stony Brook University, Stony Brook, New York 11794, USA. [165]Resources Himalaya Foundation, Kathmandu, Nepal. [166]Gunung Palung National Park, West Kalimantan, Indonesia.
‡Deceased.

LETTER

doi:10.1038/nature11421

A 61-million-person experiment in social influence and political mobilization

Robert M. Bond[1], Christopher J. Fariss[1], Jason J. Jones[2], Adam D. I. Kramer[3], Cameron Marlow[3], Jaime E. Settle[1] & James H. Fowler[1,4]

Human behaviour is thought to spread through face-to-face social networks, but it is difficult to identify social influence effects in observational studies[9–13], and it is unknown whether online social networks operate in the same way[14–19]. Here we report results from a randomized controlled trial of political mobilization messages delivered to 61 million Facebook users during the 2010 US congressional elections. The results show that the messages directly influenced political self-expression, information seeking and real-world voting behaviour of millions of people. Furthermore, the messages not only influenced the users who received them but also the users' friends, and friends of friends. The effect of social transmission on real-world voting was greater than the direct effect of the messages themselves, and nearly all the transmission occurred between 'close friends' who were more likely to have a face-to-face relationship. These results suggest that strong ties are instrumental for spreading both online and real-world behaviour in human social networks.

Recent experimental studies[6,14–16] have attempted to measure the causal effect of social influence online. At the same time, there is increasing interest in the ability to use online social networks to study and influence real-world behaviour[17–19]. However, online social networks are also made up of many 'weak-tie' relationships[20] that may not facilitate social influence[21], and some studies suggest that online communication may not be an effective medium for influence[22]. An open question is whether online networks, which harness social information from face-to-face networks, can be used effectively to increase the likelihood of behaviour change and social contagion.

One behaviour that has been proposed to spread through networks is the act of voting in national elections. Voter turnout is significantly correlated among friends, family members and co-workers in observational studies[23,24]. Voter mobilization efforts are effective at increasing turnout[25], particularly those conducted face-to-face and those that appeal to social pressure[26] and social identity[27]. There is also evidence from one face-to-face field experiment that voting is 'contagious', in the sense that mobilization can spread from person to person within two-person households[28]. Although anecdotal accounts suggest that online mobilization has made a big difference in recent elections[21], a meta-analysis of email experiments suggests that online appeals to vote are ineffective[24].

Voter mobilization experiments[26–28] have shown that most methods of contacting potential voters have small effects (if any) on turnout rates, ranging from 1% to 10%. However, the ability to reach large populations online means that even small effects could yield behaviour changes for millions of people. Furthermore, as many elections are competitive, these changes could affect electoral outcomes. For example, in the 2000 US presidential election, George Bush beat Al Gore in Florida by 537 votes (less than 0.01% of votes cast in Florida). Had Gore won Florida, he would have won the election.

To test the hypothesis that political behaviour can spread through an online social network, we conducted a randomized controlled trial with all users of at least 18 years of age in the United States who accessed the Facebook website on 2 November 2010, the day of the US congressional elections. Users were randomly assigned to a 'social message' group, an 'informational message' group or a control group. The social message group ($n = 60{,}055{,}176$) was shown a statement at the top of their 'News Feed'. This message encouraged the user to vote, provided a link to find local polling places, showed a clickable button reading 'I Voted', showed a counter indicating how many other Facebook users had previously reported voting, and displayed up to six small randomly selected 'profile pictures' of the user's Facebook friends who had already clicked the I Voted button (Fig. 1). The informational message group ($n = 611{,}044$) was shown the message, poll information, counter and button, but they were not shown any faces of friends. The control group ($n = 613{,}096$) did not receive any message at the top of their News Feed.

The design of the experiment allowed us to assess the impact that the treatments had on three user actions; clicking the I Voted button, clicking the polling-place link and voting in the election. Clicking the I Voted button is similar to traditional measures of self-reported voting, but here users reported their vote to their social community rather than to a researcher. We therefore use this action to measure political self-expression, as it is likely to be affected by the extent to which a user desires to be seen as a voter by others. In contrast, social desirability should not affect other user actions in the same way. Clicking the polling-place link took users to a separate website that helped them to find a polling location, and this action was not reported to the user's social community. We therefore use this action to measure a user's desire to seek information about the election. Finally, we used a group-level process to study the validated voting behaviour of 6.3 million users matched to publicly available voter records (see Supplementary Information).

We first analyse direct effects. We cannot compare the treatment groups with the control group to assess the effect of the treatment on self-expression and information seeking, because the control group did not have the option to click an I Voted button or click on a polling-place link. However, we can compare the proportion of users between the two treatment groups to estimate the causal effect of seeing the faces of friends who have identified themselves as voters (Fig. 1). Users who received the social message were 2.08% (s.e.m., 0.05%; t-test, $P < 0.01$) more likely to click on the I Voted button than those who received the informational message (20.04% in the social message group versus 17.96% in the informational message group). Users who received the social message were also 0.26% (s.e.m., 0.02%; $P < 0.01$) more likely to click the polling-place information link than users who received the informational message (Fig. 1).

Although acts of political self-expression and information seeking are important in their own right, they do not necessarily guarantee that a particular user will actually vote. As such, we also measured the effect that the experimental treatment had on validated voting, through examination of public voting records. The results show that users

[1]Political Science Department, University of California, San Diego, La Jolla, California 92093, USA. [2]Psychology Department, University of California, San Diego, La Jolla, California 92093, USA. [3]Data Science, Facebook, Inc., Menlo Park, California 94025, USA. [4]Medical Genetics Division, University of California, San Diego, La Jolla, California 92093, USA.

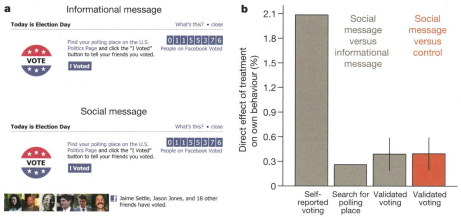
a
Informational message
Today is Election Day
What's this? • close
Find your polling place on the U.S. Politics Page and click the "I Voted" button to tell your friends you voted.
I Voted
2,151,537 People on Facebook Voted
Social message
Today is Election Day
What's this? • close
Find your polling place on the U.S. Politics Page and click the "I Voted" button to tell your friends you voted.
I Voted
2,151,537 People on Facebook Voted
Jaime Settle, Jason Jones, and 18 other friends have voted.
b
Direct effect of treatment on own behaviour (%)
2.1
1.8
1.5
1.2
0.9
0.6
0.3
0
Social message versus informational message
Social message versus control
Self-reported voting
Search for polling place
Validated voting
Validated voting

Figure 1 | The experiment and direct effects. a, b. Examples of the informational message and social message Facebook treatments (**a**) and their direct effect on voting behaviour (**b**). Vertical lines indicate s.e.m. (they are too small to be seen for the first two bars).

who received the social message were 0.39% (s.e.m., 0.17%; *t*-test, $P = 0.02$) more likely to vote than users who received no message at all. Similarly, the difference in voting between those who received the social message and those who received the informational message was 0.39% (s.e.m., 0.17%; *t*-test, $P = 0.02$), suggesting that seeing faces of friends significantly contributed to the overall effect of the message on real-world voting. In fact, turnout among those who received the informational message was identical to turnout among those in the control group (treatment effect 0.00%, s.e.m., 0.28%; $P = 0.98$), which raises doubts about the effectiveness of information-only appeals to vote in this context.

These results show that online political mobilization can have a direct effect on political self-expression, information seeking and real-world voting behaviour, and that messages including cues from an individual's social network are more effective than information-only appeals. But what about indirect effects that spread from person to person in the social network? Users in our sample had on average 149 Facebook friends, with whom they share social information, although many of these relationships constitute 'weak ties'. Past research indicates that close friends have a stronger behavioural effect on each other than do acquaintances or strangers[9,11,13,21]. We therefore expected mobilization to spread more effectively online through 'strong ties'.

To distinguish users who are likely to have close relationships, we used the degree to which Facebook friends interacted with each other on the site (see Supplementary Information for more detail). Higher levels of interaction indicate that friends are more likely to be physically proximate and suggest a higher level of commitment to the friendship, more positive affect between the friends, and a desire for the friendship to be socially recognized[29]. We counted the number of interactions between each pair of friends and categorized them by decile, ranking them from the lowest to highest percentage of interactions. A validation study (see Supplementary Information) shows that friends in the highest decile are those most likely to be close friends in real life (Fig. 2a).

We then used these categories to estimate the effect of the mobilization message on a user's friends. Random assignment means that any relationship between the message a user receives and a friend's behaviour is not due to shared attributes, as these attributes are not correlated with the treatment (see Supplementary Information). To measure a per-friend treatment effect, we compared behaviour in the friends connected to a user who received the social message to behaviour in the friends connected to a user in the control group. To account for dependencies in the network, we simulate the null distribution using a network permutation method (see the Supplementary Information). Monte Carlo simulations suggest that this method minimizes the risk of false positives and recovers true causal effects without bias (see Supplementary Information).

Figure 2 shows that the observed per-friend treatment effects increase as tie-strength increases. All of the observed treatment effects fall outside the null distribution for expressed vote (Fig. 2b), suggesting that they are significantly different from chance outcomes. For validated vote (Fig. 2c), the observed treatment effect is near zero for weak ties, but it spikes upwards and falls outside the null distribution for the top two deciles. This suggests that strong ties are important for the spread of real-world voting behaviour. Finally, the treatment effect for polling place search gradually increases (Fig. 2d), with several of the effects falling outside the 95% confidence interval of the null distribution.

To simplify the analysis and reporting of results, we arbitrarily define 'close friends' as people who were in the eightieth percentile or higher (decile 9) of frequency of interaction among all friendships in the sample (see the Supplementary Information). 'Friends' are all other Facebook friends who had less interaction. A total of 60,491,898 (98%) users in our sample had at least 1 close friend, with the average user having about 10 close friends (compared with an average of 139 friends who were not close).

The results suggest that users were about 0.011% (95% confidence interval (CI) of null distribution −0.009% to 0.010%) more likely to engage in an act of political self-expression by clicking on the I Voted button than they would have been had their friend seen no message. Similarly, for each close friend who received the social message, an individual was on average 0.099% (null 95% CI −0.042% to 0.048%) more likely to express voting.

We also found an effect in the validated vote sample. For each close friend who received the social message, a user was 0.224% (null 95% CI −0.181% to 0.174%) more likely to vote than they would have been had their close friend received no message. Similarly, for information-seeking behaviour we found that for each close friend who received the social message, a user was 0.012% (null 95% CI −0.012% to 0.012%) more likely to click the link to find their polling place than they would have been had their close friends received no message. In both cases there was no evidence that other friends had an effect (see Supplementary Information). Thus, ordinary Facebook friends may affect online expressive behaviour, but they do not seem to affect private or real-world political behaviours. In contrast, close friends seem to have influenced all three.

The magnitude of these contagion effects are small per friend, but it is important to remember that they result from a single message, and in many cases it was not possible to change the target's behaviour. For example, users may have already voted by absentee ballot before Election Day, or they may have logged in to Facebook too late to vote or to influence other users' voting behaviour. In other words, all effects measured here are intent-to-treat effects rather than treatment-on-treated effects, which would be greater if we had better information about who was eligible to receive the treatment.

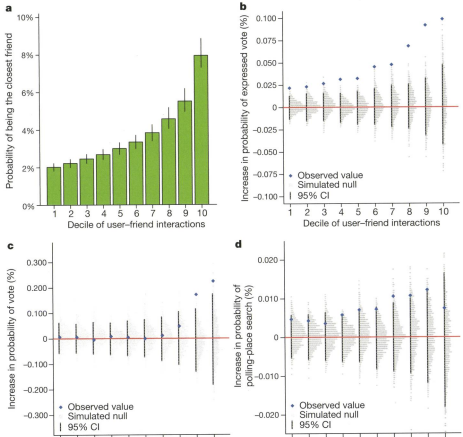

Figure 2 | The effect of mobilization treatment that a friend received on a user's behaviour. a–d, A validation study shows that at increasing levels of interaction, Facebook friends are more likely to have a close real-world relationship (**a**; see also the Supplementary Information). As the interaction increases, so does the observed per-friend effect of friend's treatment on a user's expressed voting (**b**), validated voting (**c**) and polling-place search (**d**). Blue diamonds indicate the observed treatment effect. Horizontal grey bars show the null distribution derived from simulations of identical networks in which the topology and incidence of the behaviour and treatment are the same but the assignments of treatment are randomly reassigned.

Moreover, the scale of the number of users, their friendship connections and the potential voters in a given election is very large. We estimated the per-user effect (the per-friend effect multiplied by the average number of friends per user) and the total effect (the per-user effect multiplied by the total number of users) on the behaviour of everyone in the sample (see Supplementary Information). The results suggest that friends generated an additional 886,000 expressed votes (+1.4%, null 95% CI −1.1% to 1.1%), and close friends generated a further 559,000 votes (+0.9%, null 95% CI –0.3% to 0.3%). In the Supplementary Information we also show that close friends of close friends (2 degrees of separation) generated an additional 1 million expressed votes (+1.7%, null 95% CI –0.8% to 0.9%). Thus, the treatment clearly had a significant impact on political self-expression and how it spread through the network, and even weak ties seem to be relevant to its spread.

However, the effect of the social message on real-world validated vote behaviour and polling-place search was more focused. The results suggest that close friends generated an additional 282,000 validated votes (+1.8%, null 95% CI –1.3% to 1.2%) and an additional 74,000 polling-place searches (+0.1%, null 95% CI –0.1% to 0.1%), but there is no evidence that ordinary friends had any effect on either of these two behaviours. In other words, close friendships accounted for all of the significant contagion of these behaviours, in spite of the fact that they make up only 7% of all friendships on Facebook.

To put these results in context, it is important to note that turnout has been steadily increasing in recent US midterm elections, from 36.3% of the voting age population in 2002 to 37.2% in 2006, and to 37.8% in 2010. Our results suggest that the Facebook social message increased turnout directly by about 60,000 voters and indirectly through social contagion by another 280,000 voters, for a total of 340,000 additional votes. That represents about 0.14% of the voting age population of about 236 million in 2010. However, this estimate does not include the effect of the treatment on Facebook users who were registered to vote but who we could not match because of nicknames, typographical errors, and so on. It would be complex to estimate the number of users on Facebook who are in the voter record but unmatchable, and it is not clear whether treatment effects would be of the same magnitude for these individuals, so we restrict our estimate to the matched group that we were able to sample and observe. This means it is possible that more of the 0.60% growth in turnout between 2006 and 2010 might have been caused by a single message on Facebook.

The results of this study have many implications. First and foremost, online political mobilization works. It induces political self-expression, but it also induces information gathering and real, validated voter turnout. Although previous research suggested that online messages do not work[19], it is possible that conventional sample sizes may not be large enough to detect the modest effect sizes shown here. We also show that social mobilization in online networks is significantly more effective than informational mobilization alone. Showing familiar faces to users can dramatically improve the effectiveness of a mobilization message.

Beyond the direct effects of online mobilization, we show the importance of social influence for effecting behaviour change. Our

validation study shows that close friends exerted about four times more influence on the total number of validated voters mobilized than the message itself. These results are similar to those from a prior network simulation study based on observational data that suggested each act of voting on average generates an additional three votes as this behaviour spreads through the network[30]. Thus, efforts to influence behaviour should pay close attention not only to the effect a message will have on those who receive it but also to the likelihood that the message and the behaviour it spurs will spread from person to person through the social network. And, in contrast to the results for close friends, we find that Facebook friends have less effect. Online mobilization works because it primarily spreads through strong-tie networks that probably exist offline but have an online representation. In fact, it is plausible that unobserved face-to-face interactions account for at least some of the social influence that we observed in this experiment.

More broadly, the results suggest that online messages might influence a variety of offline behaviours, and this has implications for our understanding of the role of online social media in society. Experiments are expensive and have limited external validity, but the growing availability of cheap and large-scale online social network data[17] means that these experiments can be easily conducted in the field. If we want to truly understand—and improve—our society, wellbeing and the world around us, it will be important to use these methods to identify which real world behaviours are amenable to online interventions.

Received 17 April; accepted 18 July 2012.

1. Berger, J. & Le Mens, G. How adoption speed affects the abandonment of cultural tastes. *Proc. Natl Acad. Sci. USA* **106,** 8146–8150 (2009).
2. Borgatti, S. P. *et al.* Network analysis in the social sciences. *Science* **323,** 892–895 (2009).
3. Ohtsuki, H., Hauert, C., Lieberman, E. & Nowak, M. A. A simple rule for the evolution of cooperation on graphs and social networks. *Nature* **441,** 502–505 (2006).
4. Onnela, J. P. & Reed-Tsochas, F. Spontaneous emergence of social influence in online systems. *Proc. Natl Acad. Sci. USA* **107,** 18375–18380 (2010).
5. Apicella, C. L., Marlowe, F. W., Fowler, J. H. & Christakis, N. A. Social networks and cooperation in hunter-gatherers. *Nature* **481,** 497–501 (2012).
6. Aral, S. & Walker, D. Identifying influential and susceptible members of social networks. *Science* **337,** 337–341 (2012).
7. Centola, D. An experimental study of homophily in the adoption of health behavior. *Science* **334,** 1269–1272 (2011).
8. Gonzalez-Bailon, S., Borge-Holthofer, J., Rivero, A. & Moreno, Y. The dynamics of protest recruitment through an online network. *Sci. Rep.* **1,** 197 (2011).
9. Christakis, N. A. & Fowler, J. H. Social contagion theory: examining dynamic social networks and human behavior. Preprint at http://arXiv.org/abs/1109.5235v2 (2011).
10. Aral, S., Muchnik, L. & Sundararajan, A. Distinguishing influence-based contagion from homophily-driven diffusion in dynamic networks. *Proc. Natl Acad. Sci. USA* **106,** 21544–21549 (2009).
11. Christakis, N. A. & Fowler, J. H. The spread of obesity in a large social network over 32 years. *N. Engl. J. Med.* **357,** 370–379 (2007).
12. Fowler, J. H. & Christakis, N. A. The dynamic spread of happiness in a large social network. *Br. Med. J.* **337,** a2338 (2008).
13. Christakis, N. A. & Fowler, J. H. The collective dynamics of smoking in a large social network. *N. Engl. J. Med.* **358,** 2249–2258 (2008).
14. Salganik, M. J., Dodds, P. S. & Watts, D. J. Experimental study of inequality and unpredictability in an artificial cultural market. *Science* **311,** 854–856 (2006).
15. Centola, D. The spread of behavior in an online social network experiment. *Science* **329,** 1194–1197 (2010).
16. Fowler, J. H. & Christakis, N. A. Cooperative behavior cascades in human social networks. *Proc. Natl Acad. Sci. USA* **107,** 5334–5338 (2010).
17. Lazer, D. *et al.* Computational social science. *Science* **323,** 721–723 (2009).
18. Ellison, N. B., Steinfield, C. & Lampe, C. The benefits of facebook "friends:" Social capital and college students' use of online social network sites. *J. Comput. Mediat. Commun.* **12,** 1143–1168 (2007).
19. Traud, A. L., Kelsic, E. D., Mucha, P. J. & Porter, M. A. Comparing community structure to characteristics in online collegiate social networks. *SIAM Rev.* **53,** 526–543 (2011).
20. Granovetter, M. The strength of weak ties. *Am. J. Sociol.* **78,** 1360–1380 (1973).
21. Christakis, N. A. & Fowler, J. H. *Connected: The Surprising Power of Our Social Networks and How They Shape Our Lives* (Little, Brown, and Company, 2009).
22. Nickerson, D. W. Does email boost turnout? *Q. J. Polit. Sci.* **2,** 369–379 (2007).
23. Kenny, C. B. Political participation and effects from the social environment. *Am. J. Pol. Sci.* **36,** 259–267 (1992).
24. Huckfeldt, R. & Sprague, J. *Citizens, Politics, and Social Communication: Information and Influence in an Election Campaign* (Cambridge Univ. Press, 1995).
25. Gerber, A. S. & Green, D. P. Does canvassing increase voter turnout? A field experiment. *Proc. Natl Acad. Sci. USA* **96,** 10939–10942 (1999).
26. Gerber, A. S., Green, D. P. & Larimer, C. W. Social pressure and voter turnout: evidence from a large-scale field experiment. *Am. Polit. Sci. Rev.* **102,** 33–48 (2008).
27. Bryan, C. J., Walton, G. M., Rogers, T. & Dweck, C. S. Motivating voter turnout by invoking the self. *Proc. Natl Acad. Sci. USA* **108,** 12653–12656 (2011).
28. Nickerson, D. W. Is voting contagious? Evidence from two field experiments. *Am. Polit. Sci. Rev.* **102,** 49–57 (2008).
29. Vitak, J. *et al.* It's complicated: Facebook users' political participation in the 2008 election. *Cyberpsychol. Behav. Soc. Netw.* **14,** 107–114 (2011).
30. Fowler, J. H. in *The Social Logic of Politics: Personal Networks as Contexts for Political Behavior* (ed. Zuckerman, A.) 269–287 (Temple Univ. Press, 2005).

Supplementary Information is available in the online version of the paper.

Acknowledgements We are grateful to S. Aral, J. Berger, M. Cebrian, D. Centola, N. Christakis, C. Dawes, L. Gee, D. Green, C. Kam, P. Loewen, P. Mucha, J. P. Onnela, M. Porter, O. Smirnov and C. Volden for comments on early drafts. This work was supported in part by the James S. McDonnell Foundation, and the University of Notre Dame and the John Templeton Foundation as part of the Science of Generosity Initiative.

Author Contributions All authors contributed to study design, data collection, analysis and preparation of the manuscript. J.H.F. secured funding.

Author Information Reprints and permissions information is available at www.nature.com/reprints. The authors declare no competing financial interests. Readers are welcome to comment on the online version of the paper. Correspondence and requests for materials should be addressed to J.H.F. (jhfowler@ucsd.edu).

LETTER

doi:10.1038/nature11321

Activity in motor–sensory projections reveals distributed coding in somatosensation

Leopoldo Petreanu[1]†, Diego A. Gutnisky[1], Daniel Huber[1]†, Ning-long Xu[1], Dan H. O'Connor[1], Lin Tian[1]†, Loren Looger[1] & Karel Svoboda[1]

Cortical-feedback projections to primary sensory areas terminate most heavily in layer 1 (L1) of the neocortex [1,2], where they make synapses with tuft dendrites of pyramidal neurons. L1 input is thought to provide 'contextual' information[3], but the signals transmitted by L1 feedback remain uncharacterized. In the rodent somatosensory system, the spatially diffuse[4] feedback projection from vibrissal motor cortex (vM1) to vibrissal somatosensory cortex (vS1, also known as the barrel cortex) may allow whisker touch to be interpreted in the context of whisker position to compute object location[5,6]. When mice palpate objects with their whiskers to localize object features[7,8], whisker touch excites vS1[9] and later vM1 in a somatotopic manner[10–13]. Here we use axonal calcium imaging to track activity in vM1→vS1 afferents in L1 of the barrel cortex while mice performed whisker-dependent object localization. Spatially intermingled individual axons represent whisker movements, touch and other behavioural features. In a subpopulation of axons, activity depends on object location and persists for seconds after touch. Neurons in the barrel cortex thus have information to integrate movements and touches of multiple whiskers over time, key components of object identification and navigation by active touch.

We trained head-fixed mice to perform a whisker-based object-localization task under a two-photon microscope with one whisker row (C row) (Fig. 1a)[12]. In each trial, a pole was moved into one of several locations within reach of the whiskers (sampling period, approximately 1 s; Supplementary Fig. 1a), arranged along the anterior–posterior axis on one side of the head (Fig. 1b). Mice moved their whiskers to determine whether the pole was either in one of several 'go' locations or in a 'no-go' location. Automated whisker tracking[14] measured whisker movements and shape. The force acting on the follicles, which underlies object localization[8,15,16], can be estimated from whisker shape changes induced by touch. A change in curvature at point p of the whisker is proportional to the force applied by the pole on the whisker[16]: $F \propto \Delta\kappa_p \cdot y_p$, where y_p is the bending stiffness at p. We thus present forces acting on the whiskers as the change in curvature, $\Delta\kappa$ (Supplementary Fig. 1b). Mice report their decision about object location with licking. Imaging was performed in trained mice (discriminability (d') average,

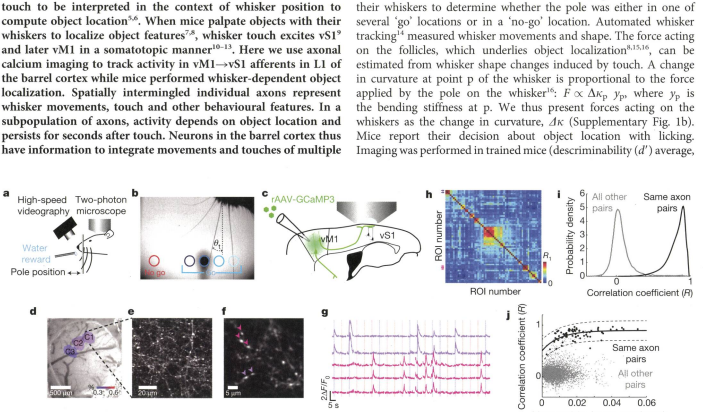

Figure 1 | Imaging activity in vM1→vS1 axons during whisker-based object localization. **a**, Head-fixed mouse performing an object-localization task under the microscope. **b**, One frame of a high-speed video sequence and typical pole positions corresponding to multiple go locations (hues of blue) and a single no-go location (red). Whisker touch was possible for all object locations for the long posterior whiskers. The azimuthal angle θ describes whisker position (θ_1 denotes azimuthal angle at first touch). **c**, vM1 neurons were infected with GCaMP3-expressing virus and their axons were imaged in L1 of vS1. **d**, Intrinsic optical-imaging signals corresponding to deflections of whiskers C1, C2 and C3, overlaid on a brightfield image of the vasculature. **e**, Two-photon images showing vM1 axons in the C1 barrel column. **f**, Field of view used for *in vivo* imaging showing varicosities (arrowheads correspond to varicosities used for fluorescence time series in **g**). **g**, Fluorescence dynamics over multiple behavioural trials. Coloured bars indicate the sampling period, when the pole is within reach (blue, go trials; red, no-go trials). **h**, Matrix of correlation coefficients for activity in different varicosities in one field of view. Arrowheads correspond to varicosities marked in **f**. **i**, Distribution of correlation coefficients for all fields of view. Black line denotes pairs of varicosities on the same axon (78 varicosities, 31 axons) and grey line denotes all other varicosity pairs (51,325 varicosities). Correlation coefficients were computed over the entire session. **j**, Correlation coefficients as a function of mean activity level (black denotes pairs of varicosities on the same axon and grey denotes all other pairs). The solid line is an exponential fit ($y = a(1 - e^{-bx}) + c$) to the black circles and the dashed lines represent the 95% confidence interval.

[1]Janelia Farm Research Campus, Howard Hughes Medical Institute, Ashburn, Virginia 20147, USA. †Present addresses: Department for Basic Neurosciences, University of Geneva, Geneva CH-1211, Switzerland (D.H.); Champalimaud Neuroscience Programme, Lisbon 1400-038, Portugal (L.P.); Department of Biochemistry and Molecular Medicine. School of Medicine, University of California, Davis California 95616, USA (L.T.).

1.8, corresponding to 80% correct trials; range, 1.2–2.6) (Supplementary Fig. 1c–e).

To image activity in vM1→vS1 axons we expressed the genetically encoded calcium indicator GCaMP3 (ref. 17) in vM1 neurons[9,12] and implanted a chronic imaging window over vS1 (ref. 18) (Fig. 1c). Imaging was in barrel columns with principal whiskers C1, C2 or C3, based on intrinsic signal imaging[18] (Fig. 1d). Fluorescent axons were abundant in L1 (Fig. 1e, f and Supplementary Fig. 2a, b). GCaMP3-positive axonal varicosities appeared as bright spots along the axon backbone[20]. Two-photon time-lapse images (field of view, 40 μm × 40 μm) were acquired using raster scanning (16 Hz) over 100–200 trials per imaging location (trial duration, 7 s) (Fig. 1f, g and Supplementary Fig. 1c, d).

Action potentials reliably invade cortical axonal arborizations and cause calcium accumulations in varicosities[21], which harbour synaptic terminals. We measured GCaMP3-mediated fluorescence transients, corresponding to trains of action potentials (≥5; Supplementary Fig. 2c–f), in regions of interest (ROIs) containing individual varicosities (range, 35–80 varicosities per field of view; 17 fields of view; 6 mice). Fluorescence transients were detected in multiple ROIs within each field of view (range, 6–20 active varicosities per field of view) (Figs 1f and 2a). As expected, the fluorescence signals from varicosities belonging to the same axon were highly correlated, whereas correlations computed across all other pairs were low (Fig. 1g). These correlations allowed us to identify varicosities on the same axon, even in cases where the local arborization could not be reconstructed morphologically (Fig. 1h–j). Below we report the activity of one varicosity per axon to represent the activity of the entire axon. Only active axons were analysed (Methods). This ensured that almost all (>99%) fluorescence signals reported neural activity rather than movement (Supplementary Fig. 3).

We aligned fluorescence time series with recordings of behavioural features, including $\Delta\kappa$, whisker movements (whisking) and lick rate, and grouped trials by trial type (Fig. 2). Axonal activity was concentrated around the sampling period, and correlated with specific behavioural variables. Some axons were active coincident with whisking before and during the sampling period (Fig. 2b–d; compare ROI1 and whisking amplitude), whereas other axons were mainly active in trials with strong whisker touch (compare ROI2 and $\Delta\kappa$). Some axons were primarily active during licking or could not obviously be explained by a single behavioural feature[12]. Correlations between activity and behaviour were apparent across trials and within trials. These data indicate that individual vM1→vS1 axons represent specific behavioural features, but the representations are diverse across the population of axons.

We used a generalized form of regression (Random Forests, Methods) to quantify how behavioural features are represented by vM1→vS1 axons[12]. Both behaviour and activity varied within trials, across individual trials and across trial types (Fig. 2b, c). For example, in some trials whisker touch was strong, whereas in other trials it was weak or absent (touch in no-go trials was typically the weakest; Supplementary Fig. 1b, e). In some trials mice whisked gingerly and late during the sampling period (Fig. 2b, trial 144), whereas in other trials they whipped their whiskers against the pole as soon as it came within reach (Fig. 2b, trial 145). Our algorithms exploit this variability and the large number of trials in our data set (Supplementary Fig. 1d)

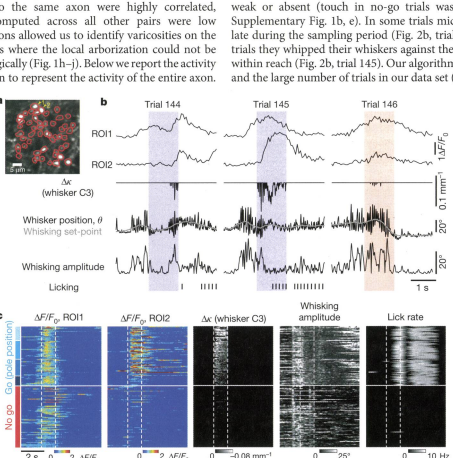

Figure 2 | Motor and sensory signals in vM1→vS1 axons. a, Image of the field of view and ROIs (red) corresponding to all visible axonal varicosities. Yellow numbers indicate ROI1 and ROI2. **b**, Activity ($\Delta F/F_0$) of two individual axons (ROI1 and ROI2) across three trials of one behavioural session, aligned with different behavioural features (whisker position, whisking set-point, whisking amplitude, $\Delta\kappa$, licking (ticks)). Protraction forces correspond to negative $\Delta\kappa$. Coloured bars indicate the sampling period (blue, go trials; red, no-go trials). **c**, Activity across an entire session for two axons ($\Delta F/F_0$ ROI1; $\Delta F/F_0$ ROI2). Each row corresponds to a trial. Dashed white lines indicate the sampling period when the pole is within reach. Trial type is indicated on the far left (hues of blue correspond to different object locations in go trials, as indicated in Fig. 1b). Only correct trials are shown. Right, behavioural variables (see Methods). $\Delta\kappa$ due to protractions; retractions are not shown. Whisking amplitude is the amplitude of the band-pass filtered (6–30 Hz) whisker angle. Lick rate is the instantaneous rate of tongue protractions. **d**, Activity (left) and behavioural variables (right) averaged across trial types. Shading represents s.e.m.

to quantify how well specific behavioural features could be decoded from axonal activity.

We first decoded the measured behavioural features ($\Delta\kappa$; whisking and licking; Methods) on the basis of activity in all axons in a field of view (Fig. 3a). The algorithms used the activity of populations of axons to fit individual behavioural features, taking into account variability within and across trials. The explained variance (R_i^2, for the ith behavioural feature) was used to measure the quality of decoding (Supplementary Fig. 4).

Population activity decoded the recorded behavioural features, including $\Delta\kappa$, whisking and lick rate (Fig. 3a). Whisking was decomposed into set-point (<1.6 Hz) and amplitude (6–30 Hz; Methods)[6,12] (Fig. 2b), but these parameters were highly correlated (Supplementary Fig. 5a) and decoding was similar for these parameters. All imaged fields of view decoded all behavioural features (R^2 larger than for trial-shuffled data; $P < 0.001$, bootstrap test for all sessions and features (Supplementary Fig. 4a)). This is despite the fact that each experiment sampled only approximately 1×10^{-5}% of the synapses in vS1 (assuming: thickness of L1 in vS1, 0.09 mm (ref. 22); vS1 area, 2 mm^2; synaptic density, 1×10^9 per mm (refs 3 and 23)). We conclude that vM1→vS1 axons relay signals related to touch, whisking, licking and other task-related variables to vS1 in a distributed and highly redundant manner.

We used similar methods to classify individual axons on the basis of their activity patterns[12] (Methods; Fig. 3b–e). One half of the active axons (78 out of 138 active axons; 56%) decoded one or more of the

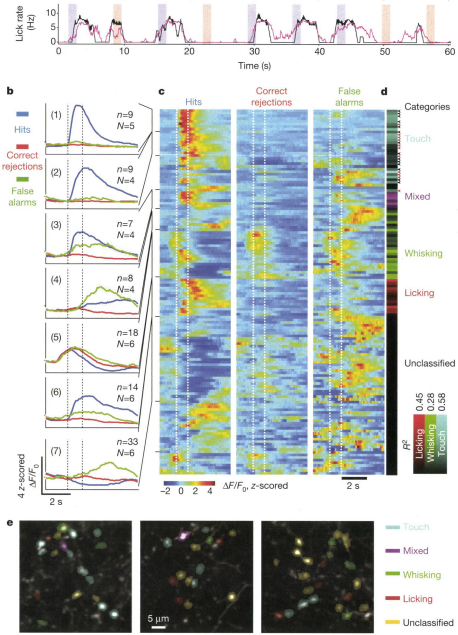

Figure 3 | Decoding behavioural variables on the basis of axonal activity. **a**, Decoding on the basis of axon populations. Time series of behavioural features down-sampled to 16 Hz (black) and the Random Forests model prediction (pink) based on the activity of all axons in one field of view. Vertical bars indicate the sampling periods and the trial type. Top, $\Delta\kappa$ induced by touch during protractions (whisker C2), a measure of contact force. Centre, whisking amplitude. Bottom, lick rate. **b**–**e**, Decoding behavioural features on the basis of the activity of individual axons. Axons were classified based on correlations with behavioural features (138 axons, 6 animals, 17 sessions). **b**, Peristimulus time histograms averaged across axons with shared activity patterns and trial types, in standardized units (z-score). Hits (blue) are correct go trials, correct rejections (red) are correct no-go trials, and false alarms (green) are incorrect no-go trials. Incorrect go trials were rare and are not shown. Correct trials and error trials were used separately in classification. N, number of animals; n, number of axons. 1, touch axons; 2, touch axons with persistent activity; 3, mixed axons; 4, whisking axons, late activity; 5, whisking axons, early activity; 6, licking axons; 7, axons that are selectively active during false alarms; these were unclassified using the behavioural features used. Grey shading represents s.e.m. **c**, Rows correspond to axons. Task-aligned activity was averaged over trials of each type. Rows were ordered on the basis of clustering by activity pattern (Methods). **d**, Correlation between the Random Forests model and different behavioural features (R_i^2) after classification (Methods). The hue indicates the strongest correlation with one of the features (cyan, touch; magenta, mixed; green, whisking; red, licking). Black and red arrowheads indicate axons showing object-location-dependent activity. Red arrowheads indicate significantly persistent axons (Fig. 4). **e**, Axons decoding different behavioural features were spatially intermingled (three sessions from three different animals). Left panel, same axons as in Fig. 2a; right panel, same axons as in Fig. 1f.

measured behavioural features (mean R^2 for best feature, 0.22). Whisking-related axons (26 out of 138 active axons) were active during whisking for all trial types, independent of touch (Fig. 2; ROI1). Whisking-related fluorescence signals lagged whisking onset (mean ± s.d., 259 ± 101 ms) (Supplementary Fig. 5b–d). However, because of the slow dynamics of calcium-dependent fluorescence we cannot exclude the possibility that the underlying spikes might lead whisking. Coding of whisking amplitude and whisking set-point is consistent with neurophysiological[6,24] and imaging experiments in vM1 (ref. 12). Touch-related axons (31 out of 138 active axons) were activated mainly in trials with touch, but not by whisking alone (Fig. 4b; Supplementary Fig. 4c). Consistently, trimming whiskers, which precluded touch during whisking, abolished activity of touch-related axons (Supplementary Fig. 6). Other axons decoded lick rate (classified as lick related)[25] or a mixture of features (classified as 'mixed' axons) (Fig. 3d).

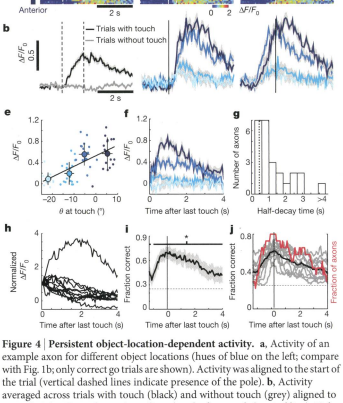

Figure 4 | Persistent object-location-dependent activity. a, Activity of an example axon for different object locations (hues of blue on the left; compare with Fig. 1b; only correct go trials are shown). Activity was aligned to the start of the trial (vertical dashed lines indicate presence of the pole). **b**, Activity averaged across trials with touch (black) and without touch (grey) aligned to start of trial. **c**, Same data as in **a**, aligned to the first touch (vertical line). Ticks, last touch in each trial. Bottom, activity averaged across object locations, aligned to first touch (hits). Grey shading indicates s.e.m. **d**, Same data as in **a**, aligned to the last touch. Bottom, activity averaged across object locations, aligned to last touch. **e**, Activity as a function of θ at touch. Same axon as in **a** is shown. For averaging, points were grouped by object location. Black line denotes linear regression (R^2, 0.41; $P = 2.5 \times 10^{-9}$). Error bars denote s.d. **f**, Activity averaged across object locations, aligned to the last touch and deconvolved to correct for the dynamics of calcium and GCaMP3 fluorescence (same axon as in **a**) (see Supplementary Fig. 8). **g**, Decay time of fluorescence after last touch for all axons showing object-location-dependent activity ($n = 25$). The dashed vertical line indicates $T_{1/2}$ for GCaMP3 fluorescence without persistent activity. **h**, Average fluorescence signals for axons showing persistent activity ($n = 11$). Activity was normalized to the value at the time of the last touch. **i**, The fraction of trials with correctly decoded object location as a function of time for the example axon shown in **a**–**d**. Dashed line indicates chance level (0.25, corresponding to four object locations). Horizontal line indicates time of significant decoding (*$P < 0.05$). Grey shading indicates s.e.m. **j**, Decoding of object location (same group as in **h**; black line, average; red line, fraction of axons decoding above chance level).

Axons representing different behavioural features were spatially intermingled over length scales of micrometres (Figs 2 and 3e); nearby varicosities were equally likely to be part of any of the representations. Repeated imaging experiments showed that the representations of individual axons were largely stable (Supplementary Fig. 6). The L1 apical tuft dendrites of individual neurons in vS1 may have access to a rich amalgam of contextual information.

Most of the touch-related axons showed activity that varied with object location (Fig. 3d, arrow heads; Fig. 4a–c and Supplementary Fig. 7) (25 out of 138 active axons). These axons became active only after first touch (Fig. 4a–c) (latencies greater than 100 ms) and might thus be driven in part by touch-triggered excitation spreading from vS1 to vM1 (refs 10, 11 and 13). In many cases, activation of these axons correlated with forces on a specific whisker. However, this whisker was typically not the principal whisker of the imaged barrel column (Supplementary Fig. 7). Touch-related activity corresponding to specific whiskers is thus broadcast widely to the barrel cortex, consistent with the diffuse nature of the vM1→vS1 projection[4]. These data implicate the primary motor cortex in somatosensation[26]. Furthermore, signals coding for object location are fed back from the motor cortex to the somatosensory cortex.

Fluorescence changes coding for object location often outlasted the presence of the pole, sometimes for several seconds (Fig. 4d–h and Supplementary Fig. 8). This is much longer than expected for the decay-time constant of GCaMP3 fluorescence after trains of action potentials in axons (half-decay time, $T_{1/2}$, 0.45 s; Supplementary Fig. 2) (Fig. 4g, h). After taking calcium dynamics and GCaMP3 fluorescence into account, significant graded, persistent activity was seen in 11 out of 25 object-location-sensitive axons (two-way mixed analysis of variance (ANOVA), $P < 0.05$), lasting from 0.5 s to more than 4 s (Fig. 3d, red arrowheads; Fig. 4g, h). Motor behaviours did not explain object-location-dependent persistent activity; licking and whisking were not different across trials with different object locations (two-way mixed ANOVA, 9 out of 11 persistent object location axons, $P > 0.05$; Supplementary Fig. 8f, g). Object location could be decoded from the activity of persistent axons for up to 4 s after the last contact (Fig. 4 i, j). This parametric persistent activity[26] represents a form of short-term memory of objects detected by specific whiskers at particular locations.

We used calcium imaging with genetically encoded indicators to track activity in specific projections (Fig. 1). Small patches of L1 in vS1 receive diverse signals from vM1, including activity coding for aspects of whisking, touch and licking (Figs 2 and 3). Most of the signals coded by L2/3 neurons in vM1 (ref. 12) were also represented in vM1 axons in L1 of the vS1. Touch-related and persistent activity was overrepresented in the vM1→vS1 axons, but this difference could be due to variations in the behavioural task or the sampled neuronal population.

Pyramidal neurons receive this rich top-down information in their tuft branches in L1, whereas bottom-up sensory input impinges mainly on the proximal basal dendrites[5]. L1 input increases neuronal gain and can promote bursting with coincident input in the proximal basal dendrites[27]. Pyramidal neurons therefore compare contextual input and ongoing sensory input.

Activity related to whisker position was a prominent component of the vM1→vS1 signals (Figs 2 and 3). Pyramidal neurons in vS1 might combine this efference copy-like positional information and touch input to compute object location in vS1 (refs 6 and 15). Whisking signals impinging on L1 dendrites might also selectively amplify activity related to touch during periods of active exploration.

Although mice responded within approximately 100 ms after touch in the object-localization task, a subpopulation of vM1→vS1 axons showed persistent object-location signals that outlasted the decision of

the animals by seconds (Fig. 4). These memory traces, which might not be relevant to solve this particular task, represent information about touches of specific whiskers in the recent past. Haptic object recognition is constructed from localization of several related object features, based on multiple touches over time[28,29] with multiple whiskers[30]. The vM1→vS1 projection links the past state of specific whiskers (input in L1) with present sensory input from other whiskers, ascending into vS1 through the sensory thalamus. The vS1↔vM1 loop thus has the capacity to integrate haptic information across time and space, key components of object recognition and somatosensory navigation. Pyramidal cells in vS1 receive L1 inputs related to past touch, whereas their proximal basal dendrites receive input signalling present touch. These neurons could selectively burst after specific sequences of touches with different whiskers, within time windows defined by the mnemonic activity in L1. In this scheme burst firing of populations of vS1 neurons codes for complex object shape (Supplementary Fig. 9).

METHODS SUMMARY

Virus expressing GCaMP3 (rAAV-synapsin (SYN)-GCaMP3, serotype 2/1, University of Pennsylvania Gene Therapy Program Vector Core) was injected (20 nl, 10 nl min^{-1}, 350 μm deep) into the left vM1 of adult (>P60) C57BL/6 male mice and a circular craniotomy was made over the ipsilateral vS1. Animals were trained in a whisker-dependent object-localization task. vM1 axons were imaged in the vS1 14–23 days after virus injection. Images of the whiskers were acquired using a high-speed camera at 500 frames per second. The whisker position (azimuthal angle at the whisker base, θ) and whisker shape were tracked using automated whisker tracking[6,14]. Licking was detected using an optical lickport.

Full Methods and any associated references are available in the online version of the paper.

Received 16 September 2011; accepted 12 June 2012.
Published online 26 August 2012.

1. Felleman, D. J. & Van Essen, D. C. Distributed hierarchical processing in the primate cerebral cortex. *Cereb. Cortex* **1,** 1–47 (1991).
2. Cauller, L. J. & Connors, B. W. Synaptic physiology of horizontal afferents to layer 1 in slices of rat S1 neocortex. *J. Neurosci.* **14,** 751–762 (1994).
3. Cauller, L. Layer I of primary sensory neocortex: where top-down converges upon bottom-up. *Behav. Brain Res.* **71,** 163–170 (1995).
4. Veinante, P. & Deschenes, M. Single-cell study of motor cortex projections to the barrel field in rats. *J. Comp. Neurol.* **464,** 98–103 (2003).
5. Petreanu, L., Mao, T., Sternson, S. M. & Svoboda, K. The subcellular organization of neocortical excitatory connections. *Nature* **457,** 1142–1145 (2009).
6. Hill, D. N., Curtis, J. C., Moore, J. D. & Kleinfeld, D. Primary motor cortex reports efferent control of vibrissa motion on multiple timescales. *Neuron* **72,** 344–356 (2011).
7. Knutsen, P. M., Pietr, M. & Ahissar, E. Haptic object localization in the vibrissal system: behavior and performance. *J. Neurosci.* **26,** 8451–8464 (2006).
8. O'Connor, D. H. *et al.* Vibrissa-based object localization in head-fixed mice. *J. Neurosci.* **30,** 1947–1967 (2010).
9. O'Connor, D. H., Peron, S. P., Huber, D. & Svoboda, K. Neural activity in barrel cortex underlying vibrissa-based object localization in mice. *Neuron* **67,** 1048–1061 (2010).
10. Ferezou, I. *et al.* Spatiotemporal dynamics of cortical sensorimotor integration in behaving mice. *Neuron* **56,** 907–923 (2007).
11. Kleinfeld, D., Sachdev, R. N., Merchant, L. M., Jarvis, M. R. & Ebner, F. F. Adaptive filtering of vibrissa input in motor cortex of rat. *Neuron* **34,** 1021–1034 (2002).
12. Huber, D. *et al.* Multiple dynamic representations in the motor cortex during sensorimotor learning. *Nature* **484,** 473–478 (2012).
13. Mao, T. *et al.* Long-range neuronal circuits underlying the interaction between sensory and motor cortex. *Neuron* **72,** 111–123 (2011).
14. Clack, N. G. *et al.* Automated tracking of whiskers in videos of head fixed rodents. *PLOS Comput. Biol.* **8,** e1002591 (2012).
15. Knutsen, P. M. & Ahissar, E. Orthogonal coding of object location. *Trends Neurosci.* **32,** 101–109 (2009).
16. Birdwell, J. A. *et al.* Biomechanical models for radial distance determination by the rat vibrissal system. *J. Neurophysiol.* **98,** 2439–2455 (2007).
17. Tian, L. *et al.* Imaging neural activity in worms, flies and mice with improved GCaMP calcium indicators. *Nature Methods* **6,** 875–881 (2009).
18. Trachtenberg, J. T. *et al.* Long-term *in vivo* imaging of experience-dependent synaptic plasticity in adult cortex. *Nature* **420,** 788–794 (2002).
19. Masino, S. A., Kwon, M. C., Dory, Y. & Frostig, R. D. Characterization of functional organization within rat barrel cortex using intrinsic signal optical imaging through a thinned skull. *Proc. Natl Acad. Sci. USA* **90,** 9998–10002 (1993).
20. De Paola, V. *et al.* Cell type-specific structural plasticity of axonal branches and boutons in the adult neocortex. *Neuron* **49,** 861–875 (2006).
21. Cox, C. L., Denk, W., Tank, D. W. & Svoboda, K. Action potentials reliably invade axonal arbors of rat neocortical neurons. *Proc. Natl Acad. Sci. USA* **97,** 9724–9728 (2000).
22. Hooks, B. M. *et al.* Laminar analysis of excitatory local circuits in vibrissal motor and sensory cortical areas. *PLoS Biol.* **9,** e1000572 (2011).
23. De Felipe, J., Marco, P., Fairen, A. & Jones, E. G. Inhibitory synaptogenesis in mouse somatosensory cortex. *Cereb. Cortex* **7,** 619–634 (1997).
24. Carvell, G. E., Miller, S. A. & Simons, D. J. The relationship of vibrissal motor cortex unit activity to whisking in the awake rat. *Somatosens. Mot. Res.* **13,** 115–127 (1996).
25. Komiyama, T. *et al.* Learning-related fine-scale specificity imaged in motor cortex circuits of behaving mice. *Nature* **464,** 1182–1186 (2010).
26. Hernández, A. *et al.* Decoding a perceptual decision process across cortex. *Neuron* **66,** 300–314 (2010).
27. Larkum, M. E., Senn, W. & Luscher, H. R. Top-down dendritic input increases the gain of layer 5 pyramidal neurons. *Cereb. Cortex* **14,** 1059–1070 (2004).
28. Anjum, F., Turni, H., Mulder, P. G., van der Burg, J. & Brecht, M. Tactile guidance of prey capture in Etruscan shrews. *Proc. Natl Acad. Sci. USA* **103,** 16544–16549 (2006).
29. Davidson, P. W. Haptic judgments of curvature by blind and sighted humans. *J. Exp. Psychol.* **93,** 43–55 (1972).
30. Krupa, D. J., Matell, M. S., Brisben, A. J., Oliveira, L. M. & Nicolelis, M. A. Behavioral properties of the trigeminal somatosensory system in rats performing whisker-dependent tactile discriminations. *J. Neurosci.* **21,** 5752–5763 (2001).

Supplementary Information is linked to the online version of the paper at www.nature.com/nature.

Acknowledgements We thank M. Hooks, N. Li, Z. Guo, J. Magee and J. Dudman for comments on the manuscript, N. Clack, V. Iyer and J. Vogelstein for help with software and D. Flickinger for help with microscope design.

Author Contributions L.P. and K.S. conceived the study. L.P. performed the experiments. L.P., D.A.G. and K.S. analysed the data. D.A.G. and D.H.O. contributed software. D.H. and D.H.O. helped with behavioural and imaging experiments. N.-I.X. performed key pilot studies. L.T. and L.L. provided reagents. L.P., D.A.G. and K.S. wrote the paper with comments from all authors.

Author Information Reprints and permissions information is available at www.nature.com/reprints. The authors declare no competing financial interests. Readers are welcome to comment on the online version of this article at www.nature.com/nature. Correspondence and requests for materials should be addressed to K.S. (svobodak@janelia.hhmi.org).

LETTER

doi:10.1038/nature11468

Increased proteasome activity in human embryonic stem cells is regulated by PSMD11

David Vilchez[1], Leah Boyer[2], Ianessa Morantte[1], Margaret Lutz[3], Carsten Merkwirth[1], Derek Joyce[1], Brian Spencer[4], Lesley Page[5], Eliezer Masliah[4], W. Travis Berggren[3], Fred H. Gage[2] & Andrew Dillin[1]

Embryonic stem cells can replicate continuously in the absence of senescence and, therefore, are immortal in culture[1,2]. Although genome stability is essential for the survival of stem cells, proteome stability may have an equally important role in stem-cell identity and function. Furthermore, with the asymmetric divisions invoked by stem cells, the passage of damaged proteins to daughter cells could potentially destroy the resulting lineage of cells. Therefore, a firm understanding of how stem cells maintain their proteome is of central importance. Here we show that human embryonic stem cells (hESCs) exhibit high proteasome activity that is correlated with increased levels of the 19S proteasome subunit PSMD11 (known as RPN-6 in *Caenorhabditis elegans*)[3–5] and a corresponding increased assembly of the 26S/30S proteasome. Ectopic expression of PSMD11 is sufficient to increase proteasome assembly and activity. FOXO4, an insulin/insulin-like growth factor-I (IGF-I) responsive transcription factor associated with long lifespan in invertebrates[6,7], regulates proteasome activity by modulating the expression of PSMD11 in hESCs. Proteasome inhibition in hESCs affects the expression of pluripotency markers and the levels of specific markers of the distinct germ layers. Our results suggest a new regulation of proteostasis in hESCs that links longevity and stress resistance in invertebrates to hESC function and identity.

Embryonic stem cells are unique among all stem-cell populations examined in that they do not seem to undergo replicative senescence[1,2]. Because proteostasis is crucial for maintaining proper cell function[8,9], hESCs could provide a new model to define proteostasis regulation and its demise in ageing. Central to proteostasis is the ubiquitin proteasome system and we examined whether proteasome activity changes as hESCs differentiate into several cell lineages. To evaluate differences in the 26S/30S proteasome activity, we monitored the degradation of specific fluorogenic peptide substrates[10]. We differentiated H9 hESCs into neural progenitors cells (NPCs) and observed a marked decrease in the chymotrypsin-like proteasome activity (Fig. 1a). Moreover, when NPCs were differentiated into neurons, we detected a further decrease in proteasome activity during the differentiation process that was observable after 2 weeks (Fig. 1a and Supplementary Fig. 1). Consistent with enhanced proteasome activity in hESCs, we found increased levels of polyubiquitinated proteins in differentiated cells compared with hESCs (Fig. 1b). Because hESCs are known to vary in their characteristics despite unlimited capacity of self-renewal[11], we differentiated a distinct hESC line, HUES-6 cells, and obtained similar results (Supplementary Figs 1 and 2). Proteasome inhibitors blocked activity from extracts of hESCs, NPCs and neurons (Supplementary Fig. 3), indicating that the increased peptidase activity was indeed due to the proteasome. In addition, the other two activities of the proteasome, the caspase-like and trypsin-like activities, were also increased in hESCs (Supplementary Fig. 4). Proteasome activity did not differ depending on the passage number (Supplementary Fig. 5).

The decrease in proteasome activity was not a specific phenomenon associated with the neural lineage as differentiation into either trophoblasts or fibroblasts induced a similar decrease (Fig. 1c, d).

Notably, hESCs lost their high proteasome activity in a continuous progressive manner during the differentiation process (Fig. 1c). Moreover, we examined other cell lines extracted from human tissues, such as astrocytes, BJ fibroblasts or immortalized HEK293T cells, and found that these cells also had lower proteasome activity compared with hESCs (Supplementary Fig. 6). We tested whether high proteasome activity in hESCs was associated with increased proliferation and found

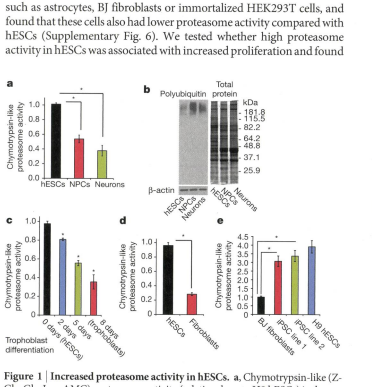

Figure 1 | Increased proteasome activity in hESCs. a, Chymotrypsin-like (Z-Gly-Gly-Leu-AMC) proteasome activity (relative slope to H9 hESCs) is shown. hESCs ($n = 11$), NPCs ($n = 13$), neurons ($n = 10$); $^*P < 0.00001$. **b**, Representative immunoblot of polyubiquitinated protein levels. β-actin is the loading control. Total protein was visualized by Coomassie staining. **c**, Chymotrypsin-like proteasome activity (relative slope to H9 hESCs) is shown. hESCs ($n = 6$), 2 days of differentiation into trophoblasts ($n = 6$), 5 days ($n = 6$), 8 days ($n = 7$). hESCs versus 2 days, $^*P < 0.001$; hESCs versus 5 days, $^*P = 7.7 \times 10^{-7}$; hESCs versus 8 days, $^*P < 0.0001$. **d**, Chymotrypsin-like proteasome activity (relative slope to H9 hESCs) is shown. hESCs ($n = 3$), fibroblasts ($n = 3$); $^*P < 0.001$. **e**, Chymotrypsin-like proteasome activity (relative slope to BJ fibroblasts) is shown. BJ fibroblasts ($n = 10$), iPSC line 1 ($n = 10$), iPSC line 2 ($n = 9$), H9 hESCs ($n = 5$). iPSC lines have increased proteasome activity compared with fibroblasts ($^*P < 0.0005$), and no significant differences compared with H9 hESCs (iPSC line 1 versus hESCs, $P = 0.11$; iPSC line 2 versus hESCs, $P = 0.29$). In **a**, **c**, **d** and **e** data represent the mean ± s.e.m. All statistical comparisons were made by Student's *t*-test for unpaired samples.

[1]Howard Hughes Medical Institute, Glenn Center for Aging Research, Molecular and Cell Biology Laboratory, The Salk Institute for Biological Studies, 10010 North Torrey Pines Road, La Jolla, California 92037, USA. [2]Laboratory of Genetics, The Salk Institute for Biological Studies, 10010 North Torrey Pines Road, La Jolla, California 92037, USA. [3]Stem Cell Core, The Salk Institute for Biological Studies, 10010 North Torrey Pines Road, La Jolla, California 92037, USA. [4]Department of Neurosciences, University of California, San Diego, 9500 Gilman Drive, La Jolla, California 92093, USA. [5]Department of Cell Biology, The Scripps Research Institute, 10550 North Torrey Pines Road, La Jolla, California 92037, USA.

that hESCs and HEK293T cells had nearly identical proliferation rates, yet hESCs had higher proteasome activity (Supplementary Fig. 7). Induced pluripotent stem cells (iPSCs) can be derived from adult somatic cells by forced expression of exogenous factors that promote cell reprogramming[12–14]. iPSC lines are similar to embryonic stem cells in many respects, such as their gene expression patterns, proteome profile and potential for differentiation[13,15]. However, the full extent of their similarity to embryonic stem cells is still being assessed[16]. We analysed two iPSC lines that had been carefully validated to ensure similar gene expression profiles, growth characteristics and developmental potentials to hESCs[17]. We discovered that these iPSC lines derived from BJ fibroblasts display increased proteasome activity similar to hESCs (Fig. 1e), indicating that proteasomal activity can indeed be reprogrammed.

The 26S/30S proteasome consists of a 20S core structure containing the proteolytic active sites and 19S cap structures that impart regulation on the activity of the holo-complex (26S, single and 30S, double capped)[18]. Although 20S particles can exist in a free form, 20S particles

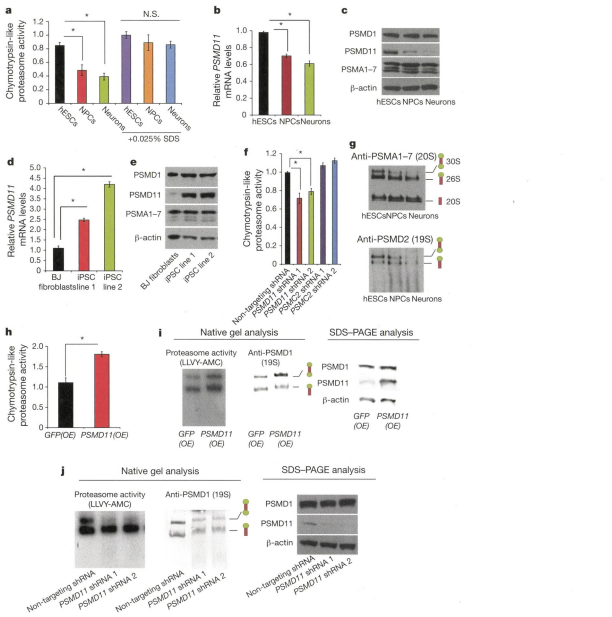

Figure 2 | Increased proteasome assembly in hESCs depends on PSMD11 expression. **a**, Chymotrypsin-like proteasome activity (relative slope to H9 hESCs + 0.025% SDS) is shown. $n = 4$–6; $^*P < 0.01$. No significant differences (N.S.) were found among the different cells when SDS was added (hESCs + SDS versus NPCs + SDS, $P = 0.25$; hESCs + SDS versus neurons + SDS, $P = 0.09$). **b**, Relative *PSMD11* expression compared with H9 hESCs. hESCs ($n = 10$), NPCs ($n = 6$), neurons ($n = 8$); $^*P < 0.00001$. **c**, **e**, Western blot analysis with antibodies against PSMA1–7, PSMD11 and PSMD1. β-actin is the loading control. **d**, Relative *PSMD11* expression compared with BJ fibroblasts. BJ fibroblasts ($n = 10$), iPSC line 1 ($n = 6$), iPSC line 2 ($n = 6$); $^*P < 0.00001$. **f**, Proteasome activity (relative slope to lentivirus non-targeting shRNA) is shown. Non-targeting shRNA ($n = 10$), *PSMD11* shRNA 1 ($n = 8$), *PSMD11* shRNA 2 ($n = 6$), *PSMC2* shRNA 1 ($n = 6$), *PSMC2* shRNA 2 ($n = 3$); $^*P < 0.01$. **g**, Native gel electrophoresis followed by western blot with PSMA1–7 (20S subunit) or PSMD2 (19S subunit) antibodies. **h**, Chymotrypsin-like proteasome activity (relative slope to green fluorescent protein (GFP) overexpressing (OE) HEK293T cells) is shown. *GFP(OE)* ($n = 4$), *PSMD11(OE)* ($n = 5$); $^*P < 0.005$. **i**, **j**, Native gel electrophoresis of HEK293T cell extracts followed by proteasome activity assay with chymotrypsin-like activity substrate Leu-Leu-Val-Tyr-AMC and immunoblotting with PSMD1 (19S subunit) antibody are shown. Extracts were resolved by SDS–PAGE and immunoblotting for analysis of PSMD11 levels and β-actin loading control. In **a**, **b**, **d**, **f** and **h**, data represent the mean ± s.e.m. All statistical comparisons were made by Student's *t*-test for unpaired samples.

in their most physiological form are inactive, unable to degrade denatured proteins or cleave peptides[10]. The 19S regulatory subunit is responsible for stimulating the 20S proteasome to degrade proteins, because ATPases of the regulatory particle open the 20S core, allowing substrates access to proteolytic active sites[19]. SDS treatment of cell extracts, a condition that activates 20S particles by allowing gate opening[20], resulted in equivalent activities among all cell types (Fig. 2a and Supplementary Fig. 8). This result suggests that all cell types have an equal number of 20S particles, but hESCs have increased levels of active 26S/30S proteasomes. We examined the expression of the different 19S proteasome subunits and observed that PSMD11 was the only 19S subunit to decrease as hESCs differentiated (Fig. 2b, c and Supplementary Figs 9–12). Consistent with the hESCs results, we observed increased PSMD11 levels in iPSCs (Fig. 2d, e). Accordingly, decreased expression of PSMD11 in hESCs (Supplementary Table 1) reduced proteasome activity (Fig. 2f), demonstrating that the increased levels of this subunit in hESCs are crucial for increased proteasome activity. PSMD11 has a vital role in stabilizing the otherwise weak interaction between the 20S core and the 19S cap[8], suggesting that hESCs might have more assembled proteasomes. We detected more 30S particles in hESCs compared with NPCs and neurons. Furthermore, as more 20S subunits are assembled into 30S particles, less free 20S is found in hESCs (Fig. 2g). Ectopic expression of PSMD11 was sufficient to increase proteasome activity and assembly in cells with relatively low proteasome activity (Fig. 2h, i). Moreover, knockdown of PSMD11 resulted in fewer assembled proteasomes (Fig. 2j).

The levels of RPN-6, the *C. elegans* orthologue of PSMD11, are increased in the long-lived *glp-1* mutant. In this mutant, increased proteasome activity, *rpn-6* expression and longevity are modulated by the forkhead box O (FOXO) transcription factor DAF-16. To examine whether FOXO transcription factors regulate proteasome activity in hESCs, we reduced expression of the closest human *daf-16* orthologues FOXO1, FOXO3 and FOXO4 (Supplementary Fig. 13 and Supplementary Table 2). Notably, we found that FOXO4 was crucial to modulate proteasome activity in hESCs, whereas FOXO1 and FOXO3, as well as a HSF1, had little or no effect on proteasome activity (Fig. 3a, b and Supplementary Fig. 14). As hESCs differentiated into neural cells, trophoblasts or fibroblasts, there was a corresponding decrease in FOXO4 expression (Supplementary Figs 15–17). Accordingly, this decrease in FOXO4 expression is reprogrammed from somatic cells to iPSCs (Supplementary Fig. 15). FOXO1 had a similar expression pattern to FOXO4 in H9 but not in HUES-6 hESCs (Supplementary Figs 15 and 16). Furthermore, reduction of FOXO4 affected proteasome activity in the multipotent NPCs, which retain partial stem-cell character, but did not affect proteasome activity in differentiated neurons (Supplementary Fig. 18 and Supplementary Table 3). These results raised the question as to whether FOXO4 regulation of proteasome activity could be a general mechanism found in dividing cells. However, we found that FOXO4 was not required for proteasome activity regulation in BJ fibroblasts or HEK293T but rather seems to be specific to hESCs (Supplementary Fig. 19). FOXO4 transcriptional activity is inhibited by phosphorylation on Thr 32, Ser 197 and Ser 262 sites, and once dephosphorylated, it translocates to the nucleus and induces target gene expression[21,22]. Expression of a constitutively active FOXO4 triple alanine mutant (FOXO4-AAA), but not wild-type FOXO4, resulted in further upregulation of proteasome activity in hESCs (Fig. 3c, Supplementary Fig. 20 and Supplementary Table 4a, b). In addition, ectopic expression of FOXO4-AAA in *FOXO4* short hairpin RNA (shRNA) cells partially restored proteasome activity of these cells (Fig. 3d and Supplementary Table 4c). We found that loss of FOXO4 resulted in reduced expression of PSMD11 in hESCs and in the multipotent NPCs, but did not affect PSMD11 in differentiated neurons (Fig. 3e, f and Supplementary Fig. 21). Knockdown of FOXO1, FOXO3 or HSF1 did not affect

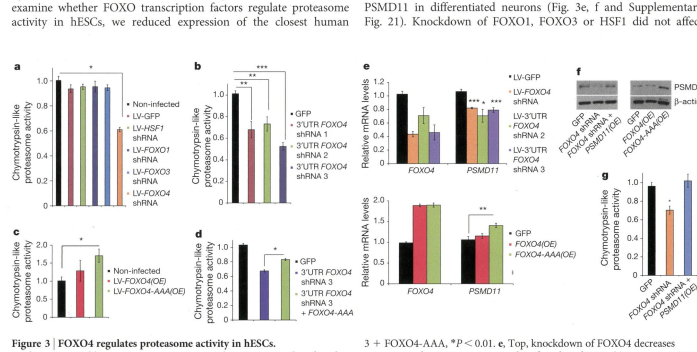

Figure 3 | FOXO4 regulates proteasome activity in hESCs. **a**, Chymotrypsin-like proteasome activity in H9 hESCs transiently infected with lentiviruses (LV; relative slope to non-infected cells) is shown. $n = 19$; $^{*}P < 0.00001$. **b**, Chymotrypsin-like proteasome activity of stable-infected hESCs (relative slope to GFP cells) is shown. GFP ($n = 7$), *FOXO4* shRNA 1 ($n = 6$), *FOXO4* shRNA 2 ($n = 3$), *FOXO4* shRNA 3 ($n = 6$). GFP versus *FOXO4* shRNA 1, $^{**}P < 0.01$; GFP versus *FOXO4* shRNA 2, $^{**}P < 0.01$; GFP versus *FOXO4* shRNA 3, $^{***}P = 4.5 \times 10^{-8}$. All shRNAs target the 3′ untranslated region (UTR) of the human genes. **c**, Proteasome activity of transiently infected hESCs (relative slope to non-infected H9 hESCs) is shown. $n = 7$; non-infected cells versus *FOXO4(OE)* cells, $^{*}P = 0.41$; non-infected cells versus *FOXO4-AAA(OE)* cells, $^{*}P < 0.05$. **d**, Proteasome activity (relative slope to GFP hESCs) is shown. $n = 4$; *FOXO4* shRNA 3 versus *FOXO4* shRNA 3 + FOXO4-AAA, $^{*}P < 0.01$. **e**, Top, knockdown of FOXO4 decreases expression of *PSMD11* in transiently infected H9 hESCs (GFP versus *FOXO4* shRNA, $^{***}P < 0.001$; GFP versus *FOXO4* shRNA 2, $^{*}P < 0.05$; GFP versus *FOXO4* shRNA 3, $^{***}P < 0.001$). GFP ($n = 15$), *FOXO4* shRNA ($n = 19$), *FOXO4* shRNA 2 ($n = 4$), *FOXO4* shRNA 3 ($n = 5$). Bottom, stable overexpression of the FOXO4-AAA mutant increases *PSMD11* expression in H9 hESCs (GFP versus *FOXO4(OE)*, $P = 0.69$; GFP versus *FOXO4-AAA(OE)*, $^{**}P < 0.01$). GFP ($n = 7$), *FOXO4(OE)* ($n = 8$), *FOXO4-AAA(OE)* ($n = 7$). **f**, Western blot analysis of PSMD11 levels. β-actin is the loading control. **g**, Proteasome activity (relative slope to GFP H9 hESCs) is shown. $n = 4$; GFP versus *FOXO4* shRNA, $^{*}P < 0.01$; GFP versus *FOXO4* shRNA + *PSMD11(OE)*, $P = 0.50$. Data in **a**–**e** and **g** represent the mean ± s.e.m. Statistical comparisons were made by Student's *t*-test for unpaired samples.

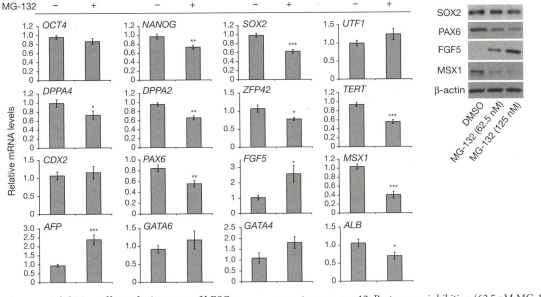

Figure 4 | Acute proteasome inhibition affects pluripotency of hESCs. **a**, Real-time PCR analysis of pluripotency (*OCT4* (also known as *POU5F1*), *NANOG*, *SOX2*, *UTF1*, *DPPA4*, *DPPA2*, *ZFP42* and *TERT*), trophectodermal (*CDX2*), ectodermal (*PAX6*, *FGF5*), mesodermal (*MSX1*) and endodermal (*AFP*, *GATA6*, *GATA4* and *ALB*) germ-layer markers. The graphs (relative expression to H9 hESCs plus dimethylsulphoxide (DMSO)) represent the mean ± s.e.m., $n = 12$. Proteasome inhibition (62.5 nM MG-132 for 24 h) in hESCs induces a decrease in pluripotency markers and modifies the levels of germ-layer markers. $^{*}P < 0.05$; $^{**}P < 0.01$; $^{***}P < 0.001$. **b**, Western blot analysis with antibodies against SOX2, PAX6, FGF5 and MSX1. β-actin is the loading control. Statistical comparisons were made by Student's *t*-test for unpaired samples.

the expression of PSMD11 in any cell type tested, including hESCs (Supplementary Tables 5–7). Moreover, overexpression of FOXO4-AAA increased PSMD11 levels in hESCs (Fig. 3e, f and Supplementary Table 5). Ectopic expression of PSMD11 in *FOXO4* shRNA hESCs rescued their proteasome activity, indicating that expression of PSMD11 by FOXO4 is sufficient to regulate proteasomal function (Fig. 3f, g).

To test the effects of proteasome inhibition on hESC identity, we induced an acute proteasome inhibition in hESCs by using the MG-132 proteasome inhibitor. Notably, hESCs were more sensitive to proteasome inhibition than were NPCs or neurons, and we had to decrease the MG-132 concentration almost 100 times to avoid cell death and detachment of hESCs (data not shown). Notably, low concentrations of MG-132 (62.5 nM) were sufficient to reduce proteasome activity and induce accumulation of polyubiquitinated proteins in hESCs (Supplementary Fig. 22). Even in the absence of differentiation treatment, we already observed that proteasome inhibition resulted in decreased levels of pluripotency markers and modified the levels of markers of the distinct germ and extraembryonic layers, while decreasing the expression of proteins involved in neurogenesis, such as PAX6 and MSX1 (Fig. 4).

Collectively, our results establish increased proteasome activity as an intrinsic characteristic of hESC identity. Our findings raise the intriguing question of why these cells need enhanced proteasome activity. One possibility is that hESCs cannot tolerate toxic, misfolded proteins, and increased proteostasis could be required to avoid hESC senescence and maintain an intact proteome for either self-renewal or the generation of an intact cell lineage. Alternatively, high proteasome activity may be tightly linked to other cellular process, such as translation, to ensure future integrity of the proteome. In addition, our results indicate that an orthologue of DAF-16, a transcription factor that regulates both lifespan and resistance to proteotoxic stress in invertebrates, crosses evolutionary boundaries and links hESC identity to invertebrate longevity modulation. It will be of particular interest to identify other genes of the proteostasis network regulated by FOXO4 in hESCs. In conclusion, our findings may trigger new advances in understanding hESC differentiation or cell reprogramming and open new possibilities for cell therapy by modulation of the proteostasis network.

METHODS SUMMARY

26S proteasome fluorogenic peptidase assays. The *in vitro* assay of 26S proteasome activities was performed as previously described[10]. Cells were collected in proteasome activity assay buffer (50 mM Tris-HCl, pH 7.5, 250 mM sucrose, 5 mM $MgCl_2$, 0.5 mM EDTA, 2 mM ATP and 1 mM dithiothreitol) and lysed by passing ten times through a 27-gauge needle. Lysate was centrifuged at 10,000*g* for 10 min at 4 °C. Fifteen to twenty-five micrograms of total protein of cell lysates were transferred to a 96-well microtiter plate (BD Falcon) and incubated with fluorogenic substrate. Fluorescence (380 nm excitation, 460 nm emission) was monitored on a microplate fluorometer (Infinite M1000, Tecan) every 5 min for 1 h at 37 °C.

Native gel immunoblotting of the proteasome. HEK293T cells were run on 3.5% native gels prepared in resolving buffer (90 mM Tris base, 90 mM boric acid, 5 mM $MgCl_2$, 0.5 mM EDTA and 1 mM ATP) with 5 mM ATP, 1 mM dithiothreitol and 3.5% acrylamide from a 40% stock solution of acrylamide and bisacrylamide in a 37.5:1 ratio (Bio-Rad). These were run at 110 V for 3 h at 4 °C. Activity assays were performed by incubating the gels in activity assay buffer for 20 min at 37 °C and developed using a BioRad Gel Doc with ultraviolet illumination. Before transfer, the gels were incubated in transfer buffer (25 mM Tris base and 192 mM glycine) with 1% SDS for 10 min followed by a 10-min incubation in transfer buffer. The protein was transferred to polyvinylidene difluoride (PVDF) membranes at 5 V for 16 h in transfer buffer using an Idea Scientific Genie Blotter. Western blot analysis was performed with anti-PSMD1 (Abcam) and analysed using the Odyssey system (LI-COR). Extracts were also analysed by SDS-PAGE to determine protein expression levels and loading control.

A detailed description of all experimental methods, including hESC culture and differentiation, is provided in Methods.

Full Methods and any associated references are available in the online version of the paper.

Received 8 August 2011; accepted 6 August 2012.

1. Evans, M. J. & Kaufman, M. H. Establishment in culture of pluripotential cells from mouse embryos. *Nature* **292,** 154–156 (1981).
2. Thomson, J. A. *et al.* Embryonic stem cell lines derived from human blastocysts. *Science* **282,** 1145–1147 (1998).
3. Isono, E., Saito, N., Kamata, N., Saeki, Y. & Toh, E. A. Functional analysis of Rpn6p, a lid component of the 26 S proteasome, using temperature-sensitive *rpn6*

mutants of the yeast *Saccharomyces cerevisiae*. *J. Biol. Chem.* **280,** 6537–6547 (2005).
4. Pathare, G. R. *et al.* The proteasomal subunit Rpn6 is a molecular clamp holding the core and regulatory subcomplexes together. *Proc. Natl Acad. Sci. USA* **109,** 149–154 (2012).
5. Santamaria, P. G., Finley, D., Ballesta, J. P. & Remacha, M. Rpn6p, a proteasome subunit from *Saccharomyces cerevisiae*, is essential for the assembly and activity of the 26 S proteasome. *J. Biol. Chem.* **278,** 6687–6695 (2003).
6. Kenyon, C., Chang, J., Gensch, E., Rudner, A. & Tabtiang, R. A *C. elegans* mutant that lives twice as long as wild type. *Nature* **366,** 461–464 (1993).
7. Tatar, M. *et al.* A mutant *Drosophila* insulin receptor homolog that extends life-span and impairs neuroendocrine function. *Science* **292,** 107–110 (2001).
8. Balch, W. E., Morimoto, R. I., Dillin, A. & Kelly, J. W. Adapting proteostasis for disease intervention. *Science* **319,** 916–919 (2008).
9. Powers, E. T., Morimoto, R. I., Dillin, A., Kelly, J. W. & Balch, W. E. Biological and chemical approaches to diseases of proteostasis deficiency. *Annu. Rev. Biochem.* **78,** 959–991 (2009).
10. Kisselev, A. F. & Goldberg, A. L. Monitoring activity and inhibition of 26S proteasomes with fluorogenic peptide substrates. *Methods Enzymol.* **398,** 364–378 (2005).
11. Osafune, K. *et al.* Marked differences in differentiation propensity among human embryonic stem cell lines. *Nature Biotechnol.* **26,** 313–315 (2008).
12. Takahashi, K. *et al.* Induction of pluripotent stem cells from adult human fibroblasts by defined factors. *Cell* **131,** 861–872 (2007).
13. Takahashi, K. & Yamanaka, S. Induction of pluripotent stem cells from mouse embryonic and adult fibroblast cultures by defined factors. *Cell* **126,** 663–676 (2006).
14. Yu, J. *et al.* Induced pluripotent stem cell lines derived from human somatic cells. *Science* **318,** 1917–1920 (2007).
15. Hanna, J. H., Saha, K. & Jaenisch, R. Pluripotency and cellular reprogramming: facts, hypotheses, unresolved issues. *Cell* **143,** 508–525 (2010).
16. Panopoulos, A. D., Ruiz, S. & Izpisua Belmonte, J. C. iPSCs: induced back to controversy. *Cell Stem Cell* **8,** 347–348 (2011).
17. Brennand, K. J. *et al.* Modelling schizophrenia using human induced pluripotent stem cells. *Nature* **473,** 221–225 (2011).
18. Finley, D. Recognition and processing of ubiquitin-protein conjugates by the proteasome. *Annu. Rev. Biochem.* **78,** 477–513 (2009).
19. Köhler, A. *et al.* The axial channel of the proteasome core particle is gated by the Rpt2 ATPase and controls both substrate entry and product release. *Mol. Cell* **7,** 1143–1152 (2001).
20. Coux, O., Tanaka, K. & Goldberg, A. L. Structure and functions of the 20S and 26S proteasomes. *Annu. Rev. Biochem.* **65,** 801–847 (1996).
21. Kops, G. J. P. L. *et al.* Direct control of the Forkhead transcription factor AFX by protein kinase B. *Nature* **398,** 630–634 (1999).
22. Matsuzaki, H., Ichino, A., Hayashi, T., Yamamoto, T. & Kikkawa, U. Regulation of intracellular localization and transcriptional activity of FOXO4 by protein kinase B through phosphorylation at the motif sites conserved among the FOXO family. *J. Biochem.* **138,** 485–491 (2005).

Supplementary Information is available in the online version of the paper.

Acknowledgements We thank W. E. Balch for critical comments on this work. We thank A. Stauffer and V. Modesto for their help with BrdU assays and cell culture, respectively. We thank S. Ruiz for advice on hESC culture and lentiviral infection. This work was supported by the Howard Hughes Medical Institute. D.V. was a recipient of the F.M. Kirby, Inc. Foundation Postdoctoral Scholar Award and Beatriu de Pinós (AGAUR) fellowship. F.H.G. acknowledges the Helmsley Foundation, JPB Foundation, Mathers Foundation, Lookout Fund and California Institute for Regenerative Medicine.

Author Contributions D.V. and A.D. planned and supervised the project. D.V. performed the experiments, data analysis and interpretation. L.B. performed neural differentiation assays and contributed to other assays. I.M. performed biochemistry experiments and contributed to other assays. M.L. performed cell culturing and trophoblast/fibroblast differentiation. C.M. performed biochemistry experiments and contributed to other assays. D.J. performed proteasome assembly experiments. B.S., L.P. and E.M. generated lentiviral constructs. W.T.B. and F.H.G. contributed with their knowledge of stem-cell biology and neural differentiation, and helped to supervise the project. The manuscript was written by D.V. and A.D. and edited by L.B., I.M., C.M., W.T.B. and F.H.G. All authors discussed the results and commented on the manuscript.

Author Information Reprints and permissions information is available at www.nature.com/reprints. The authors declare no competing financial interests. Readers are welcome to comment on the online version of the paper. Correspondence and requests for materials should be addressed to A.D. (dillin@salk.edu).

LETTER

doi:10.1038/nature11309

Chronic lymphocytic leukaemia is driven by antigen-independent cell-autonomous signalling

Marcus Dühren-von Minden[1]*, Rudolf Übelhart[1,2]*, Dunja Schneider[1]*, Thomas Wossning[1], Martina P. Bach[1], Maike Buchner[3], Daniel Hofmann[1], Elena Surova[1,2], Marie Follo[3], Fabian Köhler[1], Hedda Wardemann[4], Katja Zirlik[3], Hendrik Veelken[5] & Hassan Jumaa[1,6]

B-cell antigen receptor (BCR) expression is an important feature of chronic lymphocytic leukaemia (CLL), one of the most prevalent B-cell neoplasias in Western countries[1]. The presence of stereotyped and quasi-identical BCRs in different CLL patients suggests that recognition of specific antigens might drive CLL pathogenesis. Here we show that, in contrast to other B-cell neoplasias, CLL-derived BCRs induce antigen-independent cell-autonomous signalling, which is dependent on the heavy-chain complementarity-determining region (HCDR3) and an internal epitope of the BCR. Indeed, transferring the HCDR3 of a CLL-derived BCR provides autonomous signalling capacity to a non-autonomously active BCR, whereas mutations in the internal epitope abolish this capacity. Because BCR expression was required for the binding of secreted CLL-derived BCRs to target cells, and mutations in the internal epitope reduced this binding, our results indicate a new model for CLL pathogenesis, with cell-autonomous antigen-independent signalling as a crucial pathogenic mechanism.

CLL cases can be divided into two groups based on the mutational status of the immunoglobulin genes. Notably, in B cells from ~1% of both groups, unmutated CLL and mutated CLL cases express almost identical BCRs, and in 30% of cases the BCRs can be classified into certain stereotypes based on structural similarities and the HCDR3 (refs 2–5). This restricted BCR repertoire has been interpreted to be the result of a BCR-driven selection mechanism initiated by specific antigens that may promote the expansion of the respective CLL clone[6,7].

We have recently reported functional similarity between the pre-BCR and polyreactive BCRs, and have demonstrated that both activate cell-autonomous signalling in pre-B cells[8]. Furthermore, we have shown that the pre-BCR induces ligand-independent cell-autonomous signalling by surrogate light-chain-mediated binding to an intrinsic pre-BCR glycosylation site[9]. CLL-derived BCRs are also often polyreactive[10,11], suggesting that, in analogy to the pre-BCR, CLL BCRs might activate ligand-independent autonomous signalling through the binding of BCR-intrinsic motifs. We tested this hypothesis by comparing the signalling capacity of randomly chosen BCRs from different B-cell lymphomas in triple knockout (TKO) cells that do not express endogenous pre-BCRs or BCRs owing to inactivation of *RAG2* and *λ5* genes. An additional deficiency in SLP65 (also known as BLNK) expression makes TKO cells an ideal reconstitution system to test receptor function by transfection of receptor components and a tamoxifen-inducible ERT2–SLP65 fusion protein[12]. As shown previously[8], the pre-BCR and a polyreactive human BCR derived from an early bone marrow B cell (BCR62) activate Ca^{2+} mobilization autonomously without additional ligands, whereas a non-polyreactive human BCR derived form a selected mature B cell (BCR53) requires additional crosslinking (Supplementary Fig. 1a and data not shown). Similar to BCR53, we found that BCRs derived from multiple myeloma ($n = 4$), marginal zone lymphoma ($n = 3$), mantle cell lymphoma ($n = 4$) and follicular lymphoma ($n = 4$) required crosslinking with anti-BCR antibody in addition to SLP65 activation to induce Ca^{2+} flux (Fig. 1, Supplementary Fig. 1b, c and Supplementary Table 1; data not shown). By contrast, all tested ($n = 17$) CLL-derived BCRs, including those containing typical CLL variable heavy chain (VH) elements (for example, IGHV4-34, IGHV3-7, IGHV3-23, IGHV3-30 and IGHV1-69)[3] and stereotyped HCDR3s, induced autonomous signalling on SLP65 activation (Fig. 1, Supplementary Fig. 2a and Supplementary

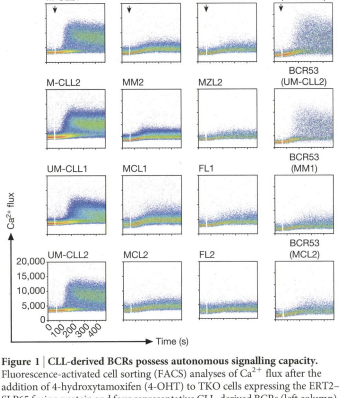

Figure 1 | CLL-derived BCRs possess autonomous signalling capacity. Fluorescence-activated cell sorting (FACS) analyses of Ca^{2+} flux after the addition of 4-hydroxytamoxifen (4-OHT) to TKO cells expressing the ERT2–SLP65 fusion protein and four representative CLL-derived BCRs (left column), two representative BCRs of multiple myeloma (MM), mantle cell lymphoma (MCL), marginal zone lymphoma (MZL) and follicular lymphoma (FL) (middle two columns) and BCR53 variants containing different HCDR3s of representative CLL, multiple myeloma or mantle cell lymphoma receptors (right column). Addition of the stimulus is indicated by black arrows. M, mutated; UM, unmutated.

[1]Centre for Biological Signaling Studies (BIOSS), Albert-Ludwigs Universität Freiburg, 79104 Freiburg, Germany. [2]Spemann Graduate School of Biology and Medicine, Albert-Ludwigs Universität Freiburg, 79104 Freiburg, Germany. [3]Department of Hematology/Oncology, University Medical Center Freiburg, 79106 Freiburg, Germany. [4]Max Planck Research Group Molecular Immunology, Max Planck Institute for Infection Biology, 10117 Berlin, Germany. [5]Department of Hematology, Leiden University Medical Center, 2333 ZA Leiden, the Netherlands. [6]Department of Molecular Immunology, Faculty of Biology, Albert Ludwigs University of Freiburg and Max Planck Institute of Immunobiology and Epigenetics, 79108 Freiburg, Germany.

*These authors contributed equally to this work.

Table 1; data not shown). No obvious difference was found between mutated ($n = 10$) and unmutated ($n = 7$) CLL BCRs (Fig. 1 and data not shown). Importantly, BCRs derived from healthy donors who possess CLL-typical VH genes such as *IGHV1-69* or *IGHV4-34* did not display autonomous signalling (Supplementary Fig. 2b).

To investigate whether autonomous signalling is also involved in lymphoproliferation in animal models of CLL, we examined TCL1 mice, which express a transgene for human T-cell leukaemia 1 (*TCL1*) under the control of the VH promotor and the Eμ enhancer[13]. TCL1 is highly expressed in unmutated CLL[14] and TCL1 transgenic mice show clonal expansion of $CD5^+$ IgM^+ B cells bearing unmutated BCRs[13,15]. To test whether transformed clones derived from TCL1 mice express autonomously active BCRs, we studied four different BCRs from TCL1 mice in the TKO reconstitution system. All four TCL1-derived BCRs showed autonomous Ca^{2+} flux similar to the human CLL BCRs and the murine pre-BCR, whereas a 4-hydroxy-3-iodo-5-nitrophenylacetyl (NIP)-specific murine BCR (B1-8) showed no autonomous signalling (Supplementary Fig. 3a, b). Similar to human B-cell CLL, TCL1-transformed murine B cells are $CD5^+$. Therefore, we tested whether autonomous signalling is a characteristic feature of murine B1a B cells that are typically $CD5^+$ and IgM^+. Interestingly, BCRs from B1a B cells did not induce autonomous signalling, indicating that this capacity is a unique feature of leukaemia-derived BCRs (Supplementary Fig. 3c). Together, our data show that, in contrast to all other B-cell lymphomas tested, BCRs derived from CLL patients and TCL1 mice possess the unique capacity to induce autonomous signalling.

The bias in VH gene usage and the high proportion of stereotyped HCDR3s in CLL suggest that HCDR3 has a critical role in the development of this disease[2,3,5]. To test whether transferring HCDR3 from a CLL-derived BCR transfers autonomous signalling capacity to a non-autonomously active BCR, we replaced the HCDR3 of BCR53 with three different CLL-derived HCDR3s. As a negative control, we replaced the HCDR3 of BCR53 with the HCDR3s of a multiple myeloma BCR and a mantle cell lymphoma BCR that contained the same VH gene as the chosen CLL BCRs. Although all modified BCR53 derivatives were expressed on the cell surface, only those containing a CLL-derived HCDR3 acquired the capacity for autonomous signalling (Fig. 1 and Supplementary Fig. 1; data not shown).

Our previous results indicated that the ability to induce autonomous Ca^{2+} flux was associated with BCR polyreactivity[8]. Because most secreted CLL-derived BCRs were reported to be polyreactive[10], we tested the chosen CLL BCRs for polyreactivity. Only three out of six randomly chosen CLL-derived BCRs—two unmutated and one mutated—showed polyreactive potential by binding to more than two antigens in enzyme-linked immunosorbent assays (ELISA) and showing cytoplasmic staining of HEp-2 slides in indirect immunofluorescence assays (Supplementary Fig. 4a, b). Furthermore, only one out of four tested TCL1 BCRs (TCL1 no. 3) showed polyreactivity in the same assays (Supplementary Fig. 4c, d). The frequent lack of polyreactivity suggests that other mechanisms induce the autonomous signalling of CLL-derived BCRs. To show that specific antigens on adjacent cells are not required for the activation of CLL BCRs, we examined autonomous Ca^{2+} signalling in isolated, single cells. We detected autonomous Ca^{2+} flux in single cells expressing a CLL-derived BCR, whereas additional stimulation with anti-BCR antibodies was required for activation of single cells expressing the BCR53 control (Fig. 2a, b).

The lack of polyreactivity suggests that antigen-independent signalling might be achieved by HCDR3-dependent binding of BCR-intrinsic motifs, suggesting mutual BCR recognition on CLL cells. Indeed, secreted CLL-derived BCRs bound to the surface of TKO cells expressing a CLL BCR or the control BCR53, although they failed to bind to TKO cells that did not express a receptor (Fig. 3a, b and Supplementary Fig. 5a). This suggests that the CLL-derived BCRs might interact with intrinsic BCR structures and that this interaction

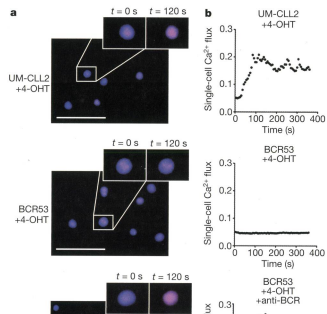

Figure 2 | CLL BCRs induce cell-autonomous signalling. **a**, Live-cell imaging of single TKO cells expressing ERT2–SLP65 and unmutated CLL2 or BCR53 after induction with 4-OHT. Images show merged channels of Indo-1 unbound (blue) and Indo-1 bound (violet). Magnification is ×40; scale bars, 25 μm. **b**, Ca^{2+} flux of representative single cells from **a**. Kinetics are representative of at least ten single cells.

could mediate antigen-independent stimulation if it takes place within the membrane of the same cell. Using a phage-display approach, a recent study identified different peptide motifs that bind to primary CLL cells in a HCDR3-dependent manner, and one of these motifs showed specific binding to each of the tested CLL samples[16]. Through sequence analysis we found that this motif possesses homology to a conserved epitope in the framework region 2 (FR2) of VH domains (Supplementary Fig. 5c). To test whether this region contains an internal epitope important for autonomous signalling, we generated point mutations of the amino acids Val 37 and Arg 38 within this motif. As a control we mutated a conserved arginine (Arg 43) outside of the motif. Our results show that mutating Val 37 or Arg 38, but not Arg 43, abolishes autonomous signalling of CLL BCRs, whereas stimulation with anti-BCR antibodies show normal Ca^{2+} flux for all mutants (Fig. 3c, d and Supplementary Fig. 5b, d; data not shown). As the introduced mutations are located outside of the antigen-recognition site of the BCR, these data indicate that the observed autonomous signalling is not induced by BCR interaction with external antigens in the environment, because such antigens should still be able to bind to and stimulate the mutated CLL BCR. To confirm this view, we mutated Val 37 and Lys 38 in the NIP-specific B1-8 BCR and found that the resulting mutant BCRs show normal antigen-dependent stimulation after incubation with NIP–bovine serum albumin (Fig. 3c and Supplementary Fig. 5b). Thus, these data indicate that the loss of autonomous signalling was caused by the inability of the CLL BCR to bind to the mutated intrinsic motif. In agreement with this, the binding of secreted CLL BCRs to TKO cells was reduced when the cells expressed a BCR with a mutated intrinsic motif (Fig. 3e). Together, our results suggest that an intrinsic BCR motif and HCDR3 mediate autonomous BCR stimulation in CLL-derived BCRs.

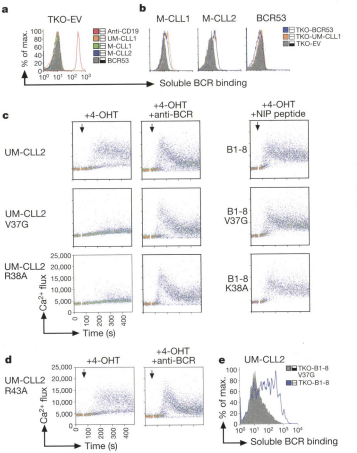

Figure 3 | Autonomous signalling of CLL-derived BCRs is mediated by the recognition of a BCR-intrinsic epitope. **a**, Surface-binding profiles of different secreted CLL BCRs on TKO cells expressing empty vector (EV). Secreted BCR53 and anti-CD19 antibody were used as negative and positive controls, respectively. The amount of secreted BCR used was >100-fold higher than for the anti-CD19 antibody. **b**, Surface-binding profiles of secreted M-CLL1, M-CLL2 and BCR53 on TKO cells expressing the indicated BCRs. **c**, **d**, FACS analysis for autonomous Ca^{2+} flux after addition of the indicated stimuli in TKO cells expressing the ERT2–SLP65 fusion protein. **c**, The UM-CLL2 mutants V37G and R38A (left) or the corresponding B1-8 mutants (right). **d**, The UM-CLL2 R43A mutant. Arrows indicate addition of the stimuli. **e**, Surface-binding profile of UM-CLL2 on TKO cells expressing B1-8 or B1-8 V37G.

To show that autonomous signalling can also be detected in primary CLL samples, we monitored Ca^{2+} flux in primary B cells from CLL patients and compared them to primary peripheral B cells from healthy donors or patients with other B-cell neoplasias. Because SLP65 function is constitutively active in primary cells, a synchronous start of autonomous signalling as in the TKO cells cannot be achieved in primary cells. However, constitutive autonomous signalling suggests that a proportion of the primary cells show increased Ca^{2+} flux. In fact, our experiments show that primary CLL samples show elevated Ca^{2+} mobilization compared with the control cells. Moreover, this signalling capacity required BCR function, as inhibition of the protein tyrosine kinase SYK, which transmits BCR signals[17], prevented this activity (Fig. 4 and Supplementary Fig. 6a). Similarly, monitoring Ca^{2+} mobilization in single cells showed periodic SYK-dependent signals in isolated primary CLL B cells but not in control cells (Fig. 4 and Supplementary Fig. 6b). As survival of CLL B cells is associated with nuclear-factor κB (NF-κB) activation[18], we investigated the expression of NF-κB-regulated survival genes[18] in primary CLL cells and found that inhibition of autonomous BCR signalling by inhibition of SYK led to a reduction in the expression of MYC and XIAP (Supplementary Fig. 6c).

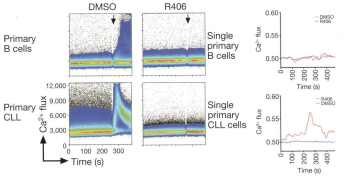

Figure 4 | Cell-autonomous Ca^{2+} signalling is elevated in primary CLL B cells. Ca^{2+} flux in primary peripheral B cells from a healthy donor or a CLL patient with or without R406 treatment (left panels; addition of an anti-BCR stimulus as a control for cell viability and Indo loading is indicated by a black arrow) and Ca^{2+} flux in single cells from a healthy donor or a CLL patient (right panels). DMSO, dimethylsulphoxide.

BCR expression is commonly used as a diagnostic marker for the characterization of CLL patients. The restricted BCR repertoire of both mutated and unmutated CLL suggests a potentially important role for BCR signalling in the transformation and expansion of CLL B cells. The restricted BCR repertoire and the observed polyautoreactivity suggested that CLL BCRs might recognize extrinsic autoantigens, thereby inducing the selective expansion of the respective B cells. Therefore, blocking such autoantigens or blocking BCR function by inhibiting downstream signalling factors, such as the tyrosine kinase SYK, are considered as potential therapies for CLL[19–22].

However, our data indicate that CLL BCRs induce cell-autonomous signalling independent of extrinsic antigens and identify an intrinsic motif that might provide new targets for the therapy of CLL by interfering with autonomous BCR stimulation. It is conceivable that additional intrinsic epitopes exist that activate the autonomous signalling of distinct CLL BCRs. In this scenario, the HCDR3-driven interaction with distinct epitopes on nearby BCRs is sufficient for the induction of autonomous signalling on CLL cells. In agreement with this, HCDR3 sequences derived from CLL BCRs were able to transfer the autonomous signalling capacity to other receptors in our experiments. Presumably, only certain HCDR3 sequences have this unique capacity, which might explain the restricted repertoire and the requirement for certain HCDR3 regions in CLL. Thus, the presence of distinct intrinsic epitopes may explain the observed structural similarities of CLL BCRs, which are probably selected on the basis of the ability of HCDR3 to interact with such intrinsic structures. It should be noted, however, that the presence of intrinsic epitopes and their role in autonomous signalling does not rule out that for certain cases, extrinsic antigens are involved in the pathogenesis of CLL. This may further potentiate the basal activity of CLL BCRs. Our study presents a new mechanism for the pathogenesis of CLL and suggests that investigating intrinsic BCR-associated epitopes may lead to the development of new therapeutic approaches based on the inhibition of the autonomous BCR activation in CLL cells.

METHODS SUMMARY

Details of lymphoma material, clinical data, mice strain data, cells and cell-culture conditions, polyreactivity assays, plasmids and retroviral transduction, flow cytometry and Ca^{2+} flux analysis, single-cell Ca^{2+} flux analysis, NF-κB-activity assays, reverse-transcriptase PCR and statistical analysis are provided in Methods.

Full Methods and any associated references are available in the online version of the paper.

Received 28 November 2011; accepted 11 June 2012.
Published online 12 August 2012.

1. Morton, L. M. *et al.* Lymphoma incidence patterns by WHO subtype in the United States, 1992–2001. *Blood* **107**, 265–276 (2006).

2. Ghiotto, F. *et al.* Remarkably similar antigen receptors among a subset of patients with chronic lymphocytic leukemia. *J. Clin. Invest.* **113,** 1008–1016 (2004).
3. Stamatopoulos, K. *et al.* Over 20% of patients with chronic lymphocytic leukemia carry stereotyped receptors: pathogenetic implications and clinical correlations. *Blood* **109,** 259–270 (2007).
4. Bikos, V. *et al.* Over 30% of patients with splenic marginal zone lymphoma express the same immunoglobulin heavy variable gene: ontogenetic implications. *Leukemia* **26,** 1638–1646 (2012).
5. Widhopf, G. F. II *et al.* Chronic lymphocytic leukemia B cells of more than 1% of patients express virtually identical immunoglobulins. *Blood* **104,** 2499–2504 (2004).
6. Ghia, P., Chiorazzi, N. & Stamatopoulos, K. Microenvironmental influences in chronic lymphocytic leukaemia: the role of antigen stimulation. *J. Intern. Med.* **264,** 549–562 (2008).
7. Stevenson, F. K., Krysov, S., Davies, A. J., Steele, A. J. & Packham, G. B-cell receptor signaling in chronic lymphocytic leukemia. *Blood* **118,** 4313–4320 (2011).
8. Köhler, F. *et al.* Autoreactive B cell receptors mimic autonomous pre-B cell receptor signaling and induce proliferation of early B cells. *Immunity* **29,** 912–921 (2008).
9. Übelhart, R. *et al.* N-linked glycosylation selectively regulates autonomous precursor BCR function. *Nature Immunol.* **11,** 759–765 (2010).
10. Hervé, M. *et al.* Unmutated and mutated chronic lymphocytic leukemias derive from self-reactive B cell precursors despite expressing different antibody reactivity. *J. Clin. Invest.* **115,** 1636–1643 (2005).
11. Sthoeger, Z. M. *et al.* Production of autoantibodies by CD5-expressing B lymphocytes from patients with chronic lymphocytic leukemia. *J. Exp. Med.* **169,** 255–268 (1989).
12. Meixlsperger, S. *et al.* Conventional light chains inhibit the autonomous signaling capacity of the B cell receptor. *Immunity* **26,** 323–333 (2007).
13. Bichi, R. *et al.* Human chronic lymphocytic leukemia modeled in mouse by targeted *TCL1* expression. *Proc. Natl Acad. Sci. USA* **99,** 6955–6960 (2002).
14. Herling, M. *et al.* High TCL1 levels are a marker of B-cell receptor pathway responsiveness and adverse outcome in chronic lymphocytic leukemia. *Blood* **114,** 4675–4686 (2009).
15. Yan, X. J. *et al.* B cell receptors in TCL1 transgenic mice resemble those of aggressive, treatment-resistant human chronic lymphocytic leukemia. *Proc. Natl Acad. Sci. USA* **103,** 11713–11718 (2006).
16. Binder, M. *et al.* B-cell receptor epitope recognition correlates with the clinical course of chronic lymphocytic leukemia. *Cancer* **117,** 1891–1900 (2011).
17. Kulathu, Y., Grothe, G. & Reth, M. Autoinhibition and adapter function of Syk. *Immunol. Rev.* **232,** 286–299 (2009).
18. Herishanu, Y. *et al.* The lymph node microenvironment promotes B-cell receptor signaling, NF-κB activation, and tumor proliferation in chronic lymphocytic leukemia. *Blood* **117,** 563–574 (2011).
19. Seiler, T. *et al.* Characterization of structurally defined epitopes recognized by monoclonal antibodies produced by chronic lymphocytic leukemia B cells. *Blood* **114,** 3615–3624 (2009).
20. Buchner, M. *et al.* Spleen tyrosine kinase inhibition prevents chemokine- and integrin-mediated stromal protective effects in chronic lymphocytic leukemia. *Blood* **115,** 4497–4506 (2010).
21. Suljagic, M. *et al.* The Syk inhibitor fostamatinib disodium (R788) inhibits tumor growth in the Eμ–TCL1 transgenic mouse model of CLL by blocking antigen-dependent B-cell receptor signaling. *Blood* **116,** 4894–4905 (2010).
22. Friedberg, J. W. *et al.* Inhibition of Syk with fostamatinib disodium has significant clinical activity in non-Hodgkin lymphoma and chronic lymphocytic leukemia. *Blood* **115,** 2578–2585 (2010).

Supplementary Information is linked to the online version of the paper at www.nature.com/nature.

Acknowledgements We thank C. Croce for providing the TCL1 mice, M. Reth and P. Nielsen for scientific discussion and reading the manuscript, C. Wehr for help cloning TCL1-derived BCRs, A. Ott, A. Würch, S. Hopitz and B. Wehrle for help with FACS experiments and cloning, and D. Pfeifer and M. Pantic for providing clinical data. This work was supported by the Deutsche Krebshilfe (Project 108935), the Deutsche Forschungsgemeinschaft (SFB746 and JU 463/2-1) and the Excellence Initiative of the German Federal and State Governments (GSC-4, Spemann Graduate School).

Author Contributions M.D.-v.M., R.Ü., D.S., F.K. and M.P.B. conducted cloning of BCRs. M.D.-v.M., R.Ü. and D.S. performed measurements of BCR surface expression and calcium flux and performed soluble BCR-binding assays. M.D.-v.M. and T.W. performed quantitative reverse-transcriptase PCR experiments. M.B. performed the NF-κB activity ELISA. E.S. analysed V$_H$ region sequences from patient samples. M.D.-v.M. and M.F. performed single-cell Ca^{2+} measurements. D.H. and H.W. tested the polyreactivity of CLL and TCL1 receptors. K.Z. and H.V. conducted the characterization of lymphoma patients and provided samples. M.D.-v.M., T.W., F.K. and H.J. wrote the manuscript. H.J. designed experiments. All authors discussed the results and commented on the manuscript.

Author Information Reprints and permissions information is available at www.nature.com/reprints. The authors declare no competing financial interests. Readers are welcome to comment on the online version of this article at www.nature.com/nature. Correspondence and requests for materials should be addressed to H.J. (jumaa@immunbio.mpg.de).

LETTER

doi:10.1038/nature11316

HDAC8 mutations in Cornelia de Lange syndrome affect the cohesin acetylation cycle

Matthew A. Deardorff[1,2]*, Masashige Bando[3]*, Ryuichiro Nakato[3]*, Erwan Watrin[4]*, Takehiko Itoh[5], Masashi Minamino[3], Katsuya Saitoh[3], Makiko Komata[3], Yuki Katou[3], Dinah Clark[1], Kathryn E. Cole[6], Elfride De Baere[7], Christophe Decroos[6], Nataliya Di Donato[8], Sarah Ernst[1], Lauren J. Francey[1], Yolanda Gyftodimou[9], Kyotaro Hirashima[10], Melanie Hullings[1], Yuuichi Ishikawa[11], Christian Jaulin[4], Maninder Kaur[1], Tohru Kiyono[12], Patrick M. Lombardi[6], Laura Magnaghi-Jaulin[4], Geert R. Mortier[13], Naohito Nozaki[14], Michael B. Petersen[9,15], Hiroyuki Seimiya[10], Victoria M. Siu[16], Yutaka Suzuki[17], Kentaro Takagaki[18], Jonathan J. Wilde[1], Patrick J. Willems[19], Claude Prigent[4], Gabriele Gillessen-Kaesbach[20], David W. Christianson[6], Frank J. Kaiser[20], Laird G. Jackson[1,21], Toru Hirota[12], Ian D. Krantz[1,2] & Katsuhiko Shirahige[3,22]

Cornelia de Lange syndrome (CdLS) is a dominantly inherited congenital malformation disorder, caused by mutations in the cohesin-loading protein NIPBL[1,2] for nearly 60% of individuals with classical CdLS[3–5], and by mutations in the core cohesin components SMC1A (~5%) and SMC3 (<1%) for a smaller fraction of probands[6,7]. In humans, the multisubunit complex cohesin is made up of SMC1, SMC3, RAD21 and a STAG protein. These form a ring structure that is proposed to encircle sister chromatids to mediate sister chromatid cohesion[8] and also has key roles in gene regulation[9]. SMC3 is acetylated during S-phase to establish cohesiveness of chromatin-loaded cohesin[10–13], and in yeast, the class I histone deacetylase Hos1 deacetylates SMC3 during anaphase[14–16]. Here we identify HDAC8 as the vertebrate SMC3 deacetylase, as well as loss-of-function *HDAC8* mutations in six CdLS probands. Loss of HDAC8 activity results in increased SMC3 acetylation and inefficient dissolution of the 'used' cohesin complex released from chromatin in both prophase and anaphase. SMC3 with retained acetylation is loaded onto chromatin, and chromatin immunoprecipitation sequencing analysis demonstrates decreased occupancy of cohesin localization sites that results in a consistent pattern of altered transcription seen in CdLS cell lines with either *NIPBL* or *HDAC8* mutations.

Human SMC3 is acetylated by ESCO1 and ESCO2, homologues of yeast Eco1, and has been shown to be important for the establishment of sister chromatid cohesion[10,11,13,17,18]. Using a monoclonal antibody specific for acetylated SMC3 (SMC3-ac)[18], we found that whereas total SMC3 levels remain stable throughout the cell cycle, SMC3-ac rapidly disappears during mitosis, suggesting coordinated deacetylation (Supplementary Fig. 1).

We therefore used RNA interference (RNAi)-based screening of all known human histone deacetylases (HDACs) and sirtuins to identify HDAC8 as the vertebrate SMC3 deacetylase (Supplementary Fig. 2). Loss of HDAC8 activity using either *HDAC8* RNAi or the HDAC8-specific inhibitor PCI-34051 (PCI; Fig. 1a, b) does not alter cell cycle progression, but clearly increases SMC3-ac in both soluble and chromatin fractions throughout the cell cycle (Fig. 1c, lanes 4 and 6, Fig. 1e, lanes 18–22 and 29–33, and Supplementary Fig. 3d, lanes 22–28 and 36–42). Nearly all HDAC8 is present in the soluble fraction in both asynchronous and synchronized cultures (Fig. 1c, e). These data indicate that HDAC8 is present and active throughout the cell cycle, and that soluble SMC3-ac is its deacetylation target, similar to Hos1 in yeast[14–16]. Notably, the increase of SMC3-ac in the soluble fraction in the absence of HDAC8 activity suggests that SMC3-ac dissociates from chromatin but fails to be deacetylated. In addition, we unexpectedly observed few sister chromatid cohesion defects with loss of HDAC8 activity alone (Supplementary Fig. 4).

To understand the role of HDAC8 in genome-wide regulation of cohesin dynamics, we performed chromatin immunoprecipitation sequencing (ChIP-Seq) analysis of synchronized HeLa cells transfected with control or *HDAC8* RNAi (Fig. 2) and immunoprecipitated with either an anti-RAD21 antibody to detect total cohesin or an anti-SMC3-ac antibody. Although total cellular cohesin shows no decrease (Supplementary Fig. 5a, b), and there is a high degree of overlap between SMC3-ac, cohesin and CTCF[19] localization sites in treated and untreated cells, high read numbers and tight correlations between experimental replicates enabled us to identify a 17% loss of total cohesin localization peaks with reduced HDAC8 activity (Fig. 2a–c and Supplementary Fig. 5d–h). Furthermore, despite using conditions that increase total SMC3-ac more than twofold (Fig. 1e and Supplementary Fig. 3d), we note a 16% loss of SMC3-ac localization sites with HDAC8 reduction (Fig. 2a–d and Supplementary Fig. 5f, g). Finally, we found that in both control and HDAC8-depleted cells, SMC3-ac preferentially localizes to downstream regions of genes relative to the distribution of RAD21 (Fig. 2c, d and Supplementary Fig. 5f, g). Together, this data demonstrates decreased occupancy of cohesin localization sites with the loss of HDAC8 activity, an observation similarly noted for *NIPBL* haploinsufficient CdLS cells[20].

With the known role of cohesin regulation in CdLS and the observations that a reduction in either HDAC8 or NIPBL leads to decreased cohesin occupancy of localization sites, we proposed that *HDAC8* mutations may cause CdLS. We screened this X-linked gene in 154 individuals with CdLS negative for mutations in *NIPBL*, *SMC1A* and

[1]Division of Human Genetics and Molecular Biology, The Children's Hospital of Philadelphia, Pennsylvania 19104, USA. [2]The Department of Pediatrics, University of Pennsylvania Perelman School of Medicine, Philadelphia, Pennsylvania 19104, USA. [3]Research Center for Epigenetic Disease, Institute for Molecular and Cellular Biosciences, The University of Tokyo, Tokyo 113-0032, Japan. [4]Centre National de la Recherche Scientifique (CNRS), Research Institute of Genetics and Development (IGDR), Faculté de Médecine, Rennes 35043, France. [5]School and Graduate School of Bioscience and Biotechnology, Tokyo Institute of Technology, Yokohama 226-8503, Japan. [6]Department of Chemistry, University of Pennsylvania, Philadelphia, Pennsylvania 19104, USA. [7]Center for Medical Genetics, Ghent University Hospital, 9000 Ghent, Belgium. [8]Institut für Klinische Genetik, Technische Universität Dresden, 01307 Dresden, Germany. [9]Department of Genetics, Institute of Child Health, 11527 Athens, Greece. [10]Division of Molecular Biotherapy, Japanese Foundation for Cancer Research, Tokyo 135-8550, Japan. [11]Department of Pathology, Japanese Foundation for Cancer Research, Tokyo 135-8550, Japan. [12]Virology Division, National Cancer Center Research Institute, Tokyo 104-0045, Japan. [13]Department of Medical Genetics, Antwerp University Hospital and University of Antwerp, B-2650 Antwerp, Belgium. [14]Bio-Frontier Research Center, Tokyo Institute of Technology, Yokohama 226-8503, Japan. [15]Department of Clinical Genetics, Aalborg Hospital, Aarhus University Hospital, 9100 Aalborg, Denmark. [16]Medical Genetics, University of Western Ontario, London, Ontario N6A 5W9, Canada. [17]Graduate School of Frontier Sciences, The University of Tokyo, Tokyo 277-8561, Japan. [18]Experimental Pathology, Japanese Foundation for Cancer Research, Tokyo 135-8550, Japan. [19]GENDIA, 2020 Antwerp, Belgium. [20]Institut für Humangenetik Lübeck, Universität zu Lübeck, 23538 Lübeck, Germany. [21]Department of Obstetrics and Gynecology, Drexel University School of Medicine, Philadelphia, Pennsylvania 19102, USA. [22]CREST, JST, K's Gobancho, 7, Gobancho, Chiyoda-ku, Tokyo 102-0076, Japan.
*These authors contributed equally to this work.

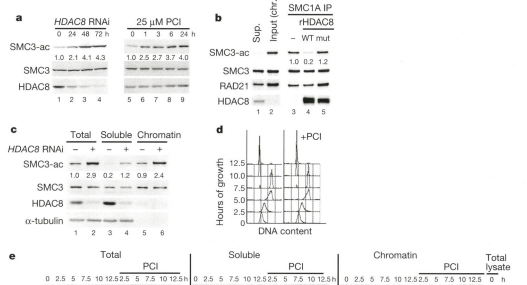

Figure 1 | HDAC8 is an SMC3 deacetylase. a, HeLa cells were transfected with *HDAC8* short interfering RNA (siRNA; lanes 1–4) or incubated with 25 μM PCI, the HDAC8-specific inhibitor (lanes 5–9), for the indicated times. Total cell lysates were prepared and analysed by immunoblotting using anti-SMC3-ac, SMC3 and HDAC8 antibodies. Numbers beneath SMC3-ac bands indicate quantification of SMC3-ac levels normalized to SMC3 levels and the 0 h time point. **b**, Acetylated SMC3 was prepared by co-immunoprecipitation with SMC1A from HeLa cell chromatin extracts. Immunoprecipitates (IP) were incubated with recombinant purified HDAC8 (rHDAC8) or mutant (mut) HDAC8 protein at 30 °C for 1 h and analysed by immunoblotting as in **a**. Chr., chromatin; Sup., supernatant; WT, wild type. **c**, Unsynchronized HeLa cells transfected with *HDAC8* siRNA for 48 h were fractionated into soluble and chromatin fractions and immunoblotted as in **a**. **d**, HeLa cells were synchronized by double thymidine arrest, and released in the presence or absence of 25 μM PCI for the indicated time and verified by FACS analysis for cell cycle progression. **e**, Cell extracts of the PCI-treated cells in **d** were fractionated into soluble and chromatin fractions and analysed by immunoblotting as in **a**. Histone H3 Ser 10 phosphorylation (H3S10P) is a marker of prophase and the onset of mitosis.

SMC3, as well as *RAD21* (also known as *SSC1*), *STAG2*, *ESCO1*, *ESCO2* and *MAU2* (also known as *SCC4*). We identified four *de novo* missense mutations and one *de novo* nonsense mutation in *HDAC8* (Supplementary Table 1 and Fig. 3a). In addition, one familial mutation (c.1001A>G; p.H334R) was identified in a boy, his mildly affected sister and his unaffected mother, in which the mutant allele was inactivated in her blood. This mutation was also one of the *de novo* mutations in an unrelated girl. None of the mutations was seen in 290 ethnically matched control chromosomes or in 629 individuals of the 1000 Genomes Project[21]. Despite the small numbers and the varied clinical features in females due to random X-chromosome inactivation, these children demonstrate growth, cognitive and facial features consistent with those caused by mutations in *NIPBL* ('classical' CdLS). Both expression studies (Supplementary Fig. 6a) and X-chromosome inactivation studies (data not shown) demonstrate complete skewing towards the normal allele in the blood of females with *HDAC8* mutations, indicating strong selection against the mutation. This limited the number of cell lines available for subsequent studies. However, immunoblotting demonstrated minimal HDAC8 protein expression in lymphoblastoid cell lines (LCLs) from a hemizygous boy with a p.G320R mutation as well as the skin fibroblasts from a female lyonized to express a p.H180R mutant allele (Fig. 3b), indicating protein instability in each case. Consistent with this, assessment of SMC3-ac demonstrates increased levels in both the p.G320R LCLs and the p.H180R fibroblasts, whereas the total amount of SMC3 (Fig. 3b) and cell cycle distribution for the LCLs are unchanged (Supplementary Fig. 6b).

We expressed the HDAC8 missense mutations in *Escherichia coli*, purified and assayed each for deacetylase activity. These data (Fig. 3c) demonstrate that the p.H180R mutation severely abrogates HDAC8 deacetylase activity, and demonstrate significant activity losses for the p.G320R, p.T311M and p.H334R mutations, consistent with high conservation of each residue and position in the structure of HDAC8–substrate complexes[22,23] (Fig. 3d and Supplementary Fig. 6c–e). Finally, purified wild-type, but not mutant HDAC8, can rescue the SMC3 overacetylation seen in *HDAC8* mutant LCLs (Supplementary Fig. 6g, h).

We have previously demonstrated that mutations in *NIPBL*, the primary cause of CdLS, result in consistent, reproducible changes of genes expressed from LCLs derived from individuals with CdLS[20]. Using Nanostring multiplex expression analysis to avoid variation introduced by PCR or RNA amplification-based assessments and a previously validated 32-gene CdLS classifier set[20], we compared the expression of LCLs from the male with the p.G320R mutation and from two girls (with the p.H180R and p.H334R mutations) who express only the normal allele in these cells, to 10 normal controls and 12 LCLs with loss of function *NIPBL* mutations. In this assay, the aggregate 32-gene LCL expression profile of the single male with an *HDAC8* mutation strongly correlates with that seen in *NIPBL*-mutant cell lines, whereas the profile for the two female lines, which express the wild-type allele, correlates with normal controls (Fig. 3e). These data support the hypothesis that loss of HDAC8 activity results in widespread transcriptional dysregulation as seen in *NIPBL*-mutated CdLS cells. The loss of cohesin-binding sites in *HDAC8* RNAi-depleted HeLa cells and in *NIPBL*-mutant LCLs[20] was also noted in the p.G320R HDAC8-mutant LCLs and fibroblasts derived from the girl with the p.H180R mutation, in which small but consistent changes in transcriptional dysregulation were also noted (Supplementary Figs 6a, 7 and 8). Together, these data suggest that loss of HDAC8 activity leads to a common pathogenic mechanism for classical CdLS that converges on the reduction of bound cohesin complexes.

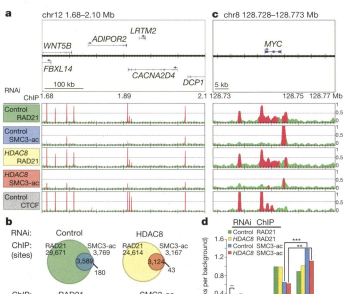

Figure 2 | Cohesin and SMC3-ac localization sites in control and *HDAC8* RNAi-treated HeLa cells. **a**, Example of ChIP-Seq data (Ensemble gene position 1.68–2.10 Mb of human chromosome 12). ChIP-Seq data are shown in reads per million. Regions in which signals were significantly enriched (see Methods) are in red. Binding profiles for RAD21 and SMC3-ac in control and *HDAC8* RNAi-treated HeLa cells are shown. **b**, Venn diagrams showing numbers and overlap of localization sites. **c**, Example of region-specific localization showing binding sites for RAD21 and SMC3-ac in the *MYC* gene locus. Ensemble gene position 128,728–128,773 Mb of human chromosome 8 is shown. **d**, Classification of RAD21 and SMC3-ac localization sites as a log ratio to background reads. Significance was calculated using a two-sample test for equality of proportions. $*P < 0.05$; $**P < 0.001$; $***P < 0.0001$; $-P > 0.05$. Upstream and downstream are defined as within 5 kb from gene boundaries, respectively. SMC3-ac preferentially localizes to the downstream end of genes.

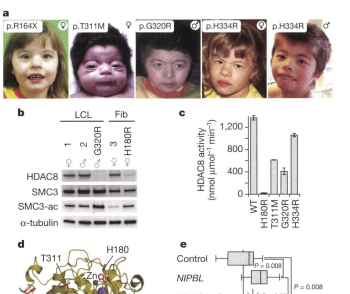

Figure 3 | HDAC8 mutations in CdLS. **a**, Facial features of individuals with *HDAC8* mutations labelled with corresponding mutation and sex. **b**, Western blotting of protein from LCLs and fibroblasts (Fib). Sex is indicated under controls (1, 2 and 3) or mutation designation. **c**, HDAC8 mutations disrupt deacetylase activity. Bar graphs demonstrate the effect of HDAC8 mutations on deacetylase specific activity (nmol substrate μmol enzyme^{-1} min^{-1}). All assays were performed in triplicate. Error bars indicate standard deviation. Enzymatic activity for all mutations is significantly less than wild type ($P < 0.05$). **d**, Localization of HDAC8 mutations on the crystal structure (PDB accession code 3F06; ref. 23). Mutated residues are in red. **e**, The expression profile of *HDAC8*-mutant LCL is consistent with that seen in cell lines with *NIPBL* mutations. The summed standard deviations of gene expression compared with *NIPBL* mutant from control LCLs for 32 genes was determined for each sample. Box graphs demonstrate twenty-fifth, median and seventy-fifth percentiles of each group. Whiskers indicate minimum and maximum values. Note that for the *HDAC8* male (p.G320R) the values are for biological replicate samples for a single cell line (denoted by asterisk). Unpaired two-tailed *t*-test significances are indicated.

To understand the endogenous effect of HDAC8 loss on cohesin further, we compared each cohesin subunit in chromatin-bound and unbound fractions in the LCLs with a hemizygous p.G320R mutation versus control LCLs, and unexpectedly noted accumulation of RAD21 fragments in HDAC8-mutant cells (Supplementary Fig. 9a, lanes 2, 4 and 6). Using a RAD21 amino terminal-specific antibody, we verified accumulation of the RAD21 N-terminal separase cleavage fragment (RAD21-N) in mutant LCLs, *HDAC8* RNAi-treated HeLa cells and HDAC8-mutated fibroblasts expressing catalytically inactive HDAC8 compared with wild-type HDAC8 (Fig. 4 and Supplementary Fig. 9). The accumulation of this cleavage fragment in the chromatin-bound fraction of HDAC8-mutant cells suggests that it may remain bound to the cohesin complex, so we assessed whether RAD21-N co-immunoprecipitates with other cohesin subunits. In HDAC8-mutant cells, RAD21-N co-immunoprecipitates with SMC1A, SMC3, STAG1 and STAG2 (Fig. 4b), strongly suggesting that without functional HDAC8, the cleaved N terminus of RAD21 remains attached to the cohesin complex, presumably via acetylated SMC3 (ref. 24). To confirm that clearance of cleaved RAD21 is dependent on HDAC8, we performed complementary analyses in synchronized HeLa cells with or without the HDAC8 inhibitor PCI (Fig. 4c, d). These data demonstrate the appearance of the N-terminal and carboxy-terminal RAD21 fragments after entry into mitosis (marked by histone H3 Ser10 phosphorylation; H3S10P) and activation of separase (Fig. 4d, lanes 9–12 and 21–24) as well as their persistence in both soluble and chromatin fractions (Fig. 4d, lanes 18–20) when most cells are in G1 phase (data not shown). By contrast, in untreated cells, these cleavage products are predominantly detected in the soluble fraction (Fig. 4d, lanes 2–4), and largely disappear 3 h after release.

We also made several observations about HDAC8 activity in the prophase removal of cohesin[25,26]. Loss of HDAC8 activity does not disrupt the prophase pathway of cohesin removal from chromatin, as demonstrated by a consistent reduction of chromatin-bound cohesin in the presence of metaphase inhibitors in either control or PCI-treated cells (Fig. 4d, lanes 13 and 17 versus 21–24). However, HDAC8 activity is necessary after prophase removal of cohesin, because in metaphase inhibitor-treated cells, soluble SMC3-ac is markedly increased in the presence of PCI (Fig. 4d, lanes 9–12). Finally, with WAPAL depletion, which diminishes prophase removal of cohesin[18,27,28], we noted that SMC3-ac is substantially increased (Supplementary Fig. 9e).

To test whether other cohesin-promoting proteins might remain associated with SMC3-ac in the absence of HDAC8 activity, we analysed HeLa and patient-derived cells, which also demonstrated increased retention of sororin (also known as CDCA5)[18,29] and RAD21-N, but not WAPAL, on soluble SMC3-ac (Fig. 4e–g and Supplementary Fig. 9d). Taken together, these data strongly suggest that HDAC8 is necessary for the deacetylation of SMC3 after its removal from chromatin in both prophase and anaphase pathways to enable proper

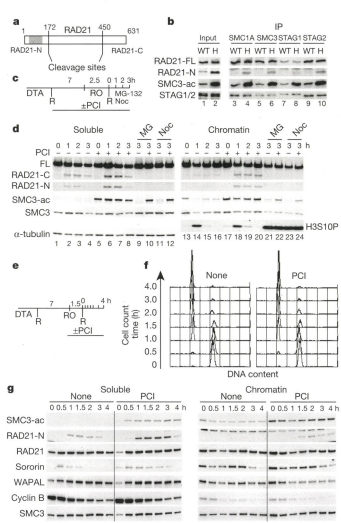

Figure 4 | Retention of RAD21-N and sororin on cohesin in the absence of HDAC8. **a**, RAD21 separase cleavage sites. Vertical lines indicate cleavage sites. Grey region indicates the RAD21-N antibody epitope. **b**, SMC3, STAG1 and STAG2 were immunoprecipitated from soluble extracts from normal (WT) and *HDAC8*-mutant (H) cell lines. Full-length RAD21 (FL), the cleaved N-terminal RAD21 fragment, SMC3-ac and STAG1/2 were analysed by SDS–PAGE and immunoblotting. **c**, Experimental schema of **d**. HeLa cells were synchronized by double thymidine arrest (DTA) and released (R) in the presence or absence of PCI. Seven hours after release, cells were treated with RO-3306 (RO) to arrest at the G2/M boundary. After removing RO-3306, cells were cultured in the presence or absence of nocodazole (Noc) or MG-132 (MG) to arrest in metaphase. Cells were collected at indicated time points after release from RO-3306 arrest. **d**, Cell extracts were fractionated into soluble and chromatin-bound fractions. Full-length RAD21, cleaved C- and N-terminal RAD21 fragments, SMC3-ac, SMC3, H3S10P and α-tubulin were analysed by SDS–PAGE and immunoblotting. H3S10P is used as a metaphase marker. **e**, Experimental schema of **f** and **g**. HeLa cells were synchronized and released and treated with RO-3306 as in **d**. After removing RO-3306, cells were cultured in the presence or absence of PCI and collected at the indicated times. **f**, FACS analysis of HeLa cells in **g**. **g**, Cell extracts were fractionated into soluble and chromatin-bound fractions. Levels of SMC3-ac, RAD21-N, full-length RAD21, sororin, WAPAL, cyclin B (a G2 marker) and SMC3 were analysed by SDS–PAGE and immunoblotting.

dissolution of pro-cohesive elements and allow for recycling of 'refreshed' cohesin for the next cell cycle (Supplementary Fig. 10).

In summary, this work demonstrates that HDAC8 functions as a vertebrate SMC3 deacetylase to facilitate the renewal of cohesin after its removal from chromatin in prophase or anaphase, and that loss of HDAC8 activity results in decreased cohesin at localized sites to cause both cellular and clinical features of CdLS.

METHODS SUMMARY

Cell culture and synchronization, chromatin fractionation, purification of recombinant HDAC8 in baculovirus and *E. coli*, SMC3-ac deacetylation assays, RNA interference, immunofluorescence microscopy, human subjects, mutation screening, HDAC8 conservation analysis, crystal structure analysis, expression profiling, assessment of X-chromosome inactivation, chromatin immunoprecipitation, ChIP-Seq and RNA-Seq analyses are described in detail in the Methods.

Full Methods and any associated references are available in the online version of the paper.

Received 20 January; accepted 12 June 2012.
Published online 12 August 2012.

1. Gillespie, P. J. & Hirano, T. Scc2 couples replication licensing to sister chromatid cohesion in *Xenopus* egg extracts. *Curr. Biol.* **14,** 1598–1603 (2004).
2. Takahashi, T. S., Yiu, P., Chou, M. F., Gygi, S. & Walter, J. C. Recruitment of *Xenopus* Scc2 and cohesin to chromatin requires the pre-replication complex. *Nature Cell Biol.* **6,** 991–996 (2004).
3. Gillis, L. A. *et al.* NIPBL mutational analysis in 120 individuals with Cornelia de Lange syndrome and evaluation of genotype-phenotype correlations. *Am. J. Hum. Genet.* **75,** 610–623 (2004).
4. Krantz, I. D. *et al.* Cornelia de Lange syndrome is caused by mutations in NIPBL, the human homolog of *Drosophila melanogaster* Nipped-B. *Nature Genet.* **36,** 631–635 (2004).
5. Tonkin, E. T., Wang, T. J., Lisgo, S., Bamshad, M. J. & Strachan, T. *NIPBL*, encoding a homolog of fungal Scc2-type sister chromatid cohesion proteins and fly Nipped-B, is mutated in Cornelia de Lange syndrome. *Nature Genet.* **36,** 636–641 (2004).
6. Deardorff, M. A. *et al.* Mutations in cohesin complex members SMC3 and SMC1A cause a mild variant of Cornelia de Lange syndrome with predominant mental retardation. *Am. J. Hum. Genet.* **80,** 485–494 (2007).
7. Musio, A. *et al.* X-linked Cornelia de Lange syndrome owing to *SMC1L1* mutations. *Nature Genet.* **38,** 528–530 (2006).
8. Nasmyth, K. & Haering, C. H. Cohesin: its roles and mechanisms. *Annu. Rev. Genet.* **43,** 525–558 (2009).
9. Dorsett, D. Cohesin: genomic insights into controlling gene transcription and development. *Curr. Opin. Genet. Dev.* **21,** 199–206 (2011).
10. Rolef Ben-Shahar, T. *et al.* Eco1-dependent cohesin acetylation during establishment of sister chromatid cohesion. *Science* **321,** 563–566 (2008).
11. Unal, E. *et al.* A molecular determinant for the establishment of sister chromatid cohesion. *Science* **321,** 566–569 (2008).
12. Zhang, B. *et al.* Dosage effects of cohesin regulatory factor PDS5 on mammalian development: implications for cohesinopathies. *PLoS ONE* **4,** e5232 (2009).
13. Heidinger-Pauli, J. M., Unal, E. & Koshland, D. Distinct targets of the Eco1 acetyltransferase modulate cohesion in S phase and in response to DNA damage. *Mol. Cell* **34,** 311–321 (2009).
14. Beckouët, F. *et al.* An Smc3 acetylation cycle is essential for establishment of sister chromatid cohesion. *Mol. Cell* **39,** 689–699 (2010).
15. Xiong, B., Lu, S. & Gerton, J. L. Hos1 is a lysine deacetylase for the Smc3 subunit of cohesin. *Curr. Biol.* **20,** 1660–1665 (2010).
16. Borges, V. *et al.* Hos1 deacetylates Smc3 to close the cohesin acetylation cycle. *Mol. Cell* **39,** 677–688 (2010).
17. Zhang, J. *et al.* Acetylation of Smc3 by Eco1 is required for S phase sister chromatid cohesion in both human and yeast. *Mol. Cell* **31,** 143–151 (2008).
18. Nishiyama, T. *et al.* Sororin mediates sister chromatid cohesion by antagonizing Wapl. *Cell* **143,** 737–749 (2010).
19. Wendt, K. S. *et al.* Cohesin mediates transcriptional insulation by CCCTC-binding factor. *Nature* **451,** 796–801 (2008).
20. Liu, J. *et al.* Transcriptional dysregulation in NIPBL and cohesin mutant human cells. *PLoS Biol.* **7,** e1000119 (2009).
21. The 1000 Genomes Project Consortium. A map of human genome variation from population-scale sequencing. *Nature* **467,** 1061–1073 (2010).
22. Vannini, A. *et al.* Substrate binding to histone deacetylases as shown by the crystal structure of the HDAC8-substrate complex. *EMBO Rep.* **8,** 879–884 (2007).
23. Dowling, D. P., Gantt, S. L., Gattis, S. G., Fierke, C. A. & Christianson, D. W. Structural studies of human histone deacetylase 8 and its site-specific variants complexed with substrate and inhibitors. *Biochemistry* **47,** 13554–13563 (2008).
24. Haering, C. H., Lowe, J., Hochwagen, A. & Nasmyth, K. Molecular architecture of SMC proteins and the yeast cohesin complex. *Mol. Cell* **9,** 773–788 (2002).
25. Waizenegger, I. C., Hauf, S., Meinke, A. & Peters, J. M. Two distinct pathways remove mammalian cohesin from chromosome arms in prophase and from centromeres in anaphase. *Cell* **103,** 399–410 (2000).
26. Giménez-Abian, J. F. *et al.* Regulation of sister chromatid cohesion between chromosome arms. *Curr. Biol.* **14,** 1187–1193 (2004).
27. Gandhi, R., Gillespie, P. J. & Hirano, T. Human Wapl is a cohesin-binding protein that promotes sister-chromatid resolution in mitotic prophase. *Curr. Biol.* **16,** 2406–2417 (2006).
28. Kueng, S. *et al.* Wapl controls the dynamic association of cohesin with chromatin. *Cell* **127,** 955–967 (2006).
29. Schmitz, J., Watrin, E., Lenart, P., Mechtler, K. & Peters, J. M. Sororin is required for stable binding of cohesin to chromatin and for sister chromatid cohesion in interphase. *Curr. Biol.* **17,** 630–636 (2007).

Supplementary Information is linked to the online version of the paper at www.nature.com/nature.

Acknowledgements We are grateful to the individuals and families with Cornelia de Lange syndrome who participated in this study, as well as to the referring physicians and colleagues who have contributed samples and clinical information. We thank Riken Omics Science Center, K. Nakagawa, S. Watanabe, M. Albrecht and J. Eckhold for technical support. We thank J.-M. Peters for the sororin and RAD21 antibodies. We thank F. Beckouët and K. Nasmyth for sharing unpublished results. We are indebted to the continued support of the US and International Cornelia de Lange Syndrome Foundations. This work was supported by National Institutes of Health grants K08HD055488 (NICHD, M.A.D.), GM49758 (D.W.C.) and P01 HD052860 (NICHD; I.D.K.), research grants from the US CdLS Foundation, institutional funds from the Children's Hospital of Philadelphia, Intramural funding from the University of Lübeck (Schwerpunktprogramm, Medizinische Genetik: Von seltenen Varianten zur Krankheitsentstehung; F.J.K., G.G.-K.), Research Program of Innovative Cell Biology by Innovative Technology, Grant-in-Aid for Scientific Research (S) and for innovative science from MEXT (K.Sh.).

Author Contributions M.B. and K.Sh. designed and performed the biochemical analyses; M.B., E.W., C.J., L.M.-J. and K.Sh. performed HDAC screening. M.B., K.Sa., E.W. and L.M.-J. performed chromatin spreading assays; N.N. monoclonal isolation; M.B., R.N., T.I., M.K., Y.K. and K.Sh. the ChIP sequencing and analysis; M.B., R.N. and Y.S. RNA sequencing; M.M., K.T. and T.H. microscopy. M.A.D., G.G.-K., L.G.J., F.J.K. and I.D.K. initiated the human studies. M.A.D., D.C., E.D.B., G.R.M., V.M.S., P.W., N.T., Y.G., M.B.P., G.G.-K. and I.D.K. identified and characterized clinical data. M.A.D., M.K., S.E., L.J.F., M.H. and F.J.K. performed mutation screening, inactivation and lymphoblastoid expression studies. K.H., T.K. and H.S. established fibroblast cell lines. M.A.D., J.J.W., K.E.C., P.M.L., C.D. and D.W.C. performed enzymatic and structural analysis. M.A.D., M.B. and K.Sh. drafted the manuscript. All authors analysed data, discussed the results and commented on the manuscript.

Author Information ChIP-Seq and RNA-Seq data from this study are available from the Sequence Read Archive (SRA) database (http://www.ncbi.nlm.nih.gov/sra) under the accession number SRP011927. Reprints and permissions information is available at www.nature.com/reprints. The authors declare no competing financial interests. Readers are welcome to comment on the online version of this article at www.nature.com/nature. Correspondence and requests for materials should be addressed to M.A.D. (deardorff@email.chop.edu), I.D.K. (ian2@mail.med.upenn.edu) or K.Sh. (kshirah@iam.u-tokyo.ac.jp).

LETTER

doi:10.1038/nature11432

Impact of caloric restriction on health and survival in rhesus monkeys from the NIA study

Julie A. Mattison[1], George S. Roth[2], T. Mark Beasley[3], Edward M. Tilmont[1], April M. Handy[1,4], Richard L. Herbert[5], Dan L. Longo[6], David B. Allison[7], Jennifer E. Young[1], Mark Bryant[8], Dennis Barnard[9], Walter F. Ward[10], Wenbo Qi[11], Donald K. Ingram[12] & Rafael de Cabo[13]

Calorie restriction (CR), a reduction of 10–40% in intake of a nutritious diet, is often reported as the most robust non-genetic mechanism to extend lifespan and healthspan. CR is frequently used as a tool to understand mechanisms behind ageing and age-associated diseases. In addition to and independently of increasing lifespan, CR has been reported to delay or prevent the occurrence of many chronic diseases in a variety of animals. Beneficial effects of CR on outcomes such as immune function[1,2], motor coordination[3] and resistance to sarcopenia[4] in rhesus monkeys have recently been reported. We report here that a CR regimen implemented in young and older age rhesus monkeys at the National Institute on Aging (NIA) has not improved survival outcomes. Our findings contrast with an ongoing study at the Wisconsin National Primate Research Center (WNPRC), which reported improved survival associated with 30% CR initiated in adult rhesus monkeys (7–14 years)[5] and a preliminary report with a small number of CR monkeys[6]. Over the years, both NIA and WNPRC have extensively documented beneficial health effects of CR in these two apparently parallel studies. The implications of the WNPRC findings were important as they extended CR findings beyond the laboratory rodent and to a long-lived primate. Our study suggests a separation between health effects, morbidity and mortality, and similar to what has been shown in rodents[7–9], study design, husbandry and diet composition may strongly affect the life-prolonging effect of CR in a long-lived nonhuman primate.

For over 20 years, the NIA has studied the effects of CR in long-lived nonhuman primates (NHPs) (*Macaca mulatta*, average lifespan in captivity is ~27 years and maximum reported lifespan is ~40 years), to verify whether the life-prolonging effects observed in lower organisms also occur in monkeys and thus, might plausibly translate to human ageing[10,11]. The NIA CR study began in 1987 at the NIH Animal Center[12]. CR was initiated in monkeys of varying ages to evaluate the impact of age of onset of CR on its biological effects. Study design has been reported elsewhere[12,13]. Male and female monkeys were enrolled into the study at young, middle and older ages[12]. Data reported here are grouped as either young-onset (includes juvenile, adolescent and adult) or old-onset monkeys. Supplementary Table 1 reports the current census.

Any animal that died underwent a complete necropsy by a board-certified pathologist. A gross description of the pathology related to each organ was provided along with the probable cause of death and any contributing factors. Survival data were analysed in two ways: all-cause mortality and age-related deaths; a distinction also reported previously[5]. In both studies (NIA and WNPRC), age-related survival excluded deaths due to acute conditions that do not have an age-related increase in risk such as gastrointestinal bloat, anaesthesia, injury or endometriosis. Pathology details are in the Supplementary Information.

Old-onset CR monkeys (16–23 years) did not live longer than controls in either the all-cause (Fig. 1a) or age-related survival analysis (there were three cases of non-age related deaths in the CR group and 2 in the control group, graph not shown). In this group, males had significantly longer survival compared to females ($P = 0.0003$) and neither sex benefitted from CR. To date, four CR monkeys and one control from the old-onset group have lived beyond 40 years. Although CR has not increased mean or maximum lifespan relative to control, 50% survival for the females is 27.8 years and 35.4 years for the males, exceeding the ~27 year median lifespan previously reported for monkeys in captivity[14]. These monkeys may have benefitted from excellent husbandry conditions and thus CR started at older ages provided no additional increase in survival. Furthermore, there were no apparent differences in causes of death between the two diet groups. Neoplasia, cardiovascular disease, amyloidosis and general organism deterioration in the oldest animals were equally represented in both diet groups.

Old-onset CR was beneficial on several measures of metabolic health and overall function. Both male and female CR monkeys weighed less than the control counterparts, although the diet effect was greater in the males. In longitudinal measures from serum of fasted monkeys, triglycerides, cholesterol and glucose levels increased with age for both male and female controls. However, triglycerides were significantly lower in the CR monkeys ($F_{(1,21)} = 5.76$, $P = 0.026$) (Fig. 1b), and cholesterol remained significantly lower in the CR males (Fig. 1c) ($F_{(40,774)} = 1.53$, $P = 0.02$). At the oldest ages, fasting glucose was numerically lower in the CR monkeys (Fig. 1d) and significantly lower in CR males compared to controls ($P = 0.04$). On a single measure of plasma-free isoprostane, an indicator of oxidative stress, control males had significantly higher levels than the CR monkeys (23.24 ± 1.25 versus 15.93 ± 1.97 pg ml^{-1}; $P = 0.009$). In contrast, we previously reported that old-onset CR may negatively affect immune function[1,5].

Current survival curves for the young-onset male and females are shown in Fig. 2a (all-cause mortality) and Fig. 2b (age-related mortality). No significant diet effects are noted in survival between control and CR

[1]Laboratory of Experimental Gerontology, National Institute on Aging, NIH Animal Center, 16701 Elmer School Road Building 103, Dickerson, Maryland 20842, USA. [2]GeroScience, 1124 Ridge Road Pylesville, Maryland 21132, USA. [3]Department of Biostatistics, Ryals Public Health Bldg 343C University of Alabama at Birmingham, 1530 3rd Avenue S, Birmingham, Alabama 35294, USA. [4]SoBran, Inc., 4000 Blackburn Lane, Suite 100, Burtonsville, Maryland 20866, USA. [5]National Institute of Allergy and Infectious Disease, NIH Animal Center, 16701 Elmer School Road, Building 102, Dickerson, Maryland 20842, USA. [6]Laboratory of Molecular Biology and Immunology, National Institute on Aging, NIH, 251 Bayview Boulevard Room 08C228, Baltimore, Maryland 21224, USA. [7]Office of Energetics, University of Alabama at Birmingham, 1665 University Boulevard, RPH 140J Birmingham, Alabama 35294, USA. [8]Office of the Director, Diagnostic and Research Services Branch, NIH, Bldg 28A, Room 114, 28 Service Road West, Bethesda, Maryland 20814, USA. [9]Office of the Director, Diagnostic and Research Services Branch, NIH, Building 14A, Room 119A, 14 Service Road West, Bethesda, Maryland 20814, USA. [10]Department of Physiology/Barshop Institute for Longevity and Aging Studies, University of Texas Health Science Center at San Antonio, 7703 Floyd Curl Drive, San Antonio, Texas 78229, USA. [11]Department of Cellular and Structural Biology/ Barshop Institute for Longevity and Aging Studies, University of Texas Health Science Center at San Antonio, 7703 Floyd Curl Drive, San Antonio, Texas 78229, USA. [12]Nutritional Neuroscience and Aging Laboratory, Pennington Biomedical Research Center, Louisiana State University, 6400 Perkins Road, Baton Rouge, Louisiana 70808, USA. [13]Laboratory of Experimental Gerontology, National Institute on Aging, NIH, 251 Bayview Boulevard Suite 100, Baltimore, Maryland 21224, USA.

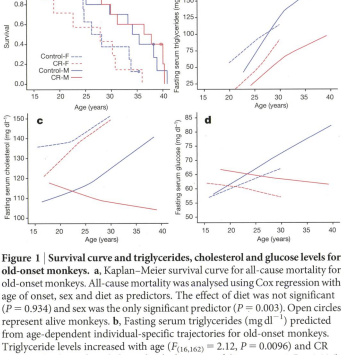

Figure 1 | Survival curve and triglycerides, cholesterol and glucose levels for old-onset monkeys. **a**, Kaplan–Meier survival curve for all-cause mortality for old-onset monkeys. All-cause mortality was analysed using Cox regression with age of onset, sex and diet as predictors. The effect of diet was not significant ($P = 0.934$) and sex was the only significant predictor ($P = 0.003$). Open circles represent alive monkeys. **b**, Fasting serum triglycerides (mg dl^{-1}) predicted from age-dependent individual-specific trajectories for old-onset monkeys. Triglyceride levels increased with age ($F_{(16,162)} = 2.12$, $P = 0.0096$) and CR monkeys had significantly lower levels than control ($F_{(1,21)} = 5.76$, $P = 0.026$). F, female; M, male. Overall triglyceride trajectories were based on 243 observations for 34 monkeys (50 observations for 8 control-F; 81 for 10 control-M; 32 for 7 CR-F; 80 for 9 CR-M). Age breakdowns for all figures are in the supplementary material. **c**, Cholesterol predicted from age-dependent individual-specific trajectories for old-onset monkeys. Cholesterol levels increased with age ($F_{(53,774)} = 1.54$, $P = 0.009$), and male monkeys had significantly lower levels than females ($F_{(1,24)} = 23.60$, $P < 0.0001$). A significant three-way diet–sex–age interaction ($F_{(40,774)} = 1.53$, $P = 0.02$) indicated that cholesterol levels increased with age for control males whereas CR males tended to have a slight reduction in cholesterol. Thus, at older ages (>30 years), CR male monkeys have significantly lower cholesterol levels compared to controls. Overall cholesterol trajectories were based on 994 observations for 28 animals (204 for 7 control-F; 301 for 7 control-M; 134 for 5 CR-F; and 355 for 9 CR-Male). **d**, Fasting serum glucose (mg dl^{-1}) levels predicted from age-dependent individual-specific trajectories for old-onset monkeys. Five glucose measurements above 100 mg dl^{-1} for one diabetic control-M were omitted to remove the influence of these outliers on the analyses and graphs. There were significant changes in glucose over time ($F_{(20,285)} = 10.48$, $P < 0.0001$) and males and females were significantly different in the trends over time ($F_{(18,285)} = 3.58$, $P < 0.0001$) with males having increases in glucose levels over time, whereas the glucose levels of the females slightly decreased. The overall CR difference was not significant, $F_{(1,22)} = 1.18$, $P = 0.288$, and the CR differences in trend over time were not significant, $F_{(20,285)} = 1.23$, = 0.2259. Additional analyses stratified by sex conditions showed that control males had significantly higher glucose levels compared to CR males, $F_{(1,\ 14)} = 5.27$, $P = 0.04$. Overall glucose trajectories were based on 387 observations for 34 monkeys (79 observations for 8 control-F; 131 for 10 control-M; 48 for 7 CR-F; 129 for 9 CR-M).

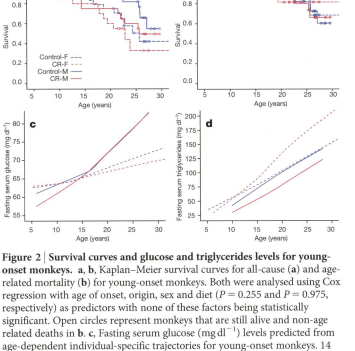

Figure 2 | Survival curves and glucose and triglycerides levels for young-onset monkeys. **a**, **b**, Kaplan–Meier survival curves for all-cause (**a**) and age-related mortality (**b**) for young-onset monkeys. Both were analysed using Cox regression with age of onset, origin, sex and diet ($P = 0.255$ and $P = 0.975$, respectively) as predictors with none of these factors being statistically significant. Open circles represent monkeys that are still alive and non-age related deaths in **b**. **c**, Fasting serum glucose (mg dl^{-1}) levels predicted from age-dependent individual-specific trajectories for young-onset monkeys. 14 glucose measurements above 100 mg dl^{-1} in diabetic monkeys (7 observations for 3 control-M; 5 for 2 CR-M; 2 for 1 control-F) were omitted to remove the influence of these outliers on the analyses and graphs. There were significant changes in glucose over time ($F_{(18.1,112)} = 11.24$, $P < 0.0001$), and males and females were significantly different in the trends over time ($F_{(18,112)} = 1.98$, $P = 0.0088$) with males having a larger increase in glucose levels over time. There was no significant difference due to diet group. Overall glucose trajectories were based on 1,260 observations for 81 monkeys (346 observations for 23 control-F; 350 for 20 control-M; 281 for 20 CR-F; 283 for 18 CR-M). **d**, Fasting serum triglycerides (mg dl^{-1}) predicted from age-dependent individual-specific trajectories for young-onset monkeys. There were significant changes in triglycerides over time ($F_{(14,843)} = 17.59$, $P < 0.0001$) and males and females were significantly different in the trends over time ($F_{(14,843)} = 5.36$, $P < 0.0001$). Furthermore, there was a diet–sex interaction indicating that the overall effect of CR on triglycerides was significantly different for male and female monkeys ($F_{(1,68)} = 5.07$, $P = 0.0276$). Specifically, CR males had lower triglycerides than control males. By contrast, CR females had higher triglyceride levels than control females. Overall triglyceride trajectories were based on 973 observations for 81 monkeys (266 observations for 23 control-F; 280 for 20 control-M; 213 for 20 CR-F; 214 for 18 CR-M).

monkeys for either analysis. Statistical controls are described in Methods. Of the original 86 monkeys in the young-onset cohorts, 24% (11/46) of the control animals and 20% (8/40) of the CR group died of age-related causes. The NIA findings contrast with the adult-onset study at WNPRC that demonstrated a beneficial CR effect in which 37% of the control monkeys had died from age-related causes compared to only 13% in the CR group. When accounting for all deaths, the trend persisted with 9 control and 13 CR animals dying of non-age related causes. Survival probabilities for all NIA age groups combined are shown in Supplementary Fig. 1a, b.

Considering that just less than 50% of young monkeys are still alive, these data do not represent final lifespan curves in this study. On the basis of lifespan projections using the hazard function[16], most animals are projected to be dead 10 years from now and the estimated probability statistics indicates a likelihood of less than 0.1% chance that the overall survival outcome would favour the CR group. The probability that a significantly different effect on mean survival will emerge in the next 5–10 years of the study is very low; however, a potential effect on maximum lifespan cannot be ruled out.

As there is a clear difference in CR effect on mortality between the colonies at NIA and WNPRC, further comparisons of these two longitudinal studies are warranted and planned. In an estimate of NIA's current data (as of 1 December 2011) to the published WNPRC data summarized as of 22 February 2008 and reported in ref. 5, NIA monkeys, both control and CR, may have a lifespan advantage comparable to the WNPRC CR monkeys.

Although they eat less (Supplementary Table 2) and weigh less[13], young-onset CR monkeys lack many of the expected CR benefits. Fasting serum glucose levels were not significantly lower in the CR monkeys compared to control (Fig. 2c), and only the CR males had somewhat lower triglycerides compared to respective controls ($P = 0.051$) (Fig. 2d). However, in a ligature-induced model of

inflammation in the oral cavity[1], we have shown an improved immune response in young-onset CR monkeys and beneficial effects in T cells isolated from adolescent-onset males[2].

The incidence of cancer was markedly improved in young-onset CR monkeys ($P = 0.028$ compared to controls); in fact, neoplasia has not been identified in any monkey from this group (Fig. 3a). In contrast, five of the six cases in young-onset control monkeys were considered the cause of death with a mean age at diagnosis of 22.8 ± 1.7 years. Glucoregulatory function was also improved in CR monkeys (Fig. 3a). However, two cases of diabetes have been diagnosed in CR monkeys; thus, the prevention of obesity did not prevent the occurrence of insulin-dependent diabetes and further investigation of the aetiology of such cases is of interest. Interestingly, CR did not reduce the incidence of cardiovascular disease as was reported in the WNPRC colony. Our findings are based on tissue pathology because these diagnoses were identified after death.

An analysis of first occurrence of age-related disease was done on the NIA monkeys using the same disease criteria as defined by the WNPRC study. These conditions included: cancer, diabetes, arthritis, diverticulosis and cardiovascular disease. Although age-related diseases were detected in control monkeys at an earlier age than in CR monkeys, the incident curves were not significantly different ($P = 0.06$) (Fig. 3b).

Considering that these two projects maintain high quality veterinary support in comparable experimental settings, study the same species of primates, and test the same intervention, what could account for the differences in survival outcome?

A notable difference between the two studies is diet composition. The NIA-1-87 formulation (Labdiet, PMI Nutrition International) has a natural ingredient base whereas WNPRC diet is purified (Harlan Teklad). Although natural ingredient diets risk having some variation between batches, they contain components that may have an impact on health such as phytochemicals, ultra-trace minerals and other unidentified elements[17]. In purified diets, each ingredient supplies a specific nutrient and each required mineral and vitamin is added as a separate component. Nutrient sources were also different. Protein was derived from wheat, corn, soybean, fish and alfalfa meal for the NIA diet, whereas the WNPRC diet protein source was lactalbumin. The NIA diet also contained flavonoids, known for their antioxidant activity, and fat from soy oil and the oils from the other natural ingredients (that is, corn, wheat and fish). Fish meal contains approximately 8–12% fat and is rich in omega-3 fatty acids. The WNPRC study dietary fat was derived from corn oil. Carbohydrate content was also notably different; although both diets had 57–61% carbohydrate by weight, the NIA study diet was comprised primarily of ground wheat and corn, whereas the WNPRC study diet contained corn starch and sucrose. Indeed, the WNPRC diet was 28.5% sucrose, whereas the NIA study diet was only 3.9% sucrose. This latter point may be particularly important as a diet high in sucrose may contribute to the incidence of type II diabetes[18,19].

The NIA and WNPRC studies also approached vitamin and mineral supplementation differently. The NIA study used one diet for both CR and control monkeys, which was supplemented with an additional 40% of the daily-recommended allowance to insure adequate nutrition for the CR monkeys. Thus, the NIA diet formulation supersupplemented the control monkeys. The WNPRC study fed two different diets and only the CR monkeys were supplemented.

Another important difference in study design was that the NIA study control monkeys were not truly fed *ad libitum*, unlike the WNPRC study. The regulated portioning of food for the NIA control monkeys may be a slight restriction and thus, largely prevented obesity. It has been reported that 10% CR increased lifespan in rats compared to *ad libitum*, even more than 25 and 40% CR[20]. The NIA control monkeys may experience survival benefits from this slight restriction.

Calorie restriction effectively lowered body weight in the NIA and WNPRC monkeys (Supplementary Table 2)[13,21]. However, WNPRC monkeys generally weighed more than corresponding NIA monkeys. For example, at 17 years of age, WNPRC males weighed approximately 12% more than corresponding NIA males and the difference was approximately 18% for the females. Thus, the NIA monkeys may be in an optimal weight range.

NIA monkeys originated from both China and India, and have greater genetic diversity compared to the strictly Indian colony at WNPRC. In rodent studies, genetic differences have affected the survival outcome in CR studies, even shortening it in some recombinant inbred mouse strains[22]. In genetically heterogeneous wild-caught mice, although hormonal and weight loss effects were consistent with CR, there was no overall mean longevity effect[23]. It is apparent that the effect of CR is not straightforward, and genetic differences may have a larger role than has been considered to date. A final analysis which includes all monkeys and controls for genetic origin can address this confounding variable.

Lastly, as in rodent studies[24], the age of onset of the CR regimen for the two studies could certainly impact survival outcome as it has other measures. CR initiated in the youngest male monkeys delayed maturation[25] and slowed skeletal growth[26]. Additionally, only the immune response of the adolescent males was improved by CR[15].

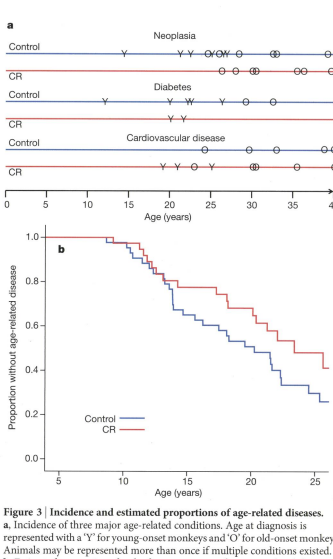

Figure 3 | Incidence and estimated proportions of age-related diseases. **a**, Incidence of three major age-related conditions. Age at diagnosis is represented with a 'Y' for young-onset monkeys and 'O' for old-onset monkeys. Animals may be represented more than once if multiple conditions existed. **b**, Estimated proportions for the first occurrence of any age-related disease in each monkey from the young-onset age group (males and females combined) statistically controlling for sex and sex–CR interaction. These conditions included: cancer, diabetes, arthritis, diverticulosis and cardiovascular disease. The difference between control and CR is not statistically significant, $P = 0.06$. Old-onset monkeys are not represented.

In the first randomized trial in humans, 6 months of CR improved several biomarkers of ageing and improved cardiovascular health, suggesting a reduction in risk of age-related disease. However, a lifespan study in humans is improbable[27]. Even a self-imposed CR regimen in lean individuals improved several metabolic, inflammatory and cardiovascular measures[28]. Current findings show that in nonhuman and human primates, CR evokes very similar metabolic, hormonal and physiological changes that are linked to longevity in CR rodents[28]. It will be valuable to continue to compare findings from ongoing monkey CR studies to dissect the mechanisms behind the improvement in health that occurred with and without significant effects on survival.

METHODS SUMMARY

Approval. This study was approved by the Animal Care and Use Committee of the NIA, NIH and was conducted in an AALAC-accredited facility.

Diagnostics. In live animals, diagnostic evaluations were made on the basis of clinical presentation. Radiographs confirmed conditions of osteoarthritis; endoscopic evaluation of diverticulosis revealed hernia-like outpouching in the mucosa of the descending colon with trapped faecal material in the diverticula; diabetes was confirmed by consistent elevated fasting glucose and glucose response during an intravenous glucose tolerance test; surgical biopsy or removal of tumours confirmed neoplasia. Cardiovascular abnormalities such as myofibre loss and fibrosis were diagnosed at necropsy as well as death due to acute congestive heart failure.

Blood sampling. For longitudinal measures, blood samples were obtained under ketamine (7–10 mg kg^{-1}, intramuscular) or Telazol (3.5 mg kg^{-1}, intramuscular) anaesthesia following an overnight fast. Serum samples were stored at −80 °C until analysed. Plasma free isoprostane samples were collected in 2005 and measured according to the description in ref. 29.

Full Methods and any associated references are available in the online version of the paper.

Received 27 October 2011; accepted 23 July 2012.
Published online 29 August 2012.

1. Branch-Mays, G. L. *et al.* The effects of a calorie-reduced diet on periodontal inflammation and disease in a non-human primate model. *J. Periodontol.* **79,** 1184–1191 (2008).
2. Messaoudi, I. *et al.* Delay of T cell senescence by caloric restriction in aged long-lived nonhuman primates. *Proc. Natl Acad. Sci. USA* **103,** 19448–19453 (2006).
3. Kastman, E. K. *et al.* A calorie-restricted diet decreases brain iron accumulation and preserves motor performance in old rhesus monkeys. *J. Neurosci.* **30,** 7940–7947 (2010).
4. Colman, R. J., Beasley, T. M., Allison, D. B. & Weindruch, R. Attenuation of sarcopenia by dietary restriction in rhesus monkeys. *J. Gerontol. A* **63,** 556–559 (2008).
5. Colman, R. J. *et al.* Caloric restriction delays disease onset and mortality in rhesus monkeys. *Science* **325,** 201–204 (2009).
6. Bodkin, N. L., Alexander, T. M., Ortmeyer, H. K., Johnson, E. & Hansen, B. C. Mortality and morbidity in laboratory-maintained Rhesus monkeys and effects of long-term dietary restriction. *J. Gerontol. A* **58,** B212–B219 (2003).
7. Forster, M. J., Morris, P. & Sohal, R. S. Genotype and age influence the effect of caloric intake on mortality in mice. *FASEB J.* **17,** 690–692 (2003).
8. Murtagh-Mark, C. M., Reiser, K. M., Harris, R. Jr & McDonald, R. B. Source of dietary carbohydrate affects life span of Fischer 344 rats independent of caloric restriction. *J. Gerontol. A* **50A,** B148–B154 (1995).
9. Swindell, W. R. Dietary restriction in rats and mice: a meta-analysis and review of the evidence for genotype-dependent effects on lifespan. *Ageing Res. Rev.* **11,** 254–270 (2012).
10. Messaoudi, I. *et al.* in *Calorie Restriction, Aging, and Longevity* (eds Everitt, A. V., Rattan, S., Le Couteur, D. & de Cabo, R.) 55–78 (Springer, 2010).
11. Roth, G. S. *et al.* Aging in rhesus monkeys: relevance to human health interventions. *Science* **305,** 1423–1426 (2004).
12. Ingram, D. K. *et al.* Dietary restriction and aging: the initiation of a primate study. *J. Gerontol.* **45,** B148–B163 (1990).
13. Mattison, J. A. *et al.* Age-related decline in caloric intake and motivation for food in rhesus monkeys. *Neurobiol. Aging* **26,** 1147–1127 (2005).
14. Colman, R. J. & Kemnitz, J. W. in *Methods in Aging Research* (ed. Yu, B. P.) 249–267 (CRC, 1998).
15. Messaoudi, I. *et al.* Optimal window of caloric restriction onset limits its beneficial impact on T-cell senescence in primates. *Aging Cell* **7,** 908–919 (2008).
16. Allison, P. D. *Survival Analysis Using SAS: A Practical Guide* (SAS Institute, 1995).
17. Nadon, N. L. Exploiting the rodent model for studies on the pharmacology of lifespan extension. *Aging Cell* **5,** 9–15 (2006).
18. Lomba, A. *et al.* A high-sucrose isocaloric pair-fed model induces obesity and impairs NDUFB6 gene function in rat adipose tissue. *J. Nutrigenet. Nutrigenomics* **2,** 267–272 (2009).
19. Roncal-Jimenez, C. A. *et al.* Sucrose induces fatty liver and pancreatic inflammation in male breeder rats independent of excess energy intake. *Metabolism* **60,** 1259–1270 (2011).
20. Duffy, P. H. *et al.* The effects of different levels of dietary restriction on aging and survival in the Sprague-Dawley rat: implications for chronic studies. *Aging (Milano)* **13,** 263–272 (2001).
21. Raman, A. *et al.* Influences of calorie restriction and age on energy expenditure in the rhesus monkey. *Am. J. Physiol. Endocrinol. Metab.* **292,** E101–E106 (2007).
22. Liao, C. Y., Rikke, B. A., Johnson, T. E., Diaz, V. & Nelson, J. F. Genetic variation in the murine lifespan response to dietary restriction: from life extension to life shortening. *Aging Cell* **9,** 92–95 (2010).
23. Harper, J. M., Leathers, C. W. & Austad, S. N. Does caloric restriction extend life in wild mice? *Aging Cell* **5,** 441–449 (2006).
24. Speakman, J. R. & Hambly, C. Starving for life: what animal studies can and cannot tell us about the use of caloric restriction to prolong human lifespan. *J. Nutr.* **137,** 1078–1086 (2007).
25. Roth, G. S. *et al.* Age-related changes in androgen levels of rhesus monkeys subjected to diet restriction. *Endocr. J.* **1,** 227–234 (1993).
26. Lane, M. A. *et al.* Aging and food restriction alter some indices of bone metabolism in male rhesus monkeys (*Macaca mulatta*). *J. Nutr.* **125,** 1600–1610 (1995).
27. Redman, L. M. & Ravussin, E. Caloric restriction in humans: impact on physiological, psychological, and behavioral outcomes. *Antioxid. Redox Signal.* **14,** 275–287 (2011).
28. Omodei, D. & Fontana, L. Calorie restriction and prevention of age-associated chronic disease. *FEBS Lett.* **585,** 1537–1542 (2011).
29. Ward, W. F. *et al.* Effects of age and caloric restriction on lipid peroxidation: measurement of oxidative stress by F2-isoprostane levels. *J. Gerontol. A* **60,** 847–851 (2005).

Supplementary Information is available in the online version of the paper.

Acknowledgements We thank the animal care staff and technicians, both past and present, especially J. Travis and M. Szarowicz; K. Vaughan for her editorial help; and the many collaborators that have contributed to this project. This research was supported by the Intramural Research Program of the NIH, National Institute on Aging.

Author Contributions G.S.R. and D.K.I. jointly conceived the original study and implemented it. J.A.M., R.d.C., D.K.I. and G.S.R. designed experiments, analysed and discussed data. J.A.M., R.d.C. and D.K.I. wrote the paper. T.M.B. and D.B.A. conducted statistical analyses and consultation. E.M.T., A.M.H. and J.E.Y. provided many years of technical support, data collection and supervision. R.L.H. provided veterinary support. D.L.L. assisted with data interpretation, discussion and paper edits. M.B. performed pathology assessments. D.B. assisted with initial diet formulation and all diet analyses and comparisons. W.F.W. and W.Q. designed and performed the isoprostane assays.

Author Information Reprints and permissions information is available at www.nature.com/reprints. Readers are welcome to comment on the online version of the paper. The authors declare competing financial interests: details accompany the full-text HTML version of the paper at www.nature.com. Correspondence and requests for materials should be addressed to J.A.M. (mattisonj@mail.nih.gov), R.d.C. (deCaboRa@grc.nia.nih.gov) or D.K.I. (Donald.Ingram@pbrc.edu).

LETTER

doi:10.1038/nature11317

Human ES-cell-derived cardiomyocytes electrically couple and suppress arrhythmias in injured hearts

Yuji Shiba[1,2]*, Sarah Fernandes[1]*, Wei-Zhong Zhu[1], Dominic Filice[1,3], Veronica Muskheli[1], Jonathan Kim[1], Nathan J. Palpant[1], Jay Gantz[1,3], Kara White Moyes[1], Hans Reinecke[1], Benjamin Van Biber[1], Todd Dardas[4], John L. Mignone[4], Atsushi Izawa[2], Ramy Hanna[4], Mohan Viswanathan[4], Joseph D. Gold[5], Michael I. Kotlikoff[6], Narine Sarvazyan[7], Matthew W. Kay[7,8], Charles E. Murry[1,3,4] & Michael A. Laflamme[1]

Transplantation studies in mice and rats have shown that human embryonic-stem-cell-derived cardiomyocytes (hESC-CMs) can improve the function of infarcted hearts[1–3], but two critical issues related to their electrophysiological behaviour *in vivo* remain unresolved. First, the risk of arrhythmias following hESC-CM transplantation in injured hearts has not been determined. Second, the electromechanical integration of hESC-CMs in injured hearts has not been demonstrated, so it is unclear whether these cells improve contractile function directly through addition of new force-generating units. Here we use a guinea-pig model to show that hESC-CM grafts in injured hearts protect against arrhythmias and can contract synchronously with host muscle. Injured hearts with hESC-CM grafts show improved mechanical function and a significantly reduced incidence of both spontaneous and induced ventricular tachycardia. To assess the activity of hESC-CM grafts *in vivo*, we transplanted hESC-CMs expressing the genetically encoded calcium sensor, GCaMP3 (refs 4, 5). By correlating the GCaMP3 fluorescent signal with the host ECG, we found that grafts in uninjured hearts have consistent 1:1 host–graft coupling. Grafts in injured hearts are more heterogeneous and typically include both coupled and uncoupled regions. Thus, human myocardial grafts meet physiological criteria for true heart regeneration, providing support for the continued development of hESC-based cardiac therapies for both mechanical and electrical repair.

Although hESC-CMs form gap junctions and beat synchronously *in vitro*[6,7], there is only indirect evidence for their electromechanical integration after transplantation[6–8]. We do not know whether hESC-CM grafts contract synchronously at physiological human rates, integrate in injured hearts despite scar tissue, or affect electrical stability. Indeed, both pro-arrhythmic[9] and anti-arrhythmic[10] effects have been reported for mouse cardiomyocyte grafts in injured mouse hearts. Human cardiac grafts could plausibly contribute to arrhythmogenesis through automaticity[11–14] and triggered activity[15], and their irregular graft geometry could promote reentry[1–3,16].

To address these uncertainties, we employed a new guinea-pig model of cardiac injury. Prior work with hESC-CMs in infarcted hearts was carried out in mice and rats[1–3], but these species' rapid heart rates (approximately 600 and 400 beats per minute (b.p.m.), respectively[17]) may prevent host–graft coupling or arrhythmias that could occur in humans. *In vitro* hESC-CMs show a spontaneous rate of approximately 50 to 150 b.p.m.[12,13,18] and can be paced up to 240 b.p.m., suggesting that they can keep up with the guinea-pig heart (approximately 200 to 250 b.p.m.[19]).

We first examined the structural, mechanical and electrocardiographic consequences of hESC-CM transplantation in injured hearts of immunosuppressed guinea-pigs (Supplementary Fig. 1a). hESC-CMs were derived from H7 hESCs, as previously described[2,20]. Adult guinea-pigs were subjected to cardiac cryoinjury and implanted with telemetric electrocardiographic (ECG) transmitters. Ten days later, they underwent a repeat thoracotomy and intra-cardiac injection of either 1×10^8 hESC-CMs in a pro-survival cocktail (PSC) of factors previously shown to enhance hESC-CM engraftment[2] ($n = 15$), 1×10^8 non-cardiac hESC-derivatives in PSC (non-CMs; $n = 13$), or PSC vehicle alone ($n = 14$). hESC-CMs were 63% pure by anti-α-actinin flow cytometry, whereas non-CMs included no detectable cardiomyocytes (Supplementary Fig. 2).

Twenty-eight days after transplantation, all animals showed transmural scar and thinning of the left ventricle. Scar area was not different among the groups (13.2 ± 0.9% of the left ventricle in hESC-CM, 14.8 ± 1.4% in non-CM, and 15.3 ± 1.9% in PSC-only recipients). However, hESC-CM recipients showed partial remuscularization with islands of human myocardium occupying 8.4 ± 1.5% of the scar area (Fig. 1a). The human origin of these grafts was confirmed by *in situ* hybridization with a human pan-centromeric probe, and more than 99% of the human cells immunostained positively with the cardiac marker β-myosin heavy chain (βMHC; also known as MYH7) (Fig. 1b and Supplementary Fig. 3a–f). No teratomas developed, and hESC-CM grafts were negative for multiple non-cardiac markers (Supplementary Fig. 3g–k). Most of the graft myocardium was located in the central scar, but there were occasional points of host–graft contact in the border zone with shared intercalated discs identified by anti-connexin 43 and cadherin immunostaining (Fig. 1c–h and Supplementary Fig. 3d, e). Minimal immune reaction was observed in sections stained with a guinea-pig-specific pan-leukocyte marker (Supplementary Fig. 3l). Grafts were supplied by host-derived neovessels that contained erythrocytes, indicating perfusion by the host coronary circulation (Supplementary Fig. 3h, m–o).

Surviving human cells were found in only 7 of 13 non-CM recipients at 28 days after transplantation, and these grafts were smaller than those in hESC-CM recipients (less than 1% of the scar area). No βMHC-positive graft was detected in non-CM recipients; instead, the surviving human cells consisted of small epithelial nests and scattered fibroblastic cells (Supplementary Fig. 4).

Hearts receiving hESC-CMs, non-CMs and PSC only, were assessed by echocardiography on days −2 and +28 relative to cell transplantation. All groups showed increased left-ventricle dimensions and reduced fractional shortening on day −2 relative to uninjured controls

[1]Department of Pathology, Center for Cardiovascular Biology, Institute for Stem Cell and Regenerative Medicine, University of Washington, 850 Republican Street, Seattle, Washington 98109, USA. [2]Department of Cardiovascular Medicine, Shinshu University, 3-1-1 Asahi, Matsumoto, Nagano 390-8621, Japan. [3]Department of Bioengineering, Center for Cardiovascular Biology, Institute for Stem Cell and Regenerative Medicine, University of Washington, 850 Republican Street, Seattle, Washington 98109, USA. [4]Department of Medicine and Cardiology, Center for Cardiovascular Biology, Institute for Stem Cell and Regenerative Medicine, University of Washington, 1959 NE Pacific Street, Seattle, Washington 98195, USA. [5]Geron Corporation, 230 Constitution Drive, Menlo Park, California 94025 USA. [6]Department of Biomedical Sciences, College of Veterinary Medicine, Cornell University, Ithaca, New York 14853, USA. [7]Department of Pharmacology and Physiology, The George Washington University, 2300 I Street NW, Washington DC 20037 USA. [8]Department of Electrical and Computer Engineering, The George Washington University, 2300 I Street NW, Washington DC 20037 USA.
*These authors contributed equally to this work.

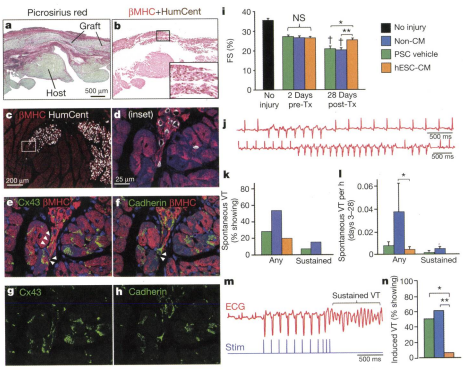

Figure 1 | Transplanted hESC-CMs partially remuscularize injured guinea-pig hearts, preserve mechanical function and reduce arrhythmia susceptibility. **a**, **b**, Twenty-eight-day-old hESC-CM grafts in a cryoinjured heart stained with picrosirius red (**a**), and anti-β-myosin heavy chain (βMHC, red) plus human-specific *in situ* probe (HumCent, brown) (**b**). **c**–**h**, Confocal image of host–graft contact, dual-labelled for HumCent (white) and βMHC (red) (**c**; a higher magnification image of the area in the white box in **c** is shown in **d**), de-stained and then immunostained for βMHC (red) and either connexin 43 (Cx43, green; **e** and **g**) or cadherins (green; **f** and **h**). Arrows indicate Cx43 and cadherin shared between graft and host myocytes. **i**, Left-ventricle fractional shortening (FS) by echocardiography in uninjured animals and cryoinjured recipients of PSC vehicle only, non-CMs or hESC-CMs at 2 days prior to and 28 days after transplantation (Tx). **j**, Representative telemetric ECGs, including non-sustained ventricular tachycardia (VT) in an hESC-CM recipient (top trace), as well as sustained VT and triplet PVCs in a non-CM recipient (bottom trace). **k**, Percentage of animals by group that showed spontaneous VT during monitoring from days 3 to 28 after transplantation. **l**, Frequency of spontaneous VT by group. **m**, ECG (red) and stimulation (blue) traces from a cryoinjured non-CM recipient induced to sustained VT by PES. **n**, Percentage of animals in each group induced to VT. All data are presented as mean ± s.e.m.; $n \geq 13$ per group. NS, not significant. $^*P < 0.05$; $^{**}P < 0.01$. $^\dagger P < 0.05$ versus day −2.

($n = 11$), but there were no differences among the cryoinjured groups (Fig. 1i and Supplementary Fig. 5). The two control groups exhibited further left ventricle dilation and deterioration of fractional shortening between days −2 and +28 ($P < 0.05$ for all pairwise comparisons between time points). This deterioration was completely attenuated in cryoinjured hESC-CM recipients, which showed significantly greater fractional shortening on day +28 than cryoinjured PSC-only or non-CM recipients ($P < 0.05$ and $P < 0.01$, respectively) (Fig. 1i).

Ambulatory telemetric ECG recordings were obtained regularly from 1 day after injury to 28 days after transplantation. Pilot studies revealed only rare premature ventricular contractions (PVCs) in uninjured animals, whereas cryoinjured but not transplanted animals showed occasional PVCs and runs of ventricular tachycardia (Supplementary Table 1). Interestingly, the hESC-CM group had the lowest fraction of animals with PVCs after transplantation and the lowest rate of couplet PVCs per hour (Supplementary Fig. 6). Moreover, fewer hESC-CM recipients showed spontaneous ventricular tachycardia, and hESC-CM recipients were the only group with no sustained ventricular tachycardia (Fig. 1j, k). Next, we counted all episodes of ventricular tachycardia from day 3 to 28 and found that non-CM recipients showed 785% more ventricular tachycardia episodes than hESC-CM recipients (95% confidence interval: 74% to +4,370%, $P < 0.01$; Fig. 1l).

As a final test of electrical stability, we induced arrhythmias through programmed electrical stimulation (PES). To detect either a positive or negative effect of cell transplantation, we developed a PES protocol that induced ventricular tachycardia in 40% of non-transplanted animals at 38 days after cryoinjury ($n = 5$), but not in uninjured animals ($n = 8$). When cryoinjured hESC-CM recipients were challenged with PES at 28 days after transplantation, ventricular tachycardia was induced in only 6.7% of these animals versus 61.5% and 50% of cryoinjured non-CM and PSC-only recipients, respectively ($P < 0.01$ by Fisher's exact test, Fig. 1m, n).

To explore the mechanism by which hESC-CMs improved mechanical and electrical function, we investigated whether the grafts were coupled and beat synchronously with host myocardium. We used zinc-finger nuclease (ZFN)-mediated transgenesis[21] to create hESC-CMs that stably expressed the genetically encoded fluorescent calcium sensor, GCaMP3 (refs 4, 5), and these myocytes exhibited robust fluorescence transients with each contractile cycle *in vitro* (Supplementary Fig. 7 and Supplementary Movie 1). We transplanted 1×10^8 GCaMP3-positive hESC-CMs (cardiac purity of 74 ± 10%) into intact and cryoinjured guinea-pig hearts and carried out intravital imaging at 2 or 4 weeks after transplantation (Supplementary Fig. 1b). Epicardial fluorescent transients indicated activation of the graft *in vivo*, and these were correlated with the ECG to determine their synchrony with host myocardium[10].

The GCaMP3-positive hESC-CM grafts in uninjured hearts had extensive host–graft contact with little intervening fibrosis (Fig. 2a and Supplementary Fig. 8a). Correspondingly, these hearts showed an impressive degree of host–graft electromechanical integration. We found large GCaMP3-positive hESC-CMs grafts in all uninjured recipients at 14 days after transplantation ($n = 9$), and 100% of the visible graft in each animal showed calcium fluorescence transients that synchronized 1:1 with systole in the host ECG (Fig. 2b). These hearts were also imaged *ex vivo* during mechanical arrest with either 2,3-butanedione monoxime (BDM) or blebbistatin ($n = 11$). 1:1 host–graft coupling continued under these conditions, ruling out confounding motion artefacts and the possibility of indirect graft activation by passive stretch (Supplementary Fig. 8 b, c and Supplementary Movie 2). hESC-CM grafts in uninjured hearts remained fully coupled during pacing at rates ≥5 Hz (Fig. 2c).

Next, we transplanted GCaMP3-positive hESC-CMs at 10 days after cryoinjury and carried out intravital imaging at 14 and 28 days after transplantation ($n = 7$ and $n = 15$ animals, respectively). By histology, surviving grafts at both time points were mostly located within the central scar, although occasional points of host–graft contact in the border zone were identified (Fig. 3a and Supplementary Fig. 9a). Dual labelling with a guinea-pig-specific *in situ* probe and anti-green fluorescent protein (GFP) immunostaining ruled out a meaningful

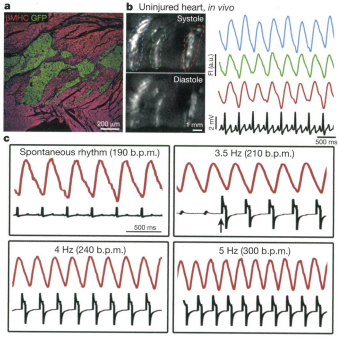

Figure 2 | hESC-CM grafts in uninjured hearts show 1:1 coupling with host myocardium. **a**, GCaMP3-positive hESC-CM graft in an uninjured heart immunostained for GFP (green) and βMHC (red), showing extensive host–graft contact with minimal intervening scar. **b**, Left, GCaMP3-positive hESC-CM graft in an uninjured heart during systole and diastole, acquired using an open-chest preparation at 14 days after transplantation. Right, GCaMP3 fluorescence intensity (FI) versus time for the red, green and blue regions of interest indicated in the left panel, as well as the host ECG (black). GCaMP3 fluorescent transients in all three regions occurred with 1:1 coupling with QRS complexes of the host ECG. a.u. arbitrary units. **c**, GCaMP3 fluorescent signal (red) and ECG (black) from a representative hESC-CM graft in an uninjured heart, imaged *ex vivo* under mechanical arrest. 1:1 host–graft coupling occurred during spontaneous beating and pacing at rates ≤5 Hz. Arrow, onset of pacing.

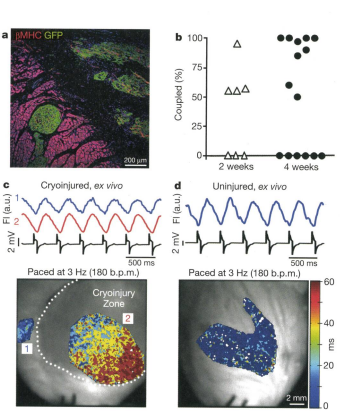

Figure 3 | hESC-CM grafts show 1:1 host–graft coupling in the majority of injured recipient hearts, but the extent of coupling and pattern of activation is variable. **a**, GCaMP3-positive hESC-CM graft in a cryoinjured heart immunostained for GFP (green) and βMHC (red). Small graft nests were located in host muscle within the border zone, but most of the graft was in scar. **b**, Percentage of visible GCaMP3-positive hESC-CM graft in each cryoinjured heart that showed 1:1 host–graft coupling at 14 and 28 days after transplantation ($n = 7$ and $n = 15$ animals, respectively). **c**, Representative 28-day-old GCaMP3-positive hESC-CM graft in a cryoinjured heart imaged *ex vivo* during mechanical arrest with blebbistatin and pacing at 3 Hz. Top, traces of mean fluorescent intensity versus time for graft regions located within host muscle (1, blue font) and the cryoinjury zone (2, red font). Both were activated in a 1:1 correlation with the host ECG (black). Bottom, corresponding activation map showing the interval (in ms) between the stimulus pulse and the local rise in GCaMP3 fluorescence. Graft in host muscle (1) showed uniformly rapid activation, whereas the graft in the scar (2) activated first in centre of the scar and then gradually progressed towards the border zone. On other occasions, graft activation started at the border zone and radiated into the scar. **d**, Top, traces of GCaMP3 fluorescence and EGG. Bottom, the activation map for a representative GCaMP3-positive hESC-CM graft in a blebbistatin-arrested uninjured heart. This graft showed 1:1 host–graft coupling and a brief interval between stimulus and GCaMP3 transient upstroke.

contribution of cell fusion to the observed GCaMP3 signals (Supplementary Fig. 9b and Supplementary Movie 3).

Cryoinjured hearts with GCaMP3-positive hESC-CM grafts showed robust epicardial fluorescence transients, but their behaviour was more heterogeneous than that of grafts in uninjured animals, with greater variation in size, distribution and temporal relationship to the host ECG. Given this complicated behaviour, we focused on imaging mechanically arrested hearts *ex vivo*, so that the grafts could be more completely visualized and the proportion of coupled and uncoupled graft could be quantified better (Supplementary Movies 4 and 5). We found regions of GCaMP3-positive graft with consistent 1:1 host–graft coupling in approximately 60% of hearts at both 14 and 28 days after transplantation (4 out of 7 animals, and 9 out of 15 animals, respectively; Fig. 3b and Supplementary Tables 2 and 3). Although there was no significant difference in the fraction of animals with coupled grafts between the two time points, in the subset of animals with at least some coupling, there was a trend towards greater host–graft coupling over time (66 ± 10% versus 87 ± 6% of visible graft at 14 and 28 days, respectively). No grafts with intermittent or partial coupling (for example, 1:2 or 1:3 host–graft coupling) were observed. Uncoupled graft regions showed regular GCaMP3 fluorescent transients, but these occurred with a periodicity unrelated to the ECG or neighbouring graft domains, usually at a rate slower than the host (at 28 days, 96 ± 11 b.p.m. versus a host rate of 176 ± 9 b.p.m.). By marking the coupled and non-coupled graft regions with indelible inks that survive histological processing, we found many examples of reliably coupled graft located within the central scar region, proving that coupling is not limited to grafts at the border zone (data not shown). When injured hearts with GCaMP3-positive hESC-CM grafts were paced, most of the initially coupled graft regions remained coupled up to 4 Hz, after which some loss of coupling was observed (Supplementary Fig. 10).

We next attempted to perform voltage mapping of graft and host myocardium in cryoinjured hearts but, unexpectedly, hESC-CM grafts failed to label with the potentiometric dyes RH237 and di-4-ANEPPS (Supplementary Fig. 11). hESC-CMs were readily labelled *in vitro* (Supplementary Fig. 12), so their poor staining *in vivo* probably reflects sluggish perfusion of the graft tissue and perhaps reduced membrane staining because of undeveloped T-tubules[22]. However, we did obtain good labelling of host myocardium with RH237 and we therefore compared voltage maps from cryoinjured hearts with and without grafts ($n = 6$ and $n = 4$ animals, respectively). As expected, both groups showed robust propagation in uninjured myocardium, whereas optical action potential amplitudes and epicardial conduction velocities were reduced in the cryoinjury zone. The two groups showed no significant differences in the amplitudes of optical action potentials within the injured zone or the kinetics of activation and repolarization

(Supplementary Figs 13 and 14), suggesting that hESC-CM transplantation does not exert major paracrine effects on host electrical behaviour.

Because the electrical activity of hESC-CM grafts could not be evaluated with potentiometric dyes, we used instead the GCaMP3 signal to assess graft activation and propagation. GCaMP3 transients lag depolarization owing to slow binding of calcium, but this delay should be the same throughout the graft[19,23], so graft activation maps can be generated using the time interval between electrical stimulation (or host QRS complex of the ECG) and the GCaMP3 transient. This revealed a marked difference in activation between grafts located in viable host muscle versus those in scar tissue (Fig. 3c, d). Grafts in intact myocardium were activated uniformly and within approximately 10 ms, probably reflecting synchronous activation through multiple points of contact with the host. In contrast, graft activation within scar tissue was spatially and temporally heterogeneous, even in regions with 1:1 coupling. These coupled grafts showed initial activation within approximately 10 to 20 ms, but the spread of activation was slower, such that some areas required >50 ms for activation. This probably reflects the more limited contacts between graft and host, as well as slower propagation within the immature graft myocardium.

These intravital imaging studies are, to our knowledge, the first direct demonstration that human cardiomyocytes can integrate and contract synchronously with host myocardium. Although additional paracrine mechanisms cannot be excluded, the demonstration of electromechanically coupled grafts in injured hearts supports the idea that hESC-CMs can improve mechanical function by creating new force-generating units, a sine qua non for heart regeneration. However, hESC-CM grafts in injured hearts were not always fully integrated, implying that enhancing their integration may further benefit contractile function. The model developed here represents a reasonably high-throughput platform to test strategies to improve host–graft integration (for example, tissue engineering, attenuating graft cell death and reducing fibrosis).

Our study also provides reassurance about the arrhythmogenic risk of cardiac repair with immature stem-cell-derived cardiomyocytes. Consistent with prior transplantation studies with primary fetal mouse cardiomyocytes[10], we observed an arrhythmia-suppressive effect that was unique to cardiomyocyte grafts and occurred despite incomplete host–graft coupling. Although this is encouraging, before clinical translation of hESC-based therapies, it will be necessary to carry out safety and efficacy studies with longer follow-up durations and in a large animal model.

METHODS SUMMARY

GCaMP3-positive hESCs were generated by ZFN-mediated targeting, following a method described previously[21] (Supplementary Fig. 7), and these transgenic and wild-type hESCs were differentiated into cardiomyocytes, as previously reported[2,20]. Guinea-pigs underwent cryoinjury, immunosuppression with cyclosporine plus methylprednisolone, cell transplantation and physiological monitoring as detailed in the Supplementary Methods and Supplementary Fig. 1. Intravital imaging of GCaMP3-positive hESC-CM grafts was carried out on day 14 or 28 after transplantation, using open chest and *ex vivo* Langendorff preparations. GCaMP3 and RH237 fluorescent signals were acquired with a high-speed camera (Andor iXon 860 EM-CCD) on an epifluorescence stereomicroscope. All procedures complied with regulations of the University of Washington Institutional Animal Care and Use Committee.

Full Methods and any associated references are available in the online version of the paper.

Received 26 April 2011; accepted 12 June 2012.
Published online 5 August 2012.

1. Caspi, O. *et al.* Transplantation of human embryonic stem cell-derived cardiomyocytes improves myocardial performance in infarcted rat hearts. *J. Am. Coll. Cardiol.* **50,** 1884–1893 (2007).
2. Laflamme, M. A. *et al.* Cardiomyocytes derived from human embryonic stem cells in pro-survival factors enhance function of infarcted rat hearts. *Nature Biotechnol.* **25,** 1015–1024 (2007).
3. van Laake, L. W. *et al.* Human embryonic stem cell-derived cardiomyocytes survive and mature in the mouse heart and transiently improve function after myocardial infarction. *Stem Cell Res.* **1,** 9–24 (2007).
4. Tallini, Y. N. *et al.* Imaging cellular signals in the heart *in vivo*: cardiac expression of the high-signal Ca^{2+} indicator GCaMP2. *Proc. Natl Acad. Sci. USA* **103,** 4753–4758 (2006).
5. Tian, L. *et al.* Imaging neural activity in worms, flies and mice with improved GCaMP calcium indicators. *Nature Methods* **6,** 875–881 (2009).
6. Kehat, I. *et al.* Electromechanical integration of cardiomyocytes derived from human embryonic stem cells. *Nature Biotechnol.* **22,** 1282–1289 (2004).
7. Xue, T. *et al.* Functional integration of electrically active cardiac derivatives from genetically engineered human embryonic stem cells with quiescent recipient ventricular cardiomyocytes: insights into the development of cell-based pacemakers. *Circulation* **111,** 11–20 (2005).
8. Gepstein, L. *et al. In vivo* assessment of the electrophysiological integration and arrhythmogenic risk of myocardial cell transplantation strategies. *Stem Cells* **28,** 2151–2161 (2010); erratum **29,** 1475 (2011).
9. Liao, S. Y. *et al.* Proarrhythmic risk of embryonic stem cell-derived cardiomyocyte transplantation in infarcted myocardium. *Heart Rhythm* **7,** 1852–1859 (2010).
10. Roell, W. *et al.* Engraftment of connexin 43-expressing cells prevents post-infarct arrhythmia. *Nature* **450,** 819–824 (2007).
11. Kehat, I. *et al.* Human embryonic stem cells can differentiate into myocytes with structural and functional properties of cardiomyocytes. *J. Clin. Invest.* **108,** 407–414 (2001).
12. He, J. Q., Ma, Y., Lee, Y., Thomson, J. A. & Kamp, T. J. Human embryonic stem cells develop into multiple types of cardiac myocytes: action potential characterization. *Circ. Res.* **93,** 32–39 (2003).
13. Zhu, W. Z. *et al.* Neuregulin/ErbB signaling regulates cardiac subtype specification in differentiating human embryonic stem cells. *Circ. Res.* **107,** 776–786 (2010).
14. Mandel, Y. *et al.* Human embryonic and induced pluripotent stem cell-derived cardiomyocytes exhibit beat rate variability and power-law behavior. *Circulation* **125,** 883–893 (2012).
15. Jonsson, M. K. *et al.* Quantified proarrhythmic potential of selected human embryonic stem cell-derived cardiomyocytes. *Stem Cell Res.* **4,** 189–200 (2010).
16. Chen, H. S., Kim, C. & Mercola, M. Electrophysiological challenges of cell-based myocardial repair. *Circulation* **120,** 2496–2508 (2009).
17. Swoap, S. J., Overton, J. M. & Garber, G. Effect of ambient temperature on cardiovascular parameters in rats and mice: a comparative approach. *Am. J. Physiol. Regul. Integr. Comp. Physiol.* **287,** R391–R396 (2004).
18. Mummery, C. *et al.* Differentiation of human embryonic stem cells to cardiomyocytes: role of coculture with visceral endoderm-like cells. *Circulation* **107,** 2733–2740 (2003).
19. Shiotani, M., Harada, T., Abe, J., Hamada, Y. & Horii, I. Methodological validation of an existing telemetry system for QT evaluation in conscious guinea pigs. *J. Pharmacol. Toxicol. Methods* **55,** 27–34 (2007).
20. Zhu, W. Z., Van Biber, B. & Laflamme, M. A. Methods for the derivation and use of cardiomyocytes from human pluripotent stem cells. *Methods Mol. Biol.* **767,** 419–431 (2011).
21. Hockemeyer, D. *et al.* Efficient targeting of expressed and silent genes in human ESCs and iPSCs using zinc-finger nucleases. *Nature Biotechnol.* **27,** 851–857 (2009).
22. Lieu, D. K. *et al.* Absence of transverse tubules contributes to non-uniform $Ca^{(2+)}$ wavefronts in mouse and human embryonic stem cell-derived cardiomyocytes. *Stem Cells Dev.* **18,** 1493–1500 (2009).
23. Kotlikoff, M. I. Genetically encoded Ca^{2+} indicators: using genetics and molecular design to understand complex physiology. *J. Physiol. (Lond.)* **578,** 55–67 (2007).

Supplementary Information is linked to the online version of the paper at www.nature.com/nature.

Acknowledgements We thank Y. Tallini, L. Linares, B. Johnson and S. Dupras for advice and technical assistance. This work was partly supported by a grant from Geron Corporation (M.A.L.), as well as by US National Institutes of Health grants K08-HL80431 (M.A.L.), R01-HL064387 (M.A.L. and C.E.M.), P01-HL094374 (M.A.L. and C.E.M.), R01-HL084642 (C.E.M.), P01-GM81619 (C.E.M.), U01-HL100405 (M.A.L. and C.E.M.) and R01-HL095828 (N.S. and M.W.K.). Animal experiments were supported in part by the University of Washington's Mouse Metabolic Phenotyping Center, U24-DK076126.

Author Contributions S.F., Y.S., W.-Z.Z., D.F., M.I.K., J.D.G., C.E.M. and M.A.L. designed the study. Y.S. and S.F. led the arrhythmia and calcium imaging experiments, respectively. Y.S. developed and performed the telemetry and programmed electrical stimulation. T.D., J.L.M., A.I., R.H. and M.V. performed telemetric ECG interpretation. The GCaMP3-expressing hESC line was generated by J.G., N.J.P. and B.V.B.V.M., J.K., K.W.M., S.F. and Y.S. carried out and analysed immunohistochemistry experiments. S.F., H.R. and M.A.L. developed and performed guinea-pig-specific *in situ* hybridization. S.F., W.-Z.Z. and D.F. carried out and analysed the GCaMP3 imaging experiments. D.F., M.W.K. and N.S. developed and analysed the voltage mapping experiments. All authors contributed to data analysis and interpretation. Y.S. created the figures with the assistance of S.F., W.-Z.Z., K.W.M. and D.F. C.E.M. and M.A.L. wrote the manuscript.

Author Information Reprints and permissions information is available at www.nature.com/reprints. The authors declare competing financial interests: details are available in the online version of the paper. Readers are welcome to comment on the online version of this article at www.nature.com/nature. Correspondence and requests for materials should be addressed to M.A.L. (laflamme@u.washington.edu) or C.E.M. (murry@uw.edu).

CORRECTIONS & AMENDMENTS

CORRIGENDUM

doi:10.1038/nature11372

Corrigendum: Recurrent network activity drives striatal synaptogenesis

Yevgenia Kozorovitskiy, Arpiar Saunders, Caroline A. Johnson, Bradford B. Lowell & Bernardo L. Sabatini

Nature **485,** 646–650 (2012); doi:10.1038/nature11052

On page 3 of the PDF and print version of this Letter, column two, in the text describing the mEPSC frequency and dendritic spine density values shown in Fig. 3b and 3c, the words 'saline' and 'cno' were erroneously exchanged. The correct text should read: (D1-Cre, direct pathway MSNs: frequency, saline 0.8 ± 0.1 Hz, $n = 18$; cno 0.36 ± 0.07 Hz, $n = 25$; spine density, saline 0.96 ± 0.04 spines per μm, $n = 5$; cno 0.49 ± 0.05 spines per μm, $n = 5$; D2-Cre, indirect pathway MSNs: frequency, saline 0.04 ± 0.01 Hz, $n = 7$; cno, 0.27 ± 0.09 Hz, $n = 8$; spine density, saline 0.54 ± 0.05 spines per μm, $n = 5$; cno 0.98 ± 0.06 spines per μm, $n = 5$). This has been corrected online in the PDF and HTML of the original paper.

ERRATUM

doi:10.1038/nature11423

Erratum: Non-invasive prenatal measurement of the fetal genome

H. Christina Fan, Wei Gu, JianbinWang, Yair J. Blumenfeld, Yasser Y. El-Sayed & Stephen R. Quake

Nature **487,** 320–324 (2012); doi:10.1038/nature11251

In this Article, the statement of the competing financial interests was inadvertently omitted in the print version. The statement was corrected online on 18 July 2012.

CORRIGENDUM

doi:10.1038/nature11373

Corrigendum: Biodiversity loss and its impact on humanity

Bradley J. Cardinale, J. Emmett Duffy, Andrew Gonzalez, David U. Hooper, Charles Perrings, Patrick Venail, Anita Narwani, Georgina M. Mace, David Tilman, David A.Wardle, Ann P. Kinzig, Gretchen C. Daily, Michel Loreau, James B. Grace, Anne Larigauderie, Diane S. Srivastava & Shahid Naeem

Nature **486,** 59–67 (2012); doi:10.1038/nature11148

In Table 1 and Supplementary Table 2 of this Review, under the 'Category of service' called 'Regulating', the first two 'Measures of service provision' related to 'Biocontrol' should read 'Abundance of herbivorous pests' instead of 'Control of herbivorous pests'. With this word change, a downward arrow for either the predicted or actual diversity–service relationship would indicate that the abundance of herbivorous pests declines (and biocontrol increases) with increasing plant diversity. This does not alter any of our conclusions, because all diversity–service relationships were correctly described in the text of the manuscript itself. These errors have been corrected online in the HTML and PDF versions of the original Review, and in the original Supplementary Information.

ERRATUM

doi:10.1038/nature11425

Erratum: An origin of the radio jet in M87 at the location of the central black hole

Kazuhiro Hada, Akihiro Doi, Motoki Kino, Hiroshi Nagai, Yoshiaki Hagiwara & Noriyuki Kawaguchi

Nature **477,** 185–187 (2011); doi:10.1038/nature10387

In Fig. 3 of this Letter, the axes labels were inadvertently exchanged. The *y*-axis label should read "Declination offset from 43-GHz core (mas)" and the *x*-axis label should read: "RA offset from 43-GHz core (mas)". The PDF and HTML versions have been corrected online.

CAREERS

TURNING POINT Astrobiologist's passion for Mars science creates opportunities **p.328**

@NATUREJOBS Follow us on Twitter for the latest news and features **go.nature.com/e492gf**

NATUREJOBS For the latest career listings and advice **www.naturejobs.com**

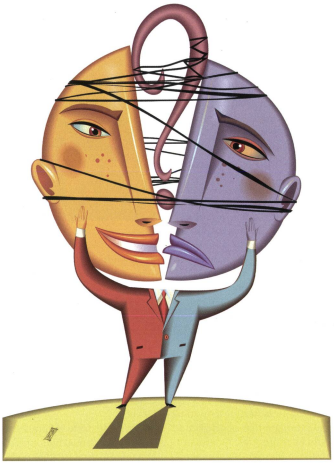

IMAGES.COM/CORBIS

COLUMN

Working together

The right administrative system can ease the job search for dual-career couples, argues **Mary Anne Holmes**.

It is a process common on university campuses around the world. A faculty search committee ploughs through piles of applications, sorts them, evaluates them, brings the best candidates to campus and interviews the top few. It eventually arrives at the perfect person for the job. The head of the department makes the offer — only to discover that the perfect candidate has a partner, and the dreaded two-body problem must be addressed.

It can be a nightmare: the whole search collapsing as the clock runs out and the committee tries to find a position for the partner. But at the University of Nebraska–Lincoln (UNL), we have developed a means of dealing with the problem to help both candidate and recruiter.

By the time a job offer is made, a substantial amount of time and money has been invested. At the UNL, departments spend between US$9,000 and $18,000 simply advertising a position. Factor in the time spent by faculty members on reviewing applications — 10–20 hours, depending on the size of the pile — and the costs are even higher. No one wants a candidate to turn down an offer.

The joint hiring of academic couples has quadrupled since the 1970s. By 2008, 36% of academics in the United States had a partner who also worked in academia. And the rate was highest among scientists: 54% of male and 83% of female scientists had a partner in academic science, most in a similar field (L. Schiebinger *et al. Dual-Career Academic Couples: What Universities Need to Know*; Stanford University, 2008). With so many female scientists partnered with an academic, strategies to increase the number of women employed as faculty members in science, technology, engineering and mathematics should include a means of addressing dual-career opportunities.

The UNL tackled this question using an Institutional Transformation award from the US National Science Foundation's ADVANCE programme, which aims to improve the representation of women in academic scientific careers. The university came up with a process that should transfer well to other institutions.

FROM THE START

The UNL Dual Career Assistance initiative addresses the two-body problem early in the negotiation and recruiting process. Primary candidates are informed about the programme once they have been shortlisted, but before they are interviewed. They are told that if they have a partner who is qualified for a faculty position, the partner should send a letter of interest, a CV and a statement of research and teaching interests to the ADVANCE office. The director of the ADVANCE programme notifies the appropriate department chair and the college dean of the potential dual-career hire.

This initiative gives the candidate a safe place to disclose their relationship status without making it a factor in deliberations, and provides a relay office to alert all parties. The extra time allows the university to bring the partner to campus for an interview as soon as the offer for the primary candidate is put together. The original search committee is left out of the flow of information, so that it doesn't inappropriately weigh relationship status as a criterion for selection. After all, it may be hard to resist the urge to speculate on how having a partner will affect a candidate's likelihood of accepting an offer. But relationship status, of course, has little to do with the candidate's suitability for the position.

If a candidate with an academic partner is ▶

ultimately selected for a faculty position and the partner's target college and department are interested, the partner is flown to Lincoln for an interview. If the interview goes well and faculty members in the target department vote to make an offer to the partner, two offers go forward. If the department is not interested, the process stops and the primary candidate and their partner have to decide whether to come to the university with just one job (we have lost a few candidates this way).

The ADVANCE grant supplies one-quarter of the salary for the partner for up to three years, with the department, college and provost's office each supplying a further quarter. The university's office of research provides start-up funds. This three-year bridge funding buys time for all the administrators to find a permanent funding stream for the partner, which might be provided by a new funding line or the retirement of an existing faculty member.

Sometimes, the primary candidate has a partner who does not want to stay in academia. We can assist with external job searches through our networks and the local chamber of commerce, or the partner can look for a job independently.

The UNL's original ADVANCE grant was for five years, and we anticipated that as many as eight dual-career hires would be made over that time. In fact, after four years we have hired 12 partners.

What happens when the ADVANCE funding runs out? Bridge funding could help. But there are ways, in principle, for universities to institutionalize this process without any grants. One model could be to reserve a proportion of new positions for dual-career hires. The provost or dean could refrain from filling a few positions each year, or could raise an endowment.

Overall, the UNL has had more success with these formal procedures than with informal last-minute requests to accommodate a partner. The programme works in large part because department chairs agree to cooperate: if we accept a partner now, the reasoning goes, another department will help us in the future. Some administrators have expressed concern that a formal dual-career programme will raise the expectations of partners, only for these to be dashed when no position is forthcoming. However, we find that prospective faculty members appreciate the transparency of the process.

Dual-career partnership is not a passing fad. Addressing this need must be an integral part of future universities if we are to attract and keep the best and the brightest. ■

Mary Anne Holmes *is a professor of Earth and atmospheric sciences at the University of Nebraska–Lincoln and director of ADVANCE-Nebraska.*

TURNING POINT
Alberto Gonzalez Fairén

As a teenager in Spain, Alberto Gonzalez Fairén watched US astronomer Carl Sagan's television series Cosmos, *read the book based on the series and knew that he wanted to be a scientist. He is now an astrobiologist at the SETI Institute's Carl Sagan Center for the Study of Life in the Universe in Mountain View, California, and the NASA Ames Research Center in Moffett Field, California. In October, Fairén will collect the Harold C. Urey Prize for outstanding achievement in planetary science from the American Astronomical Society, based in Washington DC.*

What was it about *Cosmos* that sparked your interest in science?

Listening to Sagan telling stories about how science is done and how scientists work, and describing the thrill of scientific discovery, I said to myself, "That's what I want to do."

You did a master's degree in genetics. How did you move from that to Martian environments?

It was the other way around. I've been very interested in planetary science and astrobiology since I was a teenager, but there were no university programmes in the field in Spain at the time. Genetics was a distant second interest to me, but I needed to graduate to start my PhD and begin working as a planetary scientist. Astrobiology was starting to become respectable, and I thought that a background in genetics would be appropriate for an astrobiologist interested in Martian environments.

What are your plans for the future?

I'm leaving the SETI Institute because 'soft money' — working solely off grants — is no longer an option for me. When you have a family, you need some kind of stability. I've been offered two academic positions in the United States, and I've won a starting grant from the European Research Council. If I accept one of the offers here, I will stay in US Mars science, which is very attractive right now, especially after the success with the Curiosity rover landing. If I go back to Europe, I will have substantial funding to launch my own group, which seems the logical next step.

Describe your biggest career milestone.

Carbonates are minerals produced in water; the fact that none had been found on Mars had long been used to argue that there were never oceans on Mars. But my adviser told me about a river in Spain that was very acidic; I knew that carbonates do not form in acidic water. I was two years into my PhD and proposed that oceans on Mars were also acidic and that this acidity inhibited the formation of carbonates. A team including me and my adviser submitted a paper on the subject to *Nature* on 7 January 2004. NASA's rover Opportunity landed on Mars days later — and found direct evidence for such acidic environments. We had accurately anticipated the rover's results. Our paper was published on 23 September 2004, and was central to the completion of my PhD.

Does the Urey prize have a special meaning for you?

It won't help me to get grants or positions, but it is a high personal honour. There is a long list of names of very, very, very important people in planetary science who have won this award.

Has it been difficult to adjust to living and working in the United States?

Not really. Life in California is not so different from life in Spain, and I already had a good command of English. The biggest difference is that the United States rewards effort and merit.

Do you have any regrets about your career?

No. Some time ago I realized that my errors were necessary to bring me to where I am now. I didn't begin to pursue my PhD until I was 30, and while I was away from science I worked as a bartender, a taxi driver, a film-rating classifier and a teacher, among other things. But I got my PhD in 2006 and started working for NASA, and that was a turning point in my career. It offered me the freedom and resources to pursue my own investigations. My career would have been totally different without the NASA experience. ■

INTERVIEW BY KAREN KAPLAN

a nature conference

2012 *Nature* / Institute for Genomic Medicine Symposium

Building upon the outstanding success of the Inaugural and 2011 Symposia at the Institute for Genomic Medicine at University of California, San Diego, this year's symposium, in partnership with *Nature*, is aimed at the international scientific community, with the goal of fostering and facilitating communication and collaborative initiatives in medical genomics.

The following topics will be covered at the conference: Cancer Genomics, Gene & Cell Therapies, Complex Human Traits, Personalized Genomics for Implementation of Genetic Information.

November 4-5, 2012
UCSD School of Medicine Campus
La Jolla, CA, USA

KEYNOTE SPEAKER:
Eric Green (National Human Genome Research Institute, NIH, USA)

CONFIRMED SPEAKERS:

Robin Ali
Ines Barosso
Jean Bennett
George Church
Mark Daly
Richard Gilbertson
Joseph Gleeson
Joe Gray
David Haussler
Vanessa Hayes
Jonathan Sebat
Mike Snyder
Mike Stratton
Doug Turnbull

ORGANIZERS:
Kelly Frazer (University of California, San Diego, USA)
Xiang-dong Fu (University of California, San Diego, USA)
Magdalena Skipper (*Nature*, UK)
Kang Zhang (University of California, San Diego, USA)
Kun Zhang (University of California, San Diego, USA)

For more information and to register visit:
www.nature.com/natureconferences/nigm2012

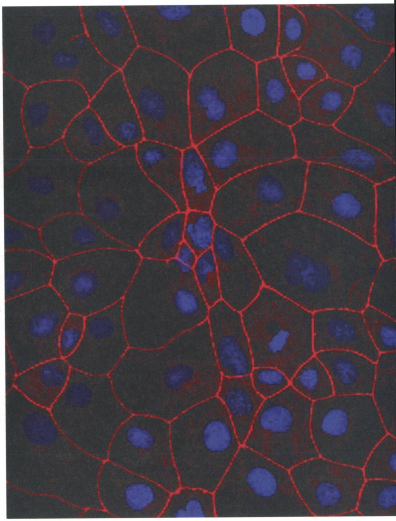

IGM Institute for Genomic Medicine

UC San Diego Health Sciences

nature

IN226557E

SPOTLIGHT ON LATIN AMERICA

Latin America: talent magnet

Unprecedented scientific growth is drawing more scientists south of the U.S. border. And clever schemes to tap into existing global R&D expertise, rather than build it from scratch, is forging new partnerships

"In the last decade, the Latin American and Caribbean region has had the fastest increase in number of scientists and publications."

Mario Albornoz, coordinator of Ricyt

WHEN PHYSICIST Horatiu Nastase accepted a permanent position in São Paulo two years ago, none of his colleagues considered Brazil as a career option. A lot has changed since then. "Now, many more are thinking about coming here," says the Romanian string theorist. The 40-year-old has no plans to leave his research position at São Paulo State University. "I have seen Brazilian science going up since I came here, the opposite of what you see in the U.S. or Japan, where funds are cut and hiring is made difficult," he says. Nastase did his PhD at Stony Brook University in New York, and then worked at Princeton University, and the Tokyo Institute of Technology. "The idea of coming to Brazil doesn't scare scientists anymore," he says.

Nastase is one of many scientists surfing the wave of Latin American R&D growth. "In the last decade, the Latin American and Caribbean region has had the fastest increase in number of scientists and publications," says Mario Albornoz, coordinator of the Ibero-American and Inter-American Network of Science and Technology Indexes (Ricyt), based in Buenos Aires. Between 1999 and 2009, the number of full-time scientific positions in the region rose from 130,000 to 245,000 and publications increased from 27,000 to 62,000 (from 2.73% to 4.36% of the world's total), according to Ricyt's data.

"These trends have been sustained by a rate of increase in science funding second only to that of Asia," explains Albornoz. The amount invested in Latin America R&D has grown from US$10 billion to US$27 billion between 1999 and 2009. Although the investment has spurred growth of R&D capacity, impact through innovation lags. "There are a few success stories, but innovative companies are still not statistically significant," says Albornoz. No Latin American country, with the exception of Chile, appears in the top 50 of the United Nations innovation rankings published in August.

"We are in an excellent economic moment, but our growth is based on low added-value products like oil, food, or mining: our challenge is to make science have an impact on industry," says Glaucius Oliva, president of CNPq, Brazil's national center for scientific and technological development. Brazil invests more in R&D in the region (1.22% of its GDP) and publishes 55% of all Latin American scientific articles, according to 2010 data. However, the government wants scientists to get more involved at the sharp end of innovation.

To help this happen, in 2011 the Brazilian government launched the Science Without Borders program: 100,000 fellowships to be awarded over the next four years to scientists—from undergraduates to full professors. Recipients must go abroad, perform research in strategic technological areas (in companies or in applied research laboratories), and come home to Brazil to apply what they have learned. If they don't return, they must repay the grant. The government and private companies have assigned a total US$2.5 billion to the program. "Petrobras [the state-run oil company] and the Federation of Brazilian Banks, among others, are giving money because they see a big opportunity in the program," says Oliva.

Science Without Borders also features two schemes for attracting foreign talent. For new PhDs, the Young Talents program offers a three-year postdoc in Brazil. For more experienced scientists, the »

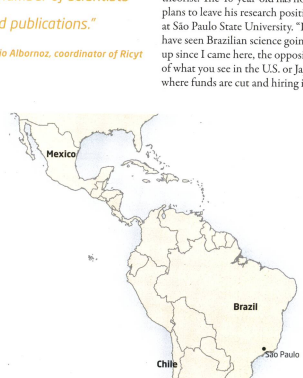

Postdoc and research **opportunities** in Brazil

Fifty percent of all science created in Brazil is produced in the State of São Paulo. The state hosts three of the most important Latin American universities: USP, UNICAMP and UNESP. Other universities and 19 research institutes are also located in São Paulo, among them the renowned Instituto Tecnológico de Aeronáutica (ITA), Instituto Nacional de Pesquisas Espaciais (INPE) and Laboratório Nacional de Luz Síncrotron, besides most of Brazilian Industrial P&D.

The São Paulo Research Foundation (FAPESP), one of the leading Brazilian agencies dedicated to the support of research, has ongoing programs and support mechanisms to bring researchers from abroad to excellence centers in São Paulo.

The **Young Investigators Awards** is part of FAPESP's strategy to strengthen the State research institutions, favoring the creation of new research groups. See more about it at www.fapesp.br/yia.

FAPESP **Post-Doctoral Scholarship** is aimed at distinguished researchers with a recent doctorate degree and a successful research track record. The scholarship enables the development of research within higher education and research institutions in São Paulo. Postdoc scholarships are available when calls for applications are issued internationally, or as individual scholarships requested on demand.

In the first case, positions are advertised at www.fapesp.br/oportunidades/en and candidates are selected through international competition. In the second, the proposal must represent an addition to a pre-existent research group and should be developed in association with faculty in higher education and research institutions in São Paulo. More information at www.fapesp.br/en/postdoc.

FAPESP 50 YEARS

FAPESP

www.fapesp.br/en

NW226836R

Visiting Senior Researcher program places international scientists in Brazilian institutions for two months per year over three years, "In both cases, we offer a packet that includes a very competitive salary, money for research and for students or postdocs, as well as the opportunity to apply for Brazilian grants," says Oliva.

In 1997 the Sao Paulo Research Foundation (FAPESP) created the Young Investigator Awards, grants for excellent senior postdocs, both from Brazil or elsewhere. The organization also sponsors a visiting researcher program for more senior scientists as well as the Sao Paulo Excellence Chair – a funding scheme that targets highly-accomplished foreign scientists and provides salary and research funds for working in Sao Paulo for twelve weeks a year over three to five years, says Carlos Henrique de Brito Cruz, FAPESP scientific director .

While Science Without Borders and FAPESP imports individuals into Latin America, some Latin American countries are bringing in entire institutions.

Conrad von Igel, executive director of InnovaChile, a program of the the Chilean Economic Development Agency (CORFO), explains the notion. "Developed countries have decades of experience in translating science into innovation: doing it from scratch would entail a large amount of risk and resources for us, so instead we want to import that capacity."

Carlos Henrique de Brito Cruz, scientific director, FAPESP - São Paulo Research Foundation

CSIRO and CORFO signing Center of Excellence agreement. From left to right: Hernán Cheyre (Executive Vice President of CORFO), Megan Clark (Chief Executive of CSIRO) and Hernán de Solminihac (Minister of Mining - Chile)

Since 2009, this public organization has attracted four branches of international excellence centers to Chile, matching strategic sectors of the country's economy: CSIRO (Australia) in mining, Wageningen University (Netherlands) in food, INRIA (France)in information and communications technology and Fraunhofer (Germany) in biotechnolgy. A new application round for the program will start in September 2012

"The government will provide a grant of up to US$13 million to each one of these centers for four to eight years depending on the type of center, but they are required to match that grant, eventually by engaging with Chilean companies to raise a part of their financing," explains von Igel. The host institution provides full or part-time scientists. "We are not competing by putting a lot of money on the table: what we offer is a stable political framework and a coherent, long-term commitment to science and innovation," says von Igel. Chile is number one in Latin America in terms of publications per million inhabitants, and it hosts two of the five best universities of the region, according to the QS ranking.

This new call for international R&D centers also reflects a new government focus on corporate R&D as well as institutional efforts. Last January, the Chilean government approved an R&D tax incentive measure that will allow companies to claim a tax credit of 35% on all R&D expenditures and a tax deduction for the remaining 65%. "This means that corporate R&D centers selected for this program – while required to contribute proportionally more resources to the project in the beginning than institutional centers – can effectively make up that difference by claiming this tax incentive," says von Igel.

He adds that these efforts will »

ICTP SAIFR
International Centre for Theoretical Physics South American Institute for Fundamental Research

ICTP-SAIFR is a new South American regional center for theoretical physics in São Paulo created through a collaboration of the International Centre for Theoretical Physics in Trieste (ICTP) with the State University of São Paulo (UNESP) and the São Paulo Research Funding Agency (FAPESP).

In addition to serving as a center of excellence for research, **ICTP-SAIFR** regularly organizes international schools and workshops for PhD students and researchers. Generous fellowships are available for postdocs and visitors, and a search is open for five permanent research professors.

To participate in activities or apply for fellowships and permanent positions, online applications are available on our webpage

www.ictp-saifr.org

NW227244R

Seeking International Centers of Excellence and Corporate R&D Labs

CORFO

CORFO, the Chilean Economic Development Agency, seeks to attract prestigious international R&D centers and corporations to set up applied R&D activities in Chile, offering grants of up to US$12.8 million.

- Top R&D centers from around the world have already taken the leap, including Fraunhofer- Gesellschaft, CSIRO, Inria and Wageningen UR.
- Outstanding corporate R&D Labs as well as institutional R&D Centers are welcome to apply.
- Chile's progressive R&D Tax Incentive in effect pays for close to 50% of out-of-pocket R&D expenditures via a 35% tax credit, with the remaining 65% being tax-deductible.

Why **Chile**

- **Highly Skilled and Competitive Human Resources**
  Close to 3.000 postgraduates returning to Chile from top 150 universities worldwide
  (National Commission on Science and Technology Research - CONICYT)
- **Outstanding Quality of Life**
  #1 in Latin America (UNDP Human Development Index 2011)
- **Globally Integrated**
  Free Trade Agreements with 59 countries provide preferential access to 86% of global GDP

For more information, contact stt@corfo.cl CORFO | Chilean Economic Development Agency

Gobierno de Chile

NW227114R

LANGEBIO
Laboratorio Nacional de Genómica para la Biodiversidad

Cinvestav

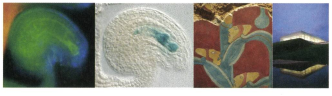

POSTDOCTORAL POSITIONS IN MOLECULAR, DEVELOPMENTAL AND EVOLUTIONARY BIOLOGY. Laboratorio Nacional de Genómica para la Biodiversidad LANGEBIO CINVESTAV Irapuato, MEXICO.

Several postdoctoral positions are available in the Group of Reproductive Development and Apomixis to study: (a) the genetic basis and molecular mechanisms that control gametogenesis and seed formation in plants, with particular emphasis on the epigenetic regulation of sexuality and apomixis; (b) the origin and domestication of maize, with particular emphasis on the genetic and epigenetic organization of its ancient genome.

Highly motivated individuals who recently obtained a PhD and have a strong background in molecular, cellular, and developmental biology, population genetics, or computational biology are encouraged to apply. Interested individuals should send their curriculum vitae, a brief description of their research interests, and the names of three references to:

Dr. Jean-Philippe Vielle-Calzada; Langebio Cinvestav Irapuato, Km 9.6 Libramiento Norte Carretera Irapuato-León Apartado Postal 629 CP36821, Irapuato Guanajuato MEXICO.
Email: avivas@ira.cinvestav.mx.

Deadline: October 14th, 2012.

www.langebio.cinvestav.mx

NW227675R

CIÊNCIA SEM FRONTEIRAS
The Brazilian Scientific Mobility Program

Opportunities for scientists from abroad to conduct projects in Brazil.

Special Visiting Researcher
Researchers recognized internationally as leaders in their areas

Young Talent Attraction
Young researchers who have a highlighted scientific or technological produtivity

Are welcome to apply

www.cienciasemfronteiras.gov.br/web/csf-eng

NW227675R

BRAZILIAN GOVERNMENT
BRASIL

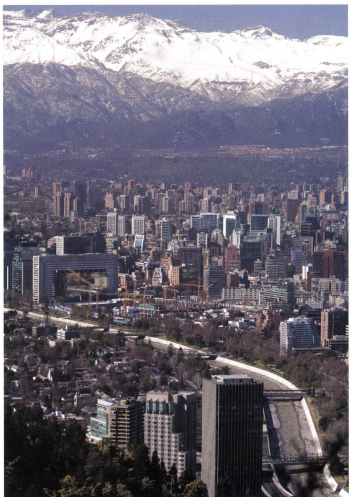

Tax incentives are being used to draw R&D companies to Santiago and Chile – the only Latin American country to make a "Top 50" United Nations list of innovative nations

open opportunities for the best among local and international scientists and says they are making very public their search for candidates. "We have published openings for the excellence centers in top newspapers of the country: it's the first time that a research institution publishes a half page announcement!" he says. "The international R&D centers that have set up operations in Chile have already begun hiring large numbers of highly skilled scientists, which is shaking the local R&D market and opening up opportunities that simply weren't available locally before."

Organizations based outside Latin America are also striving to attract scientific expertise into the region. UNESCO helped establish a branch of the Trieste-Italy-based International Center for Theoretical Physics (ICTP), to Sao Paulo. "Three years ago, ICTP's director Fernando Quevedo decided to open branches around the world, so that scientists don't have to travel all the way to Italy," explains Nathan Berkovits, director of the Sao Paulo branch. The institute remains internationally competitive by offering salaries, recruiting processes and working conditions comparable with equivalent institutions in the U.S., says Berkovits. The center also has reciprocal agreements with the Perimeter Institute in Canada and the CERN in Switzerland to promote cross applications and visits.

Another successful import comes from Germany. The Heidelberg Center, a branch of the Heidelberg University provides an example of how collaboration can prevent "brain drain," explains Walter Eckel, the center's executive director. "Six Chilean professors of psychotherapy, who did their PhD in the seventies in Germany, contacted us when the center opened with the idea of developing a joint doctoral program in their field. The German doctoral students spend some time in Santiago collecting data and the Latin American students go to Heidelberg to attend some seminars and symposia", he says.

The Heidelberg Center is managed by the University of Heidelberg, and funded by student fees and by Germany (in 2009 it won a €2.1 million grant until 2014 from the German government). One third of the staff is from Heidelberg, one third from Chile, and one third is comprised from the rest of Latin America.

"Heidelberg University is the most international of German universities: the Chilean center allows for joint programs and helps attract Latin American doctoral students," Eckel explains. "Latin America was not especially attractive a decade ago, but there has been a shift of focus in the local government which has become more aware of the need to invest in R&D," says Eckel.

All the new centers emerging in Latin America aspire to become hubs of scientific activity. "It is a very uneven area: for example, Brazil, Mexico, Chile and Argentina are much more advanced than other countries," explains Berkovits. "We want to have visitors from less strong countries, and in 2014 we are planning to organize a workshop in Lima," he adds. The Heidelberg center is exporting its expertise through training programs via collaborations with universities in Mexico, Paraguay, Argentina, and Brazil.

Beyond importing institutions and capacity for research, Latin America is striving to create its own reference centers in research. Langebio, the Mexican National Laboratory of Genomics for Biodiversity, in Irapuato, was set up in 2006. Its horizons were on show from the outset with a futuristic building and an impressive frontline infrastructure.

"Mexico is one of the five megadiverse countries in the world: we saw an area of opportunity in exploring the genetics of our national biodiversity," says Jean Philippe Vielle Calzada, a member of the founding group of the institution. Researchers at Langebio have worked on the genomics of plants specific to Mexico: sequencing the "palomero" pop corn (one of the most ancient variant of the crop) and are currently sequencing avocado, the most important "cash crop" for the Mexican economy.

The center is financed by the Federal Government of Mexico, the State Government of Guanajuato, and by international grants. It has 15 groups with plans to double the size within five years. "There are lots of openings," says Vielle Calzada. Six of the current group leaders are from outside Mexico (Holland, UK, Germany, US, and Denmark) and three are Mexican scientists who worked abroad before its opening. "The creation of Langebio and other centers of its generation has driven universities to create degrees that did not exist before, like genomic sciences, systems biology, and biochemical engineering: we are surprised by the capabilities of the new graduates," says Vielle Calzada.

Latin American scientists are enjoying a buoyant period, but they realize further investment is needed for the region's knowledge economy to really come into its own. "The investment in research is still largely insufficient," says Vielle Calzada. Although the increases have been the starting line—the percentage of GDP devoted to research—was small, leaving lots of room for growth. "However, the GDP itself has increased a lot: this is why the percentage does not reflect the large growth in investment," says Ricyt's coordinator Albornoz.

Berkovits, of ICTP in Sao Paulo, outlines areas which hinder R&D development in Latin America: "Poor public schools, lots of bureaucracy, and language requirements to access university positions are barriers that should be overcome." But he urges scientists to look past these obstacles: "The US and EU economies are not doing well, so several countries in Latin America are becoming attractive places to work," says Berkovits. "We think we can show that a scientist can do international-level research here."

Nature editorial staff have no responsibility for content

Research Scientist

Braskem 10 anos

JOB DESCRIPTION

Braskem S.A. is seeking a creative and motivated scientist for a position in the field of Metabolic Engineering with experience in any of the following areas: computational enzyme engineering, , high-throughput assay development and screening, microbial genetics, and/or metabolic pathway design. The candidate should be interested in working in a small and extensively multi-disciplinary team at our Biotechnology Laboratory in Campinas, Brazil. Braskem is an important player in global thermoplastics production with 35 industrial plants, and is the largest producer of thermoplastic resins in the Americas. With Braskem´s commitment to innovation and becoming a world leader in sustainable chemistry Biotechnology plays a key role. Today we are the largest producer of biopolymers in the world and are involved in strategic partnerships with important global biotechnology companies to develop drop-in products from renewable feedstocks such as Brazilian sugarcane.

The successful candidate will play an important role in Braskem´s metabolic engineering programs with opportunities to grow with the company.

At the scientist level, she/he will be responsible for:

1. High-level development of strategies for carbon-flux improvement in microorganism
2. Design and execution of experimental trials and data analysis
3. Management of project goals, timelines, and deliverables
4. Thorough understanding the field and ability to bring recent technologies to the team

JOB REQUIREMENTS

A Ph.D. in life sciences with 1+ years of relevant experience or a M.S./ B.S. in biological sciences with a minimum of 3 years experience in an industrial setting and the ability to work independently are required for this job. Prior research experience in microbial genetic, metabolic or enzyme engineering, computer based enzyme evolution, and/or high-throughput assay design and execution is required. The successful candidate is expected to have strong written and oral communications skills and the ability to adapt to the Brazilian scientific environment. Portuguese is recommended but not required.

Braskem offers competitive benefits and compensation package designed to attract and retain the very best.

For further information about this position and to apply please send your CV and a cover letter to
researchposition@braskem.com.br

NW226835R

UNICAMP

Opportunity for highly qualified scholars at the University of Campinas

The University of Campinas (Unicamp), one of the leading research universities in Latin America, is seeking highly qualified scholars from all over the world to participate in its Visiting Professor Program. This program allows scholars to conduct teaching and research activities at Unicamp for a period from 12 to 24 months, after which they are offered the opportunity to compete for a tenured position at the university. Participants in the program receive an annual fellowship stipend of up to about US$ 74,000, plus an airline ticket to Brazil, health insurance coverage and support for lodging in Campinas, a very pleasant 1-million-inhabitant city located some 100 kilometers from São Paulo. Applicants should be PhD holders with high academic achievement records in one of the fields covered by Unicamp's 22 schools (for a complete list, please visit **www.unicamp.br/unicamp/structure?language=en**.

If you are interested in joining us, please send your CV in English or Portuguese to **carreiras@reitoria.unicamp.br**. For further information, please visit our website at **www.unicamp.br** or send a message to **info.carreiras@reitoria.unicamp.br**.

Brazil is a fast developing country. Be part of the progress. Come work at one of the leading research universities in Latin America.

W228379R

Institut Pasteur de Montevideo

TWO YOUNG GROUP LEADER POSITIONS

The Institut Pasteur de Montevideo (IP Montevideo) is an international scientific institution now seeking young research scientists to lead **two new research groups,** one in bioinformatics and the other in biomedical research, both for a five-year period.

The proposal on bioinformatics will receive institutional funding starting at 80 000 Euros per year, final amount to be negotiated according to the project's requirements and within the budgetary envelope of this program. Group leaders are expected to develop original research in bioinformatics and to provide expertise to different ongoing local projects. Projects within the field of genomics will be considered with particular interest.

The proposal on experimental biomedical research will receive institutional funding starting at 100,000 Euros per year, final amount to be negotiated according to the project's requirements and within the budgetary envelope of this program. Group leaders will be expected to develop original science projects in any biomedical field.

Biologists, biochemists, medical doctors, other graduates in life sciences, chemists, computer scientists, engineers, mathematicians, physicists, etc may apply, provided they obtained their PhD degree within the last 6 years. Previous experience in biomedical research or related technical research is required, as well as an excellent record of publications.

This award is for 5 years. In exceptional cases it could be renewed for a supplementary two-year period.

Deadline for applications: **November 4th, 2012**

Pre-selected candidates will be interviewed by the International Scientific Committee, during February 2013 at the Institut Pasteur de Montevideo.

Additional information at: **http://www.pasteur.edu.uy/internationalcall5**

Supported by ANII (National Agency for Research & Innovation) and UruguayINNOVA (Uruguay - UE)

NW228405R

naturejobs

European Head Office, London naturejobs@nature.com
The Macmillan Building, 4 Crinan Street, London N1 9XW, UK
Tel: +44 (0) 20 7843 4961 Fax: +44 (0) 20 7843 4996

Global Head:
Nils Moeller, +44 (0) 20 7843 4953 n.moeller@nature.com

Southwest UK/RoW:
Emma Hare, +44 (0) 20 7843 4944 e.hare@nature.com

Northeast UK/Ireland:
Matthew Ward, +44 (0) 20 7014 4059 m.ward@nature.com

France/Switzerland/Belgium:
Julie Aramburu, +44 (0) 20 7843 4994 j.aramburu@nature.com

Scandinavia/Spain/Portugal/Italy:
Megan Ball, +44 (0) 20 7843 4973 m.ball@nature.com

North Germany/The Netherlands/Eastern Europe:
Kristin Doelling, +44 (0) 20 7843 4970 k.doelling@nature.com

South Germany/Austria:
Maria Kubalova, +44 (0) 20 7014 4084 m.kubalova@nature.com

Natureevents:
Matthew Clare, +44 (0) 20 7014 4015 m.clare@nature.com

Business Development Manager, Middle East:
Jon Giuliani, +44 (0) 20 7843 4922 j.giuliani@nature.com

USA Head Office, New York naturejobs@us.nature.com
75 Varick Street, 9th Floor, New York, NY 10013-1917
Tel: +1 800 989 7718 Fax: +1 800 989 7103

US Sales Manager:
Ken Finnegan, +1 212 726 9248 k.finnegan@us.nature.com

Japan Head Office, Tokyo
Chiyoda Building, 2-37 Ichigayatamachi, Shinjuku-ku, Tokyo 162-0843
Tel: +81 3 3267 8751 Fax: +81 3 3267 8746

Asia-Pacific Sales & Business Development Manager:
Yuki Fujiwara, +81-3-3267-8765 y.fujiwara@natureasia.com

Business Development Manager, Greater China/Singapore:
Gloria To, +852 2811 7191 g.to@natureasia.com

India
3a, 4th Floor, DLF Corporate Park, Gurgaon, 122 002, India

Advertisement Sales:
Vikas Chawla, +91 1242881057 v.chawla@nature.com

Memorial Sloan-Kettering Cancer Center
The Best Cancer Care. Anywhere.

TENURE TRACK FACULTY POSITION
Cancer Pharmacology or Drug Discovery

Sloan-Kettering Institute is seeking an innovative individual who wishes to address problems of relevance to cancer drug discovery and development for a tenure-track position at the Assistant or Associate Member level with strong research accomplishments in biology, biochemistry or pharmacology. Faculty will be eligible to hold graduate school appointments in the Gerstner Sloan-Kettering Graduate School of Biomedical Sciences, the Weill Graduate School of Medical Sciences of Cornell University, as well as the Tri-Institutional MD/PhD Training Program and Tri-Institutional Training Program in Chemical Biology.

MSKCC offers a unique and exciting research environment with programs in Immunology, Pharmacology, Chemistry, Molecular Biology, Computational Biology, Genetics, Cell Biology, Developmental Biology, Cellular Biochemistry and Structural Biology. The presence of world-renowned clinical programs in cancer research, treatment and prevention offers unique opportunities for creative collaboration.

Applicants should have a PhD and/or MD degree, postdoctoral experience, and dedication to important problems at the interface of biology, biochemistry or chemistry as they relate to cancer pharmacology.

The deadline for applications is **November 1, 2012**. Interested candidates should visit **http://facultysearch.ski.edu** to access the on-line faculty application. Please visit the site as soon as possible, as it contains important information on the required application materials, including deadlines for submission of letters of reference. Inquiries may be sent to **Marie Aiello** at **aiellom@mskcc.org** or to **Dr. David Scheinberg, Chairman, Molecular Pharmacology and Chemistry Program** at **scheinbd@mskcc.org**.

facultysearch.ski.edu

MSKCC is an equal opportunity and affirmative action employer committed to diversity and inclusion in all aspects of recruiting and employment. All qualified individuals are encouraged to apply.

NW228175R

Cancer Science Institute of Singapore

NUS National University of Singapore | CSI

CSI Singapore, National University of Singapore, is a state-of-the-art research center with a multifaceted and coordinated approach to cancer research, extending from basic cancer studies all the way to experimental therapeutics. The focus of the institute is on cancers endemic to Asian populations such as gastric, liver, lung, leukemia and breast cancers. The institute houses a full spectrum of research and clinical translational facilities. This major center is led by a team of world-class scientists with significant government funding from Singapore's National Research Foundation and Ministry of Education.

We are seeking individuals with exceptional scientific credentials to join a vibrant, dynamic team at CSI Singapore.

Principal Investigators

Qualified candidates at Professor, Associate Professor and Assistant Professor levels should be at the cutting edge of their field with an established record of excellence in cancer research.

Candidates should have the capability and experience of leading high-level, innovative research programs resulting in international quality publications. Successful candidates can look forward to stable funding for up to 5 years commensurate with their abilities, ample laboratory space and resources, a competitive salary package and a dynamic working environment. Candidates with research emphasis in gastric, liver and lung cancers will be strongly considered.

Applications should include full curriculum vitae, publication list, information on years of experience in research and laboratory work, and names and contact information (email and telephone numbers) of 3 references.

Professor Daniel G. Tenen
Director, Cancer Science Institute of Singapore (CSI Singapore), NUS
Email: csi_careers@nus.edu.sg
Website: www.csi.nus.edu.sg

Only shortlisted applicants will be notified.

Visit our website at www.csi.nus.edu.sg

JP228274R

Marion Hitchock wants to make the world a better place - for everyone. As a scientist at Bayer, Marion knows she is doing just that. Searching for solutions and never giving up. That is the passion that unites all of us at Bayer. We call it the Bayer Spirit. If you feel it, too, then it is high time we had a chance to talk about a career at Bayer.

Lab Head Cardiovascular Research

Bayer Pharma AG, Wuppertal, Germany

Job description In your new role you will support internal development projects. You are responsible for planning, execution and evaluation of in vivo animal models in rodents especially models for the study of progressive kidney diseases (diabetic, hypertensive and glomerulonephritis-induced nephropathy) and models for the study of kidney disease-induced cardiovascular diseases (anemia, osteopathy, vascular calcification). Moreover, the analyses include biochemical, histopathological and molecularbiological techniques. You will lead and participate in interdisciplinary teams and projects from optimization of substances to pre-clinical studies.

Your qualifications As a graduate in natural science (Biology, Biochemistry, Molecular Biology, Genetics), medical science or pharmacy with a doctorate degree you have already gained experience as postdoctoral fellow. You are interested in the field of experimental chronic kidney diseases and possess in vivo expertise in rodent models of chronic kidney diseases or chronic cardiovascular diseases. You are experienced in leading scientific staff and like to work in interdisciplinary teams. Additionally, you show a proven track record of several years successful scientific working. You are skilled in using MS Office for presentations and publications. Effective communications skills as well as a good command of German and fluent command of English is essential.

Your application We offer a competitive salary in an international environment as well as excellent opportunities for professional and personal development. If your background and personal experience fits this profile, please send us your complete application at www.myBayerjob.de (Reference Code 0000041473), submitting a cover letter, your CV and references.

www.myBayerjob.de **Fon +49 214 30 9 97 79**

W228337R

Memorial Sloan-Kettering Cancer Center

The Best Cancer Care. Anywhere.

FACULTY POSITIONS

Center for Stem Cell Biology & Developmental Biology Program

The Center for Stem Cell Biology (CSCB) and the Developmental Biology Program are seeking innovative individuals who have strong records of research accomplishments in stem cell biology for tenure-track positions at the Assistant Member level (equivalent to Assistant Professor). The CSCB was established to further the interaction of researchers with active stem cell research programs at the Center, to enhance and build novel stem cell related resources and to recruit leading-edge stem cell faculty. The CSCB is interested in research in any aspect of stem cell biology, including the study of stem cells in model organisms, tissue stem cells and the biology and application of human embryonic stem cells or induced pluripotent stem cells. Candidates with a strong interest in applying developmental approaches to studying stem cell biology are particularly encouraged to apply.

Applicants should have a PhD and/or MD degree, a productive postdoctoral experience, dedication to important problems in stem cell biology, and the potential to develop a strong independent program in stem cell research. Successful candidates will be appointed in the Developmental Biology Program and will become a member of the CSCB. Successful candidates are also eligible to hold additional appointments at the Gerstner Sloan-Kettering Graduate School of Biomedical Sciences, the Weill Cornell Graduate School of Medical Sciences, as well as the Tri-Institutional MD/PhD Training Program.

Successful applicants will have access to outstanding resources including expanded state-of-the-art facilities for human pluripotent stem cells, high-throughput chemical and genetic screening, mouse genetics, genomics, flow cytometry, advanced imaging and cancer biology. Memorial Sloan-Kettering offers a unique and exciting multidisciplinary research environment. Faculty in the CSCB participate in the Tri-Institutional stem cell initiative (with Weill Cornell and Rockefeller University) that links stem cell researchers across neighboring institutions.

The deadline for applications is **November 1, 2012**. Interested candidates should visit **facultysearch.ski.edu** to access the on-line faculty application. The site contains important information on the required application materials as well as deadlines for submission of letters of reference.

Inquiries may be sent to **Tiffany Lennon** at **lennont@mskcc.org**; to **Dr. Lorenz Studer, Director CSCB**, at **studerl@mskcc.org**; or to **Dr. Kathryn Anderson, Chair Developmental Biology Program**, at **k-anderson@ski.mskcc.org**.

facultysearch.ski.edu

MSKCC is an equal opportunity and affirmative action employer committed to diversity and inclusion in all aspects of recruiting and employment. All qualified individuals are encouraged to apply.

NW228173R

UCL

UCL Faculty of Life Sciences

Director of Sainsbury Wellcome Centre for Neural Circuits and Behaviour

University College London (UCL), the Gatsby Charitable Foundation, and the Wellcome Trust invite applications for the post of Director of a major new neuroscience centre to be based at UCL: the Sainsbury Wellcome Centre for Neural Circuits and Behaviour. This Centre will address a fundamental challenge in modern biology, determining how neural circuits process information and direct behaviour. Advances in this field will transform understanding of brain function, and ultimately lead to new ways of monitoring and regulating brain activity in health and disease.

The Sainsbury Wellcome Centre will be housed in a new state-of-the-art building embedded at the heart of UCL. It will develop and exploit new approaches for determining anatomical and functional connectivity in neural circuits and for recording, imaging and manipulating activity in genetically defined ensembles of neurons. This experimental work will be tightly integrated with the theoretical and computational neuroscience carried out by the Gatsby Computational Neuroscience Unit which will relocate to the new building in 2014.

The new Centre will comprise 12 research groups (including the Director's) and will conduct a vibrant interdisciplinary research effort, investigating information processing in neural circuits across a range of model systems and behaviours. UCL provides the ideal environment for a new Centre undertaking such a major interdisciplinary effort in neuroscience. The Centre will draw on and catalyse the rich, wide-ranging neuroscience community at UCL, currently ranked 2nd in the world for ISI citations in neuroscience and behaviour. It will also benefit from important strengths in allied fields such as physics, chemistry, engineering, nanotechnology and biomedicine.

The post of Director carries with it a professorial title and the post holder will play a significant role in the strategic development of Neuroscience at UCL. The Director will be responsible for recruiting and nurturing outstanding research groups; and for promoting links between the Centre, UCL, and the wider scientific community. Substantial and long-term resources will be available to support the scientific work of the Director and other researchers in the Centre.

The Director of the Centre will be a visionary leader with an outstanding track record in neuroscience research related to the core mission of the Centre and with substantial experience of scientific strategy and management.

The appointment will be full time and the salary is negotiable on the professorial scale, but not less than £62,110 per annum, inclusive of London Allowance. A relocation package will be available in addition. The appointment is available from Summer 2013.

For further details about the vacancy and how to apply online please go to http://www.ucl.ac.uk/hr/jobs/ and search on Reference Number 1275837.

If you have any queries regarding the application process, please contact Nick McGhee on n.mcghee@ucl.ac.uk, tel +44 (0)20 7679 8878. If you wish to discuss the post informally, please contact Professor Sir John Tooke on j.tooke@ucl.ac.uk, tel +44 (0)20 7679 0878.

Closing Date: Monday 15th October 2012.

We particularly welcome female applicants and those from an ethnic minority, as they are under-represented within UCL at this level.

Supported by wellcome trust

GATSBY

U228369R

EMBL

The European Molecular Biology Laboratory is searching for Team and Group Leaders. EMBL offers a highly collaborative, uniquely international culture. It fosters top quality, interdisciplinary research by promoting a vibrant environment consisting of young, independent researchers with access to outstanding graduate students and postdoctoral fellows. EMBL is an inclusive, equal opportunity employer offering attractive conditions and benefits appropriate to an international research organisation.

Team and Group Leader Opportunities

at EMBL Heidelberg, Germany

TEAM / GROUP LEADER

COMPUTATIONAL BIOLOGY / BIOINFORMATICS

EMBL's headquarters in Heidelberg host four research units: Cell Biology and Biophysics, Developmental Biology, Genome Biology as well as Structural and Computational Biology. Bioinformatics activities are integral to the interdisciplinary research activities at EMBL and thus we seek to recruit an outstanding Group or Team Leader, working in the broad area of computational biology and bioinformatics, who would utilise the highly interdisciplinary and collaborative environment at EMBL Heidelberg.

Our search for candidates is deliberately broad and comprises all areas of computational biology that are complementary and synergistic to existing research activities at EMBL Heidelberg. Possible research areas comprise but are not limited to structural bioinformatics (e.g. modelling of protein complexes and their interactions and/or dynamics in a cellular context), image analysis/visualisation (e.g. reading out data from GFP screens, E-tomograms or visualising a virtual cell atlas), cheminformatics (e.g. chemical-protein-network analysis), systems bioinformatics (e.g. tissue modelling, analysis network perturbations) or transcriptional regulation/epigenetics (e.g. chromatin modification analysis).

We are open to applications from candidates who wish to focus entirely on their own research projects and, because there is an increasing need to integrate and streamline the multiple computational approaches followed within EMBL, to candidates who wish to function at the interface between research and service activities. The successful candidate should demonstrate a strong motivation to work in the multidisciplinary and collaborative environment of EMBL, reaching out to the many other computational and experimental groups.

For further information about this position please contact **recruitment@embl.org**.

Interviews are planned for 6 and 7 December 2012.

GROUP LEADER

GENOME BIOLOGY

The Genome Biology Unit studies the molecular mechanisms by which genetic information is expressed and regulated to yield complex biological systems, and how genetic variation leads to phenotypic diversity. The Unit addresses questions at different scales, ranging from detailed mechanistic studies (using genetics, chemistry, biochemistry and microfluidics) to genome-wide studies (using functional genomic, proteomic and computational approaches). This powerful combination enables the unit to dissect and model complex processes going from genotype to phenotype.

This group leader position provides a very competitive package to support an independent research group in an excellent scientific and highly collaborative environment. We particularly encourage candidates applying a systems biology approach to understanding specific aspects of gene expression regulation, evolution, metabolomics, stem cell biology or genomic applications to health to apply, but welcome candidates with demonstrated excellence in any area of genome biology.

Further information about the position can be obtained from the Joint Heads of Unit Eileen Furlong (**eileen.furlong@embl.de**) or Lars Steinmetz (**lars.steinmetz@embl.de**).

Interviews are planned for 28, 29 and 30 November 2012.

APPLICATION INSTRUCTIONS

Please apply online through **www.embl.org/jobs** and include a cover letter, CV and a concise description of research interests and future research plans. Please also arrange for 3 letters of recommendation to be emailed to **references@embl.de** at the latest by 21 October 2012.

Further information on Team/Group Leader appointments can be found under **www.embl.org/gl_faq**.

For more information please visit:

www.embl.org

W22833?R

EINSTEIN

Albert Einstein College of Medicine
OF YESHIVA UNIVERSITY

Chair
Dominick P. Purpura Department of Neuroscience

The Albert Einstein College of Medicine invites applications and nominations for the position of Chair of the Dominick P. Purpura Department of Neuroscience. We seek an outstanding scientist with leadership experience and a broad vision for Neuroscience, for appointment as Professor and holder of an endowed chair.

Einstein offers a supportive research environment with numerous, well-equipped core facilities (http://www.einstein.yu.edu/home). Einstein is one of the nation's premier research-intensive medical schools, with a full-time faculty of 2,585 physicians and scientists, 759 MD students, 339 PhD students, 117 MD/PhD students, and 395 Postdoctoral fellows. Einstein has NIH funded research centers in Human Embryonic Stem Cells, Aging, AIDS, Cancer, Diabetes, Obesity, Health Disparities, Intellectual and Developmental Disabilities and Liver Diseases.

The Department of Neuroscience http://www.einstein.yu.edu/departments/neuroscience/ at Einstein offers an interactive, translational and diverse environment, including outstanding and well-funded scientists in the fields of cognitive, behavioral, physiological and cellular and molecular neuroscience. The Department of Neuroscience consists of 27 Primary Faculty, 30 Secondary Faculty, 26 post docs, 32 graduate students and 7 MSTP students. It is housed entirely within the 9 floors of the Rose F. Kennedy Research Building and has close interactions with the departments of Neurology and Psychiatry. It has 12,000 square feet of available laboratory space for new faculty recruitments. The College has made the recruitment of the Chair a primary goal and has committed substantial resources for recruitment and research support.

Please submit a letter and curriculum vitae in electronic format to Dr. Robert H. Singer, Chair, Dominick P. Purpura Department of Neuroscience Search Committee, Albert Einstein College of Medicine, Jack and Pearl Resnick Campus, 1300 Morris Park Avenue, 601-Golding, Bronx, NY. 10461. E-mail: Robert.singer@einstein.yu.edu.

We particularly welcome applicants who will add diversity to our academic leadership and faculty. Equal Opportunity Employer.

NW228448R

Tufts
UNIVERSITY

TUFTS UNIVERSITY
DEPARMENT OF CHEMISTRY

The Department of Chemistry is in the midst of a multi-year expansion.

Applications are invited for multiple positions at the assistant professor level with research interests at the interface of chemistry and life sciences, broadly defined. All areas of chemistry at this interface will be considered. Excellent resources are available for new research programs in the Life Sciences—one of the university's strengths. Teaching responsibilities will include graduate and undergraduate courses in chemistry and biochemistry, and may include biophysical, bioanalytical, bioinorganic, chemical biology, and bioinformatics. Successful candidates must demonstrate the potential to develop an internationally recognized research program and excel in teaching. The Chemistry Department at Tufts is a well-funded, thriving community of researchers with collaborations across the university and the greater Boston area. Additional information about the department can be found at http://chem.tufts.edu. **Applicants should submit a CV, a research plan, and three letters of recommendation via https://academicjobsonline.org/ajo/jobs/1748.**

Alternatively, these materials may be sent to Faculty Search Committee, Department of Chemistry, Tufts University, Medford, MA 02155.

Evaluation of candidates will begin October 10, 2012 and continue until the position(s) are filled. Tufts University is an Affirmative Action/Equal Opportunity employer.

We are committed to increasing the diversity of our faculty. Applications from women and members of underrepresented groups are strongly encouraged.

NW228325R

UMDNJ ROBERT WOOD JOHNSON MEDICAL SCHOOL
University of Medicine & Dentistry of New Jersey

The Cancer Institute of New Jersey™
Bringing research to life.

NCI CCC
A Comprehensive Cancer Center Designated by the National Cancer Institute

Cancer Research Faculty Positions

The Cancer Institute of New Jersey (CINJ) invites applications for tenure-track faculty positions specializing in cancer progression, genetic instability, metastasis, genetics, metabolism, signaling or microenvironment. Exceptional senior investigators will also be considered. CINJ is an NCI-designated, comprehensive and consortium cancer center that includes faculty members from UMDNJ-Robert Wood Johnson Medical School, Rutgers and Princeton Universities.

New faculty are expected to establish an innovative, independent and collaborative research program addressing important, fundamental questions in the area of cancer biology. Interdisciplinary approaches are encouraged and the combined CINJ consortium faculty has complementary expertise and strength in cancer biology, signal transduction, systems biology, metabolism, and genomic instability. Qualified candidates must have a Ph.D. and/or M.D., or equivalent graduate degree, and outstanding academic credentials. We seek candidates who are independent investigators interested in collaboration with basic scientists and with clinical faculty for translational research. Rank will be commensurate with experience.

Interested applicants should send their CV, a brief description of their research interests and plans, and the names of three references via email to **cinjrecruitment@gmail.com** or mail to: **Search Committee, c/o Larissa Varela, Faculty Recruitment Office, Cancer Institute of New Jersey, 120 Albany St, Tower 2, 5th Floor, New Brunswick, NJ 08901**.

CINJ website http://www.cinj.org/

UMDNJ is an EEO/AA employer, m/f/h/v, and a member of the University Health System of New Jersey.

NW227752RL

2013 Izaak Walton Killam Postdoctoral Fellowships

Izaak Walton Killam Postdoctoral Fellowships (KPDF) in most fields of study are tenable for up to two years at Dalhousie University, located in Halifax, Nova Scotia, Canada. KPDFs are valued at $44,000 CDN per year plus travel allowance, a one-time $3,000 research grant, and a $1,000 conference travel grant. Applicants must have recently completed a PhD (Jan 2011 or later) at a recognised university and have no current affiliation with Dalhousie University. Applications must be submitted no later than 17-Dec-12. Full details available at:

dalgrad.dal.ca/kpdf

DALHOUSIE UNIVERSITY
Inspiring Minds

Save time!
Save your searches on **naturejobs.com** as a Job Alert email or RSS feed

nature jobs
making science work

Imperial College London

Imperial College Healthcare NHS Trust

Grow with a leading, internationally-recognised centre of excellence for neuroscience and mental health

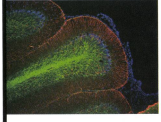

Imperial College London is making a substantial investment in a new Division of Brain Sciences. We are extending a search that is expected to lead to more than a dozen new full staff appointments within its Centres for Neuroscience, Neuropsychopharmacology and Mental Health. We will enhance existing strengths to develop a world-leading portfolio of experimental and translational neuroscience/ mental health in collaboration with the Imperial College Academic Health Sciences Centre.

Imperial College London provides an outstanding multidisciplinary environment for basic, clinical and translational research. The Division has substantial research facilities including recently constructed laboratory space at the Hammersmith Hospital and will build on unique resources of its strong patient base (with significant research network support), the embedded Multiple Sclerosis Society and Parkinson's UK Tissue Banks, the new Wellcome Trust McMichael Clinical Research Facility, clinical and preclinical MRI and PET and the co-localised Imanova Ltd, one of Europe's most modern and comprehensive PET molecular imaging centres.

The Division will work closely with the Neurosciences Faculty across the College to develop research particularly in areas of:

- Neuroinflammation and neurodegeneration
- Restorative neurology
- Affective and related disorders
- Biology of addiction
- Radiochemistry and molecular neuroimaging

The new Division provides a unique career opportunity for individuals with the vision, leadership ability and ambition to be among the best. The level of appointment (Professor, Reader, Senior Lecturer or Lecturer) and a generous support package will be determined according to experience with a focus on long-term career development and success within the College. Applications are particularly (but not exclusively) encouraged from outstanding clinical or non-clinical scientists with expertise in stroke and the neurology of traumatic brain injury, neuroprotection and brain repair, neuroimmunology, the neurobiology of affective disorders and addiction, dementia, neuroimaging chemistry and neurotechnology.

Informal enquiries can be made to the new Head of Division, Professor Paul Matthews (E-mail: p.matthews@imperial.ac.uk). Applications, including a letter describing research and career objectives and a full curriculum vitae should be sent to Alice Ashley-Smith (0208 383 3299; e-mail: a.ashley-smith@imperial.ac.uk) on or before 30 November 2012.

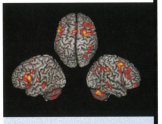

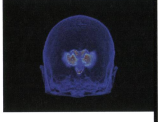

Committed to equality and valuing diversity. We are also an Athena Bronze SWAN Award winner, a Stonewall Diversity Champion and a Two Ticks Employer.

Stonewall DIVERSITY CHAMPION

U208464R

Want the best of the global market?

Make nature jobs making science work your first choice.

The University of Edinburgh

The University of Edinburgh is an exciting, vibrant, research led academic community offering opportunities to work with leading international academics whose visions are shaping tomorrow's world.

College of Science and Engineering
School of Biological Sciences

Chair of Stem Cell Biology and Associate Director of The Centre for Regenerative Medicine

Salary Scale: On the Professorial range

Applications are invited from innovative researchers of international standing for the Chair of Stem Cell Biology in the Centre for Regenerative Medicine (CRM). You will have a strong track record of international-quality publications and research funding in stem cell biology, and the vision and leadership skills to promote the development of basic and translational research programmes and form effective partnerships with colleagues from a wide range of scientific disciplines. You will have the ability to attract leading researchers and excellent students to CRM, and will contribute to the development and delivery of high-quality undergraduate and postgraduate teaching.

The mission of CRM is to study stem cells, disease and tissue repair to advance human health. The Centre comprises research groups from the School of Biological Sciences and the College of Medicine and Veterinary Medicine, co-located in a new £54M purpose-built research building. CRM has a world-leading integrated programme of research in the molecular, cellular, developmental and translational biology of stem cells. The new Chair will play a key role in shaping and leading the long-term research strategy of this exciting initiative.

The University of Edinburgh is an exciting, vibrant, research-led academic community offering opportunities to work with leading academics whose visions are shaping tomorrow's world. The University of Edinburgh aims to ensure equality of opportunity and holds an Athena Swan bronze award.

Apply online, view further details or browse more jobs at our website. Alternatively, telephone the recruitment line on 0131 650 2511. Ref: 3016254N. Closing date: 22 October 2012.

Committed to Equality and Diversity

The University of Edinburgh is a charitable body, registered in Scotland, with registration number SC005336.

www.jobs.ed.ac.uk

U228466R

National Socio-Enviromental Synthesis Center
Postdoctoral Fellowship Program

Applications due November 1, 2012
Please visit
www.sesync.org/programs/postdocs

NW228368R

You don't have to look this hard to find a job with Nature.jobs.

nature jobs
making science work

UNIVERSITY OF OXFORD

www.ox.ac.uk/jobs

University Lectureship in Biochemistry, Structural Biology and Biophysics –

in association with a Tutorial Fellowship at Lincoln College

Salary £42,883 - £57,581 per annum

Department of Biochemistry

Applications are invited for a University Lectureship in Biochemistry in the area of Structural Biology and Biophysics. This position would be held within the Department of Biochemistry, University of Oxford, leading to a permanent academic post upon the successful completion of a probationary period. A Tutorial Fellowship at Lincoln College is attached to this position.

The successful applicant will join a team of structural biologists and biophysicists which forms a key element of research within the new Biochemistry Building. The principal duty will be to establish and lead a world-class research programme in the area of experimental structural biology and/or biophysics of membrane proteins and related systems. The successful applicant will have, or show promise of, an international reputation for research and scholarship, and will contribute to and benefit from a full role in the academic life of the Biochemistry Department and of Lincoln College. He/she will be able to demonstrate the ability to teach high-achieving and challenging undergraduates and graduate students.

Please see the further particulars on the website at **http://www.admin.ox.ac.uk/fp** for more details about the post and for full instructions before making an application. For an informal discussion, please contact Professor Mark Sansom, David Phillips Professor of Molecular Biophysics and Head of Department, on: (01865) 613 212 or head@bioch.ox.ac.uk Applications should be sent by email to academicrecruitment@bioch.ox.ac.uk by 12 noon on Friday 12 October 2012.

Applications are particularly welcome from women and ethnic minorities, who are under-represented in academic posts in Oxford.

Committed to equality and valuing diversity

NW228456R

UNIVERSITY OF OXFORD

www.ox.ac.uk/jobs

University Lectureship in Biochemistry, Membrane Protein Crystallography –

in association with an Official Studentship at Christ Church

Salary £42,883 - £57,581 per annum

Department of Biochemistry

Applications are invited for a University Lectureship in Biochemistry in the area of Membrane Protein Crystallography. This position would be held within the Department of Biochemistry, University of Oxford, leading to a permanent academic post upon the successful completion of a probationary period. An Official Studentship (i.e. a tutorial fellowship) at Christ Church is attached to this position.

The successful applicant will join a team of structural biologists and biophysicists which forms a key element of research within the new Biochemistry Building. The principal duty will be to establish and lead a world-class research programme in the area of structural biology as applied to membrane proteins. The successful applicant will have, or show promise of, an international reputation for research and scholarship, and will contribute to and benefit from a full role in the academic life of the Biochemistry Department and of Christ Church. He/she will be able to demonstrate the ability to teach high-achieving and challenging undergraduates and graduate students.

Please see the further particulars on the website at **http://www.admin.ox.ac.uk/fp** for more details about the post and for full instructions before making an application. For an informal discussion, please contact Professor Mark Sansom, David Phillips Professor of Molecular Biophysics and Head of Department, on: (01865) 613212 or head@bioch.ox.ac.uk. Applications should be sent by email to academicrecruitment@bioch.ox.ac.uk by 12 noon on Friday 12 October 2012.

Applications are particularly welcome from women and ethnic minorities, who are under-represented in academic posts in Oxford.

Committed to equality and valuing diversity

U228457R

WWW.NIH.GOV
Positions@NIH
THE NATIONAL INSTITUTES OF HEALTH

The NIH Intramural Research Program is Recruiting Tenure-Track "Earl Stadtman Investigators"

The National Institutes of Health, the U.S. government's premier biomedical and behavioral research enterprise, is pleased to announce its fourth annual call for "NIH Earl Stadtman Investigators." Scientific discoveries from our intramural laboratories, with their extensive infrastructure and critical mass of expertise, have a crucial role in both maintaining America's research excellence and advancing medical treatments and cures.

Come join the team whose hallmarks are stable funding, intellectual freedom, shared resources, and access to a broad range of scientific expertise. We seek creative and independent thinkers eager to take on high-risk, high-impact research in tenure-track positions.

A variety of basic and translational/clinical positions are available, with areas of active recruitment including (but not limited to): Biostatistics/Bioinformatics; Chromatin Biology/Epigenetics; DNA Replication, Repair and Recombination; Molecular Epidemiology and Population Genetics; Molecular Immunology; Molecular Pharmacology and Toxicology; Neuroscience; Population Science; Stem Cells/iPS Cells; Structural Biology and Systems Biology; and Virology.

*****

Who we are: Among our approximately 1,200 principal investigators and 4,000 trainees are world-renowned experts in basic, translational and clinical research. Our strength is our diversity in pursuit of a common goal, to alleviate human suffering from disease. Similar to academia, we offer our scientists the opportunity to mentor outstanding trainees at all levels (e.g., graduate students and postdoctoral fellows) in a research setting.

Whom we seek: For this broad, trans-NIH recruitment effort, we seek talented, early-career scientists with a clear and creative research vision who wish to contribute to the nation's health.

Qualifications/eligibility: Candidates must have an **M.D., Ph.D., D.D.S./D.M.D., D.V.M, D.O., R.N./Ph.D.**, or equivalent doctoral degree and have an outstanding record of research accomplishments as evidenced by publications in major peer-reviewed journals. Applicants may be in early stages of their research careers or non-tenured early-to-mid career scientists. Appointees may be U.S. citizens, resident aliens, or non-resident aliens with, or eligible to obtain, a valid employment-authorization visa.

How to apply: Applicants must submit a CV, a three-page research plan, a one-page description of their vision for future research and its potential impact, and contact information for three professional references through our online application system at http://irp.nih.gov/stadtman between August 1 and October 1, 2012. You will be asked to designate a primary and secondary scientific area of expertise to aid in assigning your application to the appropriate review committee. Requests for letters of recommendation will be sent to your references when you submit your application. Reference letters will be accepted via upload to the website until 11:59 p.m. EDT October 15, 2012. We cannot accept paper applications.

What to expect: Search committees of subject-matter experts will review and evaluate applicants based on the following criteria: publication record, scientific vision and potential scientific impact of current and proposed research, demonstrated independence, awards and references. The committees will identify the most highly qualified candidates to invite to the NIH for a lecture in November or December 2012, which will be open to the NIH scientific staff, and for subsequent interviews with the search committees. The search committee chairs and NIH Scientific Directors, who lead our intramural programs, will identify finalists to be recruited as Earl Stadtman Investigators. Candidates not selected as Stadtman finalists can still be considered for other open NIH research positions. The entire process from application review to job offer may take several months, depending on the volume of applications.

****

We call upon individuals who will open our eyes to possibilities we haven't yet envisioned, to complement our scientific mission and enhance our research efforts. More information about our program is at http://irp.nih.gov. The inspiring story of Earl and Thressa Stadtman's research at the NIH is at http://history.nih.gov/exhibits/stadtman. Specific questions regarding this recruitment effort may be directed to Dr. Roland Owens, Assistant Director, NIH Office of Intramural Research, at owensrol@mail.nih.gov. DHHS and NIH are Equal Opportunity Employers.

NCCR TransCure
Excellence in Membrane Transport Research

u b
b UNIVERSITÄT BERN

Assistant Professor tenure-track – in *vivo* cancer pharmacology – University of Bern, Switzerland

The Medical Faculty of the University of Bern is accepting applications for a faculty position at the level of tenure-track Assistant Professor. We are looking for a candidate who has outstanding records of achievement and interest in the following areas:

1. Cancer biology (i.e. biology of prostate, breast and colon cancer)
2. Use of in *vivo* cancer models to validate cancer targets; in-depth experience with xenograft models
3. Experience with preclinical drug development, pharmacokinetics, ADME profiling and toxicology studies
4. Focus on transporters and ion channels as therapeutic targets
5. Teaching experience, preferably in German

The successful candidate will be an integral member of the Swiss National Center of Competence in Research called NCCR TransCure (Principal investigator Matthias A. Hediger; see: http://www.transcure.ch. TransCure is a multidisciplinary team of Swiss experts that is focused on developing therapeutic strategies for major human diseases such as cancer, diabetes, heart diseases and neurological diseases, based on scientific breakthroughs in the field of transporter and ion channel biology. He/she will provide expertise in cancer biology, experimental pharmacology and preclinical drug development to move forward the development of therapeutic lead compounds emerging from existing TransCure projects. As part of this effort, the candidate will establish an independent and internationally competitive research program which is well aligned with the focus of the NCCR TransCure. A well-documented record of independent and innovative research is a prerequisite, including significant publications in high impact journals. However, specific experience in transport or membrane biology is not required. In addition, he/she will participate in teaching medicinal physiology, cell biology, pharmacology and biochemistry to students of medicine, veterinary medicine and pharmacy.

The University of Bern is an equal opportunity employer. Women are particularly encouraged to apply in accordance with the NCCR›s initiative to support women in science.

The application documents including a letter of intent, resume, publications, funding, a short outline of planned research, and names of 3 references should be submitted electronically to the office of the Dean (bewerbungen@meddek.unibe.ch).The application deadline is October 15, 2012. For more information, please contact the Chairman of the Search Committee, Prof. Peter M. Villiger, Head, Department of Rheumatology, Clinical Immunology & Allergology, Inselspital, CH-3010 Bern, Switzerland. E-mail: peter.villiger@insel.ch.

The Dean's Office, Faculty of Medicine, University of Bern, Murtenstrasse 11, CH-3010 Bern, Switzerland

W228388R

naturejobs
Scientists stay informed of the latest:
• Hot jobs
• Career news
• Announcements
Sign-up to our FREE jobseeker newsletter:
www.naturejobs.com/newsletter

nature

the international weekly journal of science seeks to appoint a

Microbiology Editor

Nature, the international weekly journal of science, seeks to appoint a Microbiology Editor to join a team dedicated to publishing the world's best original research in the biological sciences.

The successful candidate will play a key role in determining how biological sciences are represented - through the selection and preparation of manuscripts for publication and by acting as Nature's interface with the relevant research communities. This is a demanding and intellectually stimulating position, and calls for a keen interest in the practice and communication of science.

The ideal candidate will have a strong track record of research in microbiology including medical and environmental microbiology but highly qualified candidates from other areas of the biological sciences are also encouraged to apply. Applicants should hold or expect shortly to receive a PhD or equivalent degree.

This position can potentially be based in either one of Nature's US offices or in London and may involve international travel to meetings and laboratories.

Please apply by uploading your CV, covering letter (including your class of degree, a brief account of your research and other relevant experience, and details of your current salary) and a concise discussion of recent scientific developments which you have found particularly exciting (stating why).

Please apply via http://jobs.macmillan.com/
job reference NPG/094/12.

CLOSING DATE: 24th of September

nature publishing group npg

IN228306R

"When trying to recruit good scientists for such a remote institutions like ours, in the Canary Is., the high visibility and wide-range exposure that Naturejobs provides has been crucial. I'm very happy to have international candidates who applied to our position from places ranging between St. Petersburg and Cincinnati. Thanks a lot!"

Eduardo Salido, MD, PhD,
Hospital Universitario de Canarias

naturejobs

Careers@Singapore: Research & Academia
17 – 21 September 2012
United Kingdom

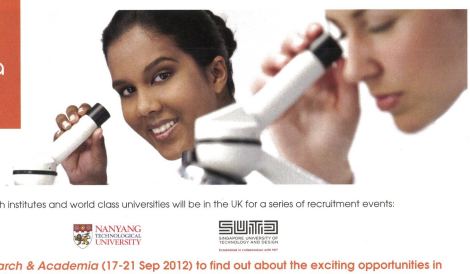

Contact Singapore and Singapore's top research institutes and world class universities will be in the UK for a series of recruitment events:

Institute of Chemical and Engineering Sciences A*STAR

NANYANG TECHNOLOGICAL UNIVERSITY

SINGAPORE UNIVERSITY OF TECHNOLOGY AND DESIGN
Established in collaboration with MIT

Sign-up for *Careers@Singapore: Research & Academia* (17-21 Sep 2012) to find out about the exciting opportunities in Research & Academia in Singapore: www.contactsingapore.sg/CareersSG/Research_Academia/Sep2012

Date	Time	Venue
Mon, 17 Sep	1230 - 1400	University of Warwick, Coventry
Tue, 18 Sep	1300 - 1430	University of Cambridge, Cambridge
Wed, 19 Sep	1300 - 1430	University of Oxford, Oxford
Wed, 19 Sep	1830 - 2000	Institute of Physics, London
Thu, 20 Sep	0900 - 1700	Naturejobs Career Expo 2012, London
Fri, 21 Sep	1800 – 2000	Holiday Inn Kensington Forum, London

Not able to meet us in person? Join us at our upcoming **Contact Singapore Virtual Career Fair for Research and Academia on 12 and 13 October 2012**. Visit **www.contactsingapore.sg/Research/VCF/Oct2012** to find out more about the event.

Contact Singapore

Contact Singapore engages overseas Singaporeans and global talent to work, invest and live in Singapore. We actively link Singapore-based employers with professionals to support the growth of our key industries.

Website: **www.contactsingapore.sg** | Job portal: **www.contactsingapore.sg/jobs** | For enquiries, email: **london@contactsingapore.sg**

Contact Singapore
contactsingapore.sg

U227290R

UNC
SCHOOL OF MEDICINE

CHAIR, DEPARTMENT OF CELL BIOLOGY AND PHYSIOLOGY

THE SCHOOL OF MEDICINE AT THE UNIVERSITY OF NORTH CAROLINA AT CHAPEL HILL is searching for an outstanding individual to provide academic and administrative leadership for the research and teaching programs of the newly formed Department of Cell Biology and Physiology. Research interests of current faculty include cardiovascular biology, neurobiology, endocrinology, cell shape motility and adhesion, imaging technology, cytoskeleton, membrane trafficking, cell polarity, protein quality control, and GI, renal and respiratory physiology. The department has outstanding facilities and collaborative relationships with other basic research and clinical departments, research centers, and institutes within the University and maintains strong ties to other academic and industrial institutions in the Research Triangle. The minimum educational requirement for this position includes a Ph.D. and/or M.D. degree in a related field. The successful candidate will have a distinguished record of scientific research and extramural funding and demonstrate outstanding skills in leadership and administration.

The Search Committee will begin reviewing candidates immediately and continue until the position is filled. Interested applicants should submit an online application at http://unc.peopleadmin.com/postings/7359 to include their detailed curriculum vitae, description of administrative experience, research goals and teaching interests.

Women and members of under-represented minority groups are especially encouraged to apply.

Questions related to this search may be emailed to the search administrator, Dede Corvinus <dede_corvinus@med.unc.edu> .

University of North Carolina is an Equal Opportunity Employer.

NW228251R

National Institute of Chemistry
Ljubljana / Slovenia / EU Member State
http://www.ki.si/

In accordance with Articles 25 and 26 of the National Institute of Chemistry Statute, the Board of Governors of the National Institute of Chemistry, Hajdrihova 19, Ljubljana, hereby announces a

PUBLIC TENDER
FOR THE APPOINTMENT OF A DIRECTOR
OF THE NATIONAL INSTITUTE OF CHEMISTRY

Candidates for the position of Director must meet the following conditions* :

- a PhD in one of the fields of activity of the Institute,
- internationally comparable research or technological/development results in the last five years,
- organisational and leadership skills.

Director will be appointed by the Board of Governors, with the consent of the Government of the Republic of Slovenia exercising its rights as founder. The Director is the organisational and professional leader of the public research institute with a five-year mandate starting on 19 April 2013.

Candidates should send their applications by and including **28 September 2012** to the following address: Kemijski inštitut, Hajdrihova 19, 1001 Ljubljana, Slovenia. Applications must be in sealed envelopes marked "For the advertised position of Director". Candidates must enclose evidence of compliance with the conditions of this tender (proof of the type and level of education, a CV stating previous experience and a bibliography) and a work and management programme for the Institute.

Candidates will be notified of the selection results within 30 days of the date the public tender was announced.

Candidates will be invited to give oral presentations at the session of the Scientific Council of the National Institute of Chemistry taking place on 8 October 2012 at 9.00 and at the session of the Board of Governors of the National Institute of Chemistry on 11 October 2012 at 15.00.

Information on the tender and the relevant information material are available in the main office of the Institute, tel. +386 1 4760 444.

**The criteria for determining compliance with the conditions are prescribed by the Rules on Criteria for the Evaluation of the Qualifications of Project Leaders (http://www.arrs.gov.si/sl/akti/prev-kriteriji-vodje-p-ckr11.asp).*

W228456R

UNIVERSITY OF OXFORD

www.ox.ac.uk/jobs

x6 Career Development Fellows

Fixed term 3x 5 years, 1x 4 years, 2x 3 years

stem BANCC
Stem Cells for Drug Discovery

All Grade 7: £29,249 - £35,983

Applications are invited to join the newly established StemBANCC programme at Oxford, funded by the Innovative Medicine Initiative (IMI). StemBANCC is a 5-year interdisciplinary programme involving academic and industry partners across 11 countries with the objective of developing human induced pluripotent stem cells as a platform for drug discovery. Led by the University of Oxford, this ambitious project brings together internationally renowned scientists and clinicians to study and develop new therapies for some of the major diseases of our time: Alzheimer's, Parkinson's, Autism, Schizophrenia, Bipolar, Migraine, Pain and Diabetes. With our European academic and industry partners, we will create a world-class research programme to improve stem cell models of disease and undertake extensive molecular and cellular characterization.

We are seeking outstanding individuals with a strong track record to join the Oxford StemBANCC programme. We have 6 career development fellow positions and three further researcher positions.

Small molecules for iPS line expansion and differentiation: One Career Development Fellow, 5 years; Dr Angela Russell and Professor Steve Davies.
Genome Engineering iPS Lines: Two Career Development Fellows, 5 years and 3 years; Dr Sally Cowley, Professor William James and Dr Richard Wade-Martins.

iPS cell-derived dopaminergic neuronal models of Parkinson's Disease One Career Development Fellow, 3 years; Dr Richard Wade-Martins.

Developing better iPS cellular models for neurological disorders One Career Development Fellow, 5 years; Dr Zameel Cader.

iPS cell-derived sensory neuronal models of neuropathic pain One Career Development Fellow, 4 years; Dr David Bennett.

Further information about StemBANCC may be found at:
Informal enquiries may be directed to the StemBANCC Academic Coordinator, Dr Zameel Cader on zameel.cader@dpag.ox.ac.uk or the relevant laboratory heads.

The closing date for applications is: Midday, Friday 5th October 2012.

Interviews will be held as soon as possible thereafter.

Applications for this vacancy are to be made online.

To apply for this role and for further details, including the job description and selection criteria, please visit **https://www.recruit.ox.ac.uk** and search using keywords 'StemBANCC' or alternatively visit **www.stembancc.org**

Committed to equality and valuing diversity

U228460R

nature materials

Associate Editor

Nature Materials is a prestigious international monthly journal (Impact Factor 32.841) covering all aspects of materials science and technology. We have an exciting opportunity available for a materials scientist to join our editorial team as an Associate Editor working on all aspects of the journal.

We are particularly interested in applicants with expertise in condensed matter physics but we would welcome applications from outstanding candidates in any area of materials science.

The ideal candidate should have a PhD and preferably postdoctoral experience with a strong research record. The successful candidate will play an important role in determining the representation of their field in the journal, and will work closely with the other editors on all aspects of the editorial process, including manuscript selection, commissioning and editing of Reviews and News & Views, and writing for the journal. A key aspect of the job is liaising with the scientific community through laboratory visits and international conferences.

This is a demanding and intellectually stimulating position. Broad scientific knowledge and training, excellent literary skills and a keen interest in the practice and communication of science are a prerequisite. The successful candidate must, therefore, be dynamic and outgoing and have excellent interpersonal skills. The salary and benefits will be competitive, reflecting the critical importance and responsibilities of this position.

The new editor will join our team in our London office. The *Nature Materials* team is part of a dynamic editorial and publishing environment that also includes *Nature*, *Nature Physics*, *Nature Nanotechnology* and *Nature Chemistry*.

Applicants should upload the following to vacancy **NPG/084/12** on http://jobs.macmillan.com/ - a CV (including their class of degree and a brief account of their research and other relevant experience), a News & View style piece (800 words or less) on a recent paper from related literature, and a brief cover letter explaining their interest in the post and their salary expectations.

Closing Date: Monday 17th September 2012

nature publishing group npg

IN227557R

***Naturejobs* gives an explosive start to your career!**

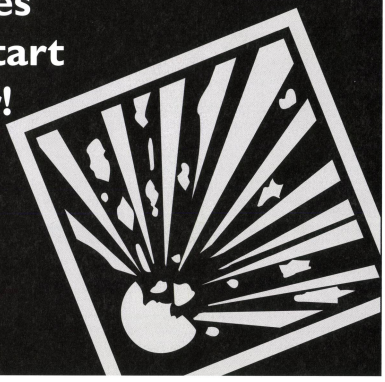

naturejobs

Max Planck Institute of Immunobiology and Epigenetics

Max-Planck-Institut für Immunbiologie und Epigenetik

The **Max Planck Institute of Immunobiology and Epigenetics** in Freiburg, Germany invites applications for the position of

Independent Junior Group Leader

in the areas of lymphopoiesis or gene regulation and nuclear architecture with an emphasis of the hematopoietic system. Candidates are expected to have a record of outstanding and internationally recognized research accomplishments.

The initial appointment will be for five years with the possibility of extension. The group will be provided with modern laboratory space in the **Department of Cellular and Molecular Immunology,** funds for equipment, running costs and technical support.

The MPI of Immunobiology and Epigenetics (www.ie-freiburg.mpg.de) offers a stimulating, international and interdisciplinary research environment. The MPI provides state-of-the-art service facilities, including Transgenic Mouse Unit, Cell Sorting, Mass Spectrometry, Bioinformatics, Deep-Sequencing and Live Cell Imaging.

The MPI of Immunobiology and Epigenetics is an international research institute with English as the working language. Salaries will be based on previous experience according to TVöD guidelines. A childcare facility is directly attached to the institute. Women are especially encouraged to apply; handicapped applicants with equal qualifications will be given preferential treatment.

Candidates should submit their applications (cover letter, C.V., description of scientific achievements and future research plans, list of publications as well as three reference letters) to our homepage: **http://www.ie-freiburg.mpg.de/jobs** Informal inquiries can be made with Rudolf Grosschedl.

Applications will be accepted until **October 30th, 2012.**

W228500R

WARNING
NO EXIT

Alternative careers if the bench gets too much.

nature jobs

INDIAN INSTITUTE OF GEOMAGNETISM

(An Autonomous Organisation of the Department of Science and Technology, Government of India)

Plot. No. 5, Sector -18, Kalamboli Highway, New Panvel, Navi Mumbai 410 218

Advt.No. 013/12

Indian Institute of Geomagnetism is a premier research Institute in the country involved in the study of all aspects of Geomagnetism. It has strong research programmes in the following three areas :

1. **Observatory and Data Analysis**
2. **Upper Atmospheric Sciences**
3. **Solid Earth Geomagnetism**

The Institute is looking for a distinguished Scientist (Citizen of India) with ability and experience to carry out

DIRECTOR

This is a top R&D management position. The Director will have the overall administrative control of the Institute and will provide high level leadership to the Institute in identification of research programmes and projects of national and international relevance in various specialized fields of research undertaken by the Institute. She/He will enthuse and motivate scientists of the Institute; promote creativity and excellence and create an atmosphere conducive to harmonious functioning of the Institute. She/He will interact and establish rapport with national and international, academic and professional institutions and specialists dealing with the domain areas of research undertaken by the Institute and will ensure multi-disciplinary and multi-institutional cooperation towards fulfilment of the objectives of the Institute.

Qualifications :

Essential : Doctorate in Earth, Atmospheric and related sciences with (a) atleast 20 years of experience in R&D in Science and Technology organizations and/or in industrial and academic institutions or as faculty/ scientist of recognized national/ international universities / research institutes/ corporate R&D Labs etc., out of which atleast 4 years should be in managerial / administrative capacity for science and technology programmes, planning and development, budget & finance, coordination and such organizational matters, (b) R&D experience in Solid Earth Geophysics / Geomagnetism / Upper Atmospheric Physics / Sun Earth relations.

Desirable : (i) Post-doctoral research (ii) Original published work of high standard (iii) Evidence of high-professional eminence by way of recognitions like fellowship of academies, national/international awards in science etc.

The appointment can also be on deputation basis. Candidates fulfilling the above norms and working in Central / State Governments /Universities / Recognised Research Institutions /Semi Government, Statutory or Autonomous Organisations in India, holding analogous post or 5 years regular service in the post carrying pay in the pay band of Rs.37400-67000 + Grade Pay of Rs.10,000/- or equivalent, can be considered for appointment on deputation basis.

Age : Not exceeding 56 years as on 1st July, 2012.

Tenure: The appointment will be for a period of 5 years or upto the date of superannuation, whichever is earlier. The tenure can be extended on recommendations of the Governing Council, by the Central Government.

Pay Scale: Rs.67,000/- (annual increment @3%) - Rs.79,000/- plus allowances, as per Central Government rules.

The Search-cum-Selection Committee constituted by the Department of Science & Technology will consider the applications and nominations received from Fellows of Academies, Directors of National Laboratories and Vice Chancellors of Universities, etc. for selection. The Committee can also consider those who may not have applied for the post, after considering all the applications and nominations and finding that no candidate is suitable. The Search-cum-Selection Committee can also invite a person of high repute for appointment. The application or nomination may be sent on the prescribed application form available on the website of the Institute, **www.iigm.res.in** to the Registrar, Indian Institute of Geomagnetism, at the above address, so as to reach him **on or before 15.10.2012.**

RW228394R **Registrar**

Faculty Position in Biophysics

University of Texas Southwestern Medical Center

The recently inaugurated Department of Biophysics at The University of Texas Southwestern Medical Center invites applications for tenure-track faculty positions at the level of assistant professor. We seek outstanding candidates who study molecular mechanisms of biological processes, in vitro or in vivo, using physical and quantitative approaches. We particularly encourage applications from those with backgrounds in single-molecule spectroscopy, quantitative imaging or cryo-electron microscopy. Scientists within the Department of Biophysics participate in a vibrant, interdisciplinary, interdepartmental, and highly collaborative research community within the University.

Applicants should submit a *curriculum vitae*, a concise description of research plans (3 page limit) and three letters of reference by **October 31, 2012** to **http://academicjobsonline.org.** The posting number is **1830.**

You may email questions to:
BiophysicsSearch@UTSouthwestern.edu.

▶ **Attention: Michael Rosen**, Chair, Biophysics Faculty Search Committee, U.T. Southwestern Medical Center, 5323 Harry Hines Blvd., Dallas, TX 75390-8816.

The University of Texas Southwestern Medical Center is an Affirmative Action/Equal Opportunity Employer. Women and minority candidates are encouraged to apply.

UT SOUTHWESTERN MEDICAL CENTER

NW228376R

UNIQUE SETTING. UNPARALLELED LEARNING.

JANELIA FARM RESEARCH CAMPUS | CONFERENCES

MARCH 3–6, 2013
INSECT VISION: CELLS, COMPUTATION, AND BEHAVIOR
Organizers: Thomas Clandinin, Karin Nordström, Michael Reiser

MARCH 6–9, 2013
DYNAMICS OF PREY CAPTURE & ESCAPE
Organizers: Gwyneth Card, Anthony Leonardo, Bill Mowrey, Katie von Reyn, Ryan Williamson

MARCH 24–27, 2013
BIOLOGICAL SEQUENCE ANALYSIS & PROBABILISTIC MODELS
Organizers: Sean Eddy, Katherine Pollard, Adam Siepel

APRIL 14–17, 2013
PLANAR CELL POLARITY
Organizers: André Goffinet, Jeremy Nathans, Tony Winshaw-Boris, Yingzi Yang, Jennifer Zallen

APRIL 21–24, 2013
SENSORY SIGNALING IN MODEL ORGANISMS
Organizers: Cori Bargmann, Craig Montell

APRIL 28–MAY 1, 2013
THE NEURAL BASIS OF VIBRISSA-BASED TACTILE SENSATION
Organizers: Alison Barth, Mitra Hartmann, David Kleinfeld, Karel Svoboda

MAY 13–16, 2013
TEMPORAL DYNAMICS IN LEARNING: NETWORKS & NEURAL DATA
Organizers: Josh Dudman, Timothy Gardner, Alla Karpova, Joseph Paton

MAY 19–22, 2013
STRUCTURAL BIOLOGY OF MEMBRANE PROTEINS
Organizers: Susan Buchanan, Tamir Gonen, Thomas Walz

Janelia conferences are small and specialized events intended to encourage rapid scientific advances and foster collaborative interactions. If you are interested in joining our robust dialogue among leading scientists, submit a research abstract today.

APPLICATION DEADLINE:
2PM ET NOVEMBER 14, 2012

www.janelia.org/conferences/nat

HHMI janelia farm research campus

NW227972E

REPROGRAPHICS: CC Media Group, London EC1V 8AR UK and **The Charlesworth Group,** Wakefield, UK.
PRINTED BY: William Gibbons & Sons Ltd, UK; **Publishers Press**, Lebanon Junction, Ky, USA and **Obun Printing Co. Inc,** Tokyo, Japan

a nature conference

Nature and VIB present:

Frontiers in plant biology: From discovery to applications

Recent years have seen an explosion of new high throughput technologies which in turn have enabled ground-breaking discoveries in plant sciences. Next generation sequencing and advances in genome assembly and analysis are helping to crack the code of even the most complex genomes. Transcriptomics, proteomics and metabolomics are leading the way in providing new insights into the inner workings of plant cells and plant cell-cell communications. Equally importantly, the cell biology toolbox – previously mainly restricted to animal and yeast cells – has finally been built up in plants allowing researchers to explore the fundamental questions in plant cell biology and compare plant solutions with those of other organisms. Importantly, the 'omics' and cell biology tools also shed light on plant-environment interactions, including responses to abiotic signals and plant-pathogen interactions.

October 3-5, 2012
Aula Ghent University, Ghent, Belgium

SPEAKERS

Julia Bailey-Serres
Dominique Bergmann
Ralph Bock
Joanna Chory
José Dinneney
Caroline Dean
Xinnian Dong
Catherine Feuillet
Jiří Friml
Maria Harrison
David Jackson
Liwen Jiang
Sophien Kamoun
Salome Prat
Pamela Ronald
Kazuki Saito
Mark Stitt
Teva Vernoux
Marc Vidal
Olivier Voinnet
Philip Wigge
Shinjiro Yamaguchi
Zhenbiao Yang
Qifa Zhang

ORGANIZERS:

Jo Bury (VIB, Belgium)
Jiří Friml (VIB / Ghent University, Belgium)
Dirk Inzé (VIB / Ghent University, Belgium)
Deepa Nath (*Nature*, UK)
Magdalena Skipper (*Nature*, UK)
Detlef Weigel (Max Plank Institute for Developmental Biology, Germany)

Abstract submission and early booking (reduced fee) deadline: July 25, 2012

For more information and to register visit:
www.nature.com/natureconferences/fpb2012

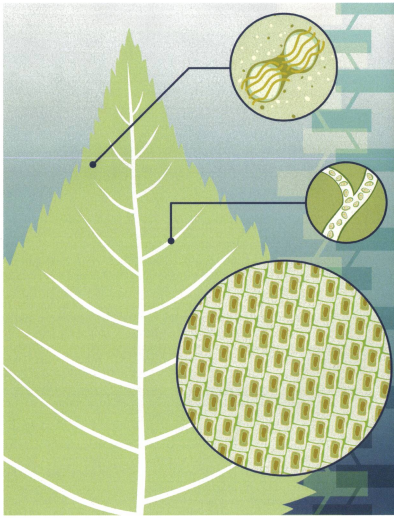

nature

VIB

IN224604E

COMMUNICANT

The ties that bind.

BY JOHN GILBEY

We'd been dating for years, but we were still tiptoeing around the question that faces many couples in our situation. It was, we agreed very late one night, a matter of commitment and trust — and not something to take on lightly.

In retrospect, it was probably me that blocked the discussion from going any further which — I realized far too late — may well have been why Helen was so enthusiastic about the Silicon Valley job. It was a wonderful opportunity: three months with a biodata start-up company in Mountain View getting them up to speed on the new techniques that she had just published.

Sure, we vowed to stay in touch, but as her work ramped up and the schedule began to bite, our conversations all but petered out. Glumly, I began to understand just what a mistake I'd made. I had, I reasoned, completely blown it — so I was really surprised when she wanted to see me the first evening after she'd got back from her trip. She had, she said, something to tell me.

We agreed to meet for dinner at the Tandoori place near the railway station — where we'd had our first date. I got there early and sat nervously scrunching poppadoms and drinking too much cold Indian lager while mentally preparing my speech of apology.

She looked fantastically alive. The Californian sun had tinted her hair slightly auburn and her skin had acquired a fresh glow of health and well-being. Helen smiled at me — the smile of someone who has important news that they are dying to share. I put two and two together and asked her if she was pregnant. Her laugh came as a relief to me, although the loud whoop I gave gained me some baleful stares from the other diners. So, if not that — then what?

Helen turned slightly in her chair and scooped her hair aside with one hand. There, at the base of her skull, was the thing we had spent so long discussing: a small, dimpled disk of alloy, anodized a fashionable lime green, laser engraved with the tiny characters defining her range of MAC addresses. Helen had got a Connection.

I can't remember everything I said, but I know I used "betrayal" a few times — and "selfish", and possibly a few worse epithets. Helen sat serenely until I'd finished my rant, then she smiled away the waiters who were trying to come to her rescue.

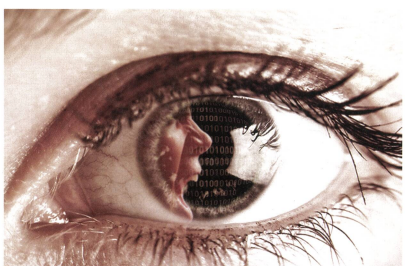

JAKOBY

She looked at me with something that I hoped was compassion — but it was the kind of look you give to a grumpy child who doesn't understand the adult world.

"I know we said we'd wait — but when I got to the lab and saw how much synergy everyone got from being Connected, I just couldn't resist. They were really kind, but I could see that I wouldn't be able to work there effectively without it. It's more than that though — it gives a wonderful sense of… well, belonging and understanding."

I asked — testily — for an example, and Helen thought for a moment. "Well, things like knowing that the X32 bus is running nine minutes late, that the guy over there in the corner is really excited about his new media job — he is here to celebrate with his friends but they are still on the bus. He thinks I'm cute, by the way — he especially likes my… Uh, never mind. Oh, and it's going to rain later — so I'd like to be home by ten…There is just so much richness and texture; I thought you, of all people, would understand."

Just because I'm a software developer doesn't mean I have to like the stuff, I thought gloomily. Having worked in the industry for years, I know just what happens when you are working against a wildly optimistic deadline with a microscopic budget — and that isn't the sort of code I want plumbed permanently into my nervous system, even if it does mean I can read my e-mail while walking down the street. I considered remonstrating with her about the lack of adequate testing protocols, the myriad unknown risks of interactions and privacy — don't get me started on privacy — but they were all old, stale arguments.

Helen now had a golden world — a world without me — with the millions of other Connected folk who obviously shared startlingly intimate details of her life. Nothing I could do or say would change her delight in this new set of senses. I have to admit, though, that I was curious about what it felt like when the software was running, so I asked her.

She wrinkled her nose, then her eyes defocused slightly while she reviewed her symbiotic systems and tried to put words to the sensations. "Kind of nice, like wearing a cosy pair of slippers — or walking with a friend. But the best bit is when an application gets upgraded, there's a sort of tingly rush of anticipation like you get on Christmas Eve when you're a kid."

Her cheeks flushed slightly in a way that I recognized from a much more private moment. "In fact," she said quietly, "the core system is updating itself right now."

I waited expectantly for a moment, and then slowly became aware of the lack of movement in the space around me. Across the table, Helen was rigid — with her pupils slowly dilating. As I watched with mounting horror, a small bead of saliva slid from one side of her mouth. Then the screaming started: sharp, guttural and inhuman — but it was a long time before I realized it was coming from me. ■

NATURE.COM
Follow Futures on Facebook at:
go.nature.com/mtoodm

John Gilbey *is currently wrestling with his first science-fiction novel,* Contextual, *and fears that it may be gaining the upper hand.*

7,000 Human Proteins Made from Human Cells.

More Assays! Better Assays!

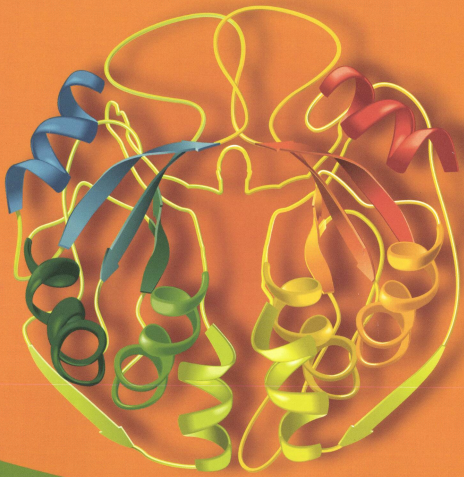

The Largest Collection of Mammalian Cell-Derived Proteins

- Protein functional studies
- Compound screening
- Immunogens for antibody production
- Assay standards: ELISA, Mass Spec, and more
- Bulk production available

Human MTOR protein activity verified in a kinase assay

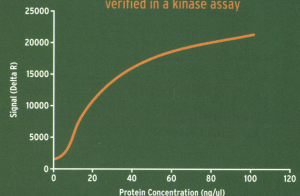

origene.com/protein

ORIGENE
Your Gene Company

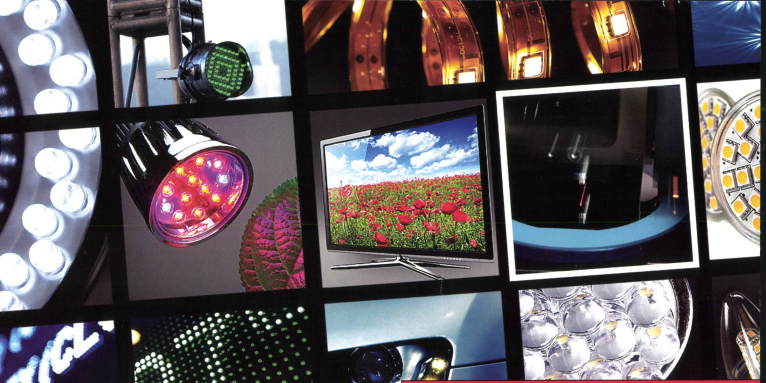

STEALTH DICED LEDs

BRIGHTER WORLD

Hamamatsu Photonics "Stealth Dicing" technology helps produce better, brighter, more affordable LEDs to enlighten our world.

Cutting an LED semiconductor wafer into individual chips with a laser, as manufacturers generally do, produces heat and destroys some of the reflective surface layers that help to channel light. This results in dimmer LEDs.

Hamamatsu Photonics solved these problems by reinventing a decade-old technology named Stealth Dicing. With Stealth Dicing, instead of cutting across the surface of the wafer, the laser is focused beneath the surface, creating a precise, "hidden" rift. The chips then break apart neatly.

No water is needed, saving a precious resource. Also, the width of the rift is nearly zero, sparing the reflective surface and thus making brighter LEDs for less money.

These improved efficiencies open the door for widespread use of these energy saving lights in general illumination and paves the way for other applications of Stealth Dicing. For example, stealth-diced silicon carbide chips could be used in next generation electronic control systems in electric cars, photovoltaics and smart grids.

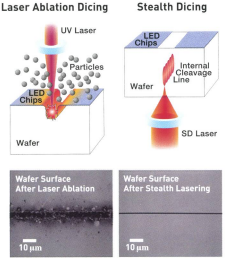

Stealth Dicing eliminates the molten debris of laser ablation dicing, so it requires no water clean-up.

Hamamatsu Photonics' expertise with light has revealed an elegant solution to a complex problem.

HAMAMATSU

PHOTON IS OUR BUSINESS

For more information, visit our site at: http://jp.hamamatsu.com/en/rd/publication

HAMAMATSU PHOTONICS K. K.

325-6, Sunayama-cho, Naka-ku, Hamamatsu City, 430-8587 Japan Telephone: (81)53-452-2141, Fax: (81)53-456-7889 URL http://www.hamamatsu.com